Magmatic Evolution and Alteration Geochemistry of the Black Mountain Southeast Porphyry Copper-Gold Deposit, Baguio Mineral District, Luzon, Philippines

Gabriel Sweet, BA

Submitted in fulfillment of the requirements for the degree of

Masters of Science

May, 2011

Abstract

The Black Mountain porphyry Cu-Au deposit is located in the central-western portion of the Baguio mineral district, Philippines, approximately six kilometers southwest of Baguio City in the Upper Bued River. It consists of two orebodies hosted within the Black Mountain Intrusive Complex (BMIC). The 'Main' or 'Kennon' orebody occurs at the northwest end of the elongate intrusive complex. Main was block caved from 1969 - 1983 and had a preproduction reserve of 47 Mt at 0.38% Cu and 0.35 g/t Au + 0.01% Mo. The Southeast orebody was block caved from 1977 – 1983 from surface at 790 meters to a subsurface elevation of 560 meters and had a preproduction reserve of 15 Mt ~0.37% Cu + 0.26 g/t Au. The Southeast orebody has a surface expression that is approximately 150 meters wide and 600 meters long, trending northwest.

Sampling and detailed mapping at a 1:1000 scale of the Black Mountain Southeast area has identified six intrusive phases, termed the Black Mountain Southeast Intrusive Suite (BMSIS). From oldest to youngest, these are: the hornblende megacrystic Liw-Liw Creek basaltic dikes (LLC), the quartz vein stockworked and quartz flooded early mineralization diorite plug that is the main host of mineralization at Black Mountain Southeast (EMD), the plagioclase and variably hornblende-phyric diorite stock and dikes (PHD), the hornblende megacrystic and clotted gabbro dikes (HMG), the hornblende clotted basalt dikes (HCB), and a series of young aphanitic to plagioclase microphenocrystic mafic dikes (AM). Over the lifetime of the porphyry system, they mark a temporal shift in composition from mafic to felsic to mafic. These rocks are derived from low- to medium-K calc-alkaline island arc melts. U-Pb and ^{40}Ar-^{39}Ar dating has confirmed the relative chronology of intrusive phases, and major and trace element whole rock geochemistry confirms the temporal shift from mafic to felsic to mafic magmas. Isotope systematics (Rb-Sr and Sm-Nd) show that both radiogenic Sr and Nd increase during the lifetime of the Black Mountain Southeast system. Major element geochemistry of hornblende phenocrysts indicate two spatially and/or temporally distinct crystallization events; one occurred at shallower levels as a product of quenching

intermediate magma, whereas the other occurred at deeper crustal levels in the presence of mafic magmas.

The magmas of Black Mountain Southeast porphyry system are a product of complex sub-arc generative mechanisms and intra-crustal modification: Liw-Liw Creek magmas were generated and emplaced prior to ~3.2 Ma, possibly as a product of resumed subduction of an aseismic seamount chain. Locally compressive tectonics facilitated intra-crustal stagnation and the subsequent fractional crystallization of a Liw-Liw Creek magma chamber. A second mafic melt (a hybrid mixture of evolved slab-derived basalt and primitive depleted mantle wedge material) was generated and, upon ascension into the crust, underplated the crystallizing Liw-Liw Creek magma chamber. The additional heat and volatiles provided by the hybrid melt resulted in partial melting at the base of the magma chamber and possibly energized the remaining melt within the intrusion, giving rise to felsic and intermediate partial melt products (as a mixture of the hybrid magma and partial melt product) as well as mineralizing fluids. A shift to local extension allowed for the emplacement of the partial melt products, and a gradual increase in the representation of the hybrid mafic melt in the upper porphyry system.

Alteration associated with the Black Mountain Southeast orebody constitutes an early sub-circular zone of potassic alteration (quartz+biotite) imposed over the central plug of EMD that is spatially and temporally linked to mineralization, followed outward by a contemporaneous propylitic alteration halo (epidote+chlorite+carbonates). A later northwest-elongate zone of pyritic and sericitic alteration overprinted both of the earlier alteration assemblages. Weak phyllic alteration is present locally in quartz-pyrite veins crosscutting the Black Mountain Southeast area.

Trace element analysis of alteration epidote demonstrated a spatial chemical zonation within the propylitic alteration halo of the Black Mountain Southeast system for a suite of pathfinder elements, originally defined by the AMIRA P765 project to be used for regional porphyry exploration (Zn, Sn, Mo, Cu, La, Y, Zr, Sr, As, Pb, Sb, U, Bi). Comparison of the alteration epidote trace element compositions with the trace element compositions of the host rocks and host phenocrysts suggested that for the majority of the suite of elements examined, host rock chemistry did not have an impact on epidote trace

element composition. However, a weak correlation between epidote, whole rock and plagioclase phenocryst Sr composition was detected. It is therefore recommended that Sr be discarded from the possible suite of pathfinder elements.

Acknowledgements

I would like to extend my heartfelt gratitude to my primary advisor, Dr. Peter Hollings, for the help, the advice, the encouragement, the patience and most of all the opportunity. Your facilitation of this project and all of the travel, lab work and wonderful experiences it entailed was (and will continue to be) deeply appreciated. To my second supervisor, Dr. David Cooke, I cannot thank you enough for the guidance you gave me while in Tasmania and the Philippines, as well as the continued input and encouragement throughout my work. Again, I thank you both for what has been an amazing formal introduction to economic geology.

All of the AMIRA P765A research team members for their input, support and friendliness towards this American standing out like a sore thumb in Tasmania; Zhaoshan Chang, Jeff Hedenquist, Nick Jansen, Bruce Gemmell, Huayong Chen, Noel White, Jamie Wilkinson and Clara Wilkinson. My thanks to Mike Baker for providing support and knowledge in the field and lab, as well as a place to live while in Hobart.

My gratitude to all of the sponsors of the P765A project, AMIRA (especially Alan Goode), the NSERC CRD program and the SEG, for providing and facilitating the financial backing for the project and my research. I would like to thank Anglo American geologists Paddy Waters and Rene Gonzales for their input on much of my work and their support in providing field materials, and Norman Tamayo for his help in Manila.

My deepest appreciation goes to the entire CODES faculty and students (and those related to them) who provided input, guidance and a much-needed break from time-to-time, and made me feel at home while in Hobart; Isa, Jam, Anita, Nathan, Lindsey, Helen, Nick, Hugo, Sarah, Karsten, Heidi, Keith, Emily, Reed, Steve, Tony, Anthony, Leonid and everyone else.

My thanks to the Lakehead University faculty, students and alumni for their support and friendship during my time there; Dr. Kissin, Dr. Conly, Dr. Hill, Scott, Corey, Marc, Ben, Larissa, John, Maura, Adam, Shankie and Roisin.

My thanks to the staff of MIT and Carleton University (Ottawa) for the use of their Laboratory equipment.

Finally, I would like to thank my family and friends back home for their seemingly unyielding support and encouragement over the last two and a half years. Thank you guys...

Table of Contents

List of Figures

List of Tables

Chapter 1

Introduction

1.1 The Baguio Mineral District and Black Mountain Southeast

Over the last three million years, porphyry (e.g., Santo Tomas II; Imai, 2001), epithermal (e.g., Acupan; Cooke et al., 1996) and skarn (e.g., Thanksgiving; Callow, 1967) mineralization has made the Baguio mineral district of Northern Luzon, Philippines, one of the world's most prolific mineral provinces (Waters and Gonzales, 2005). Current estimates of total mineral wealth contained within these deposit types are in excess of 35 million ounces of gold and over 2.7 million tons of copper (Waters and Gonzales, 2005). Active mining and production for much of the 20th century focused on gold extraction from epithermal veins, leaving the porphyry Cu-Au-(Mo) mineralization underdeveloped and the region under-explored. However, recent exploration by AngloAmerican in the 1990s lead to the discovery of multiple porphyry prospects (e.g., Mexico and Nugget Hill; Waters, 1999; Waters and Gonzales, 2005), suggesting that there are substantial Cu and Au resources yet to be uncovered.

Early research into porphyry-style mineralization noted a broad genetic relationship between the low-grade, high tonnage deposits and stocks, plugs and dikes of intermediate to felsic calc-alkaline to alkaline magmas in island and continental arcs world-wide (e.g., Sillitoe, 1972; Sillitoe, 1973; Gustafson and Hunt, 1975). Later research into the generation of the porphyry mineralization specific to the Baguio district confirmed this connection, and established a genetic link between Pliocene calc-alkaline magmatism and onset of mineralization in the Baguio district (Sillitoe and Gappe, 1984; Sillitoe, 1989). More recent work has taken this connection a step further, and attempted to identify and track the changes in the geodynamics of the northern Philippine Arc system, as they pertain to sub-arc generation and intra-crustal emplacement of fertile magmas (e.g., Defant et al., 1989; Yumul et al., 1995; Sajona et al., 1999; Hollings, 2006; Polve et al., 2007; Hollings et al., in press). As such, numerous theories have been proposed for the Pliocene tectonic and magmatic history of the northern Philippine Arc and generation of fertile magmatism in the Baguio district. These include an arc polarity reversal in the late-Miocene from dominantly westward subduction to dominantly

eastward subduction (Yang et al., 1996), tearing in the down-going slab of South China Sea below the arc in the late-Miocene to early-Pliocene (Yang et al., 1996; Bautista et al., 1996, 2001), eastward subduction of an aseismic seamount chain below northern Luzon during the early-Pliocene (Yang et al., 1996; Hollings and Cooke, 2005) and shallowing of the eastward subducting slab (Yang et al., 1996; Hollings et al., in press). Despite the abundance of models for the late-Miocene to Pliocene magmatic and tectonic evolution of the Philippine Arc, there is one aspect of the geodynamic history that appears to be a common theme linked to the onset of mineralization: a major change in arc dynamics around five million years ago.

The Black Mountain Southeast Cu-Au-(Mo) porphyry system of the Black Mountain Intrusive Complex (Waters and Gonzales, 2005) lies at the southeast end of the Baguio mineral district's westernmost Pliocene intrusive cluster. Along with the Mexico prospect (Waters, 1999; Waters and Gonzales, 2005), the Black Mountain Kennon orebody (Bureau of Mines and Geosciences, 1986) and the Thanksgiving skarn (Callow, 1967), the Black Mountain Southeast orebody represents the emergence of mineralization in the Baguio mineral district. Similarly, the magmatism genetically linked to the mineralization at Black Mountain represents the earliest fertile product of a major shift in the geodynamics of the northern Philippine Arc system. This distinct temporal setting makes the intrusive rocks of the Black Mountain system particularly attractive for a petrological study investigating the northern Philippine Arc's changing dynamics. In particular, what new processes or changes in ongoing sub-arc and intra-crustal processes could have given rise to fertile magma generation? Prior to the work presented herein, there has been little-to-no petrological data generated for the Black Mountain Southeast system or the greater Black Mountain Intrusive Complex, and no inquiry into the magmatic history of the Baguio district's mineralization through the lens of its earliest mineralized intrusive center.

1.2 This Thesis

1.2.1 Objectives

The work presented herein focuses on two aspects of Black Mountain Southeast's generation and evolution:

1. The petrogenesis of the Black Mountain Southeast's intrusive rocks, examining their sub-arc origins, their intra-crustal evolution and their intrusive history within the context of the Black Mountain Southeast system itself, and the Pliocene magmatism of the Baguio mineral district.
2. The control of host rock geochemistry on the composition of propylitic epidote. As part of AMIRA P765A, the alteration anatomy and epidote geochemistry of the Black Mountain Southeast system is given special attention in order to better constrain controlling factors on pathfinder element zonation around porphyry deposits (a method of geochemical exploration developed by the AMIRA P765 project, 2006).

Ultimately, the goal of this study was to provide insight into what aspect of the sub-arc and/or intra-crustal environment changed in the late Miocene to facilitate the production of magmas that were fertile for porphyry mineralization, and to quantify the potential control of protolith trace element composition on the trace element content of alteration epidote.

1.2.2 Methods

These topics were investigated using data collected from laboratory and field techniques, including:

1. Mapping of the lithology and alteration of the Black Mountain Southeast orebody at a scale of 1:1000, and collection of rock samples (in March of 2008; Baguio mineral district, Luzon, Northern Philippines).
2. Thin section petrography (performed at the University of Tasmania, Hobart, Tasmania; Lakehead University, Thunder Bay, Ontario; MIT University, Boston, Massachusetts).

3. Uranium-lead dating utilizing ID-TIMS zircon techniques (performed at the Pacific Centre for Isotopic and Geochemical Research at the Department of Earth and Ocean Sciences, University of British Columbia, British Columbia).
4. Argon^{39}-argon^{40} dating utilizing noble gas mass spectrometry (performed at the College of Oceanic and Atmospheric Sciences, Oregon State University, Corvallis, Oregon).
5. Analysis of Rb-Sr and Sm-Nd isotope systematics within the Black Mountain Southeast intrusive rocks (performed at the Carleton University laboratory, Ottawa, Ontario).
6. Geochemical analysis of whole rock samples using inductively coupled plasma mass spectrometry (ICPMS; performed by Acme Labs, Vancouver, British Columbia).
7. Analysis of phenocryst population major element compositions utilizing electron microprobe techniques (EMP; performed using microprobe equipment at the University of Tasmania, Hobart, Tasmania; MIT University, Boston, Massachusetts).
8. Analysis of trace element compositions of epidote and phenocryst populations using laser ablation-inductively coupled plasma mass spectrometry (LA-ICPMS; performed at the University of Tasmania, Hobart, Tasmania).
9. Analysis of trace element compositions of epidote and phenocrysts utilizing LA-ICPMS grain mapping techniques (performed at the University of Tasmania, Hobart, Tasmania).

Chapter 2

Background Geology

2.1 Geography and Location

The Baguio mineral district is located approximately 220 kilometers north of Manila in the Benguet subprovince in the southern foothills of the Central Cordillera mountain range (Fig. 2.1). The mineral district includes a wide variety of deposit types, spanning the range of epithermal (e.g., Antomok and Acupan deposits), porphyry (e.g., Santo Tomas II and Black Mountain) and skarn (e.g., Thanksgiving) style mineralization, all of which are spatially and temporally associated with the eastward subduction of the South China Sea (Waters and Gonzales, 2005; Waters et al., in press). The host stratigraphy is a volcano-sedimentary fold belt forming a 300-kilometer long, 50-kilometer wide mountain range. The topography of the Baguio mineral district is characterized by steep-walled drainage valleys and rugged peaks up to 2,900 meters above sea level. The climate is tropical monsoonal and can produce daily rainfall in excess of one meter during peak wet season (generally between June and October), contributing significantly to high regional erosion rates.

The Black Mountain Copper-Gold Porphyry system (16°21'13.99"N ; 120°36'32.63"E) is located in the central-western portion of the Baguio mineral district, approximately five kilometers southwest of Baguio City in the Upper Bued River (Fig. 2.2). It consists of two ore bodies hosted within the Black Mountain Intrusive Complex (discussed later in this chapter). The 'Main', or 'Kennon' ore body occurs at the NW end of the elongate Black Mountain Intrusive Complex and extends into the Southeast ore body (Fig. 2.2). Associated deposits include the Thanksgiving gold and base metal skarn approximately 200 meters east of the Kennon ore body (Callow, 1967), and the Mexico copper-gold prospect two kilometers to the west (Waters and Gonzales, 2005; Fig. 2.2).

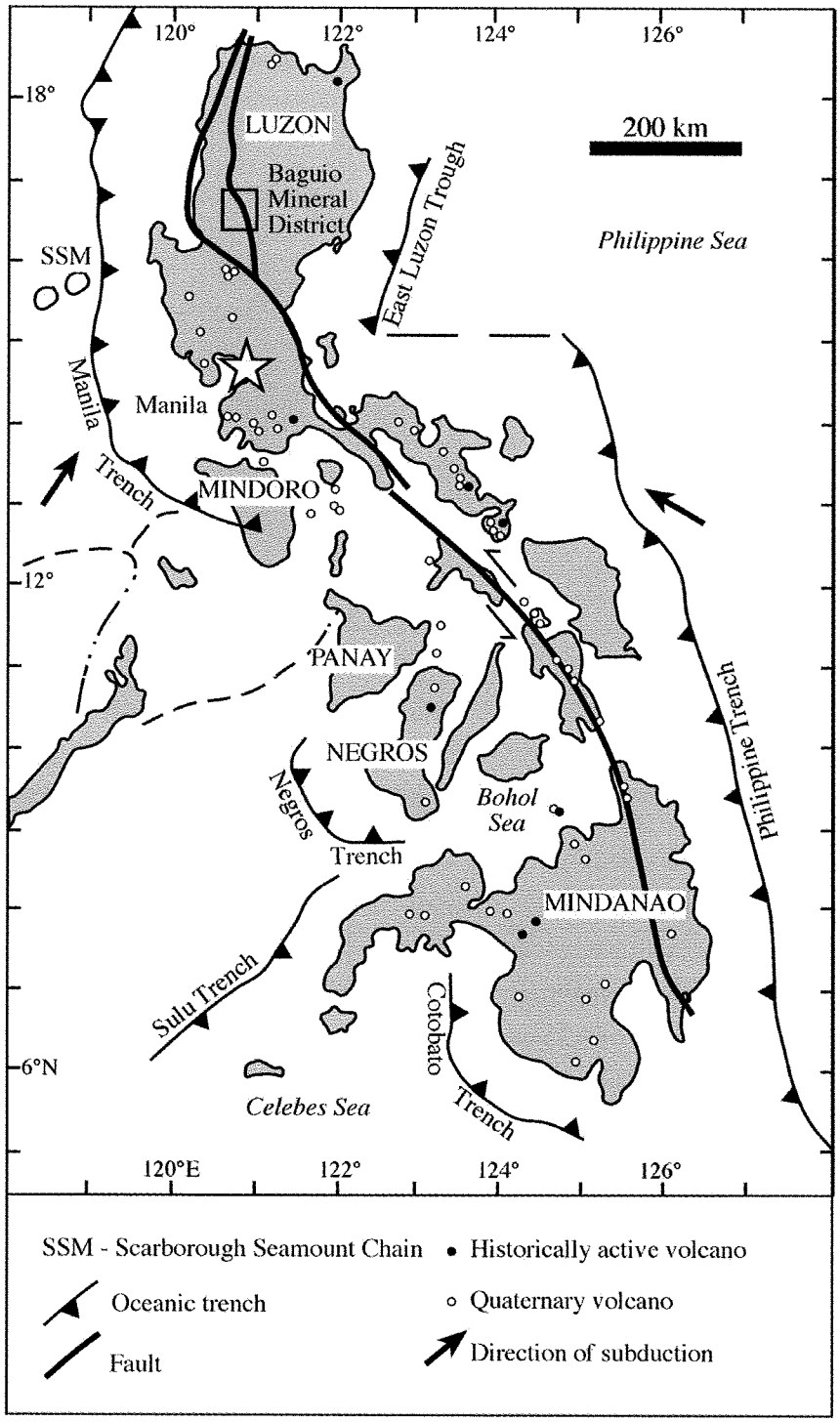

Figure 2.1 – Map of the Philippines showing submarine trenches, Philippine Fault and the subduction of the Philippine Sea and South China Sea below the northern island of Luzon, modified after Mitchell and Leach (1991). The location of the Baguio Mineral District is denoted by the black box approximately 220 kilometers north of Manila.

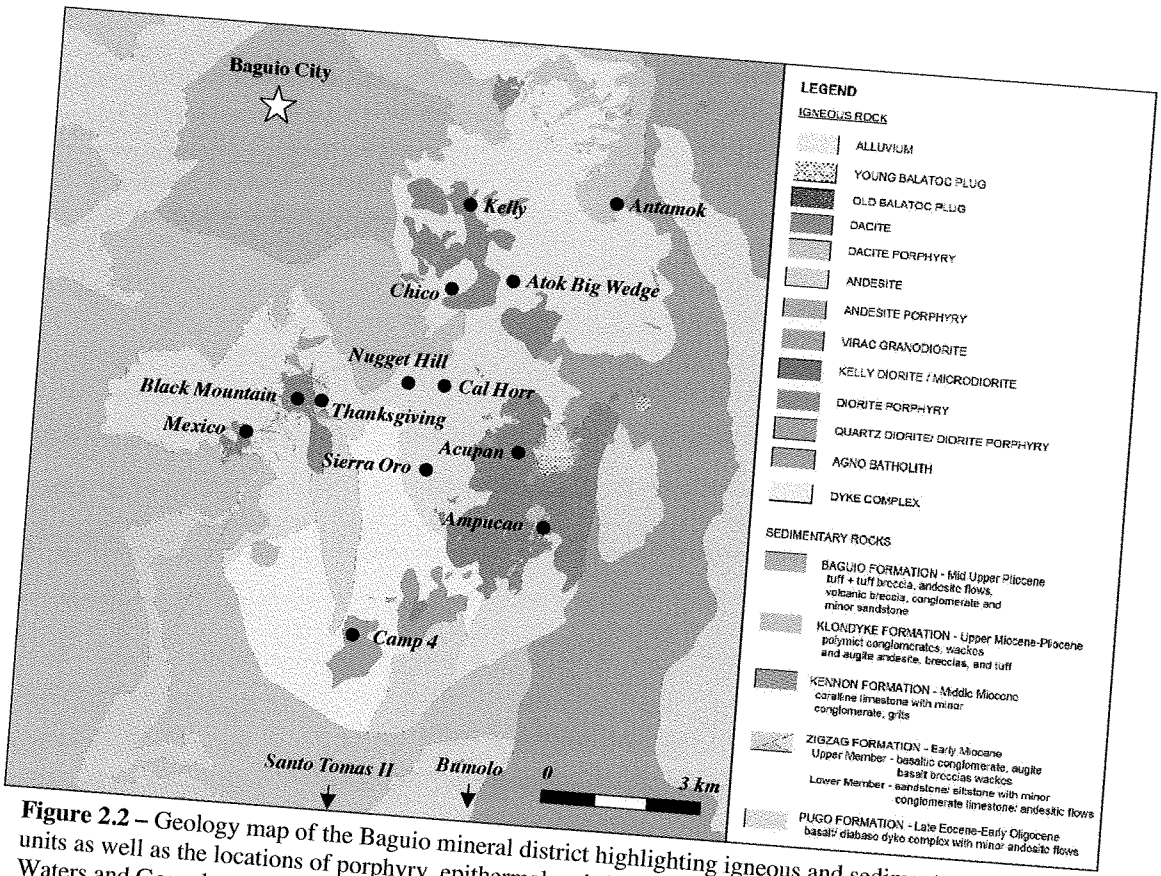

Figure 2.2 – Geology map of the Baguio mineral district highlighting igneous and sedimentary rock units as well as the locations of porphyry, epithermal and skarn deposits and prospects. Modified after Waters and Gonzales (2006).

2.2 Tectonic Framework

The history of the Philippine Arc over the last 50 million years is marked by a complicated procession of plate rotations, aseismic ridge subduction and obduction, collision, arc reversal and ophiolite emplacement. However, the development of a comprehensive reconstruction of the Luzon Arc and the Baguio mineral district's local tectonic history is complicated by multiple competing interpretations of the geological record (Hall, 1996, 1997a, 1997b, 2001; Yang et al., 1996; Bautista et al., 2001; Yumul et al., 2003; Hollings et al., in press). The debate over the local tectonic nature of Luzon is very much active. A tectonic reconstruction of Southeast Asia and the greater South Pacific was proposed by Hall (1996, 1997a, 1997b, 2001) based on paleomagnetic data. However, Yang et al. (1996), Bautista et al. (2001), Yumul et al. (2003) and Hollings et al. (in press) have proposed differing interpretations of the evolution of the Philippine Arc based on local stratigraphy and igneous products. Below is a summary of the

proposed reconstructions, highlighting the similarities and differences between the regional interpretations and the local models.

2.2.1 Regional Tectonic History of the Philippines and Southeast Asia

Hall (1996, 1997a, 1997b, 2001) modeled the tectonic evolution of southeast Asia and the South Pacific. The following section summarizes his work, highlighting the development of the Philippine Arc and its post-Miocene evolution in the context of the region. For more detail and visual schematics for Hall's reconstruction, the reader is referred to Hall (1996, 1997a, 1997b, 2001).

50+ Ma – 10 Ma

Following the breakup of the Gondwana super continent prior to 50 million years ago, the eastern Philippine islands were situated at the southern overriding subduction margin of the clockwise-rotating Philippine Sea Plate. The islands formed in an intra-oceanic arc setting of Cretaceous age (Hall, 1997b). Southward subduction of the North New Guinea-Pacific ridge beneath the Philippine Sea Plate prior to 45 Ma resulted in extension-related boninitic volcanism and the production of the Izu-Bonin-Mariana arc systems. The ophiolitic Zambales complex on Luzon is thought to be the western extent of this boninitic volcanic arc (Hall, 1997a). The east Philippines and Halmahera arcs, located on the southern margin of the Philippine Sea Plate were incorporated as the basement rocks of a growing arc system above the northward subducting Indian-Australian plate.

Between 50 and 40 Ma, Hall (1997a) suggested that extensive clockwise rotation (up to 50 degrees) of the Philippine Sea Plate was possibly linked to the aforementioned subduction of the North New Guinea-Pacific spreading ridge beneath the Philippine Sea Plate. The development of a spreading ridge in the center of the Philippine Sea Plate, resulting in the opening of the West Philippine-Celebes Sea has also been cited as a product of the North New Guinea-Pacific ridge subduction. However, Hall (1997b) also noted that the new spreading center could have also been a product of initiated southward subduction of the South China Sea beneath Luzon and Sulu arc.

Between 40 and 30 Ma, the Philippine Sea Plate ceased clockwise rotation, but was now situated such that a transform fault separated the formerly continuous Luzon and Izu-Bonin arcs. Southward subduction of the South China Sea continued beneath the Luzon arc. However, the period from 30 to 20 Ma was marked by multiple large-scale plate collisions. Collision of the New Guinea passive margin with the east Philippines-Halmahera arc system occurred at 25 Ma. This was followed immediately by the arrival of the Australian margin at the southern boundary of the Philippine Sea Plate, causing clockwise rotation of the Philippine Sea Plate. This termination and subsequent rotation initiated subduction beneath the Sulawesi-Sangihe arc extending north to Luzon, and enabling the northward migration of the east Philippine islands (Hall, 1997b)

Ongoing clockwise rotation of the Philippine Sea Plate and subduction beneath the Sulawesi-Sangihe arc between 20 and 10 Ma, drove Luzon northwestward into the Eurasian plate. The collision between Luzon and the Cagayan ridge with the passive margin in Mindoro and Palawan, forced subduction southward below the Sulu arc, continuing until approximately 10 Ma. The rest of the Philippine islands continued to migrate northwestward as the Philippine Sea Plate's clockwise rotation continued. Hall (1997a) proposed that intra-plate strike-slip and subduction structures within the east Philippine islands (linked to torsion forces derived from the plate's rotation) produced localized volcanic activity.

10 Ma – present

Hall (1997b) noted that by 10 Ma, Southeast Asia was by-and-large recognizable in its present form. During this period, the pole of the Philippine Sea Plate's clockwise rotation shifted north. Coupled with the continuing northward movement of the Australian plate, the collision of the Luzon arc with Eurasia, and the cessation of Borneo's rotation, this initiated new subduction at the Philippine and Negros trenches at approximately 5 Ma. Continued subduction at the Manila, Sangihe and Halmahera trenches was linked to the new subduction zones via a series of strike-slip systems running through the Philippine islands. Hall (1997b) inferred that these transform fault

systems produced local intra-plate deformation by effectively breaking the Philippine islands into small fragments.

The present day Philippine arc system is defined by a double arc, with the older (Miocene-Pliocene) Western Volcanic Chain (WVC) and the younger (Quaternary) Eastern Volcanic Chain (EVC) separated by 50 kilometers north of Luzon (18°N) and converging near 20°N (Yang et al., 1996). The Philippine Arc is a composite terrain, comprised of the aseismic Palawan microcontinental block and the Philippine Mobile Belt (Gervasio, 1971; McCabe et al., 1985; Yumul et al., 2003). The arc is situated between two major subduction zones (Fig. 2.1): to the west, the South China Sea plate is subducting eastward along the Manila Trench beneath Luzon, accompanied by the Southeast Sulu Sea subducting eastward along the Negros Trench further to the south. Eastward subduction/obduction of the Scarborough Ridge (an extinct spreading center) along the top of the South China Sea plate has been cited by Yang et al. (1996) and Bautista et al. (2001) as having a major role in shaping the Luzon Arc (discussed below). The eastern margin of the Philippine arc is characterized by westward subduction of the Philippine Sea at the East Luzon Trough in the north, and the Philippines Trench in the south. A series of transform faults cut the arc and are visible in Figure 2.1 as the north-northwest trending, sinistral transcurrent Philippine Fault. A series of splays off the Philippine Fault through northern Luzon, have produced a highly complex arrangement of "fragments" (Hall, 1997b).

2.2.2 Local Tectonics and Magmatism of the Baguio Mineral District

Despite the extensive paleomagnetic data set presented in work by Hall (1996, 1997a, 1997b, 2001), the regional reconstruction detailed above cannot explain the local geological record of Luzon's Central Cordillera. Based on geochemical and petrological studies of the intrusive suites across Luzon, Yang et al. (1996), Bellon and Yumul (2000), Bautista et al. (2001) and Yumul et al. (2003) proposed a different reconstruction of the Philippine Arc, noting an arc polarity reversal in the early Miocene and the subsequent subduction of the Scarborough Seamount Chain.

In contrast to the proposal that westward subduction at the Philippine Trench was not initiated until 5 Ma (Hall, 1996, 1997a, 1997b, 2001), local tectonic/magmatic

reconstructions by Yang et al. (1996) and Bautista et al. (2001) inferred a major early Miocene arc-polarity reversal in which dominant subduction shifted from westward along the pre-existing Philippine Trench, to eastward along the newly developed Manila Trench. Hall (1997a) proposed that the Philippine Trench was not active during the early Miocene, negating the possibility of a polarity reversal. Coupled with the later subduction/obduction of the aseismic Scarborough Ridge, this transition to eastward subduction has been cited as a driving force behind the Miocene double-arc development, emplacement of post-Oligocene intrusives and major local uplift (Yang et al., 1996; Bautista et al., 2001; Cooke et al., 2006). It has also been linked to the widespread mineralization of the Baguio and Mankayan Mineral Districts (e.g. Cooke et al., 2006). Noting the geodynamic model of the similar double arc system of the Lesser Antilles Arc (Bouysse and Westercamp, 1990) and the effects of ridge subduction on arc-trench systems (Vogt, 1973; Kelleher and McCann, 1976; Bogt et al., 1976; Nur and Ben-Avraham, 1983, 1989; McCann and Sykes, 1984; McGeary et al., 1985; Cloos, 1993), Yang et al. (1996) proposed a three-stage ridge subduction model (Fig. 2.3a-c) for the development of the northern Taiwan-Luzon Arc over the last six million years:

Stage 1 (6 Ma) (Fig. 2.3a)

Eastward subduction of the South China Sea Plate below the Philippine Sea Plate during the Miocene led to the formation of the West Volcanic Chain, a typical intra-oceanic island arc system. Yang et al. (1996) noted that the newly formed arc was approaching the Eurasian plate margin as the Philippine Sea Plate moved in a northwesterly direction. This northwesterly movement is consistent with the model of Hall (1997a). The Scarborough Ridge, a young, low-density extinct spreading center, had not yet reached the arc (Yang et al., 1996).

Stage 2 (5-4 Ma) (Fig. 2.3b)

After reaching the northern Philippines arc, the relatively buoyant Scarborough ridge resisted subduction and was accreted to the base of the overlying plate. This underplating was cited by Yang et al. (1996) as a driving force behind major uplift in the fore-arc basin, and the disruption of volcanic centers in northern Luzon resulting in a cessation of

volcanism. At the same time, the Taiwan-Luzon Arc collided with the Eurasion continental margin, terminating local volcanic activity in the north. Large amounts of continentally-derived sediments were subducted with the down going South China Sea Plate, enriching the mantle wedge sources of the arc magma (Defant et al., 1989, 1990; McDermott et al., 1993; Fourcade et al., 1994; Yang et al., 1994).

Stage 3 (<2 Ma) (Fig. 2.3c)

Subduction of the Scarborough Ridge resumed approximately two million years ago as the compressive forces and pull of the down going slab forced the ridge beneath the arc. However, the relative buoyancy of the ridge resulted in a significantly shallower angle of subduction for the South China Sea Plate, shifting volcanism to the east of the WVC. Continued upward forces driven by the buoyant ridge are theorized to have produced a tear in the South China Sea Plate at approximately 20°N, exposing the mantle wedge to an enriched mantle source (Yang et al., 1996).

Bautista et al. (1996, 2001) identified multiple issues stemming from the model of Yang et al. (1996), noting the lack of a seismic gap in the area of the proposed tear at 20°N, and that the WVC and EVC would diverge to the north if a tear was in fact located at 20°N. Instead, Bautista al. (2001) proposed an alternative model in which subduction of the buoyant Scarborough Ridge caused bending in the down going slab at approximately 20°N, generating extensional stresses in the overriding plate. Interpreting a seismic gap at 17°N as a trace of the down going Scarborough Ridge, Bautista et al. (2001) inferred that the slab tear was located at approximately 16°N. They concurred with Yang et al. (1996) that slab flattening produced the Taiwain-Luzon double arc feature, but discounted the Scarborough Ridge as the cause. Instead Bautista et al. (2001) invoked the subduction of a large, buoyant plateau (the Stewart Bank and Virgan High) at 20°N as the driving force behind slab flattening. They noted the Scarborough Ridge was a plane of weakness in the down going South China Sea Plate along which tearing could occur.

Recent work by Hollings et al. (in press) has challenged the arc polarity reversal from the models of Yang et al. (1996) and Bautista et al. (1996, 2001). Instead, Hollings et al. (in press) reported that the geochemistry and geochronology of the late-Oligocene

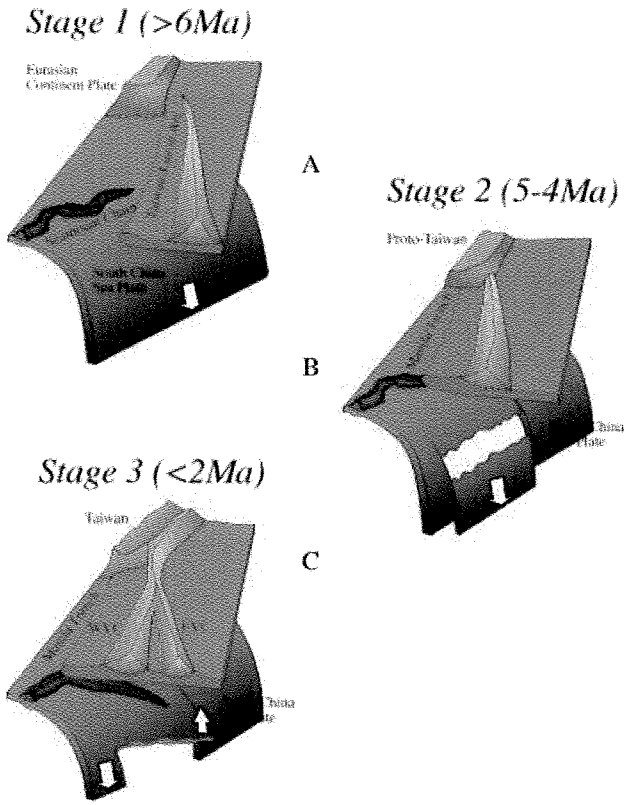

Figure 2.3 – Geodynamic model of the late Miocene onwards evolution of the Taiwan-Luzon Arc (after Yang et al., 1996). (A) Stage 1: Generation of the Taiwan-Luzon Arc by volcanism related to the eastward subduction of the South China Sea Plate. (B) Stage 2: Collision of the northern Taiwan-Luzon Arc with the Eurasian Continental margin produced proto-Taiwan. Resistance to subduction by the Scarborough Seamount Chain (and attachment beneath the overriding plate) yielded a localized cessation in volcanism. A tear in the down going slab may have occurred during this time period. (C) Stage 3: Continued downward pull by the South China Sea slab forced the aseismic Scarborough Ridge below the arc. However, the higher buoyancy of the ridge yielded a shallowing of the subduction angle, and shifted the centers of active volcanism eastward. This allowed for the distinction to be made between the older West Volcanic Chain (WVC) and the younger East Volcanic Chain (EVC). A slab break occurred at 20°N, allowing for enriched mantle component to enter the mantle wedge.

to early-Miocene intrusive rocks of the Baguio district are consistent with eastward subduction of the South China Sea plate, implying that subduction along the Manila trench generated magmatism prior to the proposed arc polarity reversal (Yang et al., 1996; Bautista et al., 1996, 2001). As well, Hollings et al. (in press) suggested that the mid Miocene-onwards geodynamic environment was largely a product of slab flattening rather than subduction of the Scarborough Ridge. In particular, they attributed the cessation in volcanism, uplift and exhumation of the Baguio district, and onset of porphyry and epithermal mineralization to shallowing of the subduction angle of the South China Sea below the Luzon arc.

2.3 Geology of the Baguio Mineral District

The stratigraphy of the Luzon Central Cordillera documents the evolution of a marginal basin depositional environment to an island arc setting. The progression from Cretaceous-Eocene marginal basin sedimentation and volcanism, to shallow marine sedimentation in the late Eocene to mid Miocene, to calc-alkaline magmatic arc construction in the mid Miocene is broadly consistent with the tectonic reconstructions of Yang et al. (1996), Bautista et al. (2001) and Hollings et al. (in press), as well as the regional models of Hall (1996, 1997a, 1997b). The shift from submarine deposition to subaerial volcanism (and the subsequent generation of a magmatic arc) is thought to be a product of the mid-Miocene initiation of the Manila Trench (Hollings and Cooke, 2005). Development of mid-Miocene and Pleistocene volcanic centers and intrusive suites described below are also directly related to the eastward subduction of the South China Sea beneath Luzon.

2.3.1 Volcanic and Sedimentary Units

Formal designation of the Baguio mineral district's stratigraphy was proposed by Pena (1970). Since then, challenges, refinements and correlative studies have been advanced by Balce et al. (1980), De los Santos (1982), UNDP (1987), Malaterre (1989), Mitchell and Leach (1991), Pena (1998), Gonzales (2004), and Waters et al. (in press). The division of units presented below represents modifications and refinements of the Pena's (1970) stratigraphy by Malaterre (1989), Pena (1998) and Waters and Gonzales (2006).

Pugo Formation

As the stratigraphic floor of the Baguio mineral district (Fig. 2.4), the Pugo Formation comprises basaltic and andesitic extrusive rocks with minor sandstone, argillite, chert and volcaniclastic interbeds (Fig. 2.5). It is laterally heterogeneous, exhibiting local greenschist facies metamorphism. The metamorphic nature of this heterogeneity has led to an internal division of the Pugo by some workers, with the metamorphosed rocks classified as the Dalupirip Schist (Balce et al., 1980). Surface exposure is prominent in the eastern margin of the Baguio mineral district as well as throughout the Bued River within and south of the Black Mountain Porphyry deposit (Fig. 2.2). The Pugo has been estimated to be 1100 to 1600 meters thick (Pena, 1998) and is correlated with the Lepanto Metavolcanic rocks and the Malitep Formation in the Cervantes-Bontoc area (Malaterre, 1989). Pena (1998) assigned the Pugo Formation a Cretaceous to Eocene age. The depositional environment is inferred to have been a subduction-related marginal basin, though Malaterre (1989) has interpreted the Pugo to be the sedimentary cover of an incomplete ophiolitic sequence.

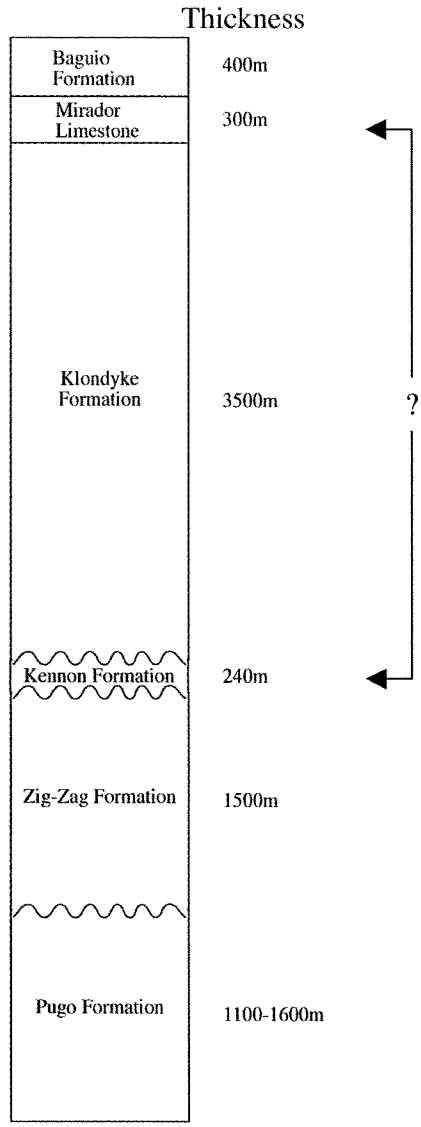

Figure 2.4 – Generalized stratigraphic column for the volcano-sedimentary units of the Baguio mineral district. After Pena (1970), Malaterre (1989), Pena (1998) and Waters and Gonzales (2006). The question mark and connecting brackets between the Mirador Limestone and the Kennon Formation indicates that these two units may be one and the same, as indicated by Balce (1980) and Malaterre (1989).

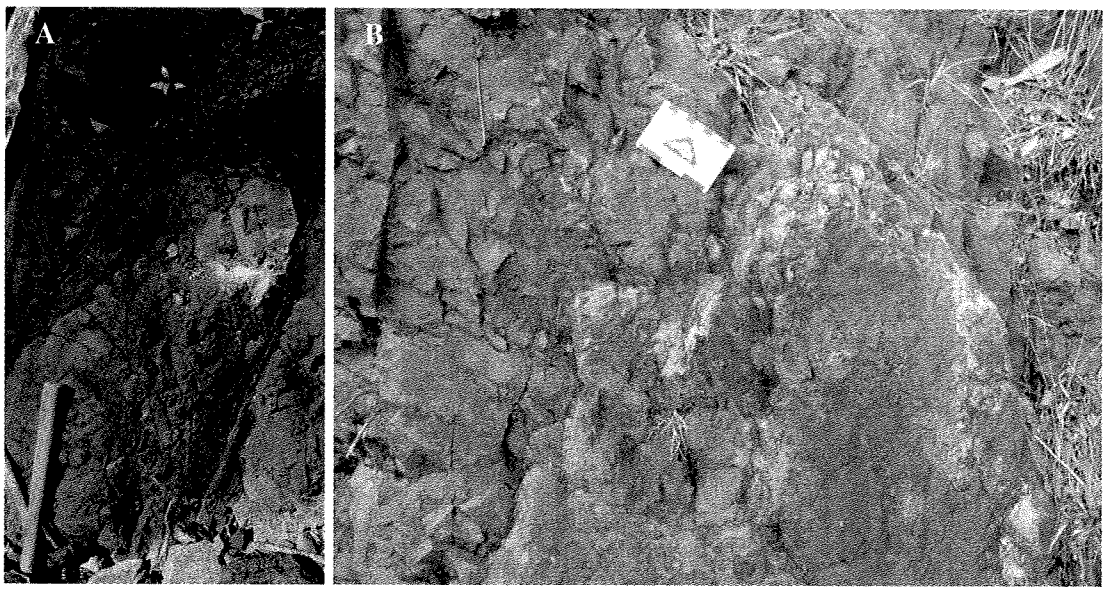

Figure 2.5 – Examples of Pugo Formation observed in the Baguio district: (A) vesicular pillow basalts in the Bued River (photo from field work conducted during the AMIRA P765 project); (B) an outcrop of extrusive mafic rock (photo by Mike Baker, 2008).

Zig-Zag Formation

The Zig-Zag Formation unconformably overlies the Pugo Formation (Fig. 2.4), and is a sequence of marine conglomerates, sandstones, shales, andesitic lavas and tuffs and rare limestones (Pena, 1970). Vertical variation within the Zig-Zag Formation has led to the recognition of an upper and lower subdivision. The lower Zig-Zag Formation is marked by inter-bedded conglomerates, wackes, siltstones and andesitic tuffs, whereas the upper Zig-Zag Formation includes conglomerates, basalt flows and minor wackes. The formation is exposed throughout the central Baguio district (Fig. 2.2), and is readily observed in the Bued River valley at Camp 6 where it appears as alternating beds of red and green-gray sandstone (Fig. 2.6). The alternation of bedding color reflects the cycling of depositional redox conditions from oxidizing to reducing (Waters and Gonzales, 2005). Correlative work by Malterre (1989) identified outcrops of Zig-Zag Formation in the western Bontoc-Cervantes area, and fossil-based dating suggests the Zig-Zag is of late Oligocene to early Miocene age. Pena (1998) estimated that the formation is between 1700 and 1800 meters thick.

Figure 2.6 – Examples of Zig-Zag Formation observed in the Baguio district: (A) clasts of diorite in a Zig-Zag Formation breccia (photo by Mike Baker, 2008); (B) alternating beds of red and green-gray sandstones in the Bued River, Camp 6 (photo by David R. Cooke, 2008).

Kennon Formation and the Mirador Limestone

The Kennon Formation unconformably overlies the Zig-Zag Formation (Fig. 2.4), and is characterized by shallow marine massive, gray, fossil-rich limestones, calcarenites and calcirudites (Pena, 1970; Gonzales, 2004; Fig. 2.7). Balce et al. (1980) noted that the Kennon Formation could be broken down into two formal units: the Kennon Limestone (massive, fossil-rich limestone) and the Twin Peaks (marl and calcareous mudstones). Exposure of the Kennon is widespread, outcropping west of the Mexico Prospect and in the northwest corner of the Baguio district (Fig. 2.2), and extending northwards into the Bontoc-Cervantes and Illocos areas (Malaterre, 1989). Pena (1998) determined that the Kennon is between 190 and 240 meters thick. Dating of faunal contents by Malaterre (1989) yielded an age of early to middle Miocene, representing a time of tectonic quiescence and reef building prior to middle Miocene volcanic arc construction.

The Mirador Limestone was originally documented by Leith (1938) to include the Kennon and Mirador limestones. Work by Corby et al. (1952) revised the stratigraphic designations of the Baguio district by establishing the Kennon Formation as an independent unit from the Mirador. However, more recent work by Balce (1980) and Malaterre (1989) indicated that due to the existence of Zig-Zag conglomerates at its base, the Mirador Limestone is analogous to the Kennon Formation, conformably overlying the Klondyke Formation at the western edge of the Baguio district (Fig. 2.2). A detailed description and correlation of specific outcrops of early-to-mid Miocene limestone in the

Baguio district was presented by Balce et al. (1980), wherein it was suggested that the classification name of "Mirador" be discontinued. Pena (1998) estimated the Mirador to be approximately 300 meters thick and to be of Miocene to Pliocene age. A second age of early-to-mid Miocene was reported by Tan (1994) based on the faunal content of the Mirador Limestone.

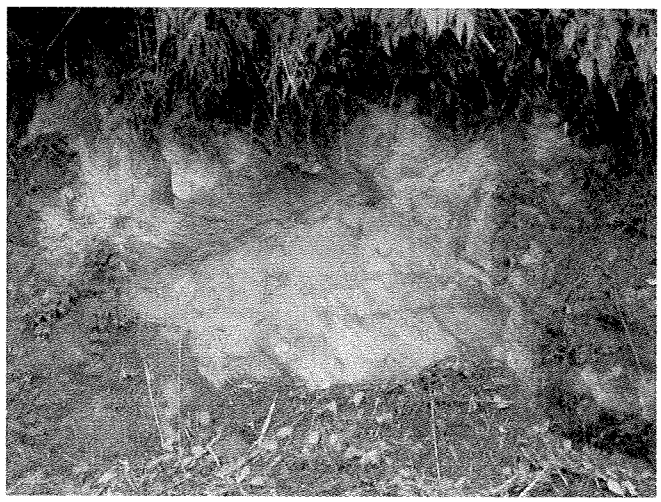

Figure 2.7 – Outcrop of Mirador limestone (photo by David R. Cooke, 2008).

Klondyke Formation

The Klondyke Formation was defined by Durkee and Pedersen (1961) and Gonzales (2004) as a thick sequence of terrestrial to shallow-marine clastic sedimentary and volcanic rocks, exposed in the western Baguio mineral district (Fig. 2.2). Unconformably overlying the Kennon Formation (Fig. 2.4), the Klondyke Formation is characterized by polymictic conglomerates interbedded with sandstones, siltstones, shales, pyroclastics, limestones and calcirudites (Fig. 2.8a). Many of the clasts in the conglomerate are well rounded, coarse boulders of the Central Cordilleran Diorite Complex (described below), possibly indicating a localized paleo-depositional setting proximal to the Central Cordilleran uplift. Dating of dacitic clasts yielded an age of 20±1.0 Ma (Bellon and Yumul, 2000), indicating a maximum age of deposition for the Klondyke Formation. Lateral variation in the Klondyke's thickness is noted by Pena (1998), with a range of 1800 meters in the east-central section of the Baguio district (near Kennon Road) thickening westward to 3500 meters thick (near the Marcos Highway). Nano-fossil

dating by Leon et al. (1991) yielded an age of middle to late Miocene for the Klondyke Formation.

Baguio Formation

Identified by Smith and Eddingfield (1911), the Baguio Formation is a series of subaerial pyroclastic and siliciclastic rocks unconformably overlying the Mirador Limestone and Klondyke Formation (Fig. 2.4). The Baguio Formation is composed primarily of tuffs, tuff breccias, volcanic breccias, conglomerates, sandstones and andesite flows (De los Santos, 1982; Pena, 1998; Fig. 2.8b), with some outcrops containing the pyroclastic and siliciclastic rocks overlying the andesite flows (southeast of Baguio City, for example). Reported thickness ranges from 200 to 400 meters, with ages ranging from an Ar-Ar age of 3.66±0.11 Ma for an andesitic pyroclastic sample (Dunlap, 2002) to a K-Ar age of 3.57 Ma for a basaltic breccia clast (Malaterre, 1989).

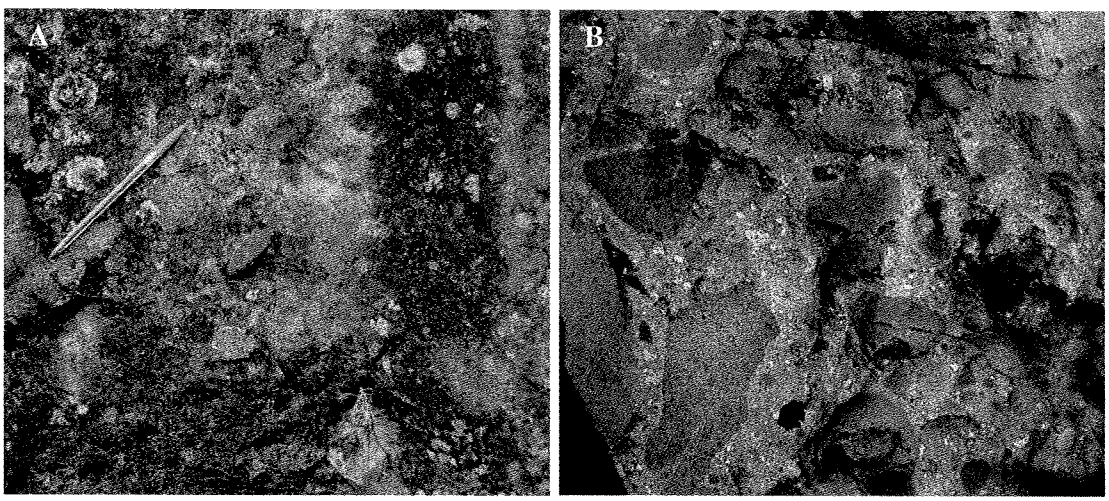

Figure 2.8 – Examples of Klondyke Formation conglomerate (A) and Baguio Formation dacitic sandstone (B) observed in the Baguio district: Both photos are from field work conducted during the AMIRA P765 project.

2.3.2 Intrusive Units

Due in part to their temporal and spatial association with porphyry, epithermal and skarn mineralization (addressed later in this chapter), the post-Oligocene intrusive rocks of the Baguio mineral district are well studied and documented. Previous work by Shannon (1979), Balce et al. (1980), JICA (1983), UNDP (1987), Pena (1998), Waters and Gonzales (2005), Waters et al. (in press) and others detailed the spatial and temporal relationship of the intrusive rocks with respect to the local stratigraphic column, whereas Bellon and Yumul (2000), Yumul et al. (2003), Polve et al. (2007) and others investigated the nature and origins of these magmas. The following descriptions of Baguio intrusive suites are based on the work of the aforementioned authors, and reflect the Miocene-onwards tectonic development of Luzon as detailed above.

A temporal division is present in the post-Oligocene igneous record of the Baguio mineral district. Specifically, a cessation of voluminous magmatism between approximately 17 and 5 Ma subdivides the intrusive suites into an early Miocene group, and a Pliocene group, the latter of which is associated temporally and spatially with the onset of mineralization within the Baguio district. However some authors have noted volumetrically minor adakitic magmatism occurring in central Luzon during the middle-to-late Miocene (Sajona et al., 1993, 1994, 1996; Sajona and Maury. 1998; Yumul et al., 2000; Castillo et al., 1999; Rae et al., 2004). Specifically within the Baguio district, Jego et al. (2005), Payot et al. (2007), and Gregoire et al. (2008) have identified the Monglo adakite.

Central Cordillera Diorite Complex

The eastern edge of the Baguio mineral district is marked by a north-south trending, elongate intrusive complex (Fig. 2.2). This multi-phase series of intermediate intrusive rocks was known as the Ango Batholith until Pena (1998) renamed it the Central Cordillera Diorite Complex (CCDC). Six intrusive phases have been recognized by Shannon (1979) in the CCDC:

1. The Kadang Trondhjemite: a medium to coarse-grained, volumetrically minor constituent of the CCDC, containing significant anhedral quartz (30%-60% by volume) and minor mafic minerals such as hornblende and biotite, and occupying

"thin slivers" along the eastern and western margins of the complex (Shannon, 1979).

2. The Itogon Quartz Diorite: a volumetrically significant intrusive phase in the southern CCDC, exhibiting a mostly medium-grained texture and a gradational contact with the Kadang Trondhjemite where modal plagioclase increases at the expense of quartz.
3. The Antamok Diorite: a volumetrically dominant phase in the northern CCDC, characterized by gradational contacts with both the Itogon (to the south) and Kadang (to the east) as plagioclase and mafic mineral contents increase at the expense of quartz.
4. The Liang Gabbro: a minor, medium to coarse-grained, multi-phased stock characterized by a gradational contact with the Antamok Diorite over short distances. Modal minerals are dominated by plagioclase, hornblende and augite.
5. The Lucbuban Gabbro: a coarse-grained, small wedge shaped stock in the southern CCDC containing predominantly plagioclase, hornblende and augite, and exhibiting a sharp contact with the Itogon Quartz Diorite.
6. The Virac Granodiorite: a medium-grained, large intrusive body on the west-central flank of the CCDC, exhibiting a subtle north-south heterogeneity and composed predominantly of plagioclase, hornblende, quartz and orthoclase. This unit was only recently included in the CCDC (Waters and Gonzales, 2005) and was formerly a member of the Virac Pluton (Shannon, 1979).

The age of the diorite complex ranges considerably, but Waters and Gonzales (2005) have inferred a middle Miocene age of emplacement for the overall complex via correlation of their Ar-Ar dates for the Lucbuban Gabbro (22.1±0.2 Ma) and Virac Granodiorite (20.10±0.13 Ma and 20.82±0.32 Ma) with K-Ar dates from Malaterre (1989) for a quartz diorite intrusive (18.8±0.9 Ma and 16.1±1.0 Ma) and Sajona (2002) for samples of diorite phases (16.6±0.8 Ma to 13.2±0.7 Ma). With respect to the stratigraphy of the district, Waters and Gonzales (2005) noted that the Virac Granodiorite has intruded both the Pugo and Zig-Zag formations, emphasizing its emplacement in the middle Miocene.

Monglo Adakite

The Monglo adakite has been defined as a hornblende- and xenolith-bearing dacite (Jego et al., 2005; Payot et al., 2007). It crops out as a 50 meter-thick sheet in a rock quarry approximately 16 kilometers northwest of Baguio City where it is observed crosscutting the Klondike formation (Fig. 2.2). Three types of xenoliths have been identified by previous workers, and include (in order of abundance), spinel dunite xenoliths, amphibole-bearing gabbro xenoliths, and amphibolite xenoliths, all of which are between 1 and 10cm in diameter (Jego et al., 2005; Payot et al., 2007; Gregoire et al., 2008). A K-Ar age of 8.65±0.23 Ma was reported for the host adakitic dacite, and an age of 115.6±8.33 Ma for an amphibolite xenolith (Payot et al., 2007). Petrographic and geochemical studies of the xenolith populations have traced the generation of the Monglo adakite magmas to multiple episodes of South China Sea plate-derived melt percolation through ophiolitic sequences within the lower crust of Luzon (Jego et al., 2005; Gregoire et al., 2008).

Mafic Dike Complex

This series of heterogeneous, mafic, pyroxene and hornblende-megacrystic dikes includes diabase, lamprophyric and appinite intrusive rocks occupying the central portion of the Baguio district (Waters and Gonzales, 2005; Fig. 2.2). Previously termed the Kias Creek Dyke Complex (UNDP, 1989), the dikes occur in tight clusters and exhibit evidence for multiple injections of magma (Waters and Gonzales, 2005). Observation of hornblende megacrysts (up to 10 cm in diameter) concentrated towards the center of the dikes indicates rapid quenching at the margins and significant flow concentration (Waters and Gonzales, 2005). Additionally, widespread amphibolite inclusions in the dikes are interpreted to represent the xenoliths of Philippine arc basement rock (Waters and Gonzales, 2005). Work by Hollings et al. (in press) suggested that these magmas were mantle derived and a product of the subduction of the Scarborough Ridge below the Manila Trench.

Hornblende Ar-Ar dating of a diabase dike from the Dike Complex, as well as two similar dikes to the south (east of Camp 4) yielded ages of 4.12±0.22 Ma, 4.55±0.15

Ma and 4.03±0.08 Ma, respectively (Waters and Gonzales, 2005). Confirming this relatively young age are field observations by Waters and Gonzales (2005) noting that the Dike Complex intrudes the Pugo Formation, the Zig-Zag Formation and the Virac Granodiorite.

Black Mountain Intrusive Complex

Located in the west-central region of the Baguio district, and approximately five kilometers southwest of Baguio City (Fig. 2.2), the Black Mountain Intrusive Complex (BMIC) is composed of felsic to mafic porphyritic intrusive plugs and dikes. Previous work by Callow (1967), Balce (1980) and Waters and Gonzales (2005) identified two main intrusive centers: the western Mexico Diorite and the eastern Black Mountain quartz diorite porphyry. In their documentation of the BMIC, Waters and Gonzales (2005) noted four primary lithologies: hornblende quartz diorite, quartz diorite, plagioclase- and hornblende-phyric andesite and hornblende megacrystic andesites and basalts.

Waters and Gonzales (2005) utilized Ar-Ar methods to date five samples from both intrusive centers of the BMIC: hornblende from a hornblende-quartz diorite porphyry of the Black Mountain intrusive body yielded an age of 2.98±0.30 Ma; secondary biotite from a quartz diorite porphyry of the Black Mountain intrusive body yielded an age of 2.95±0.05 Ma; hornblende from a plagioclase-hornblende andesite porphyry of the Black Mountain intrusive body yielded an age of 2.81±0.24 Ma; hornblende from a hornblende andesite porphyry of the Mexico intrusive body yielded ages of 3.09±0.15 Ma and 2.90±0.15 Ma. Dating of the multiple phases within the Black Mountain Intrusive Complex (both the Black Mountain and Mexico intrusive bodies) by Waters and Gonzales (2005) indicates that the BMIC was emplaced over the course of less than half a million years between approximately 2.70 and 3.20 Ma. This is slightly younger than the stratigraphy-based models of Balce et al. (1980) and Pena (1998) that assign a very late Miocene age to the Black Mountain Intrusive Complex.

Camp 4 Intrusive Complex

Located approximately ten kilometers south of Baguio City (Fig. 2.2), this intrusive suite contains at least seven separate intrusive phases (Waters and Gonzales, 2005). Rock type ranges from intermediate to mafic, and multiple phases of plagioclase hornblende andesite porphyry have been identified, as well as the Ubolan hornblende diorite porphyry, the Kidao quartz diorite porphyry, and a pyroxene hornblende lamprophyre dike (Waters and Gonzales, 2005). Dating of the complex was conducted by Waters et al. (in press): a hornblende andesite porphyry dike (previously determined to be an early intrusive phases on the basis of field observations; Waters and Gonzales, 2005), returned hornblende Ar-Ar ages of 4.56±0.28 Ma and 4.03±0.14 Ma.

Santo Tomas II-Bumolo-Clifton Cluster

Located in the southernmost Baguio mineral district (Fig. 2.2), this cluster of porphyritic intrusive rocks includes three separate intrusive centers of similar age and composition (Waters and Gonzales, 2005): the Santo Tomas II, Bumolo and Clifton intrusive centers.

Studies of drill core from Santo Tomas II (Imai, 2001) have identified three phases of pipe-like, intermediate intrusive rocks containing varying amounts of primary plagioclase and hornblende, and secondary biotite (Waters and Gonzales, 2005). Local terminology has dubbed two of these intrusive phases the "Dark Diorite" and the "Clear Diorite" (associated with mineralization at the Santo Tomas II mine, described below), the latter of which is distinguished by more pervasive silicification (Imai, 2001; Waters and Gonzales, 2005). The third intrusive phase is a quartz andesite porphyry. Age constraints on the Santo Tomas intrusive phases have been reported by multiple authors: Bellon and Yumul (2000) reported an age range of 3.71 to 2.31 Ma for the "light" and "dark" diorites based on seven K-Ar analyses; Imai (2001) reported eight Ar-Ar dates for minimally altered and biotite-altered diorites, yielding a range of 2.10-1.20 Ma; Waters and Gonzales (2005) utilized Ar-Ar dating methods on secondary biotite, reporting an age of 1.61±0.13 Ma for the Dark Diorite, and 1.52±0.17 Ma for the quartz andesite. However, it should be noted that some of these dates may reflect the age of secondary biotite alteration within the intrusive rocks, and not the age of emplacement. The Santo Tomas II intrusive suite has been emplaced within the Pugo Formation.

The Bumolo intrusive center is located approximately 1.5 kilometers to the northeast of Santo Tomas II in the southern Baguio mineral district (Fig. 2.2) and is composed of a small, multiphased quartz diorite porphyry intrusion. Waters and Gonzales (2005) and Waters et al. (in press) identified a series of four intrusive phases consisting of (from oldest to youngest) a plagioclase-hornblende diorite porphyry, two temporally distinguishable leucocratic and coarse-grained hornblende quartz diorites, and a microdiorite porphyry containing xenoliths of the aforementioned diorites. Imai (2001) reported a K-Ar age for a hornblende quartz diorite of 1.80±0.20 Ma, and Ar-Ar dating of a plagioclase-hornblende quartz diorite porphyry containing xenoliths of an earlier diorite yielded an age of 2.06±0.70 Ma.

The Clifton quartz diorite porphyry has intruded the Kennon and Klondike Formations (Waters and Gonzales, 2005; Waters et al., in press) and has been described as comprising two separate intrusive phases: a hornblende andesite porphyry and a later clinopyroxene-hornblende andesite porphyry (Imai, 2001). Dating of the later intrusive phase by K-Ar methods by Imai (2001) yielded an age of 1.70±0.60 Ma.

Ampucao-Hartwell-Balatoc Cluster

Located approximately 10 kilometers southeast of Baguio City (Fig. 2.2), this cluster includes two intrusive bodies and a major diatreme all of which have been emplaced within the last 1.5 million years. The Ampucao porphyry body (De Guzman, 1986; Cooke and Bloom, 1990) has intruded the Zig-Zag Formation and the Virac granodiorite and is crosscut by epithermal quartz veining. It is composed of three temporally distinguishable phases ranging from diorite to dacite (De Guzman, 1988; Cooke and Bloom, 1990). Dating by Waters and Gonzales (2005) of hornblende from a plagioclase-hornblende microdiorite yielded an Ar-Ar age of 0.99±0.13 Ma. A fission track age of 2.40±0.50 Ma was reported for secondary orthoclase alteration associated with the emplacement of the Ampucao in the Virac Granodiorite (Cooke and Bloom, 1990).

The Hartwell intrusive body is located approximately 400 meters north of the Ampucao porphyry (Fig. 2.2) and is a small hornblende-biotite dacite porphyry intruding the Virac granodiorite (Waters and Gonzales, 2005). Dating of hornblende via Ar-Ar methods yielded an age of 1.18±0.25 Ma (Waters and Gonzales, 2005).

The Balatoc Diatreme is located approximately 1.5 kilometers north of the Ampucao porphyry complex (Fig. 2.2) and is a subvertical polymict breccia pipe cutting through the Zig-Zag Formation and the Virac Granodiorite (De Guzman, 1988). It is represented at the surface as a 1 kilometer-wide ovoid and stretches down to a known depth of 2000 meters (Waters and Gonzales, 2005). Three phases of the diatreme were recognized by De Guzman (1988), and included two breccia facies and an intrusive dacitic plug. The breccia facies are divided into the "old breccia" and the "young breccia", both of which are polymict. The old breccia contains poorly sorted, polymictic, angular-to-rounded clasts of country rock within an andesitic matrix. The young breccia contains clasts of country rock and the old breccia, as well as carbonized wood, set in an andesitic to dacitic, fine-grained matrix (Waters and Gonzales, 2005). Sawkins et al. (1979) and Waters and Gonzales (2005) interpreted the organic content of the young breccia to indicate extensive vertical movement within the pipe, noting the presence of the charcoal at depths up to 650 meters below the present day surface. The aforementioned dacitic plug has intruded both of the breccia phases, and has truncated some epithermal veins. The dacitic plug has yielded a K-Ar age of 0.80 Ma (Defant and Drummond, 1990) and epithermal veins associated with the young breccia have yielded a K-Ar age of 0.65±0.07 Ma (Aoki et al., 1993). Carbon fourteen dating of the carbonized wood contained within the young breccia yielded an estimated age of 0.65 Ma (De Guzman, 1988).

2.4 Baguio Mineral District Deposits and Mineralization

2.4.1 History of Exploration and Development

The Baguio mineral district of Northern Luzon, Philippines, is one of the world's premier mineral provinces, with over 35 million ounces of gold and 2.7 million tons of copper contained in epithermal (e.g., Antamok; Sawkins et al., 1979; Cooke et al., 1996), porphyry (e.g., Santo Tomas II; Imai, 2001) and skarn resources (e.g., Thanksgiving; Callow, 1967). Baguio was the major gold producer in the Philippines for much of the 20th century, but mine closures in the 1990s led to a significant reduction of production. Approximately 23 million ounces of gold, 30 million ounces of silver and 1.5 million tons of copper have been recovered from the mineral district, with gold and copper

reserves of 12 million ounces and 1.2 million tons, respectively (Waters and Gonzales, 2005). In 2008, the only major mechanized mining operation in the district was the Santo Tomas II mine. Production from epithermal veins is restricted to small-scale local mines.

The porphyry, skarn and epithermal mineral deposits of the Baguio district are spatially and temporally linked to the late-Miocene to Pleistocene intrusive units described above: porphyry mineralization is centered directly above these intrusive centers while skarn and epithermal mineralization is generally more distal. Dating of alteration assemblages associated with mineralization (e.g., Ar-Ar dating of secondary biotite from the Black Mountain Kennon ore body by Waters and Gonzales, 2005) coupled with dating of primary intrusive phenocrysts (e.g., Ar-Ar dating of primary hornblendes from this study), has provided ample evidence that there is a temporal connection between the porphyritic intrusive bodies and the mineralization of the Baguio district.

2.4.2 Porphyry Centers and Related Skarn Mineralization

The majority of known copper-gold porphyry deposits of the Baguio mineral district occur in clusters around and above the Black Mountain Intrusive Complex, the Camp 4 Intrusive Complex, and the Santo Tomas II-Bumolo-Clifton intrusive cluster (Fig. 2.2). Of the identified centers of porphyry-type mineralization, only the Black Mountain deposit and the Santo Tomas II deposit have been mined on a large scale, leaving development of the associated prospects to small scale recovery. The work presented herein focuses on the Black Mountain Cu-Au Porphyry deposit, and as such the summary below emphasizes mineralization proximal to the Black Mountain Intrusive Complex.

Black Mountain Porphyry System

The Black Mountain porphyry Cu-Au deposit is located in the central western portion of the Baguio district approximately five kilometers southwest of Baguio City in the Upper Bued River (Fig. 2.2). It consists of two ore bodies hosted within the Black Mountain Intrusive Complex. The 'Main' or 'Kennon' ore body occurs at the northwest end of the elongate intrusive complex, and was block caved from 1969-1983. It had a pre-production reserve of 47mt at 0.38% Cu and 0.35g/t Au + 0.01% Mo (UNDP, 1987).

The Southeast ore body was block caved from 1977-1983 from surface at 790m to a subsurface elevation of 560 meters, and had a pre-production reserve of 15mt ~ 0.37% Cu + 0.26g/t Au (Sillitoe and Gappe, 1984: UNDP, 1987). The Southeast ore body has a surface expression that is approximately 150 meters wide (SW/NE) and 600 meters long (NW/SE).

Sulfide mineralization is chiefly chalcopyrite and pyrite, with rare molybdenite and bornite (UNDP, 1987; Waters and Gonzales, 2005). Centered over the porphyry body, the pyrite alteration halo to the Black Mountain copper porphyry system is ovoid in shape, with a long axis approximately 2.75 kilometers in length (trending NW/SE), and a 1 kilometer-wide short axis (trending SW). The mineralization occurs as yellowish-rusty outcrops with pyrite-limonite veins and can be identified along the Bued River and in some road cuts along the Kennon Road (Waters and Gonzales, 2005).

The Thanksgiving skarn is located along the Kennon Road, approximately 0.5 kilometers E/SE of the Black Mountain Kennon ore body (Fig. 2.2). Benguet Exploration Inc. extracted a total of 108,457 tons of ore with a return of over 2.7 million grams of gold from the Thanksgiving Mine between 1957 and 1965. Assayed ore from 1965 contained 33.45 g/t gold, 156.49 g/t silver, 12.11% zinc, 0.6% copper, 0.36% lead and 0.01% cadmium (Callow, 1967). Ore bodies are found as pods and irregular veins along porphyry-limestone contacts within a Zig-Zag series limestone bed. The host carbonate is striking 160° and dipping west at approximately 50° (Callow, 1967). Skarn rock at Thanksgiving is recognized by Callow (1967) as widespread, irregular lenses and veins of garnet-clinozoisite skarn along the limestone-Black Mountain Intrusive Complex porphyry contacts. Sulfide mineralization is primarily massive sphalerite and pyrite, with minor chalcopyrite, galena, and arsenopyrite. Sparsely distributed throughout the sulfide minerals (as well as chlorite and calcite) are small (<0.1mm diameter) single and composite particles of altaite, hessite, petzite and sylvanite. Petzite is recognized as the primary source of gold in the Thanksgiving deposit (Callow, 1967).

Discovered in the late 1990's by AngloAmerican, the Mexico Prospect is located approximately 2 kilometers west of the Black Mountain South East ore body (Fig. 2.2). Copper and gold-rich skarn mineralization at Mexico was produced by the intrusion of hornblende diorites and hornblende-plagioclase andesites of the Black Mountain

Intrusive Complex into Klondyke and Zig-Zag Formation carbonates. As with the Thanksgiving Skarn, ore is located in lenses and pockets, possibly reflecting the lens-like geometry of calcareous units within the Zig-Zag Formation (Waters and Gonzales, 2005). Many of the skarn bodies were identified by Waters and Gonzales (2005) as prograde massive garnet skarn, sporadically retrograded locally to sulfide-bearing phases. Copper and gold mineralization occurs predominantly in magnetite-chalcopyrite skarn, with localized replacement of garnet skarn by bornite, with grades ranging up to 6 grams per ton Au and 5% Cu (Waters and Gonzales, 2005).

Porphyry-style mineralization has been recognized at Mexico and takes the form of pyrite, chalcopyrite and molybdenite-rich quartz veins cutting across a hornblende diorite porphyry (Waters and Gonzales, 2005). Localized potassic alteration associated with these quartz veins is also noted (Waters and Gonzales, 2005). The composition and distribution of alteration at the Mexico prospect reflects that of a porphyry Cu-Au deposit: a zoned alteration assemblage is exposed over approximately one square kilometer and is associated with the copper, gold, molybdenum and selenium enrichment (Waters and Gonzales, 2005).

Camp 4

The Camp 4 Intrusive Complex is located five kilometers south-southeast of the Black Mountain Porphyry system, and is host to the Kidao and Ubolan Cu-Au porphyry prospects (Fig. 2.2). The Kidao prospect is located in the Bidlag, Jaime and Pugo Creeks and occupies approximately two square kilometers (Waters and Gonzales, 2005). Mineralization and alteration varies considerably over the surface delineation, from pervasive weakly disseminated chalcopyrite associated with magnetite (5-10%) and propylitic alteration, to quartz stockworking containing localized disseminated molybdenite and chalcopyrite-bornite viens associated with biotite-actinolite-magnetite alteration (Waters and Gonzales, 2005). Average grades for the latter are 0.27% Cu and 0.25 grams per ton Au with local values extending to 1.18% Cu and 0.64 grams per ton Au (Waters and Gonzales, 2005). De Guzman (unpublished report to Benguet Corporation, 1986) and Waters and Gonzales (2005) noted peripheral quartz-molybdenite and magnetite veinlets peripheral to the Kidao prospect.

The Ubolan prospect is a low-grade Cu-Au porphyry prospect 500 meters southwest of Kidao. It was drilled by Filmag in the 1960's (Waters and Gonzales, 2005) and crops out in the Ubolan and Gawa creeks.

Santo Tomas-Bumolo-Clifton

The Santo Tomas II porphyry deposit and the Bumolo and Clifton porphyry prospects are located approximately 10 kilometers south of the Black Mountain deposits (Fig. 2.2). The Santo Thomas II Cu-Au porphyry deposit was block caved from 1958 to 2003, extracting 809,000 tons of copper and 4.70 million ounces of gold from 288 million tons of ore (Waters et al., in press). Sulfide mineralization is predominantly chalcopyrite, bornite and molybdenite, with the majority of gold contained within the sulfides. Alteration assemblages associated with Santo Tomas II reflect a "bull's-eye" pattern in which silicification and potassic alteration are centered over the mineralizing intrusive phases, followed outwards by a pyritic halo and propylitic alteration (Bureau of Mines and Geosciences, 1986).

The Bumolo Cu-Au porphyry prospect is 1.5 kilometers northeast of Santo Tomas II (Fig. 2.2), and is hosted by a small, multiphased quartz diorite porphyry. Sulfide mineralization is present as chalcopyrite within quartz stockwork as coarse grains, and disseminated throughout the early intrusive phases (Waters and Gonzales, 2005). Grades average 0.2% Cu and 0.5 grams per ton Au (Waters and Gonzales, 2005). Alteration associated with Bumolo includes texturally destructive potassic assemblages (biotite), actinolite and magnetite alteration, intermediate argillic assemblages, and weak chloritization (Waters et al., in press).

The Clifton porphyry Cu-Au prospect is defined by a small hornfelsed and pyritized zone associated with a quartz diorite intrusion. Localized skarn was been noted by Waters et al. (in press).

Ampucao-Hartwell-Balatoc

The Ampucao Cu-Au porphyry prospect is located approximately five kilometers southeast of the Black Mountain deposit (Fig. 2.2), and is associated with high grade porphyry copper and gold mineralization. Exploration drilling southward of the Acupan

epithermal gold mine (north of the Ampucao prospect; Fig. 2.2), yielded interceptions of biotite-magnetite-orthoclase alteration and chalcopyrite-bornite mineralization, as well as chlorite-quartz-sericite alteration and pyrite-chalcopyrite mineralization (M. de Guzman, unpublished report to Benguet Corporation, 1986: Cooke and Bloom, 1990). An intercept over this interval returned assay grades of 0.18% Cu and 0.95 grams per ton Au (M. de Guzman, unpublished report to Benguet Corporation, 1986; Cooke and Bloom, 1990).

Clasts of copper-gold mineralized porphyry have been reported from the central section of the Balatoc Diatreme (Schafer, 1956; Waters and Gonzales, 2005). Coupled with reports of potassic alteration assemblages in the deeper levels of the nearby Acupan mine (more than a kilometer north of the potassic alteration of the Ampucao porphyry system), Waters and Gonzales (2005) and Waters et al. (in press) suggested that another porphyry copper-gold system may be located at the base of the diatreme.

Nugget Hill Cu-Au Porphyry Prospect

Discovered in the late 1990's by AngloAmerican, the Nugget Hill prospect is located 2.5 kilometers east of the Black Mountain deposit (Fig. 2.2), where porphyry copper and gold mineralization and alteration encompass an area of 0.5 square kilometers. Mineralization is hosted in hornfelsed andesitic breccias in the Zig-Zag Formation, as well as diabase dikes of the Dike Complex and occurs as magnetite veinlets cross-cut by quartz-magnetite-chalcopyrite-bornite stockwork veins. Assays of highly mineralized outcrops and float breccia from Liw-Liw Creek returned values up to 1.17% Cu and 4.58 grams per ton Au (Waters and Gonzales, 2005; Waters et al., in press). These high-grade veins and veinlets are associated with potassic alteration, which was then overprinted by high temperature propylitic alteration (diopside-albite) and and illite-pyrite-quartz alteration assemblage. Structurally-controlled epithermal base-metal veins (spalerite-galena-gold) overprint the porphyry system at Nugget Hill's peak (Waters and Gonzales, 2005; Waters et al., in press).

Chico Cu-Au Porphyry Prospect

Located three kilometers northeast of the Black Mountain deposit (Fig. 2.2), the Chico Cu-Au porphyry prospect hosts two zones of chalcopyrite-bornite mineralization associated with quartz-magnetite stockworking and potassic alteration. A small outcrop of porphyry-type mineralization defines the northern zone approximately 700 meters north of the Baguio Airport. Assays from this area yielded 0.97% Cu and 1.83 grams per ton Au (Waters and Gonzales, 2005). The second zone, recognized by Waters and Gonzales (2005) as porphyry-style alteration, is located approximately two kilometers southeast of the northern zone. Waters and Gonzales (2005) and Waters et al. (in press) proposed that the mineralization recognized at the Chico porphyry prospect is either part of a unique porphyry system, or related to the Nugget Hill porphyry system.

2.5.3 Epithermal-type mineralization

Development of at least seven bonanza-style epithermal veins in the Baguio mineral district has accounted for the majority of total gold production during the 20th century: of the 23 million ounces of gold extracted from Baguio, 19 million have been derived from the two largest epithermal veins systems, the Antamok and Acupan-Sangilo deposits (Waters et al., in press). Previous work by Aoki et al. (1993), Waters et al. (in press) and Cooke et al. (in press) has linked the emplacement of some of these epithermal systems with the youngest known porphyry center in the Baguio district (the Ampucao-Hartwell-Balatoc cluster).

Antamok

The Antamok mine is located seven kilometers east of Baguio City (Fig. 2.2) and was been mined by Benguet Corporation from 1907 until 1998 by open cut and underground methods. As the largest gold producer in the Philippines, Antamok yielded 11 million ounces of gold at an average grade of five grams per ton (Mitchel and Leach, 1991). Structurally controlled, northwest trending ore veins are characterized by multi-staged massive, vuggy quartz and hydrothermal breccias, hosted by the Zig-Zag Formation and the Antamok Diorite (Waters and Gonzales, 2005). Gold to silver ratios are approximately one to one, and are associated with rhodochrosite, calcite, sphalerite,

chalcopyrite, pyrite, galena and tellurides, with the sulfides occurring as colloform bands, veinlets and disseminations (Waters and Gonzales, 2005).

Acupan-Sangilo

The Acupan-Sangilo epithermal vein system is located less than a kilometer west of the Balatoc Diatreme (Fig. 2.2), and was mined underground by Benguet Corporation and Itogon-Suyoc Mines Inc. from 1929 to 1993. More than 8 million ounces of gold were extracted from the mine, with an estimated remaining resource of 3.5 million ounces (Waters and Gonzales, 2005). The epithermal veins trend northeast, with a subset trending east, and are hosted by the Virac Granodiorite and the Balatoc Diatreme. Ore bodies appear as veins, stockworks and breccias consisting of banded, vuggy quartz-adularia with calcite, sericite, pyrite, chalcopyrite, galena and sphalerite. Dating of illite by Aoki et al. (1993), yielded an age of 0.65±0.07 Ma, indicating that mineralization at Acupan-Sangilo is associated with the Ampucao-Hartwell-Balatoc cluster, dated at 1.20 to 0.80 Ma (Defant and Drummond, 1990; Waters and Gonzales, 2005; Waters et al., in press).

Cal Horr

The Cal Horr epithermal vein system is located half a kilometer east of the Nugget Hill prospect (Fig. 2.2), and was developed as an underground mine by Benguet Corporation before World War II, and was reopened briefly as an open pit mine from 1984 to 1989 (Waters and Gonzales, 2005). Mineralization is hosted within the Klondyke and Zig-Zag formations, by two east trending quartz-calcite-magnetite veins separated by a quartz stockwork zone that has undergone clay-pyrite-silica alteration (UNDP, 1987; Mitchel and Leach, 1991).

Chico

The epithermal vein system associated with the Chico Cu-Au porphyry prospect is located immediately east of Baguio City (Fig. 2.2). Eight veins extend from the nearby Kelly and Atok Big Wedge properties onto the eastern Chico claims and extend along strike for approximately two kilometers (Waters and Gonzales, 2005). Hosted by the

Zig-Zag Formation, the vein system is associated with a three meter wide pyritic-clay alteration halo, followed outwards by chlorite and epidote-pyrite alteration. Mineralization is pyrite with minor sphalerite, galena, barite and electrum (Domasig, 1990). Mining of the Chico epithermal system has been confined to a single structure (the Camaso Vein), grading approximately 5 grams per ton gold (Waters and Gonzales, 2005).

Atok Big Wedge

The Atok Big Wedge epithermal vein system is located one kilometer east of the Chico porphyry prospect (Fig. 2.2). Mineralization is hosted in east-trending quartz veins cutting Zig-Zag Formation andesitic clasts and intruded by a chloritized diorite (Waters and Gonzales, 2005). Gold grades range from 7 to 17 grams per ton (UNDP, 1987; Mitchell and Leach, 1990).

Sierra Oro

The Sierra Oro epithermal vein system is located approximately one kilometer south of the Nugget Hill porphyry prospect (Fig. 2.2). Similar to the Cal Horr mine, underground mining was initiated prior to World War II, and re-initiated from 1984 to 1987 by Benguet Corporation. Hosted by the Zig-Zag formation, four east-trending quartz-calcite-manganite veins yield ore grades of 6 to 13 grams per ton Au (UNDP, 1987; Waters and Gonzales, 2005).

Kelly

The Kelly epithermal vein system occurs four kilometers north of the Nugget Hill porphyry prospect (Fig. 2.2), and is host to an atypical mineral assemblage including high sulfidation state copper-bearing minerals enargite, tennantite-tetrahedrite and bornite (Comsti et al., 1990; Deyell and Cooke, 2003). Comsti et al. (1990) reported both magmatic-hydrothermal advanced argillic alteration and illitic alteration assemblages associated with the mineralization at Kelly.

2.5 Summary

Over the last 3.5 million years, porphyry and epithermal mineralization in the Baguio mineral district has been driven by calc-alkaline magmatism associated with the subduction of the South China Sea plate and the aseismic Scarborough Ridge beneath northern Luzon, as well as flattening of the downgoing slab. Coupled with high uplift and exhumation rates related to slab flattening and the collision of Luzon with the Eurasian continental margin, mineralization in the Baguio district has been responsible for the emplacement of over 35 million ounces of gold.

A definitive genetic link between mineralization and the emplacement of porphyritic intrusive clusters has produced a unique pattern within the Baguio mineral district in which an eastward younging direction is coupled with increased economic endowment for Pliocene-Pleistocene intrusive rocks (Waters et al., in press). The late Miocene subduction of the Scarborough Ridge was contemporaneous with the intrusion of the Mafic Dike swarm in the center of the Baguio district (4.80 to 3.20 Ma; Waters et al., in press). Cessation of voluminous mafic magmatism after this time period was marked by the onset of the copper and gold mineralization associated with the emplacement of the dioritic Black Mountain Intrusive Complex in the western-most region of the Baguio district (approximately 3.20-2.75 Ma; Waters and Gonzales, 2005). As noted above, the metal grades and resource volume of the Black Mountain deposits, Thanksgiving Mine and Mexico prospect are relatively low compared to the other porphyry intrusive centers within the district. Emplacement of the Santo Tomas II-Bumolo-Clifton cluster in south central Baguio between 2.80-1.40 Ma (Waters et al., in press) yielded a marked increase in economic potential (evidenced by the highly productive Santo Tomas II porphyry deposit). The youngest and easternmost porphyry intrusive center, the Ampucao-Hartwell-Balatoc cluster, has been temporally and spatially linked to the most prolific gold deposits in the Baguio district: the Acupan and Antamok giant epithermal vein systems. Waters et al. (in press) proposed that the apparent eastward migration of magmatism coupled with increased mineral endowment is a product of multiple factors: continued slab flattening and compressional uplift, periodic movement along the left-lateral Philippine fault system and the subsequent facilitation of

magma emplacement in strike-slip relay basins. Thus, the initiation of early-Pliocene mineralization in the Baguio district coincided with the formation of the Black Mountain Porphyry system, suggesting a shift in the geodynamic environment of the Luzon arc and a change in magmatism.

Chapter 3

Intrusive History of the Black Mountain Porphyry Southeast Cu-Au Deposit

3.1 Introduction

The Black Mountain Intrusive Complex (BMIC) is an intermediate to mafic series of porphyritic intrusive plugs and dikes spatially and temporally associated with the Black Mountain Kennon and Southeast copper-gold porphyry deposits (Waters and Gonzales, 2005; Waters et al., 2006; Waters et al., in press), as well as the Thanksgiving skarn deposit (Callow, 1967) and the Mexico prospect (Waters and Gonzales, 2005; Fig. 3.1). The BMIC is hosted by the Pugo and Zig-Zag Formations, and locally by the Klondyke Formation (Waters and Gonzales, 2005). Despite the work of multiple authors (Callow, 1967; Balce, 1979; Waters and Gonzales, 2005; Waters et al., in press), there has been little documentation of the specific intrusive history of the Black Mountain Southeast deposit. Consequently, mapping was undertaken in order to define the lithologies and alteration styles associated with mineralization, and delineate a paragenetic sequence for the Black Mountain Porphyry Southeast system (BMPSE). This chapter focuses on the intrusive rocks identified within the Black Mountain Southeast, their relative timings of emplacement and temporal changes in lithology. Thin section petrography was used to supplement and confirm field observations.

3.2 Previous work

Earlier lithological studies by Callow (1967), Balce (1979), Waters and Gonzales (2005), and Waters et al. (in press) identified a series of dioritic to andesitic intrusive rocks spatially associated with mineralization within the greater Black Mountain Intrusive Complex. Generally, these intrusive rocks were recognized as two distinct diorite porphyry phases linked to mineralizing events (at either Black Mountain Kennon, Southeast, Mexico or Thanksgiving), followed by a series of crosscutting andesitic mafic dikes. For example, a study of the Thanksgiving Mine by Callow (1967) identified three intrusive phases based on textural character and phenocryst content and crosscutting relationships:

1. An Older Diorite-porphyry

2. A Younger Diorite-porphyry
2. A series of late andesite dikes

Similarly, Balce (1979) examined the Kennon ore body, noting spatially- and temporally-associated stocks and dikes of quartz phenocryst-bearing quartz diorites. Waters and Gonzales (2005) mapped the greater Black Mountain Intrusive Complex during regional mapping of Baguio Mineral District, and confirmed the presence of a series of quartz diorites (Fig. 3.1). In particular, they delineated a succession of intrusive phases through crosscutting relationships, as well as Ar-Ar dating, to produce a rough chronology of magmatism. From oldest to youngest, these are:

1. A pre-mineralization hornblende quartz diorite porphyry at Kennon
1. An intra-mineralization quartz diorite porphyry at Kennon
1. A post-mineralization plagioclase hornblende andesite porphyry dike at Kennon

This chronology and series of rock types was corroborated by the findings of Waters et al. (in press), who also reported hornblende megacrystic dikes crosscutting (and thus post-dating) the mineralized intrusions. Though observed predominantly within the Kennon ore body, this series of intrusive rocks was inferred to represent magmatism at Southeast as well (Waters and Gonzales, 2005;Waters et al., in press).

Three intrusive rock types were recognized by Waters and Gonzales (2005) and Waters et al. (in press) at the Mexico prospect. These included hornblende diorites and plagioclase-phyric hornblende andesites, as well as stocks of the Black Mountain Intrusive Complex. The reference to stocks of "Black Mountain Intrusive Complex" is not specified in Waters et al. (in press), though it may refer to one or both of the voluminous quartz diorites identified at the Black Mountain Kennon ore body. As well, the designation of a hornblende andesite porphyry dike at Mexico as late mineral suggests that the andesitic magmatism took place after the emplacement of the dioritic intrusive bodies (Waters and Gonzales, 2005; Waters et al., in press). Waters and Gonzales (2005) and Waters et al. (in press) reported that mineralization of the Kennon, Southeast and Mexico ore bodies was a simultaneous, magmatically related event.

Previous studies of the BMIC (e.g., Waters and Gonzales, 2005; Hollings, 2006; Waters et al., in press; Hollings et al., in press) did not include the hornblende

megacrystic mafic Liw-Liw Creek dikes as part of the BMIC, and have instead treated them as a preceding, separate intrusive event. However, Hollings (2006) and Hollings et al. (in press) noted that the Liw-Liw Creek magmas could represent a parental magma of the BMIC. This is discussed further in Chapter 5.

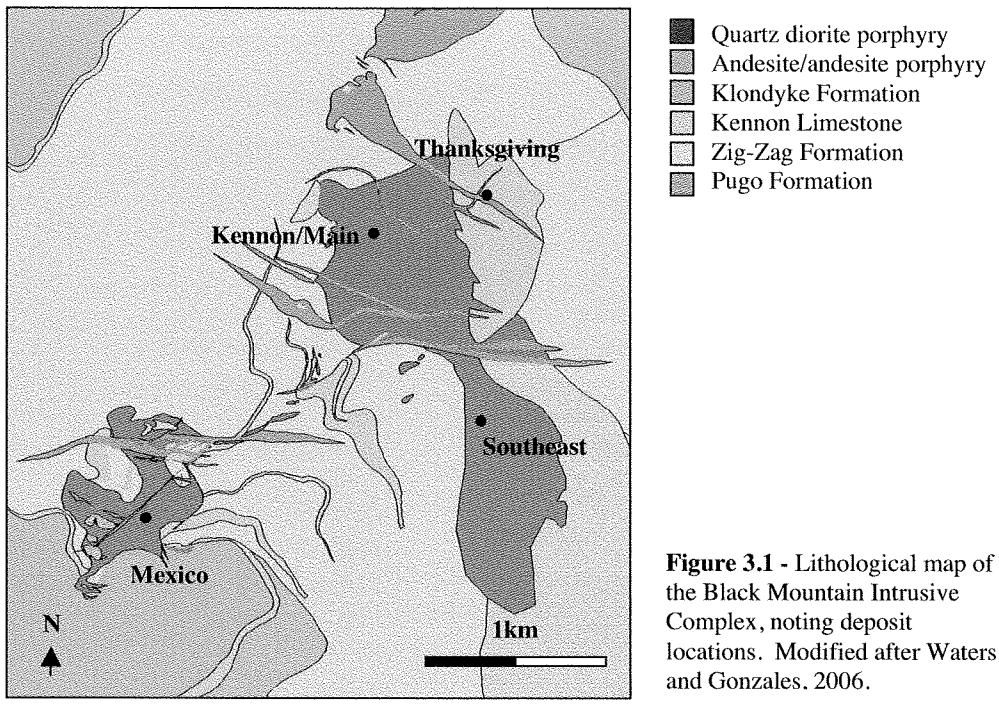

Figure 3.1 - Lithological map of the Black Mountain Intrusive Complex, noting deposit locations. Modified after Waters and Gonzales, 2006.

3.3 Methodology

Fieldwork was conducted during the first week of March 2008, and was centered in the Upper Bued River bed approximately five kilometers southwest of Baguio City center (16°21'07"N; 120°36'39"E). The mapping area was irregularly shaped, and extended northwards (up river) parallel to Kennon Road, and to the southeast up Liw-Liw Creek (Fig. 3.2). It covered a total area of approximately 0.5 km^2. Significant topographic relief and large, unstable landslide slopes (Fig. 3.3) limited outcrop documentation and examination to low-lying valley areas proximal to the Bued and Liw-Liw Creek rivers, and Kennon Road. Topographic base maps were provided by Anglo American Exploration (Philippines) Inc. at a scale of 1:1000 and were used in concert with GPS and pace and compass mapping techniques.

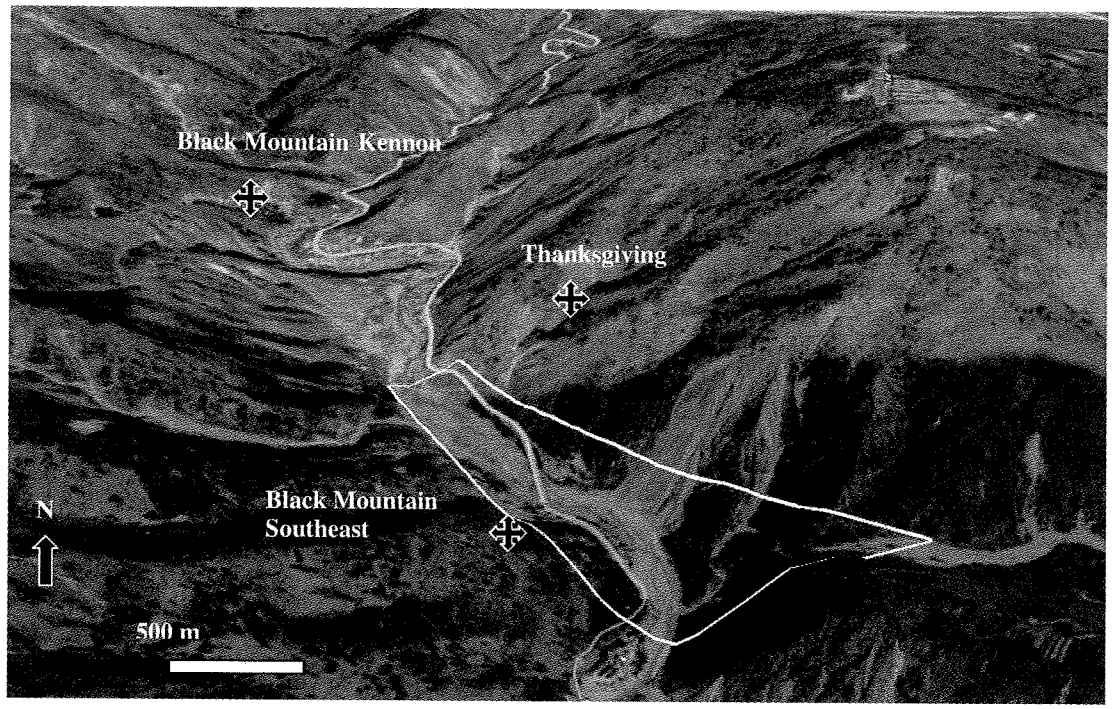

Figure 3.2 - Outline of the 2008 map area for this thesis, indicated by the white box projected on the ground. Note the location of Kennon Road (in yellow) as well as the gully leading up Liw-Liw Creek in the bottom right (Southeast) corner of the image. Image modified from Google Earth.

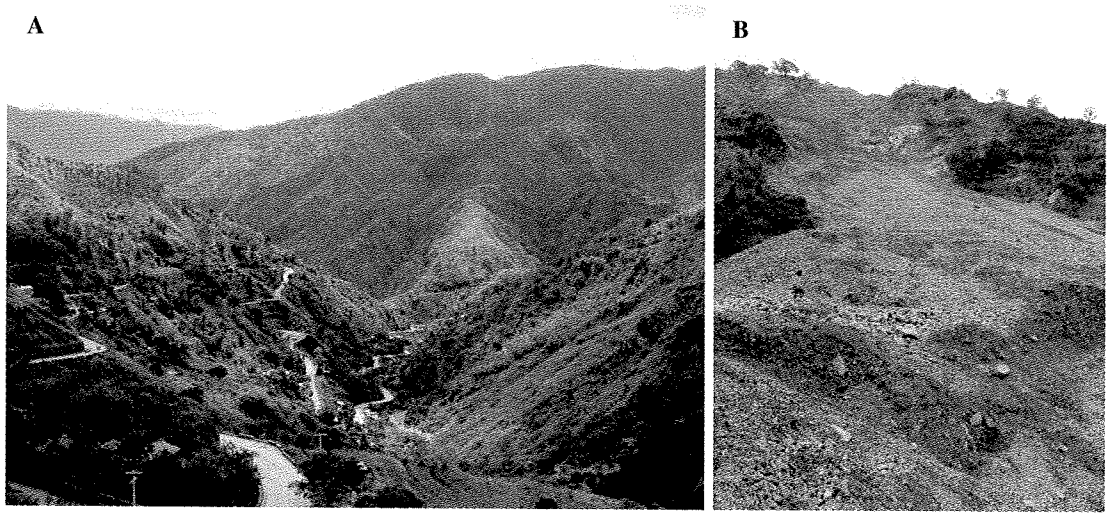

Figure 3.3 - The steep topography of the field area restricted the mapping area (Fig. 3.2) to the Bued River bed. (A) Facing southwards towards the Black Mountain field area from lookout along Kennon Road (photo by Peter Hollings, 2008); (B) facing northeast up a large landslide to the east of Kennon Road along the Bued River at the entrance to the Liw-Liw Creek runoff (photo by Peter Hollings, 2008).

3.3.1 Intrusive Phase Classification

The documentation of basic textural and mineralogical characteristics provided sufficient information to delineate unique intrusive phases at the Black Mountain Porphyry Southeast. In the field, phenocryst mineralogy and size, and overall textural character were used in conjunction with crosscutting relationships and spatial association with alteration and mineralization to distinguish intrusive events. A list of criteria, alone or in combination, was compiled by Sillitoe (2000) outlining textural, compositional and spatial characteristics for distinguishing unique intrusive phases in the field. This included: (1) abrupt truncation of early veinlets in older phases at the contacts with younger phases, (2) narrow zones of chilling in younger phases at the contacts with older phases, (3) narrow zones of flow-aligned phenocrysts in younger phases at the contacts with older phases, (4) xenoliths of older phases floating in younger phases, within close proximity to the contact with the older phase, (5) better textural preservation and lower fracture and veinlet densities in younger phases, and (6) abrupt decreases in Cu and Au content with decreasing age. Although not all pertinent to the intrusive rocks associated with the BMPSE, several of these criteria were assessed in delineating individual intrusive phases, serving as a supplement to basic textural and mineralogical characteristics.

Supplemental petrographic microscopy was used to further refine the field observations, noting:

1. Phenocrysts
    a. Mineral(s)
    a. Abundance: uncrowded (<50%) or crowded (>50%)
    a. Size
1. Groundmass character: aphanitic, very fine-grained (grain size 20-50μm), fine-grained (50-100μm), medium-grained (100-200μm)

3.4 Intrusive Phases of the Black Mountain Southeast Porphyry Deposit

Six major intrusive phases were defined through detailed (1:1000 scale) mapping of the Black Mountain Porphyry Southeast system (Fig. 3.4). In order of interpreted emplacement, these are:

1. Liw-Liw Creek hornblende megacrystic basalt [LLC]
1. Early mineralization quartz diorite [EMD]
1. Plagioclase- and variably hornblende-phyric diorite [PHD]
1. Hornblende megacrystic and "clotted" gabbro [HMG]
1. Hornblende "clotted" basalt [HCB]
1. Aphanitic to plagioclase microphenocrysitc mafics [AM]

Each intrusive phase is described below based on its distribution within the field area, outcrop characteristics, petrographic characteristics (where available) and crosscutting relationships. Descriptions are listed in their interpreted order of emplacement, from oldest to youngest. Due to the scale of the map, many of the smaller crosscutting relationships cannot be displayed and are instead referred to through field photography where available. For spatial reference in the descriptive sections below, the center of the map area is signified by a star in Figure 3.4.

3.4.1 Liw-Liw Creek basalt [LLC]

The hornblende-phyric to megacrystic and variably plagioclase-phyric mafic Liw-Liw Creek (LLC) dikes were identified at four distinct localities in the field area (Fig. 3.4). The majority of outcrops of the LLC dikes are relatively distal to the center of the mapping area, with three outcrops identified along the Liw-Liw Creek runoff in the southeastern portion of the mapping area, crosscutting Pugo Formation basalt. One outcrop was identified along Kennon Road, approximately 125 meters northeast of the map center. All occurrences of the LLC intrusive rocks took the form of dikes (<3 meter wide), striking broadly E-W (Fig. 3.5a). Weathering of the dikes resulted in a light greenish gray appearance with a yellow rust-colored staining, whereas fresh rock faces were a dark gray (Fig. 3.5b and c).

The LLC dikes contain less than 35% phenocrysts by volume, the majority of which are hornblende (30-35% volume of the total rock). The hornblendes form

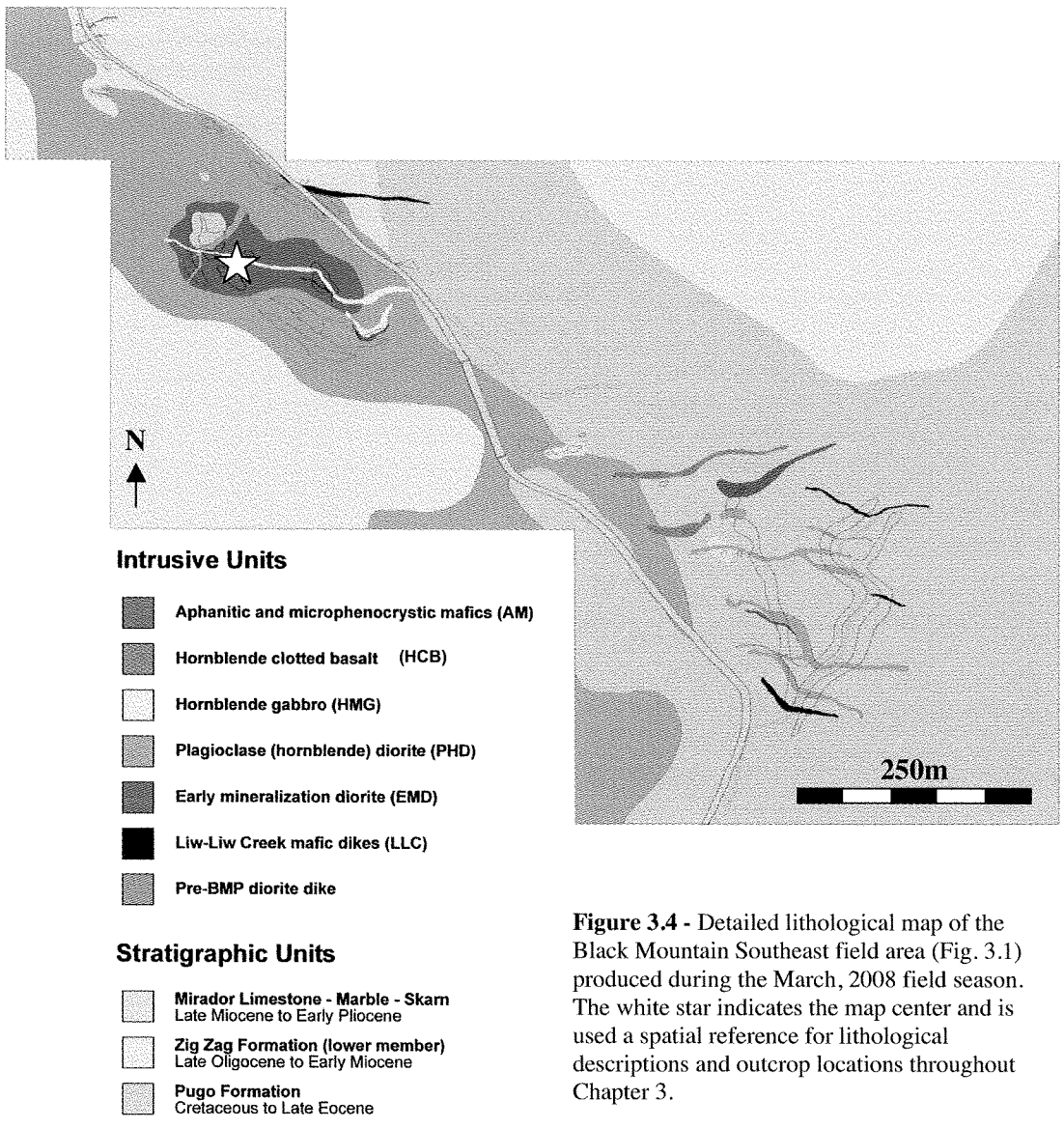

Figure 3.4 - Detailed lithological map of the Black Mountain Southeast field area (Fig. 3.1) produced during the March, 2008 field season. The white star indicates the map center and is used a spatial reference for lithological descriptions and outcrop locations throughout Chapter 3.

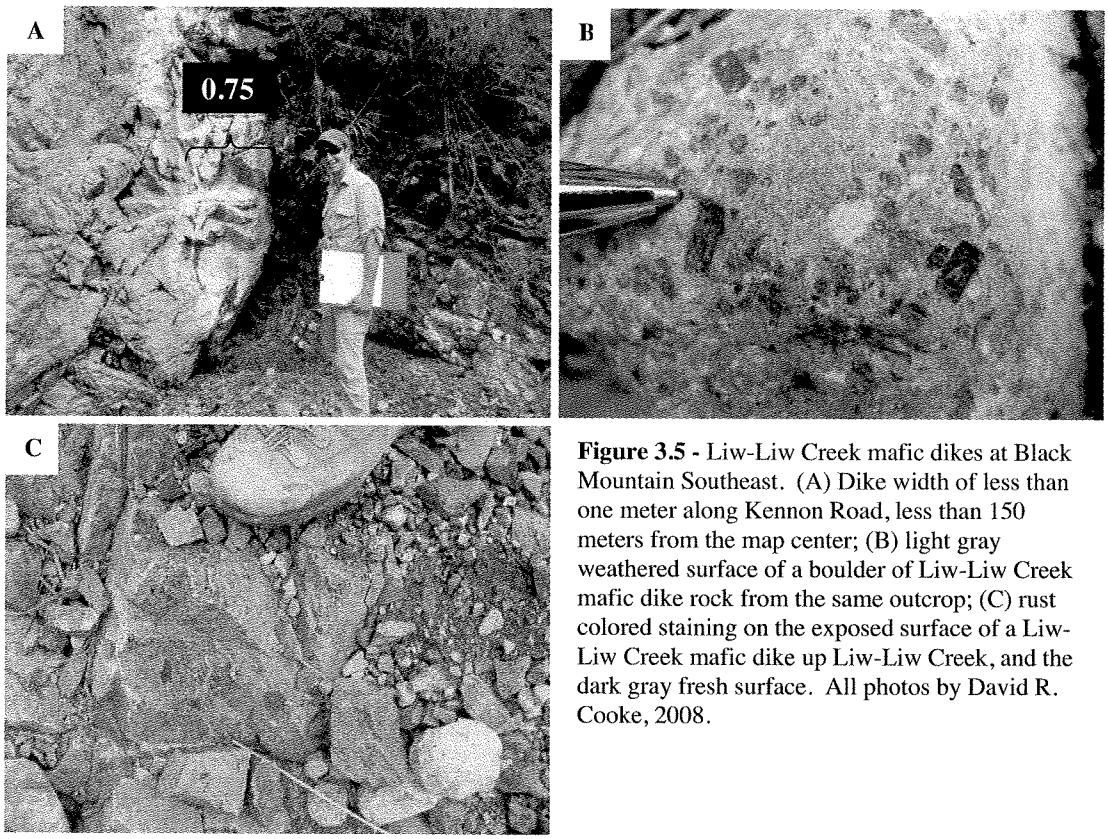

Figure 3.5 - Liw-Liw Creek mafic dikes at Black Mountain Southeast. (A) Dike width of less than one meter along Kennon Road, less than 150 meters from the map center; (B) light gray weathered surface of a boulder of Liw-Liw Creek mafic dike rock from the same outcrop; (C) rust colored staining on the exposed surface of a Liw-Liw Creek mafic dike up Liw-Liw Creek, and the dark gray fresh surface. All photos by David R. Cooke, 2008.

predominantly euhedral grains ranging from 2mm across, to more than 20mm and frequently exhibit twinning (Fig. 3.6a). Intergrowth of hornblende phenocrysts is also present, as some hornblende megacrysts are actually clusters of intergrown hornblende crystals (Fig. 3.6b). Prominent zonation is observed in a few hornblende phenocrysts, and is sometimes accompanied by degradation of the outer rim (Fig. 3.6c). Plagioclase feldspar phenocrysts (where present) represent less than 10% of the rock by volume, forming euhedral grains up to 5mm (Fig. 3.6d). The groundmass of the LLC dikes is characterized by fine- to medium-grained spindly plagioclase (>75%) crystals, with up to 25% hornblende and pyroxene.

The absence of clear crosscutting relationships makes it difficult to ascertain the temporal relationship of the LLC dikes to the rest of the Black Mountain Southeast intrusive suite. None of the dikes within the LLC runoff were observed in contact with younger Pliocene intrusive rocks. However, the dike observed closest to the map center above Kennon Road (Fig. 3.4) is implied to have been truncated by the younger intrusive

rocks. Despite the absence of a visible contact (it is paved over by the Kennon Road), there is no westward continuation of the east-striking LLC dike towards the map center (and the intrusive center). Directly below the Kennon Road outcrop in the Bued River bed, a presumably younger intrusive rock crops out without evidence of the LLC dike cutting it. The LLC dikes are therefore interpreted to be the oldest Pliocene intrusive phase present within the greater BMPSE system, in agreement with the observations and geochronology (Chapter 2; Chapter 4) of Waters and Gonzales (2005), Waters et al. (2006) and Waters et al. (in press).

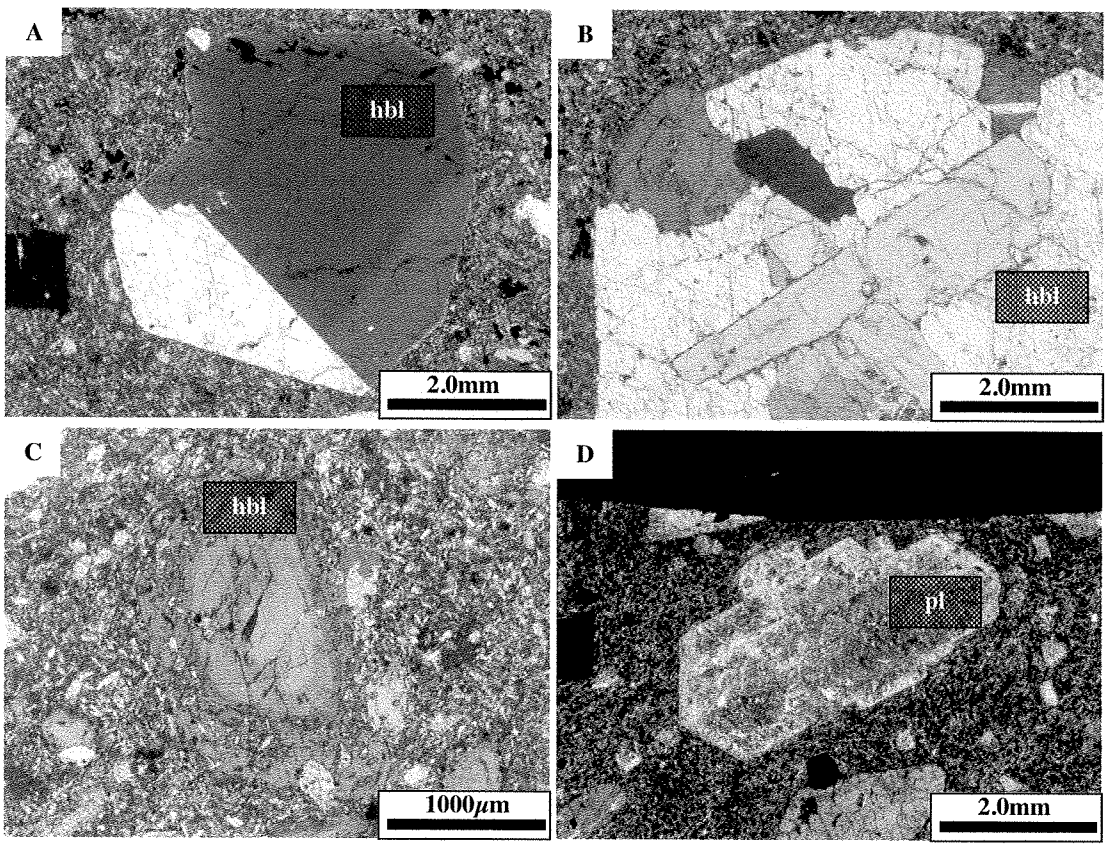

Figure 3.6 - (A) Large, twinned hornblende phenocryst [BA08GS056; 2.5X mag., polarized light]; (B) cluster of hornblende phenocrysts [BA08GS056; 2.5X mag., polarized light; (C) compositional zonation in a degraded hornblende phenocryst [BA08GS056; 5X mag., polarized light]; (D) euhedral plagioclase phenocryst [BA08GS035; 2.5X mag., polarized light]. Pl – plagioclase feldspar; hbl – hornblende

3.4.2 Early mineralization quartz diorite [EMD]

The heavily quartz-vein stock worked Early Mineralization Diorite (EMD) is found only at the center of the mapping area in the form of a large, irregularly-shaped plug (Fig. 3.4) and is the main host of porphyry-type mineralization for the Black Mountain Southeast deposit. The outcrop is ovoid, with a long axis extending approximately 100 meters southeast. The EMD crops out as a light whitish-gray rock with "splotchy" rust-colored staining (Fig. 3.7a). Three distinct quartz vein orientations were identified in the field through displacement of crosscutting sets, indicating at least three stock working events (Fig. 3.7a and b). The earliest set of veins trend between 185 and 200 degrees, and are crosscut and displaced by a second set of quartz veins trending 150 to 160 degrees. A third set of quartz veins trending between 250 and 255 degrees were not as prevalent, and did not display any displacement where they crosscut the earlier veins (Fig. 3.7b).

The quartz vein stock work and ubiquitous quartz flooding have destroyed the primary textures of the EMD rocks. In slabbed and polished hand samples, primary mineral assemblages were not observed, and the overall texture of the rock is mottled and splotchy (Fig. 3.7c and d). Defining and identifying individual phenocryst and groundmass minerals was not possible. Mineralization is hosted by EMD, and occurs as very fine, disseminated pyrite and chalcopyrite throughout the rock. Replacement of what were presumably mafic phenocrysts (hornblende?) with sulfides is common and readily observable in polished slabs (Fig. 3.7c). Although rare, thin bands of molybdenite occur in the center of the quartz veins.

The EMD is crosscut by dikes or stocks from all of the other intrusive phases (aside from the LLC dikes and HCB; Fig. 3.4). For example, near the center of the mapping area it is cut by both a hornblende- and plagioclase-phyric diorite dike (intrusive unit PHD, described below) and a small (<0.25 meters wide) aphanitic andesite/basalt dike (intrusive unit AM, described below; Fig. 3.8a and b). Further to the southwest, a finely plagioclase-phyric basalt (AM) was observed cutting through the EMD outcrop (Fig. 3.8c). The prominent quartz vein stock working is unique to EMD and is truncated at all contacts with presumably younger phases, suggesting that the stock work followed the emplacement of EMD, but preceded emplacement of the remaining intrusive phases. The definite orientations of the quartz vein sets, along with their sharp contacts with the

EMD rocks, denote emplacement via infill of a series of fractures of the EMD stock. This requires that the unaltered EMD rocks had to have been emplaced and cooled enough to allow the brittle fracturing observed.

These observations suggest that emplacement of EMD followed that of the LLC dikes, but because its original mineral content cannot be ascertained, any compositional departure from the LLC magmatism is not detectable. However, the quartz flooding and veining of the original EMD rocks represents the first voluminous felsic/intermediate magmatism within the BMPSE system. This is consistent with the geochronology and observations of Waters and Gonzales (2005) and Waters et al. (in press) for the chronology of intrusive events at the Kennon ore body.

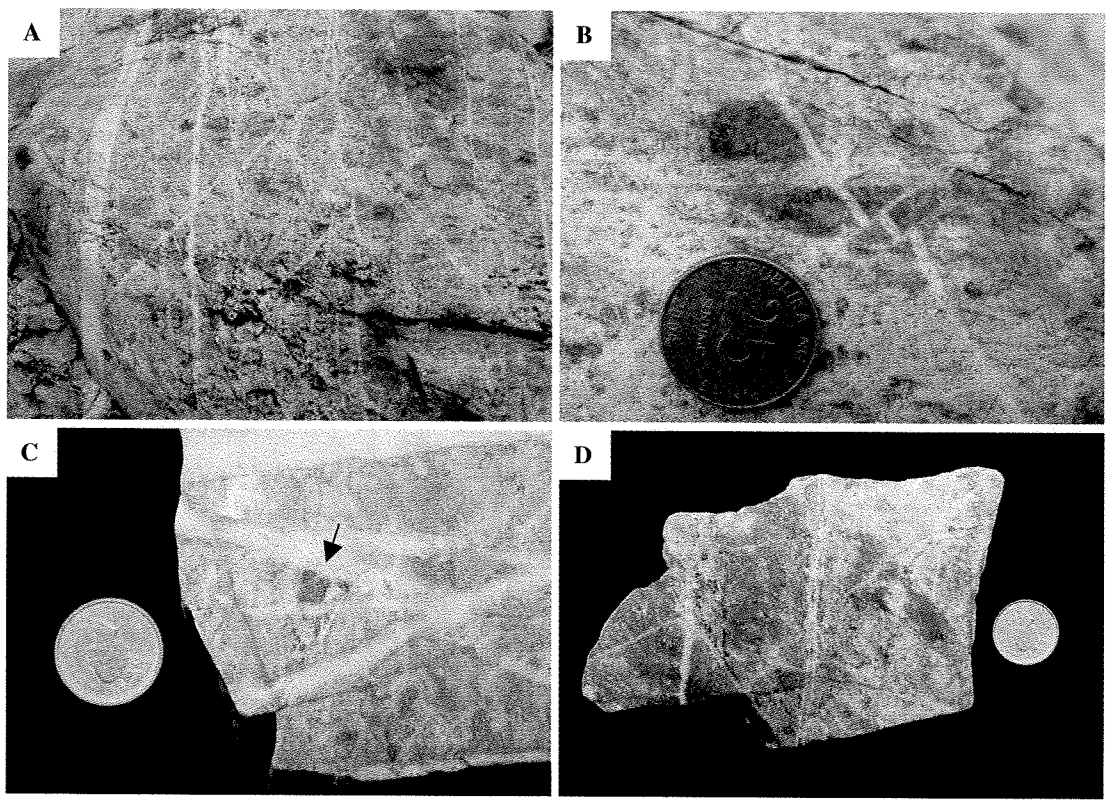

Figure 3.7 - (A) Quartz stock work veining in EMD accompanied by the typical rust-colored surface character (photo by Mike Baker, 2008); (B) offset of an early quartz vein by a later quartz veining event in the EMD (photo by Mike Baker, 2008); (C) polished slab of EMD, noting destruction of primary textures and replacement of a mafic phenocryst by very fine grained pyrite, indicated by the black arrow (sample BA08GS001); (D) destruction of primary textures in an EMD polished section (sample BA08GS012).

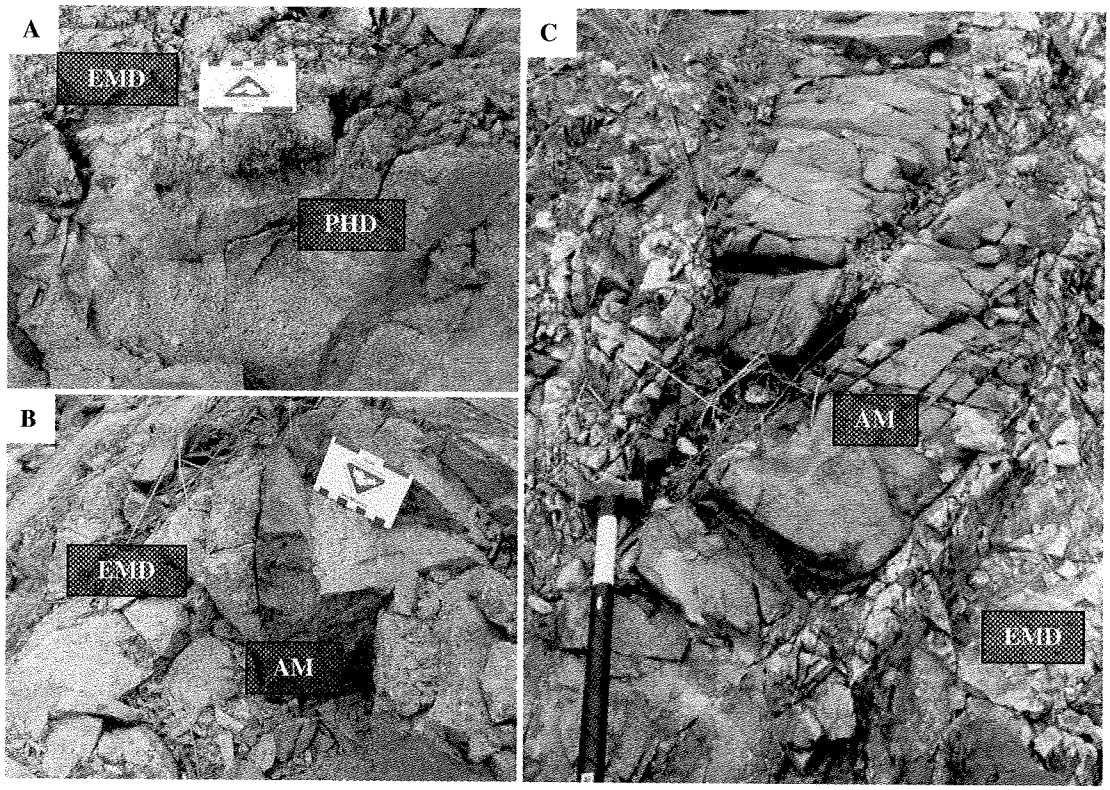

Figure 3.8 - (A) PHD dike crosscutting a plug of EMD; (B) fine grained andesite dike crosscutting an EMD plug; (C) plagioclase microphenocrystic dike displaying offset and crosscutting an outcrop of EMD. (All photos by Mike Baker, 2008)

3.4.3 Plagioclase and variably hornblende-phyric diorite (PHD)

The plagioclase and variably hornblende-phyric dioritic (PHD) rocks define the most surficially voluminous and texturally diverse intrusive phase at the BMPSE. The majority of PHD outcrop occurs as part of an irregular, oblong plug extending NW-SE through the map center, coincident with the Bued River bed (Fig. 3.4). Lateral dimensions of the plug are difficult to gauge as the long axis of the intrusive body exceeds the extent of the map area (approximately 1 km). However, the short axis (NE-SW) is approximately 100 meters at the center of the map area, covering the entire Bued River bed (Fig. 3.4). Confirmation of PHD rocks on the southwest bank of the Bued River through sampling was not possible due to the location of a river channel, however photographs of outcrop suggest that PHD extends westward beyond the riverbed (Figs.

3.4; 3.9a). As well, east-trending dikes of PHD exist in the Liw-Liw Creek runoff area, and are less than 4 meters wide. In outcrop, the rocks have a light to dark gray, mottled appearance, indicative of their relatively equigranular to crystal-crowded nature. Multiple phases of aplite and quartz dikes were identified in the central-western portion of the large PHD plug. They occur as thin (<50cm diameter), saccharoidal, pinkish-white, inter-fingering dikes (Fig. 3.9b).

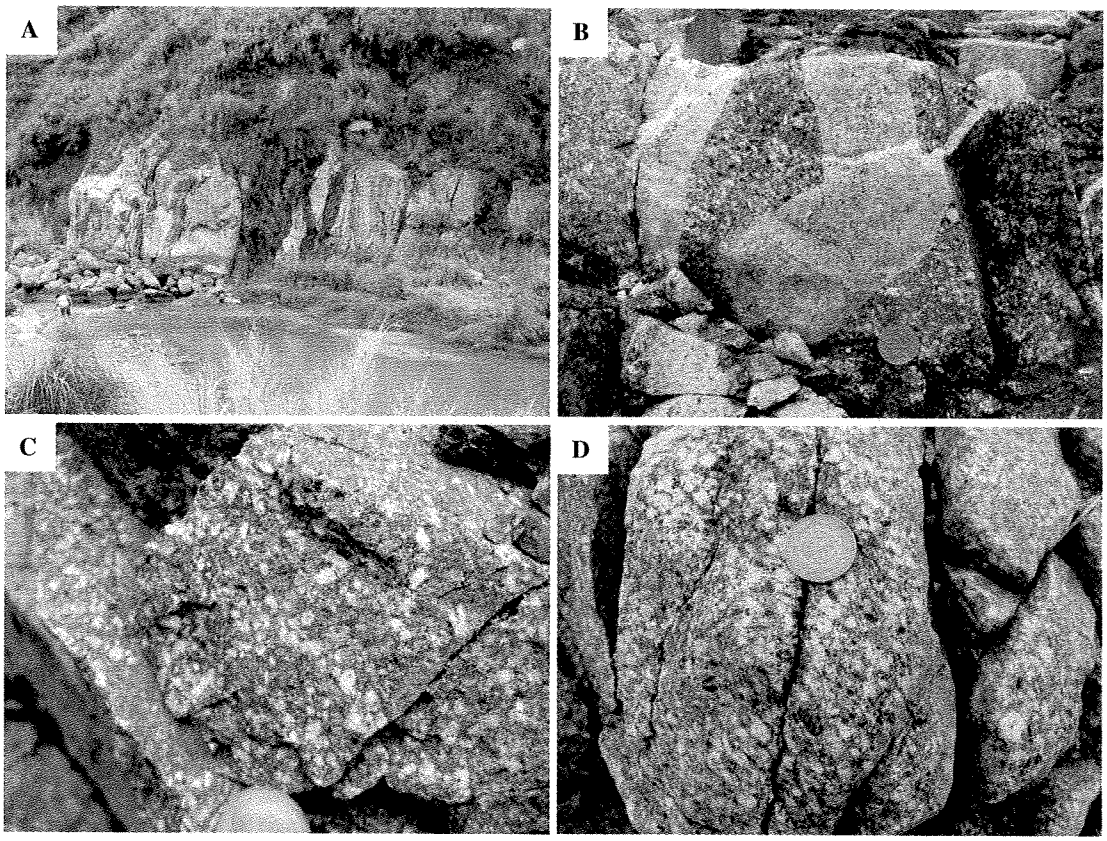

Figure 3.9 - (A) PHD dikes cropping out on the west bank of the Bued River (photo by Mike Baker, 2008); (B) aplite dikes crosscutting PHD (photo by Mike Baker, 2008); (C) plagioclase phyric PHD demonstrating a clearly porphyritic texture (sample BA08GS054; photo by David R. Cooke, 2008); (D) outcrop of PHD demonstrating a more granitic, equigranular texture (photo by Mike Baker, 2008).

There is prominent textural and mineral mode variability in the PHD rocks. In the field, outcrop varied from clearly porphyritic rocks (Fig. 3.9c), to crystal crowded, equigranular rocks (Fig. 3.9d). The majority of granitic texture was identified within the southwestern section of the large plug of PHD (Fig. 3.4); the location of the distinctly porphyritic rocks was not specific to one section of the map area. The mineral mode of the PHD varies considerably, with plagioclase as the ubiquitous phenocrystic phase alongside varying hornblende phenocryst concentrations. The variation throughout this intrusive phase suggests the existence of multiple intrusive events. However, where observed together in outcrop, the contact between dominantly plagioclase-phyric diorites and plagioclase and hornblende-phyric diorites was gradational (e.g., 50 meters southeast of the map center, on the north bank of the Bued River). The contacts between the different textures identified within the PHD are also frequently gradational. Aplite dikes were observed in outcrops of PHD less than 100 meters south of the map area center. They were sparsely distributed, occurring as E-trending, thin (<0.5 meters wide), off-white dikes.

Cumulative phenocryst contents range from ~25% to 70% by volume. Plagioclase accounts for more than 60% of the phenocryst content of any PHD sample, and forms subhedral to euhedral, tabular, zoned phenocrysts ranging from 0.5 to 8mm in length (though ranges within individual samples tends to be smaller). Carlsbad twinning of plagioclase phenocrysts is common throughout the PHD sample suite (Fig. 3.10a). In some of the crystal crowded samples, a secondary group of smaller plagioclase phenocrysts (<1mm diameter) display concentric zoning but no twinning (Fig. 3.10b). Hornblende phenocryst contents range from 5% to 20% by volume with diameters of <1-6mm. They are generally euhedral to subhedral, with a few phenocrysts in each sample exhibiting compositional zonation or twinning (Fig. 3.10c). Crystal growth habits included a range of tabular, "stocky" crystals to and long, thin "spindly" crystals (Fig. 3.10d and e). Phenocryst size ranged from 1-6mm in diameter. Groundmass in both the equigranular and distinctly porphyritic samples is predominantly very fine- to medium-grained quartz. The aplite dikes contained within PHD at the center of the map area are composed of fine- to medium-grained, equigranular, anhedral quartz (>95%; Fig. 3.11a). Trace hornblende phenocrysts were identified in a hand sample, wherein a hornblende-barren aplite dike truncated an aplite dike containing ~15% hornblende phenocrysts

(<250μm diameter; Fig. 3.11b). Thin chill margins (<1cm wide) were observed for both dikes.

Multiple dikes of PHD were observed crosscutting the plug of EMD (Fig. 3.4), suggesting a younger age of emplacement for the plagioclase- and hornblende- phyric diorites. For example, 15 meters south of the map center, a 0.75 meter wide dike of PHD displayed a chill margin at its contact with EMD (not displayed on the map due to scale). Because of its voluminous surface representation, there are also multiple examples of younger intrusives cutting across outcrops of PHD. A dike of hornblende megacrystic diorite (HMD) was observed crosscutting PHD rocks less than 200 meters southeast of the center of the map area (Fig. 3.4). A thin, plagioclase-phyric mafic dike (AM) approximately 30 meters northwest of the map center (not displayed on map due to scale) was also noted as cutting a dike of PHD. The series of aplite dikes unique to the PHD outcrops at the center of the map area suggests multiple aplite dike events prior to the emplacement of the HMG. The chill margins present in hand sample imply emplacement into PHD after the host rock had cooled somewhat.

A 1-meter wide dike of plagioclase and hornblende-phyric diorite was observed approximately 125 meters north-northwest of the map center along Kennon Road (Fig. 3.4). Mineralogically and texturally it is indistinguishable from the PHD intrusive unit, containing similar phenocryst assemblages and crystal habits. However, it is significantly older than the PHD (Chapter 4) and is thus designated as a pre-Black Mountain Porphyry dike (pre-BMP).

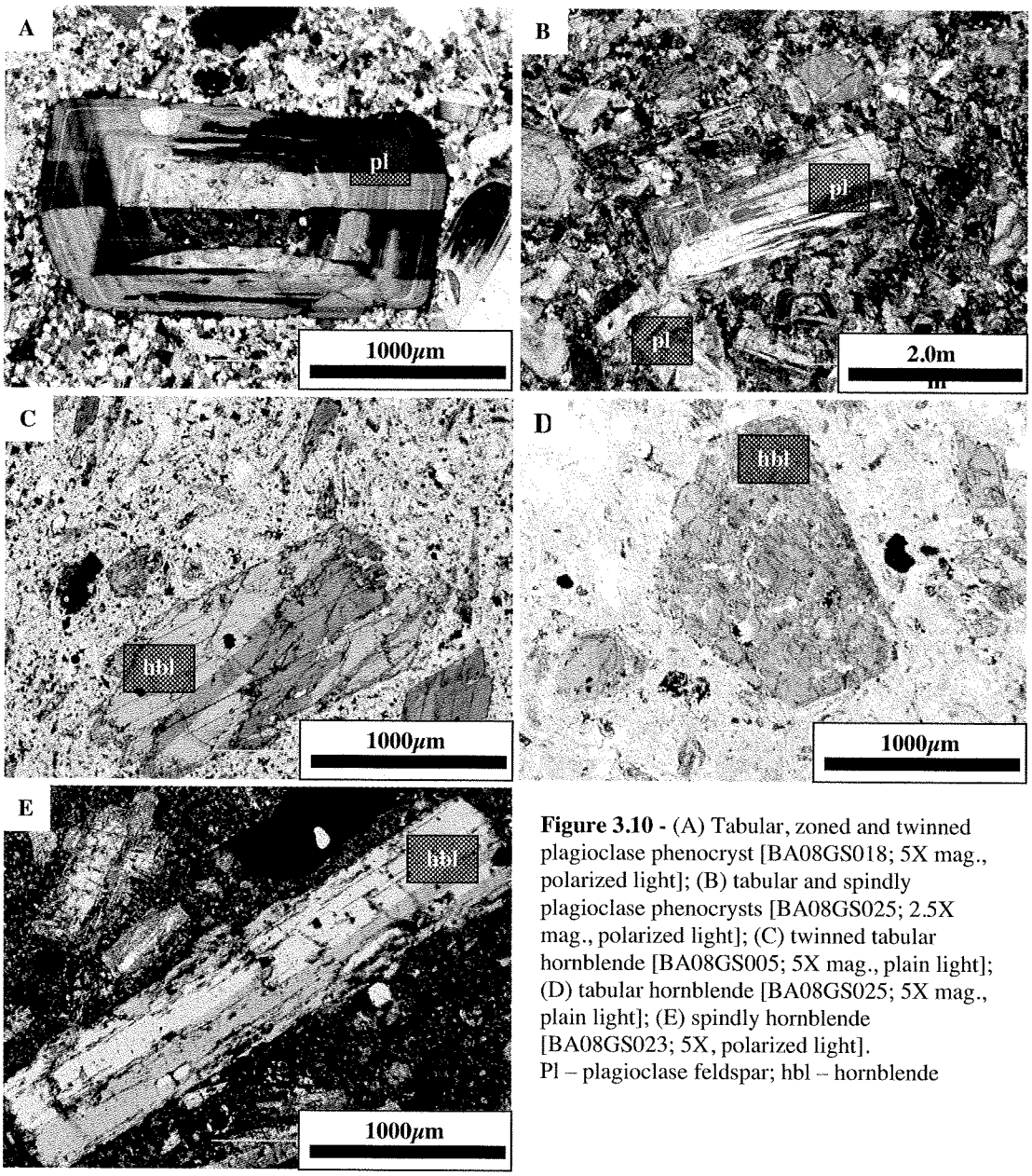

Figure 3.10 - (A) Tabular, zoned and twinned plagioclase phenocryst [BA08GS018; 5X mag., polarized light]; (B) tabular and spindly plagioclase phenocrysts [BA08GS025; 2.5X mag., polarized light]; (C) twinned tabular hornblende [BA08GS005; 5X mag., plain light]; (D) tabular hornblende [BA08GS025; 5X mag., plain light]; (E) spindly hornblende [BA08GS023; 5X, polarized light].
Pl – plagioclase feldspar; hbl – hornblende

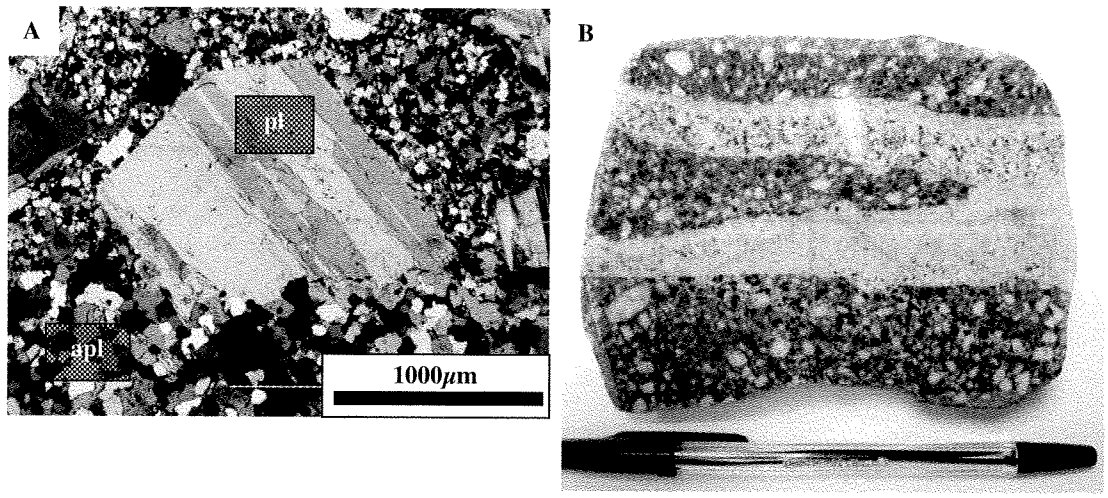

Figure 3.11 - (A) Tabular plagioclase feldspar phenocryst in PHD being cut by a dominantly quartz aplite dike; note the coarse-grained character of the aplite dike with respect to the PHD groundmass [BA08GS018; 5X mag., polarized light]; (B) a younger, hornblende-barren aplite dike cutting across an earlier hornblende-bearing aplite dike in PHD (BA08GS018).
Pl – plagioclase feldspar; apl – aplite dike

3.4.4 Hornblende megacrystic and "clotted" gabbro [HMG]

Hornblende megacrystic and clotted gabbroic rocks were identified near the center of the mapping area as broadly E-trending dikes less than two meters wide (Fig. 3.4). In weathered outcrop, they appeared as off-white to gray mottled rocks with individual hornblende phenocrysts and megacrysts, as well as large (up to 15cm across) aggregates of hornblende megacrysts (Fig. 3.12a and b). Some of the clots were zoned with respect to hornblende phenocryst size, wherein the edges of the clot were composed of smaller, non-megacrystic hornblende (Fig. 3.12b).

Phenocryst content of HMG rocks includes the hornblende megacrysts and clots, plagioclase feldspar, and both orthopyroxene and clinopyroxene. However, phenocryst content and character varies depending on the scale of observation: examination at the outcrop and hand sample scales suggests sparse hornblende megacrysts (and megacrystic clots) in a coarse-grained (up to 5mm diameter) matrix of plagioclase, hornblende and pyroxenes. However, thin section petrographic study identified a fine to very fine-grained groundmass containing the hornblende, plagioclase and pyroxene phenocrysts. Similarly, cumulative approximations for phenocryst volume are difficult to determine based on the sparse spatial distribution of the hornblende megacrysts. There were

frequently only three or four examples of individual hornblende megacrysts within a given outcrop of HMG, and even fewer hornblende aggregates. Therefore, petrographic-

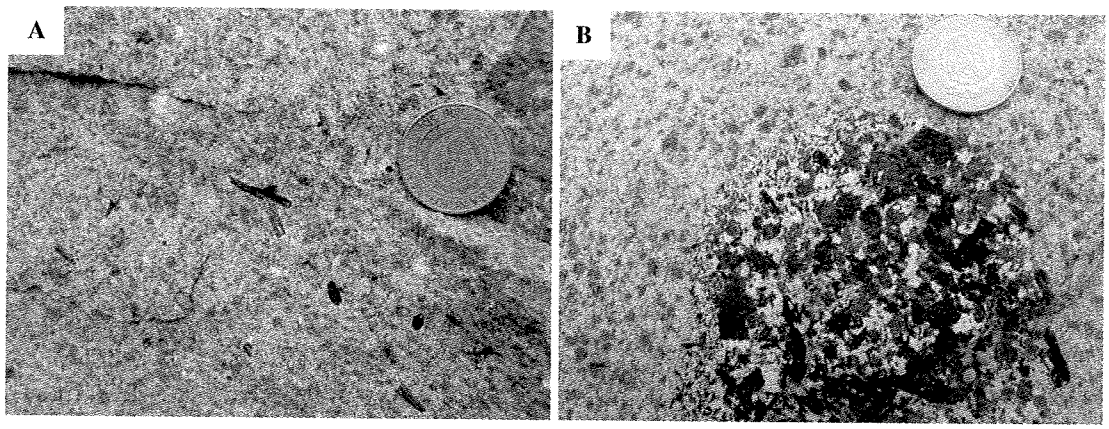

Figure 3.12 - (A) Individual hornblende megacrysts in a HMG dike; (B) hornblende megacrystic clot in HMG dike. Note the finer grained rim of the clot with respect to the coarser grained center. (Both photos by Mike Baker, 2008)

based volumetric approximations accounting for the plagioclase, non-megacrystic hornblende and pyroxene contents place total phenocryst volume between 40 and 60%. Plagioclase phenocrysts represent 30-45% of the total volume of the rock, and are between 1 and 2.5mm in diameter. They form euhedral to subhedral tabular and spindly phenocrysts, and exhibit distinct twinning (Fig. 3.13a). Unlike the previous intrusive phases, there is little-to-no zonation in the plagioclase phenocrysts of HMG. In thin section, patches of smaller (<0.5mm) spindly plagioclase crystals were observed (Fig. 3.13b). Hornblende phenocrysts account for less than 10% of total volume (not including the sparse megacrystic content), and form tabular and elongate euhedral to subhedral crystals with diameters between 1 and 7mm (Fig. 3.13c). Intergrown hornblendes are not uncommon, and compositional zoning was not identified (Fig. 3.13d). Pyroxene phenocrysts generally represent between 5 and 10% of the HMG rocks, with approximately equal concentrations of orthopyroxene and clinopyroxene. They occur as clusters of euhedral to subhedral phenocrysts with diameters between 1 and 2mm, and frequently exhibit twinning (Fig. 3.13e). The groundmass of HMG is fine-grained to very fine-grained, and is composed primarily of plagioclase feldspar.

The dikes of HMG were observed crosscutting the EMD plug in two locations: at the center of the mapping area, and about 75 meters to the east (Fig. 3.4). In both of

these outcrops, the HMG dike was also cut by a small (<0.5 meter diameter) plagioclase-microphenocrystic mafic dike and an aphanitic mafic dike (the AM unit; Fig. 3.14). As well, the HMG dikes cut outcrops of PHD about 100 meters to the southeast of the map area center (Fig. 3.4). This set of crosscutting relationships suggests a relative age of emplacement after the EMD and PHD, but prior to the aphanitic and fine-grained mafic dikes observed throughout the mapping area (HCB and AM).

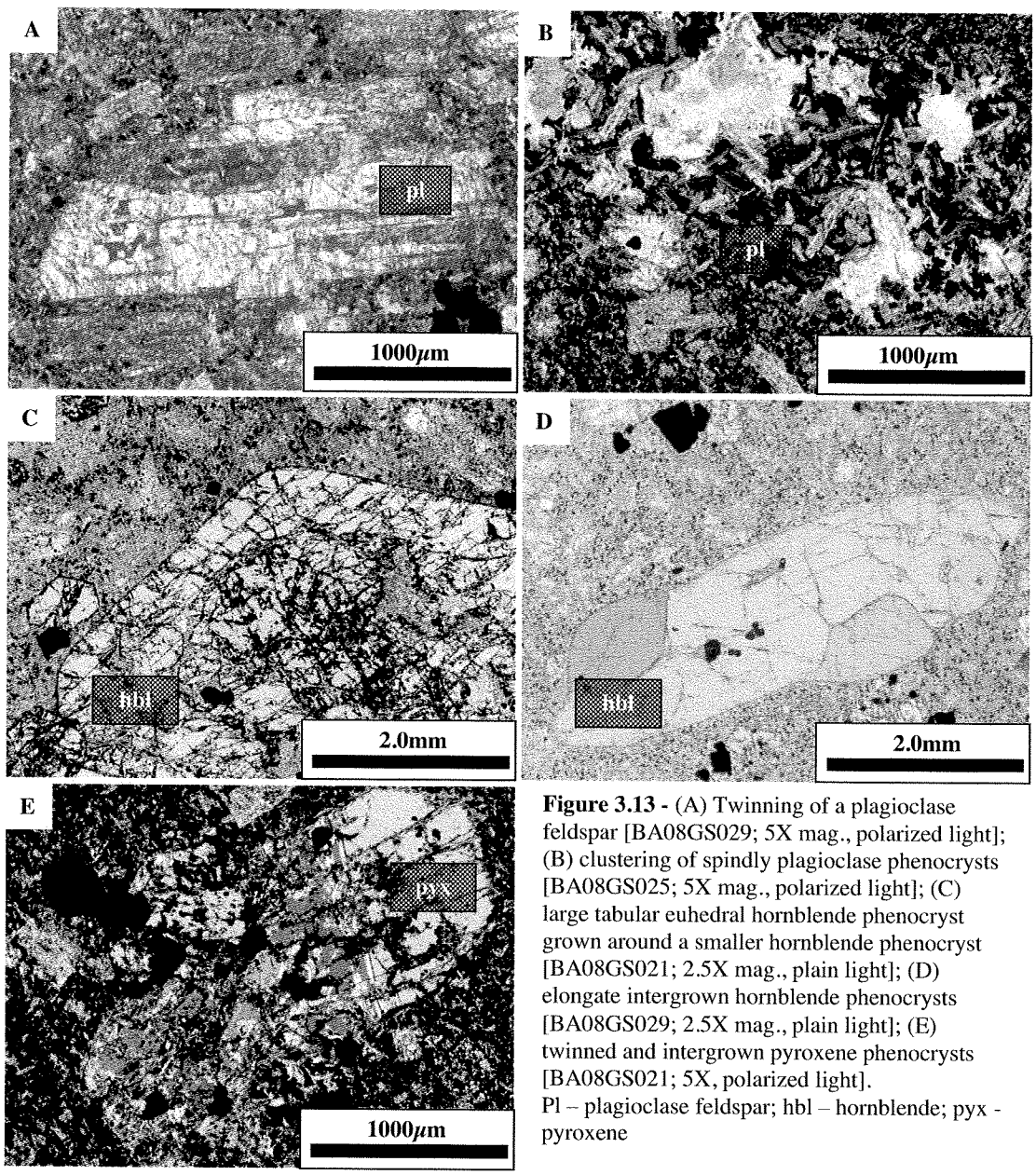

Figure 3.13 - (A) Twinning of a plagioclase feldspar [BA08GS029; 5X mag., polarized light]; (B) clustering of spindly plagioclase phenocrysts [BA08GS025; 5X mag., polarized light]; (C) large tabular euhedral hornblende phenocryst grown around a smaller hornblende phenocryst [BA08GS021; 2.5X mag., plain light]; (D) elongate intergrown hornblende phenocrysts [BA08GS029; 2.5X mag., plain light]; (E) twinned and intergrown pyroxene phenocrysts [BA08GS021; 5X, polarized light].
Pl – plagioclase feldspar; hbl – hornblende; pyx - pyroxene

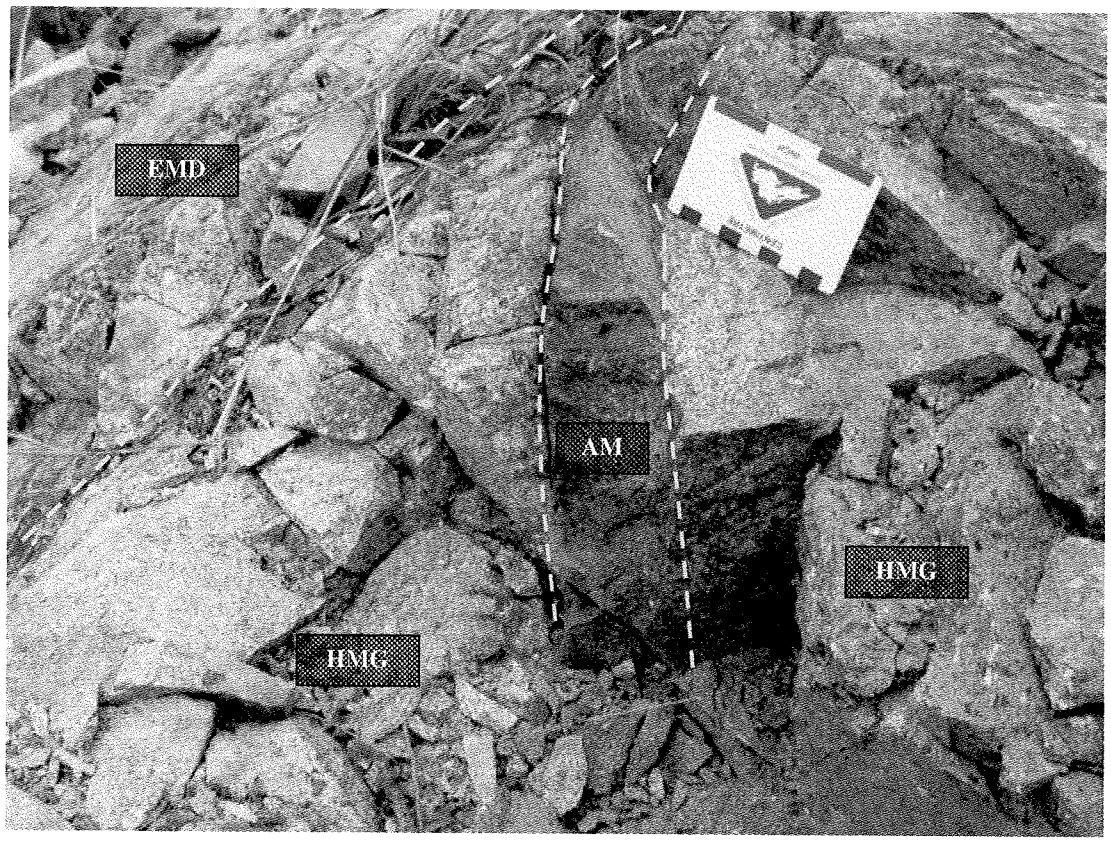

Figure 3.14 - A dike of aphanitic andesite/basalt (intrusive phase AM) contained in an HMG dike crosscutting the central EMD plug (Fig. 3.4).

3.4.5 Late-stage Mafic Intrusives

A series of fine-grained mafic dikes were noted in the field, ranging from thin (<25cm wide), aphanitic and finely plagioclase-phyric dikes at the center of the mapping area, to thicker (up to 4 meters wide) hornblende-phyric dikes containing large (up to 25cm diameter) clusters of non-megacrystic hornblende and plagioclase (500 meters southeast of the map center, along the Bued River; Fig. 3.4). The variability in the mineralogical composition and texture of this series of dikes suggests multiple intrusive phases. However, the relatively low volumetric representation within the BMPSE map area makes it difficult to establish timing relationships based on field observations. Therefore, a cautious division into two intrusive events is outlined below.

Hornblende "clotted" basalt [HCB]

The hornblende-phyric and hornblende-plagioclase clotted mafic dikes (HCB) were observed southeast of the map center in the Bued River, and take the form of thick (up to 4 meters wide), broadly E-trending dikes (Fig. 3.4). The weathered outcrops of HCB rocks was light gray, with significantly darker fresh surfaces. Despite their scarcity, the clots of hornblende and plagioclase (up to 25cm across) were apparent on both weathered and fresh faces.

Similar to the preceding HMG intrusive phase, the phenocryst content of the HCB dikes varies based on the scale of observation. Through petrographic analysis (and discounting the hornblende and plagioclase clots), the phenocryst content of HCB is between 35% and 45% by volume, and is dominantly hornblende. Euhedral to subhedral hornblende phenocrysts are up to 5mm in diameter, and occasionally exhibit zoning, twinning, or a combination of both (Fig. 3.15a and b). Smaller (<250μm diameter), subhedral or fragmental hornblendes are present as well (Fig. 3.15a). Trace amounts (<2% by volume) of subhedral clinopyroxene were observed in thin section (Fig. 3.15c). The groundmass is aphanitic. The hornblende-plagioclase clots are composed predominantly of hornblende phenocrysts (95% volume of the clots), and exhibit a zoned nature wherein hornblende phenocryst size decreases (3mm diameters dropping down to approximately 100μm) from the interior of the clot outwards towards the rim, which is sharply marked by a thin (approximately 1.5mm thick) layer of subhedral plagioclase phenocrysts (up to 1mm diameter; Fig. 3.15d-e).

Interaction between the HCB dikes and the other intrusive phases of the BMPSE was not observed in the mapping area. All contacts were with Pugo Formation rocks, and did not directly suggest a relative timing for emplacement of the HCB dikes (with respect to the BMIC). However, the broad mineralogical similarities with HMG rocks, and the presence of hornblende-plagioclase clots may suggest that the HCB dikes represent a product of magmatism similar to that of the preceding HMG unit. The major distinguishing factor between the two intrusive rock types is phenocryst abundance: because of their lower phenocryst content and finer-grained nature, the HCB dikes may represent more rapid crystallization of magmatism during the cooler, waning stages of the BMPSE porphyry system. Conversely, the HMG dikes contain more abundant

phenocrysts (and megacrysts), and may represent longer crystallization times afforded by remnant heat from the emplacement of the preceding, voluminous PHD. The HCB intrusive phase is therefore cautiously implied to have been emplaced after the HMG dikes.

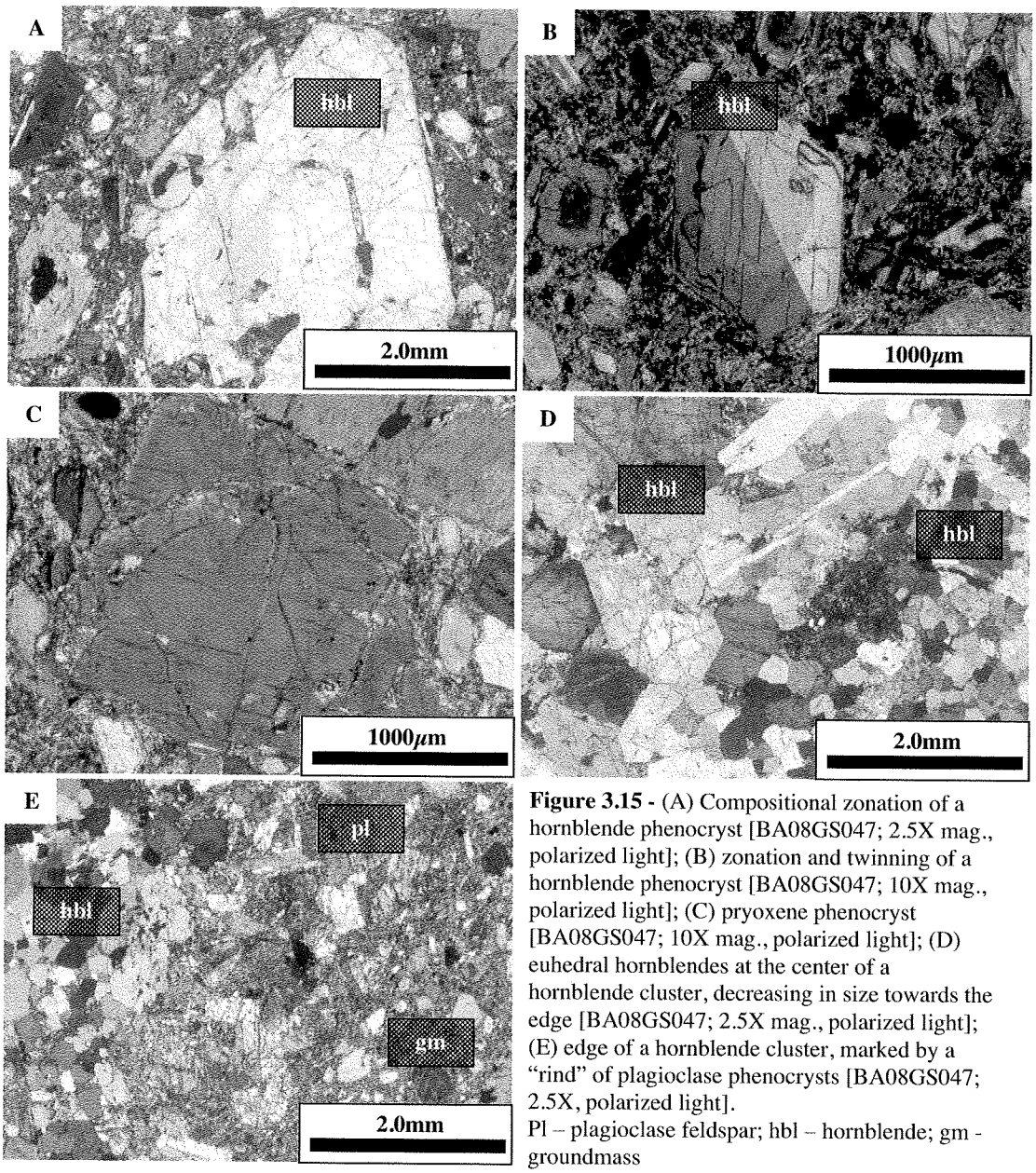

Figure 3.15 - (A) Compositional zonation of a hornblende phenocryst [BA08GS047; 2.5X mag., polarized light]; (B) zonation and twinning of a hornblende phenocryst [BA08GS047; 10X mag., polarized light]; (C) pryoxene phenocryst [BA08GS047; 10X mag., polarized light]; (D) euhedral hornblendes at the center of a hornblende cluster, decreasing in size towards the edge [BA08GS047; 2.5X mag., polarized light]; (E) edge of a hornblende cluster, marked by a "rind" of plagioclase phenocrysts [BA08GS047; 2.5X, polarized light].
Pl – plagioclase feldspar; hbl – hornblende; gm - groundmass

Aphanitic to plagioclase microphenocrystic mafics [AM]

A series of aphanitic to finely plagioclase-phyric mafic dikes were observed throughout the map area (Fig. 3.4). Termed the AM intrusive unit, most outcrops were of thin (<50cm wide), E- or NW-oriented dikes, though one outcrop (approximately 500 meters southeast of the map center) was relatively wide (10 meters thick). Four outcrops were observed within 50 meters of the center of the map area, while three were identified near the meeting point of the Liw-Liw Creek runoff and the Bued River in the southeast of the mapping area (Fig. 3.4). Weathered outcrop was a dull light to dark gray, and phenocryst content (if present) was faintly distinguishable. Fresh faces of AM dikes revealed a dark gray color, though phenocryst content was still obscured.

Textural variation between the individual dikes is minimal, as most are aphanitic with little-to-no phenocryst content. Sparse (<5% by volume) plagioclase and hornblende phenocrysts were identified at three outcrop locations, all of which are within 100 meters of the center of the map area. Plagioclase takes the form of small (<2mm diameter) tabular, subhedral phenocrysts that account for most (~95%) of the phenocryst content (where phenocrysts were observed). Trace hornblende phenocrysts were identified in one outcrop (100m southeast of the map center), and are euhedral with diameters less than 2 mm.

Interaction of AM dikes with earlier intrusive phases is confined to outcrops within 50 meters of the center of the deposit (and map area), where surface representation of EMD, PHD and HMG is the most abundant. One outcrop at the exact center of the map area illustrates the relatively late emplacement of AM dikes, as a 1 meter thick HMG dike cutting through EMD is cut by a thin (25cm thick) aphanitic mafic dike (Figs. 3.4; 3.14). Similarly, 75 meters to the southeast of the map center, a 50cm wide, finely plagioclase-phyric mafic dike exhibits a distinct chill margin where it crosscuts both EMD and HMG (Figs. 3.4; 3.16). Through these field relationships, it is clear that the broadly fine-grained, mafic magmatism of the AM intrusive phase followed that of the more porphyritic and granitic EMD, PHD and HMG.

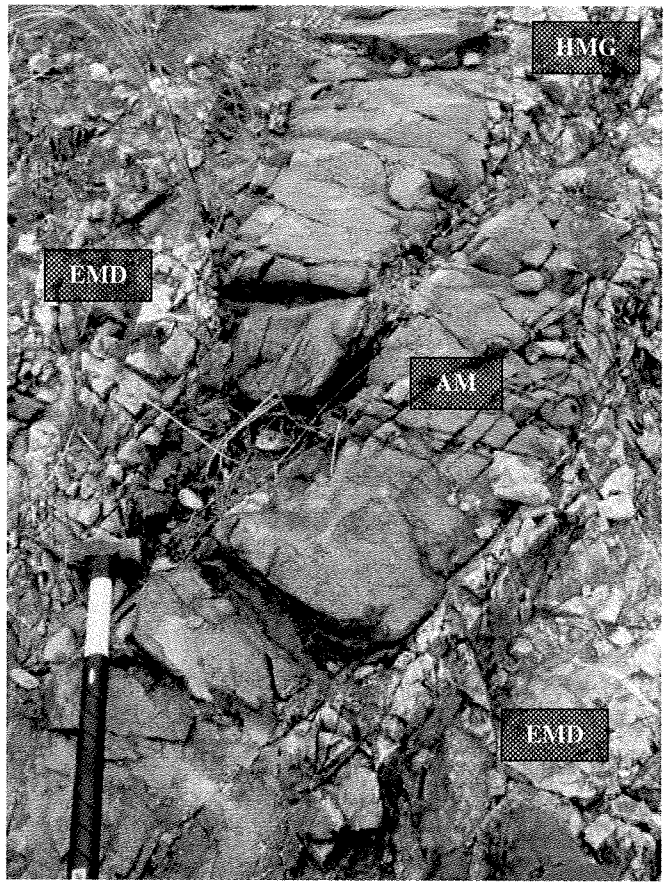

Figure 3.16 - An offset, <50cm wide plagioclase microphenocrystic mafic dike (AM) cross cutting both the EMD and HMG intrusive units (photo by Mike Baker, 2008).

3.5 Discussion

The intrusive history of the Black Mountain Southeast intrusive rocks detailed above denotes an abrupt shift from megacrystic mafic dikes, to voluminous stocks and plugs of relatively felsic equigranular and porphyritic intrusives, followed by a gradual transition to mafic fine-grained dikes. With the inclusion of the LLC mafic dikes, the Black Mountain Southeast porphyry system's magmatism appears to have evolved from mafic-to-felsic-to-mafic throughout its lifetime. Both the rock types identified and their order of emplacement are broadly concurrent with the rough petrogenetic sequence reported by Waters and Gonzales (2005) and Waters et al. (in press).

The evolving phenocryst content of the Black Mountain Southeast Intrusive Suite also emphasizes the mafic-to-felsic-to-mafic progression: the hornblende phenocryst content of the LLC dikes is supplemented with quartz and plagioclase (EMD and PHD),

followed by the addition of clinopyroxene and/or orthopyroxene and the removal of quartz with the emplacement of HMG onward. The emergence of pyroxene phenocrysts and/or microphenocrysts in a system previously dominated by hornblende is indicates of increasingly mafic magmatism. This runs contrary to what is predicted by closed system magmatic fractionation (a temporal trend of mafic to felsic), and thus suggests that a process outside of fractional crystallization played a major role the generation of the Black Mountain Southeast Intrusive Suite.

Textural changes observed within the rocks of the Black Mountain Southeast deposit are difficult to highlight, as individual intrusive phases exhibit high textural variability (e.g., the PHD intrusive phase), or no primary texture at all (e.g., EMD). However, within the intrusive phases following the EMD, there is a broad shift from crystal-crowded and distinctly porphyritic textures, to weakly porphyritic and dominantly aphanitic rocks. This advancement towards finer-grained igneous rock may be a sign of waning heat within the evolving porphyry system, limiting the growth of phenocrysts and supporting the timing relationships detailed above. This is supported by the observation of a trend towards decreased volumetric representation at the surface of the mapping area with successive intrusive events, suggesting diminishing magmatic activity in the Black Mountain Southeast porphyry system.

Previous work on the formation and evolution of porphyry systems by Keith et al. (1997), Hattori and Keith (2001), Maughan et al. (2002), Lickfold et al. (2007), Sillitoe (2010) and others suggested that the introduction of a mafic magma to the base of a porphyry system (mafic underplating) is a crucial process in the formation of mineralizing fluids and the development of porphyry-style mineralization. The increasingly mafic mineralogy of successive intrusive phases at Black Mountain Southeast could be a byproduct of such an influx of mafic magma. Were a mafic melt to be introduced into the intra-crustal parental magma body that gave rise to the Black Mountain intrusive rocks early in the system's lifetime, one would expect to see increasing lithological, mineralogical and geochemical representation of the mafic melt within shallow-crustal products. The lithological and mineralogical evidence of the mafic underplating process is observed at Black Mountain Southeast; the geochemical

and mineralogical implications of (and evidence for) mafic underplating are discussed in Chapters 5 and 6.

An explanation for the origin of the hornblende clots observed in the HMG and HCB is not clear. Waters and Gonzales (2005) observed amphibolite clusters in the Liw-Liw Creek dikes, and suggested that they were sub-arc mantle xenoliths. While this explanation is viable, the gradational sizing (and euhedral nature) of hornblende phenocrysts within the HMG and HCB clots may suggest a non-xenolithic nature. More specifically, if the finer-grained edges of the clots are interpreted to be chill margins, the clots may represent pegmatoidal "sweats" within the HMG and HCB magmas.

3.6 Summary

Six intrusive phases were identified at the Black Mountain Southeast porphyry deposit through field mapping and petrographic study. In order of oldest to youngest, these are:

1. Liw-Liw Creek hornblende megacrystic basalt [LLC]
2. Early mineralization quartz diorite [EMD]
3. Plagioclase- and variably hornblende-phyric diorite [PHD]
4. Hornblende megacrystic and "clotted" gabbro [HMG]
5. Hornblende "clotted" basalt [HCB]
6. Aphanitic to plagioclase microphenocrysitc mafics [AM]

The mineralogical and textural evolution of these intrusive rocks defines a trend of mafic-to-felsic-to-mafic magmatism in the Black Mountain Southeast system throughout its magmatic lifetime. This implies that the generation of the Black Mountain Southeast magmas was a product of processes other than fractional crystallization, such as mafic underplating.

Chapter 4

Geochronology

4.1 Introduction

Five new U-Pb dates and four new Ar-Ar ages have been generated for undated intrusive phases at the Black Mountain Southeast deposit. The samples are referred to below based on the intrusive phase subdivisions outlined in Chapter 3, and are compared with previously reported dates for the greater Black Mountain Intrusive Complex (Chapter 2). Methodology and lab procedures for the U-Pb and Ar-Ar dating techniques are summarized in Appendix 1.1 and 1.2, respectively.

4.2 Previous Work

One biotite and four amphibole Ar-Ar dates were reported by Waters and Gonzales (2005) and Waters et al. (in press) for the intrusive phases mapped by Gonzales (2004) at the Black Mountain Kennon ore body and the Mexico prospect (Chapter 2; Table 4.1). Analysis of alteration biotite from an inter-mineral quartz diorite porphyry at Kennon returned an age of 2.95±0.05 Ma, while amphibole analyses from a late-mineral hornblende andesite porphyry and a pre-mineral hornblende quartz diorite porphyry at Kennon returned ages of 2.81±0.24 Ma and 2.98±0.30 Ma, respectively. Two samples of hornblende andesite porphyry from Mexico returned hornblende Ar-Ar ages of 2.90±0.15 and 3.09±0.15 Ma.

4.3 New Dates for the Black Mountain Southeast Intrusive Suite

The new U-Pb and Ar-Ar ages generated for this study are summarized in Table 4.1 and Figure 4.1; locations of the dated samples are shown in Figure 4.2. The U-Pb ages for the Black Mountain Southeast intrusive rocks include one sample from the Liw-Liw Creek mafic dikes (LLC) and four samples from the plagioclase- and variably hornblende-phyric diorite (PHD; Chapter 3). The new Ar-Ar dates include one sample of LLC, one sample of a hornblende-plagioclase megacrystic clot contained in a dike of HMG, one sample of PHD, and one sample of a pre-BMP porphyritic dike (visually similar to the PHD; Chapter 3).

Based on the new U-Pb dates, a range of 3.00 Ma to 2.79 Ma is proposed for the PHD. The inclusion of the Ar-Ar date for PHD intrusive phase augments this range to 3.06 Ma to 2.60 Ma, as the inherently larger error involved in Ar-Ar dating eclipses the cumulative range of U-Pb error (Table 4.1). The two dates for the Liw-Liw Creek mafic dikes are 3.20±0.02 Ma (U-Pb) and 4.73±0.17 (Ar-Ar), suggesting an age range of 4.90 Ma to 3.18 Ma (Table 4.1). The clot contained in the HMG has an amphibole Ar-Ar age of 2.81±0.15 Ma. The pre-BMP porphyry dike dates at 6.39±0.49 Ma (Table 4.1). All dates produced for this study are statistically robust, with U-Pb ages calculated as 3, 4 or 5-point $^{206}Pb/^{238}U$ weighted averages, or Ar-Ar plateau ages derived from the release of between 78% and 96% ^{39}Ar (Table 4.1, Figs. 4.3 and 4.4).

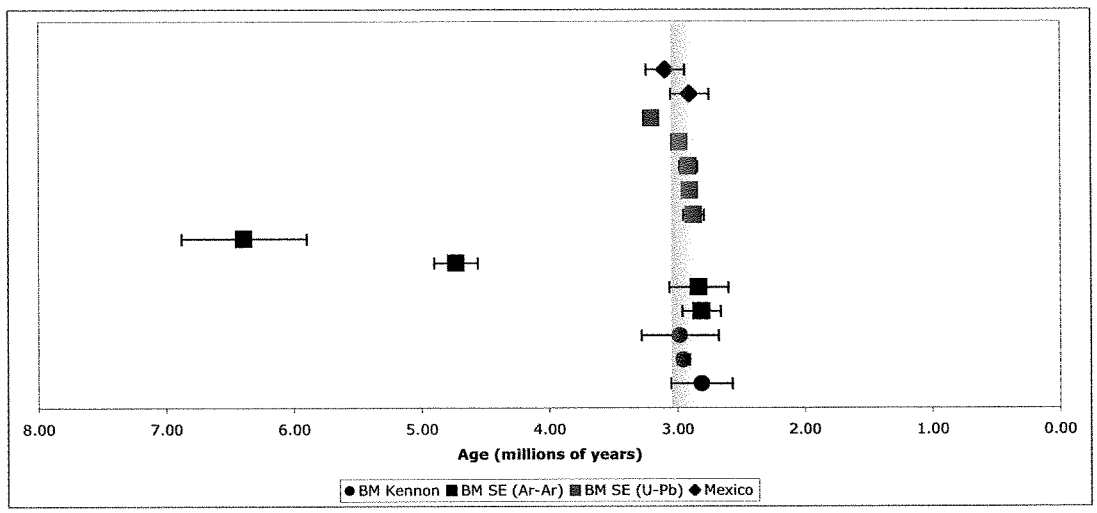

Figure 4.1 - Reported ages for the greater Black Mountain Intrusive Complex and respective 2 sigma errors. Dark blue data points indicate Ar-Ar geochronology; red indicates U-Pb. Squares indicate Black Mountain Southeast samples (from this study only); diamonds and circles indicate Mexico and Black Mountain Kennon samples, respectively (from Waters and Gonzales, 2005; Waters et al., in press). The shaded bar represents a time constraint on mineralization at Black Mountain Southeast by the observations of Waters and Gonzales, (2005) and this study.

Sample Number	Method	Locality	Min.	Rock Type	Size (#) mm	Purity (%)	Apparent Age (Ma)	± 2σ	% of ^{39}Ar	Method	Source
BA08GS007	U-Pb	BM SE	zr	hbl-pl diorite porphyry (PHD)			2.98	0.02		5-pt 206Pb/238U weighted average	This study
BA08GS013	U-Pb	BM SE	zr	pl diorite porphyry (PHD)			2.91	0.07		4-pt 206Pb/238U weighted average	This study
BA08GS019	U-Pb	BM SE	zr	pl diorite porphyry (PHD)			2.90	0.04		3-pt 206Pb/238U weighted average	This study
BA08GS040	U-Pb	BM SE	zr	hbl-pl diorite porphyry (PHD)			2.87	0.08		4-pt 206Pb/238U weighted average	This study
BA08GS054	U-Pb	BM SE	zr	pl andesite porphyry (LLC)			3.20	0.02		4-pt 206Pb/238U weighted average	This study
BA08GS009	Ar-Ar	BM SE	hbl	hbl megacrystic clot (HMG)	0.30-0.50	99	2.81	0.15	89.1	Plateau	This study
BA08GS030	Ar-Ar	BM SE	hbl	pl diorite porphyry (PHD)	0.30-0.50	99	2.83	0.23	95.5	Plateau	This study
BA08GS056	Ar-Ar	BM SE	hbl	hbl megacrystic basalt (LLC)	0.30-0.50	99	4.73	0.17	88.0	Plateau	This study
BA08GS038	Ar-Ar	BM SE	hbl	hbl-pl diorite porphyry (pre-BM)	0.30-0.50	99	6.39	0.49	77.7	Plateau	This study
806106	Ar-Ar	BM Kennon	hbl	hbl andesite porphyry	0.36-0.85	99	2.81	0.24	65.7	Plateau	Waters and Gonzales (2005)
806107	Ar-Ar	BM Kennon	bt	qtz diorite porphyry	0.36-0.85	99	2.95	0.05	25.7	Maximum	Waters and Gonzales (2005)
806108	Ar-Ar	BM Kennon	hbl	hbl-qtz diorite porphyry	0.36-0.85	98	2.98	0.30	97.8	Plateau	Waters and Gonzales (2005)
806104	Ar-Ar	Mexico	hbl	hbl andesite porphyry	0.36-0.85	99	3.09	0.15	63.7	Plateau	Waters and Gonzales (2005)
806103	Ar-Ar	Mexico	hbl	hbl andesite porphyry	0.36-0.85	98	2.90	0.15	82.5	Plateau	Waters and Gonzales (2005)

Table 4.1 – Summary of new U-Pb and Ar-Ar ages for previously undated intrusive rocks from Black Mountain Southeast, as well as reported Ar-Ar ages from Black Mountain Kennon and the Mexico Prospect intrusive rocks (Waters and Gonzales, 2005; Waters et al., in press).
Abbreviations: % of ^{39}Ar = fraction of ^{39}Ar released used to calculate the apparent ^{40}Ar-^{39}Ar age. Min. = mineral dated; zr for zircon, bt for biotite or hbl for hornblende (amphibole). Pur (%) = sample purity.

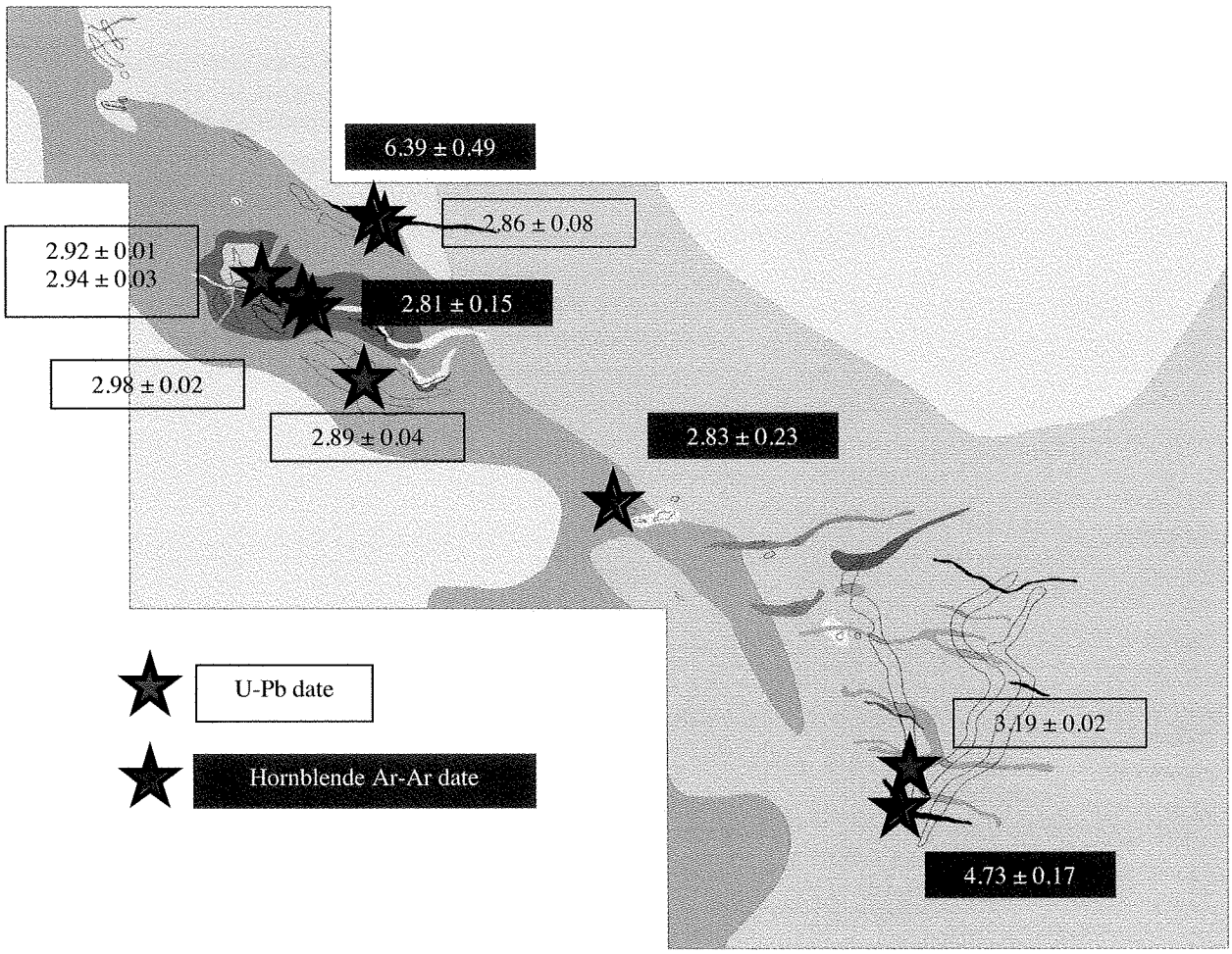

Figure 4.2 - Sample locations of the new Ar-Ar and U-Pb dates for the Black Mountain Southeast intrusive rocks (from March 2008 field season).

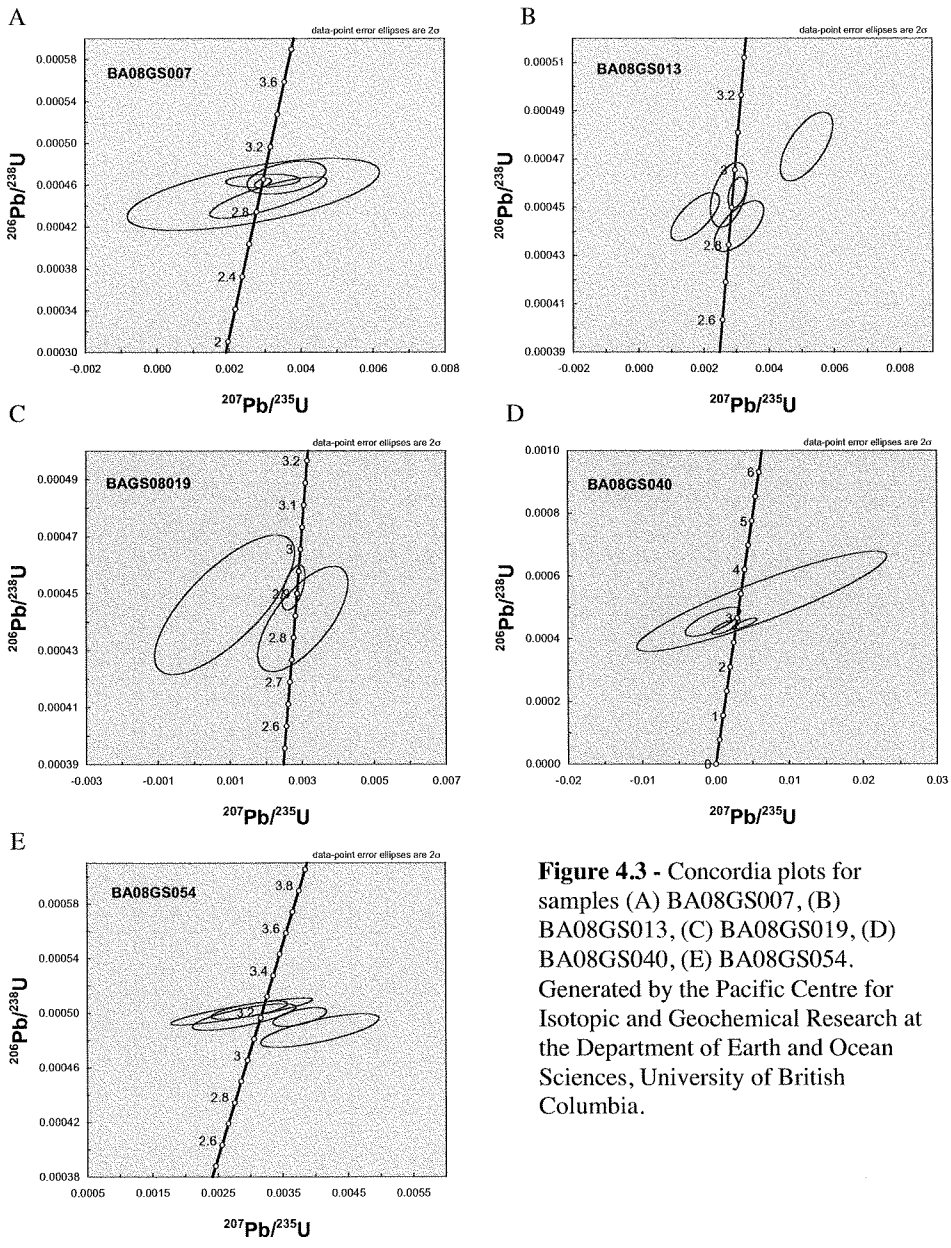

Figure 4.3 - Concordia plots for samples (A) BA08GS007, (B) BA08GS013, (C) BA08GS019, (D) BA08GS040, (E) BA08GS054. Generated by the Pacific Centre for Isotopic and Geochemical Research at the Department of Earth and Ocean Sciences, University of British Columbia.

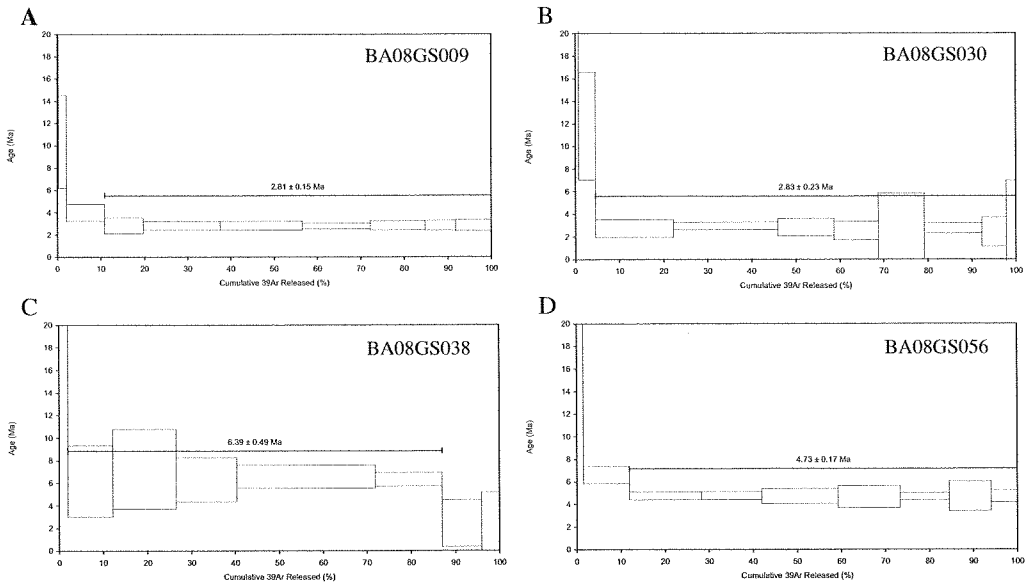

Figure 4.4 - Ar-Ar plateau ages for samples (A) BA08GS009, (B) BA08GS030, (C) BA08GS038, (D) BA08GS056. Generated by John Huard, College of Oceanic and Atmospheric Sciences, Oregon State University, Corvallis, Oregon.

4.4 Discussion

Combined with its inter- to late-mineralization timing, the age range of the PHD (ca. 3-2.79 Ma; Table 4.1) defines a minimum age of 3.00 Ma for the emplacement of the Early Mineralization Diorite (EMD; Chapter 3) and the peak of mineralization at Black Mountain Southeast. The intrusive phase hosting mineralization at the Kennon ore body was defined by Waters and Gonzales (2005) as a quartz diorite porphyry, roughly matching the description of the EMD (Chapter 3). The reported age of potassic alteration associated with mineralization from the Kennon quartz diorite porphyry (2.95±0.05 Ma; Waters and Gonzales, 2005) is consistent with the implied age of mineralization at Black Mountain Southeast (Fig. 4.1). The maximum age of mineralization at Kennon is inferred to be younger than the 2.98±0.30 Ma age of a pre-mineralization hornblende quartz diorite porphyry, which is also in agreement with the inferred age of mineralization at Southeast (Waters and Gonzales, 2005).

The reported ages for the late-mineralization hornblende andesite porphyries at the Mexico prospect suggest that they were emplaced during the waning stages of mineralization (Table 4.1; Fig. 4.1; Waters and Gonzales, 2005). This suggests that mineralization at Mexico was broadly concurrent with the formation of the Kennon or

Southeast ore bodies. The dates produced for the Liw-Liw Creek mafic dikes confirm their pre-mineralization emplacement, in agreement with Waters and Gonzales (2005).

The Ar-Ar age reported for a hornblende cluster in the HMG intrusive phase (Table 4.1) falls within the upper end of the range defined by the preceding PHD unit. The relatively young age of the hornblende clot indicates that it is not a sub-arc mantle xenolith, as originally suggested by Waters and Gonzales (2005) for the Liw-Liw Creek dikes. The presence of a ~6.4 Ma pre-BMP intermediate porphyry dike within the map area (Fig. 4.2) suggests that despite the proposed magmatic hiatus between 17 and 5 Ma (Chapter 2), volumetrically minor intermediate magmatism was occurring.

4.5 Summary

The new ages presented herein confirm the Black Mountain Intrusive Complex as the oldest mineralized intrusive suite of the Baguio Mineral District (Chapter 2), with initial emplacement of the Liw-Liw Creek mafic dikes estimated at up to ca. 4.9 Ma, and emplacement of felsic magmas beginning approximately 3.0 Ma. Within the context of the Black Mountain Southeast Intrusive Suite (Chapter 3), the new dates indicate that primitive mafic magmatism was present prior to mineralization in the form of hornblende andesite and porphyry dikes at Mexico and plagioclase and hornblende-phyric mafic dikes in Liw-Liw Creek. Coupled with its interpreted chill margin (Chapter 3), the young age of the HMG hornblende clot implies that it is not a sub-arc mantle xenolith, as suggested for similar clots in the Liw-Liw Creek mafic dikes (Waters and Gonzales, 2005), but rather a pegmatitic sweat or possibly an autolith. Despite its relative rarity within the map area, the presence of a pre-Black Mountain intermediate porphyry dike suggests that generation of small volume magmatic events did occur during late Miocene.

Chapter 5

Geochemistry and Petrogenesis

5.1 Introduction

The temporal change in magmatism from mafic-to-felsic-to-mafic compositions present within the Black Mountain Southeast Intrusive Suite (BMSIS; Chapter 3) suggests a complex sub-arc magma generation process and intra-crustal magmatic evolutionary history. Utilizing whole rock geochemistry and Rb/Sr and Sm/Nd isotopic systematics, this chapter examines the sub-arc and intra-crustal generation and evolution of the Black Mountain Southeast Intrusive Suite in its own right and within the context of the fertile Pliocene magmatism of the Baguio mineral district.

5.2 Previous Work

The geochemistry of the intrusive rocks in northern Luzon and the Baguio mineral district is well documented. The combination of world-class mineralization and young oceanic arc development and evolution has attracted the attention of industry geologists and academics alike. Regional (Luzon) and local (Baguio mineral district) geochemical data sets have been compiled and/or generated by a number of authors (e.g., Defant et al., 1989; Yumul et al., 1995, 2000, 2003a, 2003b; Yang et al., 1996; Maury et al., 1998; Sajona et al., 1999; Bellon and Yumul 2000, 2001; Bautista et al., 2001; Dimalanta and Yumul, 2003; Waters and Gonzales, 2005; Hollings, 2006; Polve et al., 2007; Hollings et al., in press; Waters et al., in press) to investigate the geodynamic and magmatic evolution of Luzon and the Baguio district.

Specific examination of the Late Miocene to Pliocene intrusive rocks of the Baguio mineral district and their associated mineralization has been conducted by Hollings and Cooke (2005), Waters and Gonzales (2005), Hollings (2006), Polve et al. (2007), Hollings et al. (in press) and Waters et al. (in press). However, geochemical data specifically from the Black Mountain Intrusive Complex (BMIC; Chapter 3) is scarce, and is limited to 18 whole rock geochemical analyses (Hollings, 2006) and seven Rb-Sr and Sm-Nd isotope analyses (Polve et al., 2007; Hollings, in press). There are no published data sets for the Black Mountain Southeast Intrusive Suite.

5.3 Whole Rock Geochemistry

This section describes the compositional range of the sampled intrusive suites through an assessment of the whole rock geochemical characteristics of the individual intrusive phases of the BMSIS (Chapter 3). The results provide insight into the apparent temporal changes in magmatic composition across the intrusive complex.

A total of 42 samples from the Black Mountain Southeast were analyzed for their major and trace element geochemistry by Acme Labs. Detailed methodology can be found in Appendix 1.3. The sample suite was selected to highlight the diversity of magmatic rocks present within the Black Mountain Southeast Intrusive Suite and to ultimately explore geochemical variations throughout the magmatic evolution of the Black Mountain Porphyry Southeast system.

Representative whole rock geochemical data from this study is presented in Appendix 2.1. All intrusive phases previously identified in Chapter 3 are represented in the sample suite: five samples are associated with the Liw-Liw Creek mafic dikes (LLC), two samples are early mineralization diorite (EMD), 14 samples of plagioclase and hornblende-phyric diorite (PHD), five samples of hornblende megacrystic gabbro (HMG), three samples of hornblende clotted basalt (HCB), and six samples of aphanitic to microphenocrystic mafic dikes (AM). Seven additional samples were analyzed that are not associated with the BMSIS, including five samples of Pugo Formation mafic extrusive rocks, one sample of Zig-Zag Formation marble, and two samples of pre-BMIC intermediate porphyry dikes (Appendix 2.1).

5.3.1 Element Mobility within the Black Mountain Southeast Intrusive Suite

The mobility of Large Ion Lithophile Elements (LILE) within porphyry environments of the Baguio district has been noted by Hollings (2006) and Hollings et al. (in press). It is therefore imperative to qualify the mobility of LILE prior to the examination and discussion of the geochemical characteristics of the Black Mountain Southeast, so that accurate classification methods are used.

Harker plots of SiO_2 versus the LIL elements/oxides K_2O and Rb, Na_2O and High Field Strength Element (HFSE) oxide TiO_2 are displayed in Figure 5.1. Despite a weak

positive correlation of K_2O and Rb with SiO_2 (as would be expected from a magma undergoing fractional crystallization; Hollings et al., in press), the scatter of data in Figures 5.1a and b demonstrates the relative mobility of LILE within the Black Mountain Southeast Intrusive Suite. Assigning a best-fit trend line for K_2O and Rb produces low R^2 values of 0.037 and 0.041, respectively (Fig. 5.1a and b). Na_2O displays a similar weak positive correlation with SiO_2, with a slightly higher R^2 value of 0.099 (Fig. 5.1c), whereas the relatively immobile TiO_2 yields a tightly clustered negative trend, with an R^2 value of 0.521 (Fig. 5.1d).

These findings are very similar to the findings of Hollings et al. (in press) for the intrusive centers of the Baguio district, wherein moderate alteration-driven remobilization of K and other LILE was confirmed. However, Hollings et al. (in press) noted that the majority of HFSEs and major elements remained unaffected, as is the case for the BMSIS samples reported here.

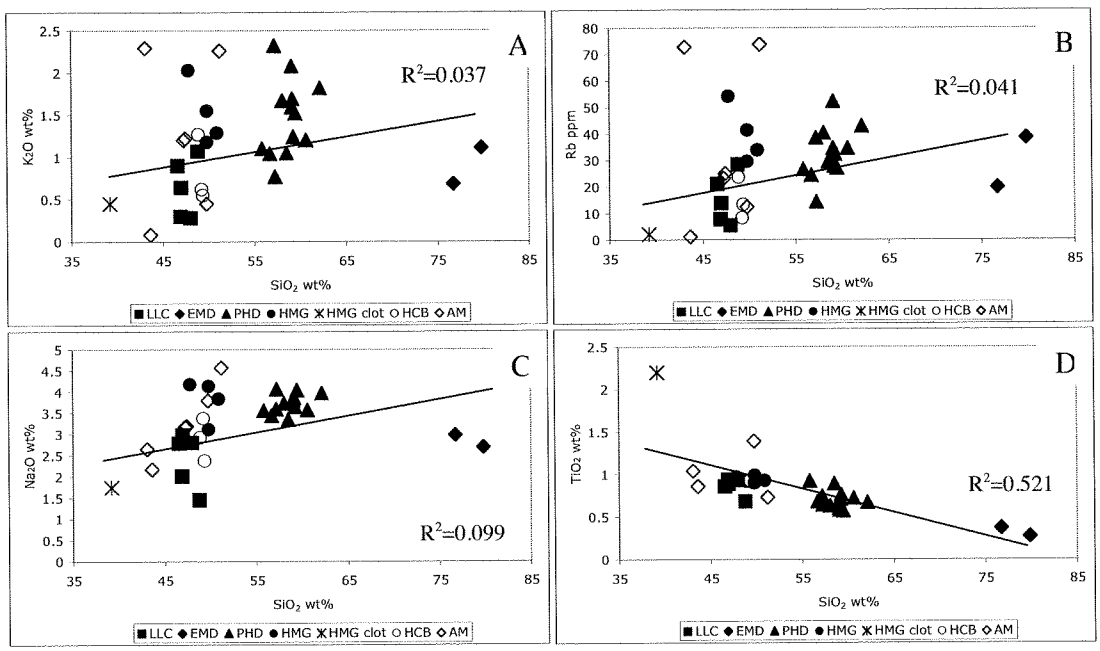

Figure 5.1 - Plots of highly mobile (A) K_2O, (B) Rb, (C) less mobile Na_2O, and (D) immobile TiO_2 versus SiO_2 for the intrusive rocks of the Black Mountain Southeast porphyry system.

5.3.2 Geochemistry of the Black Mountain Southeast Intrusive Suite

The intrusive rocks associated with the BMSIS have low- to high-K calc-alkaline affinities when plotted on a SiO_2 versus K_2O discrimination diagram (Fig. 5.2; Peccerino

and Taylor, 1976), with the majority of the suite plotting in the medium-K field. On a plot of total alkali content ($K_2O + Na_2O$) versus silica (TAS diagram; Fig. 5.3; Rollinson, 1993), the rocks of the Black Mountain Southeast plot as basalt, basaltic andesite and andesite, with broadly low- to medium-K calc-alkaline affinities. A few samples with relatively higher alkali contents plot as tephrite/basanite through trachybasalt to basaltic trachyandesite, with two samples of rhyolitic composition.

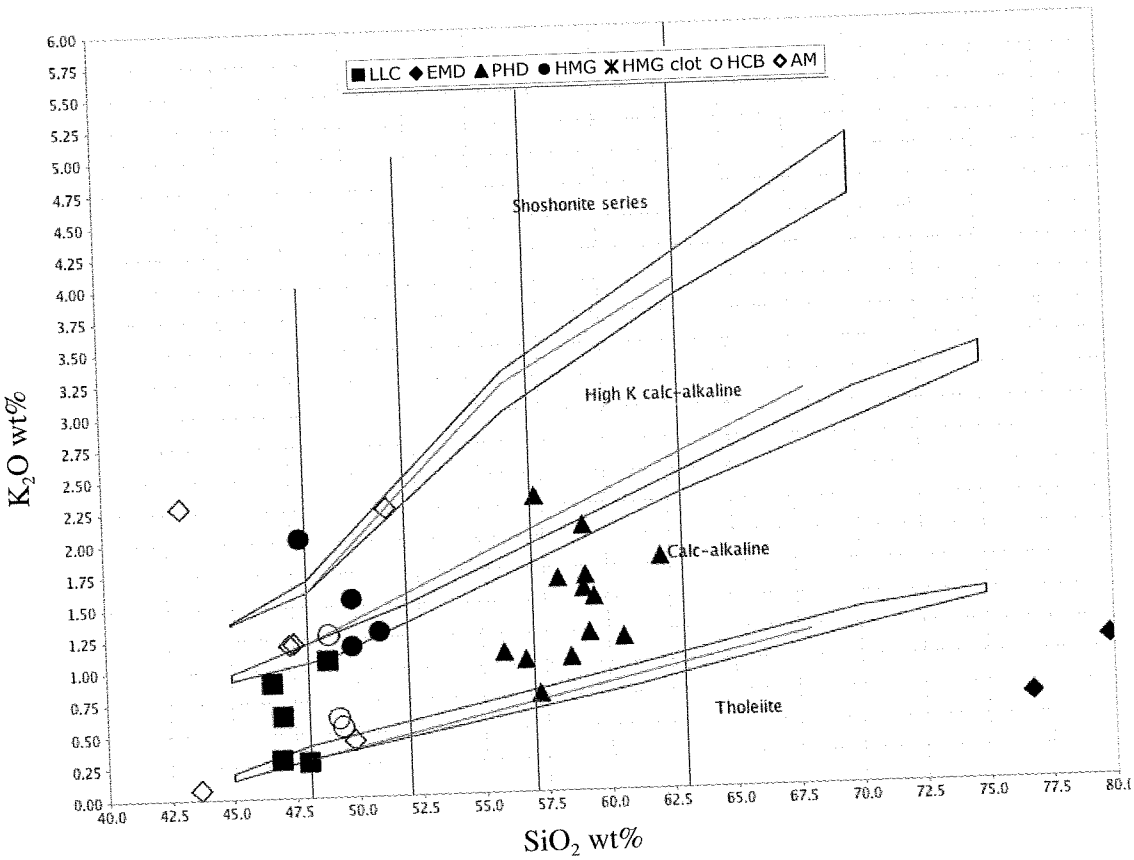

Figure 5.2 - Affinity classification for the Black Mountain Southeast Intrusive Suite, fields after Peccerillo and Taylor (1976).

The previously defined remobilization of K calls into question the reliability of the TAS and SiO_2 vs. K_2O methods for determining rock type and affinity (e.g., Hollings et al., in press). Crawford et al. (2007) proposed that this issue could be addressed by constructing a diagram of K_2O/Al_2O_3 versus P_2O_5/Al_2O_3. Plotted on the Al_2O_5-normalized discriminator diagram (Fig. 5.4), the Black Mountain Southeast intrusive suite has a low- to high-K affinity, with the majority of the samples reflecting a low- to medium-K

compositions. This is consistent with the affinities determined from Figure 5.2, with the majority of the samples plotting as medium-K calc-alkaline rocks on both diagrams. The slight disparity between the low- to medium-K affinities indicated in Figure 5.2 and Figure 5.3, and distinctly medium-K affinities in Figure 5.4 likely stems from a slight K-enrichment. Specifically, if remobilization of potassium during alteration was manifested as an overall enrichment in the sample suite, relying solely on raw K_2O values to determine rock type and affinity would readily reflect this enrichment, as seen in Figure 5.2. These observations confirm that despite apparent LILE remobilization during hydrothermal alteration (highlighted by a slight K-enrichment), other major element concentrations have remained largely unaffected, and the Peccerillo and Taylor (1976) and Robinson (1993) diagrams can be used to accurately classify the rock type and affinity of this sample suite.

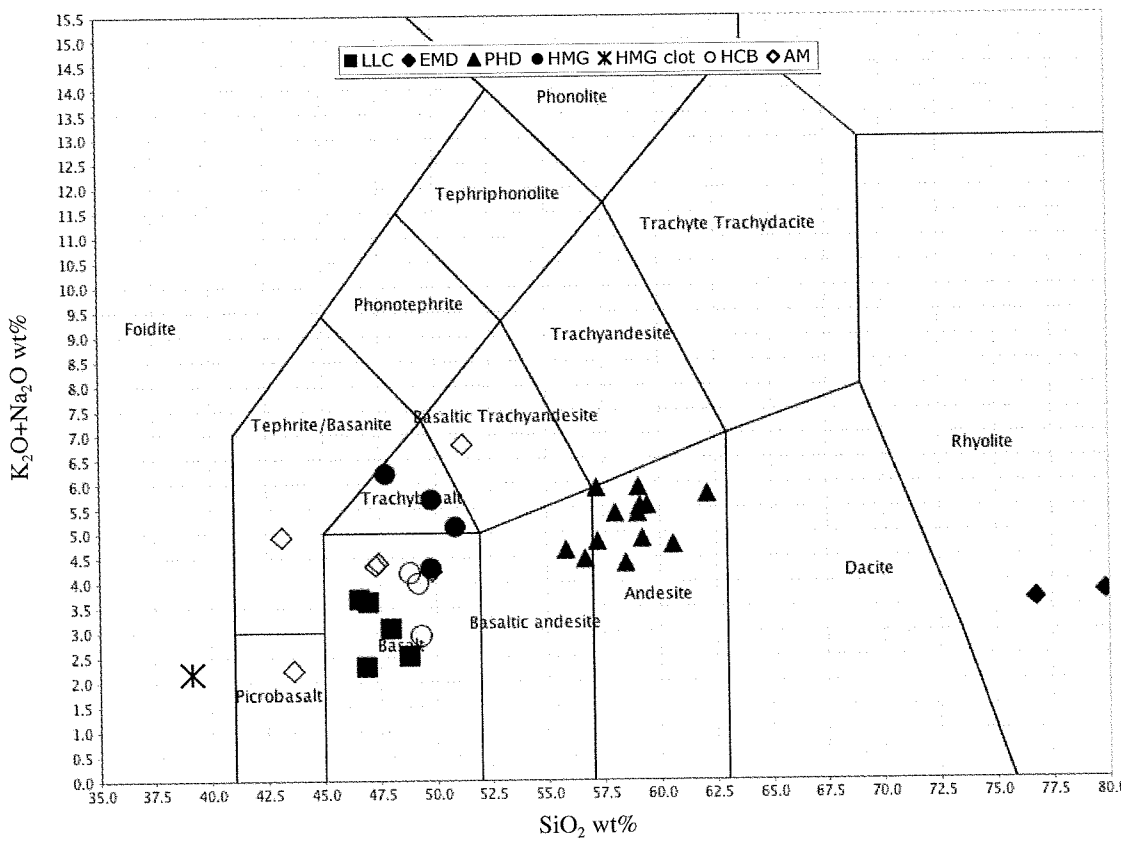

Figure 5.3 - Total Alkali-Silica diagram for the Black Mountain Southeast Intrusive Suite, after Robinson (1993).

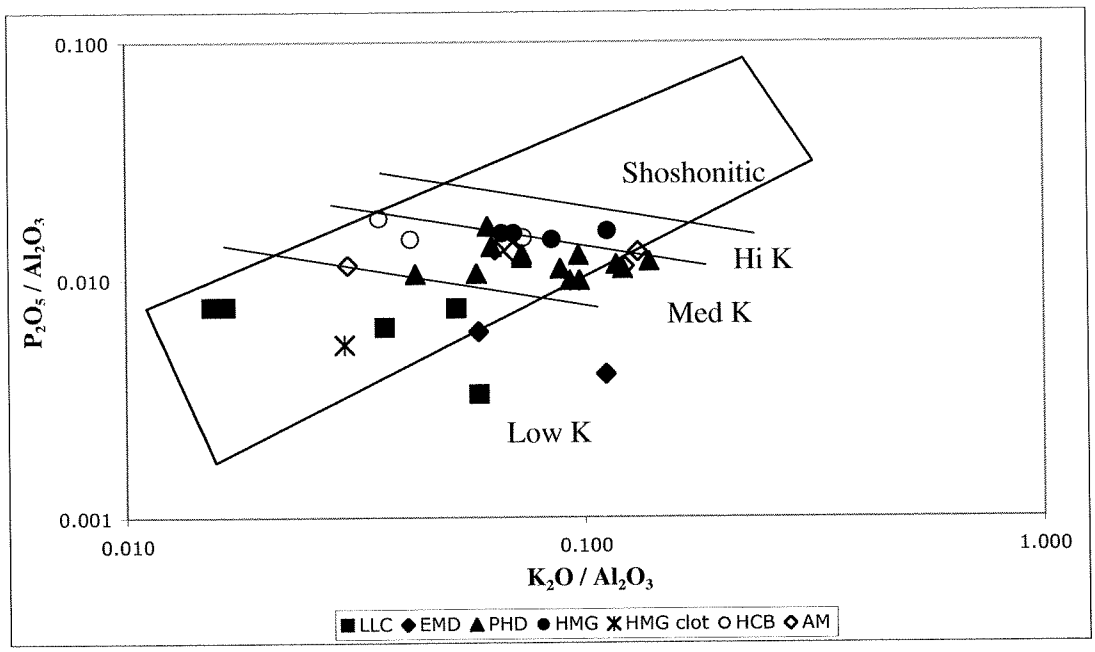

Figure 5.4 - Al-oxide normalized discriminator diagram, after Crawford et al. (2007).

Major element geochemical trends for the Black Mountain Intrusive Suite are readily discernable in Figure 5.5. Most of the major element oxides decrease with increasing SiO_2 content, with the exceptions of Na_2O and Al_2O_3. The major element oxides CaO, TiO_2 and Fe_2O_3 exhibit the most tightly clustered negative correlation with SiO_2, suggesting compatible behavior within the Black Mountain Southeast magmatic system (Fig. 5.5). It is important to note that the terms "compatible" and "incompatible" are used to describe Harker trends and do not imply liquid lines of descent. Element oxide Al_2O_3 and to some extent MgO, exhibit the same negative trends above a minimum SiO_2 content of 52.5% (Fig. 5.5; Appendix 2.1), corresponding with the SiO_2 wt% division between the PHD and HMG intrusive suites. Below this SiO_2 cutoff, the correlation is less obvious. For Al_2O_3, the scatter is represented by an overall decrease in value, as the maximum value of these elements (within the HCB and AM intrusive units) is less than that of the preceding HMG (Fig. 5.5; Appendix 2.1). Na_2O (Fig. 5.5f) displays a weak positive correlation with SiO_2, demonstrating incompatible behavior within the BMSIS (Fig. 5.5f).

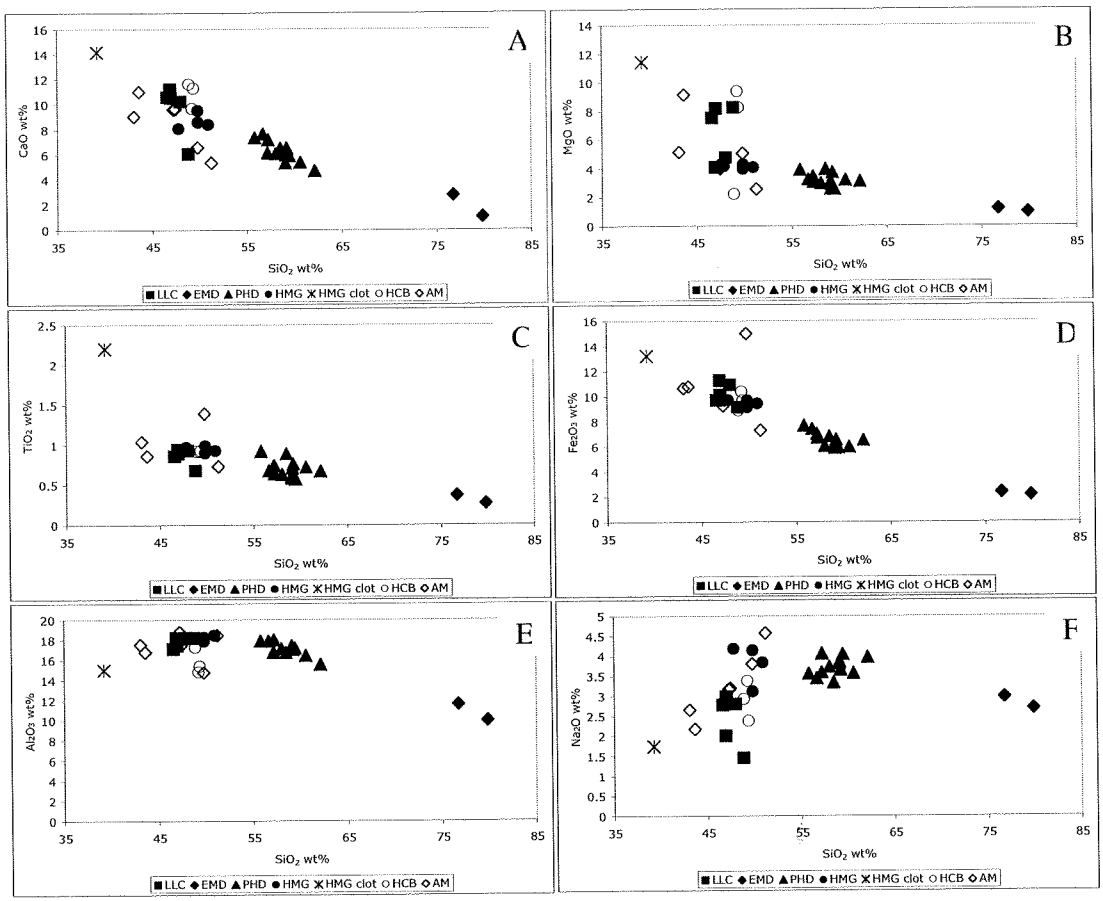

Figure 5.5 - Major element oxides plotted against SiO_2; (A) CaO vs. SiO_2, (B) MgO vs. SiO_2, (C) TiO_2 vs. SiO_2, (D) Fe_2O_3 vs. SiO_2, (E) Al_2O_3 vs. SiO_2, (F) Na_2O vs. SiO_2.

Light Rare Earth Element (LREE) enrichment and HFSE depletion characterize most of the identified intrusive phases (Fig. 5.6). However, the EMD rocks, some samples of the Liw-Liw Creek mafic dikes and the AM dikes are distinct from the other intrusive phases. Levels of LREE enrichment range considerably; the majority of samples exhibit chondrite-normalized La/Sm_{cn} values between 2.0 and 4.5 and a propensity towards higher LREE enrichment with higher silica content (Fig. 5.7). The exception to this is the EMD intrusive phase which has the highest silica content of all intrusive phases identified at Black Mountain Southeast (77-80 wt % SiO_2), but very low to unfractionated LREEs (La/Sm_{cn} ranges 1.0 to 1.5; Appendix 2.1). The Liw-Liw Creek and AM dikes also exhibit only weak LREE fractionation, with La/Sm_{cn} values all below 1.75 (Fig. 5.7). The Heavy Rare Earth Elements (HREEs) are mildly enriched on a Primitive Mantle-

normalized spider diagram (Fig. 5.6), indicating minimal fractionation during production of the BMSIS magmas.

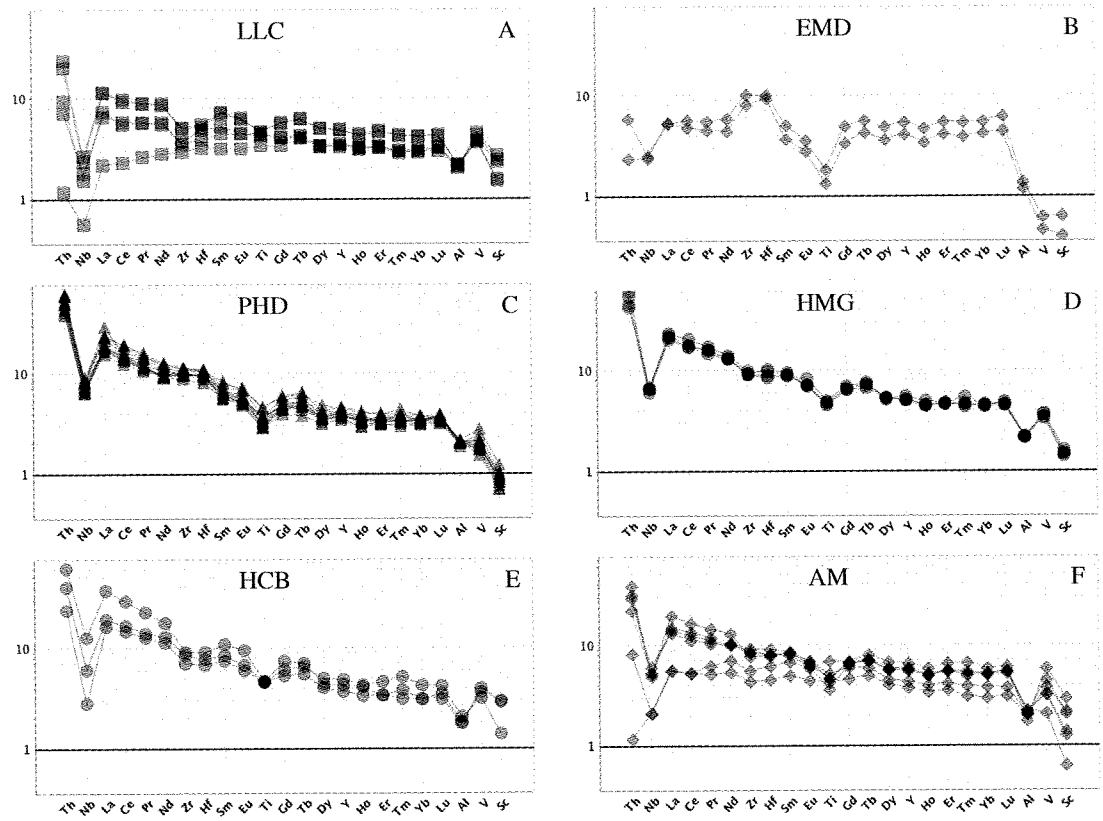

Figure 5.6 - Primitive mantle normalized plots of individual intrusive phases of the Black Mountain Southeast Intrusive Suite. Normalizing values from Sun and McDonough (1989).

Distinct HFSE anomalies are prominent through most of the sample suite (Fig. 5.6) and tend to vary systematically with increasing SiO_2 content, with negative Hf anomaly intensity decreasing, negative Zr and Hf anomalies decreasing and transitioning to positive anomalies, and negative Ti anomalies increasing in intensity. However, the LLC, EMD and AM intrusive rocks again do not follow this trend. Within these three intrusive phases, the intensity of the negative Nb anomaly broadly decreases with increasing SiO_2, and weakly negative Zr and Hf anomalies transition to weakly positive anomalies with increasing silica (Fig. 5.8a-c). EMD rocks exhibit a uniquely strong positive Zr and Hf anomaly with Zr/Zr* values ranging 1.88-2.01 and Hf/Hf* of 1.85-2.33. Negative Ti anomalies increase with higher SiO_2 (Fig. 5.8d), with the exception of some Liw-Liw Creek and AM samples that do not display a Ti anomaly (Ti/Ti* ~1).

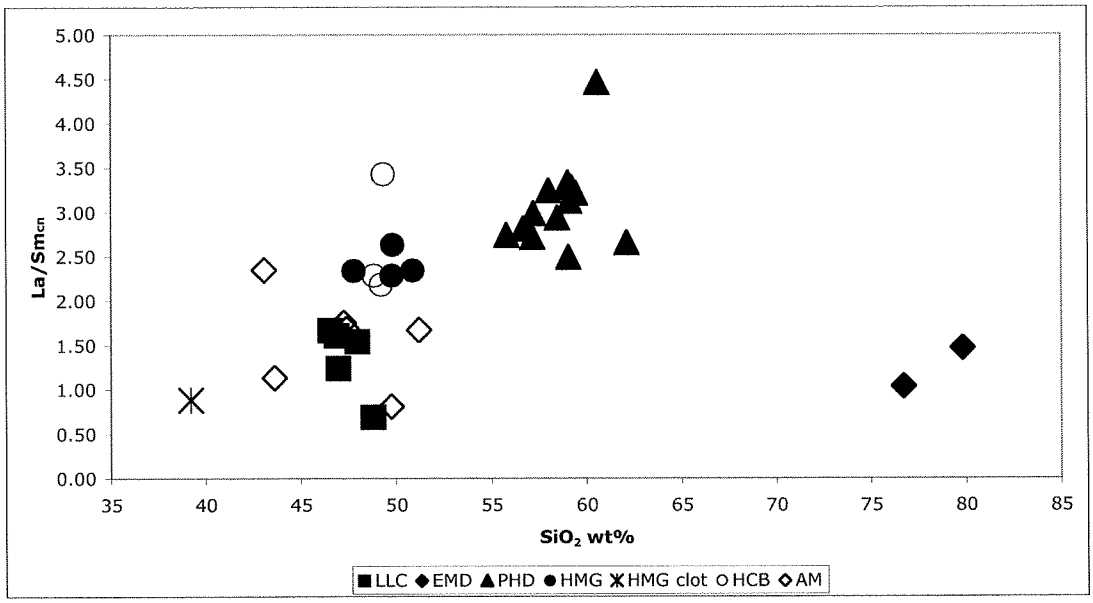

Figure 5.7 - Chondrite-normalized La/Sm_{cn} versus silica oxide for the Black Mountain Southeast Intrusive Suite.

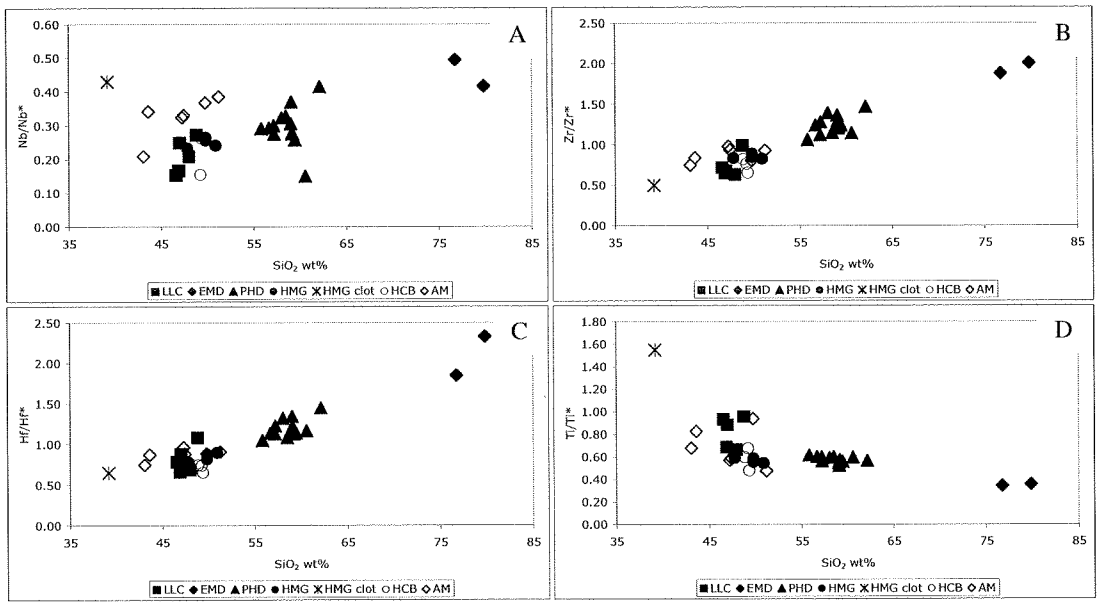

Figure 5.8 - The degree of anomaly for high field strength elements (HFSE) on primitive mantle normalized diagrams (Fig. 5.6) versus silica oxide content. (A) Nb, (B) Zr, (C) Hf, (D) Ti. The Y-axis values are calculated by comparing the logarithmic ratios of elements surrounding each HFSE such that no positive or negative anomaly is equivalent to a value of 1 (e.g., Nb/Nb*=1 means that there is no anomaly). A negative anomaly is indicated by a value of less than 1; a positive anomaly is indicated by a value greater than 1.

Transition elements commonly enriched in mafic magmas show a broad correlation with silica content within the Black Mountain Southeast Intrusive Suite. In particular, V concentrations demonstrate a near-linear negative correlation with SiO_2 (Fig. 5.9d), with maximum values of approximately 500 ppm in the mafic rocks (SiO_2 < 50 wt%) and minimum values below 50 ppm in the most felsic sample (SiO_2 ~ 80 wt%). Cr and Pt behave similarly to V, though the correlation with SiO_2 is not as clear (Fig. 5.9e and f).

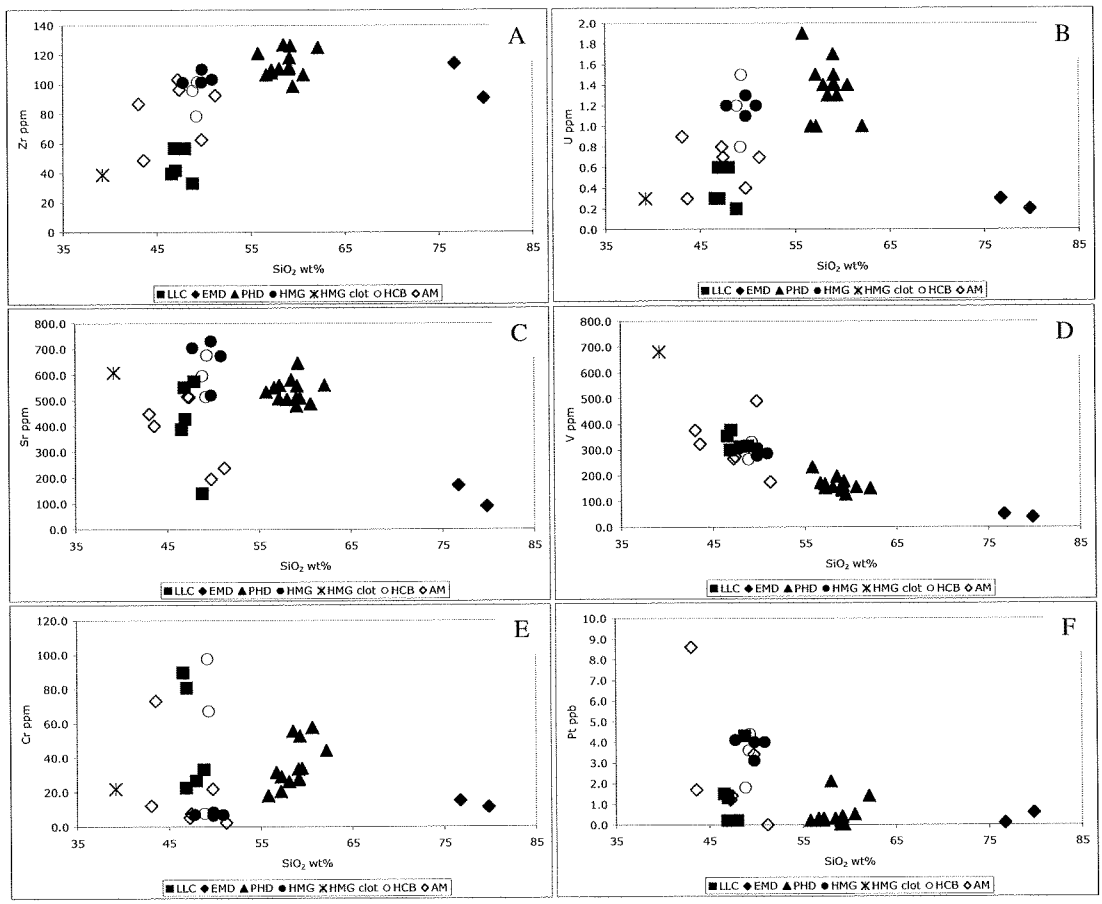

Figure 5.9 - Trace elements behavior with respect to silica oxide in the Black Mountain Southeast Intrusive Suite. (A) Zr vs. SiO_2, (B) U vs. SiO_2, (C) Sr vs. SiO_2, (D) V vs. SiO_2, (E) Cr vs. SiO_2, (F) Pt vs. SiO_2.

5.3.3 Geochemistry of Intrusive Phases

Liw-Liw Creek hornblende megacrystic basalt [LLC]

The hornblende-phyric and megacrystic mafic dikes sampled in Liw-Liw Creek plot as calc-alkaline basalts, confirming the lithological observations discussed in Chapter 3

(Figs. 5.2; 5.3). The LLC dikes represent a mafic end-member for BMSIS sample suite (47-51 wt% SiO_2). High MgO (7.5-8.2 wt%) coupled with low P_2O_5 (0.05-0.13 wt%; Appendix 2.1; Fig. 5.5b) implies a relatively primitive source for the rocks, consistent with the observations of Hollings (2006) and Hollings et al. (in press) for other hornblende-phyric Pliocene dikes from Liw-Liw Creek.

The LLC dikes contain relatively low concentrations of HFSEs and LILEs, with Hf, Zr, U, Th, Sr and Ba values as low or lower than all other intrusive phases present with respect to SiO_2 (Appendix 2.1; Fig. 5.9). For example, Zr contents for the Liw-Liw Creek dikes ranges from 31-42 ppm while the remainder of the BMSIS ranges from 49-127 ppm (Appendix 2.1; Fig. 5.9a). Similarly, Sr concentrations are 136-428 ppm compared to the 195-731 ppm for the remainder of the Black Mountain Southeast Intrusive Suite (Fig. 5.9c). Plots of SiO_2 versus transition elements commonly enriched in mafic magmas (platinum group elements, V and Cr) show some of the highest levels observed for the Black Mountain Southeast rocks (Appendix 2.1). In particular, V, Cr and Pt within the Liw-Liw Creek dikes are clearly elevated with respect to the other intrusive phases (Fig. 5.9d-f). For example, the Liw-Liw Creek intrusives have a V content range of 265-490 ppm while the remaining intrusive phases range 39-376 ppm (Fig. 5.9d).

LREE fractionation is minimal for the Liw-Liw Creek dikes, with La/Sm_{cn} ranging from 0.7-1.7, demonstrated by a relatively flat LREE slope on primitive mantle-normalized spider diagram (Figs. 5.6a and 5.7). Also, a negative Nb anomaly is prominent within the Liw-Liw Creek dikes ($Nb/Nb^* < 0.32$), though other HFSEs (Zr, Hf and Ti) display weak to no negative anomalies (Fig. 5.8b-d).

Early mineralization quartz diorite [EMD]

The EMD contains abundant quartz-rich stock-work veining, is only found at the center of the Black Mountain Southeast ore body and is the host to mineralization. With SiO_2 approaching up to 80 wt%, these samples represent the most felsic end member of the BMSIS. However, it is important to note that the rock type and affinity classification scheme presented in this thesis is of limited value for this intrusive phase (Figs. 5.2; 5.3). The intensity of the quartz stock-work has destroyed the primary mineral assemblage and

textures. As a result, the whole rock geochemistry reflects the elevated silica content and subsequent dilution of all other major elements. Additionally, varying intensity of the quartz stock-work across the outcrops of EMD (Chapter 3) controls the relative silica enrichment and major and trace element depletion. The major element composition of the EMD as plotted in Figure 5.5 likely reflects the effect of silicification, rather than the original composition of the intrusive phase. As noted in Chapter 3, the quartz vein stock-work is truncated by all other intrusive phases within the BMSIS. However, despite the classification complications caused by alteration, the EMD can be considered the first compositional departure from the LLC.

Trace element concentrations within the EMD vary considerably relative to the rest of the Black Mountain Southeast Intrusive Suite. HFSE concentrations tend to be low, with Th, Nb, U and Ta exhibiting ranges that are equal to or below those of the other intrusive phases (Appendix 2.1). For example, Th contents range from 0.2-0.5 ppm, broadly similar to those of the Liw-Liw Creek mafic dikes (0.1-0.8 ppm; Appendix 2.1). However, Hf and Zr values are elevated when compared with the other intrusive phases; Hf values range from 2.9-3.1 ppm and Zr from 91-114 ppm (Appendix 2.1). Figure 5.9a illustrates this relationship along with the rest of the Black Mountain Southeast Intrusive Suite, highlighting the relative Zr enrichment in the EMD samples. LILE concentrations mirror those of the Liw-Liw Creek mafic dikes. Plots of SiO_2 wt% versus Sr (Fig. 5.9c) highlight the depleted LILE content relative to the remainder of the BMSIS. The concentrations of compatible elements V, Cr and Pt are low within the EMD; V concentrations are 39-52 ppm, Cr 11-15 ppm and Pt 0.1-0.6 ppb (Appendix 2.1). This marks a dramatic departure from the high concentrations of the Liw-Liw Creek dikes.

LREE fractionation is minimal for the EMD samples, with little change from the preceding Liw-Liw Creek dikes. The two samples for this intrusive phase record La/Sm_{cn} values of ~1.0 and 1.5 (Fig. 5.7), and display a flat LREE slope in Figure 5.6b. However, the HFSE values differ from the Liw-Liw Creek mafic dikes and distinguish the EMD within the broader Black Mountain Southeast Intrusive Suite. The negative Nb anomaly for EMD is the weakest of all the documented intrusive phases, with Nb/Nb* values between 0.40 and 0.50 (Fig. 5.8a). Zr and Hf display positive anomalies (a unique feature of the EMD) with Zr/Zr* and Hf/Hf* values of 1.9-2.0 and 1.9-2.3, respectively

(Fig. 5.8b and c). Low Ti concentrations are illustrated by the strongest negative Ti anomaly of the Black Mountain Southeast rocks (Fig. 5.8d).

Plagioclase- and variably hornblende-phyric diorite [PHD]

The PHD samples plot as calc-alkaline basaltic andesites to andesites on Figures 5.2 and 5.3, in agreement with their mineralogy-based dioritic designation (Chapter 3). SiO_2 contents range from 55-62 wt% implying a more intermediate composition than the preceding high-silica EMD (Appendix 2.1). Virtually all major elements are enriched in the PHD (Fig. 5.5). For example, MgO ranges from 2.5-5.6 wt%, as compared to 0.96-1.19 wt% in the EMD (Fig. 5.5b).

The PHD is geochemically distinct from the preceding intrusive phase. Trace element changes mirror the aforementioned major element changes, and suggest a significant increase in HFSE, LILE and mafic indicator elements from the preceding intrusive phase. Hf, Zr, U and Th concentrations in the PHD are among the highest for the entire Black Mountain Southeast Intrusive Suite (Appendix 2.1; Fig. 5.9). LILEs behave similarly to the HFSEs, illustrated by high Sr in Figure 5.9c. However, unlike the HFSEs the relative LILE enrichment does not represent the maximum for the BMSIS. Mafic indicator elements increase from the EMD to the PHD, highlighted by the jump in V, Cr and Pt content in Figure 5.9d-f. For example, V content in the EMD (ranging from 39-52 ppm) increases to 127-232 ppm within the PHD.

LREE are enriched and fractionated within the PHD with respect to the preceding intrusive phases, with La/Sm_{cn} ranging from 2.5-4.5 (Fig. 5.7; Fig. 5.6c). As well, a negative Nb anomaly is prominent within the Liw-Liw Creek dikes ($Nb/Nb^* < 0.32$), though other HFSEs (Zr, Hf and Ti) display small to zero negative anomalies (Fig. 5.8b-d).

Hornblende megacrystic and "clotted" gabbro [HMG]

The HMG dikes of the Black Mountain Southeast Intrusive Suite plot as calc-alkaline to shoshonitic basalts and trachybasalts on Figures 5.2 and 5.3, consistent with their compositional designation in Chapter 3. Relative to the preceding PHD intrusive phase,

SiO_2 wt % (48-51%) is lower than the PHD, whereas MgO, Al_2O_3 and Na_2O values are roughly equivalent between the two (Appendix 2.1; Fig. 5.5).

The HMG samples are characterized by an increase in some mafic indicator elements and a slight increase in LILE relative to the preceding PHD. HFSE concentrations are somewhat lower than the PHD rocks, demonstrated by both a drop in maximum values and a narrower range (e.g., Zr 101-110 ppm; Fig. 5.9a). This decrease is also apparent for U (Fig. 5.9b). LILE concentrations increase slightly (e.g., Sr; Fig. 5.9c) or remain the same as the PHD (e.g., Ba; Appendix 2.1). The mafic indicator elements V and Pt are elevated within the HMG; V content rises from 127-232 ppm in the preceding PHD, to 227-307 ppm (Appendix 2.1; Fig. 5.9d and f). However, Cr contents drop considerably between the PHD and the HMG from a range of 18-125 ppm to 6.5-8.5 ppm, respectively (Appendix 2.1; Fig. 5.9e).

The HMG is less LREE enriched than the preceding PHD, falling to a lower (but still enriched) range of La/Sm_{cn} values between 2.3 and 2.6 (Figs. 5.6d, 5.7). As well, the negative Nb anomaly noted for the preceding intrusive phase is stronger for the HMG samples, with Nb/Nb* values between 0.23-0.27 (Fig. 5.8a). Zr and Hf anomalies are absent or slightly negative (Zr/Zr* of 0.83-0.89; Hf/Hf* of 0.78-0.90), marking a reduction in Zr and Hf from the PHD (Fig. 5.8b and c). A prominent negative Ti anomaly is present and is similar to the PHD (Ti/Ti* of 0.55-0.90; Fig. 5.8d).

Hornblende "clotted" basalt [HCB]

The hornblende-phyric and clotted basaltic rocks of the HCB plot as calc-alkaline basalts on Figures 5.2 and 5.3, in agreement with their mineralogical designation in Chapter 3. The HCB samples are more mafic than the preceding HMG (SiO_2 46.89-49.21 wt%; Appendix 2.1). The total alkali content is lower than the HMG samples (Na_2O+K_2O 2.9-4.2 wt%; Appendix 2.1; Fig. 5.3), and MgO increased to between 2.2-9.4 wt% from the HMG (Appendix 2.1; Fig. 5.5b).

The HCB samples are characterized by an overall drop in HFSE and LILE content relative to the preceding intrusive phase, while mafic indicator elements are more variable. The range in HFSE values drops slightly in HCB, continuing the trend noted for the PHD and the HMG intrusive phases (Appendix 2.1). LILE values are also lower

(Appendix 2.1). Mafic indicator elements vary considerably, with Cr increasing (8-98 ppm; Fig. 5.9e), V remaining equivalent (263-331 ppm; Fig. 5.9d), and Pt decreasing (1.8-4.4 ppb; Fig. 5.9f) with respect to the preceding intrusive phase.

Enrichment of LREE in the HCB is similar to that of the preceding phase, indicated by La/Sm_{cn} values between 2.2-3.4 (Figs. 5.6e; 5.7). HFSE anomalies are similar in intensity to those of the HMG, with a strongly negative Nb anomaly (Nb/Nb* of 0.15-0.27; Fig. 5.8a), a moderate negative Ti anomaly (Ti/Ti* of 0.48-0.68; Fig. 5.8d), and weak negative Zr and Hf anomalies (Zr/Zr* of 0.65 – 0.82; Hf/Hf* of 0.65 – 0.75; Fig. 5.8b and c).

Aphanitic to plagioclase microphenocrystic mafics dikes [AM]

The geochemical composition of the plagioclase microphenocrystic and aphanitic mafic dikes mapped in the Black Mountain Southeast Intrusive Suite vary considerably, ranging from calc-alkaline picrobasalt through calc-alkaline and high K calc-alkaline basalts, to borderline shoshonitic basaltic trachyandesite and tephrite/basanite (Figs. 5.2, 5.3). Due to the spread in major element concentrations in the AM rocks, there is considerable overlap with the Liw-Liw Creek mafic dikes and the HMG and HCB intrusive phases (Fig. 5.5a-f).

Trace element behavior is broadly consistent with that of the Liw-Liw Creek mafic dikes, with the exception of Zr and Hf values that overlap with HCB (Fig. 5.9; Appendix 2.1). Generally, LILE and mafic indicator elements have the same range as the Liw-Liw Creek dikes, with lower LILE values and high mafic indicator element concentrations relative to the majority of the BMSIS (Fig. 5.9c-f).

The AM samples are less LREE enriched than the preceding intrusive phases (La/Sm_{cn} 0.81-1.75; Fig. 5.6f), with primitive mantle-normalized spider plots broadly resembling those of the Liw-Liw Creek dikes (Fig. 5.6a). As well, negative HFSE anomalies are similar to the Liw-Liw Creek samples, with Zr, Hf and Ti all exhibiting moderate-to-weak negative anomalies (Fig. 5.8b-d).

5.4 Isotope Geochemistry

Sixteen samples from the Black Mountain Southeast area were analyzed for their Rb-Sr and Sm-Nd isotopic character at Carleton University, Ottowa, Ontario. Methodology for this work can be found in Appendix 1.4. The sample suite includes representative samples of all intrusive phases identified in the field (Chapter 3): two samples of the Liw-Liw Creek mafic dikes, one sample of EMD, five samples of PHD, two samples of HMG, one sample of HCB, three samples of AM, one sample of a hornblende clot from the HMG, and one sample of a hornblende-plagioclase clot from HCB. A compilation of the new data and previously reported radiogenic isotope data sets for Baguio's Pliocene intrusives is presented in Table 5.1. Hollings (2006) reported data for 11 samples of Miocene and Pliocene intrusive rocks, three of which are located within the greater Black Mountain Intrusive Complex and are incorporated herein: two are Liw-Liw Creek mafic dikes, and one is a Mexico diorite. A compilation of radiogenic isotope data for Miocene and Pliocene rocks by Polve et al. (2007) contains four samples of Pliocene Baguio district intrusives: one sample of Itogon dacite, two samples of Agoo Basalt (Sajona, 1995) and one sample of diorite collected from Kennon Road (Margoum, 2002).

The Black Mountain Southeast rocks lie along the mantle array of Zindler and Hart (2006), with a few samples of EMD and HMG deviating towards higher $^{87}Sr/^{86}Sr$ and/or higher $^{143}Nd/^{144}Nd$ values (Fig. 5.10). The $^{87}Sr/^{86}Sr$ range for the new Black Mountain Southeast data set is 0.70362-0.70423 (Table 5.1), and is within the range reported for the Philippines by McDermott and Hawkesworth (1991) of 0.70356-0.70476. However, it exceeds the range reported by Hollings (2006) of 0.70366-0.70388 and is higher than the reported range for Pacific MORB (0.70240-0.70256; Saunders et al., 1988). The $^{143}Nd/^{144}Nd$ range for the new data is 0.51290-0.51305 (Table 5.1), overlapping and exceeding the range of 0.51287-0.51298 reported by Hollings (2006), and falling approximately within the range 0.5130-0.5133 defined for Pacific MORB (Saunders et al., 1988).

Sample	Locality	Relative Age	Assigned Age (Ma)	Intrusive Phase Association	$^{143}Nd/^{144}Nd$ Initial	$^{87}Sr/^{86}Sr$ Initial	Eps Nd Present	Eps Sr Present	Eps Nd (CHUR) t	Source
354506A	BMP SE	Pliocene	3.14	diorite	0.51296	0.70369	6.36	-11.31	6.39	Hollings (2006)
354553A	Mexico	Pliocene	3.14	Mexico Diorite	0.51295	0.70410	6.14	-5.56	6.17	Hollings (2006)
BA08GS003	BMP SE	Pliocene	2.79	AM	0.51300	0.70384	7.12	-9.41	7.13	This study
BA08GS015	BMP SE	Pliocene	2.79	AM	0.51296	0.70403	6.33	-6.14	6.34	This study
BA08GS022	BMP SE	Pliocene	2.81	AM	0.51298	0.70379	6.80	-9.85	6.82	This study
BA08GS001	BMP SE	Pliocene	3.10	EMD	0.51305	0.70416	8.09	-4.13	8.10	This study
BA08GS047	Liw-Liw	Pliocene	2.83	HCB	0.51297	0.70372	6.49	-11.10	6.51	This study
BA08GS047c	Liw-Liw	Pliocene	2.83	HCB clot	0.51295	0.70367	6.23	-11.66	6.23	This study
BA08GS004	BMP SE	Pliocene	2.86	HMG	0.51297	0.70376	6.57	-10.43	6.59	This study
BA08GS011	BMP SE	Pliocene	2.86	HMG	0.51296	0.70423	6.36	-3.68	6.38	This study
BA08GS009	BMP SE	Pliocene	2.81	HMG clot	0.51296	0.70383	6.40	-9.55	6.40	This study
BA08GS005	BMP SE	Pliocene	2.90	PHD	0.51294	0.70374	5.93	-10.74	5.95	This study
BA08GS006	BMP SE	Pliocene	2.90	PHD	0.51296	0.70370	6.26	-11.32	6.28	This study
BA08GS013	BMP SE	Pliocene	2.91	PHD	0.51296	0.70362	6.34	-12.43	6.36	This study
BA08GS019	BMP SE	Pliocene	2.90	PHD	0.51296	0.70369	6.39	-11.36	6.41	This study
BA08GS040	BMP SE	Pliocene	2.87	PHD	0.51296	0.70380	6.38	-9.77	6.40	This study
353229A	Liw-Liw	Pliocene	4.00	LLC	0.51294	0.70364	6.03	-12.11	6.05	Hollings (2006)
354194A	Liw-Liw	Pliocene	4.50	LLC	0.51296	0.70358	6.34	-13.06	6.34	Hollings (2006)
BA08GS035	Liw-Liw	Pliocene	4.00	LLC	0.51290	0.70391	5.22	-8.41	5.23	This study
BA08GS057	Liw-Liw	Pliocene	4.73	LLC	0.51293	0.70374	5.81	-10.63	5.82	This study
353249	Tuba	Pliocene	3.66	basalt	0.51298	0.70377	6.81	-10.35	6.84	Hollings (2006)
PH01-08	Kennon Rd Diorite	Pliocene	1.70	diorite	0.51294	0.70402				Margoum (2002)
PH00-221	Itogon Dacite	Pliocene	0.97	dacite	0.51294	0.703852				Polve et al. (2007)
A38	Agoo	Pliocene	2.82	basalt	0.51295	0.703788				Sajona (1995)
A47	Agoo	Pliocene	2.89	basalt	0.51294	0.703774				Sajona (1995)

Table 5.1 - Nd and Sr isotopic data for Pliocene intrusive rocks of the Baguio mineral district compiled from Sajona (1995), Margoum (2002), Hollings (2006), Polve et al. (2007) and this study.

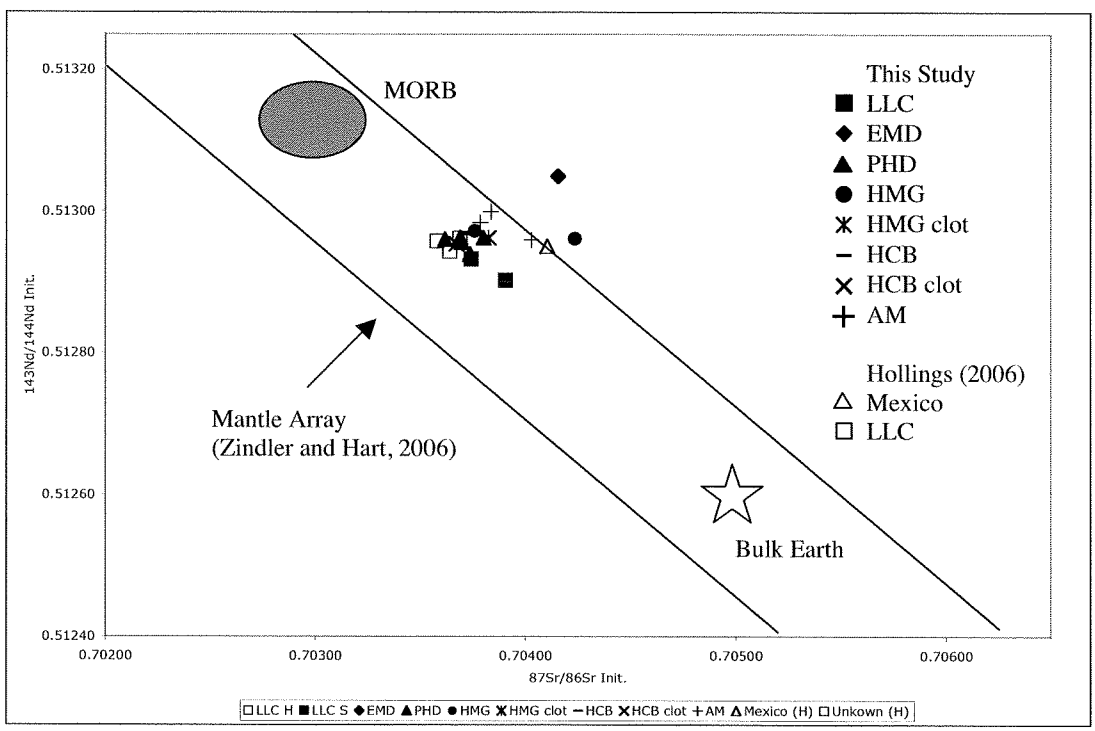

Figure 5.10 - Pliocene Nd and Sr isotopic data compiled from Hollings (2006) and this study. Mid ocean ridge basalt and bulk earth compositions shown for reference within the mantle array of Zindler and Hart (2006).

5.5 Discussion

Previous geochemical studies of the Baguio district have for the most part limited their resolution to the district scale. The geochemical variability of the successive magmatic centers documented in these studies has been used to observe large-scale shifts in tectonics and magmatism (e.g., Waters and Gonzales, 2005; Waters et al., 2005; Hollings, 2006; Hollings et al., in press). However, there has been little effort to discern temporal variations in geochemistry within individual deposits. The Black Mountain Southeast's unique setting with respect to the Baguio district's Pliocene magmatism and the recognition of a definitive temporal progression of intrusive rocks within the Black Mountain Southeast makes it possible to investigate the geochemical evolution of this porphyry system and by analogy, the Baguio mineral district as a whole.

5.5.1 The Black Mountain Porphyry Southeast System within the Context of the Baguio mineral district

Previous petrological studies of the Baguio mineral district (Defant et al., 1989; Yumul et al., 1995; Sajona et al., 1999; Waters and Gonzales, 2005; Hollings, 2006; Polve et al., 2007; Hollings et al., in press) have established an informal geochemical context for the evolution of Pliocene magma generation. This is marked by a cessation of voluminous magmatism between 17 Ma and 5 Ma that has effectively subdivided the igneous members of the Baguio district into a Miocene group and a Pliocene group. However, some authors (e.g., Polve et al., 2007) have noted volcanic activity during the Middle-Late Miocene (e.g., the ~8 Ma Monglo Adakite). Whole rock geochemical data and radiogenic isotope data for the Baguio mineral district's Pliocene intrusive centers (from Hollings, 2006 and Hollings et al., in press; Appendix 2.2) is used to supplement geochemical data from the Black Mountain Southeast.

Hollings (2006) and Hollings et al. (in press) noted that the Pliocene intrusive rocks record an increasingly evolved geochemical character over time, marked by a gradual increase in La/Sm_{cn} values with SiO_2 content, a decrease in mafic-associated elements (e.g., MgO and V), and an increase in $^{87}Sr/^{86}Sr$ (accompanied by initially high radiogenic Nd). They proposed that the early Pliocene mafic dike swarms (the Mafic Dike Complex and the Liw-Liw Creek dikes) represented a primitive, mantle-derived

parental magma that was directly related to slab melting associated with the subduction of the Scarborough Ridge beneath northern Luzon. Upon generation of this melt, Hollings (2006) further proposed that multiple mechanisms (pooling and fractional crystallization within the crust, crustal contamination and interaction with adakitic and slab sediment-derived melts) would have lead to the evolution of the fertile calc-alkaline intermediate magmatic suites associated with mineralization. By establishing the temporal and geochemical evolution of the Black Mountain Southeast Intrusive Suite within the context of the Baguio mineral district's evolving Pliocene magmatism, the geochemical data set presented in this thesis can be used to examine a more detailed interval of the early evolution of Pliocene magmatism from primitive mafic towards intermediate/felsic.

The Black Mountain Southeast Intrusive Suite (and the rest of the BMIC) represents the first voluminous intermediate magmatic event of the Pliocene within the Baguio mineral district, and is preceded by the primitive Liw-Liw Creek dikes and Mafic Dike Complex (Chapter 2). With respect to rock type and affinity, Defant et al. (1989), Hollings (2006), Polve et al., (2007) and Hollings et al. (in press) noted that the Baguio mineral district's Pliocene intrusive rocks have low- to medium-K calc-alkaline compositions. In this context, the low- to medium K calc-alkaline rocks of the BMSIS are consistent with the majority of the Baguio district (Figs. 5.11 and 5.12). Consistent with the observations of increasingly felsic magmatism during the Pliocene, the Black Mountain Southeast rocks are more mafic than the younger intrusive centers (e.g., the Santo Tomas II – Clifton – Bumolo Complex and the Ampucao – Hartwell - Balatoc Complex; Balce, 1979; Hollings and Cooke, 2005; Waters and Gonzales, 2005; Hollings, 2006; Waters et al., in press). This is clearly illustrated by lower bulk SiO_2 and higher MgO and V contents in the BMIC, despite some overlap with the younger intrusive centers (Figure 5.13a and b).

The major and trace element characteristics of the Black Mountain Southeast Intrusive Suite are broadly consistent with a supra-subduction zone setting and a sub-arc mantle magmatic source, as previously noted for the Baguio district's Miocene and Pliocene intrusives (Yumul et al., 1995; Waters and Gonzales, 2005; Hollings, 2006; Hollings et al., in press). Primitive-mantle normalized negative Nb, Zr, Hf and Ti

Figure 5.11 - Affinity classification for the Pliocene intrusive centers of the greater Baguio mineral district (after Peccerino and Taylor, 1976). Data displayed is a compilation of that reported by Hollings (2006) and Hollings (in press) and this study. The whole rock geochemical data reported by Hollings (2006; in press) can be found in Appendix 2.2. Whole rock data from this study can be found in Appendix 2.1.

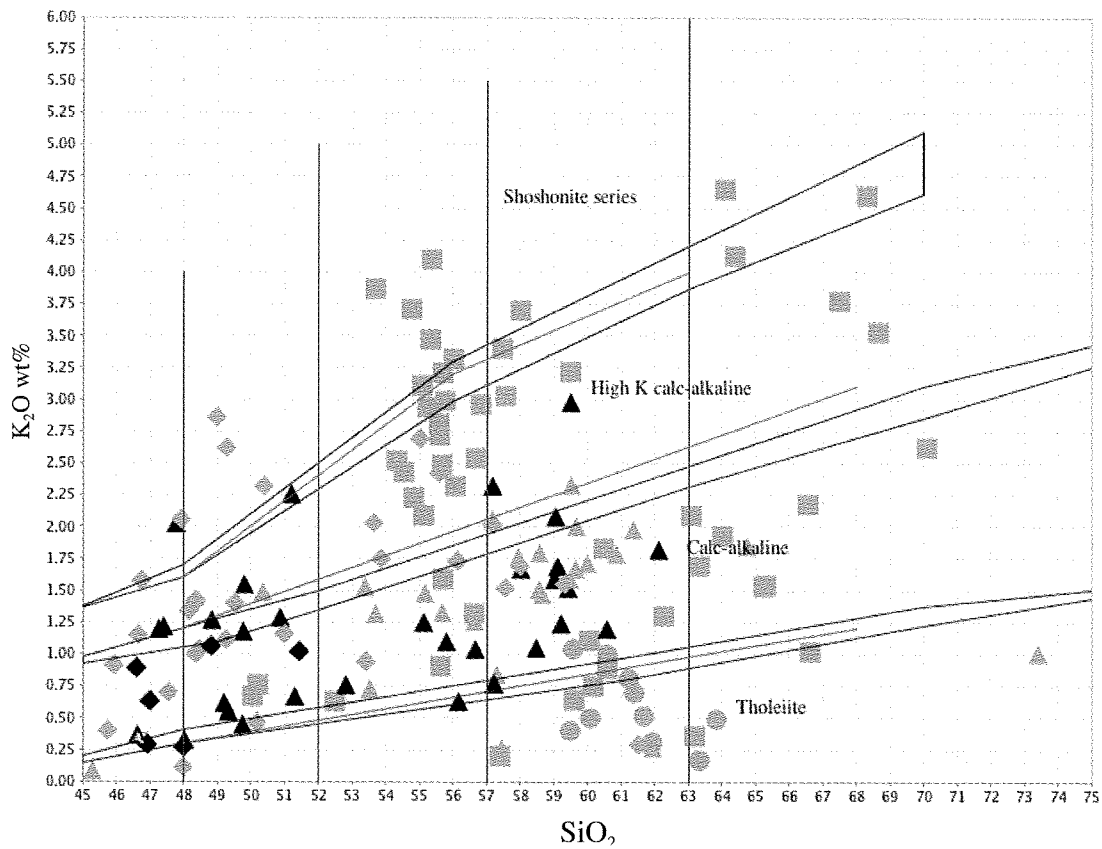

Figure 5.12 - Total alkali-silica classification for the Pliocene intrusive centers of the greater Baguio mineral district (after Robinson, 1993). Data displayed is a compilation of that reported by Hollings (2006) and Hollings (in press) and this study. The whole rock geochemical data reported by Hollings (2006; in press) can be found in Appendix 2.2. Whole rock data from this study can be found in Appendix 2.1.

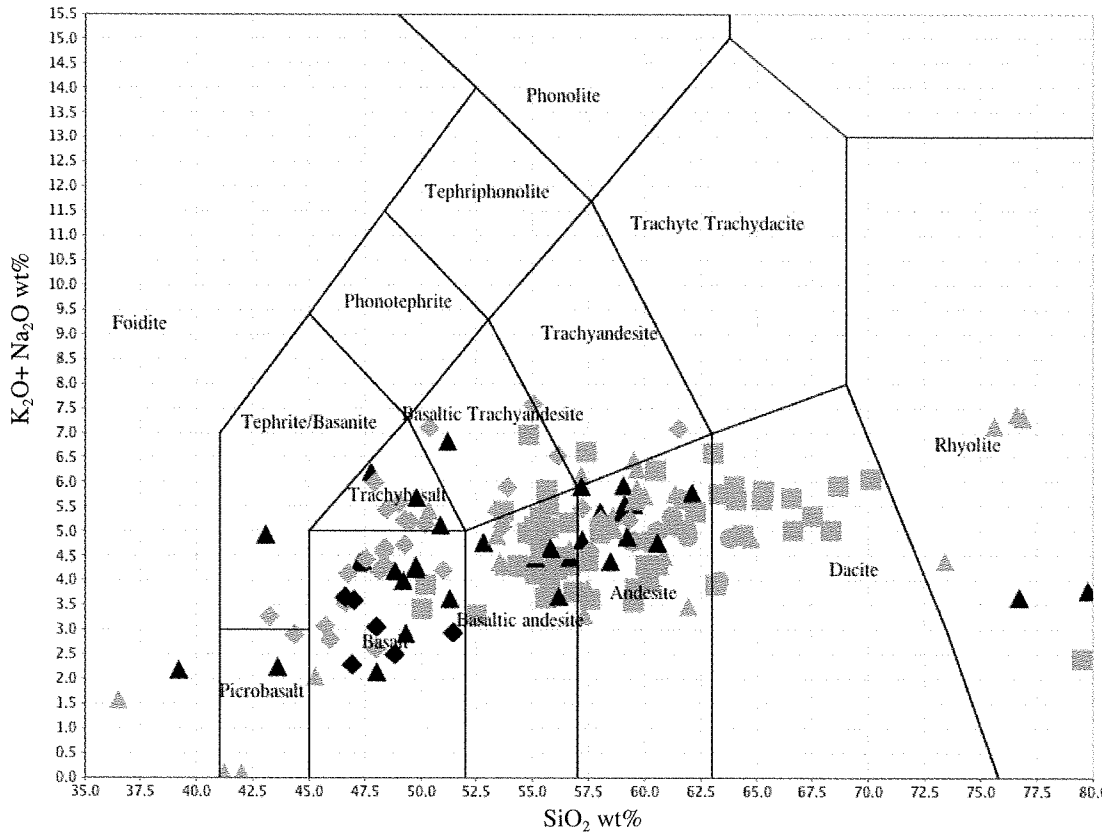

Intrusive Center
- ■ Ampucao - Hartwell - Balatoc (Antomok)
- ● Santo Tomas II - Clifton - Bumolo
- ▲ Black Mountain Intrusive Complex
- ◆ Mafic Dike - Liw-Liw Creek - Camp 4

Source
- ■ Hollings (2006)
- ■ This study

Figure 5.13 - (A) MgO vs. silica oxide, and (B) V vs. silica oxide for the Pliocene intrusive centers of the Baguio mineral district. Data displayed is a compilation of that reported by Hollings (2006) and Hollings (in press) and this study. The whole rock geochemical data reported by Hollings (2006; in press) can be found in Appendix 2.2. Whole rock data from this study can be found in Appendix 2.1.

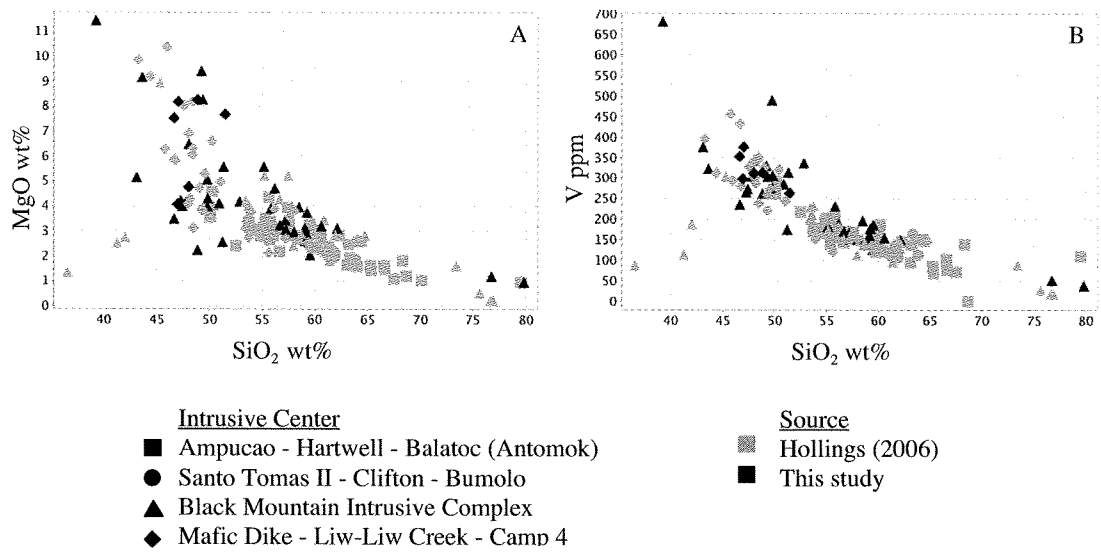

anomalies (Figs. 5.6 and 5.8a-d) and LREE enrichment (Figs. 5.6 and 5.7) in the Black Mountain Southeast rocks are characteristic of a sub-arc mantle source (Kay and Mpodozis, 2002; Hollings, 2006) and have been previously recognized throughout the Baguio district (Yumul et al., 1995: Sajona et al., 1999; Waters and Gonzales, 2005: Hollings, 2006; Hollings et al., in press). Relatively flat, unfractionated primitive mantle-normalized HREE patterns suggest magma derivation from a source above the garnet stability field (Fig. 5.6). This is consistent with the observations of Hollings (2006) and Hollings et al. (in press) for Pliocene intrusive centers throughout the Baguio district, and with local crustal thickness estimates of ~27.5±1.5 km (Dimalanta and Yumul, 2003).

The Liw-Liw Creek dikes analyzed in this study broadly conform to the model proposed by Hollings (2006) in that they appear geochemically primitive and plot as low-K calc-alkaline basalts (Figs. 5.2, 5.3 and 5.4) with minimal LREE enrichment (La/Sm_{cn} < 1.75; Fig. 5.7), and weak negative HFSE anomalies (Fig. 5.8a-d). The dikes are geochemically similar to the more mafic phases of the remainder of the Black Mountain Southeast Intrusive Suite (e.g., samples of the AM intrusive phase). Concentrations of MgO, V and Pt overlap with the more mafic intrusive phases of the BMSIS (AM, and to

a lesser extent HMG and HCB; Fig. 5.9). These observations, in conjunction with broadly similar PM-normalized spider diagrams (Fig. 5.6a and f) imply a similar source for the primitive Liw-Liw Creek dikes and the rest of the Black Mountain Southeast Intrusive Suite, and support Hollings (2006) and Hollings et al. (in press) suggestion that the BMIC may be an evolutionary product of the Liw-Liw Creek dike magmas.

Nd and Sr radiogenic isotope ranges for the Black Mountain Southeast Intrusive Suite are broadly consistent with the temporal geochemical model highlighted above, but suggest the involvement of additional magma sources. The Liw-Liw Creek mafic dikes exhibit the lowest overall $^{87}Sr/^{86}Sr$ values, concurrent with their proposed uncontaminated, mantle-derived origins (Hollings, 2006; Fig. 5.10). However, the $^{143}Nd/^{144}Nd$ values of the Liw-Liw Creek dikes plot in the middle- to lower part of the field defined by the compiled Baguio district's Pliocene data, and are lower than the $^{143}Nd/^{144}Nd$ range of the younger Black Mountain Southeast intrusive phases (Fig. 5.10). Isotope data from this study combined with the supplementary data (Sajona, 1995; Margoum, 2002; Hollings, 2006; Polve et al., 2007; Table 5.1), displays a broad decrease in maximum $^{143}Nd/^{144}Nd$ during Pliocene magmatism, but a spike to higher values in the Black Mountain Southeast rocks (particularly for the emplacement of EMD; Fig. 5.14a). If the Liw-Liw Creek and Mafic Complex dikes represent a parental magma source, then the presence of elevated radiogenic Nd in the Black Mountain Southeast rocks is suggestive of the involvement of another primitive magma. Similarly, a spike in $^{87}Sr/^{86}Sr$ within the EMD and HMG (Fig. 5.14b) implies an increased role of an evolved contaminant during the emplacement of the Black Mountain Southeast Intrusive Suite. A similar divergence of isotopic data for the Baguio district's Miocene rocks was observed by Hollings (2006) and was taken to indicate decoupling of the two isotopic systems. In a temporal sense, the isotopic divergence noted by Hollings (2006) is concurrent with the transition from generation of the Liw-Liw Creek and Mafic Dike complex magmas to the generation of the Black Mountain Southeast Intrusive Suite magmas, and may therefore be explored further by examining the geochemical and isotopic data collected for this study through the high-resolution timing relationships within the BMSIS (Chapters 3 and 4).

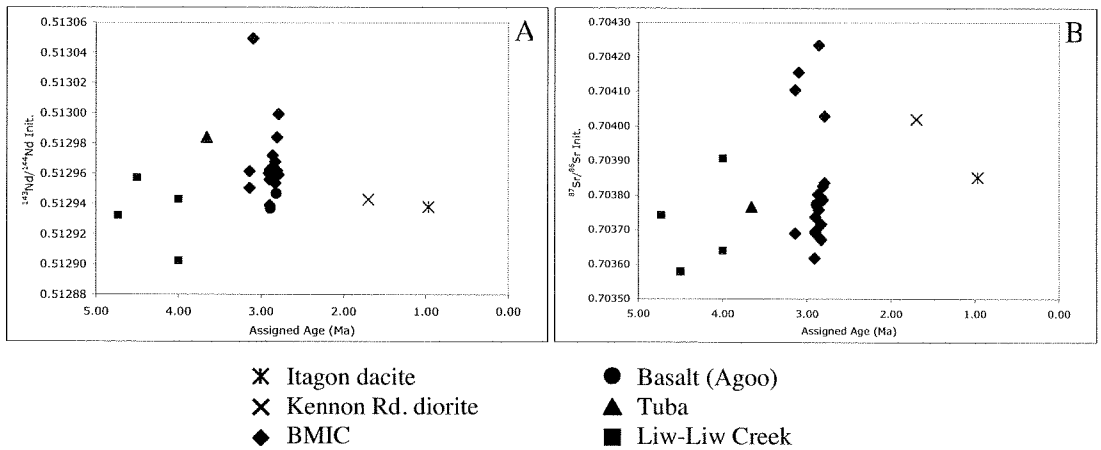

Figure 5.14 - (A) $^{143}Nd/^{144}Nd$ and (B) $^{87}Sr/^{86}Sr$ isotopic trends during the Pliocene. Compiled from Sajona (1995), Margoum (2002), Hollings (2006), Polve et al. (2007) and this study (Table 5.1).

5.5.2 Geochemical Evolution of the Black Mountain Porphyry Southeast System

The rocks of the Black Mountain Southeast broadly reflect a coherent magma suite, undergoing continual fractional crystallization of plagioclase, hornblende and a Fe-Ti oxide phase (Fig. 5.5). This is indicated by the compatible behavior of Fe_2O_3 and TiO_2 (and to a lesser extent CaO and MgO; Fig. 5.5a-d), and the recognition of plagioclase and hornblende as the dominant phenocrystic phases within the Black Mountain Southeast Intrusive Suite (Chapter 3). The inflections noted for Al_2O_3 and (to a lesser extent) Na_2O correspond with an SiO_2 content of ~52.5 wt% (Fig. 5.5e and f), and suggest contemporaneous onset of fractional crystallization of apatite and possibly alkali feldspar (though confirmation of this is hindered by the scatter of K_2O and Na_2O data through alteration-driven remobilization; Fig. 5.1a and c). Trace elements mirror this trend with highly compatible elements (e.g., V; Fig. 5.9d) decreasing with increasing SiO_2, most HFSE (aside from Ti which is likely partitioned into ilmenite) showing a positive correlation with increasing SiO_2 (Fig. 5.9a and b), and La/Sm_{cn} values demonstrating a broadly positive correlation with SiO_2 (Fig. 5.7).

Similar observations were made by Hollings (2006) and Hollings et al. (in press), wherein compatible trends of Fe_2O_3, MgO, TiO_2, P_2O_5 and CaO relative to SiO_2 were attributed to fractional crystallization of plagioclase, hornblende, apatite and a Fe-Ti oxide component within the Baguio district's Pliocene intrusive rocks. Additionally, a

positive correlation between La/Sm_{cn} and SiO_2 was interpreted to support the model of crustal ponding and fractional crystallization of the magmas. In line with Hollings (2006) and Hollings et al. (in press), the documentation of these major and trace element trends at Black Mountain Southeast lend credence to the possibility of intra-crustal magma pooling and fractional crystallization having played a major role in the production of the Black Mountain Southeast magmas. However, further examination of the whole rock geochemistry and isotope geochemistry data sets in the context of an intrusive chronology suggests a more complex geodynamic history for the BMSIS magmas.

The documentation of a distinct progression of intrusive phases at the Black Mountain Southeast calls into question some of the above implications for major and trace element concentrations versus SiO_2 (Chapter 3; Figs. 5.5 and 5.9). These Harker diagrams utilize SiO_2 wt% as an "index for fractionation". The trends derived from them assume a temporal geochemical progression from low silica to high silica rocks, in line with fractional crystallization of magma within a closed system. However, the order of magma emplacement at the Black Mountain Southeast (Chapters 3 and 4) indicates otherwise: the emplacement of the Liw-Liw Creek dikes, followed by the EMD through AM intrusive phases documents an initially mafic magma abruptly giving way to a felsic magma, and then gradually returning to a mafic component geochemically similar to the Liw-Liw Creek Dikes (Appendix 5.1). This magmatic sequence is confirmed by the reported U-Pb and Ar-Ar dates (Chapter 4), which define mafic magmatism as occurring both prior to and post felsic/intermediate magmatism (and associated mineralization) within the greater Black Mountain Intrusive Complex.

5.5.3 Isotopic Evolution of the Black Mountain Porphyry Southeast System

Data presented in this study indicates a temporal variation in the isotopic character of the Black Mountain Southeast Intrusive Suite. Given the previously defined progression of intrusive phases (Chapter 3 and 4), the Black Mountain Southeast rocks broadly increase in radiogenic character over time, marked by distinct radiogenic "spikes" coincident with the EMD. $^{143}Nd/^{144}Nd$ values show a strong negative correlation with age in Figure 5.15a, increasing with each successive intrusive phase. However, a prominent spike in $^{143}Nd/^{144}Nd$ occurs for the single sample of EMD, denoting the maximum value for the

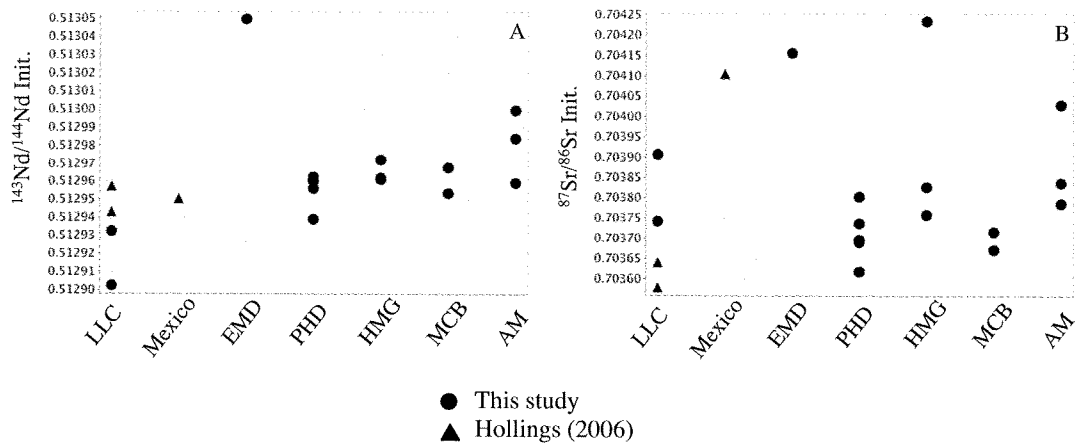

Figure 5.15 - (A) $^{143}Nd/^{144}Nd$ and (B) $^{87}Sr/^{86}Sr$ variations over time within the Black Mountain Intrusive Complex.

entire intrusive suite across all data sets (Table 5.1). Similar to the observation of increasing radiogenic Nd for the Miocene-Pliocene intrusive suite over time (Hollings, 2006), this suggests the involvement of a secondary mafic source with a more primitive isotopic character than the Liw-Liw Creek mafic magmas.

A temporal trend for $^{87}Sr/^{86}Sr$ is not as obvious (Figure 5.15b). However, apart from a few positive spikes, a broadly positive trend is apparent. Relative to the rest of Black Mountain Southeast Intrusive Suite, the Liw-Liw Creek dikes reflect low to moderate radiogenic Sr with a range of 0.70359 – 0.70391. With the emplacement of the Mexico diorite (Hollings, 2006) and EMD ($^{87}Sr/^{86}Sr$ of 0.70411 and 0.70416, respectively; Table 5.1), we see a spike in $^{87}Sr/^{86}Sr$ values, followed by an abrupt decrease back to the Liw-Liw Creek range with the PHD (0.70361-0.7038; Table 5.1). The HMG marks a second positive spike of $^{87}Sr/^{86}Sr$, with a peak value of 0.70423 (the highest $^{87}Sr/^{86}Sr$ value across all data sets). $^{87}Sr/^{86}Sr$ values then drop again with HCB, and rise slightly in the AM rocks. This erratic increase of radiogenic Sr implies sporadic but increasing involvement of an evolved component during the generation of the Black Mountain Southeast Intrusive Suite.

The increasingly radiogenic character of Black Mountain Southeast Intrusive Suite (particularly for Nd) seems to preclude the theory that the Liw-Liw Creek dikes are representative of the sole parental magma for the Baguio district's Pliocene intrusives.

More specifically, the simultaneous spikes (and negative correlations with time) in radiogenic Sr and Nd cannot be produced by a single magmatic source. Instead, the temporally increasing radiogenic Nd and Sr suggest independent generation and involvement of two additional components: a more primitive melt and the sporadic input of an evolved contaminant. However, a multi-component system does not easily explain the coincident Nd and Sr spikes within EMD, as the product of mixing an evolved contaminant (e.g., crustal material) with a primitive component (e.g., depleted mantle) would most likely plot within the mantle array (Zindler and Hart, 1986).

Decoupling of the Sm-Nd and Rb-Sr isotopic systems may explain the isotopic discrepancy in the Black Mountain Southeast Intrusive Suite. This has been noted in the Baguio district's Miocene and Pliocene intrusive rocks (Hollings, 2006) as well as in other volcanic arc environments (e.g., Conceicao et al., 2005). In particular, Conceicao et al. (2005) documented decoupling of Nd and Sr systems within mantle xenoliths from subduction-related Andean magmatism. On an $^{87}Sr/^{86}Sr$ vs $^{143}Nd/^{144}Nd$ diagram, this was manifested as a displacement of the samples to the right/above of the mantle array of Zindler and Hart (1986) indicating either an enrichment of radiogenic Sr for a given $^{143}Nd/^{144}Nd$ value, or an enrichment of radiogenic Nd for a given $^{87}Sr/^{86}Sr$ value. The BMSIS samples show a similar trend (particularly EMD; Fig. 5.10).

Conceicao et al. (2005) cited two possible causative scenarios in which $^{87}Sr/^{86}Sr$ values are elevated with minimal modification to $^{143}Nd/^{144}Nd$: (a) a chromatographic process occurring during metasomatism of mantle wedge peridotite or (b) mixing of a depleted mantle source and an evolved component. The chromatographic process involves percolation of a melt through peridotite during metasomatism of the mantle wedge, resulting in uneven movement of Sr and Nd due to differing compatibilities of the elements during equilibration along the percolation front (Conceicao et al., 2005 and sources therein). Assuming we start with an isotopically primitive melt (for example, DM), the first scenario elevates radiogenic Sr while maintaining the characteristically high $^{143}Nd/^{144}Nd$ ratio of the primitive source. This implies input of a single component into the porphyry system, and thus may account for the coincident spike in radiogenic Nd and Sr for EMD, as well as the temporal increase in overall radiogenic character during the Black Mountain Southeast's lifetime. However, elevated $^{143}Nd/^{144}Nd$ ratios do not

accompany the radiogenic Sr spike in the Mexico and HMG samples. This may illustrate a physical separation of the two isotopic systems, therefore demanding more than one source to explain the elevated $^{87}Sr/^{86}Sr$ and $^{143}Nd/^{144}Nd$ ratios.

The second scenario infers the mixing of a high $^{143}Nd/^{144}Nd$ primitive component and a high $^{87}Sr/^{86}Sr$ evolved component to produce the displacement of some of the Black Mountain Southeast samples up and/or to the right of the mantle array in Figure 5.10. Hollings (2006) and Hollings et al. (in press) proposed that an upper crustal contaminant could provide the elevated $^{87}Sr/^{86}Sr$ values observed for the BMIC rocks presumably through assimilation during intra-crustal migration or pooling of the primitive source. In the case of the Black Mountain Southeast rocks, two lines of evidence preclude this scenario: (1) the absence of elevated $^{87}Sr/^{86}Sr$ within the Liw-Liw Creek mafic magmas that presumably interacted with the same upper crustal material, and (2) the effects of isotopic contamination by continental crust would be limited due to the dominantly oceanic composition of the northern Luzon crust (Fourcade et al., 1994; Payot et al., 2007). However, White and Patchett (1984), McCulloch and Gamble (1991) and Conceicao et al. (2005) proposed that volcanic-arc basalt (a mixture of mantle- and slab-derived melts) could have an elevated Sr/Nd ratio and $^{87}Sr/^{86}Sr$ values of 0.704 to 0.705 (similar to what is observed in the Black Mountain Southeast rocks). Interaction between a volcanic-arc basalt and the mantle wedge (containing DM material) could produce a melt with elevated radiogenic Sr, but still primitive $^{143}Nd/^{144}Nd$ values (Conceicao et al., 2005). Whole rock geochemical data for the Black Mountain Southeast rocks tends to support this scenario as well, with Sr/Nd ratios of the Black Mountain Southeast rocks (range of 15-55; Appendix 2.1) comparing favorably with a modeled mixture of volcanic-arc basalt and mantle wedge material from the Antilles (Sr/Nd ratio of 33.8; White and Patchett, 1984). This scenario appears to satisfy the coinciding elevated radiogenic Sr and Nd observed within EMD. However, it does not explain the issue of the 'stand alone' elevated $^{87}Sr/^{86}Sr$ values for the Mexico sample and HMG that occur without an accompanying $^{143}Nd/^{144}Nd$ spike. Because we are dealing with a multi-component system for the second scenario, a simple consideration of mixing nature may explain this discrepancy. Despite the fact that mixing yields homogenization, an initial mixture of the evolved and primitive components could have been heterogeneous due to density and/or

temperature differences of the early melts. Early intrusive phases originating from this mixture would likely reflect the incomplete mixing, with increasing homogeneity over time. In terms of the Black Mountain Southeast Intrusive Suite, this scenario could produce the initially sporadic $^{87}Sr/^{86}Sr$ value increases, as well as the increase observed through HCB and AM as the mixture became progressively more homogeneous. Thus, based on the evolving Nd and Sr isotopic data, at least two distinct components were involved with the generation of the Black Mountain Southeast Intrusive Suite: the Liw-Liw Creek/Mafic Dike Complex magmas, and a hybrid melt derived from initially incomplete mixing of a primitive DM-sourced melt with an evolved slab/sediment derived melt.

5.5.4 Genesis of High-Si Melts in the Black Mountain Porphyry Southeast System

The evolving geochemistry of the Black Mountain Southeast Intrusive Suite provides insight into the possible intra-crustal interaction between two mafic sources. Relatively straightforward temporal geochemical trends within the Black Mountain Southeast are marked by anomalies coinciding with the EMD. As mentioned above, major and trace elements reflect the mafic-to-felsic-to-mafic temporal trend in which initial geochemistry shifts abruptly with the emplacement of EMD, and gradually returns to a composition similar to the Liw-Liw Creek dikes during the emplacement of PHD, HMG, HCB and AM intrusive phases. This supports the model of Waters et al. (in press) that mafic magmatism continued after mineralization at Black Mountain. Furthermore, the gradational shift towards a more mafic component following the emplacement of the EMD suggests that mafic magmatism was in fact ongoing throughout the generation of the Black Mountain Southeast Intrusive Suite. However, the abrupt shift to felsic/intermediate magmatism from the Liw-Liw Creek dikes to the EMD and PHD poses a problem for a dominantly mafic system. Specifically, where does the high-Si melt come from?

The generation of a felsic/intermediate melt (EMD and PHD) within a system defined by multi-component mafic magmatism requires modification of one of the mafic components within the crust. This modification could take place through magma pooling and fractional crystallization (Hollings, 2006), partial melting of an already crystallized

magmatic body in the crust, or a combination of both. As previously mentioned, major and trace element correlations with SiO_2 are interpreted to be evidence of magma pooling and fractional crystallization having taken place during the generation of the BMSIS (Figs. 5.5; 5.9). This is consistent with the observations of Hollings (2006) for the Baguio district's Pliocene intrusive rocks. Given the pre-BMIC timing of the Mafic Dike Complex and Liw-Liw Creek dikes (Waters and Gonzales, 2005; Hollings, 2006; this study), and the spike in radiogenic character contemporaneous with the onset of felsic magmatism (EMD), the work conducted for this thesis suggests a scenario wherein magmas associated with the Liw-Liw Creek mafic dikes pooled and underwent fractional crystallization within the crust. Upon generation and ascension of a second primitive magma (the hybrid mafic melt), interaction with the crystallized or crystallizing Liw-Liw magma chamber caused a partial melting event of the quenched Liw-Liw Creek magmas, leading to the generation of a more felsic component within the system.

5.7 Conclusions

In the context of a temporal progression of intrusive phases, the geochemical and isotopic data sets presented for the Black Mountain Southeast Intrusive Suite define a complicated history of sub-arc magma generation and mixing, and intra-crustal evolution. The Black Mountain magmas are the product of mixing and interaction of at least three components: (1) mafic magmas associated with the Liw-Liw Creek dikes and the Mafic Dike Complex, (2) a high Sr/Nd, volcanic arc basaltic melt with an evolved radiogenic Sr signature, and (3) a depleted mantle melt with a primitive radiogenic Nd signature. Sub-arc generation and heterogeneous mixing of the latter two components produced a hybrid melt that interacted with partially- or completely-crystallized Liw-Liw Creek and Mafic Dike magmas upon ascension into the crust.

Within the scope of the Pliocene magmatism and mineralization of the Baguio mineral district, the evolution of the Black Mountain Southeast Intrusive Suite suggests a shift towards hybrid mafic magmatism coincident with the onset of felsic magmatism and mineralization. The elevated radiogenic character of the mafic melt distinguishes it from the earlier Liw-Liw Creek magmas, and suggests a change in the nature of sub-arc magma generation. This precludes the theory that the Liw-Liw Creek dikes represent the

sole parental magma source for the Pliocene felsic magmatism (Hollings, 2006), and instead suggests that they are only one component of the Black Mountain Southeast Intrusive Suite. Distinct major and trace element trends confirm the modification of at least one of the mafic components (the Liw-Liw Creek and Mafic Dike Complex magmas) through intra-crustal pooling and fractional crystallization (Hollings, 2006), and partial melting.

Chapter 6

Hornblende Geochemistry

6.1 Introduction

Multiple authors have utilized major element composition of calcic hornblende in calc-alkaline igneous rocks as an indicator of chemical and environmental parameters of magma crystallization (e.g., pressure and temperature). For example, the Al content of hornblende has been used to infer pressure and depth of crystallization in calc-alkaline intrusive rocks (e.g., Hammarstrom and Zen, 1986; Hollister et al., 1987). Fémênias et al. (2006) reported that the Ti content of calcic amphiboles could be used to assess the temperature of amphibole crystallization, and that high alkalis (K+Na), low SiO_2 amphibole phenocryst cores were associated with basaltic andesites, andesites and trachyandesites, whereas low Na+K, high SiO_2 amphibole phenocryst cores were found in dacites and rhyolites. Similarly, Cawthorn (1976) suggested that the SiO_2 content of hornblende reflects the silica content of crystallizing magmas, implying that felsic magmas more readily crystallize amphiboles with higher silica compositions than mafic magmas.

Utilizing hornblende major element compositions (as well as supplementary feldspar geochemistry) from the Black Mountain Southeast Intrusive Suite, this chapter examines the intra-crustal modification of the Black Mountain Southeast magmas. Specifically, hornblende geobarometry (Hammarstrom and Zen, 1986; Hollister et al., 1987) and compositional variation (Cawthorn, 1976; Fémênias et al., 2006) are used to assess the intra-crustal evolution of the Black Mountain Southeast magmas, highlighting the roles of intra-crustal pooling, fractional crystallization and interaction of multiple magmatic components in the production of the Black Mountain Southeast porphyry system (Chapter 5).

6.2 Methodology

Major element geochemical data for hornblende and plagioclase feldspar phenocrysts of the Black Mountain Southeast Intrusive Suite was collected using electron microprobe (EMP) techniques at the University of Tasmania, Hobart, and the Massachusetts Institute

of Technology, Boston. Detailed methodology for the operation of both electron microprobes can be found in Appendix 1.5. The hornblende phenocrysts of three samples (BA08GS030, BA08GS035 and BA08GS056) were analyzed on both microprobes in order to constrain any variability between the two machines.

Thin section petrography conducted for this study confirmed the presence of zoned hornblende phenocrysts within the Black Mountain Southeast intrusive rocks (Chapter 3). As compositional zonation can reflect changing liquid chemistry during crystallization, care was taken to examine and compare the chemistry of phenocryst rims and cores. Consequently, at least two locations on each analyzed phenocryst were examined: a rim spot analysis and a core spot analysis. This is discussed below in greater detail. Similarly, feldspar phenocrysts were noted to have prominent zonation throughout the Black Mountain Southeast samples (Chapter 3), consequently at least one rim and one core spot analysis were made for each phenocryst.

6.3 Geochemistry

6.3.1 Micrprobe Variability

Comparison of the major element oxide output data of the two microprobes used for this study is displayed in Figure 6.1. Hornblende phenocryst populations from three samples (BA08GS030, BA08GS035 and BA08GS056) were analyzed on both machines and compared. It should be noted that the MIT and University of Tasmania data subsets for each sample do not represent analyses of the same spot locations or even the same hornblende phenocrysts. Rather, the major element oxide chemistry displayed in Figure 6.1 compares the range of hornblende compositions within individual samples. The data from the University of Tasmania and MIT laboratories show broadly similar results from each sample: the major element oxide compositions for hornblende phenocrysts group well together with little spread. Where spread is observed (e.g., MgO vs. SiO_2; Fig. 6.1c), it is present in both the MIT and University of Tasmania data sets, suggesting that there is no discrepancy between the detection of major element oxides for the two microprobes.

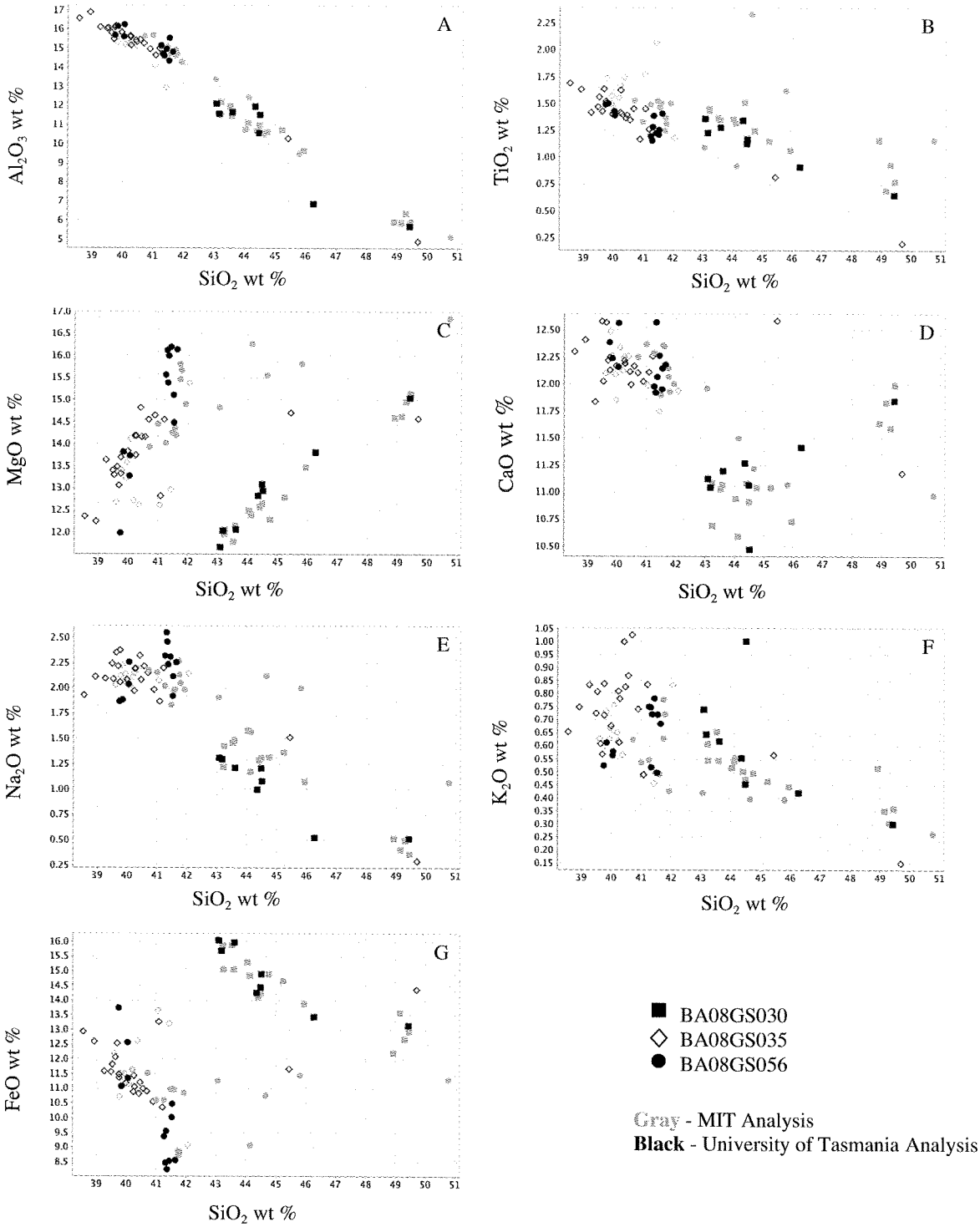

Figure 6.1 – Comparison of major element oxide variation between the MIT and University of Tasmania electron microprobes: (A) Al_2O_3, (B)TiO_2, (C) MgO, (D) CaO, (E) Na_2O, (F) K_2O, and (G) FeO.

6.3.2 Hornblende

Field mapping and petrographic studies of the Black Mountain Southeast intrusive rocks identified two hornblende phenocryst groups based on crystal nature and rock-type association. One group of hornblendes is characterized by smaller diameter phenocrysts (<5mm) that frequently constitute a phenocryst phase in the intermediate of plagioclase and variably hornblende-phyric diorite (PHD; Chapter 3). These tend to be small and/or spindly and will be referred to as *Group 1* hornblendes throughout the rest of this thesis (Fig. 6.2). The second group of hornblendes (termed *Group 2*) is characterized by larger diameter phenocrysts (>10mm) associated with the more mafic intrusive rocks at Black Mountain Southeast (the Liw-Liw Creek dikes and the HMG and HCB intrusive units, as well as the hornblende clusters; Chapter 3; Fig. 6.3). The Group 2 hornblendes are tabular and are the dominant phenocrystic mineral within their respective intrusive phase.

Martin (2007) noted that full characterization of igneous amphiboles demands a large investment of time and study beyond the examination of major elements routinely assessed in electron microprobe analyses. He inferred that the characterization of lithium, hydrogen content, the valence state of Fe and Mn, and other chemical (as well as physical) parameters are necessary for complete identification. Such an in-depth investigation of the hornblende species was beyond the scope of this study.

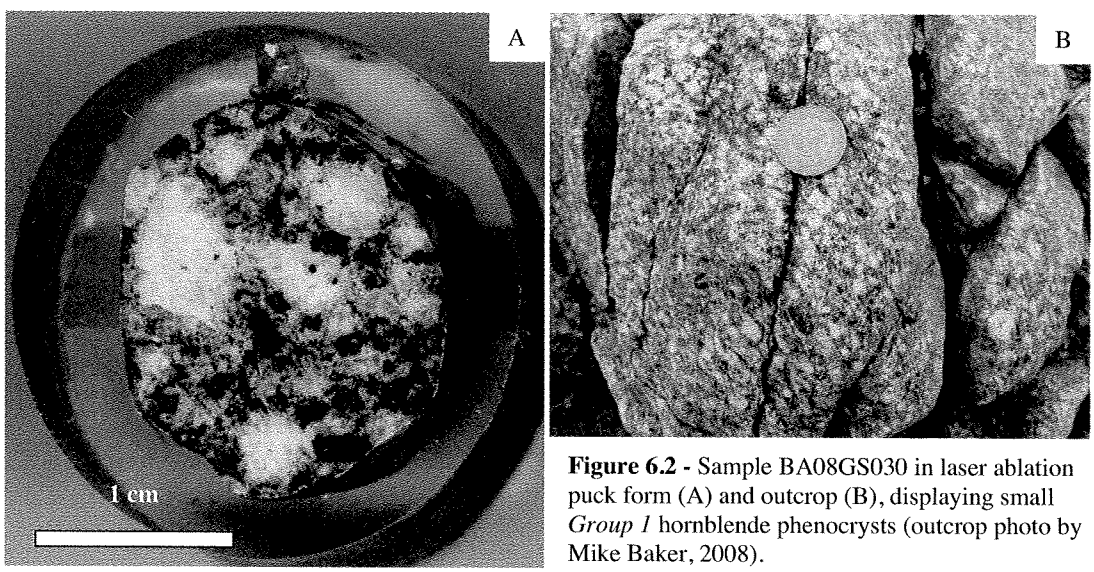

Figure 6.2 - Sample BA08GS030 in laser ablation puck form (A) and outcrop (B), displaying small *Group 1* hornblende phenocrysts (outcrop photo by Mike Baker, 2008).

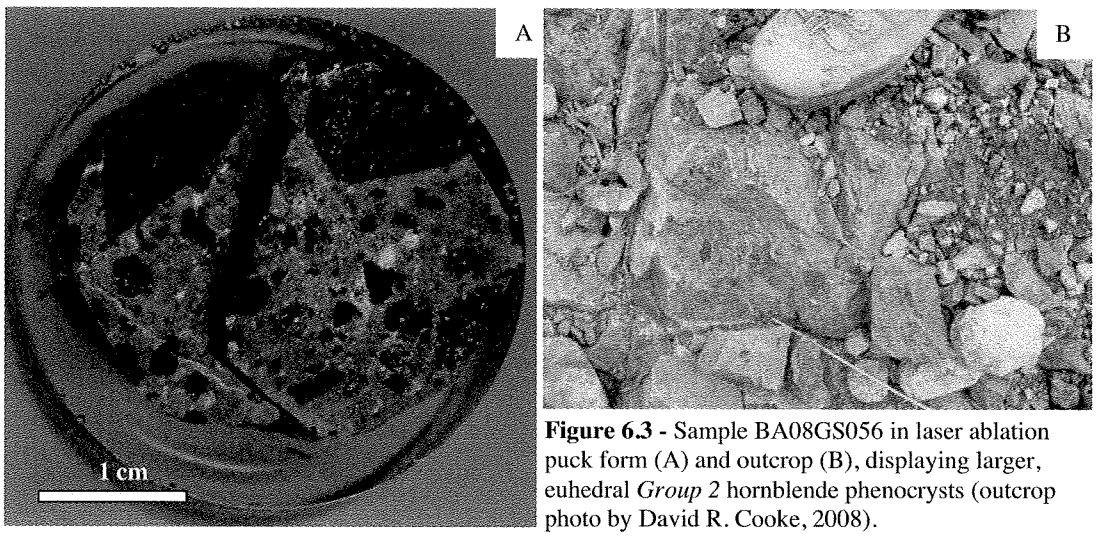

Figure 6.3 - Sample BA08GS056 in laser ablation puck form (A) and outcrop (B), displaying larger, euhedral *Group 2* hornblende phenocrysts (outcrop photo by David R. Cooke, 2008).

However, the major element data presented herein allows for broad comparison of the hornblende chemistries identified within the Black Mountain Southeast porphyry system, as well as observation of compositional variability within individual hornblende phenocrysts.

Hornblende Geochemistry

A total of 17 samples were analyzed for the major element composition of their hornblende phenocryst populations. The sample suite included three samples from the Liw-Liw Creek dikes, seven from the PHD, three from the HMG, one from the HCB, two from the hornblende-plagioclase megacrystic clusters of the HMG, and one from the hornblende clusters of the HCB. Sample locations within the map area are shown on Figure 6.4. Based strictly on rock type (and intrusive phase) associations, the sample suite can be subdivided into seven samples containing Group 1 hornblendes, and ten samples containing Group 2 hornblendes. Individual spot analyses and cations per formula unit values are presented in Appendices 2.3 and 2.4, respectively. Rim and core mean sample averages for major element oxides and atoms per formula unite are found in Tables 6.1 and 6.3, respectively.

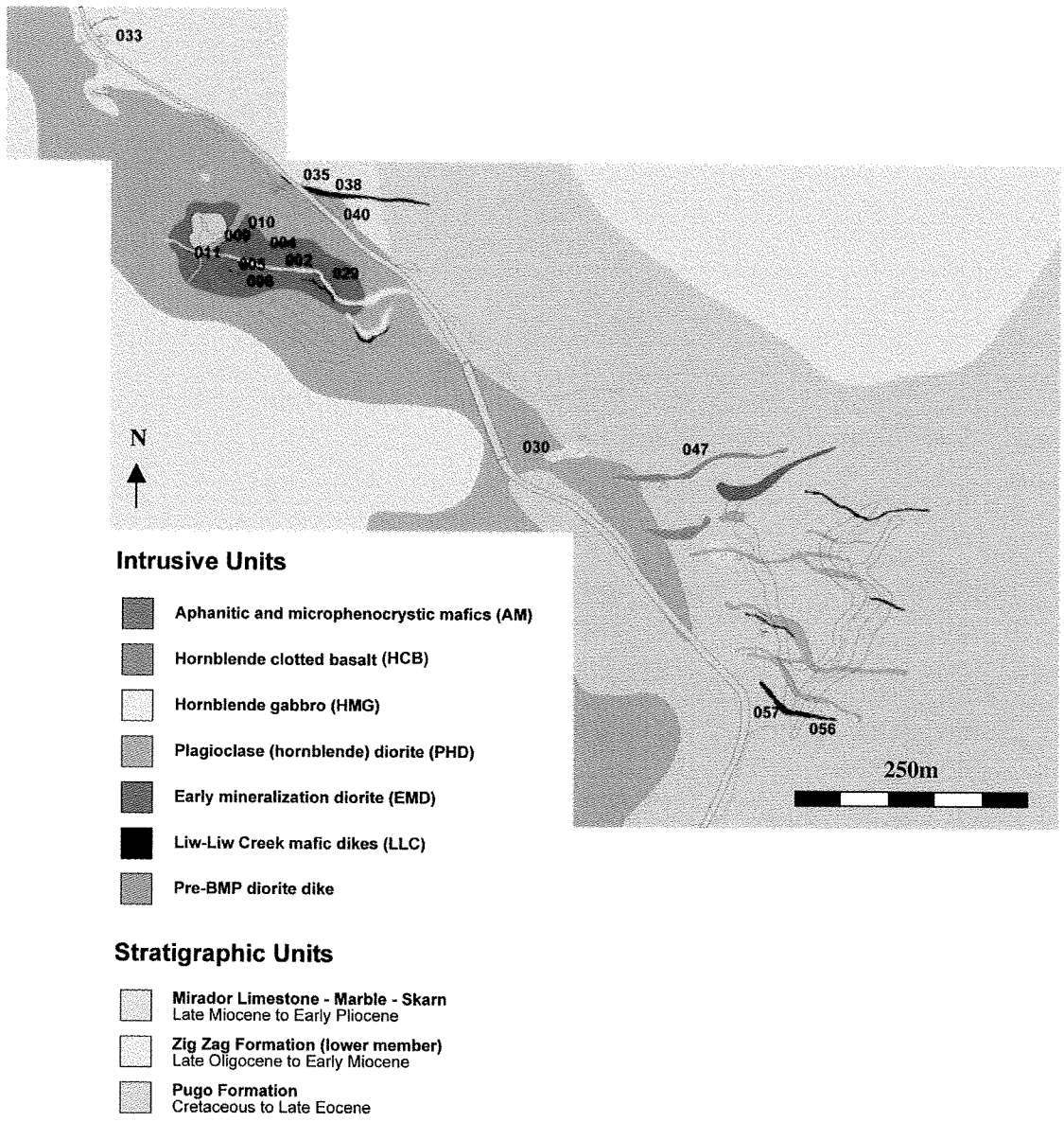

Figure 6.4 - Map showing location of hornblende samples.

Table 6.1 – Mean sample average major element oxide compositions for rim and core spot analyses.

Sample #	Spot Location	Intrusive Phase	SiO_2	TiO_2	Al_2O_3	FeO	MnO	MgO	CaO	Na_2O	K_2O	Total
BA08GS035	c	Liw-Liw	41.23	1.36	14.40	11.66	0.21	13.80	12.14	2.00	0.65	97.44
BA08GS035	r	Liw-Liw	40.04	1.55	15.50	11.68	0.15	13.52	12.16	2.12	0.73	97.46
BA08GS056	c	Liw-Liw	41.30	1.36	15.07	9.95	0.09	14.93	12.13	2.15	0.65	97.63
BA08GS056	r	Liw-Liw	42.67	1.40	13.37	10.67	0.17	15.01	11.94	1.97	0.52	97.72
BA08GS057	c	Liw-Liw	40.49	1.43	15.46	10.59	0.14	14.40	12.12	2.17	0.68	97.46
BA08GS057	r	Liw-Liw	40.97	1.37	14.76	10.05	0.06	15.13	12.19	2.15	0.57	97.26
BA08GS002	c	PHD	48.12	1.11	8.22	13.82	0.39	13.60	11.25	1.21	0.39	98.09
BA08GS002	r	PHD	47.19	1.05	8.09	13.74	0.46	14.12	11.27	1.22	0.38	97.52
BA08GS005	c	PHD	45.04	1.32	10.42	14.90	0.41	12.55	11.33	1.36	0.57	97.90
BA08GS005	r	PHD	42.92	1.84	12.09	14.76	0.33	12.22	11.58	1.60	0.62	97.98
BA08GS006	c	PHD	44.09	1.50	10.88	15.15	0.41	12.26	11.21	1.62	0.59	97.70
BA08GS006	r	PHD	45.11	1.40	9.68	14.86	0.40	12.68	11.11	1.53	0.52	97.29
BA08GS030	c	PHD	44.22	1.29	11.22	14.69	0.39	12.58	10.90	1.24	0.58	97.10
BA08GS030	r	PHD	46.16	1.09	8.88	14.33	0.48	13.36	11.36	0.94	0.48	97.08
BA08GS033A	c	PHD	44.60	1.39	9.95	14.82	0.49	12.82	11.35	1.46	0.55	97.43
BA08GS033A	r	PHD	46.50	1.04	8.54	14.17	0.58	13.82	11.19	1.28	0.39	97.50
BA08GS033B	c	PHD	43.62	1.42	11.47	13.92	0.39	13.13	11.55	1.60	0.48	97.58
BA08GS033B	r	PHD	45.59	1.20	9.12	14.42	0.54	13.55	11.18	1.34	0.43	97.37
BA08GS040	c	PHD	44.51	1.34	10.57	15.39	0.43	12.48	11.18	1.57	0.57	98.04
BA08GS040	r	PHD	44.83	1.50	10.02	14.91	0.42	12.86	11.29	1.52	0.56	97.92
BA08GS004	c	HMG	40.48	2.37	14.42	10.92	0.11	14.20	12.03	2.23	0.57	97.33
BA08GS004	r	HMG	40.73	2.71	13.89	10.88	0.15	14.08	11.94	2.31	0.66	97.34
BA08GS029	c	HMG	40.55	2.45	14.59	10.43	0.08	14.31	11.76	2.39	0.63	97.17
BA08GS029	r	HMG	40.58	2.32	14.15	10.86	0.13	14.35	12.19	2.23	0.71	97.50
BA08GS009	c	HMG Clot	39.46	2.31	14.62	11.29	0.13	14.00	12.05	2.34	0.65	96.85
BA08GS010	c	HMG Clot	40.02	2.21	15.26	10.94	0.09	14.25	12.33	2.30	0.48	97.90
BA08GS010	r	HMG Clot	41.02	2.58	13.79	11.40	0.16	14.06	11.80	2.31	0.65	97.78
BA08GS011	c	HMG Clot	40.27	2.26	14.97	10.75	0.09	14.11	11.84	2.22	0.71	97.22
BA08GS047	c	HCB	42.22	1.57	13.39	10.00	0.11	15.31	11.87	2.07	0.89	97.42
BA08GS047	r	HCB	43.06	1.59	12.57	11.02	0.17	14.89	11.78	1.84	0.80	97.71
BA08GS047	c	HCB Clot	40.88	1.58	14.22	12.24	0.19	13.22	12.18	1.98	0.68	97.17

Table 6.2 – Mean sample average atoms per formula unit (a.p.f.u.) compositions for rim and core spot analyses.

Sample #	Spot Location	Intrusive Phase	Si	Ti	Al	Fe^{2+}	Mn	Mg	Ca	Na	K	Total
BA08GS035	c	Liw-Liw	6.09	0.15	2.50	1.44	0.03	3.04	1.92	0.57	0.12	15.86
BA08GS035	r	Liw-Liw	5.93	0.17	2.70	1.45	0.02	2.98	1.93	0.61	0.14	15.92
BA08GS056	c	Liw-Liw	6.03	0.15	2.59	1.22	0.01	3.25	1.90	0.61	0.12	15.88
BA08GS056	r	Liw-Liw	6.23	0.15	2.30	1.30	0.02	3.27	1.87	0.56	0.10	15.79
BA08GS057	c	Liw-Liw	5.95	0.16	2.68	1.30	0.02	3.16	1.91	0.62	0.13	15.92
BA08GS057	r	Liw-Liw	6.02	0.15	2.55	1.23	0.01	3.31	1.92	0.61	0.11	15.92
BA08GS002	c	PHD	7.00	0.12	1.41	1.68	0.05	2.95	1.75	0.34	0.07	15.38
BA08GS002	r	PHD	6.93	0.12	1.40	1.69	0.06	3.09	1.77	0.35	0.07	15.47
BA08GS005	c	PHD	6.65	0.15	1.81	1.84	0.05	2.76	1.79	0.39	0.11	15.55
BA08GS005	r	PHD	6.36	0.21	2.11	1.83	0.04	2.70	1.84	0.46	0.12	15.67
BA08GS006	c	PHD	6.55	0.17	1.90	1.88	0.05	2.71	1.78	0.47	0.11	15.62
BA08GS006	r	PHD	6.70	0.16	1.69	1.85	0.05	2.81	1.77	0.44	0.10	15.56
BA08GS030	c	PHD	6.57	0.14	1.96	1.82	0.05	2.79	1.74	0.36	0.11	15.54
BA08GS030	r	PHD	6.83	0.12	1.55	1.77	0.06	2.95	1.80	0.27	0.09	15.45
BA08GS033A	c	PHD	6.63	0.16	1.74	1.84	0.06	2.84	1.81	0.42	0.10	15.61
BA08GS033A	r	PHD	6.85	0.11	1.48	1.75	0.07	3.04	1.77	0.37	0.07	15.51
BA08GS033B	c	PHD	6.46	0.16	2.00	1.72	0.05	2.90	1.83	0.46	0.09	15.66
BA08GS033B	r	PHD	6.75	0.13	1.59	1.78	0.07	2.99	1.77	0.38	0.08	15.55
BA08GS040	c	PHD	6.59	0.15	1.84	1.90	0.05	2.75	1.77	0.45	0.11	15.62
BA08GS040	r	PHD	6.63	0.17	1.75	1.84	0.05	2.84	1.79	0.44	0.11	15.60
BA08GS004	c	HMG	5.97	0.26	2.51	1.35	0.01	3.12	1.90	0.64	0.11	15.88
BA08GS004	r	HMG	6.01	0.30	2.42	1.34	0.02	3.10	1.89	0.66	0.12	15.87
BA08GS029	c	HMG	5.98	0.27	2.53	1.29	0.01	3.15	1.86	0.68	0.12	15.88
BA08GS029	r	HMG	5.99	0.26	2.46	1.34	0.02	3.15	1.93	0.64	0.13	15.91
BA08GS009	c	HMG Clot	5.88	0.26	2.57	1.41	0.02	3.11	1.93	0.68	0.12	15.97
BA08GS010	c	HMG Clot	5.88	0.24	2.64	1.34	0.01	3.12	1.94	0.66	0.09	15.93
BA08GS010	r	HMG Clot	6.04	0.29	2.39	1.40	0.02	3.09	1.86	0.66	0.12	15.87
BA08GS011	c	HMG Clot	5.94	0.25	2.60	1.33	0.01	3.11	1.87	0.64	0.13	15.89
BA08GS047	c	HCB	6.18	0.17	2.31	1.22	0.01	3.34	1.86	0.59	0.17	15.87
BA08GS047	r	HCB	6.30	0.17	2.17	1.35	0.02	3.25	1.85	0.52	0.15	15.78
BA08GS047	c	HCB Clot	6.07	0.18	2.49	1.52	0.02	2.93	1.94	0.57	0.13	15.85

Classification of the hornblende populations of the Black Mountain Southeast Intrusive Suite was conducted using the scheme of Féménias et al. (2006; after Leake et al., 1997) in conjunction with a plot of total Al (Al^T) versus tetrahedral Al (Al^{iv}) after Hammarstrom and Zen (1986; Fig. 6.5). Cations per formula unit were calculated on the basis of 23 oxygens for the anhydrous formula [$A_{0-1}B_2C_5T_8O_{22}(OH)_2$; Féménias et al., 2006] and total Fe as FeO, in accordance with the methodology of Hammarstrom and Zen (1986). Despite a large amount of variability in most major elements within the sample suite (Table 6.1; Appendix 2.4), a broad grouping of hornblende species can be determined. Hornblende phenocrysts identified as Group 1 hornblendes are dominantly edinite to magnesiohornblende and occur within the more intermediate PHD (Chapter 5), whereas the mafic-associated Group 2 phenocrysts are hastingsite and pargasite (Fig. 6.5). All amphibole species are calcic hornblendes, with total cation Ca>1.00 (Appendix 2.4).

Using SiO_2 as an X-axis value, nearly all major element oxides record a definitive division between hornblende phenocrysts associated with the PHD (Group 1), and those associated with the Liw-Liw Creek dikes, the HMG and HBD intrusive phases, and the hornblende megacrystic clots (Group 2; Fig. 6.6). For example, CaO content in Group 1 hornblendes ranges from 10.2-12.2 wt%, with the majority of the analyses plotting between 10.8 and 11.5 wt% (Fig. 6.6d; Appendix 2.3). However, Group 2 hornblendes range from 11.5-12.6 wt% CaO, with the majority plotting between 11.7 and 12.5 wt%. A similar division is apparent for Al_2O_3, MgO, Na_2O and K_2O (as well as TiO_2 to a lesser extent) wherein the Group 1 hornblendes are clearly distinguished by lower values (Fig. 6.6a-c, e and f; Appendix 2.3). Conversely, the Group 1 hornblendes contain higher concentrations of FeO, MnO and SiO_2 than the Group 2 hornblendes (Fig. 6.6g and h; Appendix 2.3). Therefore, the Group 1 hornblendes are defined by high Si, Mn and Fe and low Al, Ti, Ca, Mg and alkalis (K and Na), whereas Group 2 hornblendes are characteristically high Al, Ti, Ca, Mg and alkalis, and lower Si, Mn and Fe.

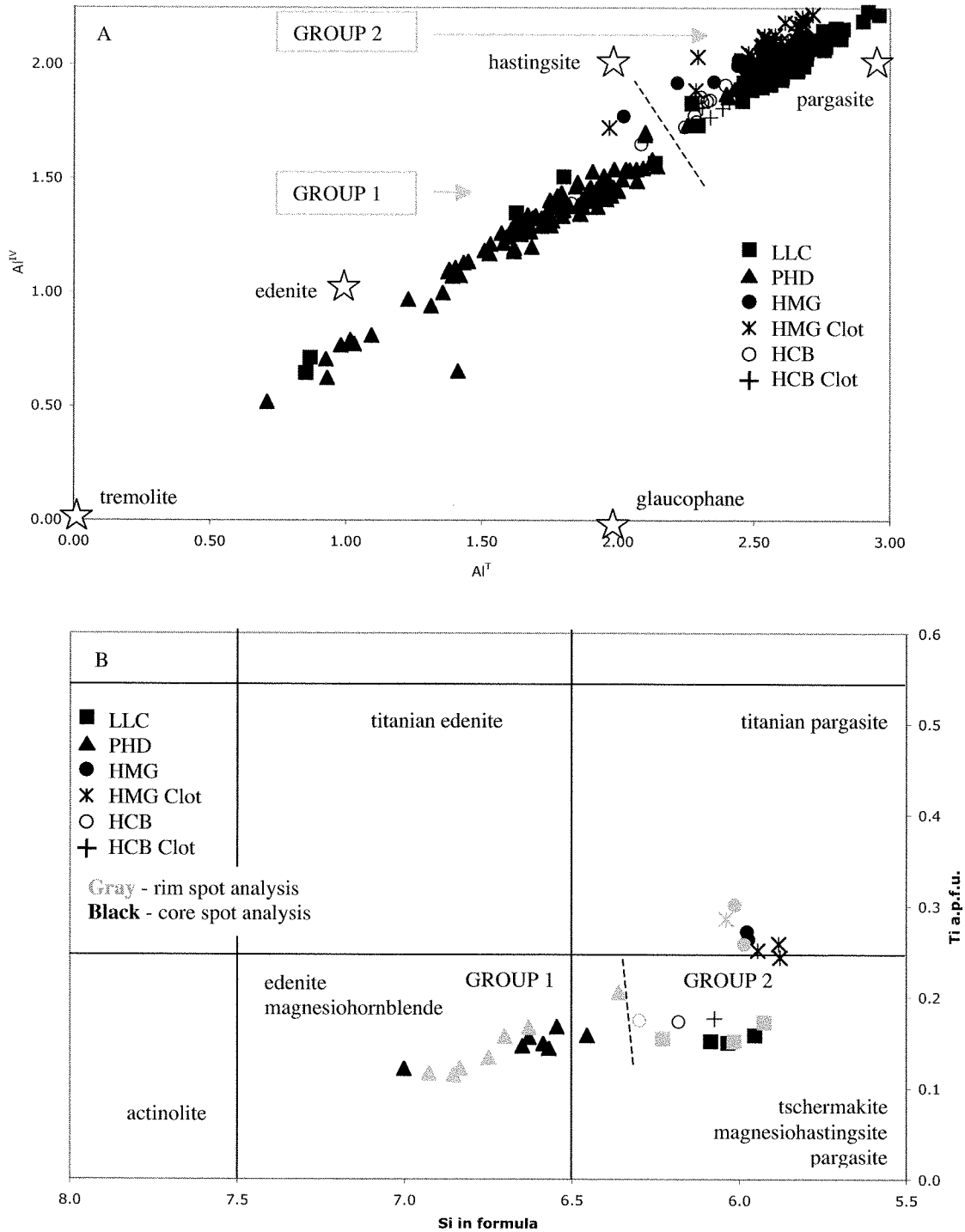

Figure 6.5 - Classification of hornblende species at Black Mountain Southeast through (A) total aluminum (Al^{T}) vs. tetrahedral aluminum (Al^{IV}) after Leake et al. (1997) and Femenias et al. (2006); (B) number of silica vs. titanium atoms per formula unit (a.p.f.u.) for sample averaged rim and core compositions, after Hammarstrom and Zen (1986). Dashed line separates Group 1 and Group 2 hornblende populations.

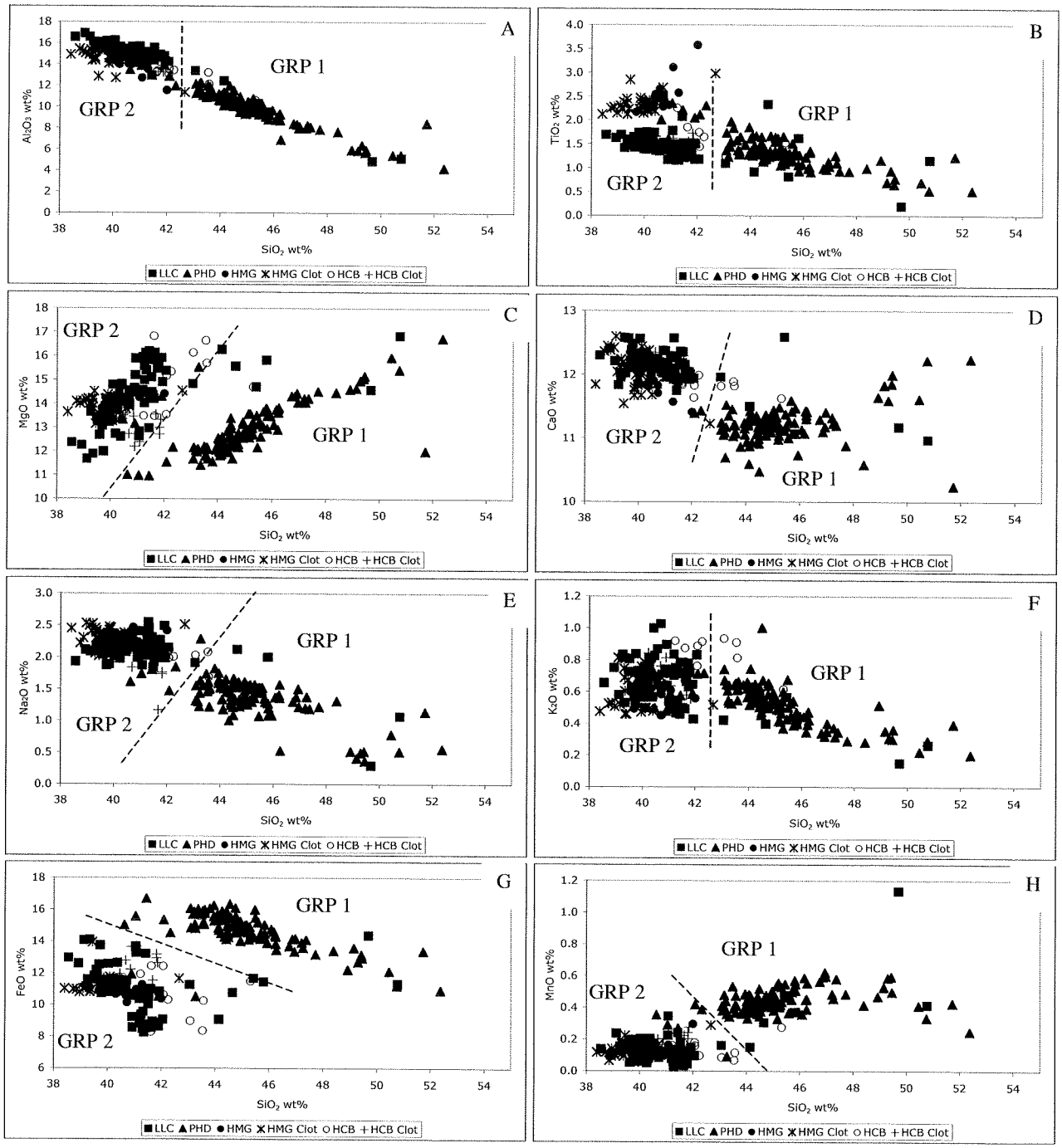

Figure 6.6 - Major element oxide geochemical divisions with respect to SiO_2 between Group 1 hornblendes (associated with the PHD intrusive rocks), and Group 2 hornblendes (associated with the Liw-Liw Creek, HMG and HCB intrusive phases, as well as the hornblende clots in the HMG and HCB): (A) Al_2O_3, (B) TiO_2, (C) MgO, (D) CaO, (E) Na_2O, (F) K_2O, (G) FeO and (H) MnO. Dashed line separates Group 1 and Group 2 hornblende populations.

Overlap between the two hornblende groups is minimal, but does occur (Fig. 6.6). The number of overlapping points varies for individual elements; on average there are less than twenty hornblende spot analyses that do not plot within their respective group ranges, the majority of which are rim compositions (Appendix 2.3; Fig. 6.6). However, the use of SiO_2 as a "discriminator" for the division of the hornblende groups yields relatively little overlap. The only samples which consistently plot across hornblende groups (i.e. both Group 1 and Group 2 hornblende phenocrysts) are samples BA08GS033B, and to a lesser extent, BA08GS005 and BA08GS035 (Fig. 6.6; Appendix 2.3). Both BA08GS033B and BA08GS005 are PHD diorites that contain Group 2 composition hornblendes. In particular, two core compositions from BA08GS033B consistently plot as Group 2 hornblendes for every major element (Fig. 6.6; Appendix 2.3). The five overlapping analyses from sample BAO8GS005 are rim compositions and do not overlap for FeO and MgO (Fig. 6.6c and d; Appendix 2.3). Sample BA08GS035 is a Liw-Liw Creek basaltic dike, and contains one core analysis that plots with Group 1 hornblendes for all major elements except CaO, FeO and MgO (Fig. 6.6b, c and d; Appendix 2.3).

Compositional Zonation

Evolving magma chemistry can be inferred through hornblende compositional zonation with the limitation that the changing mineral chemistry may not always be a product of the crystallizing magma. Féménias et al. (2006) noted "the high H_2O content of many calc-alkaline magmas results in pervasive late-emplacement deuteritic alteration to propylitization and partial modification and/or replacement of primary by secondary amphiboles." The geochemical manifestation of this late stage hydrothermal interaction varies substantially throughout the hornblende species and is dependant on the original hornblende composition (e.g., deuteric alteration of more felsic hornblendes will produce other high Si hornblende species such as actinolite). The Black Mountain Southeast rocks were derived from calc-alkaline arc melts (Chapter 5), and may have been subject to varying degrees of deuteric alteration as a result of late stage hydrothermal systems. However, the petrography of the Black Mountain Southeast hornblendes show that they

are generally unaltered, with a euhedral crystal nature and sharp crystal edges (Chapter 3).

Compositional zonation in hornblende phenocrysts varies throughout the sample suite, with some phenocrysts displaying identical core and rim major element chemistries, whereas some phenocrysts display very different core-rim compositions (Appendix 2.3). Additionally, individual samples can contain both zoned and unzoned phenocrysts. However, the high total number of analyzed hornblende crystals (approximately 200) makes it possible to overcome the individual variations by using mean average rim and core major element compositions and cation proportions (per formula unit). These were calculated for each sample, and subdivided based on intrusive phase association (Tables 6.1 and 6.2).

Compositional zoning within the Liw-Liw Creek dike hornblende phenocrysts varies between samples: two samples (BA08GS056 and BA08GS057; Table 6.1) contain phenocrysts that exhibit high SiO_2 and MgO, and low K_2O rims relative to average core composition (Fig. 6.7c and f; Table 6.1). However, the third Liw-Liw Creek sample (BA08GS035; Table 6.1) is characterized by hornblende phenocrysts with relatively little zonation. In comparison to hornblende core compositions, rims contain less SiO_2 (1 wt% difference) and slightly elevated Al_2O_3 (1.1 wt% difference); other major element values for rims and cores are broadly the same (Fig. 6.7a; Table 6.1).

On average, rim compositions of PHD hornblendes trend towards higher SiO_2 and MgO, and lower Al_2O_3, TiO_2, Na_2O and K_2O than their respective cores (Fig. 6.7a-c, e and f; Table 6.1). However, two samples (BA08GS002 and BA08GS005; Table 6.1) contain hornblende phenocrysts that reflect an average drop in rim SiO_2 wt% from core composition, with an average decrease of 1.1 and 2.1 wt% SiO_2 in the rims of BA08GS002 and BA08GS005, respectively (Table 6.1). In addition, BA08GS002 rims exhibit elevated MgO, with similar values for all other major elements with respect to core composition, whereas BA08GS005 rims are elevated in Al_2O_3, TiO_2, CaO and Na_2O, and depleted in FeO and MgO relative to the phenocryst cores (Fig. 6.7; Table 6.1).

Compositional data for HMG hornblendes suggests minimal variation between rim and core chemistry, with major elements exhibiting low levels of variation within

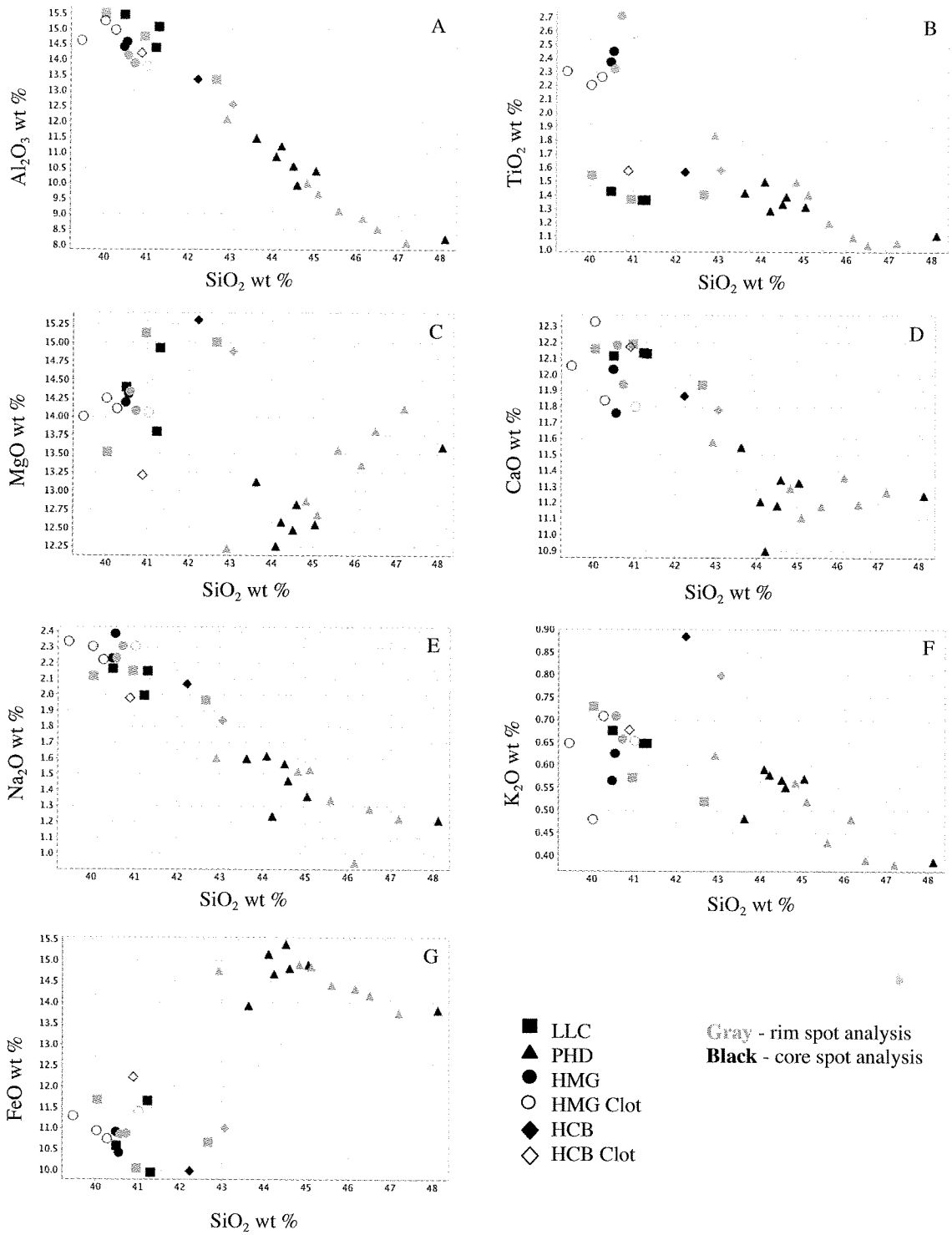

Figure 6.7 – Mean sample average major element oxide geochemistry for rim and core spot analyses: (A) Al_2O_3, (B) TiO_2, (C) MgO, (D) CaO, (E) Na_2O, (F) K_2O and (G) FeO.

individual phenocrysts (Fig. 6.7; Table 6.1). Deviation from this trend was detected in two hornblendes from sample BA08GS004, highlighted by a 1-2 wt% drop in Al_2O_3 from the core to rim (Appendix 2.3). The hornblende clusters contained in the HMG rocks are slightly less silicic than the lone phenocrysts (<1.5 wt% SiO_2 difference; Fig. 6.7; Table 6.1). Zonation in the hornblende clots is present, although it should be noted that only one sample (of three) was analyzed for both rim and core chemistry. This limit on analysis point locations is due to the nature of the cluster samples wherein individual phenocrysts are difficult to distinguish. Where rim and core spot analyses were conducted (sample BA08GS010; Appendix 2.3), average rim composition was marked by an increase in SiO_2 (1 wt%) and TiO_2 (0.4 wt%), as well as a decrease in Al_2O_3 (1.5 wt%) and CaO (0.6 wt%) over average core composition (Fig. 6.7a, b and d; Table 6.1).

HCB hornblendes are compositionally zoned, and exhibit higher rim values of SiO_2 and FeO, and lower Al_2O_3 and MgO when compared to core compositions (Fig. 6.7a,c and g; Table 6.1). Rim and core compositional analyses were not differentiated for the hornblende clusters contained within the HCB rocks as individual phenocrysts could not be identified within the clot. Nevertheless, the hornblende clots observed in the HCB rocks are characterized by higher Al_2O_3 and FeO, and lower SiO_2 and MgO than the rims and cores of individual hornblende phenocrysts (Fig. 6.7a, c and g; Table 6.1).

6.3.3 Plagioclase Feldspar

As noted in Chapter 7, plagioclase feldspar phenocrysts frequently exhibit sericitic alteration, sometimes to the point of complete destruction of the primary crystal habit. Care was taken to avoid analyzing the altered portions of phenocrysts. Due to the scarcity of plagioclase in some of the mafic samples (the HBD and the Liw-Liw Creek dikes), the population number for this data set (less than 75 phenocrysts) is smaller than that of the hornblende data set.

A total of nine samples were analyzed for the major element composition of their feldspar phenocryst populations. The sample suite included one sample from the Liw-Liw Creek dikes, seven from PHD and one from a hornblende-plagioclase clot within an HCB dike. Sample locations within the map area are provided in Fig. 6.8. Individual spot analyses are presented in Appendix 2.5.

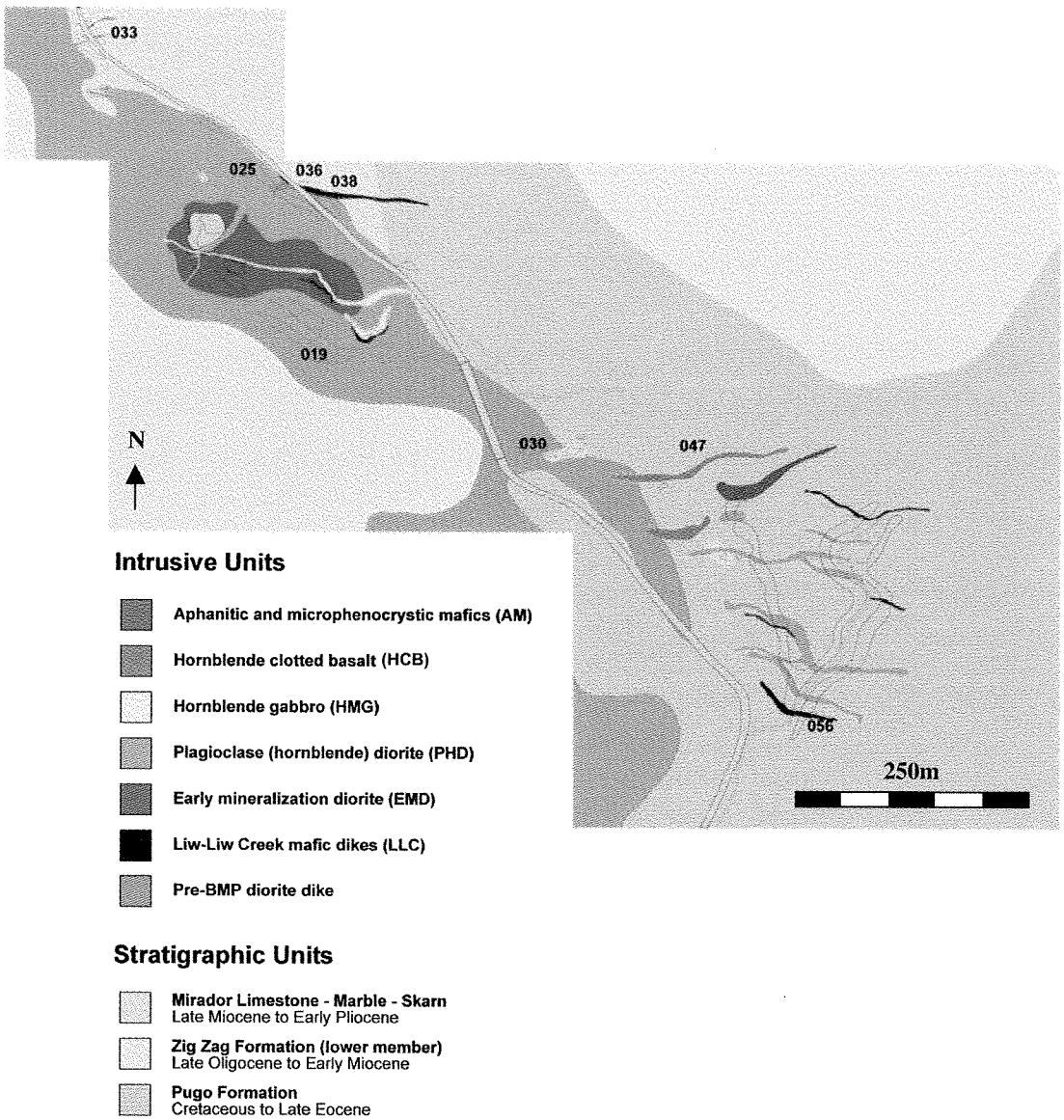

Figure 6.8 - Map of plagioclase sample locations.

The majority of feldspar phenocrysts within the Black Mountain Southeast Intrusive Suite can be broadly classified as andesine, labradorite and bytownite, with compositions ranging from An_{25} to An_{96} ($An_{\#}$, where # = 100*Ca wt%/(Ca wt% + Na wt%); Fig. 6.9; Appendix 2.5). However, there is some scatter towards orthoclase in the PHD rocks, due to the presence of weak to moderate potassic alteration (Chapter 7).

A single, unzoned feldspar phenocryst from the Liw-Liw Creek dike is labradorite, with an An_{58} core, and An_{59} rim (Fig. 6.9; Appendix 2.5). The largest spread of feldspar compositions is found in samples of the PHD. The majority of plagioclase

crystals plot as labradorite and bytownite (An_{50} to An_{70}), but the overall range is between An_{27} and An_{93} (Fig. 6.9; Appendix 2.5). Two PHD samples (BA08GS052A and BA08GS054) contain feldspars with K_2O content greater than 2.0 wt%, and are the cause of much of the scatter in Figure 6.9. Feldspars within the hornblende-plagioclase clots of HCB plot as labradorite, bytownite and anorthite, with An# between 50 and 96, though the majority of data points (five out of seven total) plot as purely anorthite (An_{90}-An_{96}; Fig. 6.9; Appendix 2.5).

Compositional zonation in Black Mountain Southeast plagioclase phenocrysts is generally very prominent (Chapter 3). However, the Electron Microprobe spot size of 35μm was frequently larger than individual compositional zones within the phenocrysts. It is therefore possible that core and rim compositions may not accurately represent the precise inner core or outermost rim chemistry. Nevertheless, one sample (BA08GS019; Fig. 6.10) was identified as containing plagioclase with a detectible variation in rim and core composition; the phenocryst cores recorded a composition of An_{54}-An_{65}, while the rim compositions were broadly lower at An_{26}-An_{58} (Appendix 2.5).

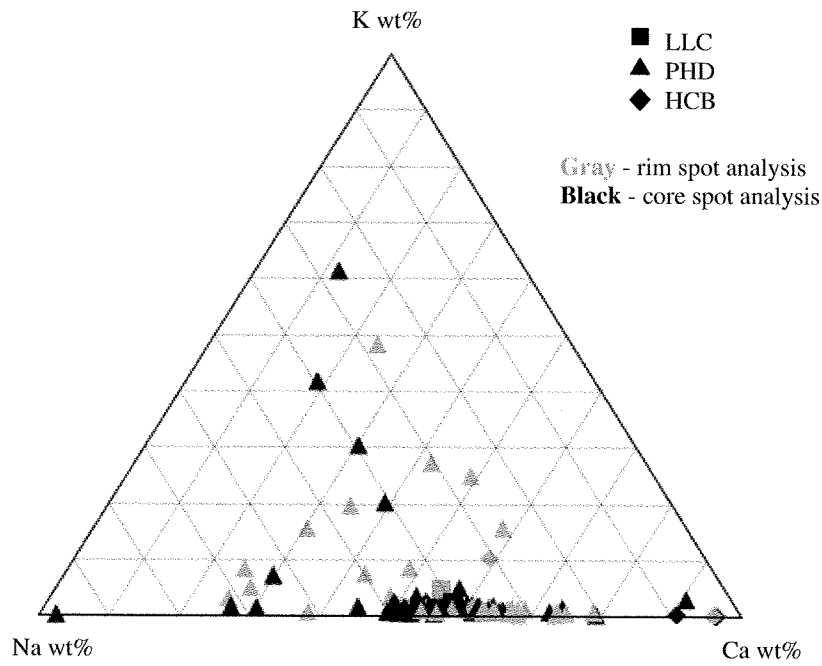

Figure 6.9 - Major element compositional variation of feldspar phenocrysts within the Black Mountain Southeast intrusive rocks.

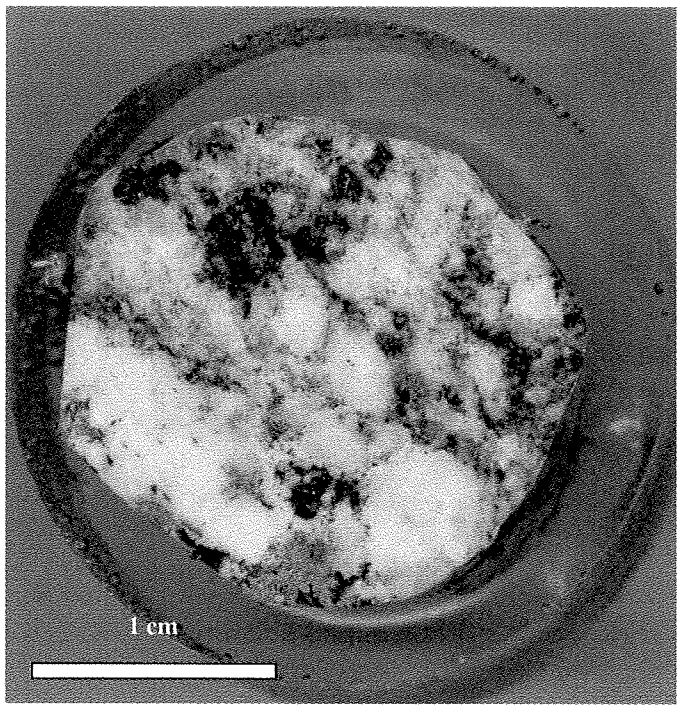

Figure 6.10 - Laser ablation puck of sample BA08GS019, containing well zoned plagioclase phenocrysts with higher core An#'s relative to rim compositions.

6.4 Discussion

As previously mentioned, the complete classification of amphibole species is a highly involved process, much of which is still contentious (e.g., Leak, 1968, 1978; Leak et al., 1997; Hawthorne and Oberti, 2006, 2007; Martin, 2007). Even within the specific igneous environment of calc-alkaline island arc magmatism, the differentiation of hornblende species is difficult due to the plethora of primary chemical and environmental variables during crystallization (Martin, 2007) as well as the potential for deuteric alteration (Féménias et al., 2006). Nevertheless, broad implications for the magmatic evolution of the Black Mountain Southeast Intrusive Suite may be made from the hornblende geochemical data set.

6.4.1 Implications for Magmatic Components and Their Interactions

In their study of amphibole species of the porphyritic Motru dike swarm (South Carpathian Mountains, Romania), Féménias et al. (2006) reported a correlation between rock type and the core composition of associated amphibole phenocrysts. Notably, more

felsic rocks (dacitic and rhyolitic dikes) contained calcic hornblendes with higher silica and lower alkali cores, whereas mafic rocks (andesites, basaltic andesites and trachyandesites) contained lower silica and higher alkali hornblende cores. These findings broadly imply that crystallization of a felsic/intermediate melt produces low alkali, high silica hornblendes, whereas crystallization of a mafic magma yields higher alkali, lower silica hornblendes. The compositional division between Group 1 and Group 2 hornblendes reflects a similar correlation within the Black Mountain Southeast rocks; the diorites of the PHD contain higher silica, lower alkali Group 1 hornblendes, and the andesites and basalts of the Liw-Liw Creek dikes and the HMG and HCB intrusive phases contain low silica, high alkalis Group 2 hornblendes (Fig. 6.6; Table 6.1; Appendix 2.3). Coupled with the intrusive timing relationships (emplacement of Group 2 hornblendes within the Liw-Liw Creek dikes followed by Group 1 hornblendes within the PHD, and finally Group 2 hornblendes within the HMG and HCB; Chapters 3 and 4), this distinct geochemical division documents physically and temporally unique crystallization events of felsic and mafic components.

Two hornblende core analysis points (out of seven total analyzed phenocrysts) from sample BA08GS033B, plot consistently within the Group 2 hornblende field and may represent inherited phenocrysts and/or changing liquid compositions (Figs. 6.4 and 6.6). The existence of an intrusive phase containing phenocrysts from both hornblende groups implies interaction of the mafic and felsic magmas at some point during the evolution of the Black Mountain Southeast porphyry. As discussed in Chapter 2, the PHD rocks show gradational textural and mineralogical variability throughout the map area, possibly the result of generation and emplacement of a heterogeneous melt. It is possible that this sample of dioritic PHD magma (represented by sample BA08GS033B) contains inherited mafic-associated hornblendes, and records a point of physical interaction between an intermediate melt and a mafic magma component. Other PHD rocks may contain Group 2 hornblendes, but given the small physical size of samples for this thesis (standard thin section or one inch diameter laser ablation "pucks"), and the relatively low volume of hornblende phenocrysts contained within many PHD rocks, the probability of encountering Group 2 hornblendes within PHD diorites is low.

Given that the Black Mountain Southeast Intrusive Suite hornblende populations experienced minimal deuteric alteration, the compositional zonation of the hornblende phenocrysts can be viewed as a product of changing magma chemistry during crystallization. Most intrusive phases exhibit a tendency towards enrichment of SiO_2 and a depletion of alkalis in the rims of hornblende phenocrysts (Fig. 6.7; Table 6.1). In particular, five of the seven PHD samples contain hornblendes with rim compositions reflecting a 0.5 to 2.5 wt% increase in SiO_2 and a 0.25 to 0.5 wt% decrease in alkali content (Fig. 6.7; Table 6.1). According to Fémênias et al. (2006), this shift in rim chemistry relative to core composition may imply crystallization in a progressively more felsic liquid, concurrent with fractional crystallization. In turn, fractional crystallization of the felsic/intermediate melt tends to support the idea that the mafic-associated and felsic-associated hornblende crystallization events were physically and/or temporally separate. However, the other two PHD samples (BA08GS005 and BA08GS002) contain hornblendes that demonstrate decreased SiO_2 and increased alkalis in rim compositions (Fig. 6.7; Table 6.1). This may imply interaction and mixing of the crystallizing felsic/intermediate melt with a more mafic magma. The prominent, closely-spaced zonation of plagioclase phenocrysts coupled with the high level of feldspar alteration within the Black Mountains Southeast Intrusive Suite (Chapter 7) prohibits quantitative calculations of magmatic evolution from the geochemical data, but does suggest that magma compositions varied during their crystallization.

6.4.2 Implications for Intra-crustal Magma Pooling and Crystallization

Hammarstrom and Zen (1986) proposed that the total aluminum content of hornblende in calc-alkaline plutons could be used to approximate pressure and depth of crystallization. This igneous barometer operates on the crystallization of minerals with octahedral Al coordination in higher pressure environments, and the supposition that crystallizing calc-alkaline plutons have enough thermodynamic restrictions (P-T-x) such that hornblende Al content is reflective of pressure only (Hollister et al., 1987). In the case of hornblende, tschermakite [$Ca_2(Fe, Mg)_3Al_2SiO_{22}(0H)_2$] is the pressure-sensitive component. The geobarometer was confirmed and calibrated by Hollister et al. (1987), and was further refined by the experimental calibrations of Johnson and Rutherford (1989) and Schmidt

(1992) to ultimately encompass a range of temperatures and pressures of 600-800 degrees C and 1.5-13 kbar. In order to restrict inferred thermodynamic variance present during magma crystallization, Hammarstrom and Zen (1986) and Hollister et al. (1987) laid down a series of mineralogical requirements that must be satisfied. These are: (1) the phases quartz, plagioclase, hornblende, biotite, orthoclase, titanite and magnetite must have crystallized together, (2) only hornblende rim compositions should be used, as they crystallized with the last remaining melt (limiting the temperature variation to a small range), and (3) the plagioclase rim compositions should be consistent (Hollister et al., 1987 suggested between An_{25} and An_{35}). Additionally, the hornblende geobarometer was established for roughly equigranular plutonic rocks (a necessity to ensure broadly contemporaneous crystallization of the aforementioned mineral phases).

The Black Mountain Southeast rocks do not fully satisfy any of the requirements laid out by Hammarstrom and Zen (1986) and Hollister et al. (1987); the mineral assemblage varies considerably between intrusive phases, plagioclase compositions range significantly and on average are above An_{50}, and the Black Mountain Southeast rocks are dominantly porphyritic, potentially negating contemporaneous crystallization of the minerals present. However, the primary reason for utilization of the igneous geobarometer is to investigate intra-crustal pooling and fractional crystallization of bimodal magmatic components within the Black Mountain Southeast system (Chapter 5). Exact depth and pressure measurements are not required to do this. Rather, a broad difference in depth of crystallization for the two hornblende groups would support the pooling and crystallization of at least two magmatic components during the lifetime of the Black Mountain Southeast system.

Within the crystalline structure of hornblende, Al is present at the T site as Al^{iv} and at the M1, M2 and M3 sites as Al^{vi}. Al^{iv} was calculated as the difference between full T site (tetrahedral) occupancy (8 cations) and the number of Si cations, implying that increasing silica yields decreasing Al^{iv} (Hammarstrom and Zen, 1986). Similarly, Al^{vi} (octahedral aluminum) was calculated by subtracting the Al^{iv} cation value from total Al cations (Al^{T}). The end result is that both Al^{iv} and Al^{vi} are dependant on Si content of the hornblendes. Thus in order to separate the effect of crystallization pressure on Al content of hornblende, Si activity needs to be determined. Cawthorn (1976) and Fémênias et al.

(2006) noted that increasingly Si-rich melts crystallize increasingly Si-rich hornblendes. However, once quartz crystallizes (and silica activity in the melt = 1), amphibole crystallization is no longer affected by melt silica contents. Therefore, the presence of quartz alongside or within hornblende phenocrysts removes silica activity as a variable in pressure-determined Al content of hornblendes. For the Black Mountain Intrusive Suite, quartz was identified alongside hornblende phenocrysts in samples of PHD and HMG, as well as possibly in a sample of Liw-Liw Creek dike.

With the observation of quartz and hornblende together, we can broadly assume that the division of the Group 1 and Group 2 hornblendes based on Al content (Figs. 6.4a; 6.6a; 6.7a) is a feature of crystallizing pressure, and thus depth. This in turn implies a physical stratigraphical division within the crust of the hornblende crystallizing events and their respective magmas, with crystallization of a mafic component taking place at a greater depth than that of the intermediate/felsic component. This observation strongly supports the idea of intracrustal pooling and fractional crystallization of the magmas that gave rise to the Liw-Liw Creek mafic dikes, as well as the emplacement and crystallization of felsic/intermediate magmas at a stratigraphically higher level.

6.5 Summary

Variations in major element geochemistry of hornblende phenocrysts provide further insight into the intracrustal evolution of the magmas that gave rise to the Black Mountain Southeast porphyry system. The distinctly different compositions of the two identified hornblende groups (Group 1 and Group 2) imply two separate hornblende crystallization events in the presence of two compositionally distinct magmas during the lifetime of the Black Mountain system. The lower total aluminum content of the Group 1 hornblendes (in comparison to the Group 2 hornblendes) is indicative of a lower pressure (and thus shallower) crystallization environment, suggesting physical separation, ponding and crystallization of at least two magmas. However, the occurrence of Group 1 and Group 2 hornblende phenocrysts within a single sample suggests that at some point during the system's evolution, the two magmas interacted. Phenocryst exchange and magma mixing would have taken place at this time.

Chapter 7

Alteration and Green Rock Geochemistry of the Black Mountain Southeast Porphyry System

7.1 Introduction

For this thesis, the alteration assemblages associated with the Cu-Au mineralization in the Southeast orebody of the Black Mountain Porphyry system were differentiated and documented through field mapping and petrographic work. As a part of the AMIRA P765A project, emphasis was placed on developing the understanding of trace element zonation within the propylitic alteration halo of the mineralized system as a function of distance from the porphyry center. Specifically, this work addressed the control of host rock geochemistry on the chemistry of secondary epidote, and whether or not element zonation in propylitic alteration is a primary feature of the hydrothermal fluids. The first part of this chapter focuses on the alteration assemblages identified at Black Mountain Southeast, including their spatial distributions and mineralogical characteristics. The second section discusses lithogeochemical controls on epidote trace element geochemistry within the propylitic alteration halo at Black Mountain.

7.2 Alteration of the Black Mountain Southeast Porphyry System

7.2.1 Previous Research: A Model for Porphyry System Alteration

The study of the spatial distribution and development of alteration assemblages in porphyry Cu deposits has evolved considerably over the last 40 years, with work by Lowell and Guilbert (1970), Gustafson and Hunt (1975), Sillitoe and Gappe (1984), Sillitoe (2010) and many others leading to a broad model for porphyry alteration anatomy. Though the petrogenetic implications differ between specific deposit models, four distinct alteration packages zoned about a central porphyry stock (or series of stocks) are generally consider to be a ubiquitous feature of porphyry Cu hydrothermal systems. These can be broadly distinguished by their mineralogy as potassic (quartz-orthoclase-biotite), phyllic (quartz-sericite-pyrite), argillic (quartz-kaolinite-montmorillonite) and propylitic (chlorite-epidote-carbonate) alteration (Meyer and Hemley, 1967; Lowell and Guilbert, 1970; Gustafson and Hunt, 1975; Sillitoe and Gappe, 1984; Sillitoe, 2010 and

others). However, the spatial distribution and petrogenesis of the alteration varies between individual deposits as a function of local structural and lithological controls, as well as depth of magmatic emplacement and magma chemistry. In their early work, Lowell and Guilbert (1970) and Gustafson and Hunt (1975) both acknowledged this variability inherent in porphyry alteration systems, and suggested that their respective models were "variations on a theme" (Gustafson and Hunt, 1975).

The development of distinct alteration assemblages in porphyry Cu systems has been attributed by Gustafson and Hunt (1975) and Sillitoe (2010) to decreasing system temperatures and a downward propagation of the hydrostatic-lithostatic transition, as a product of the solidification of underlying parental magmas. At high temperatures (>350°C), a two-phase saline liquid and vapor are responsible for potassic alteration and mineralization at depth, as well as high-level advanced argillic alteration (Sillitoe, 2010). Below 350°C, the fluid reverts to a single-phase saline liquid and is generates the sericitic and propylitic alteration assemblages (Sillitoe, 2010). However, because fluid temperature at a given location within an active porphyry system is dependent on distance from the heat source (i.e. the porphyry intrusive center), contemporaneous development of multiple alteration assemblages is thought to occur in porphyry systems (Sillitoe, 2010). For example, cooling of fluids migrating outwards from the intrusive center during early stage potassic alteration may generate propylitic alteration of country rocks peripheral to the porphyry intrusive center (Gustafson and Hunt, 1975; Sillitoe, 2010). Nevertheless, Sillitoe (2010) proposed a broad chronology for the evolution of porphyry alteration systems wherein early potassic alteration at depth of the intrusive center grades outward to propylitic (as well as advanced argillic) alteration. As the system cools and the lithostatic-hydrostatic transition collapses inwards, chlorite-sericite or phyllic alteration, and late stage advanced argillic alteration are generated overprinting the earlier potassic and propylitic assemblages. This overprinting (also known as telescoping) of alteration assemblages is also attributed to paleosurface erosion concurrent with the evolution of the hydrothermal alteration system (Sillitoe, 2010).

Previous work on the Black Mountain Kennon and Southeast porphyry systems identified potassic alteration and silicification coincident with the ore zones, defined by a well-developed quartz vein stockwork, quartz flooding and biotite alteration (Waters and

Gonzales, 2005; Waters et al., 2006). These authors identified a halo of pyrite-chlorite-epidote-gypsum alteration surrounding the potassically altered mineralized cores. An elongate pyrite alteration halo was also identified around both deposits, extending along a northwest trend for 2.75 km as a series of pyrite-limonite veins (Waters and Gonzales, 2005; Waters et al., 2006; R. Gonzales pers. com., 2008).

7.2.2 Alteration Assemblages at Black Mountain Southeast

Field observations and petrographic work undertaken as part of this study have identified three major alteration assemblages at Black Mountain Southeast: potassic, phyllic and propylitic alteration assemblages, as defined by Meyer and Hemley (1967). Spatial distribution and arrangement of alteration roughly reflects a bull's-eye pattern centered over the stock of EMD, central to the map area (Figs. 3.4 and 7.1). Alteration was assessed petrographically through the following parameters:

1. Alteration mineralogy
    a. Relict primary mineral(s)
    b. Secondary mineral(s)
2. Intensity of alteration (proportion of original mineral altered/replaced by area): none, low (up to one third replaced), moderate (one third to two thirds replaced), high (two thirds to nearly complete replacement), complete.

Potassic Alteration

Potassic alteration crops out at the center of the Black Mountain Southeast map area as a sub-circular halo approximately 150 meters in diameter (Fig. 7.1). It is limited to the EMD plug and some of the bordering PHD diorites at the center of the map area, as well as a small outcrop of PHD approximately 300 meters southeast of the map center (Figs. 3.4 and 7.1). The potassic alteration is associated with an intense quartz vein stockwork and quartz flooding, and is characterized by biotite replacement in EMD and PHD rocks (Figs. 3.4 and 7.1). In slabbed samples of EMD, the quartz stockwork veins have halos of grayish brown biotite up to 2 mm wide, as well complete destruction of primary

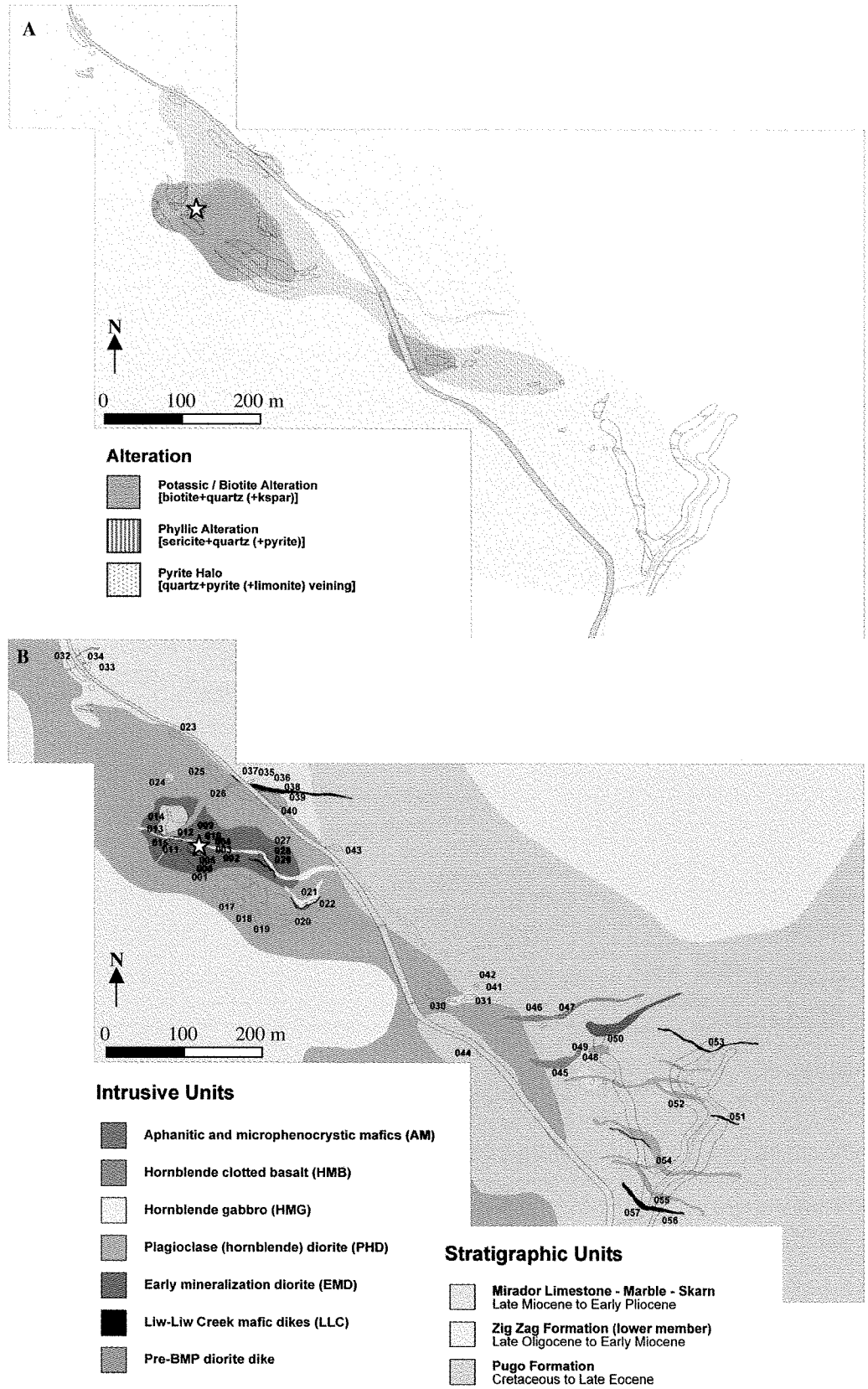

Figure 7.1 – (A) Map of distribution of alteration assemblages at the Black Mountain Southeast. (B) Corresponding lithology map of the Black Mountain Southeast and sample locations. Note the star denoting the inferred ntrusive center in the map area.

igneous textures (Fig. 7.2a). The potassic alteration of EMD rocks is spatially associated with Cu-Au-(Mo) mineralization. Minor amounts of molybdenite are observed within or bordering the quartz veins. Finely disseminated pyrite and chalcopyrite is observed throughout the groundmass as well as small (<2mm) amorphous patches of chrysocolla or malachite (presumably from leaching of copper from chalcopyrite; Fig. 7.2b).

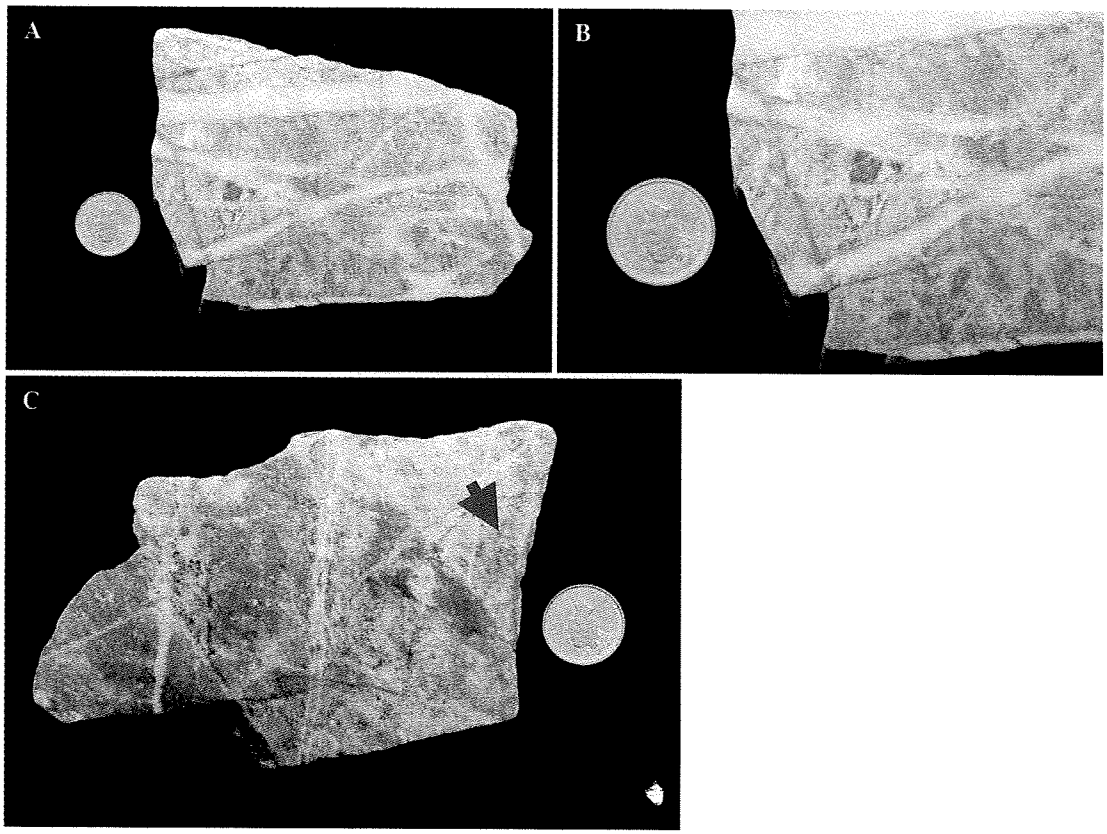

Figure 7.2 - (A) Polished slab of EMD stockwork veining (BA08GS001). Note the distinct orientation of the quartz vein sets. (B) A close up photograph of sample BA08GS001. Note the biotite alteration of EMD rock, denoted by thin brown-yellow quartz vein selvages approximately 5 mm wide. (C) Polished slab of EMD rock (sample BA08GS012). Note the disseminated pyrite and chalcopyrite throughout the sample, as well as a light green-blue copper staining (indicated by the arrow).

The nature of the pervasive potassic alteration assemblage in the central PHD diorites varies considerably. It is present as small (<25μm) replacement biotite grains in the groundmass of the rock, as well as moderate to complete biotite replacement of hornblende (Fig. 7.3a-c). Plagioclase grains are not affected (Fig. 7.3d). Small (<1cm diameter) quartz veins observed in some PHD samples display increasingly hornblende destructive biotite alteration proximal to their contacts with the groundmass (Fig. 7.3a

and e). Many hornblende phenocrysts in contact with, or cut by, the quartz veins have been completely replaced by biotite books (Fig. 7.3e), however, the veins themselves do not contain biotite.

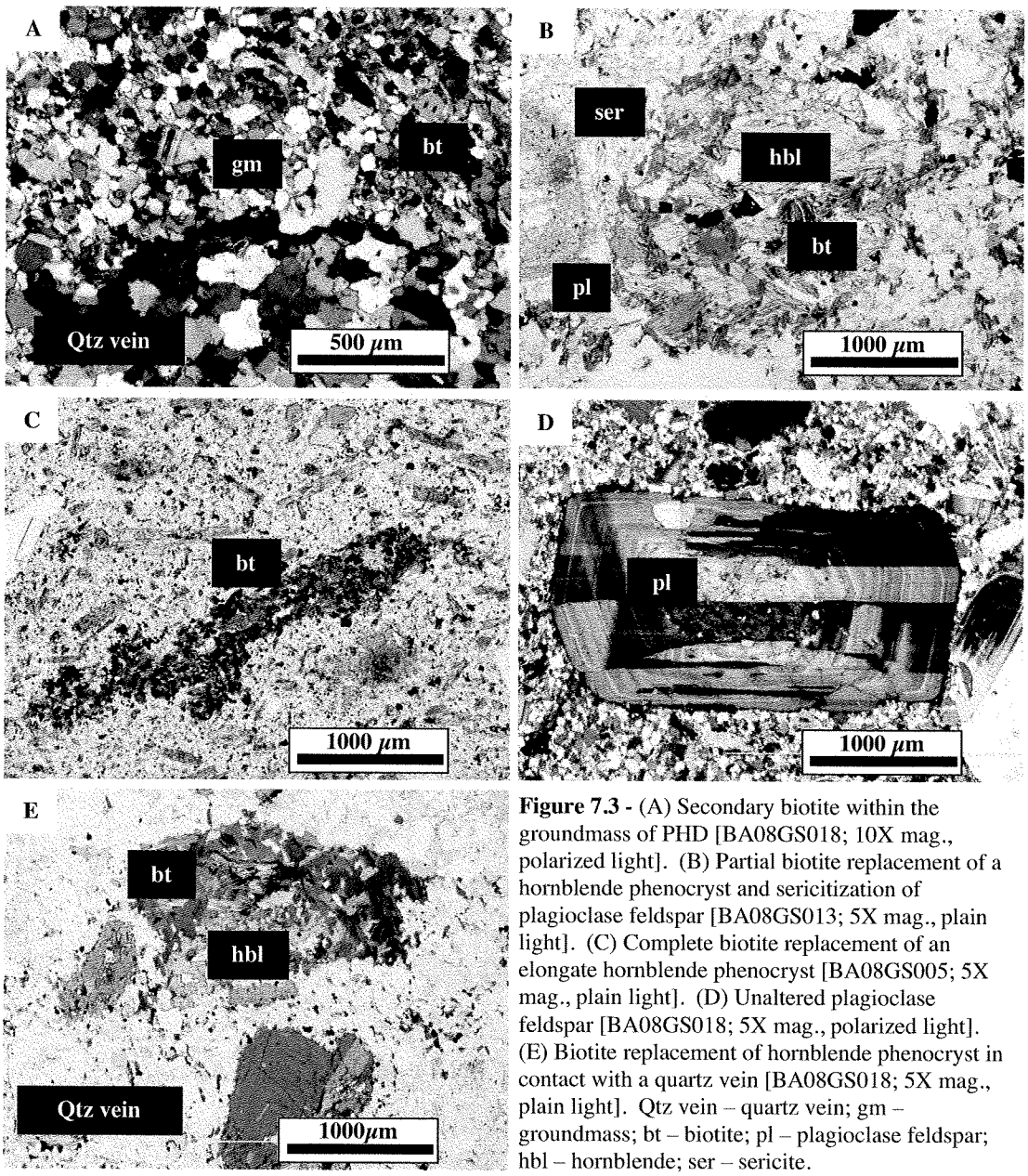

Figure 7.3 - (A) Secondary biotite within the groundmass of PHD [BA08GS018; 10X mag., polarized light]. (B) Partial biotite replacement of a hornblende phenocryst and sericitization of plagioclase feldspar [BA08GS013; 5X mag., plain light]. (C) Complete biotite replacement of an elongate hornblende phenocryst [BA08GS005; 5X mag., plain light]. (D) Unaltered plagioclase feldspar [BA08GS018; 5X mag., polarized light]. (E) Biotite replacement of hornblende phenocryst in contact with a quartz vein [BA08GS018; 5X mag., plain light]. Qtz vein – quartz vein; gm – groundmass; bt – biotite; pl – plagioclase feldspar; hbl – hornblende; ser – sericite.

Propylitic Alteration

Propylitic alteration occurs as a halo around the potassically altered and silicified core of the Black Mountain Southeast porphyry, and extends throughout the map area (Fig. 7.1). It is characterized by epidote veins and replacement, as well as minor chlorite and carbonate replacements and/or veins. Propylitic alteration is not specific to any intrusive phase, and has been identified in samples of PHD and HBC, as well as the pre-BMP diorite dikes, Liw-Liw Creek mafic dikes, Pugo mafic dikes and Mirador/Kennon limestone outcrop associated with the Thanksgiving Skarn (Chapters 2 and 3).

Epidote veins occur proximal to the deposit center, whereas selective replacement of plagioclase by epidote occurs peripheral to Black Mountain. For example, the edge of the potassic alteration halo is characterized by prominent epidote veins (<1cm wide) and moderate to complete epidote replacement of plagioclase and hornblende phenocrysts proximal to the veins (Chapter 3; Figs. 7.1 and 7.4a-c). However, in the more distal Liw-Liw Creek samples, some plagioclase phenocrysts are moderately to completely replaced by epidote (Fig. 7.4d). Epidote was also observed as amorphous, patchy groundmass replacement in samples proximal to the Southeast ore zone (Fig. 7.4e-g). Minor epidote veining was also observed at the northern edge of the map along Kennon Road, and was associated with outcrop and boulders of skarn-style mineralization (the latter of which may have originated from the nearby Thanksgiving Skarn deposit; Figs. 2.2 and 7.1; Callow, 1976).

Minor chlorite replacement of hornblende phenocrysts and carbonate veining occur around the outer edges of the central potassic alteration assemblage (Figs. 7.1, 7.4h and 7.5).

Phyllic Alteration

Phyllic alteration at Black Mountain is present as plagioclase-destructive sericitization. The domain of sericite alteration defines a crescent-shaped halo around (and overlapping with) the central potassic alteration, and extends to the southeast for approximately 700 meters, overlapping the propylitic alteration (Fig. 7.1). Although frequently found near the center of the deposit, quartz-pyrite (+limonite) veins were observed throughout the

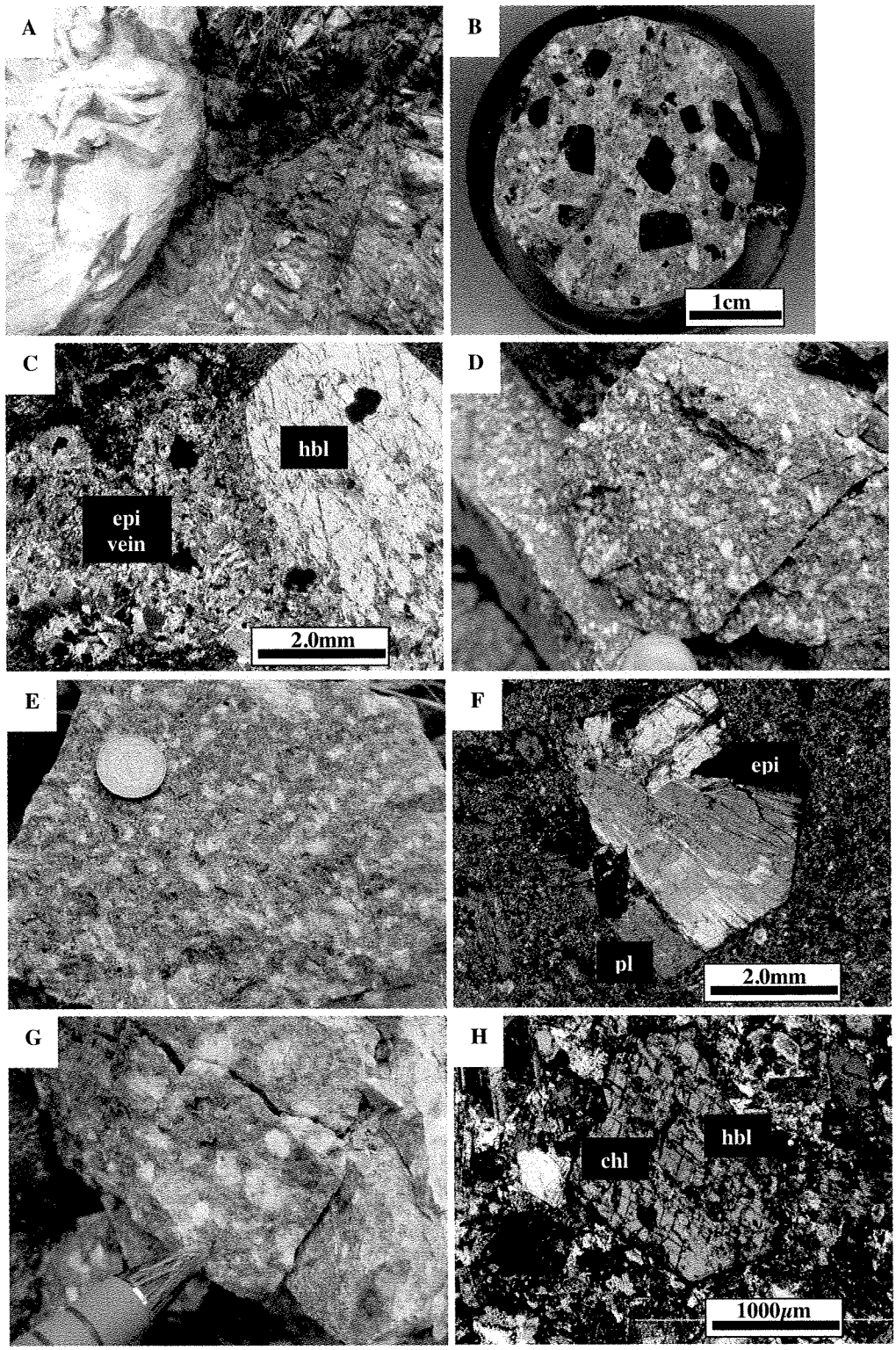

Figure 7.4 - (A) Outcrop of BA08GS035 [photo: David Cooke, March 2008] (B) Laser ablation puck of sample BA08GS035. (C) Partial replacement of hornblende by epidote proximal to epidote veining [BA08GS035; 2.5X mag., polarized light]. (D) Epidote selectively replacing plagioclase feldspar in sample BA08GS054 [photo: David Cooke, March 2008]. (E) Selective replacement of plagioclase and groundmass by epidote in sample BA08GS026 [photo: Mike Baker, March 2008]. (F) Epidote replacement of plagioclase feldspar and groundmass [BA08GS026; 2.5X mag., polarized light]. (G) Patchy replacement of groundmass and plagioclase in sample BA08GS036 [photo: David Cooke, March 2008]. (H) Minor chlorite replacement of hornblende [BA08GS025; 5X mag., polarized light]. Epi vein – epidote vein; carb vein - carbonate vein; gm – groundmass; chl – chlorite; pl – plagioclase feldspar; hbl – hornblende.

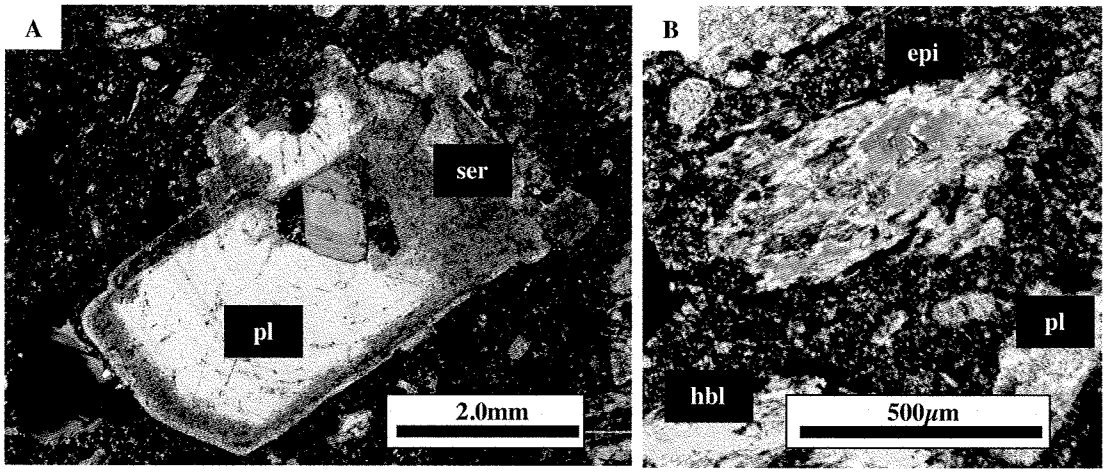

Figure 7.5 - (A) Chlorite replacement of groundmass [BA08GS025; 20X mag., plain light]. (B) Carbonate vein crosscutting a plagioclase feldspar phenocryst and groundmass [BA08GS025; 5X mag., polarized light]. Carb vein - carbonate vein; gm – groundmass; chl – chlorite; pl – plagioclase feldspar.

map area, beyond the extent of identified sericitic alteration. For example, weathering of east-trending quartz-pyrite (+limonite) veins within the central PHD rocks has resulted in rust-colored surfaces visually similar to E-trending quartz-pyrite sheet veins observed along Liw-Liw Creek (Figs. 7.1; 7.6a and b). Sericitic alteration is also present in centrally located outcrops of PHD and HMG.

Sericitic alteration varies from incipient to complete replacement of plagioclase feldspar phenocrysts (Fig. 7.6c and d). There is clear no pattern defined by complete versus weak sericitization, as intensity can vary within individual laser ablation pucks. Individual samples contain plagioclase phenocrysts that reflect the full range of sericitization, from weak to complete (Fig. 7.6e and f).

Quartz-pyrite (+limonite) veins are thin (<10cm diameter), generally E-trending features randomly spaced across the map area. However, one outcrop at the base of a large landslide in the southeastern portion of the map area contained a high concentration of closely spaced quartz-pyrite veins (Fig. 7.6g). Although not found in the outcrop, fragments of coarse, euhedral quartz-pyrite veins were found on the ground nearby (Fig. 7.6h).

7.2.3 Spatial and Temporal Implications

Although individual alteration zones are clearly definable over the map area, some overlap between potassic, propylitic and sericitic assemblages occurs near the margins of

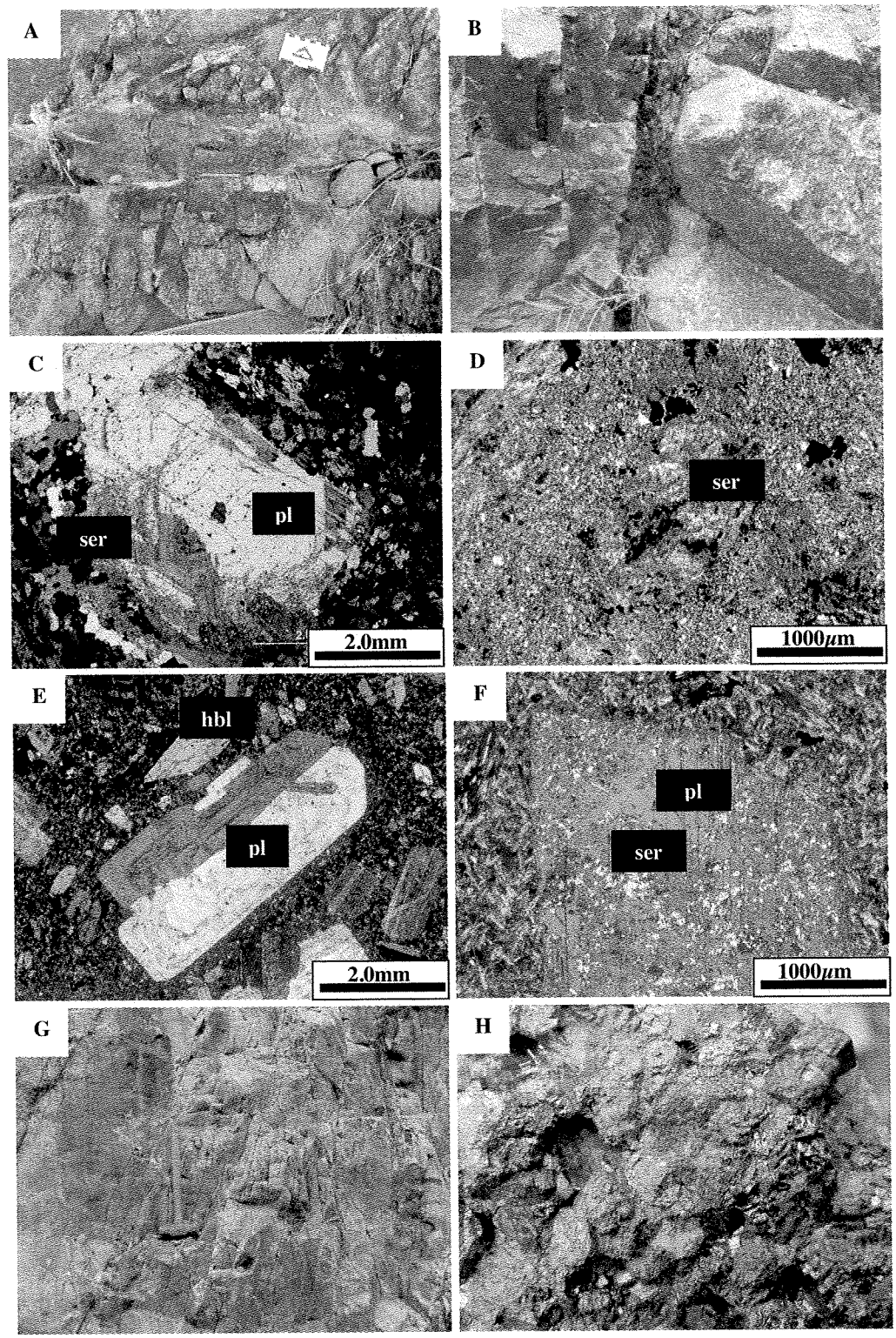

Figure 7.6 - (a) Quartz-pyrite (+limonite) veining in PHD diorite [photo: Mike Baker, March 2008] (b) Quartz-pyrite (limonite) vein in Pugo Formation up Liw-Liw Creek [photo: David Cooke, March 2008]. (c) Minor sericite replacement of phenocrystic plagioclase feldspar [BA08GS0019; 2.5X mag., polarized light]. (d) Complete replacement of plagioclase feldspar by sericite [BA08GS026; 5X mag., polarized light]. (e) Unaltered, fresh plagioclase phenocryst [BA08GS040; 2.5X mag., polarized light]. (f) Moderate sericite alteration of plagioclase felspar [BA08GS040; 5X mag., polarized light]. (g) Closely spaced quartz-pyrite veining within sample BA08GS048 [photo: David Cooke, March 2008]. Pl – plagioclase feldspar; hbl – hornblende; ser – sericite.

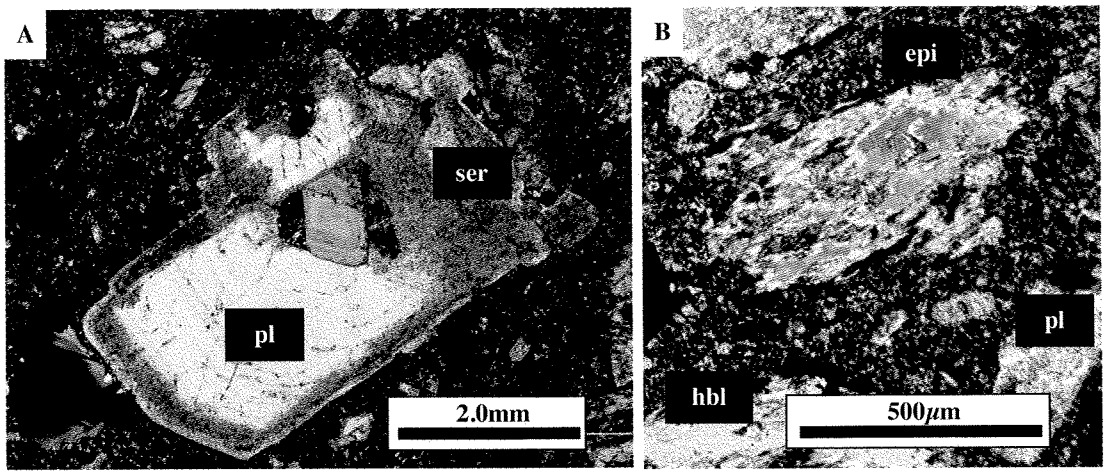

Figure 7.7 - (a) Sericitization of plagioclase feldspar phenocrysts [BA08GS023; 2.5X mag., polarized light] and (b) replacement of hornblende microphenocryst by epidote [BA08GS023; 10X mag., polarized light]. Pl – plagioclase feldspar; hbl – hornblende; epi - epidote; ser - sericite.

the central potassic alteration halo (Fig. 7.1). For example, a PHD dike approximately 50 meters to the west-northwest of the map center has undergone incipient to complete replacement of hornblende by biotite, but also exhibits moderate sericitization of associated plagioclase phenocrysts (Fig. 7.3b). Similarly, an outcrop of PHD, 170 meters north of the map center exhibits moderate sericitization of plagioclase rims and moderate to complete selective epidote replacement of hornblende phenocrysts (Fig. 7.7a and b). There is no detectable overlap between the propylitic and potassic alteration zones.

Spatial association between the Black Mountain Southeast intrusive phases (Chapter 3) and alteration zonation varies by alteration type. The propylitic alteration assemblage and the quartz-pyrite (+limonite) veins are observed throughout the Black Mountain Southeast map area (Fig. 7.1), and do not appear to have a direct spatial correlation with any specific intrusive phase. In contrast, potassic alteration is spatially correlated with and restricted to the vicinity of dikes and plugs of EMD and PHD at the center of the map area (Figs. 3.4 and 7.1). Texturally destructive biotite alteration and quartz stockwork veining and flooding is confined to the EMD plug (Figs. 3.4 and 7.1). Domains of less intense potassic alteration (including moderate biotite replacement and thinner, less visually prominent quartz veins) occur in PHD plugs and dikes (Figs. 3.4 and 7.1). This suggests a correlation between the level of potassic alteration and the intensity of quartz veining, as is common at most porphyry Cu deposits (e.g., Titley, 1982).

Sericite alteration has only affected plugs and dikes of EMD and PHD at the center of the map area. Whereas the PHD dikes that cut the EMD plug have been both potassically and sericitically altered, the HMG dikes that cut EMD rocks contain only sericitic alteration. Despite its amorphous distribution within the map area, the clear NW-trend of the sericite alteration domain indicates a structural control.

The spatial association of alteration with intrusive phases provides info as to the timing of alteration events with respect to each other and emplacement of the intrusive phases (Chapters 3 and 4). The occurrence of well-developed quartz stockwork veining and texturally destructive biotite replacement and quartz flooding only in the EMD suggests that peak potassic alteration followed the emplacement of the EMD stock, but mostly preceded the emplacement of the PHD. In particular, the formation of the observed quartz vein set orientations unique to the EMD plug requires brittle fracturing of the plug, and thus implies that quenching of the diorite magma occurred prior to potassic alteration. Conversely, the less advanced biotite replacement and less developed quartz veining (without preferred orientations) of the PHD rocks, suggests that their emplacement coincided with a later, weaker potassic alteration event. The absence of potassic alteration and the presence of sericitization within the HMG dikes suggests that the dikes were emplaced after the potassic alteration event, but prior to or during phyllic alteration (Fig. 7.1). Consequently, potassic and phyllic alteration of the BMPSE can be viewed as temporally separate events, with the potassic event preceding (and being overprinted by) the phyllic event. This is typical of porphyry Cu-Au deposits (e.g., Wilson et al., 2003; Hedenquist et al., 1998).

The relative timing of the propylitic alteration at Black Mountain Southeast is not easy to constrain. Spatially, the propylitic assemblage does not correlate with any specific intrusive phase and does not appear to have a strong structural control on its distribution. However, there is no observable overlap between the propylitic and potassic alteration zones, perhaps suggesting contemporaneous formation (unlike the later stage phyllic alteration assemblage). The pervasive quartz-pyrite (+limonite) veins cut through nearly all rock and alteration types, implying that they are a late stage feature of the Black Mountain Porphyry Southeast system.

7.2.4 Summary

The alteration zones identified within the Black Mountain Southeast map area (potassic, propylitic and phyllic) and their respective spatial distribution and relative timing are broadly consistent with other models of porphyry alteration systems (Gustafson and Hunt, 1975; Hedenquist et al., 1998; Wilson et al., 2003; Lickfold et al., 2003; Sillitoe, 2010) as well as previous observations made for the Black Mountain Kennon and Southeast orebodies (Sillitoe and Gappe, 1984; Waters and Gonzales, 2005; Waters et al., 2006). The restriction of potassic alteration to the first two intrusive phases (as well as overprinting by other alteration assemblages) implies that it developed early in the evolution of the Black Mountain Southeast alteration system. Although the timing of propylitic alteration at Black Mountain is not well defined, its existence outside of the intrusive center and the lack of overlap with the potassic alteration assemblage suggests simultaneous formation of propylitic and potassic alteration assemblages (Gustafson and Hunt, 1975; Sillitoe, 2010). Similarly, the weak "zoning" of epidote morphology away from the intrusive center is in agreement with the proposed decrease of the thermal gradient outboard of the intrusive center, and the resultant changes in alteration assemblages (Gustafson and Hunt, 1975; Bowman, 1987; Sillitoe, 2010). The observed late-stage overprinting of potassic and propylitic assemblages by structurally-controlled phyllic alteration is similar to what has been observed at many other porphyry deposits (e.g., Gustafson and Hunt, 1975), and signifies late stage alteration of the Black Mountain system, following potassic and propylitic alteration, and mineralization.

7.3 Whole Rock and Mineral Geochemistry

The AMIRA P765 project (concluded in 2006) investigated the application of alteration mineral chemistry as determined by laser ablation inductively coupled plasma mass spectrometry analysis (LA-ICPMS) in the exploration and targeting of porphyry copper-gold-molybdenum systems (Cooke et al., 2006). Trace elements in epidote were found to vary systematically with respect to proximity to porphyry centers, and also had potential to discriminate between fertile and infertile porphyry systems (Cooke et al., 2006). Research in the Baguio mineral district focused on epidote geochemistry from the propylitic alteration halos of three porphyry systems (Black Mountain, Nugget Hill and

Ampucao), one skarn deposit (Mexico) and one epithermal vein system (Acupan; Chapter 2). Cooke et al. (2006) noted systematic variations in the maximum concentrations of trace elements in epidote relative to the distance from the deposit center. The trace elements examined were subdivided into three groups based on their behavior in epidote:

1. The highest Cu, Zn, Sn and Mo abundances were found in epidote from inside pyrite halos, though the levels were frequently below the corresponding bulk rock composition.
2. Maximum rare earth element (e.g., La, Y, Zr and Sr) abundances were identified adjacent to the pyrite halo with values up to an order of magnitude greater than whole rock compositions
3. Peak As, Sb, Pb and U occurred outside the pyrite halos with values up to an order of magnitude higher than whole rock compositions

The enrichment of REE, As, Sb, Pb and U in epidote outboard of the pyritic halo was interpreted to represent amplification of the signature of porphyry-related hydrothermal alteration, potentially allowing for the detection of porphyry systems for kilometers outside of the areas of obvious mineralization (Cooke et al., 2006). In addition, the magnitude of these geochemical signals was correlated to intensity of mineralization. For example, weakly mineralized systems such as the Mexico prospect (Chapter 2) displayed weak amplification of the geochemical zoning (Cooke et al., 2006).

In order to confirm whether epidote chemistry is a viable tool in porphyry Cu-Au-Mo exploration and targeting, spatial variations in epidote trace element chemistry defined by the P765 project (Cooke et al., 2006) are tested here through a detailed appraisal of host rock controls on epidote chemistry at Black Mountain Southeast. Specifically, epidote trace element chemistry is compared to whole rock geochemistry and primary phenocryst compositions from the same samples collected from the propylitic halo to the Black Mountain Southeast ore zone to determine the controls (if any) host rock geochemistry exerts on epidote trace element compositions.

7.3.1 Previous Research

Previous research on the variability of epidote chemistry within hydrothermal systems has focused predominantly on Fe^{3+}-Al^{3+} substitution-driven compositional zoning within

individual phenocrysts and did not explore any relationships between trace element variability (e.g., Shikazono, 1984; Arnason and Bird, 1992; Arnason et al., 1993). Arnason et al. (1993) focused on thermodynamic controls of major element variability in the epidote of hydrothermal and low-pressure regional metamorphic environments. Most of their work involved the fluctuation of thermodynamic variables during epidote growth, which caused compositional zonation of Fe and Al. Although they noted that Fe^{3+} and Al^{3+} substitution in epidote is a complex function of many variables (temperature, pressure, oxygen fugacity, mineral assemblage, bulk rock composition and fluid chemistry), Arnason et al. (1993) stressed the controls of bulk rock composition and fluid composition on the formation and major element compositional zonation of secondary epidote. They reported that experimental studies by Liou (1973) and Holdaway (1972) implied a positive correlation between synthesized epidote Fe_2O_3/Al_2O_3 ratios and starting material compositions. Similarly, Shikazono (1984) noted a positive correlation between bulk rock and epidote Fe_2O_3 content through a compilation of data from active and extinct hydrothermal systems. Arnason and Bird (1992) further emphasized the controls of bulk rock major element composition on epidote chemistry in their comparison of epidote crystal zonation within different host rock types. Specifically, they noted that alteration in basalt-hosted hydrothermal systems resulted in the replacement of plagioclase phenocrysts by epidote with Al-rich rims and Fe-rich cores. However, calcareous sediment-hosted systems resulted in epidote replacement of calcite cement, wherein rims were Fe-rich and cores were Al-rich (Arnason and Bird, 1992).

Published work on the controls of epidote trace element content in porphyry and related hydrothermal systems is scarce. Though not a study of porphyry hydrothermal systems, Spieler et al. (2003) analyzed and compared the trace element chemistry of epidote, bulk rock and brines of the active, sediment-hosted Salton Sea geothermal system, California. They reported that epidote Sr and REE content did not correlate with any monitored variable during the study (depth, bulk rock composition and brine composition). Spieler et al. (2003) noted an increase in bulk rock Sr content at depths below 2000 meters from the surface within the system, and average brine concentrations roughly equivalent to maximum bulk rock compositions (~450ppm). In contrast, epidote Sr displayed no systematic relationship with brine Sr, bulk rock Sr or depth, with values

ranging from ~450ppm to nearly 6000ppm (Spieler et al., 2003). No correlation between epidote Sr and major elements (such as Fe) was identified, and individual REEs (e.g., La and Yb) varied independently of one another (Spieler et al., 2003). This research suggests that while there is a distinct control of host rock geochemistry on the major element content of alteration epidote, trace element contents appear to be a unique function of the hydrothermal system, bearing no relation to host rock composition or even the major element compositions of epidote.

The research conducted by AMIRA P765 indirectly addressed the possibility of the host rock exerting a geochemical control on epidote. In their assessment of spatial zoning of epidote trace element compositions, Cooke et al. (2006) compared epidote and corresponding whole rock compositions to highlight the hypogene geochemical dispersion halo around Black Mountain. For example, REE, As, Sb, Pb and U concentrations of epidote adjacent to and outside of the pyritic alteration halos were up to an order of magnitude greater than levels detected in bulk rock compositions. This is a feature that extends outboard of mineralization for up to four kilometers (Cooke et al., 2006). As well, enrichment of Cu, Zn, Sn and Mo within epidote from pyritic alteration halos was below the levels detected in bulk rock samples. Though not the primary intention of the comparison, the lack of a consistent correlation between epidote and the bulk composition of the rock in which it forms as a secondary mineral, broadly suggests no control of whole rock geochemistry on epidote trace element compositions, concurrent with the findings of Spieler et al. (2003).

7.3.2 Methodology and Techniques

The control of host rock geochemistry on epidote trace element composition was examined on two levels, each of which reflects a different scale of interaction between host rock and the altering fluids. Similar to the approaches of Spieler et al. (2003) and Cooke et al. (2006), the comparison of epidote trace element geochemistry and corresponding bulk rock geochemistry constitutes examination on a whole rock sample scale. This level of study provides insight into the interaction between altering fluids and host rocks, and examines the overall potential for scavenging of elements from all components of the host rock (phenocrysts and groundmass). Analytical work for this

study was similar to that of Cooke et al. (2006), and was performed exclusively at the University of Tasmania. A laser ablation inductively-coupled plasma mass spectrometry (LA-ICMPS) study was conducted on epidote from 15 Black Mountain samples (12 collected during the 2008 field season, and three collected during P765A). A total of 282 individual point analyses were produced (an additional 15 were discarded as either poor analyses or not epidote), detailing the relative concentrations of 35 elements in each analysis. Quantification of the relative concentrations was determined using stoichiometric calcium from corresponding electron microprobe (EMP) spot analyses (methodology in Appendix 1.5). Detailed analytical procedures for the use of the LA-ICPMS can be found in Appendix 1.6. Corresponding whole rock geochemical data for each sample was reported in Chapter 5. The new LA-ICPMS epidote trace element data was supplemented with the epidote and whole rock data generated from samples at Black Mountain during P765, for a combined total of 579 spot analyses from 31 samples (Appendix 2.6).

As previously noted (Section 7.2), epidote was observed as a preferential replacement phase for plagioclase phenocrysts (and to a lesser extent, hornblende) in many of the more distal plagioclase-phyric host rocks of Black Mountain (Chapter 3). Investigation of this fluid-phenocryst interaction requires a smaller, grain scale level of geochemical observation. Two methods were utilized for this section of the study: a comparison of epidote trace element chemistry with the compositions of the dominant phenocrysts in the host rocks (plagioclase and hornblende), and grain mapping. Plagioclase and hornblende phenocrysts were analyzed for their trace element concentrations through the same process described above for epidote: LA-ICPMS quantified by EMP analyses. Stoichiometric Al was used as the internal standard for plagioclase, whereas Ca was used for hornblende. A total of 204 spot analyses were used for plagioclase from 15 samples, and 141 analyses for hornblende from 11 samples.

LA-ICPMS grain mapping techniques (Appendix 1.6) were used to generate color gradient maps of variably epidote-altered phenocrysts and groundmass from five samples, for a total of eight grain maps. This technique facilitates the analysis of trace element remobilization and scavenging on the scale of individual crystals by highlighting areas of low-to-high concentrations of a given element. With the maps, it is possible to

identify enrichment and depletion halos within and around propylitic epidote of varying morphologies, and if present, confirm localized remobilization of trace elements. Similar to the raw LA-ICPMS data, the color-graded values for the grain maps are not quantitative measurements, and are shown in counts per minute. Individual laser ablation spot analyses (quantified by stoichiometric EMP data) within the grain map areas were used to provide a quantifiable reference value.

Due to the nature of LA-ICPMS data reduction, some element concentrations for certain spot analyses were below the detection limit (i.e., BDL) of the machine for those particular elements. The treatment of BDL data in the context of this thesis reflects the observations of Cooke et al. (2006) in that emphasis is placed on examination of *maximum* trace element concentrations in propylitic epidote. To this end, BDL data is not incorporated in the representation or discussion of the findings herein. However, as LA-ICPMS data is utilized differently throughout the investigation of host rock geochemical controls on propylitic epidote (for example, within whole rock sample scale and the grain scale methodology), a brief discussion and justification for the treatment of BDL data in each context is presented at the beginning of each subsection.

7.3. Geochemical Zonation Defined by Epidote Geochemistry

The first step in the investigation of epidote geochemical vectors was to test if the new samples from the Black Mountain Southeast area did in fact display the zonation pattern determined previously around Black Mountain by analysis of epidote trace element geochemistry (Cooke et al., 2006). To do this, an artificial center point was established on the Black Mountain Southeast alteration map (Fig. 7.1), and a traverse line was projected over it (Fig. 7.8). The traverse line extends northwest through the length of the map area, with a dogleg northward up Liw-Liw Creek towards the Nugget Hill porphyry prospect (Chapter 2). The locations of whole rock and analyzed epidote samples were marked on the map and projected perpendicularly onto the traverse line, yielding a

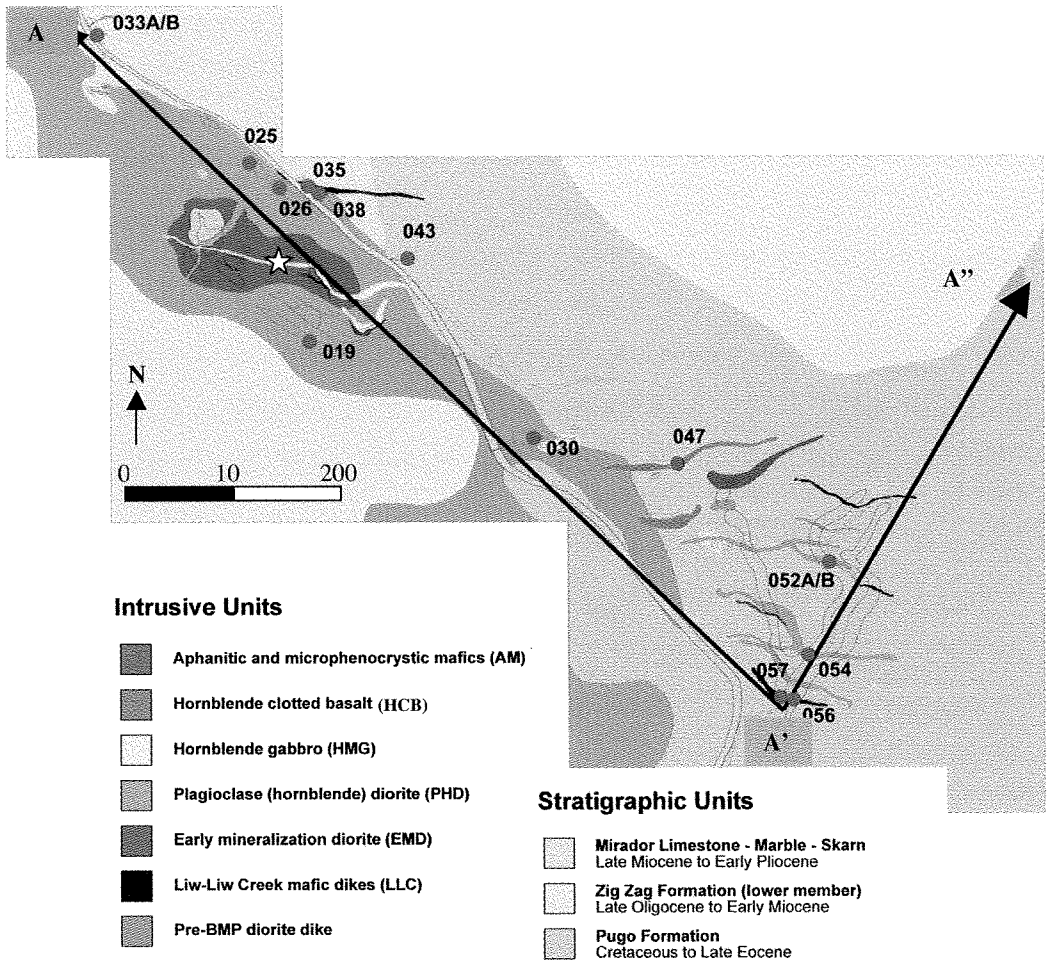

Figure 7.8 – New sample locations along a traverse line (A-A' and A'-A") for analyzed epidote and primary phenocrysts for this thesis.

broadly linear spatial distribution across the map area. This traverse line was then used as an "X-axis" to display geochemical variability across the deposit area. Rugged topography and active landslides limited sampling to rocks exposed in creek valleys, thus broadly determining the orientation of the traverse line.

Epidote morphologies for the new Black Mountain Southeast samples were subdivided into three groups based on field observations as well as hand sample descriptions: seven samples contained replacement epidote, two samples contained epidote associated with pervasive skarn-type mineralization and alteration, and three samples contained vein-type epidote (Appendix 2.6). This new data was then combined

with previously collected epidote trace element data to extend the dogleg up Liw-Liw Creek an additional 1000 meters towards Nugget Hill.

The treatment of the BDL LA-ICPMS data for this portion of the study reflects the approach of Cooke et al. (2006): only data above BDL was plotted, so as to highlight the zonation of maximum epidote trace element values.

Results

The spatial variations of trace element compositions of epidote from the Black Mountain Southeast porphyry system are displayed in Figures 7.9 and 7.10. Of the first element group identified by Cooke et al. (2006), Zn, Sn and Cu are very weakly elevated in epidote from inside the pyrite halo (Fig. 7.9a-c). However, the highest Mo concentrations in epidote occur outside the pyrite halo (Fig. 7.9d). Absolute concentrations of Zn, Cu and Mo are generally lower than the corresponding whole rock values, but Sn in epidote is equivalent to or higher than the whole rock values (Appendix 2.6). La, Y and Zr are all enriched in epidote adjacent to, but outside the Black Mountain pyrite halo (Fig. 7.9e-g). Both La and Y are significantly higher in epidote than their corresponding whole rock samples across the deposit, but Zr contents of epidote only exceed whole rock adjacent to the pyrite halo (Fig. 7.9g; Appendix 2.6). Strontium is similarly elevated in epidote at the edges of the Black Mountain pyrite halo, however the maximum Sr values occur outside the pyrite halo in both vein- and replacement-type epidote (Fig. 7.9h). The Sr content of epidote exceeds that of corresponding whole rock samples throughout the map area (Appendix 2.6). Outside the pyrite halo, both vein- and replacement-type epidote are enriched in As, Pb and Sb, with values greater than the corresponding whole rock (Fig. 7.10a-c; Appendix 2.6). However, vein epidote is similarly enriched in Pb within the potassic alteration halo (Fig. 7.9b). The single area of skarn-related epidote (along the traverse at –307 meters) does not conform to the observations above: despite its location within the pyrite halo, it is enriched in U and Sn (and Bi to a lesser degree), and depleted in Pb and As (Figs. 7.9b and 7.10a, b, d, e).

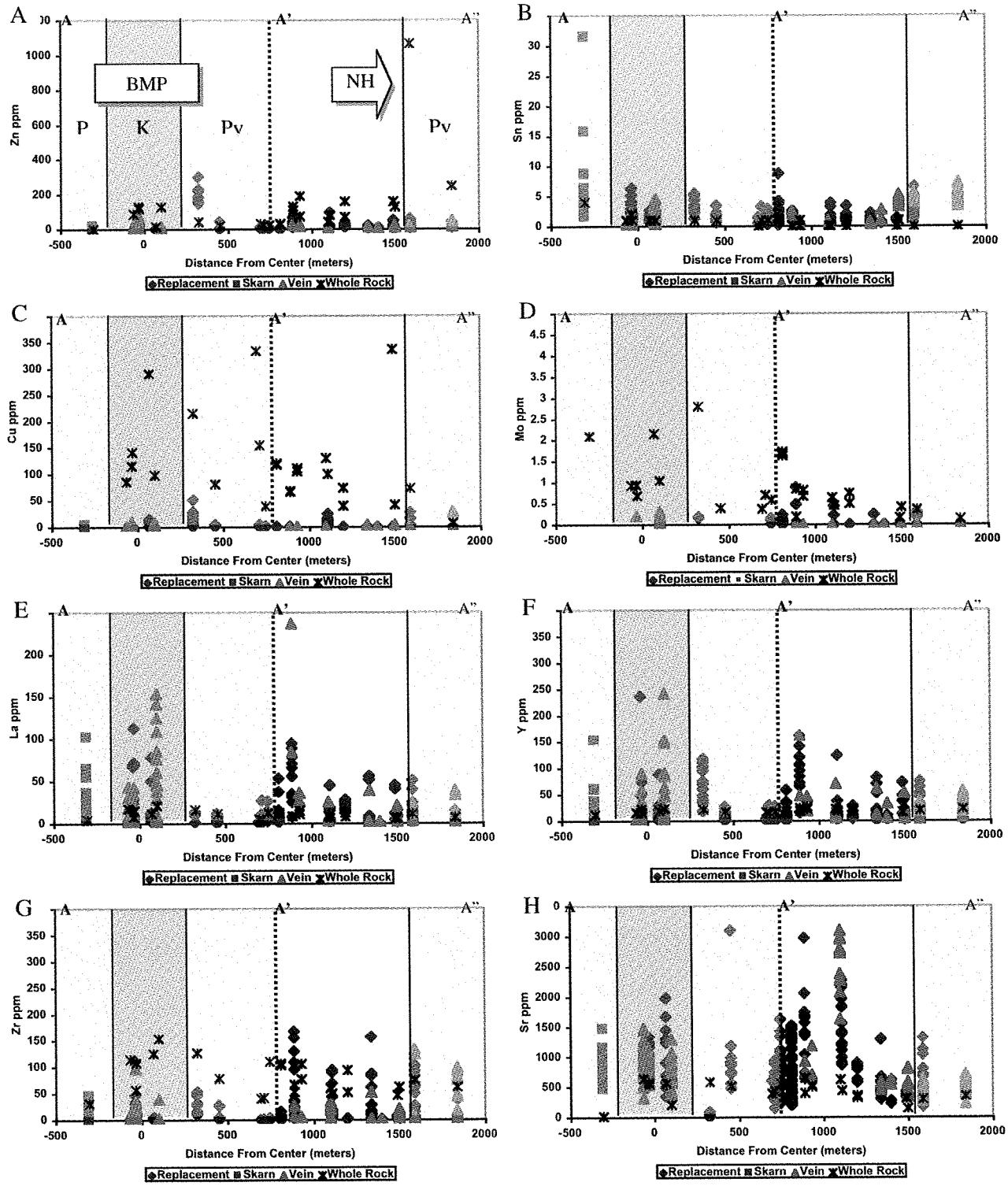

Figure 7.9 – Epidote versus sample whole rock concentrations for vector elements (Cooke et al., 2006) along Black Mountain Southeast traverse line (A-A') and Liw-Liw Creek traverse line (A'-A"; Fig. 7.8): (A) Zn; (B) Sn; (C) Cu; (D) Mo; (E) La; (F) Y; (G) Zr; (H) Sr. Extent of potassic (K Alt; dark gray shading) and pyritic (Py; light yellow shading) alteration halos indicated. "BMP SE" indicates the Black Mountain Southeast Porphyry Deposit; "NH" indicates the Nugget Hill Porphyry prospect.

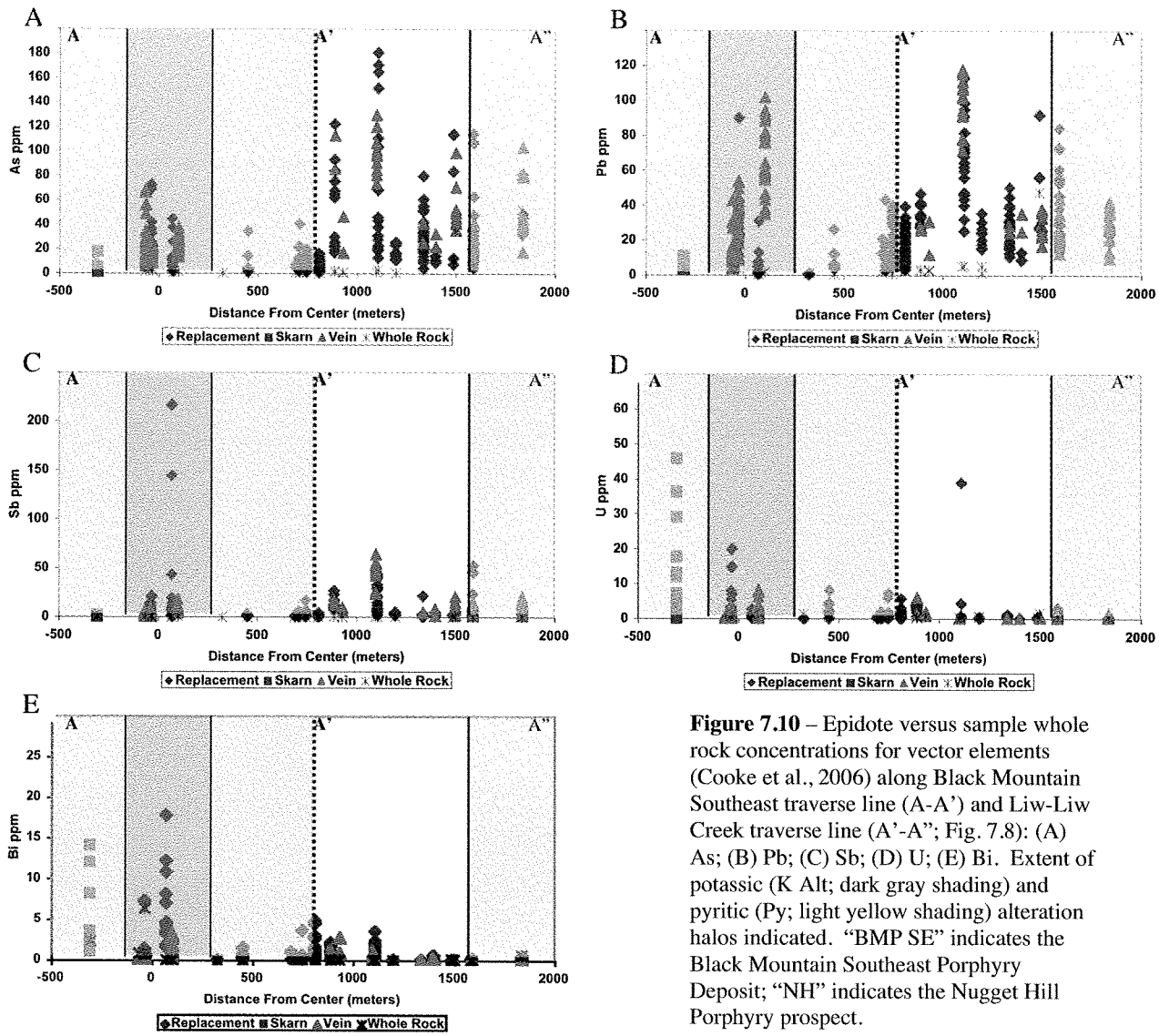

Figure 7.10 – Epidote versus sample whole rock concentrations for vector elements (Cooke et al., 2006) along Black Mountain Southeast traverse line (A-A') and Liw-Liw Creek traverse line (A'-A"; Fig. 7.8): (A) As; (B) Pb; (C) Sb; (D) U; (E) Bi. Extent of potassic (K Alt; dark gray shading) and pyritic (Py; light yellow shading) alteration halos indicated. "BMP SE" indicates the Black Mountain Southeast Porphyry Deposit; "NH" indicates the Nugget Hill Porphyry prospect.

Discussion

The substitution of trace elements in epidote around Black Mountain Southeast mostly conforms to the spatial relationships outlined by Cooke et al. (2006). Deviations were only noted in the skarn-type epidote, and also due to unexpectedly high epidote Sn values throughout the map area. Nevertheless, the verification of spatially variable epidote trace element concentrations similar to those observed by Cooke et al. (2006), suggests that the Black Mountain Southeast is a valid locality to examine the controls of bulk rock chemistry on propylitic epidote trace element composition.

7.3.4 Epidote and Whole Rock Chemistry

A map of all epidote sample locations can be viewed in Figure 7.8. The 580 spot analyses (Appendix 2.6) have been reduced to sample mean averages in order to more easily compare the epidote chemistry with the corresponding whole rock chemistry of individual samples. The averages are shown alongside the corresponding whole rock geochemical data in Table 7.1. Averages for a given sample were calculated using the mean value of epidote spot analyses that registered above the detection limit of the LA-

Sample #	**353226**	**353230**	**354019**	**354510**	**355193**	**355194**	**355195**	**355198**	**814487**	**354554**	**814495**	**353227**	**353229**	**354511**	**354555**	**354562**	**814485**	**814489**	**821173**
Date Collected	2006	2006	2006	2006	2006	2006	2006	2006	2006	2006	2006	2006	2006	2006	2006	2006	2006	2006	2006
Epidote Type	rep	rep	rep	rep	rep	rep	rep	rep	rep	skarn	skarn	vein	vein	vein	vein	vein	vein	vein	vein
Host Rock	basalt	basalt	andesite	andesite	basalt	bas-andesite	basalt	basalt	basalt		basalt	basalt	basalt	bas-andesite	dacite	dacite	dacite	basalt	lms
Epidote Avg (ppm)																			
Zn	17.0	28.3	42.8	19.5	22.2	7.6	12.1	20.5	23.1	67.6	19.7	10.2	18.3	9.9	7.8	8.3	15.4	23.9	50.2
Sn	1.0	2.1	5.2	1.8	1.1	1.4	0.9	1.4	3.6	2.0	1.3	0.4	0.5	1.6	4.8	5.9	4.5	5.1	5.7
Cu		0.0	0.4	16.9	0.0	0.0	0.0	0.8	0.4	0.1	1.7	5.8	0.1	2.3	0.0	104.8	0.0	2.4	0.0
Mo	0.1	0.2	0.0	0.3	0.0	0.0	0.0	0.0	0.1	0.0	0.0	0.0	0.0	0.0	0.0	0.0	0.0	0.0	0.2
La	118.3	67.0	665.3	68.5	25.5	1.0	8.1	21.3	12.5	0.7	0.5	6.3	31.1	13.0	11.5	30.2	7.8	10.5	11.9
Y	88.7	97.7	112.7	75.1	42.6	9.9	16.4	12.1	23.8	13.2	6.4	17.4	32.1	21.2	5.6	44.9	17.9	25.8	35.2
Zr	19.9	59.3	147.7	4.1	3.8	0.9	25.2	1.1	34.4	19.3	35.5	10.7	4.8	1.7	9.7	18.1	8.8	35.7	11.3
Sr	1493.8	1422.7	1522.1	682.3	386.4	424.1	490.0	798.5	502.4	815.4	769.2	2602.2	939.8	505.6	1051.5	1708.6	560.2	510.2	569.3
As	81.3	62.9	18.7	4.1	54.3	17.7	31.2	17.1	29.2	18.7	6.0	98.7	31.7	6.1	15.7	8.8	53.1	55.9	70.9
Pb	64.5	33.4	63.9	7.2	50.4	17.1	27.1	23.2	31.4	3.6	6.5	98.8	21.2	4.6	6.4	5.0	28.9	27.5	27.0
Sb	16.3	14.2	4.4	1.9	2.0	3.0	2.5	3.2	7.1	10.1	2.7	44.0	7.5	1.1	4.2	1.9	10.5	9.3	5.6
U	2.2	3.2	21.8	1.1	0.3	0.0	0.3	0.3	0.8	2.4	0.8	0.2	1.4	0.4	3.6	5.3	0.6	0.7	0.8
Bi	1.3	0.9	1.3	0.3	0.0	0.3	0.0	0.0	0.1	3.0	1.0	0.4	1.8	0.0	2.1	1.1	0.0	0.2	0.5
Whole Rock (ppm)																			
Zn	81.9	110.2	98.8	39.5	157.3	177.5	518.1	159.3	1064.4	37.4	37.2	42.0	73.3	109.7	4.5	13.5	128.9	247.8	427.9
Sn	0.5	0.5	0.5	0.5	0.5	0.5	0.5	1.0	0.5	0.5	0.5	0.5	0.5	0.5	0.5	0.5	1.0	0.5	0.5
Cu	99.7	68.3	217.0	113.0	336.3	32.4	15.4	39.8	72.8	4.0	4.1	129.8	111.0	35.2	16.6	5.2	41.4	7.0	60.5
Mo	0.5	0.8	1.4	1.7	0.2	0.7	0.1	0.7	0.4	65.8	1.4	0.6	0.7	0.4	0.7	10.6	0.4	0.1	1.8
La	6.5	8.7	16.9	13.2	5.8	4.1	6.0	12.5	11.6	9.7	4.1	8.6	10.9	12.1	10.2	14.3	6.8	7.0	8.6
Y	19.5	23.7	16.3	17.6	16.4	32.1	17.7	22.3	20.1	15.6	9.5	22.1	22.0	15.2	5.5	17.5	31.8	23.2	25.8
Zr	48.8	66.5	106.6	100.5	46.1	79.5	55.4	93.3	75.3	72.4	36.5	59.2	76.8	85.2	95.9	141.8	62.3	61.6	56.3
Sr	438.3	646.9	636.2	428.2	313.2	170.5	192.0	327.2	300.9	134.7	447.8	619.6	529.6	447.9	221.3	899.6	147.6	347.7	330.2
As	2.9	2.2	0.7	3.1	10.3	36.0	6.1	0.3	22.9	1.0	0.8	1.3	0.8	3.8	0.3	0.7	34.8	52.0	14.9
Pb	5.4	3.2	1.6	1.9	47.3	10.6	129.6	4.9	60.0	1.3	1.3	4.9	2.9	2.8	0.8	1.4	27.6	15.3	101.4
Sb	0.1	0.2	0.0	0.1	0.1	0.7	0.4	0.1	0.3	0.1	0.1	0.1	0.1	0.1	0.0	0.2	0.3	0.5	0.5
U	0.4	0.4	1.5	0.9	0.5	0.2	0.4	0.8	0.7	1.9	1.8	0.4	0.7	0.9	1.9	1.4	1.6	0.5	0.6
Bi	0.0	0.1	0.0	0.6	0.1	0.2	0.2	0.0	0.0	0.1	0.1	0.0	0.0	0.6	0.0	0.2	0.1	0.7	0.2
Plagioclase Avg (ppm)																			
Zn	10.5		3.3	11.5			79.8												
Sn	0.6		1.0	4.8			0.8												
Cu	0.7			95.0			1.1												
Mo	0.0			5.5			0.1												
La	0.6		4.4	2.0			4.4												
Y	0.7		0.1	0.7			5.8												
Zr	2.1		0.2	15.0			7.0												
Sr	788.7		1321.9	965.5			302.8												
As	2.3			1.7			3.2												
Pb	2.5		5.4	4.5			3.6												
Sb	0.2		0.3	1.4			2.1												
U	0.0		0.0	0.2			0.1												
Bi	0.0			0.1			0.0												
Hornblende Avg (ppm)																			
Zn	39.2		253.2																
Sn	1.3		2.8																
Cu	3.4		24.4																
Mo			0.3																
La	1.2		8.4																
Y	16.6		42.8																
Zr	19.0		36.9																
Sr	272.2		87.0																
As			1.7																
Pb	0.5		6.1																
Sb	0.2		0.5																
U	0.0		0.1																
Bi	0.0		0.0																

Table 7.1 - Mean average of pathfinder element concentrations in epidote, and plagioclase feldspar and hornblende phenocrysts for individual samples and their corresponding whole rock values. ("rep" indicates replacement-type epidote.)

Table 7.1 continued

Sample #	BA08GS019	BA08GS038	BA08GS047	BA08GS052A	BA08GS052B	BA08GS054	BA08GS057	BA08GS033A	BA08GS033B	BA08GS026	BA08GS035	BA08GS043
Date Collected	2008	2008	2008	2008	2008	2008	2008	2008	2008	2008	2008	2008
Epidote Type	rep	rep	rep	rep	rep	rep	rep	skarn	skarn	vein	vein	vein
Host Rock	andesite	bas-andesite	basalt	bas-andesite	bas-andesite	andesite	basalt	andesite	andesite	bas-andesite	bas-andesite	andesite
Epidote Avg (ppm)												
Zn	1.9	19.2	8.6	2.4	3.0	3.6	6.7	7.0	8.5	10.1	18.1	7.2
Sn	1.4	1.8	1.6	0.9	1.5	1.1	1.0	8.7	4.6	0.4	1.0	2.3
Cu	20.8	2.0	2.4	2.2	0.7	0.6	0.8	16.5	1.6	5.6		1.7
Mo				0.1	0.1	0.1					0.2	0.1
La	17.2	84.8	3.6	5.2	7.4	5.9	1.0	30.7	71.1	7.8	8.8	45.4
Y	19.2	46.6	12.2	3.4	5.0	3.5	2.2	21.5	50.6	0.6	16.8	67.2
Zr	1.4	9.9	4.0	0.9	1.8	0.5	0.4	7.4	27.2	1.0	8.9	2.5
Sr	1011.8	1241.2	1028.2	681.6	847.3	773.9	595.9	888.8	839.5	910.2	827.2	719.9
As	15.9	18.6	7.9	3.6	5.1	7.3	6.3	5.3	3.1	27.0	16.8	23.6
Pb	6.3	45.4	8.0	12.5	17.6	19.5	16.9	6.1	3.7	14.9	32.1	68.3
Sb	42.0	20.5	0.9	0.7	1.1	2.6	1.0	1.1	0.7	2.5	2.8	8.8
U	1.1	13.9	2.6	0.5	0.5	1.0	0.3	13.4	14.1	0.2	0.8	2.6
Bi	6.8	0.6	0.6	0.5	0.9	0.3	0.6	4.1	4.8	0.1	0.3	1.0
Whole Rock (ppm)												
Zn	15.2	117.4	19.7	30.6	30.6	22.6	31.9	10000.0	10000.0	86.6	127.6	128.5
Sn	1.0	1.0	1.0	1.0	1.0	1.0		4.0	4.0	1.0	2.0	1.0
Cu	290.7	141.1	81.3	119.0	119.0	39.2	333.8	1631.1	1631.1	85.3	115.6	97.9
Mo	2.2	0.7	0.4	1.7	1.7	0.6	0.4	2.1	2.1	0.9	0.9	1.0
La	11.3	14.9	11.2	11.8	11.8	12.7	5.1	3.8	3.8	17.1	7.7	21.0
Y	18.4	15.3	16.7	17.4	17.4	17.0	16.1	11.9	11.9	15.6	21.9	23.0
Zr	124.9	107.4	78.6	106.4	106.4	109.6	39.8	30.7	30.7	114.1	56.6	153.6
Sr	558.9	545.8	515.4	549.4	549.4	558.7	387.5	13.7	13.7	636.2	574.6	209.1
As	0.5	2.0		0.4	0.4	0.6	0.7	9.3	9.3	1.8	3.8	1.3
Pb	0.4	4.2	0.5	2.5	2.5	0.8	1.7	4.1	4.1	5.6	3.2	1.7
Sb	0.1	0.2	0.0	0.1	0.1	0.3	0.1	0.3	0.3	0.2	0.3	0.2
U	1.0	1.4	0.8	1.0	1.0	1.0	0.3	2.7	2.7	1.4	0.6	1.8
Bi	0.0	0.8	0.0	0.1	0.1	0.2	0.8	2.4	2.4	0.9	6.4	0.1
Plagioclase Avg (ppm)												
Zn	3.1	22.3	7.4	4.1	5.0	5.5	10.3	6.5	5.4	7.5		
Sn	0.7	0.3	1.0	0.2	0.2	0.3		0.6		0.6		
Cu	12.1	9.1	2.5	1.8	0.9	1.9	5.9	6.3	1.4			
Mo	0.3	0.5		0.1	0.0	0.1		0.3				
La	4.4	4.3	2.5	2.6	3.1	5.5	1.8	4.5	8.9	3.9		
Y	0.1	0.3	2.7	0.5	0.3	2.0	1.5	0.4	0.4	0.1		
Zr	10.5	4.2	72.2	2.7	5.5	48.8	0.5	7.5	1.0	0.2		
Sr	1147.6	1329.7	800.9	962.2	1065.8	1113.1	562.4	1095.4	1136.7	1305.3		
As		1.3		1.1	0.9	2.1	1.8			2.2		
Pb	3.6	6.4	1.3	3.3	3.5	4.9	2.1	4.5	4.4	6.0		
Sb		0.3		0.2	0.3	0.4	0.5			0.6		
U	0.1	0.1	1.0	0.1	0.1	0.6	0.2	0.3	0.0	0.1		
Bi	0.1	0.1		0.0	0.0	0.0	0.1	0.0		0.1		
Hornblende Avg (ppm)												
Zn		265.1	75.0				54.1	211.5	194.3	190.5	82.9	
Sn		1.6	1.2				1.7	2.6	1.9	2.3	1.0	
Cu		5.4	3.1				0.9	4.0	21.6	0.9	3.4	
Mo		0.1					0.1	0.2	0.2			
La		9.1	1.5				0.5	10.1	8.4	9.6	0.5	
Y		25.7	18.8				14.3	61.6	47.7	36.8	12.8	
Zr		23.7	25.3				9.9	44.4	62.0	28.1	8.5	
Sr		208.3	242.4				198.0	57.1	88.7	56.6	203.3	
As		2.3							1.1	1.0	1.5	
Pb		4.9	0.8				0.5	0.9	3.3	1.0	0.4	
Sb		0.9						0.1	0.3	0.2	0.3	
U		0.4	0.0					0.0	0.1	0.0	0.0	
Bi		0.1	0.0				0.0	0.0	0.1	0.0	0.0	

ICPMS. This methodology was preferred over a cumulative approach (a mean average of all epidote analyses for a given sample, including BDL values set to either 0.00 or the respective detection limit) as the former more readily exposes any correlation between epidote trace element values and the respective whole rock composition. Furthermore, exclusion of the BDL data in the calculated means reflects a sample average of the data used to determine spatial variations in trace element concentrations (Figs. 7.9 and 7.10; Cooke et al., 2006). Inclusion of BDL data (set to null or the respective detection limit) in the calculation of sample mean trace element values, would subdue the peaks of geochemical signals detected in the epidote, making any correlations between elevated trace elements in epidote and whole rock more difficult to detect.

Results

Distinct correlations between epidote and whole rock trace element concentrations are present within the Black Mountain Southeast data set (Fig. 7.11). Of the elements outlined by AMIRA P765 as epidote vector elements (Cooke et al., 2006), Zn and Sr (and to a lesser extent La and U) in epidote exhibit weak positive correlations with whole rock concentrations (Figs. 7.11a, d, e, h and 7.12d). Sr reflects a strong correlation between epidote and corresponding whole rock samples for the Black Mountain Southeast data set, with Sr-enriched whole rock samples generally containing Sr-rich replacement- and vein type-epidotes (Fig. 7.11h). Epidote Sr is enriched with respect to whole rock values, with epidote values generally 2-5 times that of the whole rock (Table 7.1). A linear regression run separately for the replacement- and vein-type epidote subgroups returned R^2 values of 0.5382 and 0.3377, respectively, confirming positive correlations with whole rock Sr (Fig. 7.10h). Srontium in skarn-related epidote does not reflect this positive correlation, though it should be noted that there is little statistical significance with only four data points (Fig. 7.10h). Zinc, U and La reflect similar positive correlations, but only between individual epidote subgroups and whole rock compositions. Zinc contents of vein-type epidote are positively correlated with whole rock values, with whole rock values up to an order of magnitude higher than epidote (Fig. 7.11a; Table 7.1). A linear regression of the vein-type epidote subset yields an R^2 value of 0.8499, indicating a strong positive correlation. U and La contents of vein-type epidote are also positively correlated with whole rock concentrations, with R^2 values of 0.3117 and 0.4766, respectively (Figs. 7.11e and 7.12d). Similar to Sr, epidote is enriched in U and La with values 2-3 times those of whole rock concentrations.

Relative concentrations of the other vector elements within epidote and whole rock compositions can be broadly subdivided based on the subdivisions of Cooke et al. (2006). Zirconium and Y are both enriched in epidote by less than an order of magnitude over whole rock values. Lead, Bi and As are enriched in epidote by up to an order of magnitude over whole rock values. Antimony is enriched by up to two orders of magnitude. Copper and Mo values are 10 to 100 times higher in whole rock samples than in epidote (Table 7.1). Tin is enriched in epidote by up to an order of magnitude over whole rock values.

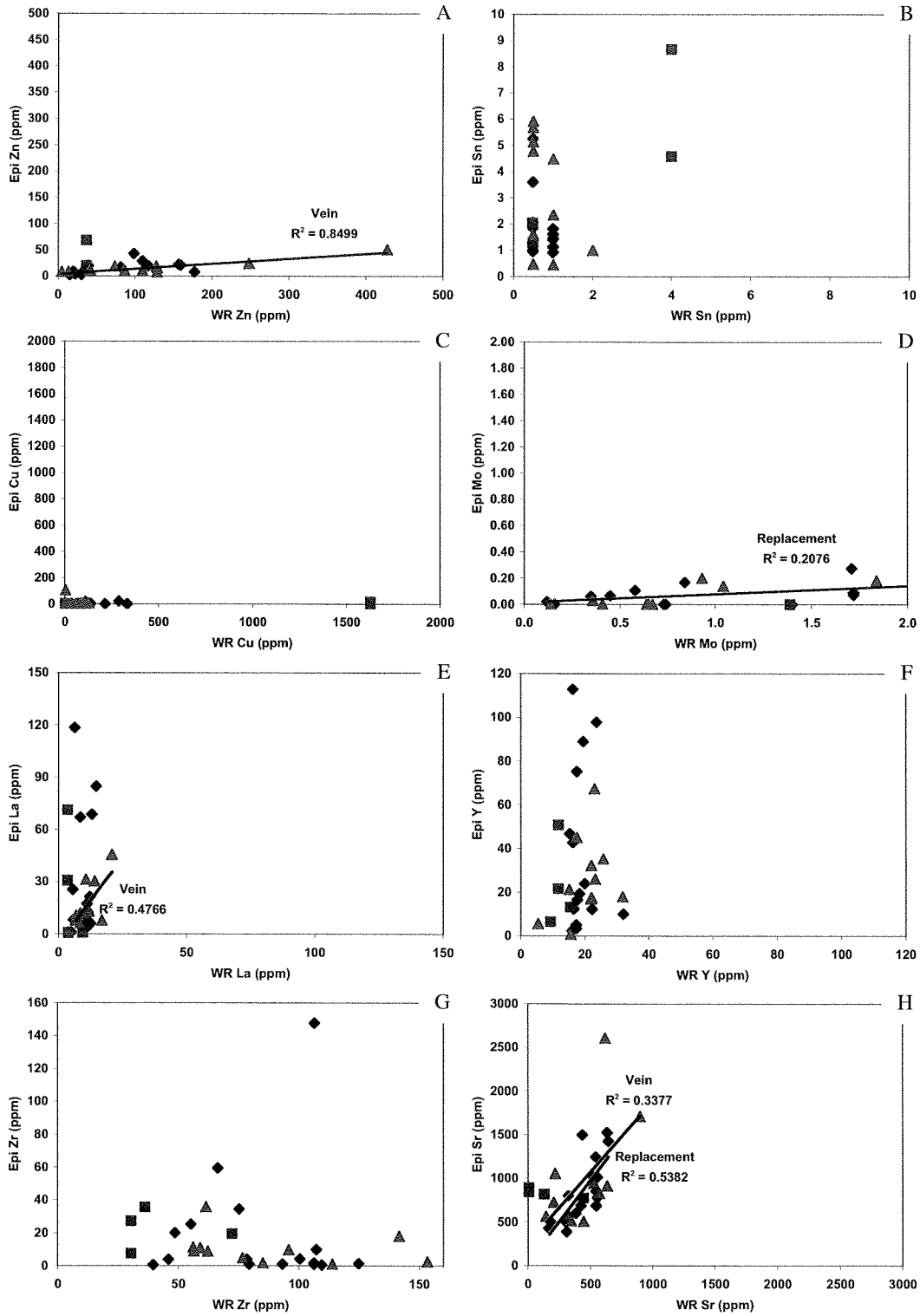

Figure 7.11 – Sample average epidote (Epi) versus whole rock (WR) concentrations for vector elements (Cooke et al., 2006): (A) Zn [linear regression for vein epidote subset R^2=0.8499]; (B) Sn; (C) Cu; (D) Mo [linear regression for replacement epidote subset R^2=0.2076]; (E) La [linear regression for vein epidote subset R^2=0.4766]; (F) Y; (G) Zr; (H) Sr [linear regression for replacement epidote subset R^2=0.5382; linear regression for vein epidote subset R^2=0.3377].

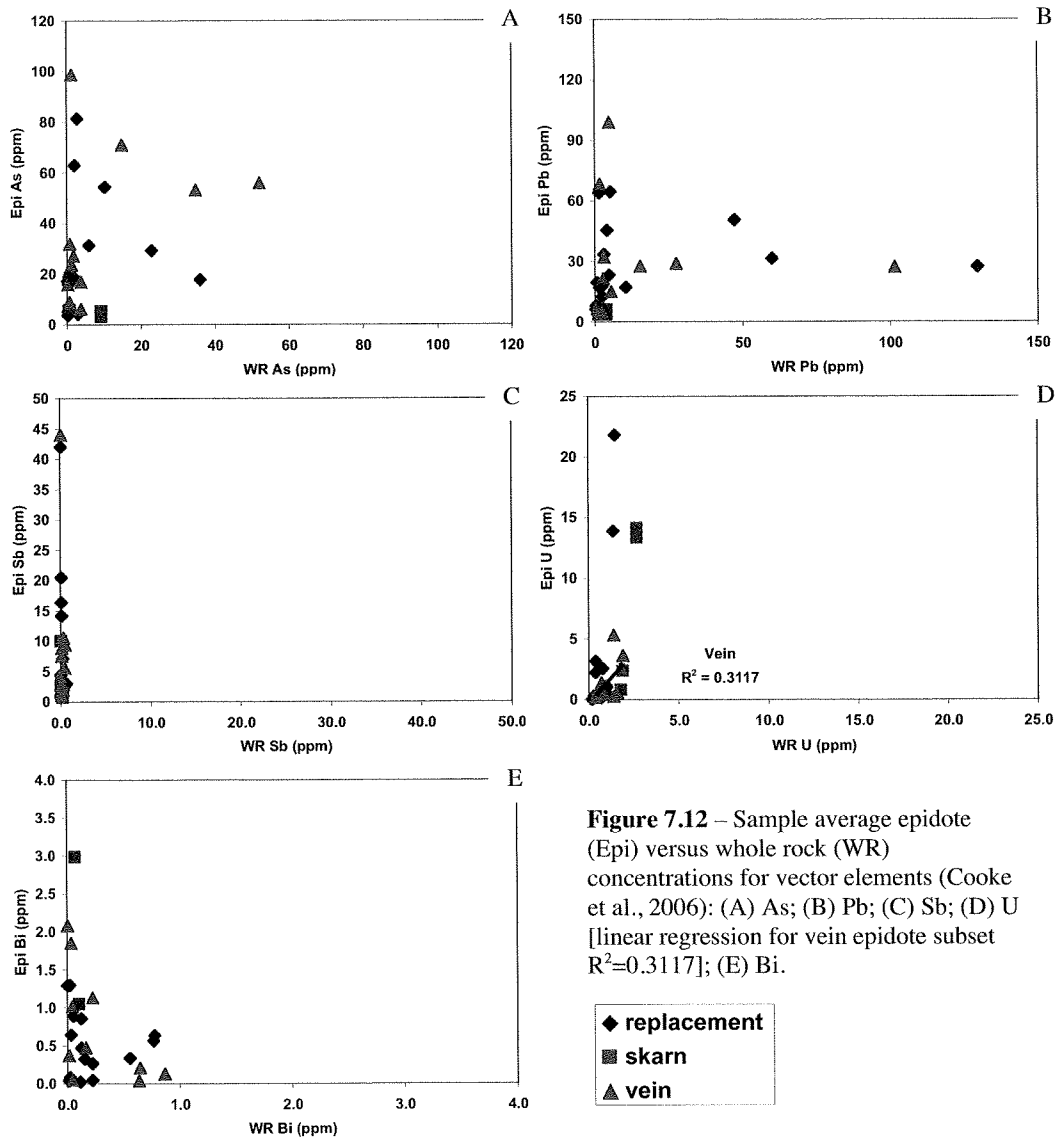

Figure 7.12 – Sample average epidote (Epi) versus whole rock (WR) concentrations for vector elements (Cooke et al., 2006): (A) As; (B) Pb; (C) Sb; (D) U [linear regression for vein epidote subset R^2=0.3117]; (E) Bi.

Discussion

The weak positive correlations between Zn, Sr, La and U from specific epidote morphologies and corresponding whole rock compositions raises the possibility that a feature (or features) of the protolith (phenocrysts and/or groundmass) exerts some influence on the trace element composition of epidote. Were groundmass compositions to supply vector elements via localized hydrothermal scavenging, similar concentrations of the trace elements monitored in both vein-type epidote (which typically replaces the groundmass around epidote veins; Fig. 7.4b) and whole rock would be expected, as the majority of samples contain over 45% groundmass by volume (Section 3.4). Given that enrichments of an order of magnitude occur for most of the pathfinder in vein-type epidote over bulk rock values, the groundmass does not appear to have influenced the trace element geochemistry of epidote. The potential control of phenocryst geochemistry on epidote composition is explored in detail below.

The positive correlations between whole rock geochemistry and vein-type epidote (Zn, Sr, La and U; Figs. 7.11a, e, h and 7.12d) may be due to propylitic alteration of vein-bearing samples yielding volumetrically greater amounts of vein-type epidote relative to other morphologies. Given the level of pathfinder element enrichment in epidote relative to whole rock values (up to an order of magnitude), the amplification of the alteration geochemical signature within the whole rock geochemical values could reflect the relative abundance of epidote. For example, samples that contain abundant vein-type epidote would yield whole rock compositions that are elevated in the elements enriched in the epidote.

With the exception of Sr, there is no evidence that phenocrysts or groundmass compositions affected the trace element compositions of epidote. Rather, it appears that hydrothermal fluids alone provided the pathfinder elements detected in the propylitic halo to Black Mountain.

7.3.5 Epidote and Primary Phenocryst Chemistry

Plagioclase and hornblende were analyzed for their trace element compositions. The raw data from the 204 plagioclase spot analyses (15 samples) and 141 hornblende analyses (11 samples) can be found in Appendices 2.7 and 2.8, respectively. As the purpose of

this investigation was to explore the potential controls of primary phenocryst compositions on secondary epidote, it was necessary to obtain trace element analyses for both epidote and the respective host phenocrysts from individual samples. However, not all samples contained plagioclase and/or hornblende phenocrysts, so some epidote-bearing samples are excluded from this portion of the study. Data sets for both epidote and plagioclase were determined from 14 samples, and epidote and hornblende from nine samples. Sample mean average plagioclase and hornblende trace element values are provided in Table 7.1.

Results

Any correlation between epidote and plagioclase trace element compositions from individual samples is minimal (Figs. 7.13 and 7.14). Of the pathfinder elements defined by P765 (Cooke et al., 2006), most show little or no correlation for any of the epidote morphologies, although for vein- and skarn-type epidote, this is also a function of the small sample population (vein-type n=1, skarn-type n=2; Table 7.1; Figs. 7.13 and 7.14). Strontium and As in replacement-style epidote are weakly correlated with plagioclase concentrations, with R^2 values of 0.3195 and 0.2700, respectively (Figs. 7.13h and 7.14a). Relative to the plagioclase values, epidote is enriched in As by an order of magnitude, and broadly equivalent in Sr values (Table 7.1).

Of the remaining vector elements, REE (La, Zr and Y) and Pb, Sb, U and Bi are all similarly enriched in epidote relative to the plagioclase phenocrysts, with most up to an order of magnitude higher in epidote. Uranium and Y are up to two orders of magnitude higher in epidote than in plagioclase. Average Zn concentrations are broadly similar in plagioclase and replacement-style epidote (Table 7.1).

There is a positive correlation between Y in epidote and hornblende, with R^2 values of 0.4948 (Fig. 7.12f). However, this positive correlation is in fact statistically weak, as the populations for each epidote subset are small (replacement-type n=5, vein-type n=2, skarn-type n=2; Table 7.1). The replacement-style epidote has Y contents broadly equivalent to hornblende (Table 7.1). No correlations can be determined between the vein- and skarn-type epidote and hornblende phenocrysts because these are two point population data subsets.

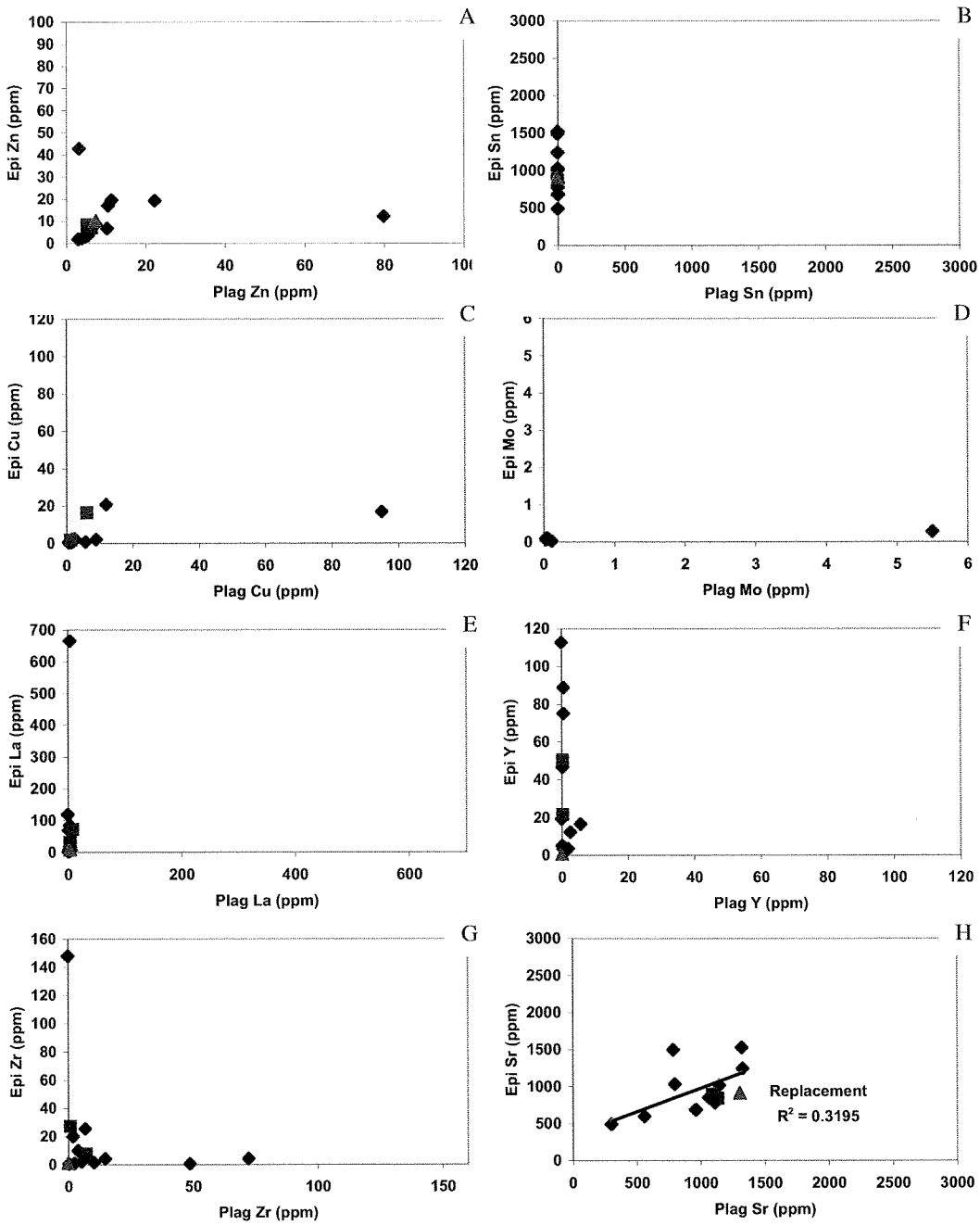

Figure 7.13 – Sample average epidote (Epi) versus sample average plagioclase (Plag) concentrations for pathfinder elements (Cooke et al., 2006): (A) Zn; (B) Sn; (C) Cu; (D) Mo; (E) La; (F) Y; (G) Zr; (H) Sr [linear regression for replacement epidote subset R^2=0.3195].

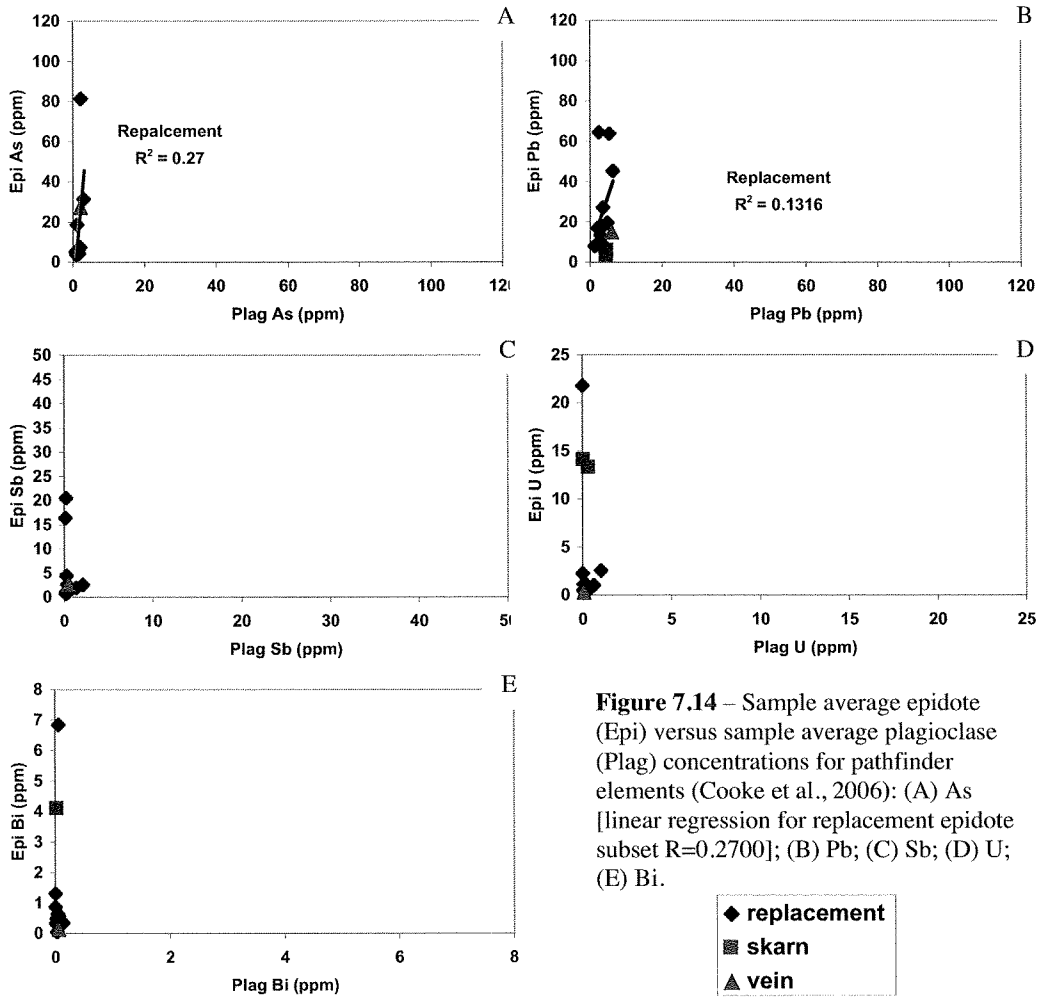

Figure 7.14 – Sample average epidote (Epi) versus sample average plagioclase (Plag) concentrations for pathfinder elements (Cooke et al., 2006): (A) As [linear regression for replacement epidote subset R=0.2700]; (B) Pb; (C) Sb; (D) U; (E) Bi.

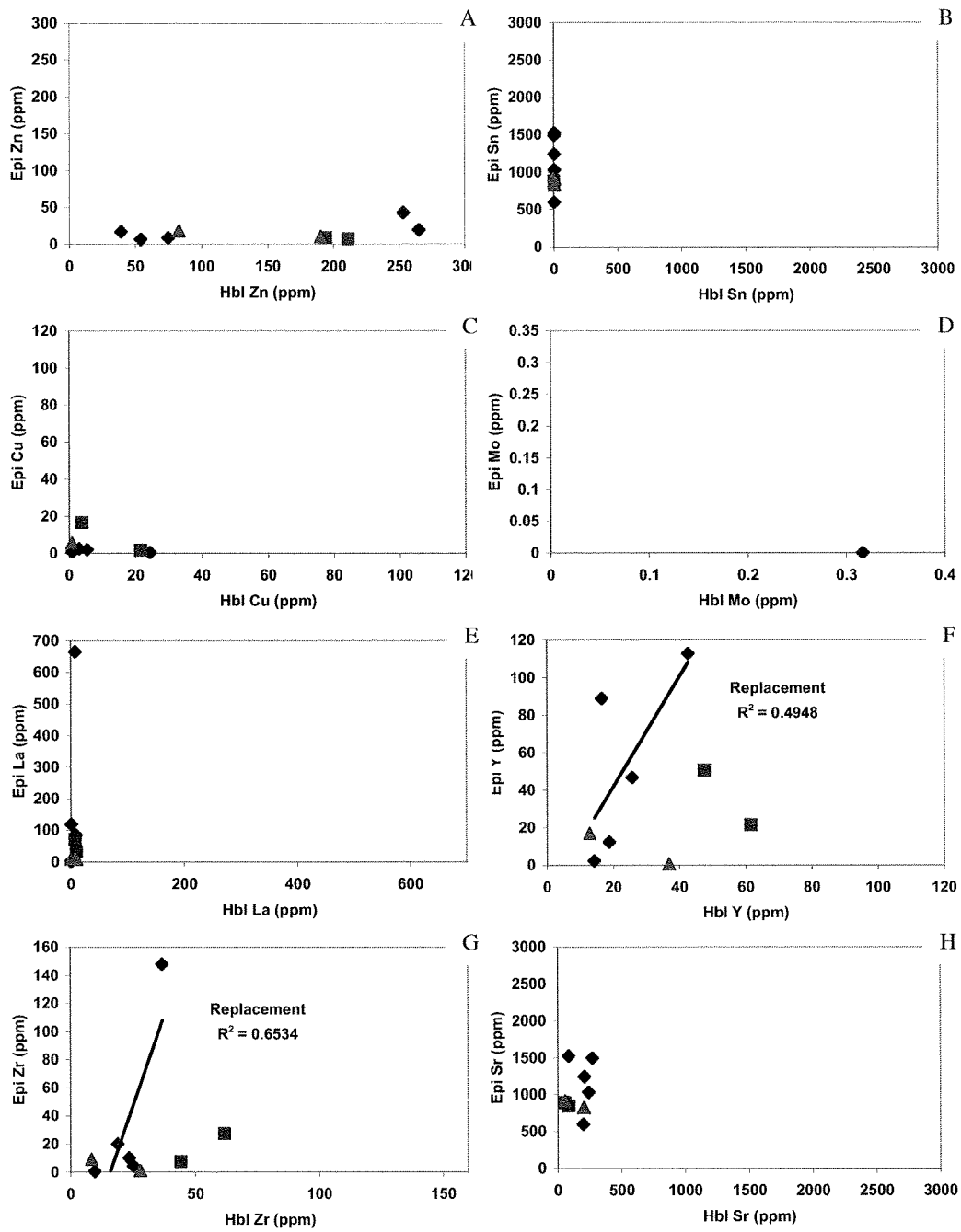

Figure 7.15 – Sample average epidote (Epi) versus sample average hornblende (Hbl) concentrations for vector elements (Cooke et al., 2006): (a) Zn; (b) Sn; (c) Cu; (d) Mo; (e) La; (f) Y [linear regression for replacement epidote subset R^2=0.4948]; (g) Zr [linear regression for replacement epidote subset R^2=0.6534]; (h) Sr.

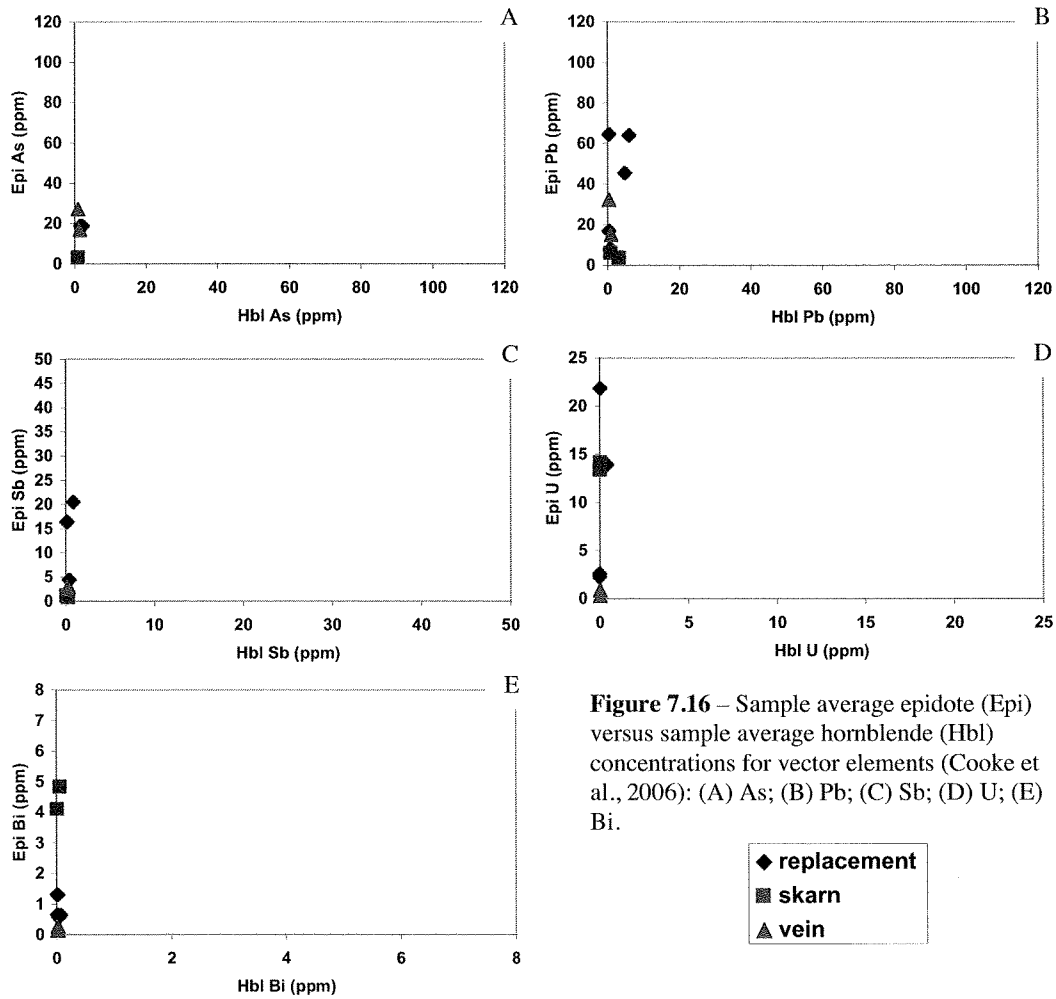

Figure 7.16 – Sample average epidote (Epi) versus sample average hornblende (Hbl) concentrations for vector elements (Cooke et al., 2006): (A) As; (B) Pb; (C) Sb; (D) U; (E) Bi.

The remaining pathfinder elements La, Zr, Sr, Pb, As, Sb, U, Bi and Sn are all enriched in epidote by up to an order of magnitude relative to hornblende, with some elements up to two (Sb, U and Bi) or three (Sn) orders of magnitude above hornblende values (Table 7.1). There are no statistical correlations between these elements.

Discussion

Coupled with the positive correlation between Sr in replacement-style epidote and primary plagioclase, the broad equivalence between the Sr values suggests that the epidote Sr could originate solely from the replaced plagioclase phenocrysts (the most commonly altered mineral in the propylitic halo to the Black Mountain; Section 7.2). Conversely, the fact that the replacement epidote values for As are up to an order of magnitude greater than plagioclase phenocrysts implies that excess As was introduced at the grain scale. Whether local scavenging of trace elements has caused their enrichment, or if their elevation in epidote is a primary feature of the hydrothermal fluids has been assessed via grain mapping techniques Section 7.3.6).

Given the statistical weakness of the correlation of Y concentrations between hornblende and replacement epidote, it is difficult to conclude that there has been any control by hornblende phenocrysts on replacement epidote chemistry. Coupled with the fact that most of the epidote is replacing plagioclase phenocrysts, it seems unlikely that the weak correlation that was observed implies a control of hornblende phenocryst geochemistry on replacement epidote.

7.3.6 Chemical Mapping

Eight chemical maps of epidote grains and their surrounding material were produced using the LA-ICPMS for five samples from across the Black Mountain Southeast map area. The samples were chosen to highlight the range of epidote morphologies (replacement of plagioclase, vein-type, replacement of hornblende), rock types, phenocryst populations and distance from the porphyry center. Figure 7.8 show the locations of the five samples, and correlating LA-ICPMS spot analyses are in Table 7.2.

Sample	BA08GS026	BA08GS026	BA08GS026	BA08GS026	BA08GS035	BA08GS035	BA08GS036	BA08GS036	BA08GS047	BA08GS047	BA08GS047	BA08GS047	BA08GS052B	BA08GS052B
Grain Map	A	A	B	B	B	B	A	A	A	A	B	B	A	A
Analysis	ma31a45	ma31a51	ma31a68	ma31a72	ma27a82	ma27a81	ap01a34	ap01a36	ap01a76	ap01a77	ap01a71	ap01a72	de04a17	de04a18
Min	epi	plag	epi	plag	epi	epi	epi	epi	epi	epi	epi	epi	epi	pl
Na		40267	51	47265	155	233	38	25	82	185	135	60	827	30999
Mg	613	211	792	35	492	448	3336	740	185	205	187	183	539	781
Al	128902	144000	138532	144000	116331	120352	105249	111514	129947	131316	127376	122533	126490	145000
K		3385	17	2077	8		51	44	3288	1072	223	36	766	11213
Ca	168000	71619	168000	61639	163000	163000	166000	166000	167000	167000	167000	167000	164000	67510
Ti	23	12	29	29	139	134	31569	7014	193	137	292	840	77	59
V	44.04	10.04	5.85		211.60	330.79	844.43	725.03	420.72	209.99	226.62	288.32	53.02	0.99
Mn	3417	246	1090	23	3403	2819	2416	1387	1767	1553	1451	1180	2363	59
Fe	109477	5822	76432	1113	119718	105937	103168	127719	109384	107741	98908	114005	113702	2634
Cu					1	1			2	2	1	1		1
Zn	6	11	10	3	7	7	20	6	7	7	6	3	5	5
Ga	46	31	24	22	32	40	58	77	45	36	47	44	45	26
As	56		8		15	19	33	16	3	3	3		8	
Sr	1443	909	779	1460	771	983	680	740	745	722	904	561	524	1059
Y	0.04	0.24	0.22		9.42	18.84	49.18	9.11	26.65	10.86	7.52	15.27	1.35	0.63
Zr		0.14			1.54	0.75	7.91	1.43	1.76	0.94	0.92	1.17	6.28	4.49
Mo					0.20									
Sn			0.54		0.89	0.99	6.35	2.62	2.25	1.12	1.07	1.13	0.44	0.18
Sb	0.41	0.89	2.13		0.64	3.96	7.78	4.00	0.58	0.41	1.00	0.20	0.64	0.23
Ba	1	600	1	92	6	8	7	2	8	3	3	2	10	510
La	4	1	9	5	7	35	38	24	9	6	2	2	2	4
Ce	4	2	10	6	16	78	72	45	17	11	3	3	3	6
Pr	0	0	1	0	2	10	8	5	2	1	0	0	0	1
Nd	1	0	2	1	10	50	31	19	11	6	2	2	1	2
Sm			0.09		2.43	10.31	6.53	3.43	3.23	1.52	0.49	0.70	0.22	0.22
Eu	0.43	0.16	0.51		1.42	4.02	5.12	3.09	4.44	1.45	1.07	1.54	0.32	0.45
Gd					2.29	8.47	7.42	2.42	4.18	2.03	0.67	1.00	0.15	0.26
Dy					1.90	4.95	9.26	1.70	5.06	2.05	1.15	2.12	0.17	0.12
Er					0.90	1.74	5.44	0.77	2.63	1.21	1.20	1.93	0.11	0.08
Yb					0.81	1.12	5.03	0.66	1.49	0.74	0.64	1.48	0.12	
Lu					0.10	0.15	0.68	0.11	0.18	0.08	0.08	0.13	0.03	0.02
Pb	14	7	10	6	22	33	31	21	4	5	5	4	30	4
Bi	0.08	0.06			0.11	0.51	0.61	0.22	0.64	0.59	0.40	0.24	0.24	
Th		0.14			0.04	0.24	0.31	0.03					0.54	0.26
U		0.10	0.06		0.60	1.24	3.22	0.97	8.06	2.43	1.43	1.45	0.15	0.07

Table 7.2 – Individual LA-ICPMS spot analyses used to quantify the chemical grain map images. Below detection limit values are left blank.

Sample BA08GS026

Two grain maps were produced for sample BA08GS026, both of which show partial epidote replacement of plagioclase phenocrysts in a plagioclase- and hornblende-phyric basaltic-andesite dike, approximately 62 meters from the center of the map area (Fig. 7.8). Chemical map BA08GS026-A (Fig. 7.17) shows epidote that has partially replaced a plagioclase phenocryst. The relative compositions of plagioclase and epidote were determined by two LA-ICPMS spot analyses (epidote: ma31a45; plagioclase: ma31a51; Table 7.2). The replacement epidote has elevated As, Pb and Sb with respect to the replaced plagioclase phenocryst (Fig. 7.17). However, the groundmass is enriched in Zr relative to epidote. High La and Y zones on the left side of the epidote grain correspond with a small hornblende microphenocryst, visible in the EMP backscatter image (Fig. 7.17). No element zonation was detected in the epidote grain apart from a weak enrichment of Sb along the irregular contact of the epidote grain with the unaltered plagioclase phenocryst. No depletion halos are identifiable in the plagioclase or groundmass surrounding the epidote grain.

Chemical map BA08GS026-B (Fig. 7.18) shows epidote that has partially replaced a plagioclase phenocryst. The relative compositions have been determined by two LA-ICPMS spot analyses (epidote: ma31a68; plagioclase: ma31a72; Table 7.2).

Elevated Sb, As, Bi, Zr, La and Y distinguish the replacement epidote from the unaltered portion of the plagioclase phenocryst. The epidote grain is coarsely zoned with higher values of Sb, La and Y occurring around the edges. A possible depletion halo for La is visible as a 200μm-wide zone of low La to the immediate left of the epidote grain (Fig. 7.18). However, examination of the photomicrograph for the grain map area identifies the area of low La as a crumbly, uneven surface (Fig. 7.18). Despite the fact that no other pathfinder elements display a uniquely low value in this area, the surficial irregularity on the polished face of the laser ablation sample may have caused the lower La value.

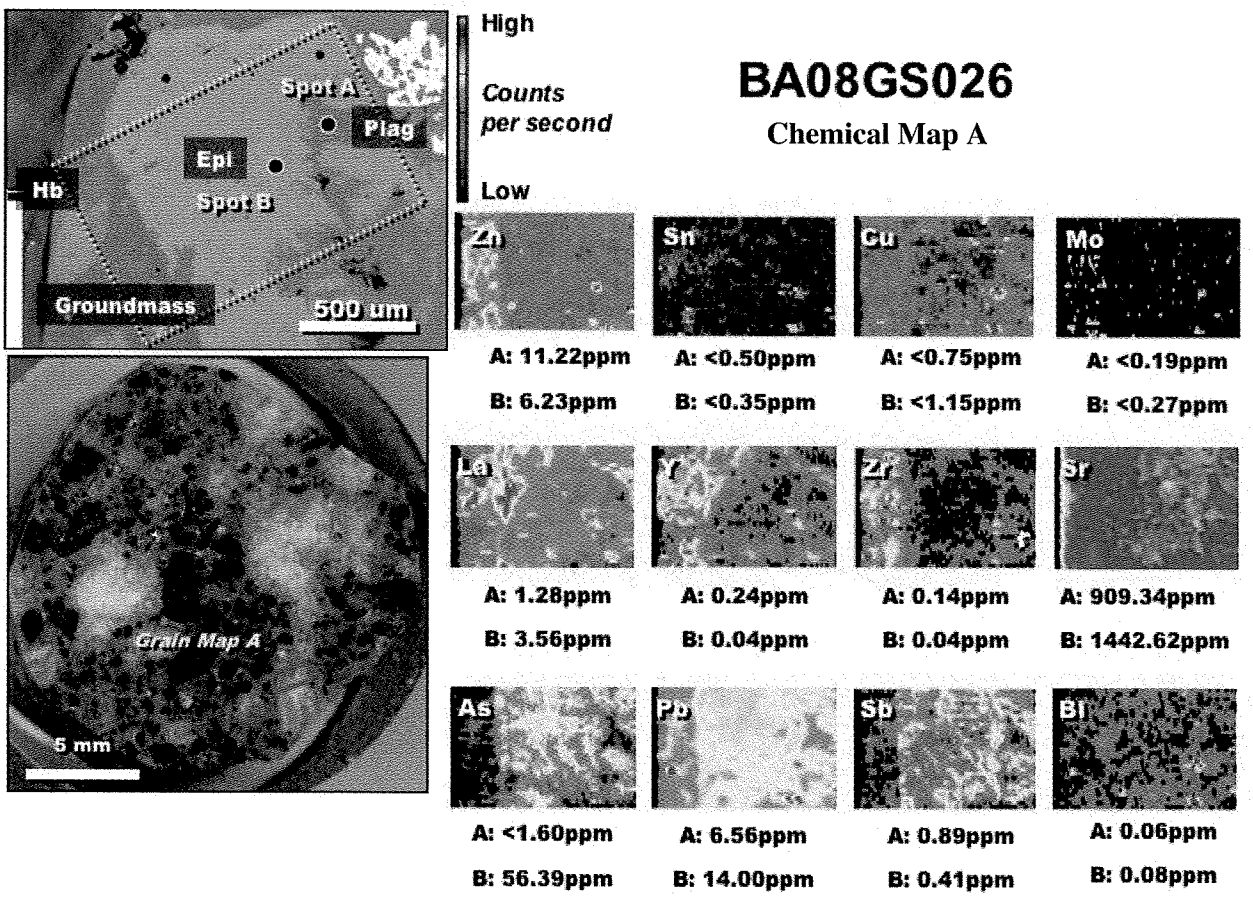

Figure 7.17 - BA08GS026 chemical map A, produced by LA-ICPMS line analyses across the red rectangle shown on the laser ablation puck photograph; partial replacement of a plagioclase feldspar phenocryst by epidote in a plagioclase- and hornblende-phyric basaltic-andesite dike approximately 62 meters from the Black Mountain Southeast map center.

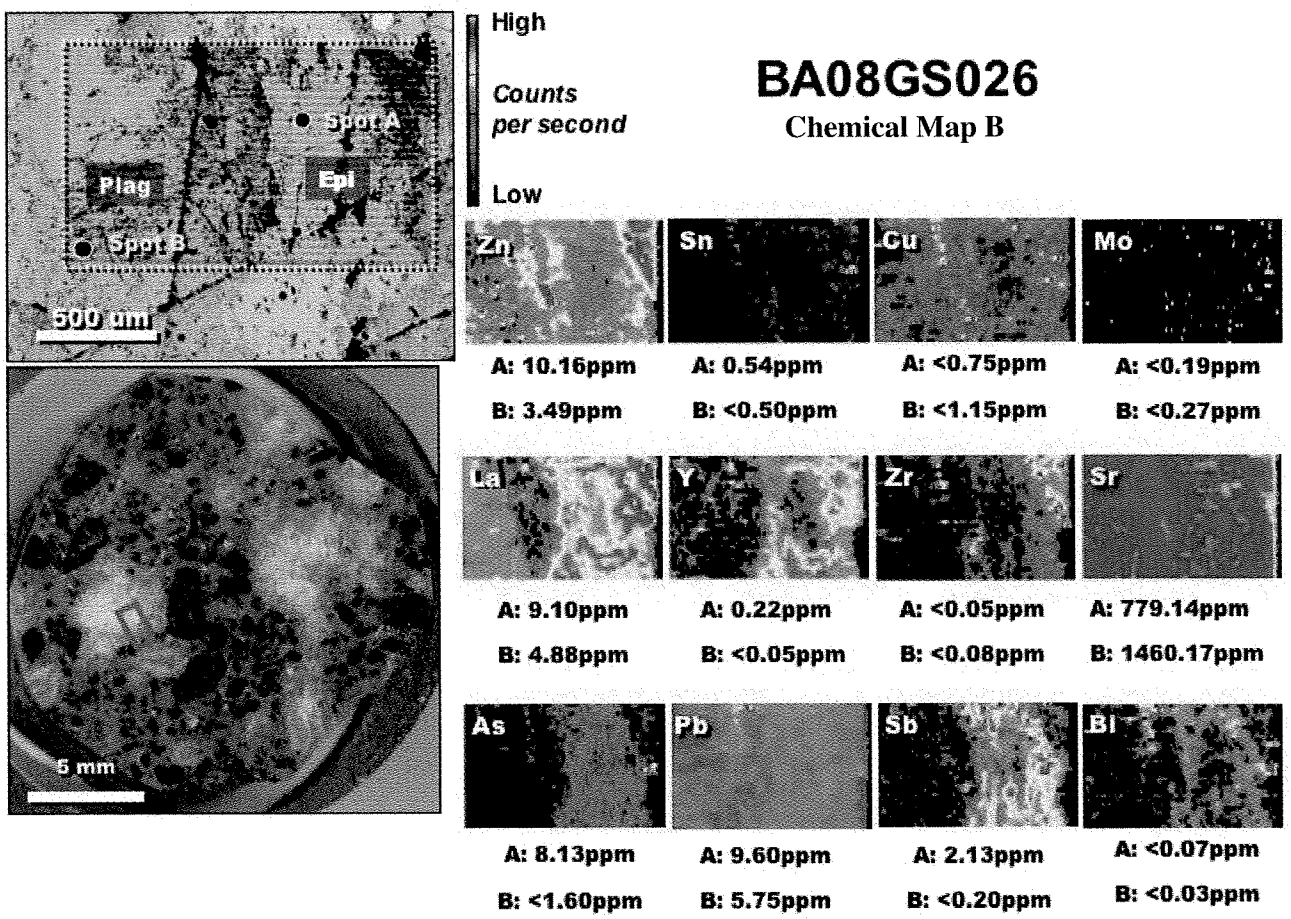

Figure 7.18 - BA08GS026 chemical map B, produced by LA-ICPMS line analyses across the red rectangle shown in the laser ablation puck photograph; partial replacement of a plagioclase feldspar phenocryst by epidote in a plagioclase- and hornblende-phyric basaltic-andesite dike approximately 62 meters from the Black Mountain Southeast map center.

Sample BA08GS035

Two chemical maps were produced for sample BA08GS035, both of which were intended to test pathfinder element zonation within epidote replacing plagioclase and hornblende phenocrysts and groundmass in contact with an epidote vein cutting a hornblende megacrystic basaltic-andesite Liw-Liw Creek mafic dike. The sample is located approximately 36 meters from the intrusive center (Fig. 7.8). Grain map BA08GS035-A (Fig. 7.19) shows epidote replacement of groundmass as well as partial replacement of a hornblende phenocryst at the edge of an epidote vein. Although no LA-ICPMS spot analyses were acquired in this grain map area, the epidote and hornblende grain boundaries are visually distinguishable for most elements. The photomicrograph of the grain map area identifies the hornblende phenocryst enveloped by smooth, continuous epidote grading outwards to a patchy, rough-looking epidote (Fig. 7.19). The transition from the hornblende phenocryst into the epidote coincides with increasing distance from the epidote vein. With respect to the hornblende phenocryst, epidote is enriched in all pathfinder elements except Zn and Cu. Arsenic, Sr, Sb and Bi are elevated in a halo around the hornblende phenocryst, coinciding with the transition from smooth to rough-textured epidote. Lanthanum and Y values increase in the patchy epidote. No zonation is present within the hornblende phenocryst, and no depletion halos are identifiable.

Chemical map BA08GS035-B is an example of replacement of a plagioclase microphenocryst by epidote approximately 5mm from an epidote vein. The plagioclase is bordered by a hornblende phenocryst (Fig. 7.20). The chemical map compositions have been quantified by two LA-ICPMS spot analyses of the epidote grain (ma27a81 and ma27a82; Table 7.2). The epidote has elevated Sb, La and Bi, and to a lesser extent As, evident around the edges of the grain (Fig. 7.20). The hornblende phenocryst at the bottom of the map area is enriched in Zn and Cu where it is in contact with the epidote. There are no depletion halos in the groundmass surrounding the epidote grain.

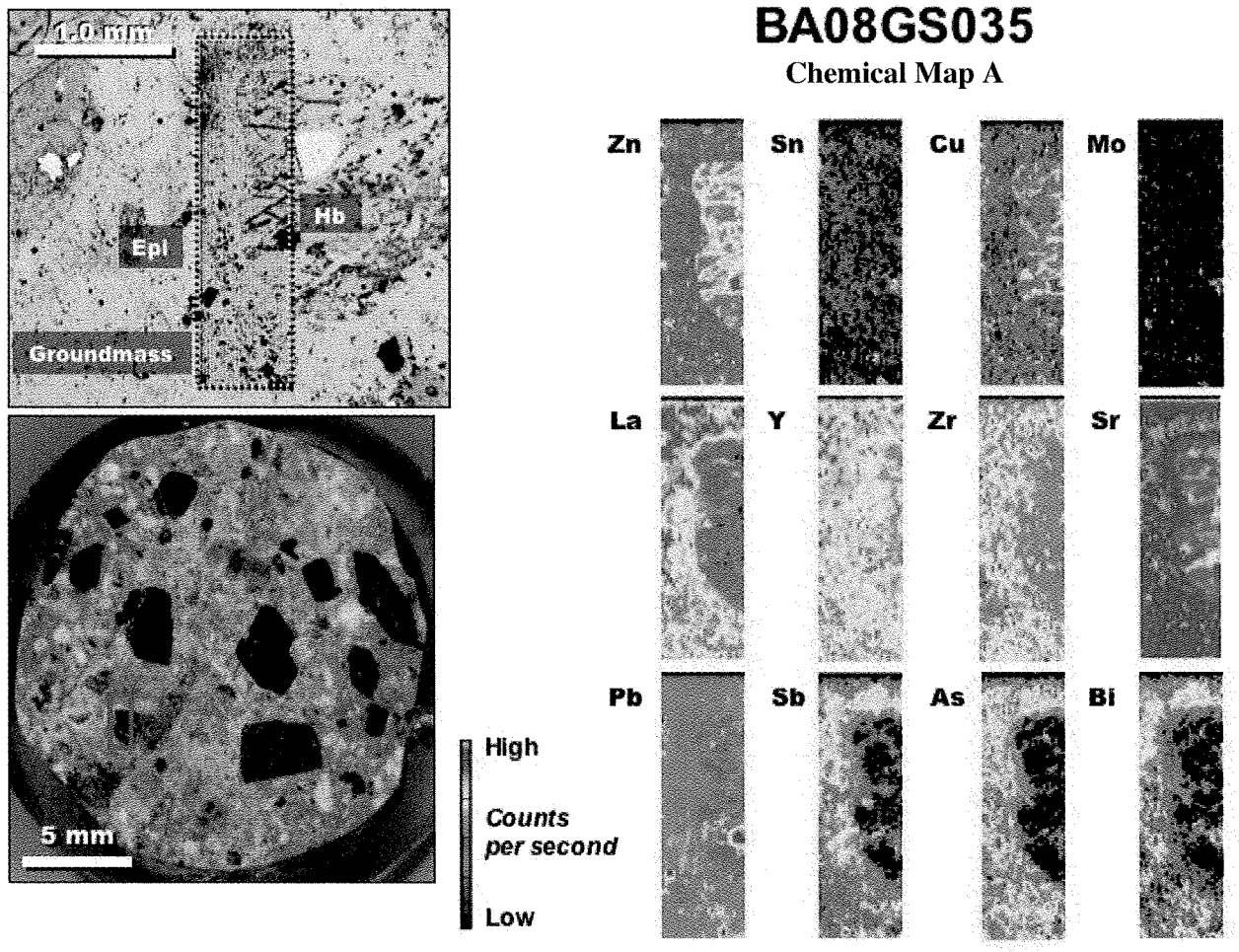

Figure 7.19 - BA08GS035 chemical map A, produced by LA-ICPMS line analyses across the red rectangle shown in the laser ablation puck photograph; partial replacement of a hornblende phenocryst in contact with an epidote vein in a Liw-Liw Creek basaltic-andesite dike approximately 36 meters from the Black Mountain Southeast map center.

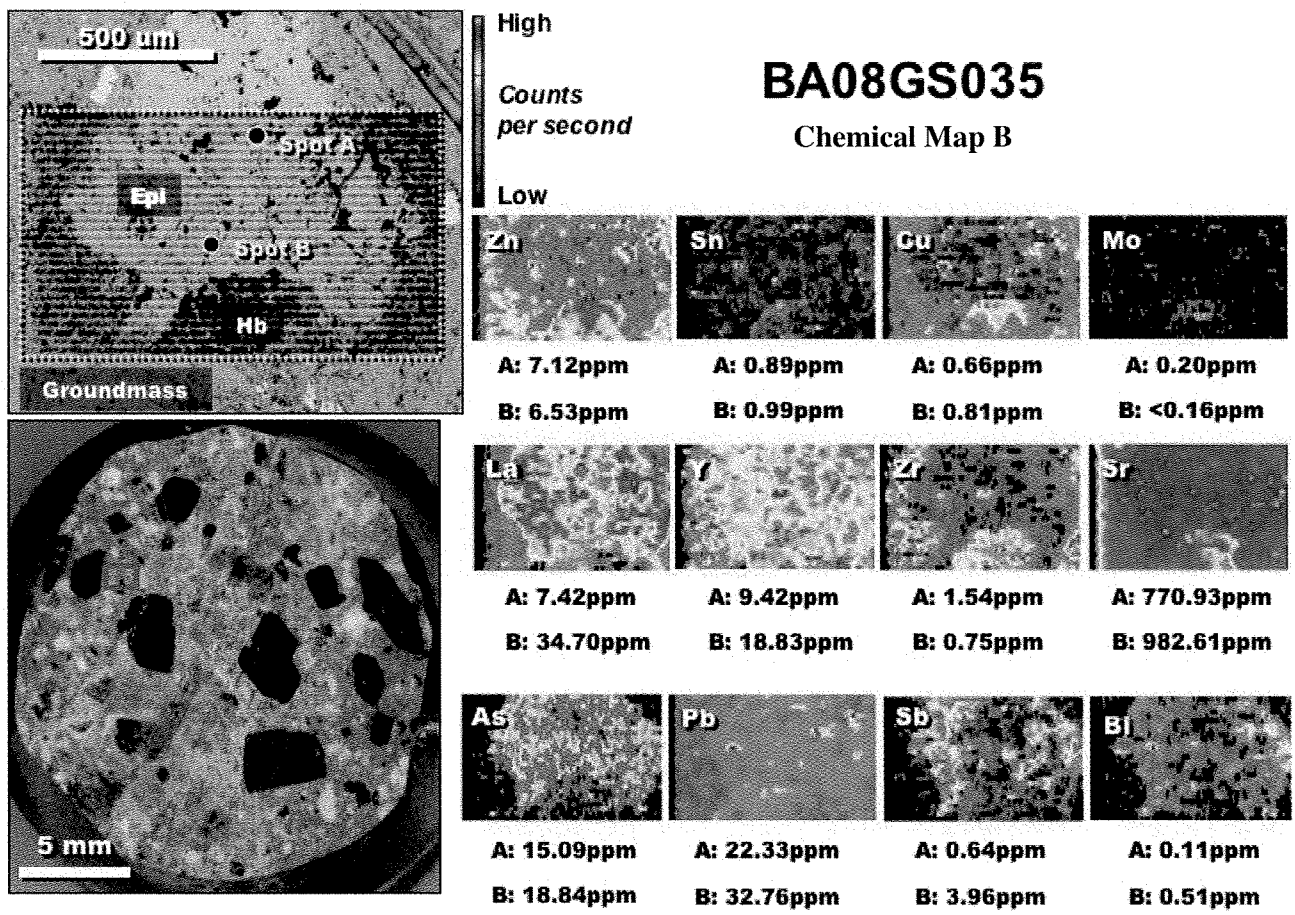

Figure 7.20 - BA08GS035 chemical map B produced by LA-ICPMS line analyses across the red rectangle shown in the laser ablation puck photograph; complete replacement of a plagioclase feldspar phenocryst by epidote, approximately 5mm from an epidote vein in a Liw-Liw Creek basaltic-andesite dike approximately 36 meters from the Black Mountain Southeast map center.

Sample BA08GS036

One chemical map (BA08GS036-A) was produced for sample BA08GS036 to examine epidote replacement of hornblende phenocrysts in a hornblende- and plagioclase-phyric diorite (Fig. 7.21). The sample was collected approximately 38 meters from the center of the porphyry (Fig. 7.8). The relative grain map compositions were quantified by two LA-ICPMS spot analyses of the epidote grain (ap01a34 and ap01a36; Table 7.2). Zonation within the epidote is defined by Zn, La and Sb enrichment at the edges of the grain, with relatively lower concentrations at the grain center (Fig. 7.21). The groundmass is enriched in Zr and Cu with respect to epidote (Fig. 7.21). No obvious depletion halos are identifiable within the groundmass.

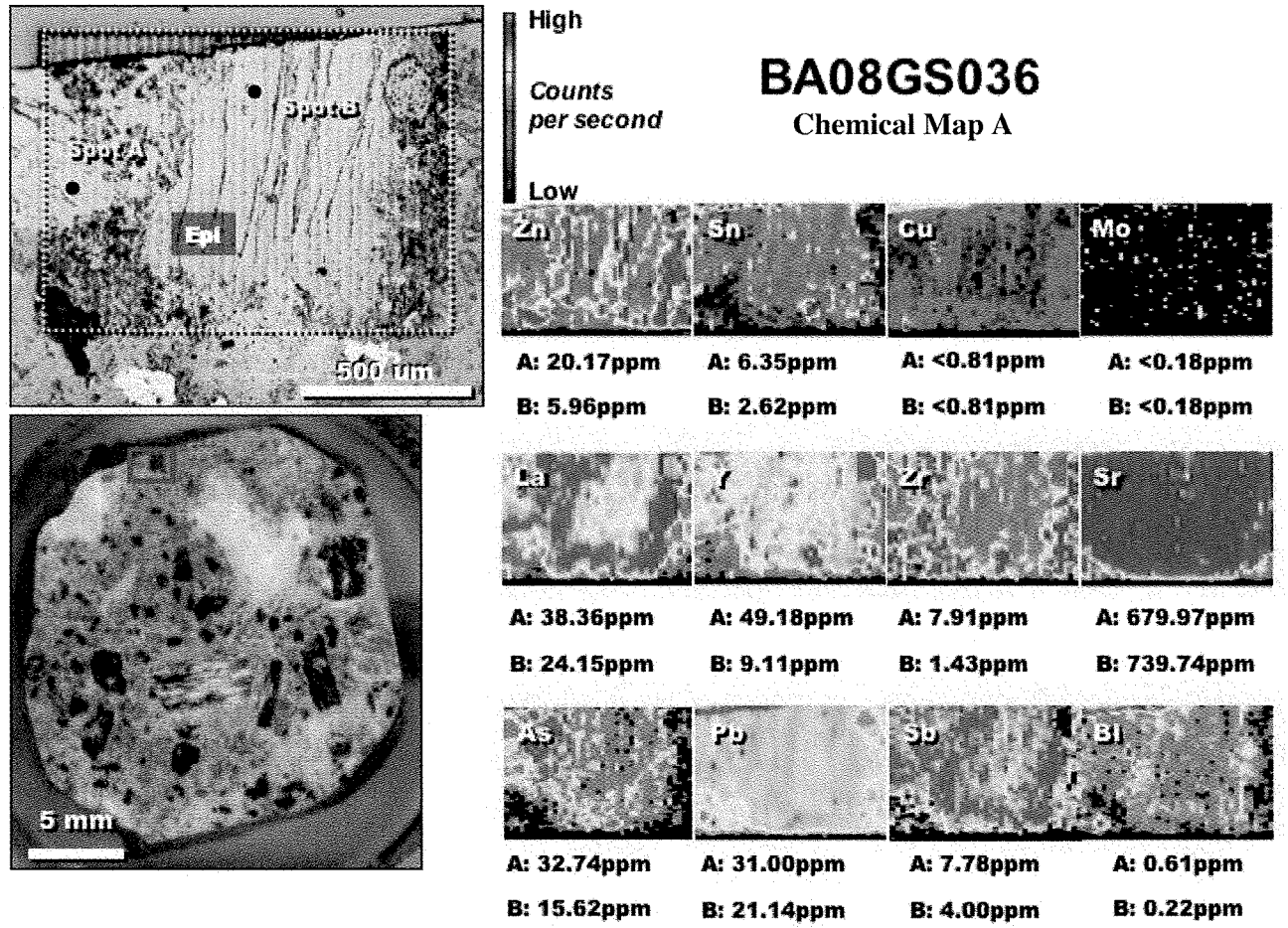

Figure 7.21 - BA08GS036 chemical map A produced by LA-ICPMS line analyses across the red rectangle shown in the laser ablation puck photograph; complete replacement of a hornblende phenocryst by epidote in a PHD plagioclase and hornblende-phyric diorite dike approximately 38 meters from the Black Mountain Southeast map center.

Sample BA08GS047

Two chemical maps were produced for sample BA08GS047. The section of sample analyzed (both for the LA-ICPMS spot analyses and grain maps) was a portion of a hornblende cluster found in the BA08GS047 basaltic dikes. Within these clusters, epidote has selectively replaced the few anhedral plagioclase phenocrysts that are surrounded by hornblende. The sample is from an outcrop of hornblende clotted basalt (HCB) approximately 458 meters from the deposit center (Fig. 7.8). The image for BA08GS047-A shows the partial, patchy replacement of anhedral plagioclase by epidote (Fig. 7.22). Element concentrations were quantified by two LA-ICPMS spot analyses of epidote in an area of more complete replacement of the plagioclase (ap01a76 and ap01a77; Table 7.2). In general, the area of more complete epidote replacement displays higher Cu, Pb and Bi contents, but lower La, Sr, As and Sb than the area where epidote

replacement was less pervasive (Fig. 7.22). Compositional zonation is minimal in the epidote, although there is a slight enrichment of Sr, As and Sb at contacts with hornblende phenocrysts. No depletion halos are present within the hornblende.

Similar to image BA08GS047-A, BA08GS047-B displays patchy epidote replacement of an anhedral plagioclase crystal (Fig. 7.23). Element concentrations were quantified by two LA-ICPMS spot analyses of areas of intense epidote replacement of the plagioclase grain (ap01a71 and ap01a72; Table 7.2). Lanthanum, Y, Sr and As are elevated within the area where epidote has only partially replacement the plagioclase grain (Fig. 7.23). Conversely, Bi is slightly elevated in the area of more pervasive epidote alteration (Fig. 7.23). The epidote is compositionally zoned with weakly elevated Sr and As values (and La and Y to a lesser extent) a the contacts between epidote and hornblende. No depletion halos were observed.

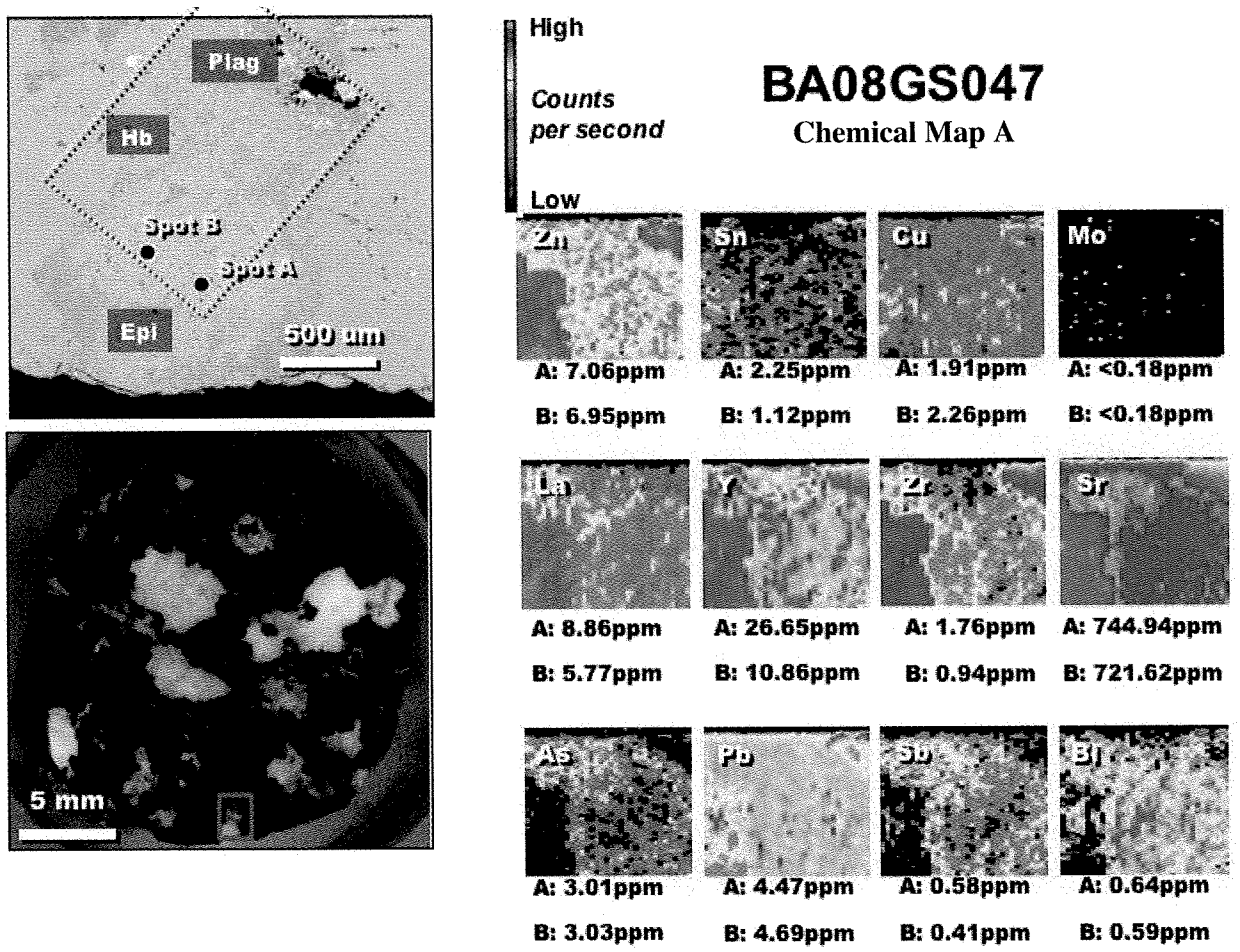

Figure 7.22 - BA08GS047 chemical map A produced by LA-ICPMS line analyses across the red rectangle shown in the laser ablation puck photograph; "patchy" replacement of a plagioclase feldspar phenocryst by epidote in a HCB hornblende-plagioclase "cluster" approximately 458 meters from the Black Mountain Southeast map center.

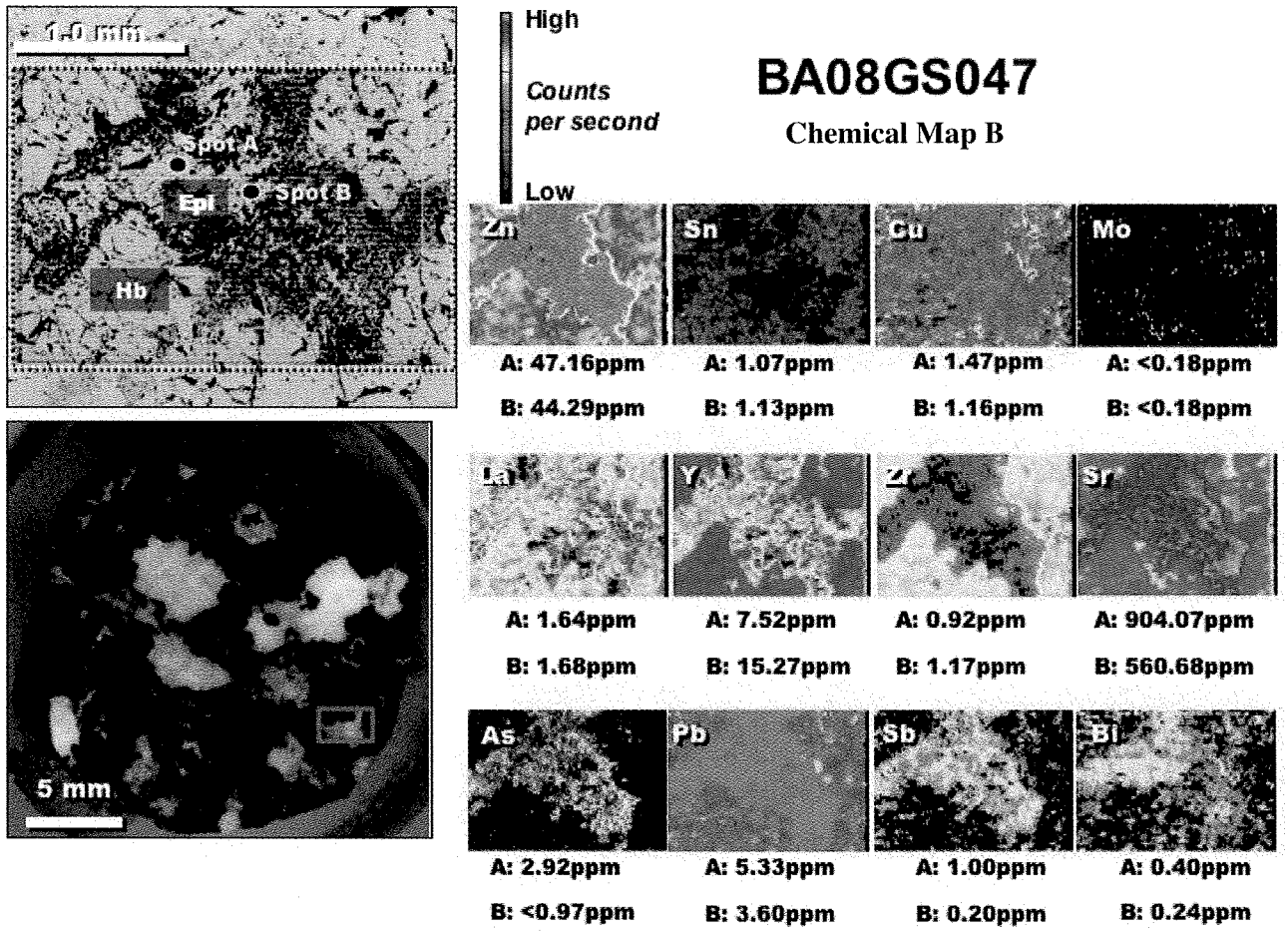

Figure 7.23 - BA08GS047 chemical map B produced by LA-ICPMS line analyses across the red rectangle shown in the laser ablation puck photograph; partial "patchy" replacement of a plagioclase feldspar phenocryst by epidote in a HCB hornblende-plagioclase "cluster" approximately 458 meters from the Black Mountain Southeast map center.

Sample BA08GS052B

One chemical map was produced for sample BA08GS052B in order to examine the distribution of trace elements in epidote replacement of plagioclase from a plagioclase- and variably hornblende-phyric diorite dike (Fig. 7.24). The sample was collected from Liw-Liw Creek, approximately 805 meters from the Southeast orebody (Fig. 7.8). Image BA08GS052B-A displays partial epidote replacement of a cluster of plagioclase grains (Fig. 7.24). Quantification of element concentrations was possible through two LA-ICPMS spot analyses, one of epidote and one of plagioclase (epidote: de04a17; plagioclase: de04a18). The epidote is enriched in La, Y, As, Pb, Sb and Bi relative to the plagioclase (Fig. 7.24). Weak zonation within the epidote is defined by a slight elevation of La and Y at the grain edges. There is no zonation of pathfinder elements with the

plagioclase. There is a slight enrichment of Zr, Zn, Cu and Y within the groundmass at the contact with the plagioclase. No depletion halos were detected within the plagioclase surrounding the epidote grain.

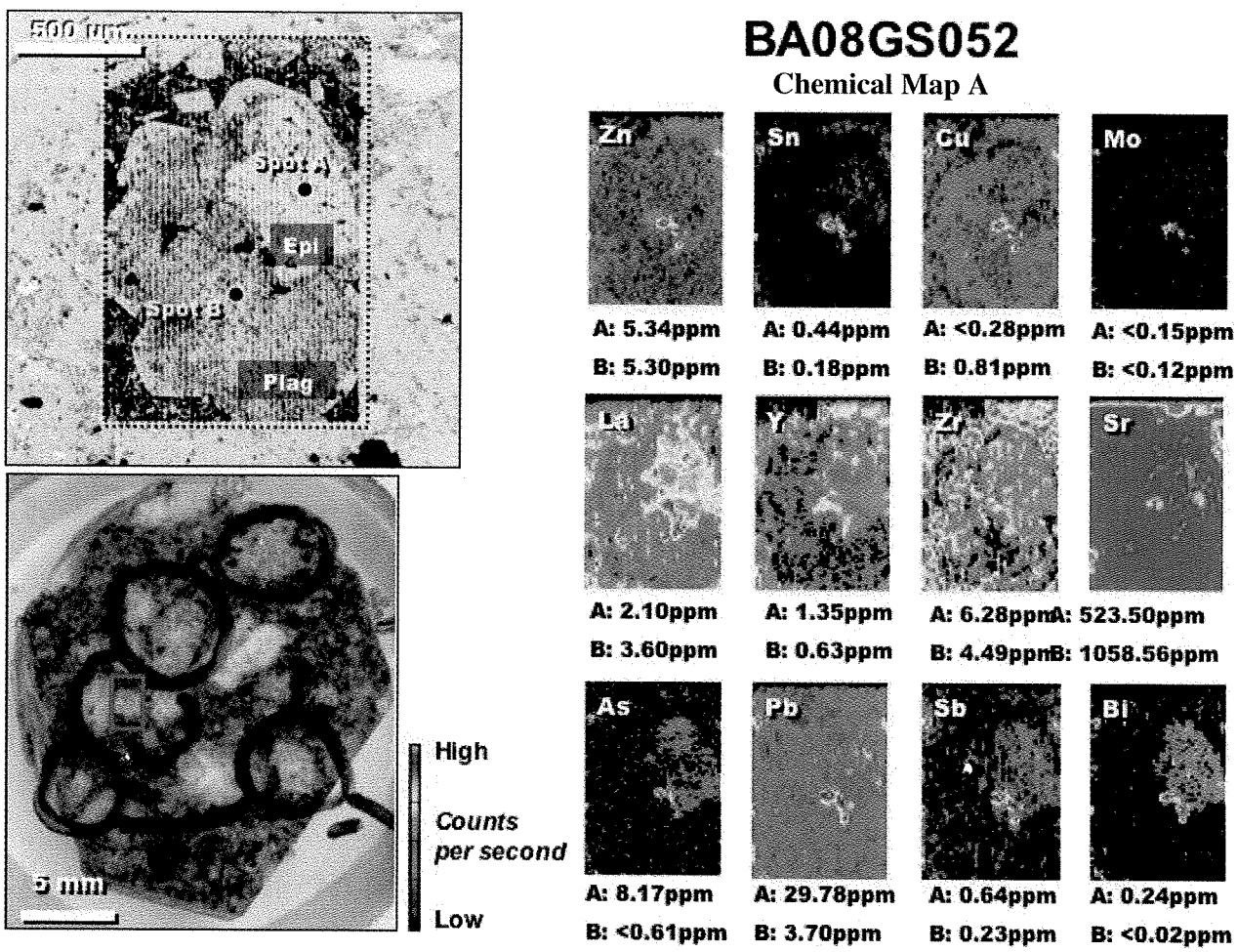

Figure 7.24 - BA08GS052B chemical map A produced by LA-ICPMS line analyses across the red rectangle shown in the laser ablation puck photograph; selective replacement of a plagioclase feldspar phenocryst by epidote in a PHD plagioclase-phyric diorite approximately 805 meters from the Black Mountain Southeast map center.

Discussion

Of the five samples examined by LA-ICPMS mapping techniques, only one demonstrated possible remobilization of vector elements on a grain scale based on the presence of a weak depletion halo in the host mineral (BA08GS026-B; Fig.7.18). Figure 7.25 displays the locations and correlative raw data output for two LA-ICPMS spot analyses in counts-per-second. The first spot analysis is located on an even-surfaced core of a hornblende grain from sample BA08GS030 (Fig. 7.25a). The raw output data for this analysis forms a clean graph of counts over time, where the number of counts for individual elements remain at a near-constant proportion to each other (signified by the parallel lines) throughout the roughly 50 second analysis run (Fig. 7.25b). Conversely, the second spot analysis is located on a rough-surfaced plagioclase phenocryst from the same sample (Fig. 7.25c). The raw data plot of counts over time displays variability in some elements (e.g., Fe) whereas others remain relatively constant (e.g., Sr; Fig. 7.25d), yielding proportionally inconsistent (i.e. non-parallel) counts per time plots. This implies that the character of the surface area can be reflected in the output data. However, it is also possible that removal of the upper surface material during ablation exposed a different mineral or inclusion directly below the analysis area. This scenario could also resulted in anomalous compositional values for this part of the grain map area.

In general, the lack of depletion halos associated with partial and complete epidote replacement grains indicates that grain-scale remobilization of trace elements during propylitic alteration did not occur at Black Mountain. The anomalously enriched elements in epidote are interpreted to have been derived from the hydrothermal fluid, rather than the host rock. The only possible exception is Sr in replacement epidote, which may be inherited from the local grains of plagioclase based on the positive correlation between epidote and whole rock Sr, as well as the equivalent sample mean concentrations of replacement epidote and plagioclase phenocrysts. However, the lack of evidence for local remobilization of any pathfinder elements from the chemical maps implies that the inheritance of plagioclase Sr content is an in-situ process. More specifically, during the alteration of plagioclase to epidote, Sr does not appear to be moved or transferred from, or to, the replaced phenocryst, but rather remains in place to be inherited by the epidote.

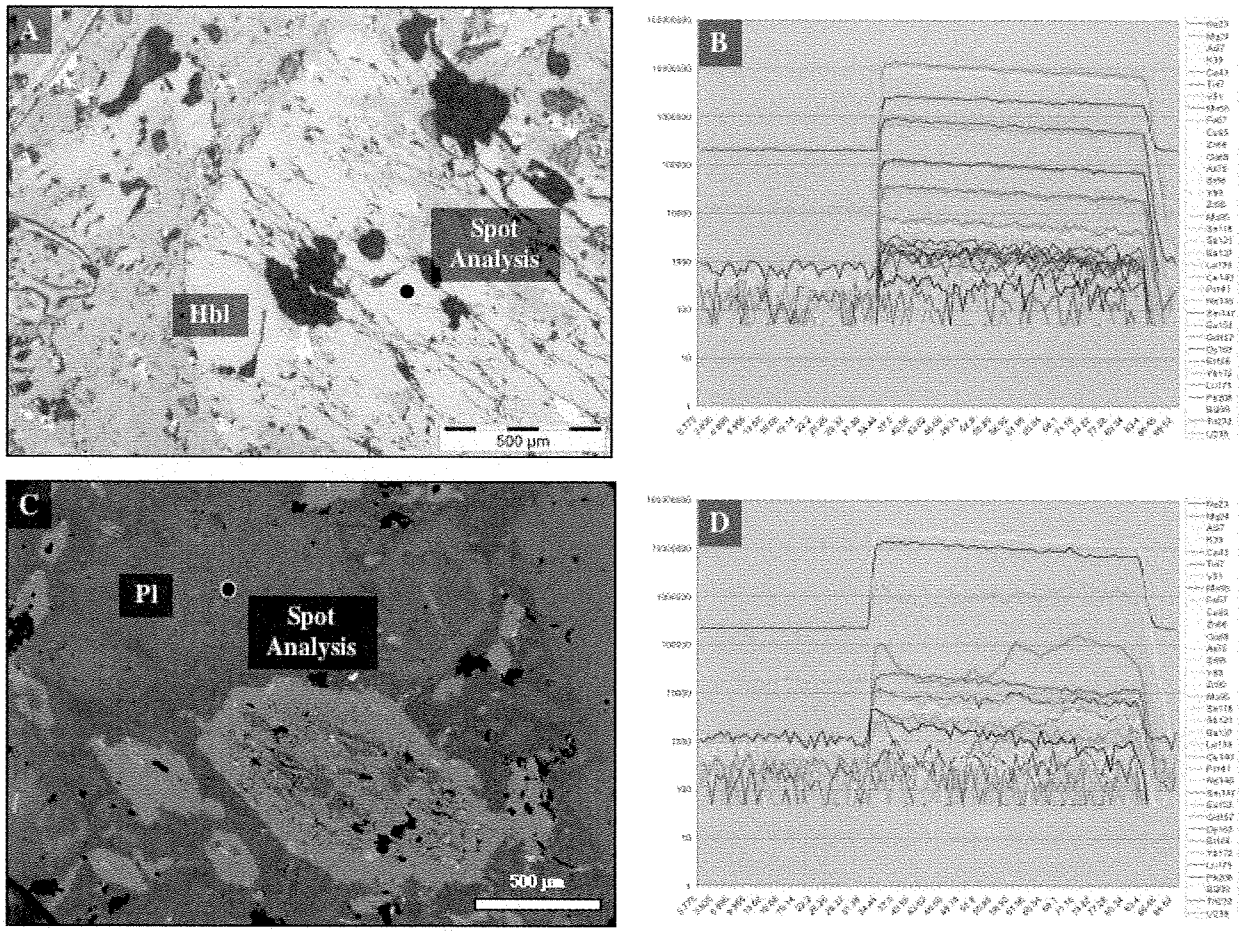

Figure 7.25 - (A) Photomicrograph of an LA-ICPMS spot analysis of a even-surfaced hornblende phenocryst core (sample BA08GS030). (B) Returned raw LA-ICPMS data (in counts per minute) for the hornblende phenocryst core. Note the broadly even element proportions over time (signified by the parallel data lines for most elements). (C) SEM back scatter image of a rough-textured plagioclase phenocryst core analysis (sample BA08GS025). (D) Raw LA-ICPMS data (in counts per minute) for the plagioclase phenocryst core. Note the variable proportions of some elements (the non-parallel data lines) along side the consistent proportions of others (the parallel data lines).

7.3.7 Summary and Implications

With the exception of Sr, sample and grain scale comparative geochemistry (as well as grain mapping techniques) suggest that the composition of epidote in the propylitic halo to Black Mountain is controlled by fluids derived from the porphyry deposit, rather than the local wall rocks. The lack of any positive correlations between pathfinder element compositions in epidote, bulk rock, plagioclase and/or hornblende analyses, the order-of-magnitude enrichment of trace elements in epidote relative to the whole rock analyses, and the lack of evidence for grain-scale scavenging of elements are indicative of a fluid-dominated geochemical signature. This finding is consistent with the spatial zonation of pathfinder elements delineated over a scale of kilometers by Cooke et al. (2006) through the study of multiple porphyry systems. In summary, the detection of similar compositional zonation patterns defined by trace elements between multiple deposits is indicative of a geochemical process that is common to the propylitic alteration environment and is independent of protolith composition.

Confirming the existence of the epidote trace element zonation patterns around porphyry deposits has been a primary objective of the AMIRA P765 and P765A projects. The identification of Sr in replacement-style epidote as a host-rock influenced geochemical feature means that it should be treated with caution when used as a pathfinder element (Cooke et al., 2006). The zonation of the remaining pathfinder elements in both replacement- and vein-type morphologies of propylitic epidote is confirmed from this study of Black Mountain and indicates they can be used to evaluate the alteration halos in porphyry systems.

Chapter 8

A Paragenetic Model for the Black Mountain Porphyry Southeast System

8.1 Introduction

Generation of the Black Mountain Porphyry system magmas and mineralization is coincident with a late-Miocene to early-Pliocene geodynamic shift in the Northern Philippine Arc, involving an arc polarity reversal, subduction of an aseismic seamount chain, shallowing of the eastward subducting South China Sea slab, and/or the formation of a slab tear beneath Luzon (Yang et al., 1996; Bautista et al., 1996 and 2001; Hollings et al., in press). Mineralogical, geochemical and isotopic data presented here suggests that the evolution of Black Mountain system itself is a product of intra-crustal magma pooling, fractional crystallization, magma mixing and partial melting as a result of the generation, ascension and interaction of two discrete magmatic components (the Liw-Liw Creek magmas and the hybrid mafic magma; Chapter 5). Interaction between the base of a stagnant Liw-Liw Creek magma chamber and the ascending hybrid mafic melt (Chapter 5) is interpreted to have produced a series of partial melting events, generating felsic magmas (the EMD and PHD intrusive phases) in an otherwise mafic-dominated system (Chapter 5). The generation of bimodal magmatism through mafic underplating is not an uncommon feature in porphyry systems, and has been previously noted in the formation of world-class porphyry systems (e.g., Keith et al., 1998, Maughan et al., 2002; Lickfold et al., 2007; Sillitoe, 2010). This chapter discusses the application of, and evidence for, mafic underplating within the Black Mountain Porphyry system and ultimately arrives at a paragenetic model.

8.2 The Mafic Underplating Model

Convective volatile exchange between an underplated mafic melt and an overlying felsic magma chamber has been cited as a driving force behind world-class porphyry mineralization (e.g. Keith et al., 1998; Maughan et al., 2001; Hattori and Keith, 2001; Lickfold et al., 2007; Sillitoe, 2010). These models argue that the metal, sulfur, volatile and/or heat budgets observed in shallow, intermediate porphyry systems may be sourced in part from the underplating of a typical intermediate/felsic calc-alkaline magma by a

volatile-rich mafic melt. However, the process of component exchange between an underplated mafic melt and the overlying magma chamber is not well constrained, leaving the nature of interaction between the two magmas open to interpretation.

Keith et al. (1998) proposed that the interaction between a wet, oxidized mafic melt and a stagnant intermediate/felsic magma chamber could result in several scenarios. Upon contact with the base of the stagnant chamber, the additional heat of the mafic melt could effectively "re-energize" the remnant liquid and promote convection of volatiles and metals already present within the overlying magma chamber (Keith et al., 1998). Similarly, crystallization of the mafic melt at the base of the magma chamber could also result in exsolution and upward release of a volatile and metal rich. Coupled with the increased heat provided by the mafic melt, a stream of volatile rich fluids and gases would rise into the overlying intermediate/felsic magma, likely accumulating near the top of the magma chamber. Alternatively, co-mingling of the two magmas could yield similar volatile and metal exchange as well as produce hybrid melts that reflect textural, mineralogical and geochemical evidence of overt mixing (Keith et al., 1998; Maughan et al., 2002; Lickfold et al., 2007). It is also possible that two (or all three) of these processes play a role in generating mineralizing fluids over the lifetime of a porphyry system. In their study of the Northparkes porphyry systems (NSW, Australia), Lickfold et al. (2007) cited a process similar to that proposed by Keith et al. (1998) wherein quenching of the underplated mafic magma expelled a "buoyant stream of volatile-rich magma and bubbles of volatiles" into the overlying felsic magma chamber (Lickfold et al., 2007). However, they also noted the presence of mineralogical, textural and geochemical indicators of overt mixing of a felsic and mafic component in late-mineralization intrusive units, indicating that the nature of interaction between the felsic and mafic components changed over time (Lickfold et al., 2007).

Although the exact nature of interaction within a subvolcanic porphyry environment is the subject of debate, the presence of mafic magmatism broadly contemporaneous with intermediate/felsic-hosted porphyry mineralization is indicative of an important role for mafic components in the generation of porphyry systems (Sillitoe, 1973; Keith et al., 1998; Maughan et al., 2001; Hattori and Keith, 2001; Lickfold et al., 2007).

8.3 Mafic Underplating at Black Mountain Southeast

8.3.1 Indications for Mafic Underplating

The data and observations cited as evidence for mafic underplating vary from system to system (e.g., Hattori and Keith, 1997; Keith et al., 1998; Maughan et al., 2002; Lickfold et al., 2007), making the construction of a comprehensive checklist of "mafic underplating indicators" all but impossible. However, within the context of the timing relationships established for the intrusive phases of the Black Mountain Southeast Intrusive Suite (Chapters 3 and 4), specific lithological and geochemical trends and features point to mafic underplating having played a role in the evolution of the system. These are:

1. The temporal trend of mafic-to-felsic-to-mafic intrusive emplacement suggests a role for ongoing mafic magmatism during the lifetime of the Black Mountain Porphyry Southeast system. This trend is evidenced by the evolving mineralogy, major and trace element geochemistry and isotope geochemistry (Chapters 3 and 5). In particular, the abrupt departure from mafic magmatism (the basaltic Liw-Liw Creek dikes) with the emplacement of the voluminous, granitic-to-dioritic EMD and PHD intrusive phases is implicative of processes other than fractional crystallization. Similarly, the following gradual return to mafic magmas geochemically similar to the Liw-Liw Creek dikes cannot be attributed to fractional crystallization (Chapter 5).
2. The identification of two temporally and spatially distinct magmatic components (the Liw-Liw Creek magmas and the hybrid mafic melt), and litho-geochemical evidence for intra-crustal ponding and fractional crystallization of the Liw-Liw Creek magmas (Chapters 3, 5 and 6) suggests a scenario wherein relatively shallow intra-crustal underplating took place between the ascending hybrid mafic melt and the base of the fully- or partially-crystallized Liw-Liw Creek magma chamber to produce an initially felsic partial melt product (the EMD and PHD intrusive phases).
3. The identification of two spatially and chemically distinct hornblende crystallization events and the presence of both hornblende populations in

individual samples implies the presence of two physically disparate crystallization events in the presence of an intermediate and a mafic melt (respectively), and a physical interaction of the two magmas at some point after hornblende crystallization (Chapter 6).

4. The presence of zoned hornblende phenocrysts with high silica, low alkali cores and low silica, high alkali rims is indicative of an increasingly mafic liquid composition during crystal growth, consistent with mixing of a felsic/intermediate melt with an increasing proportion of mafic melt (Chapter 6).

These geochemical and lithological patterns suggest a scenario wherein a partially to completely crystallized chamber of Liw-Liw Creek magma was underplated by the hybrid mafic melt (Chapter 5). The nature of interaction between the two magmas appears to have changed over time as well, with a progressively increasing proportion of the hybrid mafic component present within the upper reaches of the system (indicated by the broadly increasing radiogenic character of successive intrusive phases). More specifically, emplacement of the hybrid melt at the base of the magma chamber initially produced low degree partial melts of solidified Liw-Liw Creek chamber (giving rise to the felsic EMD and evolved PHD intrusive phases). These melts were spatially and temporally associated with the onset of mineralization of the system. However, the increasingly mafic geochemistry and mineralogy of successive intrusive phases (as well as the increasingly radiogenic character) implies a progressively higher ratio of the hybrid mafic melt to the partial melt component.

8.3.2 Paragenetic Model for the Black Mountain Southeast

Coupled with the relative timing relationships of the alteration and mineralization observed, a paragenetic model for the Black Mountain Southeast system has been constructed around the process of mafic underplating (Fig. 8.1), and is broken down into four major magmatic events:

1. (>3.20 Ma) The generation and emplacement of the Liw-Liw Creek magma chamber at shallow crustal levels under locally compressional tectonics led to intra-crustal stagnation and fractional crystallization of the magma (Fig. 8.1a). The presence of Liw-Liw Creek dikes at the current day surface (Chapter 3)

implies that small volumes of the Liw-Liw mafic magmas made their way to higher stratigraphic levels than the magma chamber, facilitated by E-trending structures. The ubiquitous presence of high-aluminum Group 2 hornblendes in the Liw-Liw Creek dikes indicates that these magmas stagnated and underwent crystallization at depth prior to their shallower level emplacement (Chapter 6). It is possible that the protolith of the EMD intrusive phase (prior to quartz flooding, stockwork veining and mineralization) was actually a mafic offshoot of the Liw-Liw Creek magma chamber, the emplacement of which was also facilitated by local structure. However, in the absence of unaltered EMD it is not possible to test this. Nevertheless, the brittle rheology required to produce the observed stockwork veining in the EMD rocks (Chapter 7) implies that it had to have cooled prior to the introduction of the quartz flooding and mineralization. This, coupled with the fact that biotite produced by potassic alteration (associated with mineralization at Kennon) was dated at 2.9-3.0 Ma (Waters and Gonzales, 2005; Chapter 4), requires that the unaltered EMD magmas had to have been emplaced prior to 2.9-3.0 Ma. This is broadly in line with upper limit of dated Liw-Liw Creek samples reported in Chapter 4 (3.18-3.22 Ma; Table 4.1).

2. (~3.20 Ma) The generation of the radiogenic hybrid mafic melt and its ascension to the base of the partially crystallized Liw-Liw Creek magma chamber resulted in a low-degree partial melt and the generation of a felsic-to-intermediate melt (Fig. 8.1b). Upon expending heat to produce partial melting of the overlying Liw-Liw Creek magma chamber, the underplating mafic melt would have quenched and exsolved volatile-rich fluids upwards in a fashion similar to that described by Maughan et al. (2002) for the Bingham system. The additional heat provided by the hybrid mafic melt would have also "re-energized" any remnant volatile-rich magma left over from ongoing fractional crystallization in the Liw-Liw Creek magma chamber. This hybrid magma-derived volatile-rich fluid would have migrated to the top of the magma chamber along with any "re-energized" fluid. Continued local compression

would have prevented large volumes of melt from reaching higher stratigraphic levels.

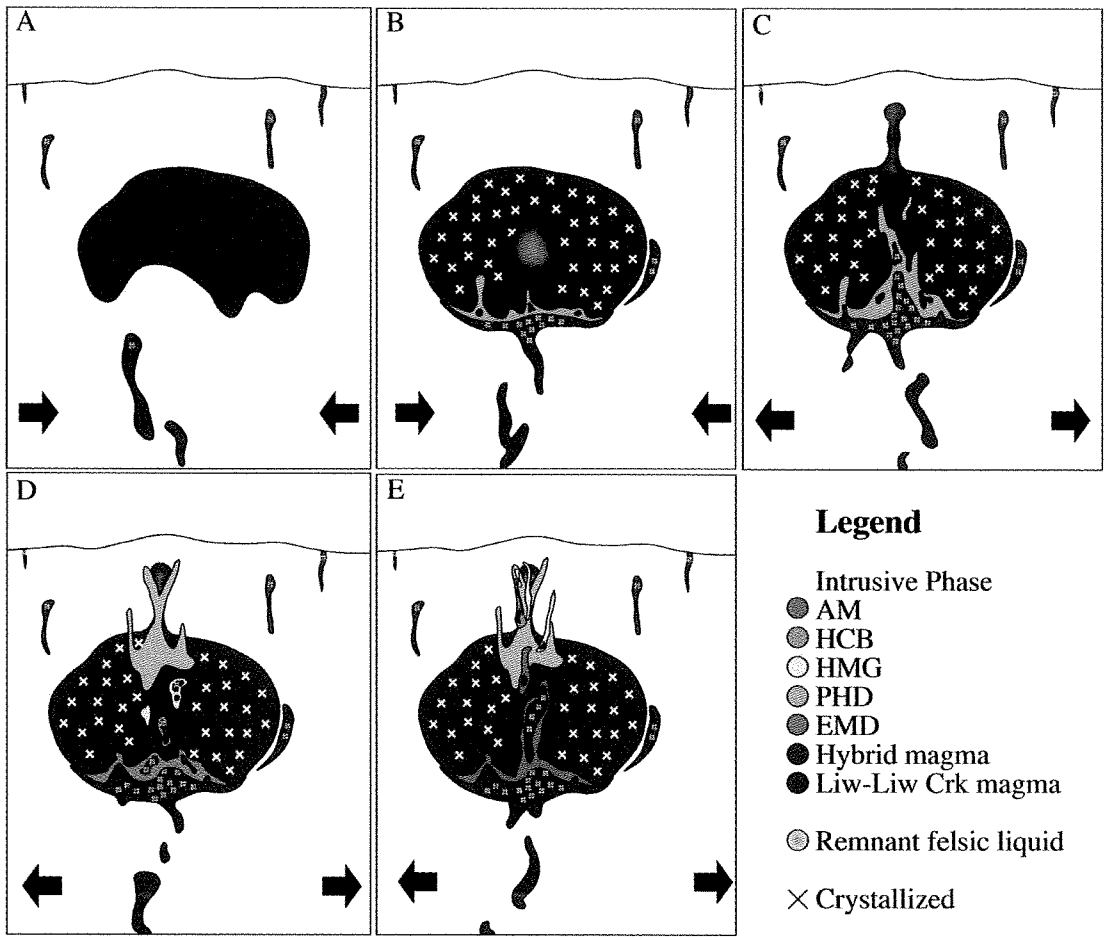

Figure 8.1 – A schematic model of the intrusive history of the Black Mountain Southeast Porphyry Cu-Au system. (A) Generation and emplacement of primitive mafic magma (Liw-Liw Creek mafic dikes) and intra-crustal stagnation under locally compressional tectonics. (B) Underplating of the partially crystallized Liw-Liw Creek magma chamber by the hybrid mafic magma yielded heat, volatile and metal budget exchange as well as partial melting "re-energizing" of remnant volatiles within the overlying chamber. Localized compression prevented significant volumes of any component from migrating upwards. (C) A shift to localized extension allowed for the emplacement of the volatile-rich fluids (leading to mineralization and early alteration) and ascension of initial partial melt components within the magma chamber. Continued addition of mafic magma to the base of the chamber resulted in mixing of hybrid mafic magma and partial melt. (D) Continued extension facilitated ascension of the hybrid mafic magma through the felsic/intermediate magma chamber, yielding lower levels of partial melt production at base of the system. (E) As a result, the ratio of hybrid mafic magma to partial melt component rose, resulting in an increasing expression of the hybrid mafic magma within the upper porphyry system.

3. (3.2 - 2.9 Ma) A shift to locally extensional tectonics (indicated by the change in magma emplacement nature from dikes of Liw-Liw Creek magma to plugs and stocks of EMD and PHD magmas; Chapter 3) would have facilitated upwards migration of the volatile-rich fluids to the cupola, leading to the quartz stockwork veining and flooding, potassic alteration and mineralization of the now cooled EMD stock (Fig. 8.1c). The derivation of much of the mineralizing and potassic-altering fluids from the underplating hybrid mafic magma would have produced the coincident Sr and Nd radiogenic spikes that are observed in the EMD rocks (Chapter 5). This would have been followed by the upward movement of the initial, intermediate partial melt product. Emplacement and crystallization of this magma proceeding the peak of mineralization (Chapter 7) and yielded the PHD intrusive phase.
4. (2.9 – 2.7 Ma) Continued generation and ascension of hybrid mafic melt to the base of the Liw-Liw Creek magma chamber during this time produced additional partial melts (Fig. 8.1d and e). However, under extensional tectonics (and ascension pathways established by the rise of previous partial melts), the hybrid mafic melt would not have had the opportunity to stagnate at the base of the magma chamber, instead ascending quickly to shallow stratigraphic levels. This resulted in the emplacement of successive intrusive phases that reflected a higher and higher hybrid mafic melt to partial melt mixing ratio, resulting in the broadly increasing radiogenic character alongside an increasingly mafic geochemical signature (Chapter 5).

8.3.2 Summary

In a broad sense, the paragenetic model for the Black Mountain Southeast system conforms to the porphyry models proposed for other porphyry systems (Keith et al., 1998, Maughan et al., 2002; Lickfold et al., 2007; Sillitoe, 2010); a hot, volatile-rich mafic magma underplated a stagnant intermediate magma chamber at shallow crustal levels, and generated a porphyry system through the addition of heat, volatiles and metals. Interaction between the underplated mafic magma and the overlying stagnant

magma chamber ranged considerably during the lifetime of the Black Mountain system: early underplating of the crystallized magma chamber generated intermediate partial melts that mixed with the underplating magma. Partial quenching of the hybrid magma released volatiles and metals into the base of the magma chamber in a fashion similar to that proposed by Maughan et al. (2002). However, a switch to a more extensional tectonic regime facilitated ascension of both the hybrid magma-derived volatile-rich fluids and the partial melt mixtures. Continued extensional tectonics and the establishment of magma pathways facilitated ascension of the underplating mafic melt, resulting in an increased presence at shallow levels within the porphyry system. This temporal variability is similar to that observed by Lickfold et al. (2007) for the porphyry systems at Northparkes, New South Wales. Similarly, the local structural control on magma emplacement at Black Mountain is mirrored by the model proposed for the Bingham porphyry system (Keith et al., 1998; Maughan et al., 2002).

8.3 Implications for Magmatism within the Baguio District

The onset of mineralization within the Baguio mineral district (concurrent with the generation and ascension of the hybrid mafic melt) at the beginning of the Pliocene indicates a contemporaneous shift in magma production within the arc (Chapter 5). The models of Yang et al. (1996), Bautista et al. (1996, 2001) and Hollings et al. (in press) dictate a major change in intra-arc geodynamics during the same time period, (Section 2.2). In particular, Hollings et al. (in press) noted that generation of the Liw-Liw Creek magmas were concurrent with subduction of the Scarborough seamount chain beneath Luzon. However, the distinct isotopic differences between the unradiogenic Liw-Liw Creek magmas and the radiogenic hybrid mafic magma suggest different generative histories. Given their radiogenic character (Chapter 5), the generation of the hybrid mafic magma may be sourced from melting of an influx of continental sediment to the sub-arc environment along the subducting South China Sea plate (Lo, 1989; Defant et al., 1989, 1990; McDermott et al., 1993; Fourcade et al., 1994; Yang et al., 1994) coupled with increased sub-arc temperatures as a byproduct of a slab tear (Yang et al., 1996; Bautista et al., 1996, 2001). Beyond this, the variety of magmatic implications for the proposed arc reversal, subduction of the aseismic Scarborough Ridge, formation of a slab

tear and/or shallowing of the subduction angle are beyond the scope of this thesis. However, the occurrence of such dynamic changes in the sub-arc environment would undoubtedly be manifested in the resultant magmatism. In the context of the Pliocene mineralization of the Baguio district, this is observable in the eastward younging direction of porphyry intrusive centers coupled with broadly increasing metal endowment (Waters and Gonzales, 2005). As the oldest and westernmost porphyry deposit in the district, the introduction of the fertile hybrid magma at Black Mountain is perhaps representative of a parental component for the younger east-lying deposits (Section 2.4).

References

Aoki M., Comsti E.C., Lazo F.B. and Matsuhisha Y., 1993. Advanced argillic alteration and geochemistry of alunite in an evolving hydrothermal system at Baguio, northern Luzon, Philippines. Resource Geology, 43, 155-164.

Arnason J., 1992. Formation of zoned epidote in hydrothermal systems. Proceedings - International Symposium on Water-Rock Interaction, 7, 1473-1476.

Arnason J., 1993. Variables controlling epidote composition in hydrothermal and low-pressure regional metamorphic rocks. Abhandlungen der Geologischen Bundesanstalt, 49, 17-25.

Balce G.R., Encina R.Y., Momongan A. and Lara E., 1980. Geology of the Baguio district and its implication on the tectonic development of the Luzon Central Cordillera: Geology and Palaeontology of Southeast Asia, 21, 265-287.

Bautista B., 1996. Implications of Recent Philippines earthquakes to the seismotectonics of southern Philippines. Eos, Transactions, American Geophysical Union, 77 (46, Suppl.), 522.

Bautista B.C., Bautista M.L., Oike K., Wu F.T. and Punongbayan R.S., 2001. A new insight on the geometry of subducting slabs in northern Luzon, Philippines. Tectonophysics, 339, 279-310.

Bellon H., 2001. Miocene to Quaternary adakites and related rocks in western Philippine Arc sequences. Comptes Rendus de l'Academie des Sciences, Serie II. Sciences de la Terre et des Planetes, 333(6), 343-350.

Bouysse P. and Westercamp D., 1990. Subduction of Atlantic aseismic ridges and Late Cenozoic evolution of the Lesser Antilles island arc. Tectonophysics, 175, 349-380.

Bowman J., 1987. Chemical and isotopic evolution of hydrothermal solutions at Bingham, Utah. Economic Geology and the Bulletin of the Society of Economic Geologists, April, 82(2), 395-428.

Bureau of Mines and Geosciences, 1986. Geology and mineral resources of the Philippines, Volume 2 – Mineral resources: Bureau of Mines and Geosciences, Ministry of Natural Resources, Metro Manila, Philippines, 446.

Callow K.J., 1967. The geology of the Thanksgiving mine, Baguio district, Mountain Province, Philippines. Economic Geology, 60, 251-268.

Castillo P., 1999. Petrology and geochemistry of Camiguin Island, southern Philippines; insights to the source of adakites and other lavas in a complex arc setting. Contributions to Mineralogy and Petrology, January, 134(1), 33-51.

Cawthorn R., 1976. Some chemical controls on igneous amphibole compositions. Geochimica et Cosmochimica Acta, November, 40(11), 1319-1328.

Cloos M., 1993. Lithospheric buoyancy and collisional orogenesis; subduction of oceanic plateaus, continental margins, island arcs, spreading ridges, and seamounts. Geological Society of America Bulletin, June, 105(6), 715-737.

Comsti M.E.C., Villones R.I., de Jesus C.V., Natividad A.R., Rollan L.A. and Duroy A.C., 1990. Mineralization at the Kelly gold mine, Baguio district, Philippines: fluid-inclusion and wall-rock alteration studies: *in* Hedenquist, J.W., White, N.C., and Siddeley, G. (eds.), Epithermal Gold Mineralization of the Circum-Pacific; Geology, Geochemistry; Origin and Exploration, I. Journal of Geochemical Exploration, 35, 297-340.

Conceicao R., 2005. Andean subduction-related mantle xenoliths; isotopic evidence of Sr-Nd decoupling during metasomatism. Lithos, June, 82(3-4), 273-287.

Cooke D.R. and Bloom M.S., 1990. Epithermal and subjacent porphyry mineralization, Acupan, Baguio District, Philippines: a fluid-inclusion and paragenetic study. Journal of Geochemical Exploration, 35, 297-340.

Cooke D.R., McPhail D.C. and Bloom M.S., 1996. Epithermal gold mineralization, Acupan, Baguio district, Philippines: geology, mineralization, alteration and the thermochemical environment of ore deposition. Economic Geology, 91, 243-272.

Cooke D.R., Wilson A.J., House M. J., Wolfe R. C., Walshe J.L., Lickfold V. and Crawford A.J., 2006. Alkalic porphyry Au-Cu and associated mineral deposits of the Ordovician to Early Silurian Macquarie Arc, NSW: Australian Journal of Earth Sciences.

Crawford A. J., Meffre S., Squire R. J., Barron L. M. and Falloon T. J., 2007. Middle and Late Ordovician magmatic evolution of the Macquarie Arc, Lachlan Orogen, New South Wales. Australian Journal of Earth Sciences, 54, 181—214.

De Guzman M.T., 1986. Geology and mineralization of the Balatoc diatreme, Acupan Mine, Benguet. Unpublished report, Benguet Consolidated, Inc., 66.

De Guzman M.T., 1988. Geology and gold mineralization of Acupan diatreme, Philippines: Unpublished poster display, Bicentennial Gold 88, Melbourne, 29.

De los Santos R. B., 1982. Geology of the Southwestern Baguio District. BMG Technical Information Series. Geology, 53, 17.

Defant M., Jacques D., Maury R., De Boer J. and Joron J.-L., 1989. Geochemistry and tectonic setting of the Luzon arc, Philippines. Geological Society of America Bulletin, 101, 663-672.

Defant M.J. and Drummond M.S., 1990. Derivation of some modern arc magmas by melting of young subducted lithosphere. Nature, 347, 662-665.

Deyell C.L. and Cooke D.R., 2003. Mineralogical and isotopic evidence for the genesis of the Kelly goldsilver deposit, Baguio District, Philippines: Diverse mineral assemblages in a hybrid epithermal system in Eliopoulos, D.G. (ed.) Mineral exploration and sustainable development. Proceedings of the 7th Biennial Meeting, Society for Geology Applied to Mineral Deposits, Milpress, Rotterdam, 4.

Dimalanta C. and Yumul G., 2003. Magmatic and amagmatic contributions to crustal growth of an island arc system: The Philippine example. International Geology Review, 45, 922-935.

Dunlap J., 2002. ^{40}Ar-^{39}Ar age determinations of hornblende and biotite samples from Mindanao and Luzon. Report R01-190 Part II and Final, March 2002, Research School of Earth Sciences, The Australian National University. Unpublished Report for Anglo American.

Durkee E.F. and Pederson S.L., 1961. Geology of Northern Luzon, Philippines. Bulletin of the American Association of Petroleum Geologists, 45, 137-168.

Femenias O., 2006. Calcic amphibole growth and compositions in calc-alkaline magmas; evidence from the Motru dike swarm (Southern Carpathians, Romania). American Mineralogist, January, 91(1), 73-81.

Fourcade S., Maury R.C., Defant M.J. and McDermott F., 1994. Mantle metasomatic enrichment versus arc crust contamination in the Philippines: Oxygen isotope study of Batan ultramafic nodules and northern Luzon arc lavas. Chemical Geology, 114, 199-215.

Gervasio F., 1971. Geotectonic development of the Philippines. Proceedings of the Pacific Science Congress, January, 12(1), 380.

Gregoire M., Jego S., Maury R. C., Polve M., Payot B., Tamayo R. A. Jr. and Yumul G. P. Jr., 2008. Metasomatic interactions between slab-derived melts and depleted mantle; insights from xenoliths within Monglo Adakite (Luzon Arc, Philippines). Lithos, July, 103(3-4), 415-430.

Gustafson L. and Hunt J., 1975. The porphyry copper deposit at El Salvador, Chile. Economic Geology and the Bulletin of the Society of Economic Geologists, August, 70(5), 857-912.

Hall R., 1996. Reconstructing Cenozoic SE Asia. In: Hall, R.,and Blundell, D. (eds.),Tectonic evolution of SE Asia. Geological Society of London Special Publication, 106, 153-184.

Hall R., 1997a. Cenozoic plate tectonic reconstructions of SE Asia. In: Fraser, A., Matthews, S., and Murphy, R., (eds.), Petroleum Geology of SE Asia. Geological Society of London Special Publication, 126, 11-23.

Hall R., 1997b. Cenozoic tectonics of SE Asia and Australasia. Indonesia: Indonesian Petroleum Association : Jakarta, Indonesia.

Hall R., 2001. Cenozoic reconstructions of SE Asia and the SW Pacific: changing patterns of land and sea. In: Metclafe, L., Smith, J., Morwood, M., and Davidson, I., (Eds), Faunal and floral migrations and evolution in SE Asia-Australasia. A.A. Balkema (Swets & Zeitlinger Publishers) Lisse, 35-56.

Hammarstrom J. and Zen E., 1986. Aluminum in hornblende; an empirical igneous geobarometer. American Mineralogist, 71(11-12), 1297-1313.

Hattori K. and Keith J., 2001. Contribution of mafic melt to porphyry copper mineralization; evidence from Mount Pinatubo, Philippines, and Bingham Canyon, Utah, USA. Mineralium Deposita, 36(8), 799-806.

Hawthorne F. and Oberti R., 2007. Classification of the amphiboles. Reviews in Mineralogy and Geochemistry 67,1, 55-88.

Hedenquist J.W., Arribas A. Jr. and Reynolds T.J., 1998. Evolution of an intrusion-centered hydrothermal system: Far Southeast–Lepanto porphyry and epithermal Cu–Au deposits, Philippines. Economic Geology, 93, 373–404.

Holdaway M., 1972. Thermal Stability of Al-Fe Epidote as a Function of f (sub O2) and Fe Content. Contributions to Mineralogy and Petrology, 37(4), 307-340.

Hollings P., 2006. Whole Rock Geochemistry of the Baguio District. AMIRA-CODES P765 Final Report, December 2006. Section 2.3, 1-53.

Hollings P. and Cooke D., 2005. Tectonic Setting and Geological Evolution of Norther Luzon, Philippines. Northern Luzon Field Guide: P765 – Transitions and Zoning in Porphyry-Epithermal Districts: Indicators, Discriminators and Vectors. April 2005, Chapter 1, 1-40.

Hollings P., Wolfe R., Cooke D. and Waters P. (in press, 2010). Geochemistry of Tertiary igneous rocks of Northern Luzon, Philippines: evidence for a back arc-setting for alkalic porphyry copper-gold deposits and a case for slab roll-back? Economic Geology Special Issue – Porphyry and Epithermal Deposits of the Philippines and Indonesia.

Hollister L., Grissom G. C., Peters E. K., Stowell H. H. and Sisson V. B., 1987. Confirmation of the empirical correlation of Al in hornblende with pressure of solidification of calc-alkaline plutons. American Mineralogist, 72(3-4), 231-239.

Imai A., 2001. Generation and evolution of ore fluids for porphyry Cu-Au mineralization of the Santo Tomas II (Philex) deposit, Philippines. Resource Geology, 51, 71-96.

Jego S., Maury R.C., Polve M., Yumul G.P., Bellon H., Tamayo R.A. and Cotton J., 2005. Geochemistry of adakites from the Philippines: Constraints on their origins. Resource Geology, 55, 161-185.

Japan International Cooperation Agency, 1983. Report on Acupan-Itogon Geothermal Development. First Phase Survey. Unpublished Report, Japan International Cooperation Agency, 94.

Johnson M. and Rutherford M., 1989. Experimental calibration of the aluminum-in-hornblende geobarometer with application to Long Valley Caldera (California) volcanic rocks. Geology, 17(9), 837-841.

Kay M. and Mpodozis C., 2002. Magmatism as a probe to the Neogene shallowing of the Nazca Plate beneath the modern Chilean flat-slab. Journal of South American Earth Sciences, 15(1), 39-57.

Keith J., Waite K., Christiansen E., Deino A. and Ballantyne G., 1997. Contributions of mafic alkaline magmas to the Bingham porphyry Cu-Au-Mo system, Utah. Abstracts with Programs. Geological Society of America, 29(6), 282.

Keith J., Christiansen E., Maughan D. and Waite K., 1998. The role of mafic alkaline magmas in felsic porphyry-Cu and Mo systems. Short Course Handbook, 26, 211-243.

Kelleher J. and McCann W., 1976. Buoyant zones, great earthquakes, and unstable boundaries of subduction. Journal of Geophysical Research, 81(26), 4885-4896.

Leake B., 1968. Amphibole from the Moine nappe in Skye. Scottish Journal of Geology, 4, Part 3, 287-289.

Leake B., 1978. Nomenclature of amphiboles. Canadian Mineralogist, 16, 4, 501-520.

Leake, B., Woolley A., Arps C., Birch W., Gilbert C., Grice J., Hawthorne F., Kato A., Kisch H., Krivovichev V., Linthout K, Laird J., Mandarino J., Maresch W., Nickel E., Rock N., Schumacher J., Smith D., Stephenson N., Ungaretti L., Whittaker E. and Guo Y., 1997. Nomenclature of amphiboles; Report of the Subcommittee on Amphiboles of the International Mineralogical Association, Commission on New Minerals and Mineral Names. American Mineralogist, 82(9-10), 1019-1037.

Leon M. and Militante-Matias P., 1991. Calcareous nannofossils from the Aksitero-Moriones area western part of Tarlac Province central Luzon Basin, Philippines. Journal of Nannoplankton Research, 13(2), 54.

Lickfold V., Cooke D., Smith S. and Ullrich T., 2003. Endeavour Copper-Gold Porphyry Deposits, Northparkes, New South Wales: Intrusive History and Fluid Evolution. Economic Geology, 98, 1607–1636

Lickfold V., Cooke D., Crawford A. and Fanning C., 2007. Shoshonitic magmatism and the formation of the Northparkes porphyry Cu - Au deposits, New South Wales. Australian Journal of Earth Sciences, 54:2, 417 – 444.

Liou J., 1973. Synthesis and Stability Relations of Epidote, Ca (sub 2) Al (sub 2) FeSi (sub 3) O (sub 12) (OH). Journal of Petrology, 14(3), 381-413.

Lowell D. and Guilbert J., 1970. Lateral and vertical alteration-mineralization zoning in porphyry ore deposits. Economic Geology and the Bulletin of the Society of Economic Geologists, 65(4), 373-408.

Maleterre P., 1989. Histoire, sedimentation, magmatique, tectonique et metallogenique d'un arc oceanique deforme en regime de transpression. PhD Thesis Universite de Bretagne Occidentale, Brest.

Margoum A., 2002. Géochimie et géochronologie du magmatisme de la région de Baguio (Ile de Luzon, Philippines). Mémoire de DEA Géosciences Marines – EDSM. Université Bretagne Occidentale, Brest.

Martin R., 2007. Amphiboles in the Igneous Environment. Reviews in Mineralogy and Geochemistry; Amphiboles: Crystal Chemistry, Occurrence, and Health Issues. 67, Ch. 9, 323–358.

Maughan D., Keith J., Christiansen E., Pulsipher T., Hattori K. and Evans N., 2002. Contributions from mafic alkaline magmas to the Bingham porphyry Cu–Au –Mo deposit, Utah, USA. Mineralium Deposita 37, 14 – 37.

Maury R., Defant M. and Bellon H., 1998. Temporal geochemical trends in northern Luzon arc lavas (Philippines: implications on metasomatic processes in the island arc mantle. Bulletin de la Societe Geologique de France, 169, 69-80.

McCabe R., Almasca J. and Diegor W., 1982. Geologic and paleomagnetic evidence for a possible Miocene collision in western Panay, Central Philippines. Geology, 10, 325-329.

McCann W. and Sykes L., 1984. Subduction of aseismic ridges beneath the Caribbean plate: implications R~r the tectonics and seismic potential of the northeastern Caribbean. Journal of Geophysical Research, 89(B6), 4493-4519.

McCulloch M. and Gamble A., 1991. Geochemical and geodynamical constraints on subduction zone magmatism. Earth and Planetary Science Letters, 102(3-4), 358-374.

McDermott F. and Hawkesworth C., 1991. Th, Pb, and Sr isotope variations in young island arc volcanics and oceanic sediments. Earth and Planetary Science Letters, 104(1), 1-15.

McDermott F., Defant M., Hawkesworth C., Maury R. and Joron J., 1993. Isotope and trace element evidence for three component mixing in the genesis of the North Luzon arc lavas (Philippines). Contributions to Mineralogy and Petrology, 113, 9-23.

McGeary S., Nur A. and Ben-Avraham Z., 1985. Spatial gaps in arc volcanism: the effect of collision or subduction of oceanic plateaus. Tectonophysics, 119, 195-221.

Meyer C. and Hemley J., 1967. Wall rock alteration. Chapter 6. International: Holt, Rinehart and Winston : New York, Toronto, and London, International.

Mitchell A. and Leach T., 1991. Epithermal Gold in the Philippines. Island Arc Metallogenesis, Geothermal Systems and Geology. Academic Press Geology Series, London, 457.

Nur A. and Ben-Avraham Z., 1983. Volcanic gaps due to oblique consumption of aseismic ridges. Tectonophysics, 99, 355-362.

Nur A. and Ben-Avraham Z., 1989. Oceanic plateaus and the Pacific ocean margins. In: Z. Ben-Avraham (Editor), The Evolution of the Pacific Ocean Margins. Oxford Univ. Press, New York. NY, 3-19.

Payot B., Jego S., Maury R., Polve M., Gregoire M., Ceuleneer G., Tamayo E.A., Yumul G., Bellon H. and Cotton J., 2007. The oceanic substratum of Northern Luzon: Evidence from xenoliths within Monglo adakite (the Philippines). Island Arc, 16, 276-290.

Peccerillo A. and Taylor S., 1976. Rare earth elements in the East Carpathian volcanic rocks. Earth and Planetary Science Letters, 32(2), 121-126.

Pena R., 1998. Further notes on the stratigraphy of the Baguio District: Journal of Geological Society of the Philippines, Vol. LIII, 3-4, 141-157

Pena R. and Reyes M., 1970. Sedimentological study of a section of the Upper Zig-Zag Formation along Bued River, Tuba, Benguet, Geological Society of the Philippines, 24, 1-19.

Polve M., Maury R.,, Jego S., Bellon H., Margoum A., Yumul G., Payot B., Tamayo R. and Cotton J., 2007. Temporal geochemical evolution of Neogene magmatism in the Baguio Gold-Copper mining district (Northern Luzon, Philippines). Resource Geology, 57, 197-218.

Rae A., Cooke D., Phillips D. and Zaide-Delfin M., 2004. The nature of magmatism at Palinpinon geothermal field, Negros island, Philippines: implications for geothermal activity and regional tectonics. Journal of Volcanology and Geothermal Research; 129, 321-342.

Rollinson H., 1993. Total alkalis versus silica (Na2+K2O vs SiO2) general igneous rocks classification diagram. Using Geochemical Data, 49-51.

Sajona F. and Maury R., 1998. Association of adakites with gold and copper mineralization in the Philippines. Comptes Rendus Academy Science Paris. Sciences de la Terre et des Planetes, 326, 27-34.

Sajona F., Maury, R., Bellon, H., Cotton, J., Pubelier, M., and Rangin., C., 1993. Initiation of subduction and the generation of slab melts in western and eastern Mindanao, Philippines. Geology, 21, 1007-1010.

Sajona, F., Bellon, H., Maury, R., Pubelier, M., Cotton, J., and Rangin., C., 1994. Magmatic response to abrupt changes in tectonic setting: Pliocene-Quaternary calc alkaline lavas and Nb-enriches basalts of Leyte and Mindanao (Philippines). Tectonophysics, 237, 47-72.

Sajona, F., Maury, R., Bellon, H., Cotton, J., and Defant, M.J., 1996. High field strength element enrichment of Pliocene-Pleistocene island arc basalts, Zamboanga Peninsula, Western Mindanao, Philippines. Journal of Petrology, 37, 693-726.

Sajona F.G., Bellon, H., Maleterre P., Ringenbach, J.C., Billedo, E.B., David, S.D., Stephan, J.F., Delteil, J., Feraud, G., Winter, W. and Cotton, J., 1999. Time and space geochemical evolution of magmatism in Luzon (Philippines) and its geodynamic implications. Unpublished manuscript.

Saunders A., Norry M. and Tarney J., 1988. Origin of MORB and chemically-depleted mantle reservoirs; trace element constraints. Journal of Petrology, 415-445.

Sawkins F., O'Neill J. and Thompson J., 1979. Fluid inclusion and geochemical studies of vein gold deposits, Baguio district, Philippines. Economic Geology, 74, 1420-1434.

Schaffer P., 1956. Progress report on the geology of the Baguio district, Philippines. Philippines Society of Mining, Metallurgical, Geological Engineers Mining Newsletter. 5, 5.

Schmidt M., 1992. Amphibole composition in tonalite as a function of pressure; an experimental calibration of the Al-in-hornblende barometer. Contributions to Mineralogy and Petrology, 110, 304-310.

Shannon, J., 1979. Igneous petrology, geochemistry and fission track ages of a portion of the Baguio Mineral District, Northern Luzon, Philippines: Unpublished MSc. Thesis, Golden, Colorado, Colorado School of Mines, 173.

Shikazono N., 1984. Composition variations in epidote from geothermal areas. Geochemical Journal, 18(4), 181-187.

Sillitoe R., 1972. A Plate Tectonic Model for the Origin of Porphyry Copper Deposits. Economic Geology and the Bulletin of the Society of Economic Geologists, 67(2), 184-197.

Sillitoe R., 1973. The tops and bottoms of porphyry copper deposits. Economic Geology and the Bulletin of the Society of Economic Geologists, 68(6), 799-815.

Sillitoe R., 1989. Gold deposits in western Pacific island arcs; the magmatic connection. Economic Geology Monographs, 6, 274-291.

Sillitoe R., 2000. Gold-rich porphyry deposits; descriptive and genetic models and their role in exploration and discovery. Reviews in Economic Geology, 13, 315-345.

Sillitoe R., 2010. Porphyry copper systems. Economic Geology and the Bulletin of the Society of Economic Geologists, 105(1), 3-41.

Sillitoe R. and Gappe I., 1984. Philippine porphyry copper deposits: geologic setting and characteristics: Technical Publication, United Nations Development Programme, Committee for Co-ordination of Joint Prospecting for Mineral Resources in Asian Offshore Areas (CCOP), 14-89.

Smith W. and Eddingfield F., 1911. Additional notes on the economic geology of the Baguio Mineral District. Philippine Journal of Sciences, 6, 429-445.

Spieler O., Kennedy B., Kueppers K., Dingwell D., Scheu B. and Taddeucci J., 2003. A fragmentation threshold for the initiation and cessation of explosive eruptions. Eos, Transactions. American Geophysical Union, 84(46), AbstractV51B-01.

Taylor H., 1974. The Application of Oxygen and Hydrogen Isotope Studies to Problems of Hydrothermal Alteration and Ore Deposition. Economic Geology and the Bulletin of the Society of Economic Geologists, 69(6), 843-883.

UNDP, 1987. Geology and mineralization in the Baguio area, Northern Luzon. UNDP BMG Technical report 5, 82.

Vogt P., 1973. Subduction and aseismic ridges. Nature, 241, 189 191.

Waters P., 1999. Exploration Potential of the Nugget Hill Cu-Au Porphyry Prospect, Baguio District, Philippines. Unpublished Internal Anglo American Report PW-99-1, 15.

Waters P. and Gonzales R., 2005. Geological Setting and Mineral Deposits of the Baguio Mineral District. AMIRA-CODES P765 Philippines Field Guide, April 2005. Chapter 6, 41-63.

Waters P., Cooke D., Gonzales R. and Phillips D., in press, 2010. Porphyry and epithermal deposits and ^{40}Ar-^{39}Ar geochronology of the Baguio district, Philippines. Economic Geology Special Issue – Porphyry and Epithermal Deposits of the Philippines and Indonesia.

Waters P., Gonzales R. and Cooke D., 2006. Geological setting and mineral deposits of the Baguio district. AMIRA-CODES P765 Final Report, December 2006. Section 2.2, 1-28.

White W. and Patchett J., 1984. Hf-Nd-Sr isotopes and incompatible element abundances in island arcs; implications for magma origins and crust-mantle evolution. Earth and Planetary Science Letters, 67(2), 167-185.

Wilson A., Cooke D. and Harper B., 2003. The Ridgeway gold-copper deposit; a high-grade alkalic porphyry deposit in the Lachlan fold belt, New South Wales, Australia. Economic Geology and the Bulletin of the Society of Economic Geologists, 98(8), 1637-1666.

Yang T., Lee T., Chen C., Cheng S., Knittel U., Punongbayan R. and Rasdas A., 1996. A double island arc between Taiwan and Luzon: consequence of ridge subduction. Tectonophysics, 258, 85-101.

Yang T., l,ee T., Chen C. and Kurz. M., 1994. Geochemical variations along the North Luzon Arc (Taiwan): An example of arc magmatism during arc-continent collision. Annual Meeting of the Geological Society of America, Seattle, WA (abstract).

Yumul G., Manjoorsa M. and Datuin R., 1995. Baguio Mining District, Luzon, Philippines: From marginal basin to mature island arc setting. II. Geochemistry of the plutonic rocks. Journal of the Geological Society of the Philippines, 50, 1-20.

Yumul G., Dimalanta C., Bellon H., Faustino D., De Jesus J., Tamayo R. and Jumawan F., 2000. Adakitic lavas in the Central Luzon back-arc region, Philippines: lower crustal partial melting products?

Yumul G., Dimalanta C., Tamayo R. and Maury R., 2003a. Collision, subduction and accretion in the Philippines: A synthesis. The Island Arc, 12, 77-91.

Yumul G., Dimalanta C., Tamayo R. and Bellon H., 2003b. Silicic arc volcanism in Central Luzon, the Philippines: Characterisation of its space, time and geochemical relationships. The Island Arc, 12, 207-218.

Zindler A. and Hart S., 1986. Chemical geodynamics. Annual Review of Earth and Planetary Sciences, 14, 493-571.

Appendix 1

Methodology

1.1 U-Pb Geochronology

New U-Pb dates for the intrusive rocks associated with the Black Mountain Southeast deposit were produced by the Pacific Centre for Isotopic and Geochemical Research at the Department of Earth and Ocean Sciences, University of British Columbia.

Zircon was separated from samples using conventional crushing, grinding, and Wilfley table techniques, followed by final concentration using heavy liquids and magnetic separations. Mineral fractions for analysis were selected on the basis of grain quality, size, magnetic susceptibility and morphology. All zircon was air abraded prior to dissolution to minimize the effects of post-crystallization Pb-loss, using the technique of Krogh (1982). Single zircon grains were dissolved in sub-boiled 48% HF and 14 M HNO_3 (ratio of ~10:1, respectively) in the presence of a mixed 233-235U-205Pb tracer for 40 hours at 240°C in 300 mL PFA or PTFE or microcapsules contained in high pressure vessels (Parr™ acid digestion vessels with 125 mL PTFE liners). Sample solutions were then dried to salts at ~130°C. Zircon residues were redissolved in ~50 mL of sub-boiled 6.2 M HCl for 12 hours at 210°C, again in high-pressure vessels. These solutions were transferred to 7 mL PFA beakers, dried to a small droplet after addition of 2 mL of 0.5 N H3PO4. Samples were loaded on single, degassed zone refined Re filaments in 5 mL of colloidal silicic acid - phosphoric acid emitter (Gerstenberger and Haase, 1997). Isotopic ratios were measured using a modified single collector VG-54R thermal ionization mass spectrometer equipped with an analogue Daly photomultiplier. All measurements were done in peak-switching mode on the Daly detector. Analytical blanks during the course of this study were 0.2 pg for U and for Pb 0.5-1.5 pg. U fractionation was determined directly on individual runs using the 233-235U tracer, and Pb isotopic ratios were corrected for fractionation of 0.23%/amu, based on replicate analyses of the NBS-982 Pb standard and the values recommended by Thirlwall (2000). Reported precisions for Pb/U and Pb/Pb dates were determined by numerically propagating all analytical uncertainties through the entire age calculation using the

technique of Roddick (1987). Standard concordia diagrams were constructed and regression intercepts, concordia ages and weighted means calculated with Isoplot 3.00 (Ludwig, 2003). All errors are quoted at the 2-sigma level unless otherwise noted.

1.2 ^{40}Ar-^{39}Ar Geochronology

Performed at the College of Oceanic and Atmospheric Sciences, Oregon State University, Corvallis, Oregon.

Incremental heating 40Ar/39Ar age determinations were performed on crystalline groundmass separates using a CO2 laserprobe combined with a MAP-215/50 mass spectrometer at Oregon State University (Corvallis). Sample preparation and acid leaching are described in Koppers et al. (2000). The mass spectrometer is a 90-sector instrument with a Nier-type source with an allmetal extraction system for 40Ar/39Ar age determinations. It has an electron multiplier for high sensitivity and an electrostatic analyzer with adjustable collector slit for an effective resolution (600) of Ar peaks from small hydrocarbon peaks. For incremental heating the system is equipped with a Merchantek integrated CO^2 laser gas extraction system connected to an ultra-clean gas cleanup line (1000 cc; Zr-Al getters). Irradiated groundmass samples were loaded into Cu-planchettes designed with a variety of pans that hold up to 50 mg of material, which are then pumped within a sample chamber fitted with a ZnSe window transparent to the CO^2 laser wavelength. Software allows for scanning across samples in a preset pattern with a defocused beam, to evenly heat the material. Ion beam currents are measured with the electron multiplier at m/z = 35, 36, 37, 38, 39, 40 and intervening baselines with an 8.5 digit integrating HP multimeter. The multiplier is operating at 2050 Volt with a system sensitivity of $4x10^{14}$ mol/volt. Peak decay is typically less than 10% during analyses and the regressed peak heights against time (normally) follow first-order and second-order polynomial fits. The background for the mass spectrometer (subsequent to 20 min isolation from pumps) is $1x10^{18}$ mol at m/z = 36, 2 $x10^{18}$ mol at m/z = 39 and 2 x 10^{16} mol at m/z = 40. The average extraction line blank is 4 $x10^{19}$ mol at m/z = 36 and 2 $x10^{16}$ mol at m/z = 40. Mass discrimination (1.0149 ± 0.0012 amu1) is monitored using zero age basaltic glass. Estimated uncertainties for the J-values are between 0.3–0.4%

standard deviation. Sample irradiation was carried out using the TRIGA CLICIT at the OSU reactor facility for 6 hours.

1.3 Whole Rock Geochemistry

Whole rock composition analysis protocols (Anglo American package AA group LITHO, ACME Lab, Vancouver, Canada).

	Unit	Detec. Limit	Method code		Unit	Detec. Limit	Method code		Unit	Detec. Limit	Method code
SiO_2	%	0.02	G4A	Cs	ppm	0.1	G4B	Mo	ppm	0.01	G1F-MS
Al_2O_3	%	0.03	G4A	Ga	ppm	0.5	G4B	Cu	ppm	0.01	G1F-MS
Fe_2O_3	%	0.04	G4A	Hf	ppm	0.5	G4B	Pb	ppm	0.01	G1F-MS
MgO	%	0.01	G4A	Nb	ppm	0.5	G4B	Zn	ppm	0.1	G1F-MS
CaO	%	0.01	G4A	Rb	ppm	0.5	G4B	Ag	ppb	2	G1F-MS
Na_2O	%	0.01	G4A	Sn	ppm	1	G4B	Ni	ppm	0.1	G1F-MS
K_2O	%	0.04	G4A	Sr	ppm	0.5	G4B	Co	ppm	0.1	G1F-MS
TiO_2	%	0.01	G4A	Ta	ppm	0.1	G4B	Mn	ppm	1	G1F-MS
P_2O_5	%	0.01	G4A	Th	ppm	0.1	G4B	As	ppm	0.1	G1F-MS
MnO	%	0.01	G4A	U	ppm	0.1	G4B	Au	ppb	0.2	G1F-MS
Cr_2O_3	%	0.001	G4A	V	ppm	5	G4B	Cd	ppm	0.01	G1F-MS
Ba	ppm	0.5	G4A	W	ppm	0.1	G4B	Sb	ppm	0.02	G1F-MS
Ni	ppm	10	G7TD	Zr	ppm	0.5	G4B	Bi	ppm	0.02	G1F-MS
Sc	ppm	0.1	G4A	Y	ppm	0.1	G4B	Cr	ppm	0.5	G1F-MS
LOI	%	0.1	G4A	La	ppm	0.5	G4B	B	ppm	1	G1F-MS
Total C	%	0.02	G4A	Ce	ppm	0.5	G4B	Tl	ppm	0.02	G1F-MS
Total S	%	0.02	G4A	Pr	ppm	0.02	G4B	Hg	ppb	5	G1F-MS
				Nd	ppm	0.4	G4B	Se	ppm	0.1	G1F-MS
				Sm	ppm	0.1	G4B	Te	ppm	0.02	G1F-MS
				Eu	ppm	0.05	G4B	Ge	ppm	0.1	G1F-MS
Au_G3B	ppb	2	G3B	Gd	ppm	0.05	G4B	In	ppm	0.02	G1F-MS
Pt_G3B	ppb	3	G3B	Tb	ppm	0.1	G4B	Re	ppb	1	G1F-MS
Pd_G3B	ppb	2	G3B	Dy	ppm	0.05	G4B	Be	ppm	0.1	G1F-MS
				Ho	ppm	0.05	G4B	Li	ppm	0.1	G1F-MS
				Er	ppm	0.05	G4B	Pd	ppb	10	G1F-MS
				Tm	ppm	0.05	G4B	Pt	ppb	2	G1F-MS
				Yb	ppm	0.05	G4B				
				Lu	ppm	0.01	G4B				

ACME Laboratories whole rock analysis package. (LOI = loss on ignition; Total C = total carbon; Total S = total sulfur)

Method G4A-G4B: A 0.2g sample split is fused at 1000°C with 1.5g of a 80:20 lithium metaborate/tetraborate mix. The cooled bead is digested in 100 mL of 5% HNO3. ICP-ES analysis determines major element concentrations reported as the common oxides. Loss on Ignition (LOI) is report as % weight loss on a 1g split is ignited at 1000°C. LECO analysis determines total C and S on a 0.2g sample split. The same whole rock fusion

solution is analysed by ICP-MS (Perkin Elmer Elan 6000) to determine absolute concentrations of these trace elements.

Method 1F-MS: A 1g subsample is digested in 6 mL of hot (95°C) modified Aqua Regia (1:1:1 HCl:HNO_3:H_2O) for 1 hour, cooled and made to 20 mL volume with 5% HCl. Solution is analysed by ICP-MS (Perkin Elmer Elan 6000 or 9000). *Some minerals of these elements may be only partly attacked. This method is effective in dissolving sulfides and other minerals soluble is strong acid such as alunite and carbonates but it may only dissolve silicates partially. Comparing with a granitic standard (TASGRAN), a basaltic standard (TASBAS), a soil power standard (GXR-2), and a copper mill-head powder standard (GXR-4) reveals that the ACME results are 0-70% lower than accepted values. In particular, Pb is 18-69% lower, but if Pb is mostly in alunite, then the error should be smaller as alunite will dissolve; Mercury is 1-10% lower.

Method G3B: A 30g sample split is custom mixed with PbO fire assay fluxes and fired for 45 minutes at 1050°C. Molten Pb + slag is poured into an iron mold, cooled and Pb button recovered. Heating at 950°C in a MgO cupel renders a Ag ± Au, Pt, Pd dore bead. The bead is parted in hot HNO3, digested by adding HCl and aspirated into a Jarrel Ash Atomcomp 875 ICP-ES to determine Au, Pt and Pd. Upper limits = 10 ppm.

Method G7TD - A 0.5g sample split is digested in 20 mL of 4-Acid solution (HNO_3:$HClO_4$:HF:H_2O) at 200°C and taken to dryness. Residue is dissolved in 16 mL of 50% HCl at ~95°C for 1 hour then made to volume in a 100 mL volumetric flask with 5% HCl. ICP-ES analysis determines total Ni

1.4 Rb/Sr and Sm/Nd Isotope Geochemistry

Performed at Carleton University Laboratories, Ottawa, Ontario.

Sample Dissolution: Between 100 and 200 milligrams of powder are dissolved in 50% HF-12N HNO_3, then attacked with 8N HNO_3 and finally 6N HCl. The residue is taken up in 1N HBr for Pb/Sr/Nd, or 2.5N HCl for Sr/Nd only.

Rb/Sr: The sample, dissolved in 2.5N HCl, is pipetted into a 14-ml Bio-Rad borosilicate glass chromatography column containing 3.0 ml of Dowex AG50-X8 cation resin. Rb and Sr are eluted in succession using 2.5 N HCl. The rare earth elements are then eluted using 6N HCl. The REE solution is dried and the residue dissolved in 0.26N HCl.

Total procedural blanks for Sr are < 250 picograms. We have two mixed $^{87}Rb/^{84}Sr$ spikes, one for felsic rocks and another for mafic to intermediate rocks. Sr is loaded onto a single Ta filament with H_3PO_4 and is run at filament temperatures of 1380-1600°C. Isotope ratios are normalized to $^{86}Sr/^{88}Sr = 0.11940$ to correct for fractionation. Two standards are run at Carleton, NIST SRM987 (TRITON: $^{87}Sr/^{86}Sr = 0.710234 \pm 14$, n=22, Sept 08 – Aug 09) and the Eimer and Amend (E&A) $SrCO_3$ (TRITON – not enough data available at this point). Rb is loaded with H_3PO_4 onto one side of a double Re filament assembly and run at temperatures of 1250-1300 °C. No correction for fractionation is made.

Sm/Nd: Samples are dissolved in 0.26N HCl and loaded onto Eichrom Ln Resin chromatographic columns containing Teflon powder coated with HDEHP [di(2-ethylhexyl) orthophosphoric acid, *Richard et al.*, 1976] . Nd is eluted using 0.26N HCl, followed by Sm in 0.5N HCl.

Total procedural blanks for Nd are < 50 picograms; < 6 picograms for Sm. Samples are spiked with a mixed ^{148}Nd-^{149}Sm spike prior to dissolution. Concentrations are precise to ± 1%, but $^{147}Sm/^{144}Nd$ ratios are reproducible to 0.5%. Samples are loaded with H_3PO_4 on one side of a Re double filament, and run at temperatures of 1700-1800 °C. Isotope ratios are normalized to $^{146}Nd/^{144}Nd = 0.72190$. Analyses of the USGS standard BCR-1 yield Nd = 29.02 ppm, Sm = 6.68 ppm, and $^{146}Nd/^{144}Nd = 0.512668 \pm 20$ (n=4). The international La Jolla standard produced: TRITON: $^{143}Nd/^{144}Nd = 0.511847 \pm 7$, n = 26 (Feb 2005 – June 2007). Internal lab standard = 0.511818 ± 8, n = 28 (Feb 2005-June 2007) and 0.511819 ± 10 n = 94 (Feb 2005 – Aug 2009).

1.5 Electron Microprobe (University of Tasmania)

Conducted at the Center of Excellence in Ore Deposit Research (CODES), University of Tasmania, Hobart, Tasmania.

Instrumentation: Cameca SX100 Electron Microprobe

1.6 Electron Microprobe (Massachusetts Institute of Technology)

Conducted at the Earth, Atmosphere and Planetary Sciences division of MIT University, Boston, Massachusetts.

Instrumentation: JEOL JXA-733 Electron Microprobe

1.7 Laser Ablation-Inductively Coupled Plasma Mass Spectrometry

Conducted at the Center of Excellence in Ore Deposit Research (CODES), University of Tasmania, Hobart, Tasmania.

Laser Ablation Spot Analysis

(Modified after Baker, unpublished, 2010)

Samples selected for mineral chemical analyses were first prepared as epoxy-mounted 1-inch diameter round mounts. Epidote bearing veins and individual grains of interest within each sample were then selected via reflected light petrography.

The internal standard (IS) values for major elements (Ca, Fe, Al etc.) were then determined using the Cameca SX100 Electron Microprobe housed at the University of Tasmania Central Science Laboratory. A single internal standard measurement was made per sample for epidote due to its reasonably consistent major element chemistry.

Raw mineral chemical data acquisition was undertaken for selected spot analyses by LA-ICPMS. During this study two instruments were used: an Agilent 7500cs Inductively Coupled Plasma-Mass Spectrometer (ICP-MS) with an attached Resonetics M50 Excimer laser ablation system, or an Agilent 7500a ICPMS with an attached New Wave 193 nm solid state laser ablation system. A typical analytical run consisted of the analysis of several unknown mineral samples, bracketed by four analyses of an external

standard (ES) material of known composition (NIST-612), with two ES analyses conducted before and two after the unknowns to correct for analytical drift over the course of the analytical run. The number of unknown analyses between the ES analyses was generally dictated by time: a rule of 1.5 hours between ES runs was adhered to. Analytical conditions for individual LA-ICPMS spot analyses included a laser spot size of ~35 μm, laser energy of 3-4 J/cm^2 and a laser pulse rate of 10 Hz. The procedure for a typical spot analysis involved initial measurement of the carrier-gas background (either Ar or He) for ~30 seconds, followed by measurement of ablated sample material for ~60 seconds. Thirty-five elements were analyzed: Na, Mg, Al, K, Ca, Ti, V, Mn, Fe, Cu, Zn, Ga, As, Sr, Y, Zr, Mo, Sn, Sb, Ba, La, Ce, Pr, Nd, Sm, Eu, Gd, Dy, Er, Yb, Lu, Pb, Bi, Th, and U. Due to sample-destructive nature of the analytical procedure, multiple analyses on a single spot were not possible. Minerals less than ~50 μm in diameter were generally not analyzed. The relatively long ablation time (~60 seconds) was necessary in order to minimize the analytical uncertainty for each spot analysis and therefore lower the detection limits for analyte elements. Longer ablation periods also enable the easier recognition of growth zones and inclusions within the mineral of interest, or where the laser beam has ablated through the mineral. These undesirable sections of the ablation period can then be screened out during the data reduction process to give a relatively clean signal.

The conversion of raw mineral chemical data to element concentrations was a multi-step process. The Laser Macro V1 automated spreadsheet (developed in 2006) was used exclusively. Raw data (measured in counts per second and recorded as .csv files) was imported into the Laser Macro V1 spreadsheet, with the four ES analyses (the two to begin the sample run and the two to end the sample run) first, followed by up to 40 unknown analyses. This established a baseline for drift of the machine during the ~1.5 hour session, as well as an assessment of data quality (mentioned above). During the importing of .csv data files, the user was able to run visual quality control, noting consistent counts per second over time (indicative of a good analysis) versus variant counts per second over time (indicative of a poor analysis). A final page was used to enter an internal standard value for the mineral analyzed in order to quantify the counts per second data. Internal standard element values were determined from correlative

microprobe spot analyses based on their consistency throughout individual samples: Ca was used for epidote and plagioclase feldspar, whereas Al was used for hornblende.

Laser Ablation Chemical Mapping

(Modified after Large et al., 2009)

Chemical imaging of selectable rectangular areas on a sample was performed to highlight zoning of trace elements within mineral grains of interest. The chemical imaging was performed by ablating sets of parallel lines in a grid across the sample. Beam size was 15-30μm, line spacing was the same size as the beam, laser pulse rate was 10Hz, and rastering was generally set at 15-30μm per second (again depending on beam size). This yielded chemical map resolution broadly equivalent to one pixel laser per spot size. Individual maps generally took between 45 minutes and 1.5 hours, with ES standard runs both before and after each map. The same suite of 35 elements were analyzed during chemical mapping as for spot analyses.

Data reduction was performed in-house by the CODES laboratory staff, and included: (1) ICPMS sensitivity drift correction for each element individually, based on the standard measurements before and after image acquisition; (2) application of a median filter to remove spikes originating from counting statistics; (3) subtraction of the average background for each element from the filtered counts; (4) assignment of the standard deviation value for each element with background-corrected counts below the standard deviation on the average background; and (5) production of images for each element using a logarithmic color scale.

Appendix 2.1 - Whole rock geochemical data for the samples collected at the Black Mountain Southeast porphyry system during the March, 2008 field season.

Sample	BA08GS001	BA08GS002	BA08GS003	BA08GS004	BA08GS005	BA08GS006	BA08GS009	BA08GS011	BA08GS012	BA08GS013	BA08GS014	BA08GS015	BA08GS019	BA08GS020	BA08GS021	BA08GS022	BA08GS023	BA08GS025	BA08GS026
Location	BMP SE	BMP SE	BMP SE	BMP SE	BMP SE	BMP SE	BMP SE	BMP SE	BMP SE	BMP SE	BMP SE	BMP SE	BMP SE	BMP SE	BMP SE	BMP SE	BMP SE	BMP SE	BMP SE
Intrusive Phase	EMD	PHD	AM	HMG	PHD	PHD	HMG clot	HMG	EMD	PHD	Pugo	AM	PHD	PHD	HMG	AM	PHD	PHD	Pre-BMP
Oxide Wt%																			
SiO2	79.81	59.06	43.61	49.81	55.81	59.12	39.20	49.78	76.72	59.22	51.31	51.21	62.12	60.58	47.78	43.08	59.03	58.02	56.17
TiO2	0.27	0.58	0.86	0.99	0.92	0.71	2.20	0.90	0.37	0.76	0.76	0.73	0.67	0.72	0.97	1.04	0.60	0.63	0.75
Al2O3	9.98	17.15	16.78	18.26	17.88	17.40	15.00	17.86	11.58	17.03	18.64	18.45	15.53	16.44	18.09	17.51	17.12	17.12	15.92
Fe2O3	2.15	5.86	10.76	9.68	7.67	6.03	13.21	9.12	2.36	6.54	8.93	7.29	6.50	5.97	9.70	10.64	6.22	6.03	6.79
MnO	0.03	0.10	0.15	0.18	0.11	0.11	0.16	0.18	0.02	0.13	0.16	0.16	0.10	0.08	0.17	0.18	0.09	0.11	0.19
MgO	0.96	2.60	9.16	4.30	3.91	2.93	11.43	3.99	1.19	3.74	5.57	2.56	3.11	3.20	4.19	5.15	3.11	2.96	4.71
CaO	1.05	5.96	11.01	8.59	7.34	6.53	14.18	9.52	2.78	6.46	9.18	5.35	4.69	5.37	8.08	9.04	5.33	6.07	8.10
Na2O	2.69	3.85	2.17	4.14	3.56	3.86	1.74	3.12	2.98	3.65	2.97	4.57	3.97	3.57	4.18	2.65	3.81	3.73	3.05
K2O	1.11	2.08	0.08	1.55	1.10	1.69	0.45	1.18	0.68	1.24	0.67	2.26	1.82	1.20	2.03	2.29	1.59	1.67	0.63
P2O5	0.04	0.19	0.12	0.27	0.30	0.22	0.08	0.28	0.07	0.21	0.07	0.21	0.18	0.21	0.29	0.23	0.17	0.17	0.20
Ti	1618.65	3477.10	5155.70	5935.05	5515.40	4256.45	13189.00	5395.50	2218.15	4556.20	4556.20	4376.35	4016.65	4316.40	5815.15	6234.80	3597.00	3776.85	4496.25
P	174.56	829.16	523.68	1178.28	1309.20	960.08	349.12	1221.92	305.48	916.44	305.48	916.44	785.52	916.44	1265.56	1003.72	741.88	741.88	872.80
Cr	11.40	33.40	73.30	8.50	18.00	27.60	21.90	6.50	15.20	52.70	37.60	2.30	44.20	57.60	7.10	12.20	27.20	26.20	125.80
Co	5.30	11.40	36.80	23.50	14.40	10.20	52.90	20.50	4.60	13.60	19.00	16.20	8.80	17.50	25.70	33.70	11.60	14.00	19.80
Ni	8.00	12.10	97.80	9.60	9.40	9.30	55.70	12.90	5.00	19.30	17.00	1.30	13.90	19.50	10.20	21.70	12.50	10.80	40.10
Rb	38.60	52.30	1.20	41.40	26.50	27.80	2.10	29.60	19.90	32.30	18.70	73.80	42.90	34.60	54.20	72.80	34.60	40.30	15.30
Sr	89.50	477.70	401.70	731.00	532.80	556.60	608.60	521.40	169.70	644.50	282.60	237.50	558.90	486.30	704.80	448.10	509.10	503.90	636.20
Cs	1.50	0.80	0.10	0.40	0.90	0.50	<.1	0.50	0.60	0.70	0.50	2.90	0.70	1.40	1.40	4.20	1.10	2.10	1.50
Ba	53.00	326.00	46.00	350.00	231.00	328.00	68.00	193.00	91.00	272.00	86.00	74.00	313.00	205.00	433.00	394.00	342.00	328.00	179.00
Sc	7.00	12.00	38.00	26.00	21.00	15.00	104.00	24.00	11.00	17.00	43.00	11.00	16.00	15.00	28.00	36.00	13.00	14.00	20.00
V	39.00	142.00	323.00	307.00	232.00	161.00	681.00	277.00	52.00	178.00	314.00	175.00	151.00	155.00	305.00	376.00	146.00	155.00	189.00
Ta	0.10	0.30	<.1	0.20	0.30	0.40	0.10	0.20	0.10	0.30	<.1	0.20	0.30	0.30	0.30	0.20	0.30	0.30	0.30
Nb	1.80	5.10	1.50	4.80	6.00	5.60	1.90	4.60	1.70	5.70	0.70	4.30	5.80	5.80	4.30	3.50	5.10	4.90	6.00
Zr	90.70	111.50	48.70	110.30	121.00	118.00	38.80	101.60	114.20	126.20	33.30	92.60	124.90	106.50	101.30	86.90	110.60	110.60	114.10
Hf	2.90	2.90	1.40	3.00	3.30	3.20	1.40	2.70	3.10	3.20	1.10	2.50	3.40	3.00	2.60	2.40	3.00	2.90	3.10
Th	0.50	3.60	0.70	5.20	4.50	5.00	1.00	3.80	0.20	4.90	0.10	2.50	3.70	5.20	3.60	3.30	4.20	4.30	5.10
U	0.20	1.70	0.30	1.30	1.90	1.50	0.30	1.10	0.30	1.40	0.10	0.70	1.00	1.40	1.20	0.90	1.40	1.40	1.40
Y	18.70	16.20	17.20	25.00	20.20	18.40	20.20	23.20	24.60	19.30	19.30	26.10	18.40	16.70	23.00	19.80	17.50	17.10	15.60
La	3.70	10.60	3.90	15.90	15.60	14.70	4.20	13.90	3.60	16.20	1.50	9.10	11.30	19.90	14.50	13.50	13.00	12.30	17.10
Ce	8.50	21.80	9.30	36.20	31.60	28.60	10.70	29.90	10.10	34.00	4.30	19.90	24.50	27.40	30.60	29.10	27.10	26.70	35.60
Pr	1.24	2.91	1.43	4.72	4.01	3.83	1.80	4.02	1.52	4.13	0.81	2.86	3.22	3.61	4.41	3.98	3.29	3.24	4.21
Nd	6.00	13.00	7.30	18.90	17.00	15.20	9.60	17.40	7.90	15.90	4.30	13.60	12.60	14.50	17.60	17.60	12.50	12.40	15.60
Sm	1.63	2.75	2.22	3.90	3.68	3.04	3.06	3.93	2.24	3.19	1.68	3.51	2.75	2.88	4.00	3.71	2.52	2.45	3.19
Eu	0.47	0.84	0.75	1.38	1.14	1.01	0.98	1.18	0.60	1.14	0.67	1.02	0.98	0.92	1.19	1.14	0.96	0.90	1.07
Gd	1.99	2.56	2.76	4.10	3.45	2.84	3.72	3.79	2.94	3.22	2.36	3.79	2.89	2.88	3.80	3.58	2.71	2.62	2.89
Tb	0.46	0.50	0.54	0.81	0.67	0.51	0.70	0.76	0.61	0.62	0.51	0.76	0.57	0.46	0.71	0.64	0.57	0.53	0.56
Dy	2.66	2.64	2.96	3.77	3.54	2.66	3.89	3.87	3.62	2.78	3.04	4.18	2.63	2.56	3.94	3.33	2.56	2.41	2.52
Ho	0.56	0.48	0.56	0.81	0.65	0.56	0.67	0.73	0.77	0.61	0.63	0.82	0.58	0.52	0.74	0.65	0.55	0.55	0.52
Er	1.99	1.63	1.72	2.20	1.92	1.60	2.04	2.23	2.63	1.60	2.06	2.67	1.57	1.46	2.21	2.02	1.53	1.65	1.41
Tm	0.29	0.24	0.23	0.40	0.28	0.24	0.26	0.34	0.40	0.28	0.30	0.40	0.29	0.23	0.34	0.29	0.25	0.25	0.24
Yb	2.09	1.69	1.47	2.17	1.88	1.67	1.74	2.13	2.71	1.67	1.93	2.56	1.65	1.55	2.24	1.88	1.57	1.62	1.28
Lu	0.33	0.26	0.23	0.36	0.26	0.27	0.24	0.33	0.46	0.27	0.30	0.40	0.28	0.23	0.34	0.28	0.27	0.28	0.23
Cu	1121.88	88.60	79.76	102.70	326.42	138.65	35.07	88.98	496.13	246.47	1131.31	37.91	290.71	903.40	97.68	116.50	173.97	157.76	85.26
Zn	14.80	25.70	58.90	53.70	34.40	37.00	43.90	53.30	9.70	31.90	29.70	75.40	15.20	43.90	58.90	79.50	91.00	42.90	86.60
Mo	156.10	0.49	0.73	0.91	1.40	0.73	0.46	0.47	9.80	0.35	5.90	0.76	2.16	1.51	1.14	0.51	0.56	7.69	0.92
Ag	284.00	23.00	103.00	45.00	28.00	38.00	28.00	39.00	55.00	13.00	116.00	13.00	74.00	169.00	62.00	110.00	51.00	40.00	79.00
Tl	0.08	0.06	<.02	0.03	0.06	0.02	<.02	0.02	0.05	0.15	0.08	0.12	0.03	0.10	0.05	0.15	0.05	0.05	0.11
Pb	2.13	0.83	2.83	3.76	0.84	1.02	8.99	3.16	0.88	0.48	1.39	2.13	0.39	1.29	6.25	5.13	2.01	1.28	5.59
Sn	1.00	1.00	1.00	1.00	2.00	<1	1.00	1.00	1.00	1.00	1.00	1.00	1.00	<1	1.00	1.00	1.00	1.00	1.00
Sb	0.11	0.13	0.19	0.13	0.04	0.06	0.56	0.03	0.05	0.02	0.06	0.12	0.11	0.10	0.20	0.46	0.14	0.09	0.15
Ga	6.80	17.70	15.20	19.90	18.40	18.90	17.80	17.50	9.20	20.30	14.10	18.00	17.80	17.90	17.30	18.30	17.90	17.40	18.90
W	2.30	1.80	0.60	1.50	2.80	1.00	1.00	0.40	1.90	0.10	0.50	0.60	1.70	0.70	0.30	0.90	1.40	0.70	0.90
Mn	222.00	537.00	795.00	957.00	350.00	379.00	871.00	858.00	129.00	410.00	343.00	1183.00	348.00	499.00	983.00	1299.00	485.00	639.00	815.00
As	1.50	0.70	2.60	2.40	0.40	0.40	5.30	1.00	1.10	0.30	0.40	0.50	0.50	<.1	1.70	1.00	0.80	0.60	1.80
Au	10.00	1.00	4.00	3.00	4.00	3.00	28.00	4.00	5.00	2.00	17.00	1.00	9.00	38.00	7.00	3.00	2.00	2.00	18.00
Cd	<.01	0.03	0.11	0.08	0.07	0.10	0.19	0.06	0.05	0.04	0.08	0.23	0.03	0.05	0.09	0.15	0.13	0.07	0.25
Bi	0.04	0.03	0.04	0.02	0.02	0.02	0.03	0.03	<.02	<.02	0.05	0.02	0.04	0.04	0.07	0.05	0.28	0.10	0.87
B *	1.00	1.00	2.00	6.00	1.00	<1	6.00	7.00	1.00	1.00	1.00	2.00	1.00	1.00	3.00	2.00	2.00	2.00	2.00
Hg	7.00	<5	<5	<5	<5	<5	<5	<5	<5	<5	<5	<5	<5	<5	<5	<5	<5	<5	<5
Se	1.50	0.20	0.10	0.20	0.30	0.10	0.20	0.10	0.90	0.30	1.30	0.10	0.20	0.80	0.10	0.10	1.20	0.50	0.60
Te	0.03	<.02	0.02	<.02	0.03	<.02	0.09	0.02	0.03	0.02	0.05	<.02	<.02	0.02	<.02	0.03	0.07	0.09	0.77
Ge	<.1	0.10	0.10	0.20	0.10	<.1	0.40	0.10	<.1	0.10	0.10	<.1	0.10	0.10	<.1	<.1	0.10	0.10	0.10
In	<.02	<.02	0.02	0.03	<.02	0.02	0.10	0.03	<.02	<.02	0.02	0.05	<.02	0.02	0.04	0.06	<.02	0.03	0.05
Re	331.00	<1	<1	<1	1.00	<1	<1	<1	9.00	<1	3.00	<1	1.00	1.00	<1	<1	<1	3.00	<1
Be	0.10	0.10	0.20	0.40	0.10	0.10	0.10	0.40	0.10	0.20	0.10	0.30	0.10	0.20	0.30	0.50	0.20	0.20	0.30
Li *	3.70	5.00	21.60	13.20	5.20	4.00	1.80	7.50	3.90	5.80	5.10	13.50	3.30	7.80	11.40	20.60	9.60	10.40	16.30
Pd	<.5	0.60	1.80	4.50	0.60	<.5	145.10	3.90	<.5	<.5	1.60	<.5	1.80	1.10	5.10	8.60	<.5	<.5	1.30
Pt	0.60	0.20	1.70	4.00	0.20	0.30	111.80	3.10	0.10	0.40	1.60	<.1	1.40	0.50	4.10	8.60	<.1	2.10	1.40
TOT/C	0.15	0.34	0.49	0.16	0.03	0.17	0.11	0.10	0.10	0.03	0.09	1.12	0.07	0.33	0.74	1.37	0.13	0.39	0.33
TOT/S	0.26	0.04	0.01	0.04	0.02	0.01	0.01	0.01	0.23	0.03	0.45	0.01	0.08	0.08	0.01	0.02	1.68	0.89	1.45
LOI	1.80	2.50	5.20	2.10	1.30	1.30	2.30	4.00	1.20	0.90	1.60	7.20	1.20	2.50	4.40	8.10	2.70	3.40	3.40

Appendix 2.1 continued

Sample	BA08GS027	BA08GS028	BA08GS029	BA08GS030	BA08GS032	BA08GS035	BA08GS037	BA08GS038	BA08GS039	BA08GS040	BA08GS043	BA08GS044	BA08GS045	BA08GS047	BA08GS049	BA08GS050	BA08GS051	BA08GS052	BA08GS053
Location	BMP SE	BMP SE	BMP SE	BMP SE	BMP SE	BMP SE	BMP SE	BMP SE	BMP SE	BMP SE	BMP SE	BMP SE	BMP SE	BMP SE	BMP SE	BMP SE	Liw-Liw Crk	BMP SE	Liw-Liw
Intrusive Phase	AM	AM	HMG	PHD	HMB	Liw-Liw	Zig-Zag	Pre-BMP	Liw-Liw	PHD	Pugo	Pugo	HMB	HMB	Pugo	AM	Pugo	PHD	Liw-Liw
Oxide Wt%																			
SiO2	47.41	47.26	50.88	58.48	48.84	47.97	46.63	55.13	46.89	57.18	59.51	52.82	49.33	49.21	48.03	49.76	51.41	56.67	48.79
TiO2	0.94	0.93	0.93	0.89	0.92	0.93	0.87	0.76	0.94	0.74	0.76	1.01	0.93	0.92	0.75	1.39	0.64	0.68	0.68
Al2O3	17.46	18.78	18.45	16.72	17.29	18.22	20.44	15.72	18.18	16.75	18.11	19.41	15.41	14.82	19.78	14.76	18.29	17.88	18.18
Fe2O3	9.70	9.23	9.44	6.81	8.90	10.92	10.53	7.49	11.26	7.01	9.08	9.27	9.68	10.38	10.36	14.99	9.21	7.40	9.12
MnO	0.21	0.18	0.18	0.12	0.20	0.26	0.12	0.21	0.35	0.12	0.16	0.17	0.17	0.14	0.15	0.18	0.16	0.11	0.15
MgO	4.00	4.23	4.11	3.96	2.24	4.78	3.49	5.58	4.09	3.44	2.03	4.18	8.27	9.40	6.48	5.06	7.69	3.24	8.27
CaO	9.63	9.60	8.39	6.50	11.62	10.24	7.49	7.41	11.22	6.13	1.70	6.05	11.29	9.67	10.23	6.57	7.35	7.65	6.07
Na2O	3.19	3.17	3.84	3.34	2.93	2.80	3.33	3.22	2.01	3.59	2.57	4.02	2.38	3.38	1.82	3.80	1.93	3.44	1.45
K2O	1.22	1.20	1.29	1.05	1.27	0.28	0.37	1.25	0.30	2.32	2.98	0.76	0.55	0.62	0.33	0.45	1.03	1.04	1.07
P2O5	0.23	0.25	0.29	0.23	0.26	0.14	0.34	0.21	0.14	0.20	0.13	0.14	0.28	0.22	0.04	0.17	0.05	0.19	0.06
Ti	5635.30	5575.35	5575.35	5335.55	5515.40	5575.35	5215.65	4556.20	5635.30	4436.30	4556.20	6054.95	5575.35	5515.40	4496.25	8333.05	3836.80	4076.60	4076.60
P	1003.72	1091.00	1265.56	1003.72	1134.64	610.96	1483.76	916.44	610.96	872.80	567.32	610.96	1221.92	960.08	174.56	741.88	218.20	829.16	261.84
Cr	7.50	5.10	7.00	55.60	7.80	26.70	13.90	111.10	22.70	20.40	17.00	24.20	67.30	97.70	26.10	22.00	26.50	31.40	33.30
Co	27.60	25.40	23.00	15.40	25.10	27.10	26.70	20.60	18.40	14.10	17.40	9.60	17.50	11.70	19.70	13.60	22.70	15.10	34.40
Ni	8.10	7.50	9.30	21.30	9.00	11.70	8.80	40.10	13.30	11.00	11.40	9.70	24.90	34.10	16.90	12.80	19.80	13.50	26.10
Rb	25.00	23.20	33.90	29.40	23.70	5.40	8.20	17.00	7.70	38.50	61.40	17.40	13.40	8.30	9.10	12.40	23.50	24.40	28.40
Sr	513.50	515.70	673.40	578.70	596.50	574.60	528.00	545.80	551.60	506.10	209.10	205.90	676.60	515.40	150.00	194.70	135.70	549.40	138.40
Cs	0.60	0.90	1.00	1.30	1.10	0.20	0.30	0.70	0.50	0.40	2.00	0.60	0.40	0.10	0.30	0.80	1.80	1.10	1.60
Ba	315.00	338.00	315.00	189.00	337.00	52.00	73.00	360.00	58.00	467.00	449.00	42.00	179.00	64.00	15.00	40.00	42.00	139.00	75.00
Sc	24.00	22.00	25.00	18.00	24.00	26.00	20.00	21.00	27.00	17.00	22.00	39.00	51.00	50.00	44.00	51.00	37.00	16.00	40.00
V	274.00	266.00	286.00	197.00	263.00	313.00	236.00	182.00	300.00	167.00	187.00	337.00	304.00	331.00	344.00	490.00	265.00	171.00	314.00
Ta	0.10	0.20	0.20	0.30	0.20	0.10	0.30	0.30	0.10	0.30	0.40	0.10	0.50	0.10	<.1	0.10	<.1	0.20	<.1
Nb	3.70	3.80	4.70	6.50	4.30	1.90	5.00	5.30	1.70	5.30	6.50	1.10	9.00	2.00	0.70	1.50	0.40	4.50	0.40
Zr	96.50	103.30	103.50	126.70	95.90	56.60	112.90	107.40	56.90	107.80	153.60	48.20	101.70	78.60	25.80	62.60	30.60	106.40	33.10
Hf	2.50	2.80	3.10	3.30	2.40	1.70	3.20	3.00	1.60	3.00	4.00	1.40	2.80	2.10	0.90	1.90	0.90	2.70	1.00
Th	1.90	2.70	4.60	5.00	3.40	2.00	2.50	4.10	1.70	4.10	5.70	0.20	5.20	2.00	0.10	0.10	0.10	3.20	0.10
U	0.70	0.80	1.20	1.30	1.20	0.60	0.80	1.40	0.60	1.50	1.80	0.20	1.50	0.80	0.10	0.40	0.10	1.00	0.20
Y	25.10	26.50	22.60	21.00	22.10	21.90	26.90	15.30	22.20	18.30	23.00	21.80	19.50	16.70	16.10	29.80	14.60	17.40	15.50
La	9.60	10.20	15.20	15.90	13.20	7.70	13.80	14.90	7.90	12.80	21.00	2.60	25.60	11.20	1.90	3.80	1.30	11.80	1.50
Ce	22.10	23.80	31.80	34.20	29.50	17.40	30.40	28.80	16.40	24.80	38.80	7.70	51.30	26.00	3.80	9.50	3.60	24.30	4.10
Pr	3.05	3.29	4.33	4.37	3.83	2.46	4.10	3.64	2.46	3.20	4.68	1.29	6.25	3.51	0.68	1.71	0.70	3.06	0.72
Nd	13.80	14.10	17.90	16.80	17.50	12.00	17.90	14.70	11.60	14.60	19.90	6.80	24.00	15.30	3.80	9.60	3.70	13.10	3.80
Sm	3.68	3.76	4.19	3.50	3.73	3.23	4.15	3.02	3.18	3.04	4.06	2.23	4.82	3.31	1.39	3.03	1.30	2.71	1.41
Eu	1.09	1.16	1.17	1.20	1.13	1.07	1.26	0.94	1.04	0.92	1.01	0.76	1.59	1.00	0.63	0.99	0.47	0.87	0.53
Gd	3.93	4.00	3.91	3.56	3.60	3.44	4.02	2.74	3.34	2.85	3.65	2.86	4.39	3.16	2.04	4.08	1.76	2.67	2.02
Tb	0.75	0.77	0.79	0.70	0.70	0.67	0.79	0.52	0.67	0.57	0.71	0.62	0.76	0.59	0.46	0.86	0.42	0.54	0.43
Dy	4.19	4.31	3.86	3.02	3.66	3.67	4.31	2.58	3.72	3.11	3.62	3.59	3.21	2.95	2.39	4.97	2.30	2.86	2.40
Ho	0.81	0.84	0.72	0.68	0.69	0.72	0.79	0.47	0.69	0.53	0.74	0.72	0.67	0.55	0.55	0.96	0.57	0.53	0.52
Er	2.63	2.66	2.27	1.83	2.20	2.28	2.66	1.37	2.21	1.78	2.41	2.26	1.62	1.62	1.57	3.17	1.61	1.76	1.60
Tm	0.37	0.38	0.32	0.32	0.38	0.31	0.40	0.22	0.32	0.27	0.35	0.35	0.28	0.23	0.25	0.49	0.24	0.24	0.22
Yb	2.49	2.54	2.22	1.79	2.08	2.07	2.58	1.36	2.03	1.66	2.28	2.15	1.51	1.54	1.49	2.90	1.49	1.75	1.52
Lu	0.39	0.41	0.33	0.29	0.31	0.31	0.39	0.20	0.32	0.24	0.35	0.32	0.26	0.23	0.26	0.45	0.24	0.27	0.24
Cu	96.01	99.20	149.02	216.11	98.13	115.57	543.18	141.14	201.88	235.53	97.93	343.28	127.12	81.31	219.77	332.55	128.14	118.95	298.63
Zn	72.60	77.00	47.20	42.60	57.00	127.60	85.50	117.40	251.20	90.90	128.50	23.20	14.80	19.70	21.60	228.60	26.30	30.60	129.10
Mo	0.78	1.06	1.49	2.80	1.25	0.93	0.60	0.68	0.67	1.61	1.04	1.28	1.44	0.39	4.64	3.98	1.32	1.72	0.44
Ag	53.00	16.00	30.00	30.00	41.00	105.00	2366.00	124.00	194.00	252.00	75.00	38.00	39.00	26.00	51.00	101.00	44.00	53.00	143.00
Tl	0.03	0.03	0.04	0.13	0.03	0.02	0.03	0.03	0.02	0.03	0.15	0.20	0.08	0.06	0.13	0.13	0.34	0.33	0.15
Pb	4.49	2.96	3.38	1.03	4.66	3.23	5.02	4.20	14.91	3.22	1.65	1.22	1.14	0.48	0.81	0.63	0.93	2.54	10.80
Sn	1.00	1.00	1.00	1.00	1.00	2.00	2.00	1.00	2.00	1.00	1.00	1.00	1.00	1.00	1.00	2.00	1.00	1.00	1.00
Sb	0.11	0.07	0.18	0.04	0.32	0.32	0.21	0.15	0.43	0.12	0.16	0.07	0.04	0.02	0.05	0.09	0.03	0.07	0.05
Ga	18.10	19.10	17.50	19.10	16.70	21.80	22.20	17.10	19.40	17.70	16.50	14.10	17.60	15.30	15.60	16.00	14.00	18.00	13.30
W	0.40	0.40	0.60	0.80	0.30	0.90	1.10	<.1	0.70	1.90	0.50	1.80	1.10	<.1	1.30	2.10	<.1	0.20	<.1
Mn	1494.00	1231.00	977.00	425.00	1363.00	809.00	650.00	939.00	1243.00	437.00	1038.00	334.00	226.00	251.00	225.00	410.00	364.00	287.00	1015.00
As	0.90	0.80	2.30	0.20	2.70	3.80	2.80	2.00	2.90	1.50	1.30	0.20	0.40	<.1	0.10	<.1	<.1	0.40	<.1
Au	6.00	3.00	4.00	5.00	2.00	47.00	430.00	16.00	27.00	47.00	3.00	6.00	8.00	3.00	7.00	10.00	4.00	56.00	12.00
Cd	0.26	0.19	0.06	0.12	0.14	0.47	0.24	0.45	1.73	0.19	0.68	0.20	0.03	0.03	0.03	0.91	0.05	0.06	0.61
Bi	0.03	0.03	0.03	<.02	0.04	6.38	4.63	0.78	5.73	2.03	0.05	0.14	0.06	0.04	0.14	0.37	0.05	0.13	0.29
B *	1.00	1.00	3.00	1.00	1.00	2.00	1.00	<1	2.00	<1	2.00	<1	1.00	<1	<1	1.00	1.00	<1	1.00
Hg	<5	<5	<5	<5	<5	<5	<5	<5	6.00	<5	<5	<5	<5	<5	<5	<5	<5	<5	<5
Se	<.1	0.10	0.10	1.00	<.1	0.80	3.30	0.20	0.70	0.60	0.10	1.90	0.40	0.20	1.40	1.10	0.40	0.60	0.80
Te	0.02	0.03	<.02	<.02	<.02	4.97	4.95	1.09	2.89	2.72	0.02	0.10	0.04	<.02	0.07	0.07	0.04	0.07	0.15
Ge	0.10	0.10	0.10	0.20	0.10	0.20	0.10	0.10	0.30	0.10	0.10	0.10	<.1	0.10	0.10	0.20	0.10	0.10	0.10
In	0.06	0.06	0.02	<.02	0.06	0.08	0.06	0.05	0.07	0.02	<.02	0.03	<.02	0.04	0.02	0.06	0.02	0.02	0.04
Re	<1	1.00	3.00	2.00	<1	<1	<1	<1	<1	<1	<1	2.00	<1	<1	5.00	45.00	6.00	<1	1.00
Be	0.20	0.30	0.20	0.20	0.30	0.10	0.20	0.20	0.10	0.10	0.40	0.10	0.30	0.10	0.10	0.10	0.10	0.10	0.10
Li *	22.90	23.40	10.80	4.10	8.00	4.40	5.60	7.90	8.70	5.20	8.00	4.20	2.40	0.50	2.90	5.10	3.20	2.60	13.80
Pd	1.00	1.00	5.00	<.5	1.50	<.5	1.00	1.30	<.5	<.5	2.60	2.40	5.30	3.00	2.00	2.00	3.10	<.5	2.30
Pt	1.40	1.20	4.00	0.30	1.80	0.20	0.90	1.50	0.20	0.20	1.00	3.40	4.40	3.60	2.20	3.40	3.00	0.30	4.30
TOT/C	1.08	0.91	0.31	0.15	1.26	0.04	0.03	0.25	0.17	0.06	0.04	0.03	0.04	0.02	0.03	0.17	0.07	0.07	0.51
TOT/S	0.01	0.02	0.05	0.49	0.01	1.78	4.91	0.70	2.00	1.39	0.15	0.84	0.31	0.10	0.91	1.24	0.19	0.34	0.49
LOI	5.90	5.10	2.10	1.80	5.30	3.40	6.30	2.90	4.40	2.40	2.90	2.00	1.60	1.00	2.00	2.80	2.10	1.50	6.00

Appendix 2.1 continued

Sample	BA08GS054	BA08GS055	BA08GS056	BA08GS057
Location	BMP SE	BMP SE	Liw-Liw	Liw-Liw
Intrusive Phase	PHD	PHD	Liw-Liw	Liw-Liw
Oxide Wt%				
SiO2	57.22	59.44	46.97	46.57
TiO2	0.64	0.57	0.89	0.86
Al2O3	17.98	17.17	17.45	17.09
Fe2O3	6.70	5.92	10.12	9.68
MnO	0.10	0.10	0.15	0.15
MgO	3.06	2.58	8.20	7.54
CaO	7.18	5.90	10.52	10.60
Na2O	4.06	4.04	2.98	2.78
K2O	0.77	1.52	0.64	0.90
P2O5	0.19	0.19	0.11	0.13
Ti	3836.80	3417.15	5335.55	5155.70
P	829.16	829.16	480.04	567.32
Cr	28.90	34.00	80.90	89.70
Co	14.50	13.80	11.20	23.80
Ni	12.90	13.40	30.40	42.90
Rb	14.30	27.10	13.80	21.00
Sr	558.70	509.10	428.40	387.50
Cs	0.40	0.70	0.60	0.90
Ba	151.00	352.00	44.00	68.00
Sc	14.00	12.00	46.00	42.00
V	152.00	127.00	377.00	354.00
Ta	0.30	0.30	<.1	0.10
Nb	4.70	4.60	1.30	1.10
Zr	109.60	98.50	41.70	39.80
Hf	2.90	2.50	1.50	1.20
Th	3.40	3.80	0.60	0.80
U	1.00	1.30	0.30	0.30
Y	17.00	15.70	14.90	16.10
La	12.70	12.50	4.50	5.10
Ce	25.20	23.40	10.40	9.70
Pr	3.20	3.15	1.58	1.59
Nd	12.80	12.10	7.80	7.50
Sm	2.75	2.51	2.35	1.98
Eu	0.84	0.81	0.75	0.75
Gd	2.67	2.34	2.44	2.42
Tb	0.50	0.41	0.46	0.44
Dy	2.75	2.30	2.50	2.47
Ho	0.54	0.48	0.51	0.53
Er	1.74	1.50	1.54	1.57
Tm	0.26	0.22	0.21	0.22
Yb	1.72	1.50	1.47	1.42
Lu	0.25	0.24	0.22	0.24
Cu	39.23	58.23	154.54	333.83
Zn	22.60	40.20	24.80	31.90
Mo	0.58	0.86	0.69	0.37
Ag	21.00	52.00	128.00	230.00
Tl	0.06	0.03	0.05	0.07
Pb	0.83	1.49	2.46	1.70
Sn	1.00	<1	1.00	<1
Sb	0.33	0.15	0.11	0.11
Ga	17.20	17.50	16.20	17.50
W	0.10	0.90	0.40	1.00
Mn	310.00	640.00	354.00	609.00
As	0.60	0.60	0.50	0.70
Au	2.00	4.00	8.00	40.00
Cd	0.21	0.12	0.10	0.08
Bi	0.16	0.02	0.40	0.77
B *	<1	1.00	<1	1.00
Hg	<5	<5	<5	<5
Se	0.10	<.1	0.30	0.80
Te	0.09	0.05	0.26	0.47
Ge	0.10	0.10	0.10	0.10
In	<.02	0.03	0.03	0.06
Re	<1	<1	<1	<1
Be	0.10	0.10	0.10	0.20
Li *	6.00	5.60	3.00	9.20
Pd	<.5	<.5	0.80	1.10
Pt	0.30	<.1	1.30	1.50
TOT/C	0.14	0.39	0.11	0.56
TOT/S	0.29	0.03	0.50	1.55
LOI	1.90	2.50	1.90	3.60

Appendix 2.2 – Whole rock geochemical data for the Pliocene intrusive centers of the Baguio mineral district (Hollings, 2006; Hollings et al., in review).

Sample	96966	96968	814451	814456	814461	814471	814474	354208	354209	354210	354211	806101	353243	353245	353246	353247	353247	353248	353248	806221	121	97031	97042	811568	811569	811570	811571
Source	Hollings (2006)	Hollings (2006)	Hollings (2006)	Hollings (2006)	Hollings (2006)	Hollings (2006)	Hollings (2006)	Hollings (2006)	Hollings (2006)	Hollings (2006)	Hollings (2006)	Hollings (2006)	Hollings (2006)	Hollings (2006)	Hollings (2006)	Hollings (2006)	Hollings (2006)	Hollings (2006)	Hollings (2006)	Hollings (2006)	Hollings (2006)	Hollings (2006)	Hollings (2006)	Hollings (2006)	Hollings (2006)	Hollings (2006)	Hollings (2006)
Assoc. Intrusive	Ampucao	Ampucao	Ampucao	Ampucao	Ampucao	Ampucao	Ampucao	Ampucao	Ampucao	Ampucao	Ampucao	Ampucao	Antamok	Antamok	Antamok	Antamok	Antamok	Antamok	Antamok	Antamok	Antamok	Balatoc	Balatoc	Balatoc	Balatoc	Balatoc	Balatoc
Age	Pliocene	Pliocene	Pliocene	Pliocene	Pliocene	Pliocene	Pliocene	Pliocene	Pliocene	Pliocene	Pliocene	Pliocene	Miocene	Miocene	Miocene	Miocene	Miocene	Miocene	Miocene	Miocene	Miocene	Pliocene	Pliocene	Pliocene	Pliocene	Pliocene	Pliocene
Oxide wt%																											
SiO2	68.7	70.1	66.6	63.1	55.4	54.8	50.2	60.5	62.3	65.3	65.3	64.0	60.1	63.2	60.2	50.1	59.6	56.6	52.5	67.5	60.6	57.4	55.6	56.1	55.3	55.7	79.5
TiO2	0.3	0.2	0.4	0.4	0.8	0.8	0.9	0.5	0.5	0.4	0.4	0.3	0.6	0.5	0.6	0.8	0.6	0.7	0.8	0.3	0.5	0.7	0.8	0.6	0.6	0.6	0.3
Al2O3	13.6	11.6	14.6	17.3	21.6	18.1	19.1	16.7	16.9	16.3	17.0	15.9	16.9	16.7	17.0	18.9	17.7	18.7	17.8	16.9	17.7	17.3	19.0	15.6	15.5	15.5	8.2
Fe2O3	6.3	7.7	6.0	5.8	6.2	7.5	10.1	5.9	6.0	4.4	4.0	5.7	6.6	5.6	6.7	8.5	6.7	6.9	8.1	3.4	6.3	6.8	7.3	5.9	6.1	6.0	3.3
MnO	0.0	0.0	0.2	0.1	0.1	0.1	0.2	0.1	0.1	0.1	0.1	0.1	0.1	0.1	0.1	0.1	0.2	0.1	0.1	0.1	0.1	0.5	0.5	0.2	0.2	0.2	0.0
MgO	1.2	1.0	1.6	1.6	3.0	2.8	4.6	2.8	2.8	1.6	1.4	1.6	2.9	2.5	3.0	3.6	3.1	2.2	2.4	1.1	2.7	3.9	4.4	2.9	3.4	3.4	1.0
CaO	3.9	3.2	2.5	3.5	0.2	6.8	10.1	3.9	4.0	3.1	4.4	3.5	6.4	6.9	7.3	10.6	6.8	7.5	10.7	5.3	7.1	6.5	6.3	6.9	5.9	6.5	1.2
Na2O	2.4	3.4	3.5	4.5	0.6	4.7	3.2	4.4	4.1	4.1	4.3	4.0	3.2	3.6	3.2	2.8	3.2	3.9	2.7	1.5	3.4	6.4	4.9	1.9	2.0	1.9	0.3
K2O	3.5	2.6	2.2	2.1	4.1	2.2	0.8	1.8	1.3	1.5	1.5	1.9	1.1	0.4	0.8	0.7	0.6	1.3	0.6	3.8	0.9	0.2	0.9	2.3	2.9	3.2	2.1
P2O5	0.1	0.1	0.1	0.2	0.4	0.2	0.2	0.2	0.2	0.1	0.1	0.1	0.2	0.2	0.2	0.2	0.2	0.3	0.3	0.1	0.1	0.2	0.2	0.2	0.1	0.1	0.0
Cr	8.3	6.7	8.8	10.5	1.2	3.7	5.3	45.6	47.1	8.0	5.9	26.1	5.1	21.2	5.0	21.0	6.6	2.0	3.6	11.5		41.1	18.8	96.5	142.6	111.4	335.7
Co			8.8	9.3	17.5	7.2	16.2	12.8	12.7	7.5	6.9	25.6	10.3	5.8	7.8	17.4	7.6	11.5	19.2	8.2				14.4	15.9	16.7	6.5
Ni			10.0	13.0	10.0	10.0	10.0	11.9	12.7	3.0	1.7		10.0	10.0	10.0	10.0	10.0	10.0	10.0	5.4				10.0	21.0	10.0	20.0
Rb	26.4	41.3	20.0	28.2	110.4	38.3	14.5	42.0	31.3	18.9	19.7	20.3	23.4	9.0	15.6	10.3	9.6	20.9	6.0	38.8	13.0	214.3	153.2	66.3	84.2	91.5	60.5
Sr	412.2	285.1	445.9	585.2	74.1	613.8	505.7	478.4	491.9	443.6	534.6	467.0	451.4	430.9	400.0	639.7	476.7	739.6	701.4	555.9	323.0	166.9	233.5	293.8	320.6	326.9	73.1
Cs			0.4	0.3	3.6	0.7	0.9	0.5	0.8	0.8	0.3		0.8	0.8	0.9	0.2	0.3	0.2	<.1	27.6				6.4	6.4	6.7	4.6
Ba	672.7	695.5	644.0	529.0	448.0	504.0	199.0	300.9	308.4	527.4	546.5	439.0	349.0	162.0	310.0	211.0	299.0	252.0	244.0	533.2	60.0	359.3	395.5	229.0	407.0	364.0	151.0
Sc	0.0		7.0	7.0	10.0	12.0	23.0	12.3	13.9	6.4	5.5	9.5	3.8	1.6	2.4	10.1	2.5	3.8	8.8	6.7				5.3	6.5	6.1	1.6
V	0.0		103.0	95.0	140.0	198.0	292.0	120.9	145.6	86.2	68.9		160.0	137.0	187.0	261.0	166.0	143.0	218.0	72.4				155.0	176.0	164.0	110.0
Ta	0.0		0.2	0.2	0.2	0.3	0.2	0.2	0.2	0.2	0.2	0.5	0.1	0.2	0.2	0.2	0.1	0.3	0.5	0.2				0.2	0.2	0.2	<.1
Nb	2.8	2.2	2.4	2.7	3.7	3.9	2.3	2.3	2.9	2.9	2.9	3.0	2.8	2.4	2.8	3.8	2.9	4.8	7.6	2.8		4.3	5.4	3.4	3.3	3.6	1.8
Zr	80.2	61.7	64.9	91.4	111.3	108.3	63.2	70.3	56.4	69.5	78.1	103.0	43.6	79.8	78.8	69.3	81.3	115.1	105.7	51.2		96.5	113.8	66.6	75.2	74.6	36.0
Hf			1.8	2.7	3.5	2.8	1.5	1.9	1.6	1.9	2.1	2.5	1.6	2.2	2.7	2.3	2.3	3.2	2.9	1.6				2.3	2.3	2.0	1.2
Th			2.3	3.2	1.9	2.4	1.2	2.7	3.0	3.1	2.9	3.3	1.4	1.2	1.9	1.4	1.2	2.6	1.7	2.1				2.1	2.0	1.7	0.6
U			0.8	1.1	0.8	1.0	0.5	0.8	0.9	0.8	0.8	0.7	0.6	0.7	0.5	0.5	0.5	0.8	0.8	0.8				0.8	0.8	0.9	0.4
Y	8.4	6.8	19.9	14.6	33.4	23.3	20.7	12.6	14.4	15.7	12.6	13.9	16.5	14.5	17.3	18.9	18.6	24.8	21.5	13.3		19.7	22.7	14.4	15.5	16.2	8.1
La	8.3	7.1	15.3	12.7	10.2	14.1	7.4	8.8	9.7	12.6	11.1	10.8	9.3	7.7	9.0	8.1	9.3	12.9	12.9	9.0		13.8	13.9	8.3	8.4	9.2	5.0
Ce	16.0	11.8	25.0	25.2	26.5	28.4	16.3	17.7	19.8	24.5	21.1	19.7	21.1	18.0	19.1	19.2	20.5	30.9	29.9	17.3		25.7	27.8	18.1	19.3	19.8	11.0
Pr	1.8	1.4	3.7	3.0	3.7	3.4	2.2	2.2	2.5	3.2	2.7	2.5	2.7	2.4	2.4	2.5	2.6	4.1	3.8	2.0		3.4	3.6	2.3	2.4	2.6	1.3
Nd	7.6	5.8	15.9	11.0	17.6	15.7	10.3	9.0	10.3	12.4	10.3	10.6	11.5	10.9	10.6	12.3	11.6	19.8	18.1	8.5		13.9	15.3	11.1	10.4	11.6	6.5
Sm	1.6	1.2	3.8	2.5	5.3	3.7	2.8	1.9	2.2	2.6	2.0	2.3	2.7	2.6	2.5	3.0	2.9	4.2	4.1	1.8		3.2	3.2	2.3	2.5	2.4	1.5
Eu	0.5	0.4	1.0	0.7	1.5	1.2	1.0	0.6	0.7	0.8	0.7	0.7	0.9	0.9	0.8	1.1	0.9	1.5	1.4	0.6		1.1	1.1	0.8	0.9	0.9	0.4
Gd	1.3	1.1	3.4	2.3	5.6	3.8	3.5	1.9	2.2	2.6	1.9	2.4	2.6	2.6	2.6	3.2	3.0	4.1	3.9	1.9		3.1	3.7	2.4	2.2	3.0	1.9
Tb	0.2	0.2	0.6	0.4	0.9	0.6	0.5	0.3	0.4	0.4	0.3		0.5	0.4	0.5	0.6	0.6	0.7	0.6	0.3		0.5	0.6	0.4	0.5	0.4	0.3
Dy	1.3	1.1	2.9	2.1	5.3	3.7	3.4	1.9	2.3	2.5	2.0	2.4	2.6	2.5	3.1	3.5	3.1	4.2	3.7	2.1		2.9	3.5	2.3	2.6	2.7	1.3
Ho	0.2	0.2	0.6	0.5	1.3	0.8	0.8	0.4	0.5	0.5	0.4	0.5	0.5	0.5	0.6	0.7	0.6	0.9	0.8	0.4		0.6	0.8	0.5	0.5	0.5	0.3
Er	0.8	0.7	2.0	1.6	3.7	2.5	2.2	1.3	1.4	1.5	1.2	1.4	1.6	1.4	1.7	1.9	1.8	2.3	2.0	1.3		1.8	2.1	1.5	1.7	1.7	0.8
Tm	0.0	0.0	0.3	0.3	0.5	0.4	0.3	0.2	0.2	0.2	0.2		0.2	0.2	0.3	0.3	0.3	0.4	0.3	0.2		0.0	0.0	0.2	0.2	0.2	0.1
Yb	0.9	0.8	1.5	1.7	3.4	2.2	1.8	1.3	1.5	1.5	1.3	1.5	1.8	1.6	1.8	1.8	2.1	2.5	2.1	1.3		1.6	1.9	1.3	1.3	1.2	0.6
Lu	0.1	0.1	0.3	0.2	0.5	0.4	0.3	0.2	0.3	0.2	0.2	0.2	0.3	0.3	0.3	0.3	0.3	0.4	0.3	0.2		0.3	0.3	0.2	0.2	0.2	0.1
Cu	1120.1	1372.0	1656.9	1195.4	79.4	15.5	276.3	630.0	635.7	1742.7	196.0		147.2	16.4	86.1	63.4	45.0	76.2	107.3	22.5		126.2	162.1	125.9	105.0	156.6	71.2
Zn	32.5	27.0	77.7	64.5	76.7	74.8	132.1	48.3	60.2	69.3	36.9		48.4	20.0	25.8	51.2	187.0	62.6	61.5	47.4		150.6	118.3	102.9	82.9	81.2	25.7
Mo			2.1	6.2	1.0	2.4	0.7	12.9	15.2	9.6	0.5		0.4	0.6	0.1	0.6	0.2	0.6	0.4			0.0	0.0	4.0	3.3	3.2	14.5
Ag			2799.0	221.0	87.0	130.0	428.0	0.2	0.1	0.3	0.1		49.0	6.0	28.0	27.0	31.0	31.0	33.0			0.0	0.0	362.0	255.0	153.0	3505.0
Tl			0.0	0.0	0.2	<.02	0.1	0.2	0.2	0.2	0.1		0.0	0.0	0.0	<.02	<.02	<.02	<.02			0.0	0.0	0.1	0.1	0.1	0.2
Pb	6.2	5.6	4.9	2.9	13.3	9.2	2.7	10.8	14.3	24.9	7.6		1.3	0.7	0.8	3.1	0.5	3.6	4.1	13.1		38.5	21.6	23.1	13.1	11.1	19.0
Sn			<1	<1	2.0	<1	<1	0.9	1.4	0.7	0.4		<1	<1	<1	<1	<1	<1	<1					<1	<1	<1	<1
Sb			0.2	0.1	0.0	0.3	0.2						0.2	0.1	0.1	0.1	0.0	0.1	0.0	1.3		3.2	6.3	0.2	0.5	1.3	4.2
Ga			16.2	18.2	19.2	19.2	19.3	16.7	19.9	21.0	20.2	13.3	17.3	18.4	17.7	21.4	18.7	22.2	21.0					16.3	17.5	18.2	9.8
W			0.8	0.5	0.5	0.3	0.2	0.5	1.8	1.1	0.3		0.3	0.1	0.1	0.1	0.6	0.2	0.4					3.0	3.7	3.0	6.3
Mn			1183.0	571.0	896.0	450.0	294.0						653.0	237.0	370.0	855.0	1007.0	895.0	968.0					1151.0	1275.0	1454.0	285.0
As			0.5	0.4	<.1	7.3	1.7	0.9	0.4	1.0	0.5		0.5	0.9	0.2	0.9	0.1	2.2	0.9					15.2	31.0	28.2	206.4
Au			1299.3	76.9	7.7	48.1	29.0	10.9	3.7	39.2	17.2		1.7	<.2	0.2	1.1	0.8	0.5	1.1					105.9	107.1	67.7	1701.1
Cd			0.1	0.0	0.6	0.2	0.4	0.1	0.1	0.1	0.1		0.0	0.0	0.0	0.1	0.1	0.1	0.1					0.2	0.1	0.1	0.1
Bi			1.8	0.3	0.6	0.0	0.1	0.2	0.1	0.2	0.1		0.2	<.02	<.02	<.02	0.0	<.02	0.0					0.2	0.2	0.2	0.1
B *			2.0	<1	<1	2.0	1.0						<1	1.0	<1	<1	<1	2.0	1.0					<1	1.0	1.0	<1
Hg			7.0	<5	<5	<5	12.0						<5	<5	<5	<5	<5	<5	<5					46.0	958.0	426.0	1341.0
Se			0.5	0.4	3.9	0.1	<.1	0.0	0.0	0.0	0.0		0.5	0.1	0.1	0.1	<.1	0.1	0.1					0.5	0.5	0.5	0.4
Te			0.2	0.0	0.2	0.1	0.1						0.0	<.02	<.02	<.02	0.1	<.02	<.02					0.3	0.2	0.1	2.5
Ge			0.1	0.2	<.1	0.1	0.1						0.2	0.2	0.1	0.2	0.1	0.2	0.2					<.1	<.1	<.1	<.1
In			0.1	0.1	<.02	<.02	0.1						0.0	<.02	<.02	0.0	<.02	0.0	0.0					0.0	0.0	0.0	<.02
Re			3.0	12.0	3.0	1.0	<1						<1	<1	<1	<1	<1	<1	<1					20.0	5.0	13.0	5.0
Be			0.2	0.2	0.1	0.1	0.1						0.1	0.1	<.1	0.2	0.1	0.4	0.2					0.2	0.2	0.2	0.2
Li *			2.2	2.8	8.5	5.3	3.8						6.9	8.0	4.1	4.1	3.1	9.8	9.1					13.0	16.1	14.8	2.8
Pd			<10	<10	<10	<10	<10						<10	<10	<10	<10	<10	<10	<10					<10	<10	<10	<10
Pt			<2	2.0	<2	<2	<2						<2	<2	<2	<2	<2	<2	<2					<2	<2	<2	<2
LOI			2.1	1.2	7.7	1.9	0.7	2.3	1.7	2.3	1.2		1.8	0.5	0.9	3.8	1.2	1.6	3.9		0.7			7.3	7.9	6.8	3.9

Appendix 2.2 continued

Sample	814101	814102	814102	814106	814107	814108	814109	814110	814111	814113	814114	814115	814116	814117	814192	814193	814194	814195	814196	814197	814198	814199	814478	814526	1.40	6	10
Source	Hollings (2006)	Hollings (2006)	Hollings (2006)	Hollings (2006)	Hollings (2006)	Hollings (2006)	Hollings (2006)	Hollings (2006)	Hollings (2006)	Hollings (2006)	Hollings (2006)	Hollings (2006)	Hollings (2006)	Hollings (2006)	Hollings (2006)	Hollings (2006)	Hollings (2006)	Hollings (2006)	Hollings (2006)	Hollings (2006)	Hollings (2006)	Hollings (2006)	Hollings (2006)	Hollings (2006)	Hollings (2006)	Hollings (2006)	Hollings (2006)
Assoc. Intrusive	Balatoc	Balatoc	Balatoc	Balatoc	Balatoc	Balatoc	Balatoc	Balatoc	Balatoc	Balatoc	Balatoc	Balatoc	Balatoc	Balatoc	Balatoc	Balatoc	Balatoc	Balatoc	Balatoc	Balatoc	Balatoc	Balatoc	Hartwell	Hartwell	Clifton-Bumolo	Clifton-Bumolo	Clifton-Bumolo
Age	Pliocene	Pliocene	Pliocene	Pliocene	Pliocene	Pliocene	Pliocene	Pliocene	Pliocene	Pliocene	Pliocene	Pliocene	Pliocene	Pliocene	Pliocene	Pliocene	Pliocene	Pliocene	Pliocene	Pliocene	Pliocene	Pliocene	Pliocene	Pliocene	Pliocene	Pliocene	Pliocene
Oxide wt%																											
SiO2	55.1	54.6	54.3	58.0	54.8	56.0	57.5	64.4	68.3	64.1	53.7	55.3	55.1	55.7	55.8	55.7	56.7	57.6	59.5	55.6	55.6	56.8	66.6	63.3	59.5	60.6	61.4
TiO2	0.7	0.7	0.7	0.6	0.6	0.6	0.6	0.6	0.5	0.6	0.7	0.7	0.7	0.8	0.7	0.7	0.7	0.6	0.6	0.7	0.6	0.7	0.4	0.4	0.6	0.6	0.5
Al2O3	16.4	16.7	16.8	15.4	15.8	15.8	15.8	15.0	13.3	16.0	16.2	16.2	16.4	18.3	17.3	17.0	16.9	16.6	16.6	16.6	16.1	16.4	17.0	17.5	18.4	17.7	17.8
Fe2O3	6.5	6.5	6.6	5.7	6.2	5.8	6.2	5.7	6.1	6.1	6.7	6.6	6.6	5.7	7.3	7.9	6.5	6.5	6.6	6.5	6.1	6.8	2.9	4.6	6.1	5.5	5.7
MnO	0.2	0.2	0.2	0.2	0.2	0.2	0.2	0.1	0.1	0.1	0.2	0.2	0.2	0.2	0.2	0.2	0.2	0.2	0.2	0.2	0.2	0.2	0.1	0.1	0.2	0.2	0.1
MgO	2.9	3.1	3.1	2.8	3.0	2.8	3.0	2.6	1.8	2.6	3.3	3.5	3.2	2.6	3.4	3.2	3.1	3.3	3.3	3.0	3.0	3.1	1.5	1.9	2.4	2.2	2.4
CaO	7.0	6.5	6.5	5.7	6.6	6.5	5.5	2.2	0.3	0.6	6.3	5.5	6.0	7.5	4.7	4.5	5.0	4.5	2.4	5.7	6.2	4.6	3.7	5.2	7.8	7.4	6.0
Na2O	2.0	1.9	1.8	1.3	1.3	1.2	1.0	0.8	0.4	1.0	1.5	1.8	2.0	3.9	1.0	1.7	1.8	0.6	0.4	0.8	0.9	0.8	4.0	4.1	4.4	4.0	4.4
K2O	2.1	2.4	2.5	3.7	3.7	3.3	3.4	4.1	4.6	4.7	3.9	3.5	3.1	1.6	3.0	2.5	2.5	3.0	3.2	2.8	2.7	3.0	1.0	1.7	0.4	1.0	0.7
P2O5	0.1	0.2	0.2	0.1	0.1	0.1	0.1	0.1	0.1	0.1	0.1	0.2	0.1	0.2	0.2	0.2	0.2	0.2	0.2	0.1	0.2	0.2	0.1	0.1	0.2	0.2	0.1
Cr	96.6	62.3	61.8	71.7	105.8	63.1	102.6	67.3	101.6	101.4	59.7	87.7	75.4	66.7	48.7	59.4	60.5	90.4	85.4	71.3	62.8	88.0	8.3	29.7	10.0	5.3	14.0
Co	15.6	13.9	14.6	14.8	15.5	14.2	14.9	14.0	13.6	14.8	18.7	18.9	16.7	10.0	16.1	15.3	15.9	16.2	17.3	15.4	15.1	16.2	5.2		10.2	11.6	8.5
Ni	16.0	10.0	<10	<10	24.0	<10	12.0	<10	<10	<10	13.0	19.0	24.0	16.0	<10	<10	<10	10.0	<10	<10	10.0	13.0	10.0	8.0	7.4	4.2	6.2
Rb	73.9	89.8	91.1	128.9	130.6	123.4	112.0	131.1	140.4	138.8	118.7	107.0	105.3	44.3	126.2	104.8	106.5	123.3	121.8	112.7	105.1	123.5	22.5	31.7	7.6	20.6	19.9
Sr	336.0	268.6	273.1	125.7	151.2	105.7	83.5	67.9	59.6	112.4	228.5	257.2	242.6	525.7	178.5	212.6	253.7	128.6	96.6	176.8	188.4	155.0	568.8	584.0	555.7	545.3	511.9
Cs	10.4	9.5	10.0	14.2	14.2	13.8	11.1	13.9	12.9	13.4	14.2	12.5	13.9	5.5	13.2	9.4	13.6	12.8	12.6	14.9	10.2	11.1	1.0				
Ba	411.0	398.0	397.0	291.0	305.0	281.0	288.0	277.0	336.0	332.0	380.0	388.0	280.0	253.0	275.0	230.0	251.0	290.0	335.0	344.0	284.0	248.0	704.0	623.0	258.8	361.0	232.1
Sc	7.1	6.4	6.5	5.1	6.6	4.9	4.6	4.1	3.3	3.4	7.8	9.4	7.2	4.8	5.7	4.9	4.6	4.2	4.3	4.9	4.7	4.9	6.0		14.9	13.3	12.1
V	167.0	169.0	178.0	150.0	167.0	156.0	155.0	147.0	139.0	152.0	171.0	184.0	203.0	193.0	203.0	201.0	172.0	168.0	167.0	164.0	156.0	171.0	77.0		142.6	124.1	125.4
Ta	0.3	0.3	0.2	0.2	0.2	0.2	0.2	0.2	0.2	0.2	0.2	0.2	0.2	0.2	0.2	0.2	0.2	0.2	0.2	0.2	0.2	0.2	0.3	0.5			
Nb	4.0	3.8	3.5	3.1	3.4	3.2	3.1	2.9	2.8	3.1	3.6	3.5	3.3	3.6	3.2	3.4	4.2	3.0	3.4	3.1	3.1	3.7	2.9	3.2	1.2	3.0	3.3
Zr	84.7	81.8	84.7	64.3	72.0	66.9	75.1	62.6	58.5	75.1	75.0	72.6	73.6	107.4	85.0	83.8	92.5	90.5	79.5	77.8	74.5	79.2	102.0	116.0	101.9	106.3	91.8
Hf	2.6	2.5	2.4	1.9	2.2	2.3	2.2	2.3	1.7	2.5	2.2	2.5	2.4	3.4	2.6	2.5	3.0	2.8	2.4	2.6	2.4	2.7	3.0	2.9			
Th	4.2	2.8	3.1	2.6	2.2	2.7	2.2	1.6	1.4	2.7	3.0	2.5	2.4	2.9	2.7	2.6	3.3	3.0	2.0	1.8	2.7	3.7	3.1	3.7	1.2	5.8	2.7
U	1.1	0.9	1.1	0.7	0.9	0.8	0.9	0.5	0.6	0.7	1.0	0.7	0.8	1.0	1.0	1.0	1.1	0.8	1.1	0.8	0.8	1.0	1.0	1.0			
Y	17.8	17.2	17.3	14.6	15.1	15.5	13.0	13.1	13.9	14.7	17.9	17.0	16.2	23.4	16.9	16.2	18.7	16.0	15.7	18.1	15.8	16.5	15.1	14.9	22.8	23.0	19.4
La	10.8	10.9	11.4	8.8	9.1	9.8	8.0	7.9	8.4	8.7	10.0	9.3	10.3	13.7	10.1	8.8	11.3	9.5	8.6	11.0	9.8	10.8	14.3	11.6	4.9	11.9	8.3
Ce	24.4	23.2	23.7	18.7	19.2	20.5	18.1	16.4	16.6	17.5	20.5	19.2	19.6	28.1	20.9	20.1	23.6	20.1	19.0	23.3	21.0	21.3	25.9	21.3	11.7	14.0	18.5
Pr	2.9	2.9	3.0	2.3	2.4	2.4	2.3	1.9	2.1	2.1	2.6	2.5	2.5	3.5	2.6	2.4	3.0	2.4	2.4	2.8	2.4	2.8	3.2	2.6			
Nd	12.6	11.8	11.9	9.6	11.4	10.2	10.4	8.4	8.7	8.8	12.8	12.1	10.6	15.4	12.0	11.4	12.2	10.5	10.8	12.0	10.5	11.2	13.8	11.5			
Sm	2.8	2.7	2.9	2.5	2.5	2.5	2.2	1.9	2.1	2.1	2.6	2.7	2.6	3.6	2.7	2.8	3.1	2.3	2.3	2.6	2.5	2.8	2.4	2.5			
Eu	0.9	0.9	0.9	0.7	0.8	0.8	0.7	0.6	0.6	0.7	0.9	0.9	0.8	1.1	0.9	0.8	0.9	0.7	0.7	0.8	0.7	0.8	0.9	0.8			
Gd	2.7	2.8	2.8	2.2	2.4	2.4	2.2	2.0	1.9	2.0	3.0	2.4	2.5	3.4	2.6	2.5	3.3	2.6	2.7	2.7	2.4	2.9	2.4	2.4			
Tb	0.5	0.5	0.5	0.4	0.4	0.4	0.4	0.3	0.3	0.4	0.5	0.5	0.4	0.7	0.5	0.4	0.5	0.4	0.5	0.5	0.4	0.4	0.4				
Dy	2.7	2.9	2.6	2.5	2.4	2.4	2.0	1.9	2.2	2.3	2.6	2.6	2.6	3.9	2.6	2.4	3.0	2.3	2.6	2.8	2.6	2.7	2.2	2.4			
Ho	0.5	0.6	0.5	0.6	0.5	0.5	0.5	0.4	0.4	0.4	0.5	0.5	0.5	0.8	0.5	0.5	0.6	0.5	0.5	0.5	0.5	0.5	0.5	0.5			
Er	1.4	1.6	1.6	1.3	1.5	1.5	1.3	1.2	1.2	1.4	1.6	1.4	1.5	2.1	1.7	1.6	1.8	1.5	1.5	1.6	1.5	1.6	1.4	1.6			
Tm	0.2	0.2	0.2	0.2	0.2	0.2	0.2	0.2	0.2	0.2	0.2	0.2	0.2	0.3	0.3	0.2	0.2	0.2	0.2	0.2	0.2	0.2	0.2				
Yb	1.6	1.6	1.7	1.6	1.3	1.5	1.5	1.3	1.2	1.3	1.5	1.4	1.5	2.4	1.7	1.5	1.9	1.5	1.5	1.5	1.3	1.6	1.6	1.6			
Lu	0.2	0.3	0.3	0.2	0.2	0.3	0.2	0.2	0.2	0.2	0.2	0.2	0.2	0.3	0.3	0.3	0.3	0.2	0.2	0.3	0.2	0.2	0.3	0.3			
Cu	122.6	157.9	159.3	113.8	99.9	97.7	110.3	90.2	102.2	105.1	118.2	126.9	111.3	335.3	130.5	164.0	107.9	125.5	141.9	97.8	137.0	144.5	99.8				
Zn	94.7	140.8	142.8	64.2	67.3	65.9	75.2	72.0	75.4	69.3	84.2	85.2	72.3	79.2	85.3	85.5	80.9	90.8	99.4	86.2	84.6	92.1	87.0		78.3	60.3	36.9
Mo	3.6	5.9	5.8	3.2	3.5	2.4	3.1	4.2	6.4	4.8	3.2	3.6	2.7	3.2	3.6	4.1	3.6	5.5	6.5	3.7	5.1	4.5	1.3				
Ag	116.0	176.0	177.0	206.0	144.0	106.0	166.0	313.0	702.0	587.0	219.0	725.0	111.0	261.0	158.0	137.0	99.0	254.0	539.0	138.0	167.0	310.0	140.0				
Tl	0.1	0.1	0.1	0.2	0.2	0.1	0.3	0.7	3.3	0.4	0.1	0.4	0.2	0.2	0.1	0.1	0.1	0.1	0.1	0.1	0.1	0.1	0.1				
Pb	19.5	36.3	36.6	10.3	5.8	9.8	11.2	12.0	12.5	14.9	6.6	11.7	6.9	3.0	18.3	17.8	15.6	16.7	23.4	18.2	15.3	16.9	19.3		2.8	5.9	1.2
Sn	<1	<1	<1	<1	<1	1.0	<1	<1	<1	<1	<1	<1	<1	<1	<1	2.0	<1	1.0	<1	<1	<1	1.0	<1				
Sb	0.3	0.3	0.3	2.0	0.5	0.6	2.5	6.6	27.7	4.4	0.6	2.6	0.8	0.4	0.2	0.2	0.1	0.2	1.2	0.2	0.2	0.2	0.1				
Ga	17.4	17.4	18.3	15.5	16.8	17.9	17.6	15.7	16.4	16.2	16.6	16.3	16.6	18.8	17.6	18.9	19.1	16.9	17.7	17.2	17.1	17.9	17.7	17.1			
W	2.8	2.7	2.8	5.6	3.2	3.9	7.9	9.4	9.1	10.9	3.2	8.1	7.0	3.0	1.9	2.6	1.7	3.1	6.0	1.7	1.9	3.2	0.5				
Mn	1313.0	1432.0	1455.0	1480.0	1401.0	1489.0	1421.0	1025.0	501.0	817.0	1657.0	1610.0	1398.0	1005.0	1383.0	1458.0	1263.0	1440.0	1236.0	1539.0	1517.0	1373.0	589.0				
As	4.5	7.9	7.9	80.4	8.6	14.1	98.6	276.0	1353.0	138.9	41.8	140.9	48.8	13.9	3.6	5.7	2.4	13.4	29.6	3.0	5.9	6.2	3.5				
Au	26.9	75.2	31.2	248.5	163.8	15.8	97.4	569.5	1718.6	1895.8	101.4	742.4	43.3	10.7	39.9	47.0	13.6	159.2	725.5	6.9	22.3	128.3	27.4				
Cd	0.2	0.4	0.4	0.1	0.1	0.1	0.1	0.1	0.1	0.1	0.2	0.2	0.1	0.3	0.2	0.2	0.3	0.2	0.4	0.2	0.2	0.2	0.3				
Bi	0.2	0.3	0.3	0.2	0.2	0.2	0.2	0.2	0.2	0.3	0.2	0.2	0.2	0.1	0.6	0.5	0.4	0.4	0.4	0.6	0.4	0.6	0.6				
B *	1.0	1.0	1.0	1.0	1.0	1.0	1.0	<1	1.0	1.0	1.0	2.0	2.0	1.0	1.0	2.0	1.0	1.0	1.0	1.0	1.0	1.0	2.0				
Hg	43.0	102.0	85.0	224.0	56.0	38.0	106.0	240.0	1475.0	210.0	20.0	522.0	166.0	71.0	37.0	156.0	71.0	58.0	53.0	38.0	57.0	89.0	9.0				
Se	0.8	1.8	1.8	0.5	0.5	0.4	0.5	0.5	0.7	0.6	0.5	0.5	0.4	0.4	3.7	3.9	1.8	1.8	1.7	1.4	2.6	2.5	0.4				
Te	0.1	0.2	0.3	0.2	0.1	0.1	0.1	0.4	0.5	0.4	0.1	0.4	0.1	0.1	0.5	0.3	0.2	0.3	0.3	0.2	0.3	0.4	0.3				
Ge	<.1	<.1	<.1	<.1	<.1	<.1	<.1	<.1	<.1	<.1	<.1	<.1	<.1	0.1	<.1	<.1	<.1	<.1	<.1	<.1	<.1	<.1	<.1				
In	0.0	0.0	0.0	0.0	0.0	0.0	0.0	0.0	0.0	0.0	0.0	0.0	0.0	0.0	0.0	0.0	0.0	0.0	0.0	0.0	0.0	0.0	0.0				
Re	13.0	8.0	10.0	2.0	8.0	8.0	4.0	9.0	15.0	9.0	3.0	4.0	5.0	10.0	15.0	49.0	15.0	18.0	14.0	15.0	21.0	34.0	1.0				
Be	0.3	0.2	0.3	0.4	0.3	0.4	0.2	0.4	0.2	0.4	0.5	0.3	0.2	0.3	0.3	0.4	0.4	0.3	0.5	0.4	0.6	0.4	0.1				
Li *	16.1	15.1	15.3	17.3	18.2	18.9	21.9	19.0	10.9	16.9	24.0	26.4	23.8	11.5	18.0	18.8	16.9	18.6	19.1	16.1	15.9	16.7	5.1				
Pd	<10	<10	<10	<10	<10	<10	<10	<10	<10	<10	<10	<10	<10	<10	<10	<10	<10	<10	<10	<10	<10	<10	<10				
Pt	<2	<2	<2	<2	<2	<2	<2	<2	<2	<2	<2	<2	<2	<2	<2	2.0	<2	<2	<2	<2	<2	<2	2.0				
LOI	6.8	7.2	7.2	6.4	7.5	7.6	6.5	4.2	4.3	4.0	7.0	6.2	6.6	3.2	6.2	6.1	6.3	6.8	7.0	7.7	8.1	7.3	2.6				

Appendix 2.2 continued

Sample	2402	354201	354202	354203	354204	354205	354206	354207	354510	354511	353224	353225	806106	806107	806108	354506	354506	354506	354508	353554	353557	354553	354555	354555	354555	354558	354558
Source	Hollings (2006)	Hollings (2006)	Hollings (2006)	Hollings (2006)	Hollings (2006)	Hollings (2006)	Hollings (2006)	Hollings (2006)	Hollings (2006)	Hollings (2006)	Hollings (2006)	Hollings (2006)	Hollings (2006)	Hollings (2006)	Hollings (2006)	Hollings (2006)	Hollings (2006)	Hollings (2006)	Hollings (2006)	Hollings (2006)	Hollings (2006)	Hollings (2006)	Hollings (2006)	Hollings (2006)	Hollings (2006)	Hollings (2006)	Hollings (2006)
Assoc. Intrusive	Clifton-Bumolo	Clifton-Bumolo	Clifton-Bumolo	Clifton-Bumolo	Santo Tomas II	Santo Tomas II	Santo Tomas II	Santo Tomas II	BMP Kennon	BMP Kennon	BMP Kennon	BMP Kennon	BMP Kennon	BMP Kennon	BMP Kennon	BMP SE	BMP SE	BMP SE	BMP SE	Mexico	Mexico	Mexico	Mexico	Mexico	Mexico	Mexico	Mexico
Age	Pliocene	Pliocene	Pliocene	Pliocene	Pliocene	Pliocene	Pliocene	Pliocene	Pliocene	Pliocene	Pliocene	Pliocene	Pliocene	Pliocene	Pliocene	Pliocene	Pliocene	Pliocene	Pliocene	Pliocene	Pliocene	Pliocene	Pliocene	Pliocene	Pliocene	Pliocene	Pliocene
Oxide wt%																											
SiO2	60.1	61.2	61.9	61.7	61.9	63.3	59.6	63.8	57.3	55.7	64.8	58.0	58.6	60.9	60.0	57.2	50.4	45.3	75.6	41.2	42.0	56.7	57.5	76.9	76.6	61.4	73.4
TiO2	0.6	0.6	0.5	0.5	0.5	0.4	0.6	0.5	0.6	0.6	0.6	0.6	0.6	0.6	0.6	0.7	0.9	0.8	0.2	0.7	0.6	0.7	0.7	0.2	0.2	0.5	0.4
Al2O3	18.2	17.6	17.3	17.3	17.5	13.4	17.2	14.9	17.8	17.6	14.5	17.3	17.0	13.6	16.8	17.5	18.8	16.5	12.4	14.4	18.4	17.3	17.1	12.9	12.9	18.2	12.8
Fe2O3	6.0	5.2	6.1	6.1	4.4	10.5	6.1	6.3	6.0	6.5	5.7	4.6	5.8	7.6	6.1	5.8	9.3	10.0	1.4	7.4	12.8	6.5	5.5	0.4	0.4	4.7	3.4
MnO	0.1	0.1	0.1	0.1	0.1	0.1	0.1	0.1	0.1	0.2	0.0	0.2	0.1	0.0	0.1	0.1	0.2	0.2	0.0	1.1	0.4	0.1	0.1	0.0	0.0	0.1	0.0
MgO	2.4	2.0	2.1	2.2	1.9	1.7	2.9	1.9	2.9	3.0	2.8	2.4	2.7	3.5	2.9	2.9	4.0	8.9	0.5	2.5	2.7	4.3	5.2	0.2	0.2	1.8	1.6
CaO	7.1	6.6	6.0	3.3	6.6	4.3	5.6	4.9	7.1	7.6	3.1	6.5	6.2	3.0	5.8	6.5	8.3	12.1	1.0	30.2	19.4	7.6	8.5	1.4	1.4	5.5	2.2
Na2O	4.3	4.5	4.6	5.1	4.7	3.8	4.5	4.4	2.5	2.6	3.0	3.2	3.5	2.7	4.0	4.1	3.9	2.0	3.0	0.1	0.0	3.4	3.6	3.3	3.4	3.8	3.4
K2O	0.5	0.8	0.3	0.5	0.3	0.2	1.0	0.5	0.8	1.3	1.9	1.8	1.8	1.8	1.7	2.1	1.5	0.1	4.2	0.0	0.1	1.3	0.3	4.0	4.0	2.0	1.0
P2O5	0.2	0.2	0.1	0.1	0.1	0.1	0.1	0.1	0.2	0.2	0.2	0.2	0.2	0.2	0.2	0.2	0.3	0.1	0.1	0.1	0.2	0.2	0.2	0.0	0.0	0.2	0.1
Cr	7.6	6.8	6.1	3.8	10.6	10.0	40.6	7.3	12.3	9.7	46.5	36.8	41.7	93.0	41.9	17.5	6.2	60.2	5.5	13.9	8.6	34.1	39.1	4.7	4.6	13.1	26.0
Co	12.2	9.3	8.9	10.5	8.2	10.3	12.2	9.1	7.4	8.3	14.2	11.2	29.3	28.2	24.9	8.9	20.7	25.7	3.4	3.3	2.1	10.2	8.5	0.6	0.5	5.6	6.4
Ni	5.6	1.9	1.5	0.4	3.1	2.8	11.7	1.9	10.0	10.0	12.7	10.2				17.0	10.0	102.0	21.0	10.0	18.0	42.0	60.0	10.0	10.0	10.0	18.0
Rb	10.9	6.3	4.6	8.8	3.0	1.4	25.5	8.6	22.7	35.2	45.8	40.0	27.9	38.1	22.1	48.2	41.2	1.5	69.7	0.9	2.7	16.1	2.9	54.0	53.9	39.6	36.0
Sr	532.7	373.1	328.8	206.6	411.8	255.4	389.8	286.0	428.2	447.9	282.1	531.5	536.0	277.0	481.0	473.5	681.7	436.2	171.1	134.7	740.5	571.6	584.3	221.3	220.7	661.2	328.0
Cs		0.2	0.2	0.3	0.1	0.2	0.5	0.2	0.9	3.2	2.5	1.3				0.7	0.4	0.1	0.9	<.1	0.4	0.2	<.1	0.3	0.3	0.7	0.4
Ba	237.5	292.9	157.2	146.0	174.8	127.4	200.6	147.4	123.0	233.0	331.0	337.5	319.0	237.0	322.0	321.0	365.0	49.0	896.0	16.0	5.0	337.0	126.0	428.0	421.0	413.0	242.0
Sc	14.6	9.4	11.3	12.8	9.2	8.4	12.9	10.6	13.0	13.0	13.5	9.9	15.6	17.1	17.0	7.0	6.5	3.3	0.9	24.0	19.0	2.0	2.5	0.6	0.5	2.8	3.6
V	135.6	110.6	119.8	138.5	105.9	164.5	139.2	113.8	174.0	166.0	154.3	113.9				153.0	285.0	304.0	28.0	114.0	188.0	154.0	172.0	18.0	18.0	96.0	89.0
Ta		0.2	0.1	0.1	0.2	0.1	0.2	0.2	0.2	0.2	0.4	0.4	0.7	0.6	0.7	0.3	0.2	<.1	0.4	0.2	0.3	0.4	0.3	0.6	0.5	0.3	0.3
Nb	1.7	2.5	2.1	2.2	2.4	1.0	2.4	1.9	4.2	4.0	5.2	5.3	4.7	5.0	5.3	3.9	4.1	1.3	2.8	2.7	3.9	5.6	4.4	5.3	6.7	5.0	4.9
Zr	100.0	112.3	100.7	88.3	112.5	68.3	96.5	92.1	100.5	85.2	99.6	130.5	123.0	99.9	129.0	86.1	96.1	43.2	55.6	72.4	89.4	101.4	89.8	95.9	93.6	135.1	103.2
Hf		2.8	2.5	2.3	2.8	1.8	2.5	2.3	3.1	2.8	2.5	3.1	3.0	2.6	3.2	2.6	3.0	1.5	1.7	2.1	2.9	2.9	2.6	3.4	3.5	3.6	2.9
Th	1.6	1.5	1.3	1.2	1.7	0.9	1.8	1.3	3.1	3.1	4.1	4.0	3.9	3.5	4.6	3.2	3.3	0.2	9.2	1.9	2.6	2.9	2.9	11.9	11.9	5.4	4.4
U		0.4	0.4	0.3	0.3	0.1	0.5	0.3	0.9	0.9	0.7	1.2	1.0	0.7	1.0	1.5	1.3	0.3	1.6	1.9	4.5	0.9	0.9	1.9	1.9	1.5	1.1
Y	22.0	22.4	15.4	19.2	16.6	6.9	14.4	15.0	17.6	15.2	13.0	16.3	17.0	14.5	18.3	19.0	24.7	18.1	3.5	15.6	18.2	17.8	16.4	5.5	5.6	18.3	12.5
La	6.8	7.3	5.8	6.2	5.9	2.5	6.4	5.1	13.2	12.1	12.0	14.9	13.3	11.2	14.6	12.1	15.5	3.9	3.6	9.7	11.0	13.1	12.8	10.2	10.2	17.3	13.0
Ce	18.0	17.7	13.0	14.8	14.0	5.7	13.9	11.3	27.2	24.7	24.0	29.7	24.8	21.2	27.5	32.3	35.6	10.4	6.0	17.6	22.1	28.3	27.5	19.3	19.1	37.0	26.9
Pr		2.5	1.8	2.1	1.9	0.8	1.8	1.5	3.5	3.1	2.9	3.6	3.1	2.7	3.4	4.0	4.3	1.5	0.5	2.3	2.8	3.2	3.0	1.9	1.8	3.9	2.8
Nd		11.0	7.8	9.4	8.5	3.3	7.6	6.5	13.6	12.7	11.2	13.8	12.7	11.5	14.5	18.8	20.9	8.5	2.5	11.6	10.7	13.9	13.3	6.3	6.3	17.1	11.1
Sm		2.8	1.8	2.4	2.1	0.8	1.8	1.7	3.3	2.6	2.3	2.8	2.9	2.7	3.4	3.7	4.6	2.5	0.5	2.5	2.7	2.9	2.6	1.0	1.0	3.4	2.1
Eu		0.9	0.7	0.8	0.7	0.4	0.6	0.6	1.0	0.9	0.8	0.9	0.9	0.8	1.1	1.3	1.4	0.9	0.4	0.8	1.1	1.0	0.9	0.3	0.3	1.0	0.7
Gd		3.1	2.1	2.6	2.3	0.9	2.0	1.9	2.9	2.4	2.2	2.6	3.0	2.8	3.4	3.3	4.1	3.0	0.4	2.7	2.7	2.9	2.7	0.8	0.7	2.7	2.2
Tb		0.5	0.4	0.4	0.4	0.2	0.3	0.3	0.5	0.5	0.4	0.4				0.6	0.7	0.5	0.1	0.4	0.5	0.5	0.4	0.1	0.1	0.4	0.3
Dy		3.5	2.4	3.0	2.6	1.0	2.1	2.3	3.4	2.8	2.2	2.6	3.0	2.6	3.3	3.2	4.1	3.1	0.6	2.7	3.2	2.9	2.7	0.9	0.7	2.9	1.9
Ho		0.8	0.5	0.7	0.6	0.2	0.5	0.5	0.6	0.5	0.5	0.6	0.6	0.6	0.6	0.7	0.8	0.7	0.1	0.6	0.6	0.6	0.6	0.2	0.2	0.6	0.4
Er		2.2	1.5	1.9	1.7	0.7	1.4	1.5	1.8	1.6	1.3	1.7	1.8	1.6	2.0	1.8	2.2	1.7	0.3	1.8	1.9	1.6	1.6	0.5	0.5	1.7	1.2
Tm		0.3	0.2	0.3	0.3	0.1	0.2	0.2	0.2	0.2	0.2	0.3				0.3	0.4	0.3	0.1	0.3	0.3	0.3	0.3	0.1	0.1	0.3	0.2
Yb		2.4	1.7	2.0	1.8	0.9	1.6	1.6	1.8	1.6	1.4	1.7	1.8	1.4	2.0	1.9	2.2	1.6	0.5	1.6	1.7	1.9	1.6	0.7	0.7	1.8	1.2
Lu		0.4	0.3	0.3	0.3	0.1	0.3	0.3	0.3	0.3	0.2	0.3	0.3	0.2	0.3	0.3	0.3	0.2	0.1	0.3	0.3	0.3	0.2	0.1	0.1	0.3	0.2
Cu		70.5	236.0	2351.0	123.8	69.5	25.4	1678.1	113.0	35.2	1952.9	31.8				53.3	105.7	97.3	611.2	4.0	28.1	19.5	214.5	16.6	15.1	140.0	295.0
Zn	54.3	44.8	36.8	45.1	22.8	36.8	36.3	25.1	39.5	109.7	28.8	138.3				26.7	69.0	83.3	11.9	37.4	30.7	18.6	11.7	4.5	4.0	41.6	38.1
Mo		0.2	0.7	12.8	0.6	2.1	1.2	1.2	1.7	0.4	0.9	0.0				0.3	1.4	0.7	2.5	65.8	0.9	0.2	0.2	0.7	0.6	0.3	0.8
Ag		0.0	0.1	0.5	0.1	0.4	0.2	0.4	110.0	542.0	0.5	0.0				23.0	28.0	46.0	151.0	24.0	75.0	35.0	144.0	28.0	29.0	80.0	81.0
Tl		0.0	0.1	0.1	0.0	0.0	0.1	0.0	0.0	0.1	0.1	0.4				0.0	<.02	<.02	0.0	<.02	0.0	<.02	<.02	<.02	<.02	<.02	<.02
Pb	0.7	5.9	4.5	7.0	2.6	9.4	5.0	3.7	1.9	2.8	4.4	6.7				1.1	8.1	4.6	0.8	1.3	1.7	1.4	0.8	0.8	0.7	1.5	1.0
Sn		0.7	0.6	0.7	0.4	1.4	0.7	0.6	<1	<1	0.6	0.7				1.0	1.0	<1	<1	<1	1.0	<1	<1	<1	<1	<1	<1
Sb									0.1	0.1						0.1	0.1	0.2	0.0	0.1	1.1	<.02	0.0	<.02	0.0	0.1	0.0
Ga		19.6	17.4	17.7	17.0	15.7	19.4	15.9	20.0	20.1	19.3	21.8	14.4	14.1	15.2	18.6	19.9	16.4	11.4	14.6	20.7	18.7	17.7	13.8	13.9	21.4	15.6
W		0.2	0.2	0.3	0.2	0.2	0.4	0.2	2.5	0.5	0.3	0.3				1.5	0.5	0.6	1.1	5.1	2.9	0.3	0.2	0.4	0.4	0.5	0.7
Mn									493.0	1036.0						467.0	1016.0	761.0	130.0	2719.0	1995.0	212.0	171.0	37.0	38.0	529.0	346.0
As		0.8	2.0	1.6	0.4	0.4	0.7	0.3	3.1	3.8	0.5	0.7				1.1	2.6	2.7	0.4	1.0	3.1	1.1	0.3	0.3	0.2	0.8	0.5
Au		3.3	41.0	56.7	30.0	17.0	4.7	25.0	94.4	429.4	22.9	2.2				0.8	1.7	5.9	22.7	3.1	1.1	3.1	14.6	0.7	0.6	4.5	11.9
Cd		0.1	0.1	0.1	0.1	0.1	0.1	0.1	0.0	0.1	0.1	0.1				0.0	0.1	0.3	0.0	0.1	0.0	0.1	0.0	<.01	<.01	0.0	0.0
Bi		0.1	0.1	0.1	0.1	0.1	0.1	0.2	0.6	0.6	0.4	0.1				0.0	0.0	0.0	0.1	0.1	0.3	0.2	0.1	<.02	<.02	<.02	<.02
B *									<1	1.0						1.0	5.0	2.0	1.0	<1	2.0	1.0	<1	<1	<1	<1	<1
Hg									<5	<5						<5	<5	<5	<5	<5	<5	<5	<5	<5	<5	<5	<5
Se		0.0	0.0	0.1	0.0	0.0	0.0	0.1	1.0	0.3	0.0	0.0				0.1	0.1	0.1	0.7	0.1	<.1	0.3	0.8	<.1	<.1	0.1	0.1
Te									0.7	2.0						<.02	<.02	<.02	0.0	0.1	0.0	0.2	0.3	<.02	<.02	<.02	<.02
Ge									<.1	<.1						0.1	0.2	0.1	<.1	0.3	0.3	0.1	<.1	0.1	<.1	0.1	0.1
In									<.02	0.0						<.02	0.0	<.02	<.02	0.1	0.2	<.02	0.0	<.02	<.02	<.02	<.02
Re									2.0	2.0						<1	1.0	<1	<1	35.0	2.0	<1	<1	<1	<1	<1	1.0
Be									0.3	0.2						0.1	0.4	0.2	0.1	0.1	0.3	0.1	0.1	0.1	0.1	0.1	0.2
Li *									6.4	6.6						11.8	16.3	19.6	2.3	1.8	1.4	1.8	1.1	0.5	0.6	3.5	3.8
Pd									<10	<10						<10	<10	<10	<10	<10	<10	<10	<10	<10	<10	<10	<10
Pt									<2	<2						<2	<2	<2	<2	<2	<2	<2	<2	<2	<2	<2	<2
LOI		0.9	0.6	1.9	1.4	1.7	1.4	1.7	4.5	4.8	2.6	5.2				3.0	2.5	4.1	1.3	2.1	3.3	1.9	1.1	0.6	0.8	1.8	1.4

Appendix 2.2 continued

Sample	354558	354561	354562	354563	354564	354564	354565	354566	354566	354566	806103	806104	354014	354015	354019	354504	1416	3416	353214	353215	353216	353217	353218	353219	353221	353223	354216
Source	Hollings (2006)	Hollings (2006)	Hollings (2006)	Hollings (2006)	Hollings (2006)	Hollings (2006)	Hollings (2006)	Hollings (2006)	Hollings (2006)	Hollings (2006)	Hollings (2006)	Hollings (2006)	Hollings (2006)	Hollings (2006)	Hollings (2006)	Hollings (2006)	Hollings (2006)	Hollings (2006)	Hollings (2006)	Hollings (2006)	Hollings (2006)	Hollings (2006)	Hollings (2006)	Hollings (2006)	Hollings (2006)	Hollings (2006)	Hollings (2006)
Assoc. Intrusive	Mexico	Mexico	Mexico	Mexico	Mexico	Mexico	Mexico	Mexico	Mexico	Mexico	Mexico	Mexico	Camp 4	Camp 4	Camp 4	Camp 4	Camp 4	Camp 4	Camp 4	Dike	Dike	Dike	Dike	Dike	Dike	Dike	Dike
Age	Pliocene	Pliocene	Pliocene	Pliocene	Pliocene	Pliocene	Pliocene	Pliocene	Pliocene	Pliocene	Pliocene	Pliocene	Pliocene	Pliocene	Pliocene	Pliocene	Pliocene	Pliocene	Pliocene	Pliocene	Pliocene	Pliocene	Pliocene	Pliocene	Pliocene	Pliocene	Pliocene
Oxide wt%																											
SiO2	58.7	53.7	62.0	59.5	59.7	58.6	53.5	55.2	36.5	53.4	59.7	59.5	57.5	48.4	58.0	49.2	61.5	55.0	56.1	50.4	46.7	51.0	50.2	53.8	57.2	47.9	48.3
TiO2	0.6	0.8	0.7	0.6	0.6	0.6	0.8	0.7	0.3	0.8	0.5	0.5	0.7	0.9	0.7	1.0	0.4	0.7	0.6	0.8	0.9	0.8	1.0	0.6	0.6	1.0	1.0
Al2O3	17.6	17.9	15.5	17.3	17.4	17.2	18.1	15.7	13.4	17.7	17.3	17.3	16.5	17.4	17.0	19.6	18.0	18.0	17.1	19.5	16.6	18.0	17.6	17.7	17.7	18.8	17.4
Fe2O3	5.9	8.1	4.8	5.5	4.2	5.7	7.7	6.6	6.7	8.2	5.2	5.5	6.0	8.3	6.0	9.3	4.1	6.6	5.6	9.3	8.1	7.4	8.5	7.8	6.3	10.7	9.1
MnO	0.1	0.2	0.2	0.1	0.1	0.1	0.1	0.1	0.4	0.1	0.1	0.1	0.2	0.2	0.2	0.2	0.1	0.2	0.1	0.1	0.2	0.2	0.3	0.2	0.2	0.2	0.2
MgO	2.9	4.0	2.9	2.5	2.3	2.7	3.6	5.2	1.4	4.2	2.3	2.5	3.6	3.1	3.8	3.9	2.3	3.0	3.9	4.6	5.8	5.0	6.6	3.8	2.7	4.1	6.1
CaO	6.8	8.4	9.0	5.5	6.8	6.5	9.2	7.4	25.2	8.2	5.5	6.1	6.6	7.1	6.1	8.0	5.1	6.0	6.6	4.7	10.0	9.3	7.5	5.1	5.6	7.2	9.7
Na2O	3.6	3.0	3.2	4.1	4.2	3.6	3.7	3.1	0.6	3.4	4.3	4.0	3.1	4.4	3.6	3.6	6.8	4.9	4.8	4.8	2.6	3.1	4.7	4.2	3.5	4.0	2.9
K2O	1.5	1.3	0.3	2.3	1.7	1.5	0.7	1.5	1.0	1.5	2.0	1.6	1.5	1.0	1.7	1.1	0.3	2.7	1.7	2.3	1.6	1.2	0.5	1.8	2.0	2.1	1.4
P2O5	0.2	0.2	0.2	0.2	0.2	0.2	0.3	0.2	0.1	0.2	0.2	0.2	0.2	0.2	0.2	0.2	0.2	0.3	0.2	0.1	0.1	0.1	0.3	0.2	0.2	0.3	0.2
Cr	20.4	13.4	12.1	17.3	12.6	17.9	28.9	120.5	4.1	15.6	36.6	40.2	59.4	<.5	72.8	0.6	25.5	15.3	63.4	124.4	92.7	189.7	134.8	46.3	5.1	11.3	54.9
Co	7.1	15.7	2.9	6.4	7.2	9.6	13.9	15.5	2.9	18.0	29.5	22.7	15.1	18.1	13.8	21.6	7.8	13.5	18.9	23.4	29.2	25.8	16.7	10.9	3.8	13.4	31.5
Ni	23.0	26.0	27.0	15.0	15.0	15.0	20.0	39.0	10.0	14.0			21.0	10.0	38.0	10.0	11.8	11.0	17.2	7.9	34.0	27.2	34.9	10.4	3.9	10.3	22.8
Rb	38.0	34.0	3.0	61.8	26.0	33.9	16.1	29.5	30.7	41.1	35.6	27.0	35.3	34.8	34.2	18.6	5.5	36.6	35.2	67.3	31.9	19.1	8.9	43.3	44.6	36.9	38.8
Sr	588.4	480.7	899.6	576.9	755.7	587.7	1041.6	610.4	590.7	497.7	564.0	554.0	626.4	602.8	636.2	649.8	1182.4	1427.8	845.0	209.5	420.1	515.8	471.9	351.2	356.5	527.0	604.0
Cs	0.7	0.6	0.1	4.5	1.1	1.6	0.6	0.6	1.4	0.4			1.2	1.7	0.8	0.4			0.5	1.7	2.2	0.3	0.2	1.2	1.4	0.6	0.2
Ba	347.0	294.0	120.0	329.0	388.0	326.0	174.0	335.0	129.0	327.0	310.0	319.0	326.0	92.0	335.0	353.0	233.1	644.1	372.4	181.5	208.9	192.2	150.7	358.5	593.6	399.8	211.8
Sc	4.1	5.9	14.0	3.7	3.5	5.9	3.5	7.5	8.0	3.2	12.9	14.2	7.1	9.4	5.9	8.5	10.5	13.6	19.7	44.0	32.4	27.2	30.6	14.7	14.4	17.3	43.4
V	145.0	233.0	150.0	129.0	120.0	137.0	212.0	175.0	87.0	229.0			162.0	240.0	153.0	261.0	112.3	197.8	181.3	322.8	282.2	245.9	278.6	153.2	149.4	341.2	307.8
Ta	0.3	0.2	0.4	0.3	0.3	0.4	0.3	0.4	<.1	0.2	0.6	0.6	0.4	0.2	0.4	0.3			0.1	0.0	0.1	0.1	0.2	0.1	0.2	0.2	0.2
Nb	5.7	2.9	5.8	4.4	4.6	4.9	4.5	4.6	0.9	2.8	4.7	4.8	5.7	3.6	5.5	3.6	2.1	4.4	2.1	0.7	1.6	1.7	4.2	1.6	3.6	2.8	2.9
Zr	108.6	88.5	141.8	106.2	140.5	101.4	124.2	99.7	45.3	85.6	122.0	130.0	112.1	94.3	106.6	103.0	77.8	98.4	74.2	37.7	59.2	65.2	99.6	75.0	119.5	92.1	76.5
Hf	3.0	2.4	4.3	3.0	3.7	3.0	3.8	2.7	1.6	2.6	2.9	3.1	3.3	2.9	3.4	3.3			2.0	1.1	1.7	1.7	2.4	1.9	3.1	2.3	2.1
Th	3.9	4.0	4.9	3.5	4.8	3.6	3.1	4.0	0.5	4.0	4.1	4.0	3.9	3.1	4.6	3.2	1.1	3.8	2.1	0.3	1.2	1.3	3.4	1.4	4.4	3.3	1.8
U	1.2	1.2	1.4	1.3	1.3	1.3	0.9	1.2	1.6	1.2	1.1	1.1	1.5	1.0	1.5	1.0			0.9	0.3	0.3	0.4	0.7	0.4	1.3	0.9	0.6
Y	17.7	20.0	17.5	16.8	19.5	17.3	28.3	15.5	8.9	19.8	15.8	17.1	17.2	28.3	16.3	30.8	11.2	14.3	10.1	19.1	19.6	20.5	19.9	19.6	22.1	22.8	22.2
La	12.9	10.9	14.3	13.2	18.8	13.1	16.2	14.7	4.0	10.4	12.9	13.6	17.0	10.5	16.9	11.4	7.1	19.3	9.1	3.4	6.1	6.8	14.2	7.0	11.9	14.6	9.5
Ce	27.4	24.8	30.4	27.2	40.4	29.0	37.7	31.9	8.0	24.0	24.2	25.0	36.7	25.4	36.4	28.0	31.3	24.4	20.0	7.5	14.4	15.8	31.1	16.3	25.9	32.3	20.8
Pr	3.1	3.1	3.9	3.1	4.4	3.3	4.5	3.5	1.1	2.9	3.0	3.1	4.1	3.2	4.0	3.5			2.6	1.1	2.0	2.2	4.1	2.3	3.3	4.3	3.0
Nd	14.1	13.9	14.8	13.2	17.6	14.2	19.6	15.2	4.3	12.9	12.5	13.1	18.6	16.2	18.5	18.9			11.2	5.1	9.3	10.0	17.0	10.2	14.3	17.6	13.0
Sm	3.0	3.2	2.9	2.8	3.4	3.0	4.5	3.3	1.1	3.2	2.8	2.9	3.7	4.1	3.6	4.7			2.3	1.7	2.6	2.6	3.8	2.6	3.1	4.1	3.3
Eu	1.0	1.0	1.0	1.0	1.0	1.0	1.5	1.1	0.5	0.9	0.9	0.9	1.0	1.2	1.1	1.4			0.7	0.7	0.9	0.9	1.2	1.0	0.9	1.3	1.1
Gd	2.9	3.2	2.7	2.7	2.9	2.7	4.5	3.0	1.0	3.2	2.8	3.0	3.1	4.4	3.1	4.7			2.1	2.3	3.0	3.0	3.7	2.7	3.4	4.0	3.6
Tb	0.5	0.5	0.5	0.4	0.5	0.4	0.8	0.4	0.3	0.5			0.5	0.8	0.5	0.8			0.3	0.4	0.5	0.5	0.6	0.5	0.6	0.6	0.6
Dy	2.8	3.3	3.2	2.7	3.1	2.9	4.7	2.8	1.5	3.3	2.9	3.0	2.9	4.8	2.7	5.1			1.8	3.0	3.3	3.2	3.5	3.1	3.6	3.9	3.9
Ho	0.6	0.7	0.6	0.6	0.6	0.6	1.0	0.5	0.3	0.7	0.6	0.6	0.6	1.0	0.6	1.1			0.4	0.7	0.7	0.7	0.7	0.7	0.8	0.8	0.8
Er	1.6	1.9	1.7	1.5	1.8	1.6	2.7	1.4	0.9	1.9	1.8	1.7	1.5	2.8	1.5	3.0			1.0	2.0	2.0	1.9	2.0	1.9	2.2	2.3	2.1
Tm	0.3	0.4	0.3	0.3	0.3	0.3	0.5	0.2	0.1	0.3			0.3	0.5	0.3	0.5			0.1	0.3	0.3	0.3	0.3	0.3	0.3	0.3	0.3
Yb	1.8	2.1	1.7	1.6	2.0	1.7	2.7	1.3	0.8	2.0	1.8	1.7	1.6	2.8	1.3	3.1			0.9	2.0	1.9	1.9	1.9	1.9	2.3	2.2	1.9
Lu	0.3	0.3	0.3	0.2	0.3	0.2	0.4	0.2	0.2	0.3	0.3	0.3	0.3	0.4	0.2	0.5			0.1	0.3	0.3	0.3	0.3	0.3	0.4	0.3	0.3
Cu	26.2	133.4	5.2	19.4	31.4	16.8	73.0	39.0	2.3	131.0			63.4	131.8	217.0	153.3			18.0	981.5	85.1	37.9	3.5	111.8	14.6	306.0	91.4
Zn	25.6	61.4	13.5	29.6	22.9	36.8	38.3	89.9	33.0	68.7			366.0	358.0	98.8	101.8	27.3	259.9	42.7	36.8	61.2	67.5	131.8	92.7	107.0	72.9	71.3
Mo	0.1	1.4	10.6	0.1	1.5	0.1	1.0	0.2	3.9	1.2			0.4	0.5	1.4	0.6			0.4	6.8	0.4	0.1	0.0	0.0	1.8	0.6	0.3
Ag	17.0	51.0	34.0	21.0	66.0	89.0	77.0	17.0	15.0	59.0			140.0	111.0	172.0	168.0			0.0	0.2	0.0	0.0	0.0	0.1	0.0	0.2	0.0
Tl	<.02	<.02	<.02	0.0	0.0	0.0	0.0	<.02	0.1	<.02			<.02	0.0	0.0	<.02			0.1	0.2	0.1	0.1	0.1	0.2	0.3	0.2	0.1
Pb	2.3	5.2	1.4	3.3	3.9	31.6	1.6	1.4	1.6	11.3			45.5	1.9	1.6	10.8	3.2	10.1	7.3	6.6	6.2	4.6	2.9	8.7	8.9	2.8	5.8
Sn	<1	<1	<1	<1	<1	<1	1.0	<1	2.0	<1			<1	1.0	<1	1.0			0.6	1.4	0.7	0.7	1.2	0.9	0.8	0.9	1.0
Sb	0.1	0.1	0.2	0.1	0.1	0.2	0.1	0.0	0.2	0.1			0.1	0.1	0.0	0.2											
Ga	20.8	20.2	16.8	19.7	21.7	21.5	23.5	20.5	14.2	20.8	14.4	14.6	19.8	18.5	19.4	20.8			21.5	18.4	18.1	18.8	19.4	20.9	24.6	23.4	17.7
W	0.3	0.6	1.3	0.3	0.4	0.2	0.2	0.5	1.5	0.6			0.5	0.9	0.4	0.6			0.2	0.4	0.2	0.3	0.3	0.3	0.5	0.4	0.3
Mn	430.0	798.0	346.0	502.0	537.0	707.0	506.0	841.0	2021.0	715.0			1457.0	1768.0	931.0	1271.0											
As	1.8	2.5	0.7	1.4	18.1	1.1	2.2	0.4	0.4	2.1			1.1	1.7	0.7	11.5			1.2	0.6	1.3	1.4	4.5	4.3	9.3	2.2	0.7
Au	0.5	2.4	1.4	<.2	0.7	1.4	1.5	<.2	3.2	1.8			5.5	0.9	4.4	5.9			8.0	34.1	2.7	5.0	2.7	5.1	4.9	12.9	6.4
Cd	0.0	0.1	0.0	0.0	0.1	0.1	0.2	0.0	0.1	0.3			2.1	0.1	0.1	0.1			0.1	0.1	0.1	0.1	0.1	0.1	0.1	0.1	0.1
Bi	0.0	0.0	0.2	0.0	0.0	0.0	0.1	0.0	0.3	0.0			0.0	0.0	<.02	0.1			0.2	0.2	0.2	0.1	0.2	0.3	0.1	0.1	0.1
B *	1.0	<1	<1	<1	<1	1.0	<1	<1	<1	4.0			1.0	2.0	1.0	3.0											
Hg	<5	<5	<5	<5	<5	<5	<5	<5	5.0	<5			<5	<5	<5	<5											
Se	<.1	<.1	<.1	<.1	0.1	<.1	0.3	<.1	0.1	<.1			<.1	<.1	<.1	0.4											
Te	<.02	<.02	0.1	<.02	0.1	<.02	0.1	<.02	0.1	<.02			0.2	<.02	0.8	0.0			0.0	0.0	0.0	0.1	0.1	0.0	0.0	0.1	0.0
Ge	0.1	0.1	0.1	0.1	0.1	0.1	0.1	0.1	0.1	0.2			0.1	<.1	0.1	0.2											
In	0.0	0.0	0.0	<.02	0.0	0.0	0.0	0.0	0.2	0.0			0.0	0.1	0.0	0.0											
Re	<1	<1	<1	<1	<1	<1	2.0	<1	<1	<1			<1	<1	26.0	<1											
Be	0.1	0.1	0.1	<.1	0.2	0.2	0.1	0.1	0.2	0.1			0.2	0.2	0.1	0.5											
Li *	7.1	3.6	1.6	7.7	8.1	13.8	3.5	7.2	2.3	10.8			10.6	30.9	8.0	21.1											
Pd	<10	<10	<10	<10	<10	<10	<10	<10	<10	<10			<10	<10	<10	<10											
Pt	<2	<2	<2	<2	<2	<2	<2	2.0	<2	<2			<2	2.0	<2	2.0											
LOI	2.1	2.5	1.3	2.3	2.8	3.2	2.1	4.1	14.5	2.3			3.9	8.8	2.7	3.9			2.8	2.2	6.3	3.6	2.5	4.2	3.1	2.8	2.6

Appendix 2.2 continued

Sample	353226	353227	353228	353229	353229	353230	353230	353231	353231	353232	354194	355192	355192	355192	355193	355198	355198
Source	Hollings (2006)	Hollings (2006)	Hollings (2006)	Hollings (2006)	Hollings (2006)	Hollings (2006)	Hollings (2006)	Hollings (2006)	Hollings (2006)	Hollings (2006)	Hollings (2006)	Hollings (2006)	Hollings (2006)	Hollings (2006)	Hollings (2006)	Hollings (2006)	Hollings (2006)
Assoc. Intrusive	Liw-Liw	Liw-Liw	Liw-Liw	Liw-Liw	Liw-Liw	Liw-Liw	Liw-Liw	Liw-Liw	Liw-Liw	Liw-Liw	Liw-Liw	Liw-Liw	Liw-Liw	Liw-Liw	Liw-Liw	Liw-Liw	Liw-Liw
Age	Pliocene	Pliocene	Pliocene	Pliocene	Pliocene	Pliocene	Pliocene	Pliocene	Pliocene	Pliocene	Pliocene	Pliocene	Pliocene	Pliocene	Pliocene	Pliocene	Pliocene
Oxide wt%																	
SiO2	46.6	49.0	59.3	48.1	45.7	44.3	53.4	55.6	53.6	48.4	48.0	47.5	48.3	49.5	43.2	45.9	49.3
TiO2	0.9	0.9	0.6	1.0	1.2	0.8	0.7	0.5	0.7	1.0	1.0	0.9	0.9	0.8	1.1	0.8	0.9
Al2O3	17.9	17.9	16.7	17.6	16.9	14.5	18.1	17.5	16.6	16.1	16.5	16.4	15.9	17.6	15.9	14.5	16.7
Fe2O3	10.5	10.3	5.5	9.8	11.3	10.1	8.2	5.6	7.2	9.7	10.1	9.5	9.7	9.5	8.9	10.0	8.4
MnO	0.2	0.2	0.1	0.2	0.2	0.2	0.2	0.2	0.2	0.2	0.2	0.3	0.3	0.3	0.4	0.2	0.2
MgO	5.9	4.7	2.6	4.3	6.3	9.2	3.1	2.1	2.8	6.3	6.9	8.0	8.2	5.3	9.9	10.4	3.8
CaO	10.8	9.5	6.3	9.3	11.5	10.4	7.6	6.3	6.4	9.0	10.4	9.0	9.1	8.5	11.0	10.1	8.1
Na2O	2.4	2.7	3.7	2.9	2.7	2.0	4.5	2.7	3.1	3.3	2.5	3.7	3.6	3.8	2.3	1.9	2.6
K2O	1.2	2.9	1.6	1.4	0.4	0.9	1.0	2.4	2.0	1.4	0.1	0.7	1.0	1.4	1.0	0.9	2.6
P2O5	0.1	0.2	0.2	0.4	0.2	0.2	0.2	0.2	0.4	0.2	0.1	0.2	0.2	0.2	0.1	0.2	0.3
Cr	61.8	6.0	36.3	43.3	35.9	184.5	24.3	9.4	1.0	52.7	23.2	90.8	62.0	24.8	106.8	122.0	20.6
Co	18.5	18.7	13.2	24.1	17.7	33.5	15.5	10.6	18.3	23.0	26.8	18.5	21.8	20.5	30.3	26.6	23.8
Ni	35.0	10.0	10.0	17.0	26.0	136.0	10.0	10.0	10.0	25.0	39.0	56.0	65.0	38.0	89.0	182.0	19.0
Rb	21.4	55.6	36.4	21.5	6.4	17.4	14.5	72.3	55.6	37.6	2.6	15.3	20.5	25.9	21.9	18.7	57.7
Sr	438.3	619.6	586.4	504.1	529.6	401.7	646.9	329.2	284.7	550.5	330.8	403.5	446.1	472.0	313.2	358.9	327.2
Cs	0.9	0.3	0.9	0.5	0.5	1.5	0.3	5.3	4.1	2.3	0.6	0.2	0.4	0.2	1.1	1.2	2.4
Ba	359.0	304.0	378.0	203.0	93.0	153.0	451.0	241.0	324.0	240.0	56.0	151.0	203.0	198.0	264.0	177.0	363.0
Sc	5.9	2.4	7.2	9.8	5.1	14.0	2.7	3.4	6.5	10.3	7.4	10.8	8.9	6.1	16.1	9.7	9.0
V	434.0	328.0	137.0	288.0	457.0	314.0	194.0	122.0	176.0	353.0	304.0	329.0	346.0	276.0	397.0	295.0	223.0
Ta	<.1	0.1	0.3	0.3	0.1	<.1	<.1	0.2	0.7	0.2	<.1	<.1	<.1	<.1	<.1	<.1	0.2
Nb	1.2	2.0	4.7	5.0	2.5	1.8	1.7	3.1	11.5	1.9	1.3	1.6	1.8	1.6	1.7	1.7	3.4
Zr	48.8	59.2	93.4	105.5	76.8	52.6	66.5	103.6	169.2	67.6	50.5	50.7	49.1	55.8	46.1	52.2	93.3
Hf	1.7	1.8	2.6	3.2	2.2	1.5	2.1	3.1	4.3	1.8	1.9	1.6	1.7	1.8	1.5	1.8	2.6
Th	1.4	1.8	4.2	2.6	2.1	1.6	1.9	2.2	7.5	1.4	0.8	1.8	1.7	2.0	1.1	1.6	2.5
U	0.4	0.4	1.2	0.7	0.7	0.5	0.4	0.8	2.3	0.4	0.3	0.5	0.6	0.6	0.5	0.5	0.8
Y	19.5	22.1	16.4	26.6	22.0	18.2	23.7	20.6	23.3	22.3	22.3	19.2	17.9	20.6	16.4	17.7	22.3
La	6.5	8.6	13.2	14.9	10.9	8.3	8.7	11.9	33.9	7.4	4.7	8.1	8.2	7.3	5.8	7.9	12.5
Ce	15.8	20.5	27.1	34.7	26.5	19.4	20.7	26.4	65.7	18.6	12.7	19.9	18.6	16.6	13.7	18.4	28.2
Pr	2.1	2.7	3.0	4.2	3.4	2.5	2.8	3.2	7.3	2.5	1.8	2.6	2.4	2.2	1.9	2.4	3.4
Nd	9.7	13.2	12.8	19.3	15.9	11.8	13.8	14.7	29.9	11.8	9.6	12.7	12.0	11.7	9.6	11.8	16.6
Sm	2.8	3.5	2.9	4.7	4.0	3.2	3.5	3.3	5.7	3.3	3.1	3.0	3.0	2.9	2.4	2.8	3.7
Eu	1.0	1.1	1.0	1.6	1.4	1.0	1.2	1.0	1.6	1.1	1.1	1.1	1.0	1.1	0.9	1.0	1.2
Gd	3.2	3.7	2.6	4.7	4.2	3.3	3.6	3.1	4.8	3.6	3.3	3.3	3.4	3.4	3.2	3.2	3.7
Tb	0.6	0.6	0.4	0.8	0.7	0.5	0.6	0.6	0.8	0.6	0.6	0.5	0.5	0.6	0.5	0.6	0.7
Dy	3.3	3.5	2.6	4.8	4.0	3.1	3.7	3.3	3.8	3.7	3.8	3.3	3.2	3.5	2.9	3.2	3.9
Ho	0.7	0.8	0.5	1.0	0.8	0.6	0.8	0.7	0.8	0.8	0.9	0.7	0.6	0.7	0.6	0.6	0.8
Er	1.9	2.2	1.5	2.6	2.1	1.7	2.4	2.0	2.2	2.1	2.1	1.8	1.8	2.1	1.7	1.8	2.2
Tm	0.3	0.3	0.2	0.4	0.3	0.3	0.4	0.3	0.3	0.3	0.4	0.3	0.3	0.3	0.3	0.2	0.3
Yb	1.9	2.0	1.5	2.4	1.9	1.7	2.5	2.1	2.3	2.1	2.1	1.7	1.8	2.2	1.6	1.7	2.4
Lu	0.3	0.3	0.3	0.4	0.3	0.2	0.4	0.4	0.4	0.3	0.3	0.3	0.3	0.3	0.2	0.3	0.3
Cu	99.7	129.8	33.6	105.3	111.0	66.2	68.3	19.3	201.1	82.6	79.8	355.0	116.2	95.2	336.3	74.2	39.8
Zn	81.9	42.0	44.7	190.0	73.3	129.9	110.2	77.6	121.7	65.1	111.7	155.7	95.9	104.1	157.3	71.1	159.3
Mo	0.5	0.6	0.3	0.8	0.7	0.2	0.8	0.2	3.3	0.6	0.5	0.2	0.2	0.3	0.2	0.5	0.7
Ag	93.0	67.0	60.0	121.0	150.0	108.0	89.0	35.0	202.0	71.0	124.0	161.0	81.0	62.0	354.0	49.0	40.0
Tl	0.0	0.0	0.0	0.0	<.02	0.0	<.02	0.1	0.1	0.0	<.02	<.02	0.0	<.02	0.0	0.0	0.1
Pb	5.4	4.9	3.7	2.6	2.9	2.1	3.2	4.1	5.7	4.2	6.1	23.6	8.4	2.6	47.3	1.2	4.9
Sn	<1	<1	<1	1.0	<1	<1	<1	<1	2.0	1.0	<1	<1	<1	<1	<1	<1	1.0
Sb	0.1	0.1	0.1	0.1	0.1	0.1	0.2	0.1	0.1	0.1	0.1	0.2	0.2	0.2	0.1	0.1	0.1
Ga	19.3	20.7	18.7	21.1	19.5	16.5	19.9	19.6	16.8	20.2	16.9	18.2	17.2	18.2	18.1	16.3	19.0
W	<.1	0.1	0.5	0.3	0.2	0.2	0.1	0.4	1.1	0.2	0.2	0.2	0.3	0.2	0.4	0.2	0.5
Mn	1057.0	670.0	925.0	1413.0	928.0	1589.0	1341.0	1188.0	1447.0	947.0	1251.0	2051.0	1454.0	1073.0	2729.0	1033.0	2015.0
As	2.9	1.3	1.5	1.1	0.8	0.7	2.2	0.6	0.6	1.4	1.3	2.0	3.2	2.8	10.3	0.5	0.3
Au	1.8	0.6	0.2	5.7	6.1	6.0	6.5	0.8	2.4	<.2	2.4	0.6	2.0	0.3	4.9	1.4	1.0
Cd	0.1	0.1	0.1	0.1	0.1	0.0	0.1	0.1	0.1	0.2	0.1	0.3	0.1	0.0	0.3	0.0	0.1
Bi	0.0	0.0	0.0	0.1	0.0	0.0	0.1	0.1	0.0	0.0	0.0	<.02	<.02	<.02	0.1	<.02	0.0
B *	<1	1.0	1.0	<1	<1	<1	1.0	1.0	1.0	1.0	<1	1.0	2.0	3.0	6.0	1.0	1.0
Hg	5.0	6.0	<5	<5	<5	<5	<5	<5	<5	<5	<5	<5	<5	<5	<5	<5	<5
Se	0.1	0.1	0.1	<.1	0.1	0.1	0.2	0.1	0.3	0.2	0.1	<.1	0.1	<.1	0.4	0.1	<.1
Te	<.02	<.02	<.02	0.1	0.1	<.02	0.6	<.02	0.0	<.02	<.02	0.1	0.1	<.02	0.5	<.02	<.02
Ge	0.2	0.1	0.2	0.2	0.2	0.2	0.1	<.1	0.1	0.1	0.1	0.1	0.2	0.2	0.1	0.1	0.1
In	0.0	<.02	0.0	0.1	0.0	0.0	0.0	0.0	0.0	0.0	0.0	<.02	0.0	0.0	0.0	0.0	0.0
Re	<1	<1	<1	<1	<1	<1	<1	<1	3.0	<1	1.0	<1	<1	<1	<1	<1	<1
Be	0.1	0.1	0.2	0.1	0.2	0.2	<.1	0.3	0.5	0.1	0.1	0.1	0.1	<.1	0.2	0.3	0.1
Li *	9.9	7.4	12.3	11.6	8.7	18.3	9.6	7.5	11.6	7.4	12.1	16.4	13.5	18.6	16.2	8.7	11.5
Pd	<10	<10	<10	<10	<10	<10	<10	<10	<10	<10	<10	<10	<10	<10	10.0	<10	<10
Pt	<2	<2	<2	<2	<2	3.0	<2	<2	<2	2.0	<2	2.0	4.0	<2	3.0	<2	<2
LOI	3.4	1.6	3.4	5.1	3.6	7.1	3.0	6.8	7.0	4.4	4.2	3.5	2.8	2.9	6.0	5.0	7.0

Appendix 2.3 – Major element oxide composition for rim and core spot analyses of hornblendes of the Black Mountain Southeast Intrusive Suite. (r = phenocryst rim analyses; c = phenocryst core analysis; all values in wt%)

Sample #	Spot Location	Intrusive Phase	Lab Location	SiO_2	TiO_2	Al_2O_3	FeO	MnO	MgO	CaO	Na_2O	K_2O	Total
BA08GS035	c	Liw-Liw	MIT	41.06	1.78	14.11	13.66	0.22	12.62	11.99	2.08	0.49	98.01
BA08GS035	r	Liw-Liw	MIT	40.38	1.74	14.97	12.63	0.20	12.61	12.26	2.19	0.57	97.55
BA08GS035	c	Liw-Liw	MIT	39.83	1.51	15.32	11.55	0.08	13.78	12.26	2.22	0.73	97.28
BA08GS035	r	Liw-Liw	MIT	40.09	1.45	15.20	11.17	0.10	14.12	12.34	2.02	0.76	97.25
BA08GS035	c	Liw-Liw	MIT	40.23	1.67	15.26	11.62	0.11	13.73	12.25	2.15	0.62	97.64
BA08GS035	r	Liw-Liw	MIT	41.43	2.07	12.95	13.21	0.24	12.96	11.75	2.24	0.46	97.31
BA08GS035	c	Liw-Liw	MIT	42.06	1.18	14.24	9.07	0.10	15.38	11.94	2.15	0.83	96.95
BA08GS035	r	Liw-Liw	MIT	39.78	1.74	15.51	10.72	0.15	13.40	12.49	2.12	0.60	96.50
BA08GS035	c	Liw-Liw	MIT	39.97	1.57	15.83	11.32	0.19	13.59	11.85	2.05	0.67	97.04
BA08GS035	r	Liw-Liw	MIT	39.60	1.65	16.09	12.18	0.18	12.68	12.10	2.04	0.63	97.14
BA08GS035	c	Liw-Liw	MIT	40.19	1.56	15.23	11.62	0.16	12.72	12.12	2.12	0.65	96.36
BA08GS035	r	Liw-Liw	MIT	39.95	1.50	15.75	11.50	0.08	13.22	12.09	2.14	0.62	96.85
BA08GS035	c	Liw-Liw	Tas	39.70	1.64	15.49	12.52	0.20	13.06	12.22	2.22	0.57	97.61
BA08GS035	r	Liw-Liw	Tas	39.26	1.42	16.12	11.58	0.15	13.64	11.84	2.10	0.83	96.94
BA08GS035	c	Liw-Liw	Tas	40.26	1.63	15.65	11.43	0.05	13.76	12.19	2.20	0.61	97.78
BA08GS035	r	Liw-Liw	Tas	39.52	1.56	16.09	11.82	0.15	13.30	12.02	2.09	0.81	97.35
BA08GS035	r	Liw-Liw	Tas	39.49	1.47	16.07	11.56	0.17	13.41	12.58	2.24	0.72	97.71
BA08GS035	c	Liw-Liw	Tas	49.69	0.20	4.90	14.37	1.13	14.58	11.17	0.29	0.15	96.49
BA08GS035	c	Liw-Liw	Tas	39.63	1.43	15.83	12.07	0.05	13.49	12.57	2.35	0.61	98.02
BA08GS035	r	Liw-Liw	Tas	39.76	1.52	16.18	11.49	0.17	13.33	12.25	2.06	0.72	97.48
BA08GS035	c	Liw-Liw	Tas	45.43	0.82	10.30	11.66	0.48	14.70	12.59	1.52	0.57	98.06
BA08GS035	r	Liw-Liw	Tas	39.75	1.50	16.12	11.38	0.10	13.70	12.13	2.38	0.84	97.90
BA08GS035	r	Liw-Liw	Tas	40.69	1.45	15.27	10.90	0.13	14.55	12.11	2.15	1.03	98.28
BA08GS035	c	Liw-Liw	Tas	38.92	1.63	16.91	12.59	0.10	12.25	12.41	2.11	0.75	97.67
BA08GS035	r	Liw-Liw	Tas	38.56	1.69	16.56	12.94	0.14	12.36	12.30	1.93	0.65	97.14
BA08GS035	c	Liw-Liw	Tas	41.20	1.26	15.02	10.36	0.11	14.55	12.26	2.20	0.84	97.79
BA08GS035	r	Liw-Liw	Tas	41.08	1.46	14.65	13.27	0.34	12.82	12.11	1.87	0.49	98.09
BA08GS035	c	Liw-Liw	Tas	40.57	1.35	15.46	10.99	0.16	14.17	12.17	2.22	0.87	97.95
BA08GS035	r	Liw-Liw	Tas	40.42	1.37	15.42	10.82	0.10	14.81	12.12	2.32	1.00	98.38
BA08GS035	c	Liw-Liw	Tas	40.89	1.17	14.97	10.54	0.11	14.65	12.02	1.99	0.74	97.08
BA08GS035	r	Liw-Liw	Tas	40.46	1.40	15.35	11.20	0.11	14.16	12.00	2.08	0.83	97.58
BA08GS035	r	Liw-Liw	Tas	40.24	1.42	15.59	10.89	0.13	14.19	12.22	1.97	0.81	97.46
BA08GS035	c	Liw-Liw	Tas	39.97	1.40	15.84	11.18	0.13	13.83	12.17	2.08	0.68	97.28
BA08GS035	r	Liw-Liw	Tas	40.27	1.41	15.19	11.05	0.06	14.19	12.19	2.19	0.78	97.33
BA08GS056	c	Liw-Liw	MIT	41.61	1.51	14.70	10.96	0.13	14.20	12.35	1.98	0.49	97.93
BA08GS056	r	Liw-Liw	MIT	50.77	1.16	5.14	11.31	0.41	16.85	10.97	1.07	0.26	97.95
BA08GS056	c	Liw-Liw	MIT	41.00	1.33	15.68	10.59	0.11	14.45	12.37	2.15	0.54	98.23
BA08GS056	r	Liw-Liw	MIT	45.80	1.62	9.51	11.45	0.37	15.82	11.07	2.00	0.39	98.04
BA08GS056	c	Liw-Liw	MIT	40.72	1.53	15.65	11.51	0.09	13.93	12.25	2.18	0.62	98.48
BA08GS056	r	Liw-Liw	MIT	41.57	1.47	14.70	10.99	0.10	14.36	12.36	1.98	0.72	98.25
BA08GS056	c	Liw-Liw	MIT	41.48	1.53	15.09	10.97	0.08	14.26	11.90	1.83	0.50	97.63
BA08GS056	r	Liw-Liw	MIT	41.26	1.50	15.05	10.61	0.11	14.02	12.29	2.02	0.55	97.40
BA08GS056	c	Liw-Liw	MIT	41.79	1.31	14.70	8.85	0.04	15.67	11.93	2.05	0.72	97.07
BA08GS056	r	Liw-Liw	MIT	41.93	1.51	14.30	10.84	0.15	14.90	12.00	1.98	0.43	98.04
BA08GS056	c	Liw-Liw	MIT	41.74	1.25	14.62	8.87	0.07	15.81	12.15	2.27	0.78	97.56
BA08GS056	r	Liw-Liw	MIT	43.06	1.10	13.38	11.27	0.16	14.83	11.96	1.91	0.42	98.09
BA08GS056	r	Liw-Liw	MIT	44.65	2.34	10.51	10.76	0.31	15.56	11.22	2.12	0.40	97.86
BA08GS056	c	Liw-Liw	MIT	41.75	1.37	14.90	8.73	0.09	15.46	12.07	2.13	0.63	97.13
BA08GS056	r	Liw-Liw	MIT	44.14	0.92	12.44	9.07	0.15	16.27	11.50	1.57	0.55	96.61
BA08GS056	c	Liw-Liw	Tas	41.64	1.41	14.83	8.56	0.06	16.14	12.18	2.26	0.69	97.76
BA08GS056	r	Liw-Liw	Tas	40.05	1.39	16.25	11.36	0.08	13.73	12.57	2.26	0.58	98.27
BA08GS056	c	Liw-Liw	Tas	41.26	1.20	15.16	9.37	0.06	15.57	11.98	2.32	0.75	97.67
BA08GS056	r	Liw-Liw	Tas	41.52	1.21	14.36	10.02	0.13	15.11	11.95	1.92	0.50	96.73
BA08GS056	c	Liw-Liw	Tas	41.53	1.26	15.55	10.48	0.18	14.49	12.15	2.12	0.72	98.47
BA08GS056	r	Liw-Liw	Tas	41.32	1.28	14.74	9.56	0.14	15.39	12.57	2.46	0.52	97.98
BA08GS056	r	Liw-Liw	Tas	40.04	1.43	15.62	12.57	0.20	13.28	12.16	2.04	0.56	97.90
BA08GS056	c	Liw-Liw	Tas	41.31	1.16	14.72	8.47	0.03	16.13	11.92	2.55	0.75	97.03
BA08GS056	r	Liw-Liw	Tas	41.43	1.23	14.98	8.53	0.04	16.20	12.26	2.31	0.78	97.77
BA08GS056	c	Liw-Liw	Tas	39.74	1.49	15.69	13.75	0.15	11.98	12.39	1.87	0.52	97.58
BA08GS056	r	Liw-Liw	Tas	39.83	1.50	16.16	11.08	0.08	13.82	12.24	1.89	0.61	97.21
BA08GS056	r	Liw-Liw	Tas	41.36	1.39	14.62	8.25	0.05	16.00	12.07	2.24	0.72	96.69
BA08GS057	c	Liw-Liw	Tas	39.12	1.70	16.58	14.05	0.24	11.67	12.21	2.08	0.58	98.23
BA08GS057	r	Liw-Liw	Tas	41.27	1.18	14.33	10.82	0.03	14.98	12.10	2.10	0.47	97.26
BA08GS057	c	Liw-Liw	Tas	39.35	1.59	15.73	14.11	0.17	11.88	11.98	2.16	0.53	97.49
BA08GS057	r	Liw-Liw	Tas	39.91	1.44	15.20	11.09	0.06	14.17	12.26	2.10	0.59	96.82
BA08GS057	c	Liw-Liw	Tas	40.93	1.38	15.48	9.22	0.12	15.19	12.14	2.41	0.90	97.76
BA08GS057	r	Liw-Liw	Tas	40.09	1.75	14.80	10.79	0.09	14.79	12.21	2.02	0.50	97.02

Appendix 2.3 continued

Sample #	Spot Location	Intrusive Phase	Lab Location	SiO_2	TiO_2	Al_2O_3	FeO	MnO	MgO	CaO	Na_2O	K_2O	Total
BA08GS057	c	Liw-Liw	Tas	40.93	1.50	15.10	8.57	0.12	15.89	12.38	2.07	0.64	97.19
BA08GS057	r	Liw-Liw	Tas	41.66	1.32	14.69	8.95	0.03	15.82	12.36	2.05	0.66	97.54
BA08GS057	c	Liw-Liw	Tas	41.41	1.24	14.85	8.77	0.11	15.83	11.93	2.23	0.71	97.07
BA08GS057	c	Liw-Liw	Tas	41.20	1.16	15.02	8.82	0.08	15.95	12.06	2.05	0.70	97.05
BA08GS057	r	Liw-Liw	Tas	41.90	1.17	14.77	8.61	0.10	15.92	12.04	2.49	0.65	97.64
BA08GS002	c	PHD	MIT	45.59	1.13	10.11	15.19	0.37	12.60	11.26	1.52	0.44	98.21
BA08GS002	r	PHD	MIT	46.24	1.32	8.69	13.83	0.45	13.76	11.30	1.36	0.47	97.42
BA08GS002	c	PHD	MIT	45.58	1.51	9.26	15.16	0.37	13.16	11.00	1.47	0.53	98.03
BA08GS002	r	PHD	MIT	44.75	1.30	9.93	16.09	0.42	12.15	11.30	1.31	0.65	97.91
BA08GS002	c	PHD	MIT	52.37	0.52	4.22	10.92	0.25	16.73	12.24	0.55	0.20	97.99
BA08GS002	r	PHD	MIT	50.45	0.69	5.44	12.10	0.41	15.93	11.61	0.78	0.22	97.63
BA08GS002	c	PHD	MIT	51.73	1.23	8.44	13.38	0.43	11.99	10.24	1.14	0.39	98.96
BA08GS002	r	PHD	MIT	46.74	0.99	8.38	13.68	0.56	14.31	11.29	1.30	0.34	97.58
BA08GS002	c	PHD	MIT	46.22	1.01	9.30	14.37	0.45	12.89	11.43	1.40	0.39	97.46
BA08GS002	r	PHD	MIT	47.72	0.92	7.85	13.18	0.48	14.50	10.88	1.21	0.29	97.04
BA08GS002	c	PHD	MIT	47.20	1.25	7.98	13.91	0.48	14.20	11.32	1.19	0.37	97.91
BA08GS002	r	PHD	MIT	47.25	1.10	8.22	13.58	0.46	14.04	11.23	1.37	0.31	97.56
BA08GS005	c	PHD	MIT	43.62	1.65	11.85	15.75	0.41	11.67	11.08	1.51	0.66	98.19
BA08GS005	r	PHD	MIT	45.47	1.30	9.88	15.98	0.46	12.15	11.37	1.07	0.67	98.35
BA08GS005	c	PHD	MIT	50.75	0.52	5.44	11.20	0.33	15.41	12.22	0.51	0.29	96.67
BA08GS005	r	PHD	MIT	44.42	1.65	10.30	15.74	0.47	12.20	11.06	1.38	0.61	97.83
BA08GS005	c	PHD	MIT	45.49	1.17	10.12	15.46	0.47	13.12	11.18	1.52	0.50	99.03
BA08GS005	r	PHD	MIT	41.05	2.35	13.86	15.56	0.29	10.96	11.96	1.73	0.59	98.36
BA08GS005	c	PHD	MIT	45.03	1.62	10.44	14.60	0.43	12.86	11.44	1.25	0.52	98.18
BA08GS005	r	PHD	MIT	40.63	2.00	13.49	15.02	0.35	11.00	12.25	1.61	0.64	97.00
BA08GS005	c	PHD	MIT	44.74	1.35	10.91	15.46	0.43	12.17	11.28	1.33	0.58	98.25
BA08GS005	r	PHD	MIT	44.54	1.39	10.75	16.33	0.40	11.67	11.14	1.34	0.67	98.24
BA08GS005	c	PHD	MIT	44.06	1.27	11.13	15.54	0.39	11.99	11.25	1.58	0.60	97.81
BA08GS005	r	PHD	MIT	42.09	2.11	12.85	15.34	0.42	11.53	11.39	1.46	0.71	97.91
BA08GS005	c	PHD	MIT	44.45	1.28	10.99	14.59	0.45	12.69	11.08	1.55	0.58	97.66
BA08GS005	r	PHD	MIT	44.41	1.37	10.70	15.90	0.46	11.95	11.27	1.24	0.63	97.93
BA08GS005	c	PHD	MIT	44.13	1.38	11.35	15.35	0.37	11.86	11.32	1.53	0.63	97.92
BA08GS005	r	PHD	MIT	41.44	2.21	12.95	16.68	0.27	10.95	11.92	1.80	0.57	98.79
BA08GS005	c	PHD	MIT	44.08	1.67	10.77	15.67	0.38	11.81	11.23	1.33	0.74	97.69
BA08GS005	r	PHD	MIT	43.27	1.96	12.24	10.50	0.09	15.52	11.52	2.28	0.53	97.92
BA08GS005	c	PHD	MIT	44.09	1.26	11.16	15.37	0.48	11.94	11.20	1.52	0.60	97.61
BA08GS005	r	PHD	MIT	41.90	2.05	13.92	10.52	0.12	14.30	11.93	2.11	0.59	97.44
BA08GS006	c	PHD	MIT	43.26	1.55	11.53	14.80	0.36	12.08	11.17	1.63	0.64	97.01
BA08GS006	r	PHD	MIT	45.02	1.57	9.73	14.85	0.38	12.73	11.41	1.55	0.52	97.76
BA08GS006	c	PHD	MIT	44.93	1.32	9.95	15.23	0.42	12.55	11.31	1.60	0.59	97.91
BA08GS006	r	PHD	MIT	44.14	1.28	10.09	14.70	0.48	12.12	10.87	1.52	0.58	95.78
BA08GS006	c	PHD	MIT	43.95	1.85	10.60	15.56	0.48	12.16	11.24	1.74	0.66	98.25
BA08GS006	r	PHD	MIT	43.36	1.83	11.04	16.01	0.34	11.40	11.35	1.55	0.52	97.41
BA08GS006	c	PHD	MIT	44.22	1.35	11.27	14.49	0.43	12.17	10.93	1.65	0.53	97.04
BA08GS006	r	PHD	MIT	44.92	1.35	9.81	14.72	0.43	12.71	11.24	1.61	0.56	97.35
BA08GS006	c	PHD	MIT	44.16	1.47	10.88	15.62	0.40	12.19	11.35	1.50	0.57	98.14
BA08GS006	r	PHD	MIT	45.14	1.43	9.69	14.91	0.43	12.89	11.33	1.56	0.52	97.90
BA08GS006	c	PHD	MIT	42.33	2.30	11.95	14.52	0.39	12.16	11.43	1.84	0.72	97.63
BA08GS006	r	PHD	MIT	44.93	1.55	9.55	14.74	0.40	13.21	11.19	1.46	0.53	97.56
BA08GS006	c	PHD	MIT	43.96	1.30	10.98	15.28	0.40	12.11	11.05	1.64	0.56	97.29
BA08GS006	r	PHD	MIT	48.39	0.99	7.64	13.40	0.41	14.45	10.58	1.31	0.28	97.45
BA08GS006	c	PHD	MIT	44.25	1.34	11.11	15.88	0.43	12.03	11.30	1.45	0.65	98.44
BA08GS006	r	PHD	MIT	43.80	1.48	10.91	16.06	0.36	11.55	10.86	1.82	0.64	97.48
BA08GS006	c	PHD	MIT	45.16	1.29	10.08	15.02	0.33	12.57	11.16	1.49	0.49	97.59
BA08GS006	r	PHD	MIT	46.07	1.22	8.75	14.73	0.36	13.10	11.13	1.36	0.44	97.16
BA08GS006	c	PHD	MIT	44.70	1.23	10.43	15.14	0.41	12.57	11.15	1.61	0.52	97.75
BA08GS006	r	PHD	MIT	45.31	1.33	9.58	14.45	0.43	12.68	11.14	1.57	0.60	97.09
BA08GS030	c	PHD	MIT	45.94	1.07	9.65	13.89	0.37	13.47	10.73	1.08	0.44	96.64
BA08GS030	r	PHD	MIT	48.92	1.16	5.92	12.21	0.47	14.60	11.64	0.51	0.52	95.95
BA08GS030	c	PHD	MIT	44.41	1.51	10.64	14.11	0.36	12.57	11.08	1.29	0.50	96.47
BA08GS030	r	PHD	MIT	44.04	1.36	10.75	15.30	0.33	12.49	10.94	1.58	0.52	97.31
BA08GS030	c	PHD	MIT	44.12	1.32	11.11	14.84	0.44	12.39	10.59	1.17	0.54	96.53
BA08GS030	r	PHD	MIT	49.15	0.69	5.87	13.58	0.53	14.63	11.83	0.41	0.35	97.04
BA08GS030	c	PHD	MIT	44.49	1.18	10.97	14.24	0.34	12.65	10.91	1.31	0.47	96.56
BA08GS030	r	PHD	MIT	49.30	0.93	6.37	12.68	0.59	14.96	11.59	0.49	0.31	97.22
BA08GS030	r	PHD	MIT	43.22	1.45	11.52	15.86	0.44	11.96	11.09	1.22	0.61	97.37
BA08GS030	r	PHD	MIT	49.45	0.77	5.92	12.94	0.50	15.15	11.99	0.36	0.36	97.44

Appendix 2.3 continued

Sample #	Spot Location	Intrusive Phase	Lab Location	SiO_2	TiO_2	Al_2O_3	FeO	MnO	MgO	CaO	Na_2O	K_2O	Total
BA08GS030	r	PHD	MIT	43.53	1.37	11.97	15.88	0.39	11.79	11.03	1.46	0.65	98.07
BA08GS030	c	PHD	MIT	43.59	1.35	11.46	15.06	0.37	12.15	11.07	1.49	0.54	97.08
BA08GS030	r	PHD	MIT	44.75	1.25	10.62	14.89	0.45	12.29	11.04	1.32	0.50	97.10
BA08GS030	c	PHD	MIT	43.24	1.44	12.20	15.06	0.38	12.06	10.69	1.43	0.54	97.04
BA08GS030	r	PHD	MIT	45.23	1.15	10.73	14.66	0.40	12.79	11.04	1.37	0.46	97.83
BA08GS030	c	PHD	Tas	44.48	1.13	10.57	14.46	0.38	13.09	11.07	1.21	0.45	96.84
BA08GS030	r	PHD	Tas	46.26	0.91	6.87	13.44	0.55	13.82	11.42	0.52	0.42	94.22
BA08GS030	c	PHD	Tas	44.50	1.17	11.52	14.90	0.44	12.94	10.47	1.08	1.00	98.03
BA08GS030	r	PHD	Tas	43.17	1.23	11.58	15.69	0.48	12.04	11.05	1.30	0.64	97.18
BA08GS030	c	PHD	Tas	44.35	1.35	11.96	14.26	0.38	12.83	11.27	1.00	0.55	97.95
BA08GS030	r	PHD	Tas	49.42	0.65	5.69	13.15	0.59	15.05	11.85	0.51	0.30	97.22
BA08GS030	c	PHD	Tas	43.08	1.36	12.11	16.05	0.41	11.66	11.13	1.31	0.74	97.85
BA08GS030	r	PHD	Tas	43.60	1.28	11.66	15.97	0.47	12.07	11.20	1.21	0.62	98.09
BA08GS033A	r	PHD	Tas	46.94	1.12	7.97	13.34	0.62	14.42	11.18	1.50	0.35	97.43
BA08GS033A	c	PHD	Tas	45.68	1.35	9.44	14.12	0.45	13.04	11.59	1.35	0.54	97.55
BA08GS033A	r	PHD	Tas	45.44	1.18	9.27	14.22	0.55	13.48	11.12	1.43	0.43	97.11
BA08GS033A	c	PHD	Tas	44.48	1.32	10.02	14.95	0.52	13.38	10.99	1.54	0.51	97.69
BA08GS033A	c	PHD	Tas	43.49	1.57	10.88	15.66	0.53	12.18	11.45	1.73	0.64	98.13
BA08GS033A	r	PHD	Tas	45.83	0.93	9.25	15.02	0.55	12.93	11.07	1.08	0.43	97.08
BA08GS033A	r	PHD	Tas	47.36	0.93	8.08	14.08	0.58	14.21	11.20	1.18	0.34	97.95
BA08GS033A	c	PHD	Tas	44.74	1.33	9.49	14.54	0.48	12.69	11.36	1.22	0.51	96.35
BA08GS033A	r	PHD	Tas	46.96	1.03	8.12	14.17	0.60	14.04	11.40	1.22	0.40	97.92
BA08GS033B	c	PHD	Tas	44.15	1.36	10.23	15.60	0.47	12.59	11.43	1.54	0.53	97.90
BA08GS033B	r	PHD	Tas	46.86	0.96	8.30	14.13	0.59	14.31	11.10	1.37	0.32	97.94
BA08GS033B	c	PHD	Tas	45.70	1.27	9.05	14.50	0.50	13.66	11.42	1.29	0.39	97.77
BA08GS033B	r	PHD	Tas	44.94	1.64	9.30	13.99	0.47	13.15	11.09	1.39	0.54	96.50
BA08GS033B	c	PHD	Tas	40.46	1.54	15.23	11.59	0.20	13.32	12.22	2.19	0.50	97.25
BA08GS033B	r	PHD	Tas	45.13	1.05	9.47	14.68	0.54	13.55	11.27	1.32	0.41	97.43
BA08GS033B	c	PHD	Tas	45.20	1.15	9.98	14.55	0.55	13.56	10.97	1.29	0.41	97.67
BA08GS033B	r	PHD	Tas	45.30	1.08	9.55	14.62	0.53	13.20	11.14	1.35	0.37	97.13
BA08GS033B	c	PHD	Tas	40.90	1.61	15.35	11.91	0.12	13.14	12.10	2.14	0.48	97.75
BA08GS033B	r	PHD	Tas	46.16	0.98	9.13	14.59	0.59	13.73	11.07	1.37	0.34	97.98
BA08GS033B	c	PHD	Tas	45.83	1.27	9.20	14.47	0.51	13.46	11.46	1.19	0.40	97.79
BA08GS033B	r	PHD	Tas	45.80	1.06	8.77	14.19	0.57	13.80	11.24	1.27	0.47	97.17
BA08GS033B	c	PHD	Tas	43.10	1.73	11.24	14.83	0.38	12.15	11.24	1.55	0.67	96.90
BA08GS033B	r	PHD	Tas	44.96	1.61	9.33	14.71	0.50	13.13	11.37	1.28	0.56	97.45
BA08GS040	c	PHD	MIT	44.59	1.18	10.22	15.44	0.43	12.34	11.14	1.52	0.54	97.40
BA08GS040	r	PHD	MIT	44.22	1.67	10.25	15.46	0.43	12.36	11.35	1.55	0.61	97.90
BA08GS040	c	PHD	MIT	45.08	1.25	10.37	14.87	0.46	12.89	11.16	1.54	0.49	98.11
BA08GS040	r	PHD	MIT	45.27	1.25	9.97	14.89	0.42	12.96	11.13	1.51	0.54	97.94
BA08GS040	c	PHD	MIT	45.10	1.29	9.94	15.00	0.41	12.62	11.22	1.53	0.53	97.65
BA08GS040	r	PHD	MIT	44.45	1.45	10.27	14.99	0.43	12.64	11.17	1.54	0.59	97.52
BA08GS040	c	PHD	MIT	43.57	1.28	11.15	15.19	0.41	12.15	11.21	1.60	0.61	97.17
BA08GS040	r	PHD	MIT	44.40	1.50	10.29	15.30	0.45	12.86	11.35	1.44	0.58	98.17
BA08GS040	c	PHD	MIT	44.52	1.42	10.90	15.44	0.38	12.55	11.13	1.66	0.55	98.54
BA08GS040	r	PHD	MIT	45.24	1.65	9.56	14.09	0.40	13.07	11.48	1.51	0.50	97.51
BA08GS040	c	PHD	MIT	43.95	1.27	11.16	16.25	0.48	12.04	11.15	1.59	0.62	98.51
BA08GS040	r	PHD	MIT	46.24	1.36	9.24	14.29	0.39	13.62	11.36	1.57	0.47	98.53
BA08GS040	c	PHD	MIT	44.76	1.66	10.26	15.56	0.47	12.74	11.28	1.53	0.64	98.90
BA08GS040	r	PHD	MIT	44.01	1.62	10.54	15.33	0.44	12.54	11.22	1.51	0.64	97.85
BA08GS004	c	HMG	MIT	41.29	2.58	13.56	11.26	0.11	14.42	11.57	2.26	0.46	97.51
BA08GS004	r	HMG	MIT	40.33	2.30	14.71	10.79	0.10	14.05	12.17	2.22	0.73	97.41
BA08GS004	c	HMG	MIT	40.72	2.53	14.04	11.34	0.12	14.18	11.83	2.26	0.58	97.60
BA08GS004	r	HMG	MIT	40.57	2.65	14.06	11.42	0.18	14.06	11.90	2.36	0.66	97.86
BA08GS004	c	HMG	MIT	40.70	2.29	14.15	10.53	0.13	14.19	12.08	2.38	0.45	96.90
BA08GS004	r	HMG	MIT	42.00	3.58	11.56	10.38	0.30	14.41	11.41	2.42	0.56	96.61
BA08GS004	c	HMG	MIT	40.16	2.33	14.84	10.85	0.08	14.09	12.21	2.10	0.71	97.38
BA08GS004	r	HMG	MIT	39.99	2.41	14.44	10.88	0.12	14.29	12.00	2.38	0.66	97.16
BA08GS004	c	HMG	MIT	40.31	2.34	14.56	10.66	0.11	14.49	12.16	2.19	0.69	97.52
BA08GS004	r	HMG	MIT	41.07	3.11	12.71	10.96	0.16	14.26	11.95	2.41	0.61	97.25
BA08GS004	c	HMG	MIT	39.68	2.17	15.39	10.88	0.11	13.81	12.35	2.19	0.49	97.07
BA08GS004	r	HMG	MIT	40.71	2.38	14.70	10.69	0.09	14.19	12.24	2.14	0.71	97.85
BA08GS011	c	HMG	MIT	40.27	2.26	14.97	10.75	0.09	14.11	11.84	2.22	0.71	97.22
BA08GS011	r	HMG	MIT	40.41	2.55	15.02	11.02	0.13	13.33	11.90	2.21	0.69	97.25
BA08GS029	r	HMG	MIT	40.92	2.32	14.30	10.71	0.10	14.56	12.20	2.24	0.71	98.05
BA08GS029	c	HMG	MIT	40.36	2.48	14.85	10.72	0.07	14.12	11.81	2.30	0.80	97.51
BA08GS029	r	HMG	MIT	40.23	2.33	14.00	11.01	0.16	14.13	12.17	2.22	0.71	96.96
BA08GS029	c	HMG	MIT	40.73	2.42	14.32	10.13	0.09	14.50	11.71	2.47	0.45	96.83

Appendix 2.3 continued

Sample #	Spot Location	Intrusive Phase	Lab Location	SiO_2	TiO_2	Al_2O_3	FeO	MnO	MgO	CaO	Na_2O	K_2O	Total
BA08GS009	c	HMG Clot	Tas	39.45	2.85	12.86	13.94	0.22	13.14	11.54	2.02	0.67	96.70
BA08GS009	c	HMG Clot	Tas	38.96	2.15	15.06	10.78	0.14	14.10	12.38	2.53	0.51	96.61
BA08GS009	c	HMG Clot	Tas	38.85	2.28	15.22	10.95	0.07	14.00	12.44	2.30	0.53	96.65
BA08GS009	c	HMG Clot	Tas	39.31	2.36	14.48	11.33	0.12	14.01	12.11	2.06	0.75	96.52
BA08GS009	c	HMG Clot	Tas	39.35	2.12	15.25	10.80	0.19	14.17	12.23	2.42	0.46	96.99
BA08GS009	c	HMG Clot	Tas	38.40	2.12	14.89	11.00	0.12	13.65	11.84	2.45	0.48	94.95
BA08GS009	c	HMG Clot	Tas	40.17	2.42	14.55	11.55	0.15	14.08	12.02	2.36	0.72	98.01
BA08GS009	c	HMG Clot	Tas	40.10	2.23	14.77	11.12	0.13	14.04	11.99	2.24	0.67	97.30
BA08GS009	c	HMG Clot	Tas	39.21	2.38	14.37	11.12	0.13	14.00	12.04	2.53	0.81	96.59
BA08GS009	c	HMG Clot	Tas	39.90	2.27	14.50	10.97	0.14	14.37	11.99	2.46	0.61	97.22
BA08GS009	c	HMG Clot	Tas	39.35	2.13	15.39	10.83	0.11	14.22	12.24	2.39	0.60	97.26
BA08GS009	c	HMG Clot	Tas	39.83	2.39	14.08	11.19	0.15	14.04	11.76	2.48	0.68	96.60
BA08GS009	c	HMG Clot	Tas	40.10	2.18	12.72	11.74	0.12	13.39	11.67	2.10	0.78	94.81
BA08GS009	c	HMG Clot	Tas	39.80	2.24	15.32	11.13	0.06	14.19	12.26	2.26	0.53	97.77
BA08GS009	c	HMG Clot	Tas	39.84	2.46	14.58	11.56	0.10	14.08	11.67	2.42	0.69	97.41
BA08GS009	c	HMG Clot	Tas	39.85	2.19	14.77	11.47	0.12	14.22	11.80	2.43	0.67	97.51
BA08GS009	c	HMG Clot	Tas	38.73	2.25	15.44	10.97	0.12	14.09	12.36	2.22	0.52	96.70
BA08GS009	c	HMG Clot	Tas	39.16	2.23	15.35	11.04	0.12	14.20	12.60	2.41	0.52	97.62
BA08GS009	c	HMG Clot	Tas	39.33	2.45	14.39	11.39	0.14	13.99	11.96	2.30	0.69	96.62
BA08GS009	c	HMG Clot	Tas	39.32	2.35	14.64	11.25	0.17	13.84	12.04	2.45	0.81	96.88
BA08GS009	c	HMG Clot	Tas	39.09	2.31	14.91	11.00	0.09	14.16	12.42	2.50	0.81	97.30
BA08GS009	c	HMG Clot	Tas	39.97	2.36	14.18	11.27	0.13	14.08	11.83	2.10	0.76	96.68
BA08GS010	c	HMG Clot	MIT	40.39	2.19	15.12	11.04	0.11	14.50	12.38	2.38	0.48	98.59
BA08GS010	r	HMG Clot	MIT	40.69	2.68	14.17	11.59	0.12	13.88	12.05	2.30	0.65	98.13
BA08GS010	c	HMG Clot	MIT	40.12	2.21	15.34	11.08	0.09	13.84	12.44	2.24	0.50	97.86
BA08GS010	r	HMG Clot	MIT	42.67	2.98	11.35	11.65	0.29	14.54	11.23	2.51	0.52	97.74
BA08GS010	c	HMG Clot	MIT	39.95	2.15	15.29	10.86	0.08	14.10	12.27	2.25	0.47	97.42
BA08GS010	r	HMG Clot	MIT	40.69	2.41	14.40	11.25	0.16	13.98	11.85	2.38	0.69	97.81
BA08GS010	c	HMG Clot	MIT	39.40	2.24	15.37	10.93	0.09	14.51	12.19	2.28	0.46	97.47
BA08GS010	r	HMG Clot	MIT	40.57	2.43	14.44	11.29	0.10	13.78	12.19	2.22	0.71	97.73
BA08GS010	c	HMG Clot	MIT	40.26	2.24	15.20	10.81	0.10	14.29	12.37	2.37	0.49	98.13
BA08GS010	r	HMG Clot	MIT	40.50	2.42	14.61	11.20	0.14	14.11	11.68	2.12	0.70	97.48
BA08GS047	c	HCB	MIT	41.61	1.20	13.24	8.29	0.05	16.83	11.86	2.13	0.87	96.09
BA08GS047	r	HCB	MIT	42.25	1.65	13.43	10.31	0.10	15.34	11.99	2.01	0.92	97.99
BA08GS047	c	HCB	MIT	43.54	1.31	13.22	8.36	0.07	16.65	11.89	2.08	0.91	98.03
BA08GS047	r	HCB	MIT	42.08	1.45	13.56	10.62	0.16	15.17	11.83	2.12	0.89	97.88
BA08GS047	c	HCB	MIT	41.23	2.26	13.76	11.92	0.16	13.48	11.94	2.04	0.92	97.71
BA08GS047	r	HCB	MIT	45.31	1.53	10.63	11.49	0.28	14.70	11.63	1.40	0.62	97.59
BA08GS047	c	HCB	MIT	43.07	1.24	13.38	8.98	0.09	16.14	11.82	2.03	0.94	97.68
BA08GS047	r	HCB	MIT	43.57	1.56	12.14	10.26	0.12	15.70	11.82	1.69	0.81	97.67
BA08GS047	c	HCB	MIT	41.63	1.85	13.34	12.44	0.18	13.47	11.84	2.07	0.79	97.60
BA08GS047	r	HCB	MIT	42.07	1.75	13.08	12.42	0.18	13.54	11.64	1.99	0.76	97.43
BA08GS047	c	HCB Clot	MIT	41.86	1.61	13.25	12.63	0.27	13.32	12.03	2.14	0.64	97.76
BA08GS047	c	HCB Clot	MIT	41.82	1.58	13.87	13.17	0.20	12.98	12.11	1.76	0.56	98.05
BA08GS047	c	HCB Clot	MIT	40.32	1.74	14.48	11.44	0.10	14.10	12.34	2.07	0.70	97.30
BA08GS047	c	HCB Clot	MIT	40.86	1.55	14.15	12.22	0.17	13.45	12.19	2.21	0.65	97.44
BA08GS047	c	HCB Clot	MIT	41.08	1.62	14.34	13.66	0.24	12.38	12.13	1.88	0.64	97.96
BA08GS047	c	HCB Clot	MIT	41.82	1.73	13.67	12.94	0.24	12.70	12.01	1.73	0.70	97.54
BA08GS047	c	HCB Clot	Tas	41.68	1.55	13.27	11.53	0.22	13.54	12.29	1.17	0.58	95.83
BA08GS047	c	HCB Clot	Tas	40.44	1.66	14.56	11.71	0.15	13.36	12.14	2.23	0.65	96.90
BA08GS047	c	HCB Clot	Tas	40.69	1.52	14.91	12.78	0.20	12.72	12.06	1.84	0.76	97.49
BA08GS047	c	HCB Clot	Tas	40.62	1.50	14.51	11.55	0.15	13.81	12.35	2.32	0.71	97.52
BA08GS047	c	HCB Clot	Tas	39.87	1.41	14.48	11.70	0.16	13.43	12.31	1.92	0.73	96.01
BA08GS047	c	HCB Clot	Tas	40.55	1.49	14.34	11.18	0.20	13.57	12.17	2.11	0.58	96.20
BA08GS047	c	HCB Clot	Tas	40.22	1.65	14.87	11.50	0.15	13.26	12.25	1.97	0.84	96.72
BA08GS047	c	HCB Clot	Tas	40.90	1.57	14.38	13.63	0.20	12.19	11.98	2.05	0.81	97.72
BA08GS047	c	HCB Clot	Tas	40.47	1.53	14.28	11.93	0.15	13.51	12.27	2.31	0.64	97.08

Appendix 2.4 – Atoms per formula unit calculated on the basis of 23 oxygens for the anhydrous formula of hornblende (Femenias et al., 2006) and total iron as FeO, in accordance with the methodology of Hammarstrom and Zen (1986). (r = phenocryst rim analyses; c = phenocryst core analysis; Al(iv) = tetrahedral aluminum)

Sample #	Spot Location	Intrusive Phase	Lab Location	Si	Ti	Al	Fe+2	Mn	Mg	Ca	Na	K	Total	*Al (iv)*
BA08GS035	c	Liw-Liw	MIT	6.08	0.20	2.46	1.69	0.03	2.79	1.90	0.60	0.09	15.84	*1.92*
BA08GS035	r	Liw-Liw	MIT	5.99	0.19	2.62	1.57	0.03	2.79	1.95	0.63	0.11	15.87	*2.01*
BA08GS035	c	Liw-Liw	MIT	5.91	0.17	2.68	1.43	0.01	3.05	1.95	0.64	0.14	15.97	*2.09*
BA08GS035	r	Liw-Liw	MIT	5.93	0.16	2.65	1.38	0.01	3.12	1.96	0.58	0.14	15.94	*2.07*
BA08GS035	c	Liw-Liw	MIT	5.94	0.19	2.65	1.43	0.01	3.02	1.94	0.62	0.12	15.92	*2.06*
BA08GS035	r	Liw-Liw	MIT	6.17	0.23	2.27	1.64	0.03	2.88	1.87	0.65	0.09	15.83	*1.83*
BA08GS035	c	Liw-Liw	MIT	6.16	0.13	2.46	1.11	0.01	3.36	1.87	0.61	0.16	15.86	*1.84*
BA08GS035	r	Liw-Liw	MIT	5.92	0.19	2.72	1.33	0.02	2.97	1.99	0.61	0.11	15.88	*2.08*
BA08GS035	c	Liw-Liw	MIT	5.92	0.18	2.76	1.40	0.02	3.00	1.88	0.59	0.13	15.88	*2.08*
BA08GS035	r	Liw-Liw	MIT	5.89	0.18	2.82	1.51	0.02	2.81	1.93	0.59	0.12	15.87	*2.11*
BA08GS035	c	Liw-Liw	MIT	6.01	0.18	2.68	1.45	0.02	2.83	1.94	0.61	0.12	15.85	*1.99*
BA08GS035	r	Liw-Liw	MIT	5.94	0.17	2.76	1.43	0.01	2.93	1.92	0.62	0.12	15.89	*2.06*
BA08GS035	c	Liw-Liw	Tas	5.89	0.18	2.71	1.55	0.02	2.89	1.94	0.64	0.11	15.94	*2.11*
BA08GS035	r	Liw-Liw	Tas	5.84	0.16	2.83	1.44	0.02	3.03	1.89	0.61	0.16	15.97	*2.16*
BA08GS035	c	Liw-Liw	Tas	5.92	0.18	2.71	1.41	0.01	3.02	1.92	0.63	0.12	15.91	*2.08*
BA08GS035	r	Liw-Liw	Tas	5.86	0.17	2.81	1.47	0.02	2.94	1.91	0.60	0.15	15.94	*2.14*
BA08GS035	r	Liw-Liw	Tas	5.84	0.16	2.80	1.43	0.02	2.96	1.99	0.64	0.14	15.99	*2.16*
BA08GS035	c	Liw-Liw	Tas	7.35	0.02	0.85	1.78	0.14	3.22	1.77	0.08	0.03	15.25	*0.65*
BA08GS035	c	Liw-Liw	Tas	5.85	0.16	2.75	1.49	0.01	2.97	1.99	0.67	0.11	16.01	*2.15*
BA08GS035	r	Liw-Liw	Tas	5.88	0.17	2.82	1.42	0.02	2.94	1.94	0.59	0.14	15.91	*2.12*
BA08GS035	c	Liw-Liw	Tas	6.63	0.09	1.77	1.42	0.06	3.20	1.97	0.43	0.11	15.67	*1.37*
BA08GS035	r	Liw-Liw	Tas	5.86	0.17	2.80	1.40	0.01	3.01	1.91	0.68	0.16	16.00	*2.14*
BA08GS035	r	Liw-Liw	Tas	5.95	0.16	2.63	1.33	0.02	3.17	1.90	0.61	0.19	15.97	*2.05*
BA08GS035	c	Liw-Liw	Tas	5.78	0.18	2.96	1.56	0.01	2.71	1.97	0.61	0.14	15.93	*2.22*
BA08GS035	r	Liw-Liw	Tas	5.77	0.19	2.92	1.62	0.02	2.76	1.97	0.56	0.12	15.93	*2.23*
BA08GS035	c	Liw-Liw	Tas	6.03	0.14	2.59	1.27	0.01	3.18	1.92	0.62	0.16	15.92	*1.97*
BA08GS035	r	Liw-Liw	Tas	6.06	0.16	2.55	1.64	0.04	2.82	1.92	0.54	0.09	15.82	*1.94*
BA08GS035	c	Liw-Liw	Tas	5.96	0.15	2.67	1.35	0.02	3.10	1.91	0.63	0.16	15.96	*2.04*
BA08GS035	r	Liw-Liw	Tas	5.91	0.15	2.66	1.32	0.01	3.23	1.90	0.66	0.19	16.03	*2.09*
BA08GS035	c	Liw-Liw	Tas	6.03	0.13	2.60	1.30	0.01	3.22	1.90	0.57	0.14	15.90	*1.97*
BA08GS035	r	Liw-Liw	Tas	5.96	0.15	2.66	1.38	0.01	3.11	1.89	0.59	0.16	15.93	*2.04*
BA08GS035	r	Liw-Liw	Tas	5.93	0.16	2.71	1.34	0.02	3.12	1.93	0.56	0.15	15.92	*2.07*
BA08GS035	c	Liw-Liw	Tas	5.91	0.16	2.76	1.38	0.02	3.05	1.93	0.60	0.13	15.92	*2.09*
BA08GS035	r	Liw-Liw	Tas	5.95	0.16	2.64	1.37	0.01	3.13	1.93	0.63	0.15	15.96	*2.05*
BA08GS056	c	Liw-Liw	MIT	6.08	0.17	2.53	1.34	0.02	3.09	1.93	0.56	0.09	15.81	*1.92*
BA08GS056	r	Liw-Liw	MIT	7.29	0.13	0.87	1.36	0.05	3.61	1.69	0.30	0.05	15.33	*0.71*
BA08GS056	c	Liw-Liw	MIT	5.97	0.15	2.69	1.29	0.01	3.14	1.93	0.61	0.10	15.89	*2.03*
BA08GS056	r	Liw-Liw	MIT	6.65	0.18	1.63	1.39	0.05	3.42	1.72	0.56	0.07	15.68	*1.35*
BA08GS056	c	Liw-Liw	MIT	5.95	0.17	2.69	1.41	0.01	3.03	1.92	0.62	0.12	15.91	*2.05*
BA08GS056	r	Liw-Liw	MIT	6.07	0.16	2.53	1.34	0.01	3.12	1.93	0.56	0.13	15.86	*1.93*
BA08GS056	c	Liw-Liw	MIT	6.07	0.17	2.60	1.34	0.01	3.11	1.86	0.52	0.09	15.77	*1.93*
BA08GS056	r	Liw-Liw	MIT	6.06	0.17	2.60	1.30	0.01	3.07	1.93	0.58	0.10	15.82	*1.94*
BA08GS056	c	Liw-Liw	MIT	6.10	0.14	2.53	1.08	0.01	3.41	1.87	0.58	0.13	15.85	*1.90*
BA08GS056	r	Liw-Liw	MIT	6.11	0.17	2.46	1.32	0.02	3.24	1.87	0.56	0.08	15.82	*1.89*
BA08GS056	c	Liw-Liw	MIT	6.08	0.14	2.51	1.08	0.01	3.43	1.90	0.64	0.14	15.92	*1.92*
BA08GS056	r	Liw-Liw	MIT	6.27	0.12	2.30	1.37	0.02	3.22	1.87	0.54	0.08	15.77	*1.73*
BA08GS056	r	Liw-Liw	MIT	6.49	0.26	1.80	1.31	0.04	3.37	1.75	0.60	0.07	15.69	*1.51*
BA08GS056	c	Liw-Liw	MIT	6.09	0.15	2.56	1.06	0.01	3.36	1.89	0.60	0.12	15.84	*1.91*
BA08GS056	r	Liw-Liw	MIT	6.43	0.10	2.14	1.11	0.02	3.53	1.80	0.44	0.10	15.67	*1.57*
BA08GS056	c	Liw-Liw	Tas	6.04	0.15	2.54	1.04	0.01	3.49	1.89	0.63	0.13	15.92	*1.96*
BA08GS056	r	Liw-Liw	Tas	5.87	0.15	2.81	1.39	0.01	3.00	1.97	0.64	0.11	15.95	*2.13*
BA08GS056	c	Liw-Liw	Tas	6.01	0.13	2.60	1.14	0.01	3.38	1.87	0.66	0.14	15.95	*1.99*
BA08GS056	r	Liw-Liw	Tas	6.11	0.13	2.49	1.23	0.02	3.32	1.89	0.55	0.09	15.83	*1.89*
BA08GS056	c	Liw-Liw	Tas	6.03	0.14	2.66	1.27	0.02	3.13	1.89	0.60	0.13	15.87	*1.97*
BA08GS056	r	Liw-Liw	Tas	6.02	0.14	2.53	1.16	0.02	3.34	1.96	0.69	0.10	15.97	*1.98*
BA08GS056	r	Liw-Liw	Tas	5.91	0.16	2.72	1.55	0.03	2.92	1.92	0.58	0.11	15.91	*2.09*
BA08GS056	c	Liw-Liw	Tas	6.04	0.13	2.54	1.04	0.00	3.52	1.87	0.72	0.14	15.99	*1.96*
BA08GS056	r	Liw-Liw	Tas	6.02	0.13	2.56	1.04	0.01	3.51	1.91	0.65	0.15	15.97	*1.98*
BA08GS056	c	Liw-Liw	Tas	5.92	0.17	2.76	1.71	0.02	2.66	1.98	0.54	0.10	15.85	*2.08*
BA08GS056	r	Liw-Liw	Tas	5.88	0.17	2.81	1.37	0.01	3.04	1.94	0.54	0.12	15.87	*2.12*
BA08GS056	r	Liw-Liw	Tas	6.06	0.15	2.52	1.01	0.01	3.49	1.89	0.63	0.13	15.91	*1.94*
BA08GS057	c	Liw-Liw	Tas	5.81	0.19	2.90	1.74	0.03	2.58	1.94	0.60	0.11	15.91	*2.19*
BA08GS057	r	Liw-Liw	Tas	6.07	0.13	2.49	1.33	0.00	3.29	1.91	0.60	0.09	15.90	*1.93*
BA08GS057	c	Liw-Liw	Tas	5.88	0.18	2.77	1.76	0.02	2.65	1.92	0.62	0.10	15.91	*2.12*
BA08GS057	r	Liw-Liw	Tas	5.93	0.16	2.66	1.38	0.01	3.14	1.95	0.60	0.11	15.94	*2.07*
BA08GS057	c	Liw-Liw	Tas	5.97	0.15	2.66	1.13	0.01	3.30	1.90	0.68	0.17	15.97	*2.03*
BA08GS057	r	Liw-Liw	Tas	5.93	0.19	2.58	1.33	0.01	3.26	1.94	0.58	0.09	15.92	*2.07*
BA08GS057	c	Liw-Liw	Tas	5.98	0.16	2.60	1.05	0.01	3.46	1.94	0.59	0.12	15.91	*2.02*

Appendix 2.4 continued

Sample #	Spot Location	Intrusive Phase	Lab Location	Si	Ti	Al	Fe+2	Mn	Mg	Ca	Na	K	Total	*Al (iv)*
BA08GS057	r	Liw-Liw	Tas	6.06	0.14	2.52	1.09	0.00	3.43	1.93	0.58	0.12	15.88	*1.94*
BA08GS057	c	Liw-Liw	Tas	6.05	0.14	2.56	1.07	0.01	3.45	1.87	0.63	0.13	15.92	*1.95*
BA08GS057	c	Liw-Liw	Tas	6.03	0.13	2.59	1.08	0.01	3.48	1.89	0.58	0.13	15.91	*1.97*
BA08GS057	r	Liw-Liw	Tas	6.08	0.13	2.53	1.05	0.01	3.45	1.87	0.70	0.12	15.94	*1.92*
BA08GS002	c	PHD	MIT	6.71	0.13	1.75	1.87	0.05	2.76	1.77	0.43	0.08	15.55	*1.29*
BA08GS002	r	PHD	MIT	6.82	0.15	1.51	1.71	0.06	3.02	1.78	0.39	0.09	15.52	*1.18*
BA08GS002	c	PHD	MIT	6.72	0.17	1.61	1.87	0.05	2.89	1.74	0.42	0.10	15.57	*1.28*
BA08GS002	r	PHD	MIT	6.65	0.15	1.74	2.00	0.05	2.69	1.80	0.38	0.12	15.58	*1.35*
BA08GS002	c	PHD	MIT	7.48	0.06	0.71	1.30	0.03	3.56	1.87	0.15	0.04	15.20	*0.52*
BA08GS002	r	PHD	MIT	7.29	0.08	0.93	1.46	0.05	3.43	1.80	0.22	0.04	15.30	*0.71*
BA08GS002	c	PHD	MIT	7.35	0.13	1.41	1.59	0.05	2.54	1.56	0.31	0.07	15.01	*0.65*
BA08GS002	r	PHD	MIT	6.86	0.11	1.45	1.68	0.07	3.13	1.78	0.37	0.06	15.52	*1.14*
BA08GS002	c	PHD	MIT	6.82	0.11	1.62	1.77	0.06	2.84	1.81	0.40	0.07	15.50	*1.18*
BA08GS002	r	PHD	MIT	7.00	0.10	1.36	1.62	0.06	3.17	1.71	0.35	0.05	15.42	*1.00*
BA08GS002	c	PHD	MIT	6.91	0.14	1.38	1.70	0.06	3.10	1.78	0.34	0.07	15.47	*1.09*
BA08GS002	r	PHD	MIT	6.93	0.12	1.42	1.66	0.06	3.07	1.76	0.39	0.06	15.47	*1.07*
BA08GS005	c	PHD	MIT	6.46	0.18	2.07	1.95	0.05	2.58	1.76	0.43	0.12	15.60	*1.54*
BA08GS005	r	PHD	MIT	6.71	0.14	1.72	1.97	0.06	2.67	1.80	0.31	0.13	15.50	*1.29*
BA08GS005	c	PHD	MIT	7.37	0.06	0.93	1.36	0.04	3.34	1.90	0.14	0.05	15.20	*0.63*
BA08GS005	r	PHD	MIT	6.60	0.18	1.80	1.96	0.06	2.70	1.76	0.40	0.12	15.57	*1.40*
BA08GS005	c	PHD	MIT	6.65	0.13	1.74	1.89	0.06	2.86	1.75	0.43	0.09	15.61	*1.35*
BA08GS005	r	PHD	MIT	6.11	0.26	2.43	1.94	0.04	2.43	1.91	0.50	0.11	15.72	*1.89*
BA08GS005	c	PHD	MIT	6.62	0.18	1.81	1.79	0.05	2.82	1.80	0.36	0.10	15.53	*1.38*
BA08GS005	r	PHD	MIT	6.13	0.23	2.40	1.89	0.05	2.47	1.98	0.47	0.12	15.74	*1.87*
BA08GS005	c	PHD	MIT	6.60	0.15	1.90	1.91	0.05	2.68	1.78	0.38	0.11	15.55	*1.40*
BA08GS005	r	PHD	MIT	6.60	0.15	1.88	2.02	0.05	2.58	1.77	0.39	0.13	15.56	*1.40*
BA08GS005	c	PHD	MIT	6.54	0.14	1.95	1.93	0.05	2.65	1.79	0.45	0.11	15.62	*1.46*
BA08GS005	r	PHD	MIT	6.26	0.24	2.25	1.91	0.05	2.56	1.82	0.42	0.14	15.65	*1.74*
BA08GS005	c	PHD	MIT	6.57	0.14	1.92	1.80	0.06	2.80	1.76	0.44	0.11	15.60	*1.43*
BA08GS005	r	PHD	MIT	6.59	0.15	1.87	1.97	0.06	2.64	1.79	0.36	0.12	15.56	*1.41*
BA08GS005	c	PHD	MIT	6.54	0.15	1.98	1.90	0.05	2.62	1.80	0.44	0.12	15.60	*1.46*
BA08GS005	r	PHD	MIT	6.17	0.25	2.27	2.08	0.03	2.43	1.90	0.52	0.11	15.76	*1.83*
BA08GS005	c	PHD	MIT	6.56	0.19	1.89	1.95	0.05	2.62	1.79	0.38	0.14	15.57	*1.44*
BA08GS005	r	PHD	MIT	6.30	0.22	2.10	1.28	0.01	3.37	1.80	0.64	0.10	15.81	*1.70*
BA08GS005	c	PHD	MIT	6.55	0.14	1.96	1.91	0.06	2.65	1.78	0.44	0.11	15.60	*1.45*
BA08GS005	r	PHD	MIT	6.14	0.23	2.40	1.29	0.01	3.12	1.87	0.60	0.11	15.79	*1.86*
BA08GS006	c	PHD	MIT	6.47	0.17	2.03	1.85	0.05	2.69	1.79	0.47	0.12	15.64	*1.53*
BA08GS006	r	PHD	MIT	6.66	0.17	1.70	1.84	0.05	2.81	1.81	0.44	0.10	15.58	*1.34*
BA08GS006	c	PHD	MIT	6.65	0.15	1.74	1.89	0.05	2.77	1.79	0.46	0.11	15.62	*1.35*
BA08GS006	r	PHD	MIT	6.67	0.15	1.80	1.86	0.06	2.73	1.76	0.44	0.11	15.57	*1.33*
BA08GS006	c	PHD	MIT	6.52	0.21	1.85	1.93	0.06	2.69	1.79	0.50	0.12	15.66	*1.48*
BA08GS006	r	PHD	MIT	6.49	0.21	1.95	2.00	0.04	2.54	1.82	0.45	0.10	15.60	*1.51*
BA08GS006	c	PHD	MIT	6.58	0.15	1.98	1.80	0.05	2.70	1.74	0.47	0.10	15.57	*1.42*
BA08GS006	r	PHD	MIT	6.67	0.15	1.72	1.83	0.05	2.82	1.79	0.46	0.11	15.60	*1.33*
BA08GS006	c	PHD	MIT	6.54	0.16	1.90	1.93	0.05	2.69	1.80	0.43	0.11	15.62	*1.46*
BA08GS006	r	PHD	MIT	6.67	0.16	1.69	1.84	0.05	2.84	1.79	0.45	0.10	15.60	*1.33*
BA08GS006	c	PHD	MIT	6.31	0.26	2.10	1.81	0.05	2.70	1.83	0.53	0.14	15.72	*1.69*
BA08GS006	r	PHD	MIT	6.66	0.17	1.67	1.83	0.05	2.92	1.78	0.42	0.10	15.59	*1.34*
BA08GS006	c	PHD	MIT	6.55	0.15	1.93	1.91	0.05	2.69	1.77	0.47	0.11	15.62	*1.45*
BA08GS006	r	PHD	MIT	7.06	0.11	1.31	1.63	0.05	3.14	1.65	0.37	0.05	15.39	*0.94*
BA08GS006	c	PHD	MIT	6.54	0.15	1.93	1.96	0.05	2.65	1.79	0.42	0.12	15.61	*1.46*
BA08GS006	r	PHD	MIT	6.55	0.17	1.92	2.01	0.05	2.57	1.74	0.53	0.12	15.65	*1.45*
BA08GS006	c	PHD	MIT	6.69	0.14	1.76	1.86	0.04	2.77	1.77	0.43	0.09	15.55	*1.31*
BA08GS006	r	PHD	MIT	6.83	0.14	1.53	1.83	0.04	2.90	1.77	0.39	0.08	15.51	*1.17*
BA08GS006	c	PHD	MIT	6.62	0.14	1.82	1.88	0.05	2.78	1.77	0.46	0.10	15.61	*1.38*
BA08GS006	r	PHD	MIT	6.73	0.15	1.68	1.80	0.05	2.81	1.77	0.45	0.11	15.56	*1.27*
BA08GS030	c	PHD	MIT	6.80	0.12	1.68	1.72	0.05	2.97	1.70	0.31	0.08	15.44	*1.20*
BA08GS030	r	PHD	MIT	7.23	0.13	1.03	1.51	0.06	3.21	1.84	0.15	0.10	15.25	*0.77*
BA08GS030	c	PHD	MIT	6.62	0.17	1.87	1.76	0.05	2.80	1.77	0.37	0.10	15.50	*1.38*
BA08GS030	r	PHD	MIT	6.56	0.15	1.89	1.91	0.04	2.77	1.75	0.46	0.10	15.62	*1.44*
BA08GS030	c	PHD	MIT	6.59	0.15	1.96	1.85	0.06	2.76	1.70	0.34	0.10	15.50	*1.41*
BA08GS030	r	PHD	MIT	7.22	0.08	1.02	1.67	0.07	3.20	1.86	0.12	0.07	15.29	*0.78*
BA08GS030	c	PHD	MIT	6.62	0.13	1.93	1.77	0.04	2.81	1.74	0.38	0.09	15.51	*1.38*
BA08GS030	r	PHD	MIT	7.19	0.10	1.09	1.55	0.07	3.25	1.81	0.14	0.06	15.26	*0.81*
BA08GS030	r	PHD	MIT	6.46	0.16	2.03	1.98	0.06	2.66	1.78	0.35	0.12	15.60	*1.54*
BA08GS030	r	PHD	MIT	7.21	0.08	1.02	1.58	0.06	3.29	1.87	0.10	0.07	15.28	*0.79*
BA08GS030	r	PHD	MIT	6.45	0.15	2.09	1.97	0.05	2.61	1.75	0.42	0.12	15.62	*1.55*
BA08GS030	c	PHD	MIT	6.50	0.15	2.02	1.88	0.05	2.70	1.77	0.43	0.10	15.60	*1.50*

Appendix 2.4 continued

Sample #	Spot Location	Intrusive Phase	Lab Location	Si	Ti	Al	Fe+2	Mn	Mg	Ca	Na	K	Total	*Al (iv)*
BA08GS030	r	PHD	MIT	6.65	0.14	1.86	1.85	0.06	2.72	1.76	0.38	0.09	15.51	*1.35*
BA08GS030	c	PHD	MIT	6.45	0.16	2.14	1.88	0.05	2.68	1.71	0.41	0.10	15.58	*1.55*
BA08GS030	r	PHD	MIT	6.66	0.13	1.86	1.80	0.05	2.81	1.74	0.39	0.09	15.52	*1.34*
BA08GS030	c	PHD	Tas	6.62	0.13	1.85	1.80	0.05	2.90	1.76	0.35	0.09	15.55	*1.38*
BA08GS030	r	PHD	Tas	7.03	0.10	1.23	1.71	0.07	3.13	1.86	0.15	0.08	15.37	*0.97*
BA08GS030	c	PHD	Tas	6.55	0.13	2.00	1.83	0.06	2.84	1.65	0.31	0.19	15.56	*1.45*
BA08GS030	r	PHD	Tas	6.46	0.14	2.04	1.96	0.06	2.69	1.77	0.38	0.12	15.63	*1.54*
BA08GS030	c	PHD	Tas	6.51	0.15	2.07	1.75	0.05	2.81	1.77	0.28	0.10	15.50	*1.49*
BA08GS030	r	PHD	Tas	7.23	0.07	0.98	1.61	0.07	3.28	1.86	0.15	0.06	15.31	*0.77*
BA08GS030	c	PHD	Tas	6.42	0.15	2.13	2.00	0.05	2.59	1.78	0.38	0.14	15.63	*1.58*
BA08GS030	r	PHD	Tas	6.47	0.14	2.04	1.98	0.06	2.67	1.78	0.35	0.12	15.60	*1.53*
BA08GS033A	r	PHD	Tas	6.90	0.12	1.38	1.64	0.08	3.16	1.76	0.43	0.07	15.53	*1.10*
BA08GS033A	c	PHD	Tas	6.74	0.15	1.64	1.74	0.06	2.87	1.83	0.39	0.10	15.53	*1.26*
BA08GS033A	r	PHD	Tas	6.74	0.13	1.62	1.76	0.07	2.98	1.77	0.41	0.08	15.56	*1.26*
BA08GS033A	c	PHD	Tas	6.60	0.15	1.75	1.85	0.06	2.96	1.75	0.44	0.10	15.65	*1.40*
BA08GS033A	c	PHD	Tas	6.47	0.18	1.91	1.95	0.07	2.70	1.82	0.50	0.12	15.71	*1.53*
BA08GS033A	r	PHD	Tas	6.81	0.10	1.62	1.87	0.07	2.86	1.76	0.31	0.08	15.48	*1.19*
BA08GS033A	r	PHD	Tas	6.93	0.10	1.39	1.72	0.07	3.10	1.76	0.34	0.06	15.47	*1.07*
BA08GS033A	c	PHD	Tas	6.71	0.15	1.68	1.82	0.06	2.84	1.82	0.36	0.10	15.53	*1.29*
BA08GS033A	r	PHD	Tas	6.89	0.11	1.40	1.74	0.07	3.07	1.79	0.35	0.07	15.50	*1.11*
BA08GS033B	c	PHD	Tas	6.56	0.15	1.79	1.94	0.06	2.79	1.82	0.44	0.10	15.66	*1.44*
BA08GS033B	r	PHD	Tas	6.87	0.11	1.43	1.73	0.07	3.13	1.74	0.39	0.06	15.53	*1.13*
BA08GS033B	c	PHD	Tas	6.74	0.14	1.57	1.79	0.06	3.00	1.80	0.37	0.07	15.55	*1.26*
BA08GS033B	r	PHD	Tas	6.71	0.18	1.64	1.75	0.06	2.93	1.77	0.40	0.10	15.54	*1.29*
BA08GS033B	c	PHD	Tas	5.99	0.17	2.66	1.43	0.02	2.94	1.94	0.63	0.09	15.87	*2.01*
BA08GS033B	r	PHD	Tas	6.69	0.12	1.66	1.82	0.07	3.00	1.79	0.38	0.08	15.59	*1.31*
BA08GS033B	c	PHD	Tas	6.67	0.13	1.73	1.80	0.07	2.98	1.73	0.37	0.08	15.56	*1.33*
BA08GS033B	r	PHD	Tas	6.72	0.12	1.67	1.82	0.07	2.92	1.77	0.39	0.07	15.55	*1.28*
BA08GS033B	c	PHD	Tas	6.02	0.18	2.66	1.47	0.02	2.88	1.91	0.61	0.09	15.82	*1.98*
BA08GS033B	r	PHD	Tas	6.78	0.11	1.58	1.79	0.07	3.01	1.74	0.39	0.06	15.55	*1.22*
BA08GS033B	c	PHD	Tas	6.75	0.14	1.60	1.78	0.06	2.96	1.81	0.34	0.07	15.52	*1.25*
BA08GS033B	r	PHD	Tas	6.79	0.12	1.53	1.76	0.07	3.05	1.78	0.37	0.09	15.56	*1.21*
BA08GS033B	c	PHD	Tas	6.46	0.20	1.99	1.86	0.05	2.71	1.80	0.45	0.13	15.64	*1.54*
BA08GS033B	r	PHD	Tas	6.68	0.18	1.63	1.83	0.06	2.91	1.81	0.37	0.11	15.56	*1.32*
BA08GS040	c	PHD	MIT	6.64	0.13	1.79	1.92	0.05	2.74	1.78	0.44	0.10	15.60	*1.36*
BA08GS040	r	PHD	MIT	6.57	0.19	1.79	1.92	0.05	2.74	1.81	0.45	0.12	15.63	*1.43*
BA08GS040	c	PHD	MIT	6.64	0.14	1.80	1.83	0.06	2.83	1.76	0.44	0.09	15.59	*1.36*
BA08GS040	r	PHD	MIT	6.68	0.14	1.73	1.84	0.05	2.85	1.76	0.43	0.10	15.58	*1.32*
BA08GS040	c	PHD	MIT	6.68	0.14	1.74	1.86	0.05	2.79	1.78	0.44	0.10	15.58	*1.32*
BA08GS040	r	PHD	MIT	6.60	0.16	1.80	1.86	0.05	2.80	1.78	0.44	0.11	15.61	*1.40*
BA08GS040	c	PHD	MIT	6.51	0.14	1.96	1.90	0.05	2.71	1.80	0.47	0.12	15.65	*1.49*
BA08GS040	r	PHD	MIT	6.57	0.17	1.79	1.89	0.06	2.84	1.80	0.41	0.11	15.63	*1.43*
BA08GS040	c	PHD	MIT	6.55	0.16	1.89	1.90	0.05	2.75	1.76	0.47	0.10	15.63	*1.45*
BA08GS040	r	PHD	MIT	6.69	0.18	1.67	1.74	0.05	2.88	1.82	0.43	0.10	15.56	*1.31*
BA08GS040	c	PHD	MIT	6.51	0.14	1.95	2.01	0.06	2.66	1.77	0.46	0.12	15.66	*1.49*
BA08GS040	r	PHD	MIT	6.76	0.15	1.59	1.75	0.05	2.97	1.78	0.44	0.09	15.57	*1.24*
BA08GS040	c	PHD	MIT	6.58	0.18	1.78	1.91	0.06	2.79	1.78	0.44	0.12	15.63	*1.42*
BA08GS040	r	PHD	MIT	6.54	0.18	1.84	1.90	0.06	2.78	1.79	0.44	0.12	15.64	*1.46*
BA08GS004	c	HMG	MIT	6.08	0.29	2.35	1.39	0.01	3.16	1.82	0.65	0.09	15.83	*1.92*
BA08GS004	r	HMG	MIT	5.95	0.26	2.56	1.33	0.01	3.09	1.92	0.64	0.14	15.90	*2.05*
BA08GS004	c	HMG	MIT	6.00	0.28	2.44	1.40	0.01	3.12	1.87	0.64	0.11	15.87	*2.00*
BA08GS004	r	HMG	MIT	5.98	0.29	2.44	1.41	0.02	3.09	1.88	0.67	0.12	15.91	*2.02*
BA08GS004	c	HMG	MIT	6.02	0.25	2.47	1.30	0.02	3.13	1.91	0.68	0.08	15.87	*1.98*
BA08GS004	r	HMG	MIT	6.23	0.40	2.02	1.29	0.04	3.18	1.81	0.70	0.11	15.77	*1.77*
BA08GS004	c	HMG	MIT	5.93	0.26	2.58	1.34	0.01	3.10	1.93	0.60	0.13	15.89	*2.07*
BA08GS004	r	HMG	MIT	5.93	0.27	2.52	1.35	0.02	3.16	1.91	0.68	0.12	15.95	*2.07*
BA08GS004	c	HMG	MIT	5.94	0.26	2.53	1.31	0.01	3.18	1.92	0.63	0.13	15.92	*2.06*
BA08GS004	r	HMG	MIT	6.08	0.35	2.22	1.36	0.02	3.15	1.90	0.69	0.11	15.87	*1.92*
BA08GS004	c	HMG	MIT	5.88	0.24	2.69	1.35	0.01	3.05	1.96	0.63	0.09	15.90	*2.12*
BA08GS004	r	HMG	MIT	5.97	0.26	2.54	1.31	0.01	3.10	1.92	0.61	0.13	15.87	*2.03*
BA08GS011	c	HMG	MIT	5.94	0.25	2.60	1.33	0.01	3.11	1.87	0.64	0.13	15.89	*2.06*
BA08GS011	r	HMG	MIT	5.97	0.28	2.61	1.36	0.02	2.93	1.88	0.63	0.13	15.82	*2.03*
BA08GS029	r	HMG	MIT	5.99	0.26	2.47	1.31	0.01	3.18	1.91	0.64	0.13	15.90	*2.01*
BA08GS029	c	HMG	MIT	5.94	0.27	2.58	1.32	0.01	3.10	1.86	0.66	0.15	15.90	*2.06*
BA08GS029	r	HMG	MIT	5.98	0.26	2.45	1.37	0.02	3.13	1.94	0.64	0.13	15.92	*2.02*
BA08GS029	c	HMG	MIT	6.01	0.27	2.49	1.25	0.01	3.19	1.85	0.71	0.09	15.87	*1.99*
BA08GS009	c	HMG Clot	Tas	5.96	0.32	2.29	1.76	0.03	2.96	1.87	0.59	0.13	15.93	*2.04*
BA08GS009	c	HMG Clot	Tas	5.82	0.24	2.65	1.35	0.02	3.14	1.98	0.73	0.10	16.03	*2.18*

Appendix 2.4 continued

Sample #	Spot Location	Intrusive Phase	Lab Location	Si	Ti	Al	Fe+2	Mn	Mg	Ca	Na	K	Total	*Al (iv)*
BA08GS009	c	HMG Clot	Tas	5.80	0.26	2.68	1.37	0.01	3.12	1.99	0.67	0.10	15.99	*2.20*
BA08GS009	c	HMG Clot	Tas	5.88	0.27	2.55	1.42	0.02	3.13	1.94	0.60	0.14	15.94	*2.12*
BA08GS009	c	HMG Clot	Tas	5.84	0.24	2.67	1.34	0.02	3.14	1.95	0.70	0.09	15.98	*2.16*
BA08GS009	c	HMG Clot	Tas	5.84	0.24	2.67	1.40	0.02	3.09	1.93	0.72	0.09	15.99	*2.16*
BA08GS009	c	HMG Clot	Tas	5.92	0.27	2.53	1.42	0.02	3.09	1.90	0.67	0.14	15.95	*2.08*
BA08GS009	c	HMG Clot	Tas	5.93	0.25	2.58	1.38	0.02	3.10	1.90	0.64	0.13	15.92	*2.07*
BA08GS009	c	HMG Clot	Tas	5.87	0.27	2.54	1.39	0.02	3.13	1.93	0.73	0.15	16.03	*2.13*
BA08GS009	c	HMG Clot	Tas	5.91	0.25	2.53	1.36	0.02	3.18	1.90	0.71	0.12	15.98	*2.09*
BA08GS009	c	HMG Clot	Tas	5.83	0.24	2.69	1.34	0.01	3.14	1.94	0.69	0.11	15.99	*2.17*
BA08GS009	c	HMG Clot	Tas	5.95	0.27	2.48	1.40	0.02	3.13	1.88	0.72	0.13	15.97	*2.05*
BA08GS009	c	HMG Clot	Tas	6.11	0.25	2.28	1.50	0.02	3.04	1.91	0.62	0.15	15.88	*1.89*
BA08GS009	c	HMG Clot	Tas	5.86	0.25	2.66	1.37	0.01	3.11	1.93	0.64	0.10	15.93	*2.14*
BA08GS009	c	HMG Clot	Tas	5.90	0.27	2.55	1.43	0.01	3.11	1.85	0.70	0.13	15.96	*2.10*
BA08GS009	c	HMG Clot	Tas	5.90	0.24	2.58	1.42	0.01	3.14	1.87	0.70	0.13	15.98	*2.10*
BA08GS009	c	HMG Clot	Tas	5.78	0.25	2.72	1.37	0.01	3.13	1.98	0.64	0.10	15.98	*2.22*
BA08GS009	c	HMG Clot	Tas	5.79	0.25	2.68	1.37	0.01	3.13	2.00	0.69	0.10	16.01	*2.21*
BA08GS009	c	HMG Clot	Tas	5.88	0.28	2.54	1.43	0.02	3.12	1.92	0.67	0.13	15.97	*2.12*
BA08GS009	c	HMG Clot	Tas	5.87	0.26	2.58	1.40	0.02	3.08	1.93	0.71	0.15	16.01	*2.13*
BA08GS009	c	HMG Clot	Tas	5.81	0.26	2.61	1.37	0.01	3.14	1.98	0.72	0.15	16.06	*2.19*
BA08GS009	c	HMG Clot	Tas	5.96	0.27	2.49	1.41	0.02	3.13	1.89	0.61	0.14	15.91	*2.04*
BA08GS010	c	HMG Clot	MIT	5.89	0.24	2.60	1.35	0.01	3.15	1.94	0.67	0.09	15.95	*2.11*
BA08GS010	r	HMG Clot	MIT	5.98	0.30	2.45	1.42	0.01	3.04	1.90	0.66	0.12	15.89	*2.02*
BA08GS010	c	HMG Clot	MIT	5.90	0.24	2.66	1.36	0.01	3.03	1.96	0.64	0.09	15.90	*2.10*
BA08GS010	r	HMG Clot	MIT	6.28	0.33	1.97	1.43	0.04	3.19	1.77	0.72	0.10	15.82	*1.72*
BA08GS010	c	HMG Clot	MIT	5.89	0.24	2.66	1.34	0.01	3.10	1.94	0.64	0.09	15.91	*2.11*
BA08GS010	r	HMG Clot	MIT	5.99	0.27	2.50	1.38	0.02	3.07	1.87	0.68	0.13	15.90	*2.01*
BA08GS010	c	HMG Clot	MIT	5.82	0.25	2.67	1.35	0.01	3.19	1.93	0.65	0.09	15.97	*2.18*
BA08GS010	r	HMG Clot	MIT	5.98	0.27	2.51	1.39	0.01	3.03	1.92	0.63	0.13	15.88	*2.02*
BA08GS010	c	HMG Clot	MIT	5.90	0.25	2.62	1.32	0.01	3.12	1.94	0.67	0.09	15.93	*2.10*
BA08GS010	r	HMG Clot	MIT	5.97	0.27	2.54	1.38	0.02	3.10	1.84	0.61	0.13	15.86	*2.03*
BA08GS047	c	HCB	MIT	6.14	0.13	2.30	1.02	0.01	3.70	1.88	0.61	0.16	15.96	*1.86*
BA08GS047	r	HCB	MIT	6.16	0.18	2.31	1.26	0.01	3.34	1.87	0.57	0.17	15.87	*1.84*
BA08GS047	c	HCB	MIT	6.27	0.14	2.24	1.01	0.01	3.58	1.84	0.58	0.17	15.84	*1.73*
BA08GS047	r	HCB	MIT	6.16	0.16	2.34	1.30	0.02	3.31	1.85	0.60	0.17	15.90	*1.84*
BA08GS047	c	HCB	MIT	6.09	0.25	2.39	1.47	0.02	2.97	1.89	0.59	0.17	15.84	*1.91*
BA08GS047	r	HCB	MIT	6.61	0.17	1.83	1.40	0.03	3.20	1.82	0.40	0.11	15.57	*1.39*
BA08GS047	c	HCB	MIT	6.25	0.13	2.29	1.09	0.01	3.49	1.84	0.57	0.17	15.84	*1.75*
BA08GS047	r	HCB	MIT	6.35	0.17	2.08	1.25	0.01	3.41	1.85	0.48	0.15	15.75	*1.65*
BA08GS047	c	HCB	MIT	6.16	0.21	2.33	1.54	0.02	2.97	1.88	0.59	0.15	15.84	*1.84*
BA08GS047	r	HCB	MIT	6.22	0.19	2.28	1.54	0.02	2.99	1.84	0.57	0.14	15.80	*1.78*
BA08GS047	c	HCB Clot	MIT	6.19	0.18	2.31	1.56	0.03	2.94	1.91	0.61	0.12	15.85	*1.81*
BA08GS047	c	HCB Clot	MIT	6.16	0.18	2.41	1.62	0.03	2.85	1.91	0.50	0.10	15.76	*1.84*
BA08GS047	c	HCB Clot	MIT	5.98	0.19	2.53	1.42	0.01	3.11	1.96	0.60	0.13	15.93	*2.02*
BA08GS047	c	HCB Clot	MIT	6.06	0.17	2.47	1.52	0.02	2.97	1.94	0.63	0.12	15.91	*1.94*
BA08GS047	c	HCB Clot	MIT	6.09	0.18	2.50	1.69	0.03	2.73	1.93	0.54	0.12	15.81	*1.91*
BA08GS047	c	HCB Clot	MIT	6.19	0.19	2.39	1.60	0.03	2.80	1.91	0.50	0.13	15.74	*1.81*
BA08GS047	c	HCB Clot	Tas	6.23	0.17	2.34	1.44	0.03	3.02	1.97	0.34	0.11	15.65	*1.77*
BA08GS047	c	HCB Clot	Tas	6.02	0.19	2.55	1.46	0.02	2.96	1.94	0.64	0.12	15.90	*1.98*
BA08GS047	c	HCB Clot	Tas	6.04	0.17	2.61	1.59	0.03	2.81	1.92	0.53	0.14	15.83	*1.96*
BA08GS047	c	HCB Clot	Tas	6.01	0.17	2.53	1.43	0.02	3.05	1.96	0.66	0.13	15.96	*1.99*
BA08GS047	c	HCB Clot	Tas	6.00	0.16	2.57	1.47	0.02	3.01	1.98	0.56	0.14	15.91	*2.00*
BA08GS047	c	HCB Clot	Tas	6.06	0.17	2.53	1.40	0.03	3.02	1.95	0.61	0.11	15.87	*1.94*
BA08GS047	c	HCB Clot	Tas	6.00	0.19	2.61	1.43	0.02	2.95	1.96	0.57	0.16	15.88	*2.00*
BA08GS047	c	HCB Clot	Tas	6.08	0.18	2.52	1.70	0.03	2.70	1.91	0.59	0.15	15.86	*1.92*
BA08GS047	c	HCB Clot	Tas	6.02	0.17	2.50	1.49	0.02	3.00	1.96	0.67	0.12	15.95	*1.98*

Appendix 2.5 – Major element oxide composition for rim and core spot analyses of plagioclase of the Black Mountain Southeast Intrusive Suite. (r = phenocryst rim analyses; c = phenocryst core analysis; all values in wt%)

Sample #	Spot Location	Intrusive Phase	Lab Location	SiO_2	TiO_2	Al_2O_3	FeO	MnO	MgO	CaO	Na_2O	K_2O	Total
BA08GS026	c	pre-BMP	Tas	51.52	0.03	30.22	0.03	0.05	0.00	12.59	4.36	0.25	99.06
BA08GS026	c	pre-BMP	Tas	55.40	0.00	28.38	0.06	0.00	0.11	9.42	5.14	0.35	98.87
BA08GS026	c	pre-BMP	Tas	53.81	-0.01	29.16	0.14	0.02	0.03	10.23	4.79	0.39	98.57
BA08GS026	c	pre-BMP	Tas	52.67	-0.01	29.89	0.08	0.02	-0.01	11.53	4.75	0.37	99.29
BA08GS026	c	pre-BMP	Tas	57.07	0.00	26.84	0.15	0.01	0.01	8.23	6.53	0.22	99.06
BA08GS026	r	pre-BMP	Tas	56.95	-0.02	26.95	0.05	0.01	0.03	8.20	6.04	0.26	98.48
BA08GS038	c	pre-BMP	Tas	52.94	0.01	29.00	0.12	0.03	0.00	9.98	5.08	0.20	97.36
BA08GS038	r	pre-BMP	Tas	51.34	0.04	30.22	0.29	0.03	0.01	11.68	4.19	0.19	97.98
353226	c	LLC	Tas	47.40	0.05	33.69	0.68	0.02	0.08	16.29	1.97	0.08	100.27
353226	c	LLC	Tas	61.20	0.03	24.36	0.15	0.04	0.02	3.41	6.69	4.01	99.90
353226	r	LLC	Tas	58.82	-0.01	26.15	0.35	-0.01	0.01	6.83	5.59	2.53	100.24
353226	c	LLC	Tas	45.42	0.03	35.22	0.68	-0.01	0.06	17.59	0.99	0.02	99.99
353226	r	LLC	Tas	65.41	0.01	22.39	0.14	-0.01	0.00	2.29	9.98	0.13	100.34
353226	c	LLC	Tas	44.73	-0.03	36.07	0.47	0.01	0.04	18.19	1.07	0.02	100.57
353226	r	LLC	Tas	43.12	0.04	22.77	3.15	0.09	0.00	25.90	0.05	0.06	95.17
353226	c	LLC	Tas	45.34	0.00	35.77	0.68	0.03	0.09	17.95	1.44	0.07	101.37
353226	r	LLC	Tas	47.25	0.01	34.24	0.64	-0.01	0.06	16.47	2.12	0.07	100.85
BA08GS056	r	LLC	Tas	56.34	0.01	28.52	0.17	0.00	0.02	8.58	6.05	0.66	100.35
354510	c	PHD (Kennon)	Tas	53.19	-0.01	30.58	0.32	0.00	0.31	10.54	4.22	0.69	99.84
354510	r	PHD (Kennon)	Tas	48.78	-0.01	30.15	0.27	0.02	0.03	15.19	3.58	0.22	98.24
354510	c	PHD (Kennon)	Tas	52.41	-0.01	31.05	0.28	-0.02	0.01	12.67	4.39	0.11	100.90
354510	r	PHD (Kennon)	Tas	52.74	0.00	30.68	0.36	0.05	0.02	12.10	4.33	0.09	100.37
354510	c	PHD (Kennon)	Tas	51.04	0.02	31.98	0.17	0.05	0.01	13.63	3.56	0.05	100.51
354510	r	PHD (Kennon)	Tas	51.00	0.00	32.43	0.02	-0.04	0.00	13.88	3.54	0.05	100.88
354510	c	PHD (Kennon)	Tas	50.12	0.00	32.13	0.19	-0.02	-0.01	13.99	3.27	0.14	99.81
354510	r	PHD (Kennon)	Tas	51.04	0.00	31.84	0.16	-0.05	0.01	12.77	3.87	0.11	99.75
354510	c	PHD (Kennon)	Tas	53.61	-0.04	29.31	0.17	0.01	0.00	10.69	4.95	0.14	98.84
354510	r	PHD (Kennon)	Tas	51.27	-0.01	31.70	0.30	0.01	0.03	13.06	3.83	0.12	100.29
354510	c	PHD (Kennon)	Tas	49.70	-0.03	32.44	0.09	0.00	-0.01	14.31	3.33	0.02	99.85
354510	r	PHD (Kennon)	Tas	52.10	-0.01	31.34	0.29	0.04	0.01	12.79	3.95	0.22	100.72
354510	c	PHD (Kennon)	Tas	51.87	0.02	30.92	0.18	0.04	0.01	12.33	4.34	0.07	99.76
354510	r	PHD (Kennon)	Tas	49.07	0.01	33.62	0.09	0.00	-0.01	14.63	2.85	0.36	100.62
BA08GS019	c	PHD	Tas	57.64	0.00	27.65	0.15	-0.03	-0.01	8.57	6.34	0.33	100.62
BA08GS019	r	PHD	Tas	63.60	-0.01	22.90	0.11	-0.01	-0.02	3.36	9.05	0.37	99.35
BA08GS019	c	PHD	Tas	56.66	-0.02	27.89	0.19	-0.04	0.00	9.04	5.87	0.31	99.90
BA08GS019	r	PHD	Tas	56.77	-0.02	27.74	0.19	-0.04	0.00	8.82	6.06	0.26	99.78
BA08GS019	c	PHD	Tas	57.74	-0.02	27.10	0.22	0.00	0.09	7.71	6.33	0.47	99.64
BA08GS019	r	PHD	Tas	63.38	-0.03	22.89	0.16	0.00	0.01	3.36	8.53	0.98	99.28
BA08GS019	c	PHD	Tas	56.53	-0.02	27.87	0.21	-0.02	0.02	8.79	5.95	0.32	99.64
BA08GS019	r	PHD	Tas	58.12	0.00	26.31	0.25	-0.03	0.01	7.64	7.07	0.27	99.64
BA08GS019	c	PHD	Tas	54.92	0.04	29.05	0.11	-0.02	0.01	10.17	5.26	0.25	99.80
BA08GS019	r	PHD	Tas	62.99	0.00	23.25	0.18	0.00	0.02	3.69	8.63	0.59	99.35
BA08GS025	c	PHD	Tas	52.08	0.02	31.32	0.25	0.02	0.02	12.49	3.98	0.15	100.34
BA08GS025	r	PHD	Tas	54.72	-0.01	28.86	0.27	-0.01	0.00	10.21	5.05	0.16	99.24
BA08GS025	c	PHD	Tas	57.11	-0.01	28.03	0.17	-0.01	-0.01	8.65	5.86	0.24	100.04
BA08GS025	r	PHD	Tas	53.68	0.00	29.84	0.16	0.02	0.01	11.04	4.87	0.18	99.79
BA08GS025	c	PHD	Tas	56.59	0.00	27.62	0.34	0.04	0.02	8.62	5.94	0.30	99.46
BA08GS025	r	PHD	Tas	58.26	-0.01	26.68	0.16	0.01	0.01	7.82	7.18	0.29	100.41
BA08GS025	c	PHD	Tas	55.03	0.03	28.82	0.32	0.01	-0.01	10.13	5.72	0.24	100.30
BA08GS025	r	PHD	Tas	56.62	-0.02	27.44	0.19	-0.04	0.02	8.39	6.16	0.22	98.97
BA08GS025	c	PHD	Tas	55.01	-0.01	28.57	0.28	0.01	0.01	9.79	5.63	0.19	99.47
BA08GS025	r	PHD	Tas	57.53	0.01	27.20	0.19	0.03	0.02	8.34	5.95	0.35	99.62
BA08GS030	c	PHD	Tas	54.29	-0.01	30.14	0.17	-0.05	0.00	10.87	5.47	0.14	101.01
BA08GS030	r	PHD	Tas	53.68	0.02	29.97	0.32	0.01	0.01	11.00	4.89	0.04	99.93
BA08GS030	c	PHD	Tas	56.93	-0.01	27.96	0.14	-0.03	0.01	8.77	6.02	0.22	100.00
BA08GS030	r	PHD	Tas	55.54	0.03	28.93	0.25	-0.01	0.02	9.71	5.18	0.14	99.78
BA08GS030	c	PHD	Tas	55.41	0.01	28.39	0.18	-0.03	0.00	9.36	5.56	0.10	98.98
BA08GS030	r	PHD	Tas	57.89	-0.01	27.19	0.08	0.00	0.01	8.24	6.93	0.11	100.44
BA08GS030	c	PHD	Tas	57.00	0.01	28.37	0.19	0.04	0.00	9.01	6.22	0.39	101.22
BA08GS030	c	PHD	Tas	56.70	0.05	27.58	0.12	0.06	0.01	8.68	6.47	0.16	99.82
BA08GS033A	c	PHD	Tas	56.29	0.00	28.81	0.29	-0.05	0.01	9.76	5.74	0.20	101.05
BA08GS033A	r	PHD	Tas	55.76	0.03	28.92	0.20	0.03	0.01	9.99	5.69	0.20	100.83
BA08GS033A	c	PHD	Tas	56.55	0.02	28.09	0.27	0.04	0.01	9.23	5.60	0.29	100.10
BA08GS033A	c	PHD	Tas	54.24	0.01	30.09	0.24	0.00	0.00	10.70	5.23	0.15	100.66
BA08GS033A	r	PHD	Tas	54.75	0.04	29.54	0.22	0.00	0.02	10.47	4.96	0.17	100.17
BA08GS033A	c	PHD	Tas	56.06	0.01	28.08	0.26	0.00	0.01	9.79	5.73	0.19	100.11
BA08GS033A	r	PHD	Tas	59.01	0.00	25.94	0.13	-0.02	0.01	6.66	4.61	3.71	100.05
BA08GS033A	c	PHD	Tas	56.27	-0.02	28.48	0.27	0.01	0.00	9.59	5.77	0.24	100.61
BA08GS033A	r	PHD	Tas	57.31	0.00	27.97	0.22	0.03	0.01	8.74	5.88	0.27	100.42
BA08GS033B	c	PHD	Tas	57.50	0.04	27.67	0.23	0.02	0.00	8.33	6.47	0.36	100.62
BA08GS033B	r	PHD	Tas	56.46	0.03	28.08	0.23	0.01	0.02	8.60	6.30	0.33	100.05
BA08GS033B	c	PHD	Tas	52.50	0.02	31.28	0.30	0.01	0.01	12.61	4.50	0.12	101.34
BA08GS033B	r	PHD	Tas	56.01	0.00	28.96	0.22	-0.01	0.00	9.70	5.44	0.25	100.57
BA08GS033B	c	PHD	Tas	58.13	-0.01	27.18	0.24	0.00	0.01	8.44	6.65	0.28	100.92
BA08GS033B	r	PHD	Tas	54.88	0.02	29.66	0.26	0.05	0.02	10.66	4.90	0.22	100.67
BA08GS033B	c	PHD	Tas	52.40	0.02	31.17	0.34	0.01	0.00	12.29	3.96	0.21	100.39
BA08GS033B	r	PHD	Tas	57.54	0.04	27.44	0.18	0.03	-0.01	8.31	6.47	0.24	100.25

Appendix 2.5 continued

Sample #	Spot Location	Intrusive Phase	Lab Location	SiO_2	TiO_2	Al_2O_3	FeO	MnO	MgO	CaO	Na_2O	K_2O	Total
BA08GS033B	c	PHD	Tas	55.76	0.01	28.43	0.27	-0.02	0.00	9.57	5.64	0.28	99.94
BA08GS033B	r	PHD	Tas	55.29	0.01	29.07	0.20	-0.01	0.00	10.06	5.37	0.23	100.21
BA08GS036	c	PHD	Tas	57.55	-0.02	27.42	0.15	0.02	0.01	8.34	6.38	0.26	100.11
BA08GS036	r	PHD	Tas	53.42	0.00	30.14	0.12	0.01	0.00	11.25	4.75	0.19	99.86
BA08GS036	c	PHD	Tas	57.55	-0.02	26.90	0.15	-0.02	0.02	7.88	6.44	0.28	99.18
BA08GS047	c	HCB	Tas	43.42	-0.02	35.60	0.60	0.03	0.05	18.46	0.91	-0.01	99.04
BA08GS047	r	HCB	Tas	54.08	0.03	28.98	0.33	0.05	0.04	9.06	4.52	1.36	98.44
BA08GS047	c	HCB	Tas	43.43	0.00	36.20	0.51	0.01	0.00	19.04	0.66	0.02	99.85
BA08GS047	r	HCB	Tas	43.43	-0.02	36.20	0.53	0.02	0.02	19.36	0.63	0.03	100.20
BA08GS047	c	HCB	Tas	45.91	0.02	34.49	0.54	0.00	0.00	17.16	1.64	0.06	99.80
BA08GS047	r	HCB	Tas	44.92	0.02	35.76	0.52	0.01	0.02	18.58	0.69	0.03	100.56
354019	c	Andesite dike	Tas	56.90	0.03	27.72	0.15	0.00	0.01	8.47	6.33	0.23	99.84
354019	r	Andesite dike	Tas	50.65	0.00	23.47	0.13	0.00	0.05	5.68	5.98	0.21	86.18
354019	c	Andesite dike	Tas	54.22	-0.04	25.12	0.18	0.01	0.00	6.94	6.48	0.26	93.17
354019	r	Andesite dike	Tas	56.64	-0.02	26.63	0.07	-0.01	0.01	8.30	6.44	0.23	98.29
354019	c	Andesite dike	Tas	55.36	-0.01	28.22	0.17	0.00	0.01	9.35	5.77	0.20	99.06
354019	r	Andesite dike	Tas	55.64	0.01	27.19	0.14	0.01	0.01	8.71	6.28	0.27	98.25
354019	c	Andesite dike	Tas	44.15	0.03	24.21	0.09	-0.01	0.02	6.82	4.51	0.14	79.96
354019	r	Andesite dike	Tas	56.32	0.00	27.58	0.15	-0.03	0.02	9.09	5.82	0.22	99.17
354019	c	Andesite dike	Tas	66.36	-0.01	19.92	0.02	0.01	0.02	0.23	10.31	0.03	96.89
354019	r	Andesite dike	Tas	59.73	0.00	22.87	0.30	-0.01	0.31	0.50	7.76	2.24	93.71

Appendix 2.6 – Individual laser ablation-inductively coupled plasma mass spectrometry spot analyses of epidote (LA-ICPMS) used for this thesis. A "Year Analyzed" of 2008 indicates newly generated data; a "Year Analyzed" of 2006 indicates data generated during AMIRA P765. Blank spaces represent either below detection limit values, or elements not measured for that particular analysis run. All values for the newly collected data are reported in ppm. Calcium and aluminum values for P765 data are reported in wt%; the remaining elements are reported in ppm. (rep = replacement epidote; skarn assoc. = skarn associated epidote)

Sample #	Year Analyzed	Year Collected	Epi Type	Na	Mg	Al	K	Ca	Ti	V	Mn	Fe	Cu	Zn	Ga	As	Sr	Y	Zr	Mo	Sn	Sb	Ba	La	Ce	Pr	Nd	Sm	Eu	Gd	Dy	Er	Yb	Lu	Pb	Bi	Th	U
BA08GS019	2008	2008	rep	143	302	118494	5	160000	319	327	1431	105600	14.46	2.24	44.21	25.30	901.26	30.45	2.97		2.02	216.39	0.46	7.23	16.78	2.20	10.26	2.75	2.86	3.14	5.12	3.90	2.74	0.38	13.01	10.85	1.16	2.67
BA08GS019	2008	2008	rep	538	221	119422	12	160000	342	643	2019	99666	2.06	2.21	51.39	11.22	1296.32	6.78	0.79		1.80	19.41	0.93	4.83	7.88	0.99	3.04	0.54	1.05	0.72	0.98	0.65	1.04	0.15	7.62	7.06	0.15	0.52
BA08GS019	2008	2008	rep		121	109111	5	160000	44	9	690	123764		0.98	26.72	10.73	578.06	0.44			1.38	13.63	0.70	2.74	3.11	0.24	0.58	0.09	0.56		0.06	0.07		0.01	0.60	3.24		0.15
BA08GS019	2008	2008	rep	390	344	114135	24	160000	434	402	2337	120958	0.89	1.43	32.88	6.42	1451.89	19.69	0.62		2.62	4.40	1.79	50.34	113.53	14.21	62.23	13.12	6.90	10.99	5.13	1.62	1.54	0.26	5.08	4.67	0.24	1.63
BA08GS019	2008	2008	rep		255	104111		160000	256	58	472	137599		1.05	31.11	8.07	349.03	5.43	0.61		0.82	0.53	0.16	4.09	7.81	1.01	4.17	1.15	1.14	1.03	0.98	0.56	0.56	0.08		1.85	0.07	0.59
BA08GS019	2008	2008	rep		326	126963		160000	986	619	3541	98522	9.67	2.80	86.17	11.09	1978.86	3.19	4.43		1.84	43.38	0.91	10.97	18.49	1.87	6.56	1.02	1.45	0.77	0.64	0.38	0.38	0.05	30.90	17.82	0.09	0.29
BA08GS019	2008	2008	rep	98	224	118939	348	160000	202	66	1279	108548		1.71	36.75	37.13	1670.86	22.33	0.55		0.95	144.52	12.96	12.25	25.61	3.09	14.20	3.25	3.54	4.16	4.06	2.58	2.46	0.40	1.93	12.22	0.20	0.98
BA08GS019	2008	2008	rep		235	105063		160000	250	126	474	138986		1.25	48.59	1.69	478.72	12.08	0.15		0.68	0.41	0.18	6.39	13.47	1.75	7.94	2.19	2.62	2.45	2.26	1.23	0.93	0.11	0.57	1.65	0.06	0.56
BA08GS019	2008	2008	rep	21	510	103277	27	160000	2953	165	961	131559		3.68	44.48	13.34	498.50	89.06	2.66		1.07	9.88	2.19	78.02	238.65	34.96	159.80	37.74	5.32	30.71	21.05	7.58	4.58	0.50	0.68	4.25	2.40	1.58
BA08GS019	2008	2008	rep		300	107141		160000	317	92	1169	135769		1.58	44.12	5.06	693.46	7.63	0.28		0.83	1.70	0.62	4.10	5.73	0.61	2.22	0.59	2.15	0.76	1.21	1.00	0.91	0.11	0.80	3.45	0.06	0.70
BA08GS019	2008	2008	rep		529	117663	40	160000	163	98	3192	120477	1.11	1.65	51.73	44.71	1233.12	13.72	0.61		1.65	7.24	2.68	8.76	14.97	1.78	7.61	1.90	5.02	2.07	2.24	1.70	1.80	0.37	1.51	8.14	4.49	2.64
BA08GS026	2008	2008	vein		618	132901		168000	44	26	1234	92293		6.13	35.84	13.78	1072.87	0.14	0.09			3.91	0.51	4.65	4.66	0.32	0.79		0.50						12.59		0.11	0.05
BA08GS026	2008	2008	vein	111	1100	141890	150	168000	83	25	2566	65601		9.91	30.37	10.93	549.48	0.30	0.84		0.49	2.65	1.64	9.23	11.02	0.75	2.04	0.25	0.48	0.09	0.06				4.26	0.10	0.18	0.12
BA08GS026	2008	2008	vein	156	826	133331	12	168000	33	4	1187	82467		11.01	27.59	19.84	655.08	0.11				1.81	0.94	6.12	6.58	0.42	1.18		0.37	0.09					10.33	0.07		
BA08GS026	2008	2008	vein	515	820	138937	23	168000	281	112	1675	77033		12.36	37.00	8.19	772.58	0.78	10.11			4.07	1.19	8.25	10.61	0.79	2.36	0.27	0.58	0.27	0.18	0.07	0.11	0.02	13.04		5.90	0.51
BA08GS026	2008	2008	vein	283	977	124167	13	168000	82	246	806	102981		12.15	50.88	25.07	682.57	0.48	0.10		0.36	3.29	1.03	4.53	5.07	0.39	0.99	0.15	0.65		0.07	0.04	0.09		27.07	0.11		0.08
BA08GS026	2008	2008	vein		687	126479	7	168000	51	191	877	104129		8.77	64.86	20.81	882.49	0.42	0.51		0.42	3.61	0.56	5.31	6.39	0.49	1.29	0.11	0.43	0.09	0.11				42.76	0.14		0.12
BA08GS026	2008	2008	vein	416	725	131476	24	168000	46	73	1559	96665		7.05	44.89	49.09	1044.47	0.08	0.09		0.47	2.25	2.08	5.42	6.35	0.44	1.03		0.44						15.86	0.10		0.05
BA08GS026	2008	2008	vein	885	814	135619	3596	168000	250	340	1315	96057		12.93	54.74	23.77	1270.30	3.90	1.57		0.62	5.81	88.75	8.80	11.53	1.03	3.40	0.40	1.35	0.64	0.60	0.29	0.32	0.04	42.95	0.13	0.67	0.89
BA08GS026	2008	2008	vein	178	855	129523	18	168000	33	20	2279	105163		7.17	45.90	66.40	1110.41	0.05				1.81	1.18	5.63	6.32	0.40	1.14	0.11	0.44						13.12	0.16		
BA08GS026	2008	2008	vein		613	128902		168000	23	44	3417	109477		6.23	46.29	56.39	1442.62	0.04				0.41	0.55	3.56	3.64	0.24	0.63		0.43						14.00	0.08		
BA08GS026	2008	2008	vein	55	898	133100	13	168000	29	11	1035	90345		13.48	26.67	28.81	547.06					1.99	1.56	5.32	5.52	0.34	0.58		0.36						8.30			
BA08GS026	2008	2008	vein	24	782	132164		168000	56	124	1634	88113		9.34	36.06	33.72	1158.60	0.47	0.07		0.42	1.64	2.00	8.27	9.44	0.74	1.93	0.21	0.83	0.19	0.10	0.05	0.06		14.89	0.08		0.17
BA08GS026	2008	2008	vein	141	748	128663	99	168000	29	52	1924	101618		23.40	38.31	35.44	1072.20	1.48			0.35	6.20	1.77	17.46	22.81	1.96	7.01	0.98	0.76	0.70	0.38	0.11		0.01	16.66	0.10		0.36
BA08GS026	2008	2008	vein	26	804	130276		168000	75	52	777	94105		6.27	35.43	5.95	321.36	0.44				0.22	0.13	2.51	2.89	0.19	0.55		0.42			0.07	0.07		4.29			0.27
BA08GS026	2008	2008	vein		993	135395		168000	23	52	1626	85541		11.67	33.50	14.33	691.44	0.05				1.34	0.47	4.74	5.22	0.37	0.94	0.10	0.35						8.14			
BA08GS026	2008	2008	vein	27	737	134699		168000	26	7	1300	88527		9.53	26.57	26.40	975.68	0.04			0.38	2.14	0.85	3.79	3.91	0.23	0.51		0.36						11.98			
BA08GS026	2008	2008	vein	27	710	133147	47	168000	43	118	1894	92136		8.77	38.66	24.18	1100.50	0.58	0.06			1.94	1.64	2.63	2.97	0.26	0.94	0.24	0.46	0.16	0.12	0.07			9.45	0.08	0.03	0.19
BA08GS026	2008	2008	vein		596	131265	6	168000	24	16	949	99464		9.71	32.95	16.66	706.10	0.09			0.37	2.38	0.69	2.18	2.52	0.18	0.44		0.30						8.90			
BA08GS026	2008	2008	vein	341	759	135954	21	168000	46	20	1678	90503		8.70	31.53	11.93	841.04	0.13	0.38			1.38	1.35	6.50	7.30	0.55	1.21		0.50						10.44		0.05	0.09
BA08GS026	2008	2008	vein	1178	830	134337	354	168000	61	21	1349	94240		8.21	32.29	34.17	842.02	0.13	0.43		0.56	0.97	5.71	8.33	10.04	0.78	1.54	0.10	0.45		0.12		0.06		10.92	0.13	0.32	0.04
BA08GS026	2008	2008	vein	51	792	138532	17	168000	29	6	1090	76432		10.16	23.59	8.13	779.14	0.22			0.54	2.13	0.82	9.10	9.55	0.61	1.62	0.09	0.51						9.60			0.06
BA08GS026	2008	2008	vein	34	854	138183	8	168000	57	18	1623	74593		10.34	29.82	10.00	753.77	0.11	0.10		0.36	5.40	0.84	4.72	5.17	0.33	1.10	0.13	0.46						7.61			0.10
BA08GS026	2008	2008	vein		600	128875	10	168000	38	112	1285	101744	0.75	9.87	44.45	15.28	1023.81	0.18	0.35			2.69	0.64	3.29	3.90	0.25	0.70		0.38	0.08					13.28	0.07		0.17
BA08GS026	2008	2008	vein	267	682	127854	32	168000	80	151	1071	100348		14.87	51.55	21.24	906.39	3.96	0.44		0.37	4.89	2.68	30.33	44.01	4.06	13.20	1.96	1.34	1.58	0.92	0.31	0.22	0.03	31.20	0.18	0.02	0.67
BA08GS026	2008	2008	vein	46	777	138504	454	168000	39	42	3114	93229		7.81	43.15	69.30	1479.45	3.36				2.79	2.68	42.88	50.48	4.24	15.43	2.92	2.85	2.43	0.97	0.23	0.15	0.02	16.35	0.25		1.10
BA08GS026	2008	2008	vein		752	142278	263	168000	41	4	1404	72735		10.13	26.57	10.57	1030.15	0.10				1.73	2.27	4.67	4.96	0.32	0.89	0.10	0.38						8.90			
BA08GS026	2008	2008	vein		1179	131039		168000	49	25	1274	99341		14.97	37.34	17.00	1035.22	0.23	0.64			2.89	0.70	5.54	6.61	0.52	1.48	0.13	0.57	0.08					11.44	0.07		0.07
BA08GS026	2008	2008	vein		468	132391		168000	25	46	762	95294		4.47	32.46	9.24	490.52				0.42	0.27		1.80	1.97	0.12	0.30		0.28						3.90			
BA08GS026	2008	2008	vein	1441	723	135559	50	168000	33	35	2343	98161		8.82	44.97	67.14	1194.12	0.17	0.05		0.36	1.00	3.08	3.75	4.01	0.26	0.74		0.39						30.19	0.15		0.04
BA08GS026	2008	2008	vein	396	881	123022	30	168000	23	48	1393	94772	0.83	9.91	40.04	55.90	875.73	0.15				1.55	1.55	5.66	6.41	0.45	1.35	0.11	0.49						13.63	0.16		0.05
BA08GS033A	2008	2008	skarn assoc.	4055	302	132167	1157	165000	124	234	1990	106365	0.71	4.58	71.62	2.38	789.12	18.15	0.26		15.81	0.99	24.56	13.40	16.02	1.54	5.69	1.10	8.72	2.05	2.50	2.06	2.08	0.38	3.28	1.38	0.01	29.05
BA08GS033A	2008	2008	skarn assoc.	105	410	114569	31	165000	40	40	1205	120238	0.61	3.27	49.34	1.12	464.30	0.64			1.56	0.21	6.95	5.07	8.21	0.76	2.49	0.38	0.41	0.13	0.13	0.04	0.06		3.08	1.09		0.05
BA08GS033A	2008	2008	skarn assoc.	20	1387	132711	341	165000	70	123	5134	115878	2.00	6.28	53.96	17.66	1464.78	1.72	1.61		2.42	1.29	44.09	8.55	16.12	1.79	6.94	0.97	0.78	0.66	0.34	0.17	0.16	0.02	11.10	3.53	0.07	0.14
BA08GS033A	2008	2008	skarn assoc.		738	123168	10	165000	79	128	1872	112950		6.60	47.30	5.02	546.74	2.95	0.32		1.92	1.75	9.41	5.72	10.04	1.02	4.23	0.88	0.85	0.68	0.42	0.34	0.50	0.06	4.15	3.55		1.96
BA08GS033A	2008	2008	skarn assoc.		603	128855	156	165000	415	524	3566	111253	3.26	6.99	68.58	1.90	1142.87	59.03	0.85		31.51	0.29	13.25	25.15	37.19	3.99	16.71	4.39	15.00	6.21	8.79	6.86	7.23	1.12	4.36	1.99		45.88
BA08GS033A	2008	2008	skarn assoc.		1804	118738	126	165000	837	434	1645	124648		12.46	72.06	4.17	832.32	36.46	7.53		5.53	1.50	10.78	102.36	160.25	16.98	67.76	13.02	9.53	12.12	7.66	2.69	1.59	0.22	7.67	3.13	1.36	12.06
BA08GS033A	2008	2008	skarn assoc.	36	788	121008		165000	511	305	3263	120443		9.00	56.16	5.06	981.26	31.32	33.70		1.83	1.88	32.40	54.34	94.76	10.17	41.56	8.74	2.51	7.12	6.42	2.48	1.86	0.25	9.28	14.04	8.80	4.40
BA08GS033B	2008	2008	skarn assoc.	143	6027	117047	2782	161000	2624	1168	1830	117055		17.42	69.99	2.63	598.44	59.92	29.21		2.14	0.46	17.94	64.40	128.71	14.69	61.10	11.68	4.98	12.32	10.14	5.45	4.47	0.60	3.45	2.20	8.13	13.00
BA08GS033B	2008	2008	skarn assoc.		882	125111		161000	1090	946	2784	93908		7.50	71.62	4.29	762.59	153.33	44.65		8.68	0.88	9.66	252.78	440.57	47.73	188.95	32.59	15.08	30.12	23.61	14.76	15.38	2.45	3.41	2.65	23.06	36.22
BA08GS033B	2008	2008	skarn assoc.		594	124818		161000	1921	604	1401	88498		3.79	50.72	3.06	997.16	32.63	18.36		2.88	1.52	31.29	21.13	38.88	4.14	18.12	4.06	2.68	4.68	4.78	3.22	2.99	0.43	4.60	1.93	4.59	7.14
BA08GS033B	2008	2008	skarn assoc.		1053	122798		161000	828	609	4960	110131		7.77	65.73	3.62	1135.76	16.00	23.26		3.37	0.66	31.13	35.72	50.12	4.67	16.19	2.86	2.89	2.38	2.53	1.54	2.12	0.34	3.36	12.03	4.85	6.64
BA08GS033B	2008	2008	skarn assoc.	177	1071	121123		161000	883	597	5013	108437		7.78	69.64	2.98	1074.67	12.92	27.35		4.10	0.77	22.20	21.51	33.04	3.24	11.73	2.13	1.84	2.13	2.16	1.30	1.77	0.30	3.26	8.13	3.99	4.18
BA08GS033B	2008	2008	skarn assoc.		920	115841		161000	1761	1250	1581	106982		6.75	78.53	1.93	468.59	28.72	20.21		6.29	0.18	4.68	31.22	49.36	5.01	19.55	4.12	6.09	4.79	4.96	2.89	2.55	0.28	3.85	2.09	6.65	17.63
BA08GS035	2008	2008	vein	120	11977	117641	50	163000	2526	932	2618	128258	1.23	45.43	76.47	25.28	1075.40	90.12	3.00		2.34	6.19	5.92	42.22	88.25	10.86	50.47	12.37	11.91	14.68	14.96	8.72	6.77	0.94	26.08	0.52	0.16	3.64
BA08GS035	2008	2008	vein	324	740	115520	30	163000	1666	269	2195	115686	0.94	13.44	43.96	19.69	724.14	13.13	9.71		0.83	1.99	7.55	10.47	16.31	1.84	8.42	1.94	1.59	2.22	2.17	1.29	1.09	0.15	49.66	0.35	0.31	0.88
BA08GS035	2008	2008	vein	407	582	112872	147	163000	86	149	2050	122408		10.23	27.64	16.87	655.99	3.19	1.01			1.01	6.34	2.94	3.62	0.41	1.35	0.25	0.65	0.57	0.48	0.37	0.27	0.05	38.91	0.07		0.16
BA08GS035	2008	2008	vein	333	708	110842	42	163000	171	177	1983	125902		17.90	25.52	19.84	535.30	0.95	0.65		0.36	0.73	9.37	0.99	1.81	0.22	0.77	0.28	0.40	0.20	0.17	0.12	0.13	0.01	26.60	0.11	0.03	0.07
BA08GS035	2008	2008	vein	169	341	120038	55	163000	193	305	3209	108647	0.85	24.81	44.54	23.96	930.50	11.44	3.12		0.75	6.23	7.72	4.03	7.79	0.89	4.58	1.17	1.25	1.73	2.00	1.35	0.90	0.17	39.63	0.45		0.62
BA08GS035	2008	2008	vein	268	1235	114592	53	163000	165	247	2469	119146	0.87	23.31	33.57	20.27	691.11	8.89	1.57		0.57	1.47	9.70	10.51	20.46	2.34	11.21	2.47	1.54	2.58	1.84	0.78	0.55	0.06	42.52	0.20	0.04	0.57
BA08GS035	2008	2008	vein	307	397	117252	24	163000	186	174	2853	109924		11.73	29.07	19.14	952.61	9.43	2.74			2.05	6.25	3.00	6.03	0.72	3.62	0.95	0.97	1.26	1.52	1.13	1.01	0.11	18.38	0.14	0.07	0.48
BA08GS035	2008	2008	vein	338	2605	113205	36	163000	737	400	2974	116499	0.93	20.39	40.58	13.80	941.65	31.19	33.83		0.75	2.91	7.18	25.47	52.01	6.86	31.93	8.67	5.91	8.70	6.57	2.69	2.32	0.35	23.60	0.37	1.38	2.15
BA08GS035	2008	2008	vein	50	576	110276	19	163000	331	267	1750	122351		10.64	33.45	8.59	835.12	4.64	0.83			1.97	9.39	1.14	2.28	0.30	1.49	0.47	1.17	0.73	0.85	0.50	0.36	0.07	38.57	0.15		0.33
BA08GS035	2008	2008	vein	185	4459	110874	56	163000	6549	388	2714	115431	3.30	33.01	33.53	15.81	747.08	20.75	23.81		1.24	2.42	8.92	6.87	13.57	1.76	8.91	2.65	2.29	3.46	3.72	2.00	1.91	0.25	36.09	0.60	0.70	0.99
BA08GS035	2008	2008	vein	89	190	120816	53	163000	435	2122	2436	100181	6.53	18.10	73.30	20.13	964.23	58.28	2.76		1.99	6.91	2.22	14.05	33.86	5.66	32.46	9.63	14.71	11.00	9.65	5.36	4.98	0.77	45.04	0.02	0.14	1.51
BA08GS035	2008	2008	vein	673	457	115947	23	163000	174	260	1977	114178		11.43	42.36	21.61	731.73	5.51	5.25		0.35	2.56	5.73	3.49	7.87	0.96	4.49	0.94	0.54	1.13	1.11	0.67	0.70	0.09	29.62	0.22		0.42
BA08GS035	2008	2008	vein	39	1361	110467	14	163000	7747	160	3315	118676		9.67	27.57	16.60	649.93	15.45	96.32		1.38	1.51	4.51	2.39	5.06	0.85	4.93	2.37	0.90	2.31	3.04	1.71	2.01	0.31	10.29	0.12	0.39	0.87
BA08GS035	2008	2008	vein	62	343	110288		163000	22	142	1948	129584		4.34	39.32	9.01	576.90	2.26	0.09			0.65	4.00	4.29	8.59	1.08	5.41	1.36	0.55	0.88	0.46	0.16	0.06	0.02	30.31	0.15		0.13
BA08GS035	2008	2008	vein	197	444	113202	5	163000	59	225	2449	119508		6.13	40.46	16.46	733.48	2.67	0.43			1.88	8.39	2.27	4.88	0.62	3.08	0.55	0.56	0.74	0.49	0.28	0.17	0.03	44.58	0.20		0.19
BA08GS035	2008	2008	vein	233	448	120352		163000	134	331	2819	105937	0.81	6.53	39.60	18.84	982.61	18.84	0.75		0.99	3.96	7.85	34.70	78.01	10.17	49.92	10.31	4.02	8.47	4.95	1.74	1.12	0.15	32.76	0.51	0.24	1.24
BA08GS035	2008	2008	vein	155	492	116331	8	163000	139	212	3403	119718	0.66	7.12	32.04	15.09	770.93	9.42	1.54	0.20	0.89	0.64	6.05	7.42	16.31	2.14	10.17	2.43	1.42	2.29	1.90	0.90	0.81	0.10	22.33	0.11	0.04	0.60
BA08GS035	2008	2008	vein	168	4343	117468	62	163000	513	846	2444	115195		17.27	63.38	19.65	948.15	13.82	2.17		1.05	4.62	3.75	2.08	4.20	0.61	3.11	1.00	1.52	1.38	2.05	1.38	1.69	0.21	37.29	0.13	0.03	0.76
BA08GS035	2008	2008	vein	281	1010	118742	52	163000	2965	1076	2605	102220	0.76	13.17	59.25	12.24	1013.44	36.50	10.92		1.44	8.02	4.02	7.48	16.04	2.25	11.16	3.43	3.65	4.42	5.53	3.75	3.77	0.50	38.04	0.11	0.30	2.01
BA08GS035	2008	2008	vein	73	3197	116574	57	163000	543	675	3787	113700	0.72	27.53	61.69	10.10	884.25	9.25	2.15		0.82	2.20	4.89	1.73	3.66	0.54	2.98	0.72	1.31	1.40	1.47	0.91	0.92	0.12	13.21	0.20	0.04	0.69
BA08GS035	2008	2008	vein	457	1438	116863	16	163000	86	85	1547	116432		8.67	23.06	17.92	584.34	3.78	0.78			1.49	5.77	7.88	17.39	2.26	10.15	2.28	1.05	1.79	1.11	0.31	0.14	0.02	22.06	0.11	0.06	0.21
BA08GS035	2008	2008	vein	243	483	119865	8	163000	119	153	3269	108039		7.57	34.36	22.68	979.56	17.28	0.80		0.66	1.36	13.14	11.44	21.58	2.74	13.54	4.03	4.53	5.08	4.49	1.44	0.75	0.10	54.13	0.23		1.36
BA08GS035	2008	2008	vein	486	6063	115556	102	163000	317	257	3547	110741		35.44	35.94	18.82	923.29	10.84	5.07		0.82	5.09	8.18	5.18	10.90	1.38	6.52	1.57	1.63	1.85	2.12	1.01	1.22	0.17	32.87	0.39	0.35	0.67
BA08GS035	2008	2008	vein	69	1712	114658	28	163000	512	354	2965	117302	0.58	13.35	38.56	14.00	845.84	20.25	5.08		1.10	1.85	8.35	10.24	20.75	2.81	12.89	3.70	2.77	4.25	3.63	1.96	1.68	0.24	40.56	0.30	0.03	0.94
BA08GS035	2008	2008	vein		542	114118		163000	517	304	3067	119341		7.91	41.21	9.85	1038.98	27.36	21.98		0.82	1.85	5.20	10.37	24.02	3.31	15.56	4.06	2.18	4.97	5.24	2.86	2.23	0.25	25.38	0.16	0.07	1.30
BA08GS035	2008	2008	vein	409	7119	108172	44	163000	3982	227	2320	116192	1.58	27.04	22.61	16.63	651.16	22.81	18.80		0.78	1.07	5.79	12.07	17.26	1.70	7.79	2.40	1.12	2.62	3.53	2.31	2.55	0.38	8.85	0.09	0.26	0.48
BA08GS035	2008	2008	vein	199	692	115789	65	163000	134	181	3035	120548		13.59	40.38	19.34	909.63	3.66	1.62		0.57	5.81	7.86	2.93	6.11	0.80	3.80	0.77	0.59	0.79	0.70	0.35	0.21	0.06	52.99	0.47	0.03	0.26
BA08GS035	2008	2008	vein	16	930	110772	7	163000	40	31	1090	122969		5.19	22.36	9.43	569.83	1.43	0.24			0.37	1.76	0.67	1.00	0.10	0.51	0.13	0.15	0.13	0.23	0.16	0.11	0.02	10.80			0.04
BA08GS035	2008	2008	vein	340	14019	117726	63	163000	169	389	3127	117537	8.92	74.26	45.50	14.49	1142.67	13.82	1.97		1.19	3.02	5.28	6.45	13.20	1.63	7.68	2.02	1.75	2.40	2.46	1.32	1.09	0.15	39.03	0.53	0.01	0.79
BA08GS036	2008	2008	rep	47	828	125838		166000	43	46	2999	115462		11.00	29.21	68.47	844.31	0.21	0.18		0.34	2.54	8.16	3.87	4.07	0.29	0.68		0.34						21.17	0.13		0.09
BA08GS036	2008	2008	rep	34	3132	114096	77	166000	13335	625	2944	120865		22.90	67.48	25.14	811.23	9.78	3.90		2.28	6.04	3.55	7.39	14.07	1.73	6.99	1.46	2.74	1.66	1.63	0.98	0.82	0.11	15.65	0.24	0.17	0.94
BA08GS036	2008	2008	rep	26	739	114190	79	166000	8701	615	1493	122674		7.21	76.86	23.14	705.03	7.22	1.52		1.74	8.03	3.94	8.17	17.25	2.16	8.76	1.85	2.26	1.51	1.07	0.61	0.42	0.05	26.10	0.34	0.06	0.78
BA08GS036	2008	2008	rep	31	962	107050	72	166000	17752	703	1652	117606	1.25	8.68	63.41	25.07	676.41	9.75	2.81		3.00	6.87	4.15	6.39	14.13	1.89	7.26	1.59	2.46	1.57	1.63	1.01	0.84	0.11	22.66	0.34	0.03	0.86
BA08GS036	2008	2008	rep	796	1320	128507	120	166000	985	357	2381	104592		24.22	46.63	72.39	729.41	8.80	33.02		1.88	5.75	14.12	10.13	19.84	2.39	10.52	2.08	2.07	2.23	1.57	0.88	0.79	0.11	26.03	0.35	2.19	1.36
BA08GS036	2008	2008	rep	120	2240	126600	233	166000	721	522	3128	102772		17.54	47.47	36.10	1037.46	19.09	33.19		0.90	6.34	12.95	8.49	23.78	3.74	19.49	4.41	2.20	4.34	3.12	1.99	2.02	0.32	26.97	0.15	0.29	1.02
BA08GS036	2008	2008	rep	47	1729	130283	55	166000	701	434	4254	100654		14.31	53.60	19.58	1184.45	14.61	30.82		0.99	10.64	3.69	6.45	17.08	2.70	13.26	2.84	1.22	2.68	2.58	1.46	1.84	0.26	32.01	0.19	0.14	0.93
BA08GS036	2008	2008	rep	424	363	132604	8	166000	910	1422	2928	147489	0.90	9.39	89.27	14.10	1254.25	236.81	20.42		6.23	14.18	3.74	1565.63	3639.66	326.22	958.46	102.80	35.59	71.07	49.51	25.34	22.60	3.77	25.02	7.28	1.24	5.40
BA08GS036	2008	2008	rep		510	127117	11	166000	494	1032	3317	95794		9.09	76.19	19.38	1213.16	48.33	110.14		5.21	14.53	3.96	70.00	140.67	17.27	72.75	15.23	9.85	13.36	9.13	4.25	4.31	0.79	17.41	1.44	0.34	7.97
BA08GS036	2008	2008	rep	62	8401	131728	47	166000	563	290	5234	90877	1.81	47.21	44.02	14.34	929.37	12.31	5.00		0.78	7.65	3.51	6.08	12.55	1.65	8.21	2.20	1.33	2.82	2.41	1.29	1.30	0.16	20.17	0.17	0.04	0.88
BA08GS036	2008	2008	rep	32	1031	122419	38	166000	641	393	1973	113179		9.19	45.55	41.80	738.92	8.94	46.56		1.05	5.55	5.78	4.32	7.87	0.88	3.81	1.01	2.31	1.20	1.21	0.88	1.14	0.15	18.63	0.09	3.22	1.56
BA08GS036	2008	2008	rep	17	10961	110845	58	166000	18119	799	1741	125752	0.99	40.65	71.94	18.72	678.05	20.02	3.13		4.11	5.11	3.44	28.04	56.68	6.82	27.83	4.93	4.51	4.22	3.27	1.82	1.52	0.24	18.38	0.42	0.06	1.38
BA08GS036	2008	2008	rep	38	3336	105249	51	166000	31569	844	2416	103168		20.17	57.84	32.74	679.97	49.18	7.91		6.35	7.78	6.67	38.36	71.65	8.28	30.66	6.53	5.12	7.42	9.26	5.44	5.03	0.68	31.00	0.61	0.31	3.22
BA08GS036	2008	2008	rep	24	2151	110364	56	166000	17229	683	2136	115863		13.97	64.72	20.59	842.47	17.69	3.42		3.75	5.83	4.27	27.69	51.94	6.13	24.34	4.60	5.04	4.08	3.05	1.58	1.35	0.21	18.36	0.46	0.11	1.80
BA08GS036	2008	2008	rep	25	740	111514	44	166000	7014	725	1387	127719		5.96	76.86	15.62	739.74	9.11	1.43		2.62	4.00	2.16	24.15	45.07	5.04	19.37	3.43	3.09	2.42	1.70	0.77	0.66	0.11	21.14	0.22	0.03	0.97
BA08GS036	2008	2008	rep	27	1829	113437	30	166000	10720	831	1492	120773		9.60	79.02	15.45	753.90	17.75	1.39		2.40	4.41	2.48	29.53	59.11	6.25	24.57	3.40	8.74	3.73	3.26	2.00	1.69	0.27	24.14	0.22	0.02	0.41

Appendix 2.6 continued

Sample #	Year Analyzed	Year Collected	Epi Type	Na	Mg	Al	K	Ca	Ti	V	Mn	Fe	Cu	Zn	Ga	As	Sr	Y	Zr	Mo	Sn	Sb	Ba	La	Ce	Pr	Nd	Sm	Eu	Gd	Dy	Er	Yb	Lu	Pb	Bi	Th	U
BA08GS036	2008	2008	rep	62	1171	135354	7	166000	120	225	3650	78254		18.89	43.93	14.02	626.92	12.65	7.01		1.19	14.52	2.06	67.33	112.26	11.66	43.39	7.43	4.07	5.73	2.85	0.98	0.59	0.07	10.29	0.17	0.09	3.40
BA08GS036	2008	2008	rep		856	131963		166000	124	120	2473	88141		10.86	42.49	17.91	1037.54	1.22	0.77		0.32	6.94	2.59	2.88	4.14	0.31	1.12	0.17	0.51	0.18	0.13	0.08	0.12	0.02	16.70	0.04	0.07	0.30
BA08GS036	2008	2008	rep	58	1146	131499	12	166000	93	62	2897	91555		16.80	33.75	23.45	725.13	0.28	0.46			8.60	5.50	6.55	7.10	0.49	1.33	0.13	0.50						18.99	0.03	0.09	0.07
BA08GS036	2008	2008	rep	88	623	134980	5	166000	97	247	3542	85867		8.43	40.39	10.54	748.47	7.49	0.47		1.66	2.16	2.29	20.54	31.99	3.57	14.12	2.85	2.06	2.46	1.70	0.63	0.36	0.06	12.51	0.14		1.35
BA08GS036	2008	2008	rep	174	501	133260	29	166000	85	29	3321	88399		15.36	31.42	9.20	590.00	0.34	0.30			2.92	4.98	5.78	6.76	0.50	1.52	0.18	0.42	0.15	0.08				8.55			0.25
BA08GS036	2008	2008	rep	65	564	137105		166000	79	120	3341	82306		8.52	35.24	6.37	875.72	2.70	0.73		1.56	2.92	1.34	8.66	13.68	1.38	4.75	0.69	0.66	0.67	0.44	0.22	0.18	0.03	12.08	0.09	0.11	0.47
BA08GS038	2008	2008	rep		2494	122194	13	160000	8134	687	4154	93396	1.45	27.62	65.24	16.55	1158.89	73.24	11.88		2.11	21.26	1.85	113.09	207.88	21.56	78.93	13.28	5.03	12.65	11.42	6.65	5.13	0.63	22.87	0.48	0.80	14.78
BA08GS038	2008	2008	rep		2106	128670	4	160000	764	678	5645	101742	1.96	27.98	69.57	16.37	1332.96	52.09	9.97		2.01	20.09	1.54	71.48	120.29	10.61	36.14	5.98	2.24	6.62	7.75	4.98	3.69	0.48	23.48	0.71	0.49	19.85
BA08GS038	2008	2008	rep	24	239	124714		160000	276	650	1045	96212		2.07	85.75	22.79	1231.69	14.59	7.84		1.33	20.06	0.69	69.80	90.48	8.50	30.73	3.55	10.08	3.10	1.87	0.94	0.97	0.13	89.79	0.70	1.02	7.05
BA08GS043	2008	2008	vein	11	255	121550		163000	214	571	1241	106757		5.53	67.38	31.04	604.43	154.06	0.04		3.06	9.63	3.12	141.81	248.22	28.81	120.82	25.19	6.75	25.49	21.18	10.74	12.76	1.93	76.62	1.82	0.05	3.11
BA08GS043	2008	2008	vein	457	214	129380	12	163000	488	208	3437	102045	3.78	9.14	44.92	27.51	799.09	5.35	0.72	0.14	2.68	10.45	4.60	9.50	15.68	1.58	6.50	1.31	0.75	1.06	0.95	0.50	0.51	0.07	90.32	0.41	0.02	1.97
BA08GS043	2008	2008	vein		220	116191	6	163000	178	512	1808	124448	1.48	5.07	66.59	13.85	595.70	46.55	0.07		3.60	4.04	2.73	60.35	104.85	11.23	45.26	7.44	3.05	7.44	5.88	3.34	3.48	0.61	37.85	0.96	0.01	2.56
BA08GS043	2008	2008	vein	34	285	125060	19	163000	545	446	2160	106382	3.92	5.65	59.40	28.40	681.46	147.99	1.04	0.09	3.21	9.18	4.26	124.84	220.32	25.48	106.53	24.55	6.06	25.53	21.49	10.88	11.32	1.75	64.20	2.64	0.42	8.27
BA08GS043	2008	2008	vein	64	229	124660	31	163000	550	442	1856	108396	7.10	14.79	64.52	22.49	685.33	84.27	1.21	0.11	4.59	10.05	3.01	76.50	136.00	15.80	67.17	16.75	5.06	16.47	12.46	6.11	6.84	1.01	75.90	3.13	0.04	7.73
BA08GS043	2008	2008	vein	11531	944	140444	544	163000	437	410	1838	105262	5.31	15.73	59.63	21.09	650.23	50.01	0.73		2.76	9.21	12.50	38.05	67.28	7.99	35.43	8.76	3.42	8.85	7.51	4.08	4.05	0.68	56.52	0.87	0.16	3.24
BA08GS043	2008	2008	vein	81	225	122762		163000	101	191	6154	109931		8.17	57.45	33.85	1293.02	3.67	0.67	0.16	2.49	10.33	7.00	3.27	6.65	0.81	2.69	0.78	0.75	0.56	0.54	0.46	0.52	0.04	102.02	0.42	0.07	1.65
BA08GS043	2008	2008	vein	73	127	118448		163000	140	181	2224	120781		4.23	59.20	20.90	872.98	3.37	0.46	0.22	2.00	9.85	3.81	2.33	4.17	0.45	1.92	0.52	0.45	0.52	0.59	0.45	0.44	0.08	88.45	0.27	0.01	2.09
BA08GS043	2008	2008	vein	152	240	114795	8	163000	228	131	3129	124083	0.91	6.13	50.07	23.81	865.44	8.85	2.65	0.23	0.84	6.61	3.99	6.46	11.26	1.27	5.49	1.28	1.38	1.53	1.20	0.81	0.99	0.17	60.86	0.64	0.11	0.38
BA08GS043	2008	2008	vein	166	173	121778	13	163000	352	219	3381	115432		7.40	53.48	28.22	1066.51	6.09	0.41	0.20	2.47	18.17	6.24	2.78	5.87	0.71	2.79	0.71	0.81	0.85	0.67	0.54	0.56	0.15	94.11	0.61	0.05	2.89
BA08GS043	2008	2008	vein	110	270	120024	6	163000	194	286	1939	102064		6.51	56.45	18.13	570.23	1.85		0.00	1.82	9.28	6.29	1.83	2.90	0.29	1.61	0.25	0.99	0.34	0.28	0.15	0.14	0.03	58.26	0.63		1.43
BA08GS043	2008	2008	vein	103	255	120531	12	163000	406	332	1813	111336	2.72	7.77	46.22	19.08	686.82	14.05	0.71		1.62	6.66	2.71	7.42	13.86	1.78	8.26	1.80	2.06	2.25	1.99	1.18	1.32	0.22	76.52	0.34	0.22	1.22
BA08GS043	2008	2008	vein	67	268	116823	8	163000	16938	303	2557	90678		7.43	41.87	26.09	987.69	403.81	38.69	0.15	1.41	8.96	3.56	153.58	298.53	38.34	172.82	39.72	13.22	49.12	48.43	34.38	40.66	6.93	81.97	0.55	0.68	1.85
BA08GS043	2008	2008	vein	113	208	121132	8	163000	238	388	1560	110740	0.51	5.45	64.57	23.68	708.81	89.72	0.44	0.31	2.64	10.15	4.47	108.99	175.43	19.16	77.92	14.64	5.11	15.07	12.82	6.83	7.13	1.19	58.91	1.87	0.03	3.85
BA08GS043	2008	2008	vein	167	287	119980	8	163000	84	368	1445	111312	1.67	5.61	63.66	21.82	442.80	0.83	0.04	0.05	3.00	8.51	5.44	1.31	2.58	0.31	0.96	0.30	0.44	0.17	0.18	0.10	0.10	0.01	54.88	0.55	0.01	0.37
BA08GS043	2008	2008	vein	398	213	122763	8	163000	170	427	1703	108780	0.99	4.53	65.89	19.94	633.06	25.64	0.06	0.13	3.20	8.93	4.72	47.71	69.98	6.31	22.34	3.11	3.01	3.16	2.33	2.02	2.48	0.43	59.90	1.20		3.54
BA08GS043	2008	2008	vein	289	282	121807	8	163000	432	298	2033	110415	2.35	6.06	53.63	21.25	620.14	242.34	0.47		2.97	5.71	3.65	85.41	165.32	22.01	101.06	24.23	12.36	31.76	31.76	20.59	21.86	3.60	43.44	0.62	0.21	2.35
BA08GS043	2008	2008	vein	213	280	121272	8	163000	66	93	1153	113474	0.34	5.40	38.20	15.20	362.55	0.96	1.68		0.52	3.80	3.65	1.50	2.81	0.31	1.23	0.33	0.18	0.23	0.20	0.13	0.10	0.01	34.95	0.27	0.20	0.15
BA08GS043	2008	2008	vein	72	256	129972	73	163000	300	398	2133	98391		5.42	62.38	37.37	696.68	47.10	0.08		3.13	11.86	10.34	45.57	74.19	8.36	34.26	7.35	4.30	7.81	6.29	3.52	3.91	0.59	79.63	2.91	0.02	6.31
BA08GS043	2008	2008	vein	594	288	122120	8	163000	65	77	1247	111720		5.13	42.66	18.23	387.29	11.40	0.45	0.04	0.41	6.84	3.41	6.23	9.68	0.95	4.09	1.17	0.51	1.71	2.23	1.12	1.20	0.13	46.48	0.51	0.02	0.11
BA08GS043	2008	2008	vein	115	257	117023	5	163000	139	34	3425	124742	0.26	9.14	20.60	22.80	906.61	63.02	0.21		0.59	6.99	4.90	28.91	57.19	7.79	35.93	8.00	11.85	9.81	7.83	4.65	3.95	0.67	91.90	0.11	0.02	0.53
BA08GS047	2008	2008	rep	38	195	125983	12	167000	870	296	1377	112483		2.63	52.87	1.23	481.10	3.09	0.56		1.74	0.62	4.35	0.57	1.15	0.15	0.73	0.19	0.63	0.36	0.42	0.46	0.38	0.05	4.20	0.15		4.64
BA08GS047	2008	2008	rep	685	269	133975	1227	167000	341	696	1331	101586	1.31	6.85	77.17	14.31	1175.36	17.34	4.99		3.44	1.90	2.34	11.11	19.83	2.49	10.98	2.89	3.25	3.58	3.48	1.75	1.26	0.15	26.39	1.45	0.03	4.01
BA08GS047	2008	2008	rep	1663	192	130736	311	167000	343	382	1763	109572	4.40	5.37	50.35	3.95	892.86	9.07	0.90		1.24	0.26	2.38	1.78	3.43	0.46	2.00	0.49	1.34	0.84	1.36	1.18	1.02	0.13	12.33	0.80		2.13
BA08GS047	2008	2008	rep		115	126756	9	167000	103	169	2379	113174		2.48	34.57		864.78	5.88	0.32		1.17	0.13	3.74	2.49	4.28	0.52	2.55	0.85	1.84	1.27	1.25	0.62	0.50	0.05	3.53	0.14		1.47
BA08GS047	2008	2008	rep	135	154	127291	13	167000	32	95	3452	112092		4.14	22.55	3.13	880.73	0.45			0.68	0.33	6.21	0.61	1.00	0.07	0.54		0.21		0.10	0.09	0.08		5.47	0.32		0.15
BA08GS047	2008	2008	rep	135	187	127376	223	167000	292	227	1451	98908	1.47	5.62	47.16	2.92	904.07	7.52	0.92		1.07	1.00	2.95	1.64	2.69	0.33	1.59	0.49	1.07	0.67	1.15	1.20	0.64	0.08	5.33	0.40		1.43
BA08GS047	2008	2008	rep	60	183	122533	36	167000	840	288	1180	114005	1.16	2.53	44.29		560.68	15.27	1.17		1.13	0.20	2.28	1.68	3.16	0.42	1.85	0.70	1.54	1.00	2.12	1.93	1.48	0.13	3.60	0.24		1.45
BA08GS047	2008	2008	rep	612	161	130740	6073	167000	541	286	1546	105040		7.83	51.64	4.69	986.15	15.65	1.33		2.05	1.35	31.03	3.18	5.76	0.77	3.76	1.13	1.91	1.69	2.28	2.04	1.55	0.18	6.24	0.72	0.02	2.32
BA08GS047	2008	2008	rep	2474	36027	122095	1366	167000	4113	778	1800	122549	2.57	43.04	55.03	34.73	3098.23	22.92	27.11		1.77	3.53	10.40	2.29	8.45	1.58	9.88	3.53	1.30	4.12	4.61	2.45	2.11	0.33	12.01	1.59	0.09	0.09
BA08GS047	2008	2008	rep	82	185	129947	3288	167000	193	421	1767	109384	1.91	7.06	44.52	3.01	744.94	26.65	1.76		2.25	0.58	8.06	8.86	16.61	2.21	10.94	3.23	4.44	4.18	5.06	2.63	1.49	0.18	4.47	0.64		8.06
BA08GS047	2008	2008	rep	185	205	131316	1072	167000	137	210	1553	107741	2.26	6.95	35.86	3.03	721.62	10.86	0.94		1.12	0.41	2.53	5.77	10.72	1.35	6.50	1.52	1.45	2.03	2.05	1.21	0.74	0.08	4.69	0.59		2.43
BA08GS052A	2008	2008	rep	441	431	124326	864	163000	27	2	1314	96291	0.30	3.52	24.55	2.81	301.36	0.39	0.41		0.24	0.15	7.69	11.78	14.14	0.76	2.03		0.26	0.09	0.04	0.04		0.01	4.08	0.28	0.22	0.01
BA08GS052A	2008	2008	rep	190	228	122747	7	163000	23	1	1493	114343		2.54	30.44	2.67	797.11	0.07	0.19	0.05	0.76	0.40	2.33	4.23	5.13	0.41	1.08	0.06	0.48	0.04					12.81	0.32	0.03	
BA08GS052A	2008	2008	rep		131	123255		163000	90	144	1188	115153	0.47	1.38	43.23	2.61	1144.13	10.83	0.11	0.01	2.58	0.88	0.33	4.29	7.48	0.88	4.21	1.10	3.18	1.45	1.37	1.06	0.82	0.11	33.31	2.72		1.16
BA08GS052A	2008	2008	rep	394	282	126497	31	163000	28	0	1915	110231		2.43	25.33	1.61	453.31	0.22	0.04		0.28	0.27	8.19	3.09	3.90	0.33	0.71	0.10	0.35		0.05	0.02			4.75	0.05	0.01	
BA08GS052A	2008	2008	rep	683	236	126514	28	163000	19		1214	110013		2.12	26.50	1.79	394.09	0.05	0.01		0.39	0.17	2.82	3.98	4.84	0.33	0.90	0.08	0.43			0.03			4.17	0.16		
BA08GS052A	2008	2008	rep	429	314	127037	8	163000	27	37	4265	110967		2.58	43.39	1.05	949.78	1.55	0.14		0.87	0.11	7.64	5.09	6.40	0.62	1.73		0.99	0.16	0.16	0.13	0.12	0.01	22.73	0.33	0.01	0.71
BA08GS052A	2008	2008	rep		336	120521	1	163000	60	172	1646	108420		4.39	38.83	10.74	392.39	0.28	0.02		0.57	1.19	3.90	2.47	3.18	0.30	0.59	0.06	0.49		0.04	0.04		0.02	26.59	0.41	0.01	0.34
BA08GS052A	2008	2008	rep		291	122508	5	163000	38	20	4368	118434		3.01	43.83	1.23	970.74	0.96	0.23	0.12	0.62	0.10	6.97	3.93	4.78	0.36	0.95	0.17	0.47	0.09	0.16	0.10	0.06	0.01	22.55	0.24	0.02	0.07
BA08GS052A	2008	2008	rep		128	121195		163000	32	8	1255	115512		1.73	45.17		305.64	0.28	0.01	0.09	0.41		0.40	3.81	4.67	0.38	1.02	0.12	0.46	0.09	0.06	0.03			4.33	0.05		0.05
BA08GS052A	2008	2008	rep	19	276	120887	1	163000	21	0	1430	112112		3.37	37.56	2.53	218.56	0.06		0.04	0.37		0.28	3.74	4.42	0.34	0.82	0.08	0.39		0.01				8.00	0.08	0.00	
BA08GS052A	2008	2008	rep	41	244	117836	4	163000	47	21	1370	116523		3.16	50.58	0.74	296.66	0.17	0.12		0.53		0.70	2.32	2.83	0.25	0.57	0.08	0.34				0.03	0.01	11.38	0.12		0.05
BA08GS052A	2008	2008	rep	13	82	127750	14	163000	51	72	1659	102687		0.99	41.97		512.28	4.79	0.52		1.09		0.87	5.36	8.15	0.76	3.07	0.62	0.76	0.84	0.84	0.45	0.41	0.03	8.47	0.09		0.86
BA08GS052A	2008	2008	rep		166	119529	10	163000	38	2	1387	107309		1.93	36.86		272.50	0.43	0.39	0.00	0.38		0.57	4.32	6.05	0.44	1.57	0.10	0.51	0.08		0.04	0.05	0.01	4.57	0.06	0.04	0.07
BA08GS052A	2008	2008	rep		126	123565	3	163000	32	8	1527	112423		2.04	40.81		593.96	0.83	0.24	0.13	0.95	0.14	1.01	3.87	4.16	0.34	1.03	0.16	0.36	0.17	0.11	0.07	0.08	0.01	7.99	0.10	0.01	0.08
BA08GS052A	2008	2008	rep		332	121064	3	163000	34	4	796	109034		1.84	23.85	1.80	218.89	0.47	0.16		0.35	0.06	0.27	5.00	6.34	0.48	1.54	0.14	0.47	0.07	0.13	0.08	0.06		3.14	0.12	0.04	0.10
BA08GS052A	2008	2008	rep		117	131753		163000	71	355	2883	94475		0.99	70.55		1351.61	0.54			3.79		0.49	2.49	2.80	0.19	0.63		1.02		0.04	0.06	0.15	0.02	14.29	0.95		0.51
BA08GS052A	2008	2008	rep	586	401	116362	92	163000	164	24	1570	116891		5.18	31.51	4.60	448.08	5.94	1.92		0.61	0.10	20.09	10.53	17.15	1.78	7.07	1.55	1.01	1.39	1.21	0.48	0.36	0.03	17.82	0.24	0.43	0.56
BA08GS052A	2008	2008	rep	31	377	121500	47	163000	38	5	6251	107932		1.34	28.41	1.31	1385.94	0.32	0.14		1.14	0.28	8.50	5.01	6.61	0.59	1.26	0.17	0.73	0.08	0.07		0.03		18.47	0.44	0.03	0.01
BA08GS052A	2008	2008	rep	308	324	121193	73	163000	42	38	3823	118319		2.71	33.87	1.24	993.36	9.58	0.49		0.78	0.20	4.88	11.74	17.44	1.78	6.71	1.41	1.75	1.63	1.54	0.90	0.50	0.08	8.36	0.38		0.78
BA08GS052A	2008	2008	rep		152	128830	2	163000	33	6	3141	97834		1.96	31.17	7.12	1477.80	0.08		0.12	0.49	1.99	12.70	5.88	6.96	0.52	1.22		0.59				0.02		29.91	0.52	0.00	0.04
BA08GS052A	2008	2008	rep	28	352	120730	1	163000	15	2	1363	109037		3.28	24.89	4.81	725.58	0.05				1.12	1.40	4.03	5.02	0.34	1.00	0.11	0.40		0.03			0.00	15.73	0.59	0.01	
BA08GS052A	2008	2008	rep	116	229	121867	35	163000	62	34	1382	112192		1.99	29.63	2.32	725.94	11.85	0.65		0.68	0.54	2.43	10.18	14.76	1.47	5.54	1.34	1.97	1.64	2.04	0.95	0.71	0.10	7.45	0.49	0.01	1.15
BA08GS052A	2008	2008	rep	100	168	119873	2	163000	26	1	2828	112505		0.79	27.16	3.86	1305.09	0.46		0.05	0.64	0.96	9.40	5.07	6.27	0.54	1.53	0.14	0.49	0.13	0.05	0.04	0.05		8.20	0.31		0.02
BA08GS052A	2008	2008	rep		339	120421		163000	50	116	2100	113754		2.28	55.05	13.51	691.84	0.51	0.28	0.09	1.70	2.76	2.17	4.40	5.83	0.41	1.37	0.20	0.65	0.14	0.09	0.05	0.06	0.02	27.16	1.62	0.03	0.17
BA08GS052A	2008	2008	rep	79	81	115576	3	163000	133	6	1062	123346		1.33	44.34	1.38	609.82	0.24	0.04		1.18	0.11	0.30	3.30	4.03	0.29	0.85		0.40	0.04	0.04			0.00	11.61	0.91		0.02
BA08GS052A	2008	2008	rep	25	225	124876	11	163000	44	130	2226	104312		2.81	39.41	8.03	1294.05	16.63	0.33	0.08	1.39	3.03	2.77	9.58	18.56	2.30	9.89	2.38	1.70	2.47	2.59	1.52	1.13	0.16	19.61	1.41	0.06	0.64
BA08GS052A	2008	2008	rep		164	114142		163000	32	1	715	124549		1.30	28.95		252.38	0.10	0.10		0.22		0.14	2.50	3.25	0.22	0.78	0.05	0.38		0.02			0.00	3.58	0.13	0.01	0.02
BA08GS052A	2008	2008	rep		197	116892	1	163000	40	20	1739	128943		2.61	48.82	6.48	752.64	1.53		0.09	0.68	0.31	2.82	2.85	3.44	0.34	0.80	0.07	0.79	0.12	0.10	0.18	0.18	0.03	7.31	0.11	0.01	0.65
BA08GS052A	2008	2008	rep	82	239	120150	5	163000	23	7	1518	116845		2.66	54.70	1.68	272.27	1.49	0.05	0.06	1.06		0.77	5.84	7.92	0.68	2.62	0.51	0.51	0.27	0.29	0.13	0.09	0.03	8.62	0.14		0.09
BA08GS052A	2008	2008	rep		135	118615	1	163000	24	6	1337	119345		2.41	59.32		239.66	2.07	0.10	0.08	0.46		0.33	7.21	10.32	0.94	3.64	0.52	0.64	0.61	0.40	0.23	0.14		6.71	0.10		0.10
BA08GS052A	2008	2008	rep		143	119179	4	163000	34	3	1291	119062		1.56	50.82	0.63	219.96	0.09	0.11		0.46		0.23	3.01	3.63	0.28	0.62	0.07	0.37		0.04		0.03		7.76	0.07	0.01	
BA08GS052A	2008	2008	rep	39	376	114149	4	163000	180	28	1447	119751		3.19	31.20	2.46	830.02	6.38	15.57		0.67	0.60	4.26	6.52	12.13	1.41	6.62	2.35	1.16	2.20	1.32	0.56	0.55	0.08	13.60	0.45	0.65	0.40
BA08GS052A	2008	2008	rep		257	120490	2	163000	37	5	1279	121194		2.42	31.81	4.05	847.46	0.18			0.42	0.93	0.37	3.64	4.39	0.37	1.15		0.32	0.07			0.00		24.39	0.92		0.02
BA08GS052A	2008	2008	rep	299	309	124706	26	163000	123	220	3889	118989	1.22	3.73	47.62	4.37	1231.89	35.62	1.67		3.69	0.26	3.30	15.59	28.28	3.41	15.33	3.97	3.87	5.56	5.63	2.80	1.63	0.19	18.26	1.15		2.21
BA08GS052A	2008	2008	rep	490	513	129449	17	163000	32	2	4771	114511		1.92	24.33	11.00	1253.76	0.31	0.73	0.13	0.30	1.45	4.05	3.95	4.77	0.38	1.10	0.04	0.35	0.04	0.05			0.00	13.02	1.25	0.06	
BA08GS052A	2008	2008	rep	65	209	120296	14	163000	225	284	1392	116930		2.30	62.98	2.50	529.38	14.60	0.24		1.56	0.43	1.32	4.13	5.40	0.44	1.47	0.25	2.94	0.74	1.38	1.64	1.68	0.20	9.58	0.34	0.02	3.03
BA08GS052A	2008	2008	rep	33	220	120958	3	163000	30	1	1258	114885		1.90	28.32		284.84	0.11			0.30		1.02	2.99	3.77	0.30	0.72	0.09	0.36	0.05	0.02	0.03		0.01	3.00	0.04		
BA08GS052A	2008	2008	rep	602	125	123450	35	163000	33	17	1593	114596		1.39	46.70	1.29	759.17	0.37	0.36		1.78	0.16	1.85	4.71	5.69	0.49	1.19	0.14	0.42	0.10	0.05	0.04	0.06		9.05	0.38	0.06	0.20
BA08GS052A	2008	2008	rep		345	121287	3	163000	135	13	1107	125152		3.10	32.13	0.84	276.71	0.69	2.47	0.03	0.30		0.54	1.47	2.03	0.19	0.54	0.10	0.22	0.06	0.12	0.08		0.02	3.63	0.07	0.07	0.01
BA08GS052B	2008	2008	rep		253	120587		164000	30	10	1914	122445	0.31	2.67	31.93	1.99	679.05	0.20	0.07	0.09	0.45	0.20	2.03	2.40	3.05	0.27	0.81	0.07	0.36			0.02	0.01		9.71	0.16	0.04	0.05
BA08GS052B	2008	2008	rep		218	120529	6	164000	53	1	1113	121089		2.09	34.10	1.24	214.97	0.07	1.35	0.05	0.33		0.66	2.65	3.52	0.28	0.78	0.08	0.32	0.06	0.01	0.02	0.01		2.88	0.08	0.05	0.02
BA08GS052B	2008	2008	rep		451	131097		164000	50	3	6696	111919		1.76	32.21	3.35	1310.98	0.13	0.02	0.23	1.46	1.08	12.15	2.67	3.92	0.35	1.22	0.17	0.36	0.07	0.05		0.04		17.72	0.58	0.01	0.01
BA08GS052B	2008	2008	rep	42	221	130381	16	164000	35	5	2672	103580		6.71	29.34	8.29	1121.52	0.71	0.08	0.10	0.43	0.99	9.32	5.06	6.28	0.49	1.46	0.12	0.56		0.10	0.06		0.01	24.35	0.45		0.08
BA08GS052B	2008	2008	rep	319	541	127060	19	164000	147	9	2035	103975		4.39	27.08	6.01	1010.39	3.05	1.87		0.60	1.54	22.57	4.16	8.44	0.93	3.76	0.85	0.34	0.79	0.54	0.26	0.24	0.03	10.95	0.23	0.41	0.08
BA08GS052B	2008	2008	rep	840	329	125627	43	164000	49	8	1941	119494		2.47	28.00	6.62	996.91	0.53	0.06		0.52	1.29	3.43	3.42	4.55	0.35	0.95	0.08	0.44	0.09	0.07	0.03		0.01	15.04	1.11	0.01	0.02
BA08GS052B	2008	2008	rep	5873	798	141726	3641	164000	150	30	2349	118781	0.70	5.05	31.84	8.42	969.85	5.01	2.66	0.04	0.91	1.39	20.63	7.06	11.22	1.15	3.76	0.85	0.77	0.79	0.63	0.48	0.39	0.07	14.02	1.30	0.15	0.44
BA08GS052B	2008	2008	rep		182	135352	4	164000	63	18	1758	96996		2.30	37.86	10.30	1519.78		0.14		1.82	4.48	1.02												39.24	4.84		
BA08GS052B	2008	2008	rep	866	449	131698	23	164000	245	57	6463	115355	0.80	3.17	50.36	1.67	1247.77	2.85	8.23	0.09	2.51	0.36	10.19	7.63	10.79	0.94	3.06	0.56	1.16	0.47	0.44	0.30	0.59	0.12	21.72	0.55	0.58	1.12
BA08GS052B	2008	2008	rep	827	539	126490	766	164000	77	53	2363	113702		5.34	45.22	8.17	523.50	1.35	6.28		0.44	0.64	9.65	2.10	2.84	0.26	0.90	0.22	0.32	0.15	0.17	0.11	0.12	0.03	29.78	0.24	0.54	0.15
BA08GS052B	2008	2008	rep	30	591	130791		164000	102	182	7030	123703		1.86	69.60	16.21	1449.02	57.99	0.29		8.75	0.70	0.96	53.01	138.34	21.04	112.84	25.47	7.70	23.44	12.30	4.44	3.94	0.51	24.51	4.56		1.69
BA08GS052B	2008	2008	rep		386	124029		164000	40	75	2696	121459		3.10	60.41	15.85	972.37	0.44			2.38	2.60	1.88	2.25	2.71	0.19	0.60	0.07	0.61	0.06	0.06	0.05	0.04	0.01	23.47	2.97		0.11
BA08GS052B	2008	2008	rep	80	154	120638	35	164000	28	5	1293	117710		1.66	28.90	0.86	535.97	0.96	0.22		0.22		2.87	4.02	4.91	0.38	1.04		0.42	0.11	0.12	0.10	0.11	0.02	5.07	0.11	0.03	0.06
BA08GS052B	2008	2008	rep	209	292	123573	8	164000	19	9	2686	115466		2.31	25.00	2.79	803.83	0.37	0.25	0.04	0.49	0.50	11.04	3.82	4.47	0.33	0.92	0.09	0.43	0.12	0.06	0.04			8.21	0.18	0.01	0.02
BA08GS052B	2008	2008	rep	50	273	124965	10	164000	119	60	3990	119384		2.75	56.77	1.89	1144.84	1.44	0.44		2.90	0.83	9.53	2.03	2.79	0.25	0.70	0.09	0.79	0.15	0.24	0.21	0.21	0.03	28.38	0.36	0.02	0.80
BA08GS052B	2008	2008	rep	2515	375	133165	301	164000	257	154	4652	102814		2.58	54.44	2.96	1253.94	32.88	5.60		4.18	0.89	15.44	37.25	61.36	6.37	28.48	6.68	5.43	6.10	5.29	3.29	3.50	0.60	23.55	0.67	2.81	5.70
BA08GS052B	2008	2008	rep		1012	121438	218	164000	93	25	1500	108853		3.04	52.29	0.90	416.10	1.17	3.46	0.07	1.44		1.09	2.77	3.27	0.27	0.77	0.11	0.48	0.18	0.16	0.12	0.21	0.04	6.88	0.09	0.32	0.56
BA08GS052B	2008	2008	rep	97	124	125488	15	164000	15	22	2558	108336	0.69	2.00	43.82	2.19	1234.74	0.22			1.28	1.07	16.14	3.72	4.63	0.33	0.88	0.11	0.73	0.07	0.03		0.07		29.09	0.35		0.20
BA08GS052B	2008	2008	rep	730	119	128405	34	164000	19	2	1602	104947		1.56	30.94	1.14	451.44	0.12	0.06		0.72	0.15	3.62	3.57	4.66	0.37	1.07	0.11	0.49		0.03	0.02		0.00	6.79	0.14	0.02	0.04

Appendix 2.6 continued

Sample #	Year Analyzed	Year Collected	Epi Type	Na	Mg	Al	K	Ca	Ti	V	Mn	Fe	Cu	Zn	Ga	As	Sr	Y	Zr	Mo	Sn	Sb	Ba	La	Ce	Pr	Nd	Sm	Eu	Gd	Dy	Er	Yb	Lu	Pb	Bi	Th	U
BA08GS052B	2008	2008	rep		205	122447		164000	23	10	2054	118304		2.62	41.07	1.59	835.93	0.17			0.61	0.33	3.24	3.52	4.53	0.34	0.86		0.43				0.03		32.91	0.28		0.10
BA08GS052B	2008	2008	rep		186	117224		164000	19	0	1001	119765		2.26	30.39		269.57	0.05			0.35		0.25	4.19	4.94	0.35	0.97		0.28	0.03	0.03	0.01		0.00	3.58	0.05	0.01	
BA08GS052B	2008	2008	rep		179	121569		164000	18	3	1172	116171		1.72	43.20	0.73	197.97	0.06			0.45		0.33	3.34	4.37	0.37	0.91	0.04	0.34	0.03					6.42	0.14		0.01
BA08GS052B	2008	2008	rep		433	117819		164000	19	73	1791	128879		5.54	48.57	9.45	328.05	0.04			0.42	0.41	2.24	1.86	2.25	0.16	0.47		0.27				0.02		21.29	0.21		0.05
BA08GS054	2008	2008	rep	121	204	135980	35	163000	87	45	2246	87036		1.68	33.93	11.64	1622.37	1.69	0.15		0.70	5.37	70.41	4.14	5.69	0.47	1.39	0.18	0.70	0.13	0.22	0.20	0.20	0.05	39.96	0.18	0.02	0.24
BA08GS054	2008	2008	rep	14	415	123844	5	163000	30	33	1715	112458		3.17	47.52	2.03	265.22	0.48			0.91		1.59	4.28	5.64	0.43	1.10	0.13	0.56	0.10	0.06	0.07	0.18	0.03	11.65	0.09	0.01	0.16
BA08GS054	2008	2008	rep		476	127490		163000	146	40	2756	107929		5.52	43.51	13.73	482.30	8.86	1.02	0.11	0.91	1.93	4.61	6.25	9.80	1.01	3.52	0.97	1.02	1.01	1.24	1.02	1.20	0.17	16.74	0.34		1.23
BA08GS054	2008	2008	rep	34	388	123201		163000	52	23	1349	108986		4.31	39.26		299.22	0.15			0.34		1.98	3.45	4.42	0.30	0.92		0.35		0.07	0.01	0.04		6.53	0.03		0.07
BA08GS054	2008	2008	rep	2294	354	131630	117	163000	28	19	2135	107068	2.12	3.17	44.02	3.94	559.53	0.25	0.03		0.44	0.61	11.14	4.18	5.74	0.49	1.32	0.19	0.45			0.04	0.04		11.69		0.07	0.04
BA08GS054	2008	2008	rep		382	125992	3	163000	26	16	3826	105598		4.42	41.87	6.90	751.59	0.38	0.05		0.77	0.82	19.00	4.40	5.49	0.38	1.22	0.07	0.48	0.05	0.04	0.05	0.08		29.15	0.33		0.04
BA08GS054	2008	2008	rep	37	378	120057		163000	135	181	3275	105015		4.58	61.64	12.78	806.91	20.45	1.21		1.77	1.98	14.03	14.42	19.87	1.80	7.39	1.73	4.50	2.43	3.38	2.53	2.29	0.26	29.72	0.17	0.04	7.27
BA08GS054	2008	2008	rep	843	352	124008	18	163000	242	165	2995	106080	0.48	5.27	58.46	8.36	943.21	27.17	3.98		2.86	1.87	15.97	26.10	36.62	3.63	13.67	3.02	4.18	4.54	4.52	2.94	2.45	0.48	23.05	0.59	0.36	6.13
BA08GS054	2008	2008	rep	174	358	120609	5	163000	79	25	1565	117830	0.60	3.07	50.95	1.29	366.76	4.09	0.73		0.77	0.21	3.06	5.50	8.09	0.79	2.74	0.54	0.87	0.65	0.68	0.32	0.35	0.04	6.84	0.13	0.02	0.71
BA08GS054	2008	2008	rep		616	125114		163000	56	37	5361	120192	0.50	4.54	53.26	4.34	1000.42	1.41	0.19		0.65	0.23	25.50	5.40	7.19	0.58	1.80	0.22	0.70	0.16	0.21	0.17	0.18	0.05	10.18	0.07		0.41
BA08GS054	2008	2008	rep	58	360	127651		163000	113	29	3265	102233		3.25	41.72	3.07	933.53	3.45	1.49		0.88	0.50	19.13	6.59	9.03	0.87	2.52	0.39	1.04	0.66	0.48	0.45	0.49	0.07	12.92	0.11		0.73
BA08GS054	2008	2008	rep	300	252	132400	24	163000	35	36	2837	96306		3.25	56.01	11.91	1095.29	2.42		0.12	2.74	5.69	30.54	5.37	6.14	0.51	1.53	0.21	1.64	0.21	0.31	0.35	0.41	0.08	32.69	0.27		1.11
BA08GS054	2008	2008	rep	12	159	120836	5	163000	33	30	1308	99488		2.24	58.00	5.24	302.77	0.24	0.04		1.65	1.85	1.57	5.10	6.14	0.41	1.09	0.07	0.54	0.10	0.05		0.03	0.00	7.89	0.60	0.00	0.08
BA08GS054	2008	2008	rep	77	348	120248	11	163000	388	243	1685	108658		4.54	55.41	16.87	1426.34	6.41	0.10		0.64	17.51	6.90	10.04	16.73	1.82	7.25	1.13	1.48	1.01	1.05	0.66	0.55	0.13	19.38	3.71	0.04	1.15
BA08GS054	2008	2008	rep		266	122411		163000	72	65	2254	113403		3.13	62.87	8.94	915.65	1.02	0.03		2.13	2.15	7.69	4.15	5.72	0.43	1.09	0.12	0.70	0.18	0.23	0.09	0.17	0.02	38.64	0.18	0.01	0.92
BA08GS054	2008	2008	rep	108	678	124156		163000	68	41	5366	118292	0.44	2.99	51.46	3.59	1066.44	0.94			1.02	0.60	26.26	3.15	3.62	0.30	0.86	0.10	0.69	0.07	0.13	0.12	0.15	0.03	9.41	0.04		0.45
BA08GS054	2008	2008	rep	8	609	128893		163000	129	18	5746	111581		3.41	50.86	7.10	1118.56	1.34	0.74	0.12	2.26	0.93	21.27	6.66	10.01	0.90	2.94	0.31	0.62	0.28	0.29	0.17	0.20	0.03	19.18	0.18	0.07	0.32
BA08GS054	2008	2008	rep	161	234	120701	11	163000	30	23	2315	111810		2.68	53.05	5.81	863.77	0.68	0.08	0.15	1.92	1.58	6.98	3.51	4.34	0.31	0.96	0.08	0.69		0.07	0.06	0.12	0.02	33.37	0.20		0.49
BA08GS054	2008	2008	rep	9	525	119673	3	163000	27	13	2721	117422		3.99	44.35	2.27	684.83	0.40	0.04		0.32	0.76	14.66	4.46	5.92	0.52	1.45	0.19	0.46	0.18	0.06	0.05	0.02	0.01	9.86	0.05	0.03	0.04
BA08GS054	2008	2008	rep	20	399	123051		163000	69	10	1470	109457		3.76	42.63	2.33	254.13	0.71	0.15		0.36	0.11	1.79	3.08	4.05	0.34	0.90	0.15	0.61	0.07	0.08	0.10	0.24	0.04	5.19		0.02	0.21
BA08GS054	2008	2008	rep	57	399	131447	11	163000	39	19	3098	93503		4.96	45.59	14.29	849.31	1.03	0.21		1.87	6.41	14.78	4.04	5.50	0.44	1.23	0.08	0.98	0.11	0.14	0.10	0.22	0.03	28.17	0.39		0.48
BA08GS054	2008	2008	rep		533	132508		163000	27	13	4226	94259		2.87	40.14	19.60	1336.14	0.22	0.05		0.81	3.40	54.49	4.80	5.84	0.43	1.14	0.08	0.63	0.07	0.04	0.03	0.08	0.01	35.56	0.11		0.07
BA08GS054	2008	2008	rep	38	326	120767	8	163000	215	21	1213	111271		2.80	45.47	1.69	225.47	1.69	0.10		0.59		1.34	2.33	3.49	0.34	1.01	0.13	0.59	0.14	0.19	0.21	0.19	0.01	5.59	0.04	0.01	0.48
BA08GS054	2008	2008	rep		422	122680		163000	59	28	1915	108245		3.60	56.01	5.53	276.92	1.51			1.09	0.14	1.34	3.26	4.25	0.31	1.17	0.12	0.52		0.16	0.19	0.26	0.04	11.35	0.04		0.29
BA08GS054	2008	2008	rep		174	130196		163000	22	5	1962	93170		1.61	39.13		746.01	0.06	0.01	0.10	0.36		8.25	3.83	4.24	0.28	0.85	0.13	0.36	0.06		0.00	0.01		4.65	0.02		
BA08GS054	2008	2008	rep		291	122677		163000	26	41	1995	112895		2.90	46.95	5.11	876.43	2.64	0.19	0.14	0.79	1.03	7.83	4.98	6.18	0.49	1.54	0.16	0.80	0.36	0.42	0.34	0.28	0.05	31.65	0.08		0.85
BA08GS054	2008	2008	rep		378	121642		163000	104	182	1813	110247		4.98	56.70	3.59	824.92	5.21	0.14	0.01	0.70	2.97	14.23	5.62	8.00	0.73	2.56	0.41	0.86	0.49	0.69	0.58	0.68	0.08	36.71	0.08		2.00
BA08GS056	2008	2008	rep	2678	314	140130	702	165000	127	234	1709	95281	3.94	7.52	47.19	40.48	934.41	5.26	0.52		0.41	5.57	7.18	3.18	6.16	0.72	3.17	0.70	1.65	0.92	0.87	0.39	0.34	0.06	43.34	0.55		0.38
BA08GS056	2008	2008	rep	6	120	119212	35	165000	6	4	919	112489		1.39	18.64	2.44	288.92	0.04	0.06				0.36	0.06	0.15	0.02			0.07						6.48			
BA08GS056	2008	2008	rep	62	140	117804	46	165000	16	35	857	120863		1.09	29.18	1.99	453.74	0.06					0.67	0.07	0.11				0.10						10.45			
BA08GS056	2008	2008	rep	45	322	122970	7	165000	102	747	852	100393		5.23	55.17	7.24	148.00	3.31			1.26		1.71	0.23	0.39	0.06	0.20		0.71	0.15	0.30	0.65	0.75	0.10	2.65	0.04		0.83
BA08GS056	2008	2008	rep	68	393	122451	14	165000	83	242	1773	114313		4.06	56.76	8.25	678.66	3.64	0.06		0.46	0.39	6.36	0.52	0.96	0.12	0.67	0.17	1.07	0.33	0.47	0.51	0.54	0.08	9.32			0.21
BA08GS056	2008	2008	rep		195	119291		165000	77	254	750	116695		3.16	66.87	3.75	270.82	10.44	0.20				1.26	1.25	2.61	0.37	1.86	0.62	1.40	1.12	1.66	1.15	1.09	0.14	2.88		0.03	0.30
BA08GS056	2008	2008	rep	158	452	123736	12	165000	730	399	1573	110006		3.55	44.83	7.30	305.68	2.83	0.80		0.73		4.82	0.53	1.04	0.14	0.66	0.14	0.52	0.23	0.41	0.31	0.66	0.09	2.71	0.08		0.27
BA08GS056	2008	2008	rep	296	220	122097	2707	165000	154	321	1228	114558		2.66	77.49	5.25	565.50	4.45	0.74		1.22	0.93	9.16	2.20	4.68	0.66	2.74	0.71	0.94	0.86	0.84	0.45	0.40	0.08	12.10	0.24	0.03	0.36
BA08GS057	2008	2008	rep		291	119383	10	167000	84	206	1350	111404		4.80	72.49	7.35	597.86	0.40			1.44	1.05	1.38	0.31	0.44	0.05	0.39		1.72						20.77	1.02		0.13
BA08GS057	2008	2008	rep	1106	2440	138540	11790	167000	452	330	1447	112993		8.62	56.08	5.30	593.98	4.07	0.44		0.51	0.85	61.63	1.74	3.42	0.45	2.15	0.50	1.24	0.71	0.64	0.42	0.39	0.06	13.02	0.10	0.03	0.50
353226	2008	2006	rep	55	213	120251	4	165000	220	1208	2002	93317	6.34	15.32	49.87	170.72	1829.69	9.63	2.11		1.39	40.59	4.88	16.11	24.89	2.84	10.32	1.36	2.81	1.69	1.15	0.95	1.68	0.40	94.96	3.58	0.02	0.14
353226	2008	2006	rep	685	3816	121989	530	165000	187	271	1597	103330	3.66	18.19	41.15	30.97	1100.27	9.86	93.52	0.22	0.60	5.22	13.96	2.57	5.90	0.72	3.73	0.67	0.85	1.00	0.87	1.15	2.00	0.30	39.83	0.39	2.75	0.41
353226	2008	2006	rep	695	23305	143197	355	165000	515	969	2818	127172	24.83	95.92	53.19	43.38	1558.60	37.56	18.55		1.07	6.07	8.05	16.08	38.77	5.49	26.81	5.88	2.64	5.78	4.92	3.02	3.36	0.62	45.82	0.47	0.42	0.14
353226	2008	2006	rep	68	258	131433		165000	249	426	2482	85216		6.60	42.05	110.70	1965.00	9.49	14.90		0.87	21.29	1.70	4.78	6.84	0.73	3.46	0.74	1.86	0.65	0.77	0.69	0.96	0.18	98.25	1.18	0.09	0.13
353226	2008	2006	rep	21	240	120956	3	165000	364	1223	1780	105861		6.95	52.73	68.43	1417.70	9.38	11.69		0.61	20.50	0.55	4.87	7.76	0.95	3.91	0.88	1.40	0.97	1.13	1.04	1.30	0.25	81.53	1.25	0.14	0.23
353226	2008	2006	rep	83	497	122131	244	165000	344	607	1542	96770	1.21	7.32	75.99	18.72	987.12	22.92	18.35		1.88	8.07	6.15	15.17	36.52	4.38	20.67	3.67	4.50	4.20	3.48	1.76	1.71	0.25	67.80	2.34	0.53	0.85
353226	2008	2006	rep	47	1008	123928	41	165000	894	947	4399	108872		23.03	127.15	22.55	982.71	1579.15	43.47		3.85	2.83	1.37	2329.79	5921.35	736.68	3193.23	630.76	74.34	522.99	368.30	136.57	77.61	7.50	46.27	1.12	8.70	38.91
353226	2008	2006	rep	88	550	118695	14	165000	326	738	1851	110901		7.08	84.42	27.47	1108.30	16.34	10.17		1.29	9.39	0.73	18.44	38.14	4.54	20.06	3.35	4.42	3.72	2.83	2.02	2.05	0.32	59.47	2.02	3.04	0.56
353226	2008	2006	rep	314	1147	112409	243	165000	178	213	883	122463		9.17	65.71	19.99	861.60	1.15	7.01		0.66	1.62	6.33	1.68	3.13	0.27	1.25	0.11	0.60	0.14	0.14	0.09	0.19	0.04	25.18	0.24	0.24	0.05
353226	2008	2006	rep	247	330	120639	395	165000	71	434	1371	106909		7.68	65.60	37.76	1208.85	1.80	0.93		0.55	8.39	1.76	0.94	1.70	0.19	0.90	0.30	0.47	0.31	0.16	0.17	0.11	0.04	55.82	0.87		0.04
353226	2008	2006	rep		353	120669		165000	1010	1771	1121	100091		4.31	107.64	12.73	1199.69	124.00	90.01		3.23	7.93		44.79	115.88	15.57	73.32	16.57	5.82	18.21	18.16	12.58	11.23	1.63	90.89	1.21	5.21	4.34
353226	2008	2006	rep	89	357	111241	187	165000	325	98	957	115876		6.26	56.23	21.28	897.48	5.81	68.55	0.44	0.57	2.91	6.67	1.86	3.96	0.45	2.18	0.64	0.48	0.60	0.66	0.82	1.22	0.20	31.84	0.21	1.93	0.48
353226	2008	2006	rep	43	187	118476	6	165000	375	937	1388	105530	1.20	11.08	58.16	151.28	2184.11	2.41	3.09			28.53	4.01	2.66	3.97	0.40	1.40	0.39	2.72	0.23	0.31	0.26	0.48	0.07	72.26	1.29		0.05
355195	2008	2006	rep	340	1151	120336	24	165000	305	339	1476	114121		15.45	32.29	50.97	433.45	18.04	27.77		1.25	0.92	0.94	4.03	9.25	1.08	4.70	1.14	0.42	1.38	2.64	2.31	2.83	0.48	27.79	0.04	0.55	0.99
355195	2008	2006	rep	11	477	115082	76	165000	14	129	1045	127591		4.97	33.61	9.23	486.14	0.81	0.16		1.09	0.21	0.45	0.92	1.80	0.23	0.84	0.19	1.34	0.09	0.14	0.08	0.08		10.44			0.11
355195	2008	2006	rep	174	621	115586	92	165000	80	163	2521	127195		5.50	34.20	25.82	567.28	0.40	0.11		0.57	0.32	1.02	0.27	0.58	0.07	0.33		0.11	0.07	0.06		0.06		15.08			0.04
355195	2008	2006	rep	854	867	118147	231	165000	119	242	2301	117102		7.97	34.56	20.25	482.93	5.73	12.51		0.90	0.57	3.31	3.32	7.75	0.97	3.42	0.95	0.33	0.90	1.11	0.69	0.98	0.14	16.71		0.53	0.54
355195	2008	2006	rep		499	118093		165000	262	320	894	119610		6.21	28.70	4.04	295.12	3.06	0.64		0.56	0.75		0.43	1.28	0.19	0.95	0.18	0.64	0.34	0.33	0.31	0.44	0.09	15.60			0.11
355195	2008	2006	rep	159	1415	121177	160	165000	21	139	1817	117812	0.64	9.22	31.04	27.04	402.76	0.69	0.25		1.02	0.75	1.62	0.69	2.02	0.23	0.77	0.20	0.13	0.16	0.18	0.10	0.18	0.01	18.19	0.02	0.13	0.08
355195	2008	2006	rep	14	645	116755	14	165000	26	402	1468	121314		10.60	37.42	10.88	423.77	82.38	0.16		1.01	2.35	0.50	8.81	53.41	13.86	74.79	18.98	4.92	17.93	13.31	5.31	4.47	0.59	28.43	0.04	0.06	0.14
355195	2008	2006	rep	178	1074	117202	153	165000	190	290	2050	119700		13.24	31.95	54.87	360.77	3.61	16.25		0.53	0.54	2.03	0.81	1.93	0.23	1.16	0.29	0.17	0.31	0.56	0.49	0.65	0.09	27.90		0.75	0.21
355195	2008	2006	rep	55	789	117651	10	165000	8760	269	3409	116939		9.14	34.36	30.80	664.13	8.05	156.90		2.20	0.43	2.02	1.59	5.65	0.64	3.02	0.84	0.31	0.94	1.21	1.08	1.31	0.28	19.37	0.03	2.76	1.16
355195	2008	2006	rep	591	932	117223	40	165000	224	333	1482	120906		9.58	31.97	28.56	455.13	8.21	61.65		1.50	1.00	1.68	2.68	6.43	0.87	3.95	0.72	0.47	0.99	1.16	1.20	1.47	0.23	26.95		2.31	0.72
355195	2008	2006	rep	2929	1413	121650	362	165000	131	321	1709	112933		13.34	29.01	60.46	429.75	7.43	2.92		0.81	1.12	4.55	1.09	2.70	0.33	1.66	0.41	0.21	0.67	1.16	0.82	1.06	0.19	39.82		0.17	0.59
355195	2008	2006	rep	72	929	121443	29	165000	228	498	1524	108312		14.20	33.62	21.09	305.76	1.14	2.28		1.02	1.60	0.68	0.49	1.07	0.13	0.54	0.17	0.25	0.12	0.24	0.10	0.23	0.04	44.63	0.04	0.02	0.25
355195	2008	2006	rep	10	485	113048		165000	23	293	972	129388		6.80	32.86	19.62	402.65	70.07	0.08		0.95	0.42	0.55	51.34	104.97	12.41	48.87	9.41	10.61	10.06	9.18	4.73	3.63	0.41	12.51			0.14
355195	2008	2006	rep	30	683	124476	13	165000	7249	352	5380	88989		12.13	47.45	38.46	1287.67	21.89	83.68	0.24	1.39	21.57	0.80	2.89	8.36	1.25	5.62	2.13	0.61	2.05	2.96	2.37	2.62	0.36	31.48	0.09	2.21	0.26
814487	2008	2006	rep	16	399	121345	68	162000	480	111	1755	120373	0.92	7.67	32.82	4.29	284.61	3.37	7.11		1.96	0.89	1.19	1.65	3.68	0.44	1.89	0.52	0.27	0.39	0.52	0.37	0.42	0.07	15.11	0.04	0.20	0.10
814487	2008	2006	rep	207	1538	120821	235	162000	6822	231	2310	117477	3.24	57.43	30.59	23.40	374.18	18.68	103.37	0.30	2.81	2.38	2.42	8.28	18.78	2.29	10.84	2.45	0.88	2.50	3.10	2.13	2.29	0.35	52.59	0.11	2.95	1.21
814487	2008	2006	rep	89	1332	122042	493	162000	577	227	1199	113668	1.02	14.61	42.43	7.29	461.02	13.81	61.55		2.30	0.81	4.92	11.86	21.66	2.68	11.57	2.50	1.05	2.44	2.31	1.55	1.66	0.25	18.15	0.04	2.30	0.83
814487	2008	2006	rep	48	596	122337	132	162000	1180	238	2724	109031	1.00	22.59	37.76	9.07	542.11	20.45	82.89		2.61	2.85	1.51	10.64	22.76	2.98	13.00	2.82	1.40	2.97	3.60	2.22	2.48	0.39	23.70	0.09	3.31	1.15
814487	2008	2006	rep	21	1315	123211	259	162000	623	537	3382	113699	1.48	29.76	40.87	36.12	660.72	74.62	6.19	0.24	1.69	6.57	1.77	40.02	77.42	9.94	43.71	10.61	3.60	12.36	12.40	6.82	6.35	0.96	45.22	0.06	0.10	1.05
814487	2008	2006	rep	27	948	115745	132	162000	13869	751	4117	94467	27.72	44.20	43.23	47.72	1117.28	19.88	22.32	0.22	2.81	23.51	23.06	9.49	16.27	1.84	8.55	2.26	1.66	2.89	3.33	1.99	2.15	0.31	54.60	0.08	0.04	0.59
814487	2008	2006	rep	35	1155	123001	172	162000	8160	622	2650	86674		15.46	35.50	30.81	679.23	32.74	15.65	0.27	1.58	9.42	4.90	8.04	12.34	1.50	7.30	2.71	1.56	3.81	5.28	3.14	3.08	0.47	20.84		0.06	0.21
814487	2008	2006	rep	51	3736	127063	1785	162000	2017	699	1807	94486	3.68	51.18	38.20	24.29	443.08	25.78	5.49		1.62	3.10	29.21	20.27	33.35	3.84	16.26	4.16	2.78	4.57	4.78	2.31	1.72	0.28	37.79	0.04	0.03	0.17
814487	2008	2006	rep	578	1661	121798	717	162000	603	459	1650	111273	3.34	30.02	54.70	14.19	435.96	30.16	91.55		4.31	1.61	9.48	24.25	49.21	5.55	23.44	4.83	2.47	4.89	5.40	3.64	3.97	0.61	18.92	0.07	3.65	2.41
814487	2008	2006	rep	20	277	125426	4	162000	680	713	3962	103993	0.66	6.45	42.21	62.98	710.27	25.88	4.65		2.09	8.31	0.76	7.28	14.52	1.90	8.47	2.09	1.46	2.98	4.24	2.99	3.73	0.62	60.81	0.08	0.04	2.84
814487	2008	2006	rep	7	252	124757	3	162000	471	1106	4631	100208	16.09	16.85	41.09	106.87	1038.57	16.09	4.20		2.19	45.64	5.55	6.33	10.51	1.14	5.08	1.52	1.62	1.50	2.03	1.86	2.04	0.35	84.36	0.05		1.46
814487	2008	2006	rep	8	255	129340		162000	209	867	8157	101652	3.49	12.41	46.69	114.12	1316.03	9.71	1.68	0.17	1.86	52.59	1.24	7.49	11.54	1.26	4.97	1.06	1.49	1.28	1.50	1.11	1.18	0.19	72.61			1.15
814487	2008	2006	rep	17	2062	116697	318	162000	447	510	1851	118475		15.80	60.45	18.48	455.98	12.18	0.67		4.00	2.70	3.76	5.63	10.67	1.29	5.74	1.36	2.52	1.45	1.86	1.29	1.58	0.24	24.22	0.07	0.08	0.69
814487	2008	2006	rep	116	1424	119868	326	162000	663	251	1629	112339		15.16	41.40	13.23	269.73	48.70	50.62		2.02	1.51	2.71	18.97	38.37	4.98	22.39	5.34	3.75	6.22	7.28	5.06	4.83	0.73	22.67	0.24	2.14	0.67
814487	2008	2006	rep	266	1629	118588	342	162000	9175	187	1004	98757	3.16	36.87	40.11	13.23	357.74	30.17	69.41		2.94	1.21	6.02	8.97	19.91	2.78	11.48	3.00	0.88	3.71	6.00	3.61	3.49	0.47	17.56	0.04	3.01	0.91
814487	2008	2006	rep	54	2611	123434	91	162000	313	246	1734	110265		17.98	58.89	20.46	223.01	9.53	0.47		1.42	1.12	0.75	3.49	6.86	0.84	3.38	1.08	1.26	1.04	1.48	1.06	1.04	0.19	13.08	0.09	0.08	0.22
353226	2006	2006	rep							590	2874	10	0.00	23.62	49.27	103.91	1376.74	5.74	3.36	0.00	0.52	14.97	4.44	3.20	5.42	0.60	2.67	0.52	1.17		0.65		0.72	0.14	112.61	2.40	0.02	0.24
353226	2006	2006	rep							540	2387	9	0.00	15.23	47.11	110.63	1841.40	4.93	4.79	0.00	0.25	12.16	10.03	2.93	4.96	0.53	2.05	0.41	1.46		0.48		0.53	0.11	74.37	1.27	0.07	0.11
353226	2006	2006	rep							330	1233	8	12.30	11.96	47.76	45.99	1221.05	4.13	4.03	0.00	0.57	7.41	11.58	1.26	2.40	0.31	1.51	0.42	0.58		0.43		0.39	0.06	43.39	0.70	0.05	0.04
353226	2006	2006	rep							477	1816	10	8.82	19.39	54.71	30.70	1183.73	10.31	8.02	0.00	0.74	7.78	34.63	2.58	6.55	0.97	4.91	1.43	1.23		1.44		0.86	0.14	46.98	0.71	0.11	0.10
353226	2006	2006	rep							894	2162	10	0.00	21.50	59.16	170.73	2195.80	2.19	2.86	0.00	0.40	43.76	2.97	3.53	4.37	0.42	1.66	0.32	3.78		0.27		0.30	0.05	64.43	1.47	0.02	0.06
353226	2006	2006	rep							987	1505	10	0.63	14.79	57.61	164.44	2151.07	1.76	3.27	0.00	0.15	29.95	3.04	3.57	5.12	0.49	1.97	0.34	2.51		0.21		0.19	0.03	61.79	1.15	0.02	0.07
353226	2006	2006	rep							910	1840	10	0.00	13.11	53.81	164.53	1829.09	3.20	5.58	0.00	0.14	33.00	2.18	4.88	7.39	0.73	2.64	0.40	2.32		0.42		0.45	0.08	69.97	1.73	0.10	0.12
353226	2006	2006	rep							1290	1624	11	16.12	18.50	72.64	180.78	2269.44	1.88	3.58	0.00	0.69	30.80	46.53	3.54	4.62	0.39	1.67	0.00	2.63		0.19		0.15	0.04	70.79	1.58	0.10	0.07
353227	2006	2006	vein							349	2632	9	0.00	10.71	68.35	100.52	3100.30	9.75	3.39	0.00	0.42	55.53	3.41	5.16	8.21	1.01	4.70	1.11	2.35		1.28		0.81	0.13	107.65	0.15	0.00	0.12
353227	2006	2006	vein							371	2220	8	0.00	18.74	56.55	80.30	2075.18	20.18	6.36	0.00	0.48	24.49	4.65	5.61	12.29	1.77	8.83	2.39	2.07		2.77		1.92	0.32	91.88	1.11	0.20	0.27
353227	2006	2006	vein							475	2399	9	0.00	10.13	62.94	90.61	2782.46	7.82	3.63	0.00	0.37	45.72	3.28	3.90	6.58	0.81	4.06	0.93	2.18		1.03		0.73	0.13	106.60	0.17	0.00	0.10
353227	2006	2006	vein							487	2255	9	0.00	10.67	67.23	97.16	2728.44	8.01	3.61	0.00	0.46	47.20	3.36	4.06	7.05	0.92	4.40	0.95	2.02		1.08		0.80	0.11	101.56	0.15	0.00	0.11
353227	2006	2006	vein							360	2560	9	0.00	9.12	67.01	107.47	2960.91	7.62	4.23	0.00	0.35	54.06	3.08	4.06	6.25	0.75	3.64	0.92	2.16		0.97		0.60	0.11	102.64	0.12	0.00	0.13
353227	2006	2006	vein							372	2439	9	0.00	8.25	67.01	106.55	2791.58	5.38	0.20	0.00	0.40	49.70	3.09	2.92	4.25	0.51	2.61	0.60	1.89		0.64		0.41	0.06	94.27	0.15	0.00	0.10
353227	2006	2006	vein							490	2919	9	0.00	14.09	67.09	129.68	2949.80	69.80	34.31	0.00	0.89	64.31	3.93	25.63	49.12	6.53	32.24	8.22	7.22		8.97		5.91	0.96	117.51	0.22	0.14	0.28

Appendix 2.6 continued

Sample #	Year Analyzed	Year Collected	Epi Type	Na	Mg	Al	K	Ca	Ti	V	Mn	Fe	Cu	Zn	Ga	As	Sr	Y	Zr	Mo	Sn	Sb	Ba	La	Ce	Pr	Nd	Sm	Eu	Gd	Dy	Er	Yb	Lu	Pb	Bi	Th	U
353227	2006	2006	vein							404	2671	9	0.00	10.83	71.85	107.34	2982.39	10.38	2.92	0.00	0.38	54.68	3.30	5.73	10.58	1.35	6.41	1.53	2.44		1.46		0.80	0.14	115.34	0.18	0.00	0.12
353227	2006	2006	vein							302	2330	9	0.64	8.73	52.44	96.63	2291.95	23.20	17.75	0.00	0.52	42.42	2.50	7.41	16.73	2.53	13.25	3.53	3.27		3.47		2.05	0.31	71.61	0.18	0.25	0.17
353227	2006	2006	vein							359	1383	8	0.00	7.90	53.89	73.66	1635.26	19.37	26.24	0.00	0.46	27.19	1.34	5.83	13.40	2.00	9.92	2.73	2.16		3.00		2.09	0.35	77.53	0.86	0.86	0.24
353227	2006	2006	vein							587	2554	9	0.00	9.92	65.43	120.28	2722.47	12.94	5.38	0.00	0.42	49.67	3.80	4.44	8.43	1.14	5.39	1.41	2.81		1.65		1.10	0.19	116.78	0.19	0.01	0.10
353227	2006	2006	vein							272	2182	8	0.39	6.55	53.22	80.41	2380.54	22.51	18.85	0.00	0.39	24.74	1.71	5.36	12.97	1.96	10.86	3.24	2.22		3.75		2.01	0.33	78.43	0.49	0.90	0.16
353227	2006	2006	vein							457	2601	9	0.00	8.58	65.52	106.66	2756.57	6.17	2.08	0.00	0.35	51.72	3.14	2.64	4.13	0.48	2.35	0.53	2.30		0.67		0.53	0.10	110.74	0.21	0.00	0.09
353227	2006	2006	vein							317	2171	8	0.00	7.96	58.50	84.61	2273.08	20.07	20.36	0.00	0.38	24.08	1.57	5.01	11.52	1.69	8.79	2.68	1.95		3.17		1.95	0.28	91.21	0.98	0.50	0.19
353227	2006	2006	vein					23.59		349	2632	9		10.71	68.35	100.52	3100.30	9.75	3.39		0.42	55.53	3.41	5.16	8.21	1.01	4.70	1.11	2.35		1.28		0.81	0.13	107.65	0.15		0.12
353227	2006	2006	vein					23.22		371	2220	8		18.74	56.55	80.30	2075.18	20.18	6.36		0.48	24.49	4.65	5.61	12.29	1.77	8.83	2.39	2.07		2.77		1.92	0.32	91.88	1.11	0.20	0.27
353227	2006	2006	vein					23.13		475	2399	9		10.13	62.94	90.61	2782.46	7.82	3.63		0.37	45.72	3.28	3.90	6.58	0.81	4.06	0.93	2.18		1.03		0.73	0.13	106.60	0.17		0.10
353227	2006	2006	vein					23.24		487	2255	9		10.67	67.23	97.16	2728.44	8.01	3.61		0.46	47.20	3.36	4.06	7.05	0.92	4.40	0.95	2.02		1.08		0.80	0.11	101.56	0.15		0.11
353227	2006	2006	vein					23.24		360	2560	9		9.12	67.01	107.47	2960.91	7.62	4.23		0.35	54.06	3.08	4.06	6.25	0.75	3.64	0.92	2.16		0.97		0.60	0.11	102.64	0.12		0.13
353227	2006	2006	vein					23.37		372	2439	9		8.25	67.01	106.55	2791.58	5.38	0.20		0.40	49.70	3.09	2.92	4.25	0.51	2.61	0.60	1.89		0.64		0.41	0.06	94.27	0.15	0.00	0.10
353227	2006	2006	vein					23.32		490	2919	9		14.09	67.09	129.68	2949.80	69.80	34.31		0.89	64.31	3.93	25.63	49.12	6.53	32.24	8.22	7.22		8.97		5.91	0.96	117.51	0.22	0.14	0.28
353227	2006	2006	vein					23.33		404	2671	9		10.83	71.85	107.34	2982.39	10.38	2.92		0.38	54.68	3.30	5.73	10.58	1.35	6.41	1.53	2.44		1.46		0.80	0.14	115.34	0.18		0.12
353227	2006	2006	vein					23.49		302	2330	9	0.64	8.73	52.44	96.63	2291.95	23.20	17.75		0.52	42.42	2.50	7.41	16.73	2.53	13.25	3.53	3.27		3.47		2.05	0.31	71.61	0.18	0.25	0.17
353227	2006	2006	vein					23.76		359	1383	8		7.90	53.89	73.66	1635.26	19.37	26.24		0.46	27.19	1.34	5.83	13.40	2.00	9.92	2.73	2.16		3.00		2.09	0.35	77.53	0.86	0.86	0.24
353227	2006	2006	vein					23.76		587	2554	9		9.92	65.43	120.28	2722.47	12.94	5.38		0.42	49.67	3.80	4.44	8.43	1.14	5.39	1.41	2.81		1.65		1.10	0.19	116.78	0.19	0.01	0.10
353227	2006	2006	vein					23.37		272	2182	8	0.39	6.55	53.22	80.41	2380.54	22.51	18.85		0.39	24.74	1.71	5.36	12.97	1.96	10.86	3.24	2.22		3.75		2.01	0.33	78.43	0.49	0.90	0.16
353227	2006	2006	vein					23.32		457	2601	9		8.58	65.52	106.66	2756.57	6.17	2.08		0.35	51.72	3.14	2.64	4.13	0.48	2.35	0.53	2.30		0.67		0.53	0.10	110.74	0.21		0.09
353227	2006	2006	vein					23.32		317	2171	8		7.96	58.50	84.61	2273.08	20.07	20.36		0.38	24.08	1.57	5.01	11.52	1.69	8.79	2.68	1.95		3.17		1.95	0.28	91.21	0.98	0.50	0.19
353229	2006	2006	vein							413	1692	13	0.00	16.80	80.70	16.91	702.31	18.74	5.07	0.00	0.92	5.33	4.14	26.33	64.04	8.95	38.25	7.80	2.88		3.39		1.39	0.15	11.75	0.87	0.00	0.92
353229	2006	2006	vein							727	2636	13	0.00	19.74	121.64	46.50	1177.32	45.42	4.62	0.00	0.00	9.69	3.61	35.97	74.98	9.35	42.49	7.61	4.75		6.71		3.04	0.27	30.62	2.82	0.00	1.85
353229	2006	2006	vein					23.45		413	1692	13		16.80	80.70	16.91	702.31	18.74	5.07		0.92	5.33	4.14	26.33	64.04	8.95	38.25	7.80	2.88		3.39		1.39	0.15	11.75	0.87		0.92
353229	2006	2006	vein					23.50		727	2636	13		19.74	121.64	46.50	1177.32	45.42	4.62			9.69	3.61	35.97	74.98	9.35	42.49	7.61	4.75		6.71		3.04	0.27	30.62	2.82		1.85
353230	2006	2006	rep							474	3749	11	1.09	26.62	61.81	67.40	1038.67	72.26	129.54	0.47	2.55	11.81	6.32	78.11	157.52	18.45	76.77	16.97	12.36		14.49		6.92	0.95	34.18	1.16	5.02	3.02
353230	2006	2006	rep							694	5404	11	0.00	11.54	75.32	16.86	1569.29	120.65	8.86	0.00	2.06	7.84	2.87	33.64	77.52	10.49	51.67	14.14	5.22		20.17		10.53	1.28	27.78	0.27	0.40	3.70
353230	2006	2006	rep							824	5328	10	0.74	35.13	66.37	22.27	2054.30	105.14	18.03	0.00	1.85	9.69	4.12	25.22	58.27	7.93	39.08	11.35	5.68		16.68		9.18	1.21	29.37	0.26	1.90	2.98
353230	2006	2006	rep							686	5781	10	0.00	11.80	68.89	19.10	1654.01	106.77	2.25	0.00	1.42	8.90	3.41	31.57	68.44	9.18	45.54	12.22	4.64		17.04		10.87	1.44	32.61	0.33	0.03	3.03
353230	2006	2006	rep							808	3868	11	0.72	26.10	69.38	64.74	1691.29	121.12	34.34	0.00	2.03	17.15	5.08	94.54	205.86	27.16	126.14	31.05	12.90		25.18		7.65	1.00	41.13	0.83	2.81	2.48
353230	2006	2006	rep							564	4252	11	0.90	38.16	60.57	61.88	1391.65	65.29	94.95	0.00	2.01	11.90	4.20	30.90	62.72	7.93	37.07	9.61	8.43		11.73		5.92	0.85	26.87	0.75	2.94	1.78
353230	2006	2006	rep							829	3950	12	0.00	20.15	85.20	121.94	736.45	161.48	17.08	0.00	2.03	26.79	3.83	88.74	196.75	26.01	120.55	31.05	10.63		29.86		9.42	1.14	33.16	2.22	0.68	3.26
353230	2006	2006	rep							725	3729	12	0.00	21.23	83.54	93.21	637.29	94.60	108.46	0.00	2.45	23.28	4.30	70.59	145.79	18.49	83.65	19.19	11.09		18.29		6.86	0.91	34.61	1.75	3.35	4.59
353230	2006	2006	rep							1070	4457	11	0.00	14.31	67.83	29.74	1746.37	141.39	36.53	0.00	2.10	11.76	3.70	55.57	129.55	17.39	80.80	20.52	6.61		23.55		12.66	1.67	39.97	0.40	2.05	3.79
353230	2006	2006	rep							954	4448	10	0.61	41.86	61.32	25.25	2971.23	15.14	24.12	0.00	1.56	12.40	9.79	7.50	13.92	1.70	7.77	1.84	1.84		2.03		2.15	0.37	46.76	0.07	0.03	0.66
353230	2006	2006	rep							743	4464	11	0.00	38.27	75.45	83.77	1412.93	83.89	167.83	0.00	2.57	12.87	4.08	34.84	70.90	9.10	42.19	10.58	8.36		14.31		7.68	1.08	27.99	0.90	5.61	4.09
353230	2006	2006	rep							756	3698	12	0.00	66.88	71.59	75.44	1353.04	71.33	155.28	0.88	2.22	13.05	5.76	65.51	123.79	14.39	62.17	13.70	12.72		12.96		6.87	0.91	40.32	1.08	4.89	3.32
353230	2006	2006	rep					21.87		474	3749	11	1.09	26.62	61.81	67.40	1038.67	72.26	129.54	0.47	2.55	11.81	6.32	78.11	157.52	18.45	76.77	16.97	12.36		14.49		6.92	0.95	34.18	1.16	5.02	3.02
353230	2006	2006	rep					23.17		694	5404	11		11.54	75.32	16.86	1569.29	120.65	8.86		2.06	7.84	2.87	33.64	77.52	10.49	51.67	14.14	5.22		20.17		10.53	1.28	27.78	0.27	0.40	3.70
353230	2006	2006	rep					22.89		824	5328	10	0.74	35.13	66.37	22.27	2054.30	105.14	18.03		1.85	9.69	4.12	25.22	58.27	7.93	39.08	11.35	5.68		16.68		9.18	1.21	29.37	0.26	1.90	2.98
353230	2006	2006	rep					23.21		686	5781	10		11.80	68.89	19.10	1654.01	106.77	2.25		1.42	8.90	3.41	31.57	68.44	9.18	45.54	12.22	4.64		17.04		10.87	1.44	32.61	0.33	0.03	3.03
353230	2006	2006	rep					22.58		808	3868	11	0.72	26.10	69.38	64.74	1691.29	121.12	34.34		2.03	17.15	5.08	94.54	205.86	27.16	126.14	31.05	12.90		25.18		7.65	1.00	41.13	0.83	2.81	2.48
353230	2006	2006	rep					22.40		564	4252	11	0.90	38.16	60.57	61.88	1391.65	65.29	94.95		2.01	11.90	4.20	30.90	62.72	7.93	37.07	9.61	8.43		11.73		5.92	0.85	26.87	0.75	2.94	1.78
353230	2006	2006	rep					23.16		829	3950	12		20.15	85.20	121.94	736.45	161.48	17.08		2.03	26.79	3.83	88.74	196.75	26.01	120.55	31.05	10.63		29.86		9.42	1.14	33.16	2.22	0.68	3.26
353230	2006	2006	rep					23.16		725	3729	12		21.23	83.54	93.21	637.29	94.60	108.46		2.45	23.28	4.30	70.59	145.79	18.49	83.65	19.19	11.09		18.29		6.86	0.91	34.61	1.75	3.35	4.59
353230	2006	2006	rep					22.84		1070	4457	11		14.31	67.83	29.74	1746.37	141.39	36.53		2.10	11.76	3.70	55.57	129.55	17.39	80.80	20.52	6.61		23.55		12.66	1.67	39.97	0.40	2.05	3.79
353230	2006	2006	rep					23.18		954	4448	10	0.61	41.86	61.32	25.25	2971.23	15.14	24.12		1.56	12.40	9.79	7.50	13.92	1.70	7.77	1.84	1.84		2.03		2.15	0.37	46.76	0.07	0.03	0.66
353230	2006	2006	rep					22.63		743	4464	11		38.27	75.45	83.77	1412.93	83.89	167.83		2.57	12.87	4.08	34.84	70.90	9.10	42.19	10.58	8.36		14.31		7.68	1.08	27.99	0.90	5.61	4.09
353230	2006	2006	rep					22.63		756	3698	12		66.88	71.59	75.44	1353.04	71.33	155.28	0.88	2.22	13.05	5.76	65.51	123.79	14.39	62.17	13.70	12.72		12.96		6.87	0.91	40.32	1.08	4.89	3.32
353230	2006	2006	rep					21.87		474	3749	11	1.09	26.62	61.81	67.40	1038.67	72.26	129.54	0.47	2.55	11.81	6.32	78.11	157.52	18.45	76.77	16.97	12.36		14.49		6.92	0.95	34.18	1.16	5.02	3.02
353230	2006	2006	rep					23.17		694	5404	11		11.54	75.32	16.86	1569.29	120.65	8.86		2.06	7.84	2.87	33.64	77.52	10.49	51.67	14.14	5.22		20.17		10.53	1.28	27.78	0.27	0.40	3.70
353230	2006	2006	rep					22.89		824	5328	10	0.74	35.13	66.37	22.27	2054.30	105.14	18.03		1.85	9.69	4.12	25.22	58.27	7.93	39.08	11.35	5.68		16.68		9.18	1.21	29.37	0.26	1.90	2.98
353230	2006	2006	rep					23.21		686	5781	10		11.80	68.89	19.10	1654.01	106.77	2.25		1.42	8.90	3.41	31.57	68.44	9.18	45.54	12.22	4.64		17.04		10.87	1.44	32.61	0.33	0.03	3.03
353230	2006	2006	rep					22.58		808	3868	11	0.72	26.10	69.38	64.74	1691.29	121.12	34.34		2.03	17.15	5.08	94.54	205.86	27.16	126.14	31.05	12.90		25.18		7.65	1.00	41.13	0.83	2.81	2.48
353230	2006	2006	rep					22.40		564	4252	11	0.90	38.16	60.57	61.88	1391.65	65.29	94.95		2.01	11.90	4.20	30.90	62.72	7.93	37.07	9.61	8.43		11.73		5.92	0.85	26.87	0.75	2.94	1.78
353230	2006	2006	rep					23.16		829	3950	12		20.15	85.20	121.94	736.45	161.48	17.08		2.03	26.79	3.83	88.74	196.75	26.01	120.55	31.05	10.63		29.86		9.42	1.14	33.16	2.22	0.68	3.26
353230	2006	2006	rep					23.16		725	3729	12		21.23	83.54	93.21	637.29	94.60	108.46		2.45	23.28	4.30	70.59	145.79	18.49	83.65	19.19	11.09		18.29		6.86	0.91	34.61	1.75	3.35	4.59
353230	2006	2006	rep					22.84		1070	4457	11		14.31	67.83	29.74	1746.37	141.39	36.53		2.10	11.76	3.70	55.57	129.55	17.39	80.80	20.52	6.61		23.55		12.66	1.67	39.97	0.40	2.05	3.79
353230	2006	2006	rep					23.18		954	4448	10	0.61	41.86	61.32	25.25	2971.23	15.14	24.12		1.56	12.40	9.79	7.50	13.92	1.70	7.77	1.84	1.84		2.03		2.15	0.37	46.76	0.07	0.03	0.66
353230	2006	2006	rep					22.63		743	4464	11		38.27	75.45	83.77	1412.93	83.89	167.83		2.57	12.87	4.08	34.84	70.90	9.10	42.19	10.58	8.36		14.31		7.68	1.08	27.99	0.90	5.61	4.09
353230	2006	2006	rep					22.63		756	3698	12		66.88	71.59	75.44	1353.04	71.33	155.28	0.88	2.22	13.05	5.76	65.51	123.79	14.39	62.17	13.70	12.72		12.96		6.87	0.91	40.32	1.08	4.89	3.32
353230	2006	2006	vein							453	3725	11	0.00	22.31	72.65	112.85	735.91	47.05	6.77	0.00	1.55	18.56	3.98	236.60	448.13	48.47	181.44	27.92	6.78		9.52		3.31	0.44	27.43	1.16	0.28	1.50
353230	2006	2006	vein							993	4054	11	0.00	22.20	77.73	85.50	925.22	162.25	26.51	0.00	2.41	12.21	3.55	84.04	186.50	24.36	110.97	26.71	8.42		29.26		12.58	1.51	25.67	1.24	4.06	6.06
353230	2006	2006	vein					22.64		453	3725	11		22.31	72.65	112.85	735.91	47.05	6.77		1.55	18.56	3.98	236.60	448.13	48.47	181.44	27.92	6.78		9.52		3.31	0.44	27.43	1.16	0.28	1.50
353230	2006	2006	vein					22.28		993	4054	11		22.20	77.73	85.50	925.22	162.25	26.51		2.41	12.21	3.55	84.04	186.50	24.36	110.97	26.71	8.42		29.26		12.58	1.51	25.67	1.24	4.06	6.06
353230	2006	2006	vein					22.64		453	3725	11		22.31	72.65	112.85	735.91	47.05	6.77		1.55	18.56	3.98	236.60	448.13	48.47	181.44	27.92	6.78		9.52		3.31	0.44	27.43	1.16	0.28	1.50
353230	2006	2006	vein					22.28		993	4054	11		22.20	77.73	85.50	925.22	162.25	26.51		2.41	12.21	3.55	84.04	186.50	24.36	110.97	26.71	8.42		29.26		12.58	1.51	25.67	1.24	4.06	6.06
354019	2006	2006	rep						335	303	3921	8	1.11	17.03	71.29	23.87	1473.32	8.22	50.50	0.00	4.01	1.22	0.69	20.76	31.44	2.97	11.14	1.85	4.30	1.72	1.32	0.63	0.71	0.11	66.62	1.04	3.83	2.78
354019	2006	2006	rep						1168	364	3415	7	1.16	30.64	76.98	27.80	933.10	156.51	347.50	0.00	7.87	9.91	3.60	1402.05	2421.17	225.19	694.91	85.91	50.10	54.58	33.62	12.89	9.83	1.24	80.16	0.83	65.65	59.87
354019	2006	2006	rep						91	71	2229	7	6.84	7.47	48.25	10.83	1189.21	10.16	2.70	0.00	3.23	1.14	11.49	50.14	106.84	10.69	37.28	5.43	1.25	3.68	2.30	0.81	0.61	0.07	46.77	0.57	0.45	3.44
354019	2006	2006	rep						795	402	5745	8	58.37	134.37	76.86	17.67	2220.52	317.62	261.40	0.00	8.03	5.59	64.04	1487.07	3248.90	345.68	1230.70	177.57	14.75	120.71	68.52	24.49	16.58	2.22	73.29	2.90	46.40	30.80
354510	2006	2006	rep							239	2846	10	0.96	42.35	33.02	7.18	862.78	5.30	2.15	1.83	1.03	2.17	59.61	9.00	17.56	1.93	7.15	1.24	0.68		0.81		0.62	0.09	6.67	0.16	0.09	0.89
354510	2006	2006	rep							182	2576	10	0.00	15.63	32.62	7.51	809.73	8.14	3.43	0.00	1.73	2.88	49.42	8.71	16.64	1.83	7.10	1.30	1.10		1.28		0.90	0.13	7.77	0.13	0.46	0.73
354510	2006	2006	rep							174	3518	8	0.51	11.42	31.59	5.49	767.45	15.00	4.27	0.43	0.92	2.15	63.14	8.80	17.60	2.06	8.66	2.23	1.66		2.49		1.50	0.22	7.77	0.08	0.24	0.76
354510	2006	2006	rep							210	2867	9	0.00	6.94	50.19	3.33	488.02	0.72	0.22	0.00	0.37	0.36	9.62	0.22	0.28	0.02	0.11	0.00	0.37		0.06		0.24	0.04	3.57	0.06	0.00	0.04
354510	2006	2006	rep							294	2779	10	1.01	19.29	38.64	4.36	621.67	4.59	1.61	0.00	0.74	0.96	26.95	2.97	6.05	0.69	2.72	0.51	0.73		0.67		0.59	0.09	5.17	0.13	0.50	0.53
354510	2006	2006	rep							647	1896	10	0.00	24.63	39.95	2.63	516.08	36.69	2.94	0.00	1.54	0.33	7.39	48.80	108.29	13.50	57.62	11.44	3.56		6.47		2.52	0.35	2.73	0.13	0.05	1.10
354510	2006	2006	rep							326	1666	10	0.86	8.34	31.78	1.76	479.94	53.83	0.55	0.00	0.96	0.13	9.53	24.53	55.37	6.88	30.59	7.11	7.46		6.81		5.04	0.71	2.87	0.12	0.02	0.93
354510	2006	2006	rep							381	1678	11	2.99	24.22	37.98	2.72	430.61	13.50	1.32	0.00	0.83	0.60	13.83	20.54	53.71	6.06	24.01	4.99	2.29		2.53		1.02	0.14	3.58	0.32	0.01	0.87
354510	2006	2006	rep							104	2745	10	0.55	28.52	29.77	6.21	417.36	1.42	0.62	0.00	0.40	1.09	29.17	2.93	4.66	0.44	1.59	0.23	1.12		0.18		0.13	0.03	5.87	0.07	0.21	0.09
354510	2006	2006	rep							207	2959	10	0.76	17.40	42.74	5.93	603.92	9.97	1.66	0.00	1.12	1.80	64.60	12.44	23.03	2.66	10.94	1.99	2.46		1.71		1.08	0.17	6.40	0.17	0.07	0.72
354510	2006	2006	rep							176	5144	9	1.31	24.29	41.54	7.00	718.73	6.04	6.51	0.00	1.30	2.15	81.88	6.00	10.30	1.15	4.90	1.04	1.67		0.86		0.60	0.11	8.37	0.16	0.31	0.51
354510	2006	2006	rep							194	2325	9	2.70	17.74	33.67	4.23	665.23	29.71	14.07	0.00	0.91	2.53	44.58	7.07	14.30	1.81	8.67	2.59	2.76		3.61		2.80	0.33	5.45	0.10	0.97	0.60
354510	2006	2006	rep							537	4332	9	18.76	22.32	72.33	8.38	703.26	53.21	1.16	0.00	10.49	6.72	26.87	49.27	102.89	13.03	56.96	12.60	7.60		9.51		3.67	0.55	8.78	3.80	0.18	2.05
354510	2006	2006	rep							625	3440	9	7.65	21.39	71.25	6.73	733.10	49.28	3.89	1.32	2.01	3.80	48.19	41.31	88.09	10.68	45.20	10.26	5.49		8.18		3.32	0.50	10.37	0.35	0.85	2.13
354510	2006	2006	vein							818	3196	8	3.18	27.11	64.61	6.17	691.51	192.39	1.05	0.00	9.95	4.11	32.79	136.32	310.29	40.26	177.43	40.18	19.07		28.76		13.30	1.79	8.49	2.05	0.07	3.61
354511	2006	2006	rep							599	1991	9	0.00	6.03	56.23	6.40	387.77	9.02	0.89	0.00	3.38	0.39	5.22	6.07	11.87	1.38	5.83	1.36	0.81		1.58		1.08	0.18	3.61	0.04	0.31	0.68
354511	2006	2006	rep							516	1632	10	0.00	3.64	61.53	4.00	413.18	3.60	0.82	0.00	3.36	0.13	1.80	3.76	6.74	0.75	2.98	0.56	0.79		0.61		0.52	0.08	3.71	0.02	0.14	0.52
354511	2006	2006	rep							609	1726	10	0.00	9.42	63.99	4.95	358.89	7.89	0.98	0.00	0.00	0.44	6.99	8.54	17.47	1.97	8.22	1.59	0.95		1.32		0.86	0.14	4.07	0.04	0.30	0.74
354511	2006	2006	rep							336	2192	10	0.00	7.22	58.58	9.51	488.97	5.80	0.99	0.00	1.80	1.45	7.59	7.85	14.99	1.57	6.00	1.16	0.93		0.93		0.74	0.12	5.40	0.03	0.80	0.52
354511	2006	2006	rep							571	1429	9	0.00	6.14	55.81	7.52	302.19	5.17	0.60	0.00	2.81	0.64	3.19	3.83	7.86	0.88	3.54	0.79	0.79		0.78		0.77	0.12	3.23	0.03	0.71	0.51
354511	2006	2006	vein							211	1673	10	0.00	11.87	54.04	8.81	352.52	7.03	3.03	0.00	1.64	0.74	11.15	3.78	7.69	0.85	3.91	0.96	0.93		1.14		0.66	0.11	2.32	0.02	0.17	0.11
354511	2006	2006	vein							277	3244	8	0.00	5.24	44.13	8.26	662.57	27.52	4.24	0.00	1.64	1.44	28.53	19.40	38.12	4.72	20.87	4.96	2.57		4.58		2.24	0.36	6.99	0.02	0.23	0.44
354511	2006	2006	vein							377	2706	9	1.36	23.89	39.52	5.66	809.55	141.83	1.20	0.00	0.92	1.66	88.18	52.42	157.28	23.62	111.52	26.96	5.45		25.41		12.93	1.92	8.43	0.05	1.04	0.48
354511	2006	2006	vein							512	1549	9	0.00	14.19	57.24	4.74	607.67	35.36	9.55	0.00	1.60	1.31	159.85	17.63	36.30	4.73	20.80	4.84	5.43		6.21		3.63	0.58	4.05	0.02	1.12	0.62
354511	2006	2006	vein							120	2160	8	0.00	7.53	47.87	9.64	707.02	1.81	0.12	0.00	1.95	3.43	25.59	4.32	7.01	0.66	2.32	0.40	0.76		0.34		0.19	0.03	7.87	0.10	0.00	0.12
354511	2006	2006	vein							171	1771	9	0.00	12.97	47.55	4.64	508.43	41.94	0.78	0.38	1.65	1.53	167.02	35.72	67.87	8.00	32.88	7.67	2.26		7.71		2.06	0.27	6.80	0.02	0.08	0.42
354511	2006	2006	vein							49	2174	10	0.00	16.38	31.11	3.14	491.25	5.68	0.26	0.00	0.49	0.51	31.95	6.74	12.49	1.23	4.48	0.93	0.76		0.89		0.51	0.06	2.77	0.00	0.04	0.15
354511	2006	2006	vein							53	1351	10	0.00	6.92	30.55	5.59	740.05	1.73	0.27	0.00	0.60	0.95	37.93	6.76	12.44	1.21	4.49	0.77	0.55		0.33		0.19	0.02	3.97	0.02	0.09	0.09

Appendix 2.6 continued

Sample #	Year Analyzed	Year Collected	Epi Type	Na	Mg	Al	K	Ca	Ti	V	Mn	Fe	Cu	Zn	Ga	As	Sr	Y	Zr	Mo	Sn	Sb	Ba	La	Ce	Pr	Nd	Sm	Eu	Gd	Dy	Er	Yb	Lu	Pb	Bi	Th	U
354511	2006	2006	vein							22	722	11	0.00	7.82	28.70	2.10	247.97	1.79	0.41	0.00	0.34	0.36	16.67	5.23	9.20	0.95	3.25	0.55	0.52		0.34		0.20	0.03	1.76	0.00	0.09	0.10
354554	2006	2006	skarn assoc.						2299	128	13399	10	0.00	461.38	20.18	16.82	7.01	4.60	18.61	0.00	0.00	0.00	0.46	0.15	1.06	0.20	2.12	1.18	0.32	0.86	0.99	0.80	1.03	0.10	0.94	0.00	0.42	0.46
354554	2006	2006	skarn assoc.						2963	96	9570	3	0.00	6.69	10.31	7.26	2.56	7.89	27.48	0.00	1.09	0.00	0.77	0.35	1.08	0.24	2.36	0.88	0.23	1.46	1.67	0.91	0.95	0.13	1.02	0.00	0.48	0.59
354554	2006	2006	skarn assoc.						298	23	4226	12	0.00	8.98	21.23	12.76	1409.17	1.98	17.54	0.00	2.27	2.10	1.82	0.97	2.43	0.39	1.77	0.56	0.14	0.62	0.47	0.23	0.17	0.00	4.00	0.86	1.11	2.92
354554	2006	2006	skarn assoc.						1103	42	3807	9	0.00	18.57	18.20	18.34	823.91	2.75	1.50	0.00	2.76	3.00	2.17	0.41	1.02	0.21	1.94	0.53	0.44	0.70	0.43	0.29	0.22	0.00	7.52	1.88	0.00	1.02
354554	2006	2006	skarn assoc.						878	264	4151	9	0.00	30.69	43.77	25.79	955.84	56.46	22.86	0.00	3.60	16.57	2.18	1.17	6.02	2.67	35.55	17.19	4.14	20.04	15.73	6.24	3.64	0.50	4.88	9.63	2.09	4.31
354554	2006	2006	skarn assoc.						1620	38	4153	13	0.00	10.17	18.02	14.18	889.57	22.95	17.25	0.00	2.07	1.42	2.70	0.49	1.98	0.73	9.30	4.77	1.53	6.09	5.36	2.44	2.08	0.31	2.51	2.38	0.53	2.98
354554	2006	2006	skarn assoc.						589	63	2890	13	0.00	18.65	18.94	40.83	1071.18	15.17	42.43	0.00	1.87	46.63	1.60	0.47	1.57	0.38	3.35	1.84	0.40	2.32	3.18	1.79	1.06	0.14	5.27	6.04	0.29	3.61
354554	2006	2006	skarn assoc.						1890	42	2190	12	0.00	9.52	21.91	11.43	550.63	4.38	13.90	0.00	2.07	0.30	0.80	0.94	2.74	0.47	2.30	0.58	0.16	0.69	1.03	0.45	0.40	0.06	1.50	0.75	0.07	2.60
354554	2006	2006	skarn assoc.						545	23	3783	9	0.00	34.00	16.85	16.39	1367.04	4.83	9.38	0.00	2.23	17.19	2.61	0.93	2.37	0.34	1.78	0.66	0.19	0.79	0.88	0.44	0.32	0.06	4.31	1.90	0.10	2.78
354554	2006	2006	skarn assoc.						630	66	5220	10	0.00	77.76	16.23	23.30	1077.28	10.67	22.18	0.00	2.32	13.40	2.16	0.78	2.58	0.78	5.96	2.84	0.76	2.88	2.85	1.02	0.68	0.10	3.66	6.42	1.07	2.41
354555	2006	2006	vein						225	11	1685	8	0.00	10.01	39.61	29.06	973.15	0.64	2.67	0.00	2.71	3.73	1.85	9.17	9.61	0.64	1.27	0.00	0.19	0.00	0.00	0.00	0.00	0.00	7.01	2.35	0.43	0.20
354555	2006	2006	vein						742	140	5179	11	0.00	0.00	73.53	0.00	1552.85	2.75	4.37	0.00	7.27	0.82	3.74	8.02	8.22	0.64	1.86	0.00	0.53	0.33	0.53	0.22	0.53	0.14	1.33	2.61	22.28	3.20
354555	2006	2006	vein						65	18	810	9	0.00	14.12	31.11	23.61	586.37	0.59	1.77	0.00	0.00	1.18	1.81	3.87	4.53	0.50	6.32	0.00	1.05	0.22	0.00	0.49	0.39	0.00	14.71	2.08	1.06	0.16
354555	2006	2006	vein						277	43	1116	11	0.00	6.18	45.38	10.80	1259.25	1.75	1.78	0.00	2.41	1.09	3.72	7.94	9.25	0.69	1.97	0.31	0.25	0.28	0.28	0.16	0.36	0.00	7.66	1.20	1.26	0.81
354555	2006	2006	vein						745	41	9063	9	1569.02	20.97	41.64	48.51	1418.99	1.74	4.65	0.00	1.90	19.94	3.37	7.84	9.03	0.56	1.55	0.39	0.30	0.32	0.21	0.13	0.18	0.00	15.01	5.05	0.15	0.48
354555	2006	2006	vein						36	979	1060	10	0.00	13.98	104.83	22.13	820.28	2.66	0.00	0.00	2.97	0.00	8.54	9.02	9.68	0.69	1.61	0.00	1.46	0.35	0.30	0.25	0.24	0.06	7.11	1.14	0.09	0.21
354555	2006	2006	vein						99	457	669	10	0.00	16.15	82.45	13.06	645.76	4.81	1.15	0.00	4.00	0.68	5.11	13.66	17.59	1.41	3.77	0.57	1.31	0.60	0.65	0.47	0.63	0.11	6.46	1.42	3.06	3.06
354555	2006	2006	vein						389	72	922	10	0.00	3.58	39.49	9.30	753.46	5.02	6.05	0.00	2.64	0.84	1.84	10.47	14.43	1.25	4.80	0.79	0.41	0.57	1.27	0.63	0.73	0.12	2.24	1.07	199.33	2.41
354555	2006	2006	vein						226	80	2140	10	0.00	9.86	48.95	20.87	937.10	3.74	9.34	0.00	1.71	29.30	1.10	6.54	8.37	0.69	1.90	0.33	0.26	0.51	0.58	0.37	0.40	0.03	10.45	3.95	14.24	3.12
354555	2006	2006	vein						1307	321	3153	11	0.00	0.00	82.94	10.14	1650.02	15.22	68.20	0.00	26.90	0.38	2.88	26.89	36.53	3.41	11.54	1.85	1.22	1.85	2.39	1.51	2.68	0.48	0.00	1.73	20.25	6.82
354555	2006	2006	vein						160	240	851	10	0.00	5.13	54.63	8.55	802.40	11.44	2.22	0.00	1.88	0.00	2.63	12.79	16.70	1.32	5.35	0.77	0.92	1.25	1.47	1.28	1.55	0.20	2.91	0.60	7.33	8.06
354555	2006	2006	vein						417	280	2297	11	3.40	2.72	73.66	8.05	1300.39	7.28	9.65	0.00	3.41	1.12	0.00	22.73	24.35	2.66	8.37	1.39	0.86	1.36	1.19	0.68	0.48	0.09	6.47	1.52	18.13	5.91
354555	2006	2006	vein						64	479	922	10	0.00	8.67	63.58	15.04	688.99	2.88	1.08	0.00	1.69	0.27	5.08	9.26	11.37	0.75	2.11	0.52	0.35	0.29	0.34	0.34	0.40	0.05	8.77	0.78	0.17	2.34
354555	2006	2006	vein						1391	405	2268	10	0.00	3.10	85.32	6.89	978.64	14.19	18.97	0.00	7.51	3.28	2.03	10.44	13.20	1.31	4.57	1.04	1.03	1.45	1.79	1.19	1.67	0.22	3.68	3.48	0.27	7.63
354555	2006	2006	vein						791	295	2053	11	0.00	2.70	68.98	10.21	1404.49	8.60	14.04	0.00	4.34	0.74	3.59	13.72	18.57	1.59	5.33	0.92	0.62	0.89	1.05	1.01	1.21	0.20	2.88	2.21	31.98	10.03
354562	2006	2006	rep						829	384	1696	12	0.00	3.97	44.35	10.11	1480.85	46.95	25.46	0.00	4.01	1.92	2.23	21.66	47.61	6.22	27.88	7.33	3.84	7.83	8.24	4.60	4.56	0.68	4.53	1.05	2.15	5.14
354562	2006	2006	rep						462	283	2212	11	0.00	5.77	61.99	9.34	1870.13	18.62	15.87	0.00	6.94	0.81	3.34	8.38	16.59	1.94	7.87	1.74	2.99	2.19	3.00	1.99	1.81	0.25	3.46	1.02	0.45	3.87
354562	2006	2006	rep						486	461	1447	12	0.00	7.13	65.60	5.25	1759.39	52.61	10.41	0.00	5.97	1.63	2.11	18.78	37.10	4.75	22.37	5.96	5.99	7.42	9.00	5.66	5.05	0.73	4.15	0.78	0.07	7.07
354562	2006	2006	rep						505	187	3853	11	0.00	8.77	34.13	15.21	2598.61	37.32	9.56	0.00	1.74	1.68	2.85	96.50	223.90	24.83	95.44	14.88	1.83	11.23	8.04	3.36	2.41	0.26	6.93	3.71	1.49	7.92
354562	2006	2006	rep						804	481	2026	12	0.00	8.13	58.02	16.40	1991.46	72.09	53.97	0.00	3.50	8.25	1.21	94.27	203.39	23.13	88.96	17.36	5.25	16.22	14.32	6.26	5.60	0.86	9.86	2.83	12.69	9.24
354562	2006	2006	vein						633	261	2355	11	0.00	7.70	49.99	7.19	1377.14	26.29	15.74	0.00	6.27	1.61	2.17	15.25	31.55	4.02	18.42	4.56	2.93	4.70	5.00	2.85	2.53	0.41	5.63	0.92	0.08	2.87
354562	2006	2006	vein						965	236	2101	12	0.00	9.34	59.04	6.52	1795.54	26.42	11.28	0.00	7.03	1.46	1.76	8.80	17.73	2.21	10.42	2.81	3.21	3.84	4.65	2.90	2.55	0.35	3.30	0.74	0.07	2.85
354562	2006	2006	vein						1175	385	2144	11	0.00	12.34	63.41	7.24	1536.13	51.48	15.55	0.00	10.11	1.26	1.94	28.20	50.59	5.65	24.43	5.82	5.70	7.49	9.01	5.25	4.91	0.73	3.40	0.61	0.04	6.13
354562	2006	2006	vein						1278	521	1350	12	0.00	12.05	64.53	7.74	1413.16	70.40	16.96	0.00	7.02	1.33	1.42	22.97	52.78	7.23	35.29	10.31	7.98	11.69	13.87	6.94	5.88	0.87	3.43	0.48	0.11	6.83
354562	2006	2006	vein						1091	419	1591	11	0.00	6.63	65.89	4.51	1376.26	48.89	15.97	0.00	8.39	1.01	1.56	20.82	45.49	6.06	29.45	7.10	5.32	8.17	9.10	4.67	4.55	0.58	4.72	0.47	0.10	4.12
354562	2006	2006	vein						496	230	2345	11	0.00	11.28	66.65	7.89	1363.54	25.28	16.62	0.00	5.47	1.22	2.95	12.74	26.20	3.29	13.26	3.31	3.22	4.08	4.28	2.58	2.13	0.32	4.67	0.80	0.20	3.52
354562	2006	2006	vein						723	519	1185	12	0.00	8.41	62.28	9.28	1628.91	63.24	14.84	0.00	5.33	1.37	1.31	25.93	56.37	7.42	35.17	9.86	6.82	10.82	12.07	6.12	5.30	0.80	5.36	0.45	0.28	6.07
354562	2006	2006	vein						614	388	1722	12	0.00	6.36	51.64	7.44	2020.68	43.53	13.06	0.00	5.02	1.31	2.15	18.72	45.67	6.36	32.21	7.37	4.40	7.87	8.04	4.59	4.96	0.79	5.85	0.81	0.06	3.41
355193	2006	2006	rep							341	4356	7	0.00	22.49	24.33	113.69	417.45	47.72	7.18	0.00	0.93	2.41	3.53	40.97	71.50	9.33	43.15	10.50	3.31		8.78		3.10	0.45	56.07	0.05	0.30	0.50
355193	2006	2006	rep							229	2777	6	0.00	50.21	21.74	83.67	420.43	72.61	3.06	0.00	0.94	2.23	5.67	44.89	100.62	14.44	71.80	17.39	4.51		13.29		3.96	0.57	91.67	0.03	0.33	0.29
355193	2006	2006	rep							323	3450	9	0.00	10.20	32.36	7.67	333.67	12.72	0.70	0.00	1.26	1.51	7.72	4.28	10.68	1.52	7.74	2.51	1.60		2.29		1.04	0.12	27.40	0.00	0.05	0.04
355193	2006	2006	rep							307	4677	7	0.00	5.87	29.96	12.33	374.09	37.29	4.40	0.00	1.39	1.90	2.27	11.89	29.10	4.17	20.53	5.96	2.23		8.42		3.10	0.40	26.53	0.00	0.12	0.31
355193	2006	2006	rep					23.74		341	4356	7		22.49	24.33	113.69	417.45	47.72	7.18		0.93	2.41	3.53	40.97	71.50	9.33	43.15	10.50	3.31		8.78		3.10	0.45	56.07	0.05	0.30	0.50
355193	2006	2006	rep					23.74		229	2777	6		50.21	21.74	83.67	420.43	72.61	3.06		0.94	2.23	5.67	44.89	100.62	14.44	71.80	17.39	4.51		13.29		3.96	0.57	91.67	0.03	0.33	0.29
355193	2006	2006	rep					22.99		323	3450	9		10.20	32.36	7.67	333.67	12.72	0.70		1.26	1.51	7.72	4.28	10.68	1.52	7.74	2.51	1.60		2.29		1.04	0.12	27.40		0.05	0.04
355193	2006	2006	rep					23.37		307	4677	7		5.87	29.96	12.33	374.09	37.29	4.40		1.39	1.90	2.27	11.89	29.10	4.17	20.53	5.96	2.23		8.42		3.10	0.40	26.53		0.12	0.31
355194	2006	2006	rep							156	3919	10	0.00	6.56	41.59	19.33	609.85	10.35	1.11	0.00	2.30	4.90	4.52	0.75	2.39	0.34	1.82	0.69	0.49		1.34		2.27	0.39	12.86	0.63	0.00	0.00
355194	2006	2006	rep							97	1056	13	0.00	5.68	40.01	14.11	273.69	2.38	0.48	0.00	0.56	0.81	1.64	0.37	1.22	0.24	1.01	0.26	0.13		0.53		0.18	0.05	8.67	0.15	0.00	0.00
355194	2006	2006	rep							153	1622	13	0.00	9.62	43.00	10.52	273.70	4.74	0.60	0.00	0.79	1.19	1.55	0.83	2.48	0.40	1.80	0.43	0.21		0.89		0.72	0.07	12.83	0.18	0.00	0.03
355194	2006	2006	rep							206	1401	13	0.00	6.56	47.77	8.69	224.49	4.05	0.45	0.00	0.79	1.13	1.75	0.59	1.98	0.28	1.47	0.48	0.25		0.92		0.61	0.06	8.50	0.20	0.08	0.00
355194	2006	2006	rep					23.54		156	3919	10		6.56	41.59	19.33	609.85	10.35	1.11		2.30	4.90	4.52	0.75	2.39	0.34	1.82	0.69	0.49		1.34		2.27	0.39	12.86	0.63		
355194	2006	2006	rep					23.30		97	1056	13		5.68	40.01	14.11	273.69	2.38	0.48		0.56	0.81	1.64	0.37	1.22	0.24	1.01	0.26	0.13		0.53		0.18	0.05	8.67	0.15		
355194	2006	2006	rep					23.14		153	1622	13		9.62	43.00	10.52	273.70	4.74	0.60		0.79	1.19	1.55	0.83	2.48	0.40	1.80	0.43	0.21		0.89		0.72	0.07	12.83	0.18		0.03
355194	2006	2006	rep					23.48		206	1401	13		6.56	47.77	8.69	224.49	4.05	0.45		0.79	1.13	1.75	0.59	1.98	0.28	1.47	0.48	0.25		0.92		0.61	0.06	8.50	0.20	0.08	
355194	2006	2006	vein							156	4130	11	0.00	8.42	41.28	21.60	618.17	5.47	0.82	0.00	1.00	1.70	1.82	0.95	2.74	0.48	2.38	0.73	0.27		1.10		0.80	0.15	35.03	0.12	0.04	0.00
355194	2006	2006	vein							1321	4459	9	0.00	8.55	71.56	32.15	544.57	32.70	1.86	0.00	2.73	8.10	0.53	2.49	7.07	1.12	6.58	2.63	1.29		4.50		3.73	0.62	24.78	0.28	0.00	0.17
355194	2006	2006	vein					23.43		156	4130	11		8.42	41.28	21.60	618.17	5.47	0.82		1.00	1.70	1.82	0.95	2.74	0.48	2.38	0.73	0.27		1.10		0.80	0.15	35.03	0.12	0.04	
355194	2006	2006	vein					23.20		1321	4459	9		8.55	71.56	32.15	544.57	32.70	1.86		2.73	8.10	0.53	2.49	7.07	1.12	6.58	2.63	1.29		4.50		3.73	0.62	24.78	0.28		0.17
355195	2006	2006	rep							276	1309	11	0.00	11.50	31.68	41.83	433.03	1.72	1.21	0.00	1.57	2.07	0.78	1.50	4.08	0.55	2.14	0.48	0.94		0.35		0.22	0.03	27.94	0.02	0.03	0.22
355195	2006	2006	rep							235	1828	11	0.00	22.14	30.58	17.76	600.58	11.68	85.49	0.00	0.61	1.21	3.78	3.76	8.86	1.07	4.65	1.10	1.00		1.59		1.93	0.36	26.35	0.02	2.67	0.48
355195	2006	2006	rep							165	2434	10	0.00	12.05	34.59	22.75	463.75	5.63	0.49	0.00	0.50	2.34	7.17	5.36	12.38	1.55	6.45	1.10	0.98		0.96		0.40	0.06	34.75	0.06	0.02	0.09
355195	2006	2006	rep							263	1905	11	0.00	21.40	28.97	79.74	363.07	5.48	8.36	0.00	0.43	0.81	2.61	2.98	6.46	0.72	3.10	0.73	0.75		0.83		0.90	0.14	38.61	0.02	0.26	0.26
355195	2006	2006	rep							248	2349	10	0.00	15.71	43.77	33.39	476.97	11.99	28.36	0.00	0.77	3.70	2.44	6.21	16.13	2.11	9.44	2.12	0.77		2.16		1.60	0.23	50.13	0.05	0.83	0.33
355195	2006	2006	rep							407	1596	10	0.00	12.52	32.85	34.40	489.82	9.52	85.93	0.00	1.52	2.69	1.30	2.40	6.79	0.92	4.22	1.16	0.42		1.68		1.58	0.26	30.32	0.04	1.85	0.89
355195	2006	2006	rep							325	1506	11	0.99	11.38	34.87	13.84	450.57	1.28	0.32	0.00	1.10	1.63	2.95	1.20	3.03	0.41	1.30	0.37	0.65		0.26		0.11	0.03	22.90	0.03	0.04	0.06
355195	2006	2006	rep							331	1488	11	0.00	17.08	31.72	51.69	448.66	5.40	1.14	0.00	0.46	2.18	8.89	2.20	5.12	0.63	2.62	0.68	0.77		0.91		0.60	0.09	28.57	0.07	0.06	0.33
355195	2006	2006	rep							320	1741	10	0.61	11.42	36.88	17.14	502.94	52.68	0.30	0.00	0.76	3.48	0.54	55.69	84.91	9.40	40.10	9.27	6.77		9.41		3.19	0.34	30.77	0.05	0.00	0.13
355195	2006	2006	vein							413	1879	10	3.94	16.68	40.19	25.17	576.76	60.94	1.75	0.00	0.71	5.26	1.09	38.51	81.26	10.34	44.80	11.45	7.35		11.81		3.58	0.44	28.27	0.05	0.06	0.17
355195	2006	2006	vein							238	1252	11	3.79	12.88	32.08	41.10	446.22	11.80	52.12	0.00	0.37	4.35	0.78	2.33	5.21	0.63	2.64	0.75	5.22		1.42		1.16	0.17	24.46	0.03	1.04	0.30
355198	2006	2006	rep							197	3931	11	0.00	15.28	52.89	16.89	847.91	26.69	1.92	0.00	2.00	3.33	81.25	25.05	51.52	6.70	30.18	7.85	3.43		5.96		1.46	0.15	26.40	0.05	0.02	0.28
355198	2006	2006	rep							176	5061	12	0.00	15.83	64.43	23.13	890.67	28.03	1.15	0.00	3.38	3.75	41.93	27.04	58.24	7.55	33.53	8.34	3.82		5.97		1.38	0.16	30.39	0.07	0.00	0.30
355198	2006	2006	rep							150	3031	12	0.00	21.18	46.90	24.45	846.22	4.48	0.69	0.00	1.42	3.82	18.22	21.36	28.42	2.52	8.27	1.35	2.37		0.96		0.47	0.07	24.58	0.06	0.00	0.23
355198	2006	2006	rep							206	2059	12	0.00	18.77	36.73	12.16	793.63	8.39	2.11	0.00	0.81	4.11	22.33	23.10	40.24	4.59	15.36	3.86	2.95		1.90		0.89	0.09	23.72	0.00	0.13	0.43
355198	2006	2006	rep							312	3821	11	0.00	27.21	45.33	25.45	834.99	17.55	2.35	0.00	1.56	5.40	54.61	28.03	50.92	6.10	24.84	5.63	3.58		4.84		1.57	0.19	35.41	0.00	0.06	0.37
355198	2006	2006	rep							149	3099	11	0.00	21.40	35.97	14.30	622.51	7.79	0.54	0.00	0.82	2.78	30.05	20.51	31.97	3.19	13.27	3.09	2.11		2.25		0.84	0.08	19.94	0.09	0.05	0.17
355198	2006	2006	rep							274	2972	11	0.00	21.20	40.68	11.59	852.26	9.87	1.06	0.00	1.04	3.10	27.97	17.41	30.18	3.47	14.30	3.41	2.09		2.31		0.83	0.13	23.87	0.00	0.21	0.41
355198	2006	2006	rep							192	2390	11	0.00	31.60	31.61	11.05	575.69	9.13	0.53	0.00	1.03	2.18	30.25	21.90	36.28	4.03	15.97	3.20	2.70		1.94		0.65	0.09	17.42	0.03	0.08	0.16
355198	2006	2006	rep							109	5174	11	0.00	14.48	32.19	15.90	845.61	4.00	0.29	0.00	1.06	1.83	16.23	12.51	18.54	1.85	6.71	1.34	1.19		0.83		0.32	0.06	15.07	0.03	0.00	0.09
355198	2006	2006	rep							162	4284	11	0.00	17.78	32.52	16.00	875.14	5.05	0.32	0.00	0.93	1.73	23.69	15.61	23.25	2.39	8.75	1.80	1.70		0.99		0.41	0.04	15.32	0.04	0.00	0.08
355198	2006	2006	rep					23.04		197	3931	11		15.28	52.89	16.89	847.91	26.69	1.92		2.00	3.33	81.25	25.05	51.52	6.70	30.18	7.85	3.43		5.96		1.46	0.15	26.40	0.05	0.02	0.28
355198	2006	2006	rep					23.18		176	5061	12		15.83	64.43	23.13	890.67	28.03	1.15		3.38	3.75	41.93	27.04	58.24	7.55	33.53	8.34	3.82		5.97		1.38	0.16	30.39	0.07		0.30
355198	2006	2006	rep					23.31		150	3031	12		21.18	46.90	24.45	846.22	4.48	0.69		1.42	3.82	18.22	21.36	28.42	2.52	8.27	1.35	2.37		0.96		0.47	0.07	24.58	0.06		0.23
355198	2006	2006	rep					22.37		206	2059	12		18.77	36.73	12.16	793.63	8.39	2.11		0.81	4.11	22.33	23.10	40.24	4.59	15.36	3.86	2.95		1.90		0.89	0.09	23.72		0.13	0.43
355198	2006	2006	rep					23.09		312	3821	11		27.21	45.33	25.45	834.99	17.55	2.35		1.56	5.40	54.61	28.03	50.92	6.10	24.84	5.63	3.58		4.84		1.57	0.19	35.41		0.06	0.37
355198	2006	2006	rep					21.99		149	3099	11		21.40	35.97	14.30	622.51	7.79	0.54		0.82	2.78	30.05	20.51	31.97	3.19	13.27	3.09	2.11		2.25		0.84	0.08	19.94	0.09	0.05	0.17
355198	2006	2006	rep					21.99		274	2972	11		21.20	40.68	11.59	852.26	9.87	1.06		1.04	3.10	27.97	17.41	30.18	3.47	14.30	3.41	2.09		2.31		0.83	0.13	23.87		0.21	0.41
355198	2006	2006	rep					23.81		192	2390	11		31.60	31.61	11.05	575.69	9.13	0.53		1.03	2.18	30.25	21.90	36.28	4.03	15.97	3.20	2.70		1.94		0.65	0.09	17.42	0.03	0.08	0.16
355198	2006	2006	rep					23.67		109	5174	11		14.48	32.19	15.90	845.61	4.00	0.29		1.06	1.83	16.23	12.51	18.54	1.85	6.71	1.34	1.19		0.83		0.32	0.06	15.07	0.03		0.09
355198	2006	2006	rep					23.67		162	4284	11		17.78	32.52	16.00	875.14	5.05	0.32		0.93	1.73	23.69	15.61	23.25	2.39	8.75	1.80	1.70		0.99		0.41	0.04	15.32	0.04		0.08
814485	2006	2006	vein						439	151	4053	10	0.00	13.27	45.09	42.04	565.83	53.25	2.12	0.00	4.97	15.12	1.31	21.08	37.37	7.12	37.12	8.54	0.78	9.69	7.99	4.23	4.11	0.63	35.62	0.08	0.00	0.80
814485	2006	2006	vein						466	168	4402	9	3.29	14.76	41.74	41.12	795.34	25.50	3.61	0.00	5.06	15.15	4.15	14.66	24.95	4.71	22.78	4.50	0.49	4.46	3.96	1.96	2.06	0.34	32.92	0.09	0.03	0.50
814485	2006	2006	vein						586	178	4687	10	0.00	20.67	44.77	52.23	820.96	18.96	21.00	0.00	3.29	21.00	1.07	12.79	20.32	4.01	17.00	3.17	0.31	2.98	2.31	1.28	1.86	0.24	37.79	0.00	0.10	0.71
814485	2006	2006	vein						598	117	1429	13	0.00	23.73	52.70	98.82	342.10	18.03	12.46	0.00	5.29	2.63	2.19	7.06	9.77	1.57	6.72	1.36	1.22	2.03	2.53	2.03	1.99	0.42	37.07	0.00	0.00	0.46
814485	2006	2006	vein						211	68	1771	11	0.00	13.60	49.69	70.54	445.85	10.32	2.23	0.00	3.75	2.46	1.21	5.29	8.44	1.45	7.74	1.42	0.50	1.90	1.15	0.92	0.87	0.11	23.47	0.05	0.00	0.30
814485	2006	2006	vein						405	111	3342	11	0.00	10.20	39.69	45.59	584.47	13.47	6.54	0.00	5.02	10.09	1.06	6.08	11.53	2.22	10.46	2.01	0.35	1.95	1.96	1.46	1.37	0.20	28.46	0.08	0.10	0.49
814485	2006	2006	vein						499	173	2610	11	0.00	17.37	44.60	42.01	552.84	8.97	11.99	0.00	4.57	11.44	1.16	1.91	3.12	0.59	3.05	1.02	0.45	0.90	1.29	1.00	1.12	0.22	21.88	0.06	0.00	0.57
814485	2006	2006	vein						387	387	2349	10	0.00	12.74	44.57	35.67	401.03	4.85	3.69	0.00	3.94	8.91	1.17	0.45	0.72	0.13	1.18	0.00	0.18	0.00	0.32	0.60	0.88	0.12	16.61	0.00	0.00	0.63
814485	2006	2006	vein						278	127	2606	12	0.00	12.28	47.11	49.70	533.38	7.45	15.17	0.00	4.32	8.11	0.87	0.79	1.19	0.25	1.33	0.46	0.44	0.76	0.90	0.84	0.94	0.14	26.00	0.04	0.00	0.49

Appendix 2.6 continued

Sample #	Year Analyzed	Year Collected	Epi Type	Na	Mg	Al	K	Ca	Ti	V	Mn	Fe	Cu	Zn	Ga	As	Sr	Y	Zr	Mo	Sn	Sb	Ba	La	Ce	Pr	Nd	Sm	Eu	Gd	Dy	Er	Yb	Lu	Pb	Bi	Th	U
814485	2006	2006	vein	36	465	25.05	140	23	439	151	4053	10		13.27	45.09	42.04	565.83	53.25	2.12		4.97	15.12	1.31	21.08	37.37	7.12	37.12	8.54	0.78	9.69	7.99	4.23	4.11	0.63	35.62	0.08		0.80
814485	2006	2006	vein		459	24.72	83	23	466	168	4402	9	3.29	14.76	41.74	41.12	795.34	25.50	3.61		5.06	15.15	4.15	14.66	24.95	4.71	22.78	4.50	0.49	4.46	3.96	1.96	2.06	0.34	32.92	0.09	0.03	0.50
814485	2006	2006	vein		698	25.69		24	586	178	4687	10		20.67	44.77	52.23	820.96	18.96	21.00		3.29	21.00	1.07	12.79	20.32	4.01	17.00	3.17	0.31	2.98	2.31	1.28	1.86	0.24	37.79		0.10	0.71
814485	2006	2006	vein	70	1494	23.08	239	24	598	117	1429	13		23.73	52.70	98.82	342.10	18.03	12.46		5.29	2.63	2.19	7.06	9.77	1.57	6.72	1.36	1.22	2.03	2.53	2.03	1.99	0.42	37.07			0.46
814485	2006	2006	vein	86	896	23.92	128	24	211	68	1771	11		13.60	49.69	70.54	445.85	10.32	2.23		3.75	2.46	1.21	5.29	8.44	1.45	7.74	1.42	0.50	1.90	1.15	0.92	0.87	0.11	23.47	0.05		0.30
814485	2006	2006	vein		595	25.19	81	24	405	111	3342	11		10.20	39.69	45.59	584.47	13.47	6.54		5.02	10.09	1.06	6.08	11.53	2.22	10.46	2.01	0.35	1.95	1.96	1.46	1.37	0.20	28.46	0.08	0.10	0.49
814485	2006	2006	vein	137	1107	23.31	89	23	499	173	2610	11		17.37	44.60	42.01	552.84	8.97	11.99		4.57	11.44	1.16	1.91	3.12	0.59	3.05	1.02	0.45	0.90	1.29	1.00	1.12	0.22	21.88	0.06		0.57
814485	2006	2006	vein	288	879	24.58	193	23	387	387	2349	10		12.74	44.57	35.67	401.03	4.85	3.69		3.94	8.91	1.17	0.45	0.72	0.13	1.18		0.18		0.32	0.60	0.88	0.12	16.61			0.63
814485	2006	2006	vein	69	1547	23.24	71	23	278	127	2606	12		12.28	47.11	49.70	533.38	7.45	15.17		4.32	8.11	0.87	0.79	1.19	0.25	1.33	0.46	0.44	0.76	0.90	0.84	0.94	0.14	26.00	0.04		0.49
814487	2006	2006	rep						30408	709	1852	10	0.00	58.07	39.37	27.81	484.35	63.62	62.70	0.00	4.57	5.98	7.82	24.44	41.02	4.79	20.92	7.24	1.80	7.98	11.01	5.83	4.62	0.63	23.37	0.04	0.06	0.19
814487	2006	2006	rep						675	532	1509	12	0.00	31.83	76.43	10.49	170.01	52.72	1.52	0.00	6.56	1.24	0.80	50.76	73.24	7.87	32.10	7.83	6.64	8.74	8.46	4.70	4.21	0.65	20.66	0.04	0.00	0.78
814487	2006	2006	rep						3947	681	933	11	0.00	14.01	35.58	9.82	320.97	2.26	5.99	0.00	5.21	0.68	12.40	1.85	3.81	0.43	1.83	0.45	0.15	0.42	0.51	0.25	0.26	0.06	17.14	0.04	0.18	0.07
814487	2006	2006	rep						31652	645	3473	10	0.00	28.15	35.35	34.70	798.23	23.09	26.57	0.00	4.70	8.33	4.70	6.99	16.44	2.24	9.22	2.69	0.70	3.33	3.18	2.36	2.39	0.44	55.17	0.03	0.04	0.52
814487	2006	2006	rep						1636	783	1027	10	0.00	37.63	27.58	35.63	343.72	1.26	3.21	0.00	4.50	1.17	19.67	0.60	1.18	0.16	0.49	0.20	0.12	0.00	0.17	0.07	0.15	0.00	28.43	0.09	0.05	0.08
814487	2006	2006	rep						8669	307	2389	11	0.00	21.43	38.99	19.83	459.54	46.32	64.06	0.00	4.71	5.36	1.25	14.20	31.31	4.04	18.64	4.44	2.80	5.52	6.28	5.48	5.96	0.92	22.19	0.12	2.16	0.82
814487	2006	2006	rep						1169	345	2508	12	0.00	8.47	34.53	24.34	380.60	32.05	101.58	0.00	4.13	2.88	0.71	12.09	29.02	3.75	16.42	3.48	2.32	4.19	4.83	3.49	4.73	0.97	29.28	0.06	3.31	1.33
814487	2006	2006	vein						313	245	2126	11	0.00	16.16	39.69	22.80	314.42	4.93	2.32	0.00	5.00	2.34	0.78	3.60	5.83	0.62	2.66	0.61	1.80	0.85	0.82	0.51	0.49	0.09	12.31	0.13	0.12	0.18
814487	2006	2006	vein						257	300	1829	12	0.00	17.36	55.17	14.91	376.83	38.18	5.70	0.00	4.80	2.01	1.10	24.60	39.72	4.52	18.59	4.57	4.78	6.26	6.54	3.39	3.04	0.51	22.33	0.08	0.22	0.32
814487	2006	2006	vein						160	254	1147	11	0.00	13.31	40.85	19.02	498.44	2.90	1.03	0.00	5.52	1.61	5.35	2.76	4.81	0.49	2.10	0.57	0.60	0.41	0.45	0.28	0.24	0.05	17.32	0.12	0.00	0.21
814487	2006	2006	vein						282	304	2077	12	0.00	11.14	45.89	19.70	347.92	15.32	0.58	0.00	5.61	3.77	0.94	9.58	16.43	1.81	8.17	2.47	1.93	2.21	2.44	1.12	1.25	0.13	19.17	0.10	0.05	0.27
814487	2006	2006	vein						655	290	1799	11	0.00	15.78	52.28	21.58	271.00	27.56	6.95	0.00	4.19	1.83	1.27	24.37	47.87	5.67	25.57	5.99	2.59	5.17	5.87	2.88	2.73	0.35	21.26	0.15	0.96	1.16
814487	2006	2006	vein						198	335	1717	11	0.00	15.37	42.29	28.54	439.81	3.37	0.78	0.00	5.13	2.45	3.49	4.33	6.62	0.67	2.73	0.44	1.12	0.58	0.55	0.25	0.46	0.00	24.16	0.13	0.06	0.12
814487	2006	2006	vein						793	289	3446	12	0.00	19.33	33.48	41.51	624.18	18.17	132.56	0.00	4.06	14.90	3.12	7.38	17.34	2.37	10.82	2.50	0.89	2.55	3.00	2.30	2.78	0.50	43.69	0.08	5.03	1.13
814487	2006	2006	vein						657	547	1631	12	0.00	14.33	40.91	28.13	375.76	13.72	123.75	0.00	4.50	1.98	0.52	7.05	15.84	2.03	7.98	1.58	0.79	2.37	2.18	1.56	1.57	0.34	34.58	0.00	3.38	0.57
814489	2006	2006	rep						22979	756	2039	9	0.00	20.36	34.76	32.14	572.58	11.10	38.08	0.00	4.54	9.08	5.82	2.70	5.60	0.75	3.90	0.79	1.30	1.60	1.80	1.00	1.26	0.12	19.66	0.28	0.04	0.34
814489	2006	2006	rep						486	519	4357	9	0.00	18.75	44.46	80.80	618.20	5.67	1.29	0.00	3.95	10.89	4.60	3.93	7.81	1.04	4.85	1.50	1.23	1.53	1.06	0.51	0.57	0.09	28.24	0.25	0.01	0.33
814489	2006	2006	rep						334	635	2062	9	0.00	40.54	41.98	36.02	424.95	19.23	2.34	0.00	4.31	7.41	20.47	14.33	30.95	4.09	19.73	5.04	2.62	4.96	3.94	2.08	1.50	0.24	23.10	0.53	0.06	0.28
814489	2006	2006	rep						95	312	1874	10	0.00	9.76	41.74	48.82	468.09	1.31	0.86	0.00	3.86	3.66	1.46	0.39	0.81	0.20	0.00	0.00	0.19	0.24	0.23	0.25	0.00	0.03	32.37	0.00	0.00	0.06
814489	2006	2006	rep		2134	24.63	163	24	22979	756	2039	9		20.36	34.76	32.14	572.58	11.10	38.08		4.54	9.08	5.82	2.70	5.60	0.75	3.90	0.79	1.30	1.60	1.80	1.00	1.26	0.12	19.66	0.28	0.04	0.34
814489	2006	2006	rep		2030	26.51	46	23	486	519	4357	9		18.75	44.46	80.80	618.20	5.67	1.29		3.95	10.89	4.60	3.93	7.81	1.04	4.85	1.50	1.23	1.53	1.06	0.51	0.57	0.09	28.24	0.25	0.01	0.33
814489	2006	2006	rep	56	1936	26.12	3545	23	334	635	2062	9		40.54	41.98	36.02	424.95	19.23	2.34		4.31	7.41	20.47	14.33	30.95	4.09	19.73	5.04	2.62	4.96	3.94	2.08	1.50	0.24	23.10	0.53	0.06	0.28
814489	2006	2006	rep		342	24.78	25	24	95	312	1874	10		9.76	41.74	48.82	468.09	1.31	0.86		3.86	3.66	1.46	0.39	0.81	0.20			0.19	0.24	0.23	0.25		0.03	32.37			0.06
814489	2006	2006	vein						1005	483	3662	10	0.00	48.13	55.99	49.83	652.90	47.33	80.80	0.00	7.08	17.79	2.73	38.88	68.30	8.09	37.00	7.40	2.28	9.02	7.36	4.61	4.32	0.59	28.50	0.18	3.23	1.43
814489	2006	2006	vein						10252	638	3681	9	0.00	27.14	41.46	79.19	569.51	37.57	91.83	0.00	7.30	12.59	6.71	9.86	25.68	3.59	18.06	4.66	1.91	5.16	5.93	3.81	4.41	0.63	30.04	0.13	1.84	1.08
814489	2006	2006	vein						28350	1249	1543	9	0.00	17.54	41.64	17.80	378.98	41.18	44.19	0.00	6.02	5.01	8.16	15.60	38.00	5.65	26.13	7.23	5.55	8.43	8.75	4.96	4.61	0.62	27.34	0.41	0.76	0.83
814489	2006	2006	vein						20847	626	1855	9	0.00	31.66	32.90	44.95	468.96	49.64	75.29	0.00	6.20	4.60	2.83	5.10	18.35	3.57	18.20	7.68	4.82	9.15	11.43	5.60	5.71	0.58	41.74	0.00	1.44	1.30
814489	2006	2006	vein						3635	940	1447	10	0.00	20.84	44.67	37.05	416.69	11.26	3.90	0.00	4.28	4.19	7.27	6.92	14.44	1.87	9.18	2.29	2.30	2.21	2.39	1.24	0.93	0.11	13.00	0.31	0.01	0.32
814489	2006	2006	vein						4443	443	5475	9	0.00	23.99	41.51	103.38	627.89	28.57	45.21	0.00	6.09	20.68	7.84	9.12	19.78	2.80	12.99	3.66	1.25	4.51	4.41	2.80	3.14	0.49	36.18	0.40	2.21	0.85
814489	2006	2006	vein						2856	691	2745	11	0.00	14.34	54.61	40.80	502.77	56.68	47.75	0.00	5.72	8.30	7.07	33.69	60.44	7.72	35.33	9.07	3.81	10.01	9.07	5.48	5.24	0.87	20.50	0.28	1.62	1.25
814489	2006	2006	vein						675	682	3106	10	0.00	13.99	58.17	41.55	713.08	47.00	98.10	0.00	4.96	14.30	3.94	9.30	23.32	3.27	15.33	4.37	1.10	5.54	6.11	5.21	4.66	0.69	28.56	0.09	2.52	1.44
814489	2006	2006	vein						216	550	3158	9	0.00	26.19	38.09	81.69	488.37	26.35	11.08	0.00	3.37	10.06	3.39	8.41	19.98	2.77	12.71	3.97	0.55	4.01	3.61	2.59	2.46	0.46	39.20	0.00	1.04	0.49
814489	2006	2006	vein						185	634	3144	9	27.97	27.78	45.36	81.09	529.98	10.27	10.24	0.00	4.31	7.68	3.83	3.08	7.52	1.02	5.84	0.91	0.38	1.24	1.40	1.21	0.95	0.14	35.16	0.08	0.15	0.44
814489	2006	2006	vein						395	639	4992	9	0.00	21.28	50.69	79.93	505.47	12.21	17.51	0.00	6.05	10.66	3.18	4.58	13.11	1.95	8.97	2.28	0.55	1.94	1.95	1.48	1.52	0.25	26.80	0.06	0.92	0.57
814489	2006	2006	vein						440	596	2570	10	0.00	20.04	45.89	38.74	225.16	7.47	2.91	0.00	3.92	1.83	3.79	1.43	3.37	0.43	1.76	0.90	0.25	0.58	0.91	1.11	1.29	0.25	9.61	0.22	0.00	0.52
814489	2006	2006	vein	550	724	26.72	239	24	1005	483	3662	10		48.13	55.99	49.83	652.90	47.33	80.80		7.08	17.79	2.73	38.88	68.30	8.09	37.00	7.40	2.28	9.02	7.36	4.61	4.32	0.59	28.50	0.18	3.23	1.43
814489	2006	2006	vein	402	698	24.60	119	24	10252	638	3681	9		27.14	41.46	79.19	569.51	37.57	91.83		7.30	12.59	6.71	9.86	25.68	3.59	18.06	4.66	1.91	5.16	5.93	3.81	4.41	0.63	30.04	0.13	1.84	1.08
814489	2006	2006	vein	50	1003	21.07	387	24	28350	1249	1543	9		17.54	41.64	17.80	378.98	41.18	44.19		6.02	5.01	8.16	15.60	38.00	5.65	26.13	7.23	5.55	8.43	8.75	4.96	4.61	0.62	27.34	0.41	0.76	0.83
814489	2006	2006	vein		597	21.33	22	24	20847	626	1855	9		31.66	32.90	44.95	468.96	49.64	75.29		6.20	4.60	2.83	5.10	18.35	3.57	18.20	7.68	4.82	9.15	11.43	5.60	5.71	0.58	41.74		1.44	1.30
814489	2006	2006	vein	148	2202	25.29	530	24	3635	940	1447	10		20.84	44.67	37.05	416.69	11.26	3.90		4.28	4.19	7.27	6.92	14.44	1.87	9.18	2.29	2.30	2.21	2.39	1.24	0.93	0.11	13.00	0.31	0.01	0.32
814489	2006	2006	vein	115	1090	23.87	113	24	4443	443	5475	9		23.99	41.51	103.38	627.89	28.57	45.21		6.09	20.68	7.84	9.12	19.78	2.80	12.99	3.66	1.25	4.51	4.41	2.80	3.14	0.49	36.18	0.40	2.21	0.85
814489	2006	2006	vein	366	750	24.21	281	24	2856	691	2745	11		14.34	54.61	40.80	502.77	56.68	47.75		5.72	8.30	7.07	33.69	60.44	7.72	35.33	9.07	3.81	10.01	9.07	5.48	5.24	0.87	20.50	0.28	1.62	1.25
814489	2006	2006	vein	125	319	24.83	27	24	675	682	3106	10		13.99	58.17	41.55	713.08	47.00	98.10		4.96	14.30	3.94	9.30	23.32	3.27	15.33	4.37	1.10	5.54	6.11	5.21	4.66	0.69	28.56	0.09	2.52	1.44
814489	2006	2006	vein		672	24.61	29	24	216	550	3158	9		26.19	38.09	81.69	488.37	26.35	11.08		3.37	10.06	3.39	8.41	19.98	2.77	12.71	3.97	0.55	4.01	3.61	2.59	2.46	0.46	39.20		1.04	0.49
814489	2006	2006	vein	94	656	26.79	29	24	185	634	3144	9	27.97	27.78	45.36	81.09	529.98	10.27	10.24		4.31	7.68	3.83	3.08	7.52	1.02	5.84	0.91	0.38	1.24	1.40	1.21	0.95	0.14	35.16	0.08	0.15	0.44
814489	2006	2006	vein	73	705	26.92	30	24	395	639	4992	9		21.28	50.69	79.93	505.47	12.21	17.51		6.05	10.66	3.18	4.58	13.11	1.95	8.97	2.28	0.55	1.94	1.95	1.48	1.52	0.25	26.80	0.06	0.92	0.57
814489	2006	2006	vein	59	984	24.91	32	24	440	596	2570	10		20.04	45.89	38.74	225.16	7.47	2.91		3.92	1.83	3.79	1.43	3.37	0.43	1.76	0.90	0.25	0.58	0.91	1.11	1.29	0.25	9.61	0.22		0.52
814495	2006	2006	skarn assoc.						448	122	2722	10	0.00	6.85	22.72	6.68	748.59	6.95	9.92	0.00	0.00	19.69	1.89	0.54	1.31	0.13	1.10	0.39	0.66	0.54	1.07	0.63	1.16	0.19	8.45	1.83	0.00	0.78
814495	2006	2006	skarn assoc.						525	107	2962	13	0.00	4.01	24.07	0.00	966.94	2.90	18.33	0.00	0.88	0.00	4.60	0.15	0.35	0.06	0.28	0.27	0.21	0.00	0.39	0.43	0.44	0.05	7.73	0.69	0.00	0.45
814495	2006	2006	skarn assoc.						1918	20	1655	11	0.00	8.40	17.56	8.10	373.45	2.07	26.28	0.00	1.48	0.61	0.74	0.35	0.74	0.11	0.55	0.00	0.21	0.23	0.34	0.16	0.00	0.03	1.61	0.23	0.16	1.28
814495	2006	2006	skarn assoc.						2004	76	1919	11	0.00	4.45	18.20	6.14	604.54	3.80	19.87	0.00	1.77	0.76	1.20	0.54	1.05	0.14	0.77	0.41	0.29	0.25	0.58	0.44	0.43	0.07	5.83	0.75	0.00	0.58
814495	2006	2006	skarn assoc.						1273	63	2387	11	0.00	6.70	20.79	6.54	765.48	4.68	25.20	0.00	1.21	1.53	2.57	1.53	3.15	0.36	1.69	0.33	0.32	0.57	0.72	0.49	0.53	0.09	6.70	0.83	0.06	0.88
814495	2006	2006	skarn assoc.						722	46	1777	11	0.00	9.29	19.64	11.27	384.54	2.43	3.93	0.00	1.69	0.60	0.74	0.00	0.18	0.00	0.27	0.00	0.21	0.21	0.28	0.26	0.50	0.06	2.71	0.35	0.00	0.34
814495	2006	2006	skarn assoc.						813	88	5860	11	0.00	8.12	23.59	8.10	1192.32	8.46	42.47	0.00	2.30	1.24	8.29	1.11	1.95	0.38	1.92	0.85	0.33	1.54	1.50	1.00	1.17	0.20	7.37	2.30	0.14	0.53
814495	2006	2006	skarn assoc.						1910	121	3251	11	0.00	7.05	25.31	6.53	1124.62	11.36	110.65	0.00	1.92	1.73	4.87	0.97	2.79	0.49	2.74	0.90	0.62	1.48	1.76	1.43	1.95	0.52	12.38	2.34	0.25	1.70
814495	2006	2006	skarn assoc.						1067	83	3597	16	0.00	186.22	26.28	0.00	995.79	8.14	123.52	0.00	3.37	1.41	3.44	0.63	1.30	0.22	1.17	0.00	0.32	1.32	1.51	0.66	0.98	0.31	9.05	0.91	0.17	1.53
814495	2006	2006	skarn assoc.						1329	416	2411	11	0.00	6.19	39.22	9.01	692.15	2.00	33.73	0.00	1.73	1.91	2.31	0.35	0.76	0.07	0.46	0.21	0.20	0.39	0.24	0.29	0.41	0.07	7.87	1.13	0.21	0.84
814495	2006	2006	skarn assoc.						1478	47	3109	11	0.00	5.90	21.10	12.52	851.89	4.80	20.45	0.00	0.00	1.34	4.19	0.31	1.27	0.20	1.29	0.85	0.13	0.72	0.69	0.40	0.71	0.10	6.16	0.98	0.06	0.60
814495	2006	2006	skarn assoc.						174	37	1915	1	0.00	0.00	3.44	2.80	534.21	5.61	2.48	0.00	0.39	3.17	0.63	0.11	0.40	0.08	0.70	0.30	0.22	0.56	0.70	0.54	0.97	0.17	3.27	0.63	0.02	0.31
814495	2006	2006	skarn assoc.						2119	158	2204	12	0.00	2.81	21.24	0.00	764.70	19.56	25.03	0.00	0.00	0.72	1.79	0.33	0.93	0.22	2.13	1.40	0.28	1.99	2.76	2.63	3.36	0.56	5.10	0.66	0.00	0.93
821173	2006	2006	vein						847	689	4274	11	0.00	20.71	42.83	71.88	735.95	50.90	6.44	0.25	3.74	11.57	5.26	26.23	60.91	8.71	41.24	11.19	4.29	12.53	10.64	4.37	3.60	0.47	30.57	0.49	0.35	1.74
821173	2006	2006	vein						739	628	3411	11	1.50	28.99	39.58	84.52	645.78	36.14	6.37	0.00	3.87	6.76	6.15	20.88	47.19	6.60	31.92	8.36	3.29	9.20	7.21	3.31	2.38	0.33	32.81	0.43	0.21	1.34
821173	2006	2006	vein						670	567	3234	12	86.53	38.53	41.43	83.57	614.08	35.61	4.63	0.00	3.94	6.50	6.13	21.06	46.19	6.15	29.59	7.45	3.54	8.06	6.74	3.12	2.11	0.32	30.58	0.36	0.12	1.20
821173	2006	2006	vein						535	522	2603	12	49.87	67.58	38.79	53.17	351.62	13.61	2.36	1.19	3.94	2.67	6.87	4.61	10.25	1.39	7.08	2.09	1.15	2.53	2.51	1.39	1.35	0.20	18.87	0.64	0.01	0.43
821173	2006	2006	vein						541	575	3783	13	73.19	127.22	50.41	40.86	668.20	17.85	1.05	0.00	3.44	3.89	4.77	7.03	14.98	2.05	10.00	3.02	1.28	3.31	3.26	1.66	1.32	0.19	22.69	0.24	0.01	0.71
821173	2006	2006	vein						2029	555	3423	11	5.33	29.03	36.02	95.14	642.68	12.29	44.43	0.00	4.17	6.85	5.59	3.75	8.99	1.35	6.68	1.76	0.67	2.09	2.08	1.41	1.45	0.25	24.09	0.43	1.18	0.45
821173	2006	2006	vein						385	552	3149	12	45.08	57.48	37.10	88.50	692.11	29.01	1.89	0.00	4.73	3.62	4.88	13.87	30.11	4.21	19.60	5.67	2.15	6.00	5.17	2.64	2.19	0.32	29.23	0.45	0.02	0.76
821173	2006	2006	vein						860	515	3091	12	7.50	30.23	38.29	76.43	532.90	16.11	7.30	0.24	4.70	4.20	5.36	5.89	13.37	1.89	9.37	2.83	1.42	3.38	3.11	1.62	1.36	0.21	27.87	0.35	0.08	0.58
821173	2006	2006	vein						1099	645	2978	10	2.41	27.49	42.62	69.48	482.32	27.02	20.47	0.00	15.27	5.04	6.14	4.79	13.34	2.05	11.33	3.59	1.10	4.14	4.49	3.37	3.52	0.51	21.72	0.74	0.94	1.14
821173	2006	2006	vein						1021	661	3859	11	6.92	81.29	46.87	69.26	775.76	28.71	18.15	1.06	6.03	8.19	5.63	8.24	20.68	3.20	15.94	4.69	1.49	5.10	5.12	3.24	3.54	0.51	27.83	0.61	2.58	1.15
821173	2006	2006	vein						1222	657	2823	10	12.38	44.69	37.91	92.29	418.65	20.27	41.46	0.00	4.95	3.35	14.26	4.79	12.59	1.90	9.95	3.09	0.91	3.34	3.43	2.38	2.69	0.38	35.93	0.80	4.35	0.61
821173	2006	2006	vein						620	563	3227	11	6.45	73.70	38.62	65.85	732.25	65.84	6.50	0.00	5.57	10.00	10.82	15.18	36.92	5.39	26.25	6.53	2.75	9.20	10.05	5.82	4.29	0.61	33.00	0.29	0.16	0.52
821173	2006	2006	vein						320	577	2930	12	12.10	78.48	48.51	44.64	624.78	132.24	1.89	0.00	6.78	7.32	8.07	28.40	72.91	10.64	52.81	15.11	3.41	19.63	22.23	12.91	10.22	1.43	37.95	0.44	0.20	0.74
821173	2006	2006	vein						471	477	1930	11	1.04	24.21	48.33	40.81	314.79	35.20	6.92	0.00	7.04	1.66	4.63	11.18	27.63	4.16	21.76	6.25	2.60	7.39	6.76	3.38	2.78	0.36	13.60	0.36	0.02	0.91
821173	2006	2006	vein						65	379	2661	13	1.38	23.72	37.51	86.72	307.44	7.49	0.37	0.00	6.84	2.07	4.65	2.36	5.03	0.75	3.36	1.07	1.08	1.32	1.36	0.79	0.78	0.11	18.81	0.35	0.00	0.34

Appendix 2.7 – Individual laser ablation-inductively coupled plasma mass spectrometry spot analyses of plagioclase (LA-ICPMS) generated for this thesis. All values reported in ppm; blank values indicate below detection limit concentrations.

Sample #	Mineral	Date Collected	Na	Mg	Al	K	Ca	Ti	V	Mn	Fe	Cu	Zn	Ga	As	Sr	Y	Zr	Mo	Sn	Sb	Ba	La	Ce	Pr	Nd	Sm	Eu	Gd	Dy	Er	Yb	Lu	Pb	Bi	Th	U
353226	plag	2008	24963	4564	130000	12627	108282	279.09	149.14	506.35	12734.72	0.14	15.50	18.95	12.25	495.76	2.65	5.93	0.06	0.25	0.20	142.39	1.29	3.10	0.42	1.92	0.37	0.22	0.56	0.44	0.31	0.31	0.07	7.36		0.11	
353226	plag	2008	10442	1515	130000	11564	187496	107.69	3.57	2475.79	5589.24	1.87	8.83	15.61	0.50	742.83	1.18	0.09	0.00	2.11	0.33	50.09	1.46	2.76	0.40	2.04	0.39	0.27	0.26	0.19	0.11	0.08	0.02	10.11	0.02	0.02	
353226	plag	2008	57127	9230	130000	21173	23358	18.13	53.00	397.96	14564.93	0.18	33.61	15.09	0.66	857.31	0.21	2.89	0.00	0.30	0.21	330.11	0.18	0.31	0.05	0.16	0.05	0.04	0.05	0.08	0.01	0.04	0.02	1.44		0.08	0.02
353226	plag	2008	50942	2921	130000	5201	50175	371.95	19.72	196.68	6002.35	0.91	9.83	13.04	1.25	1013.26	0.77	3.53	0.05	0.71	0.25	135.50	0.61	1.35	0.18	0.74	0.17	0.16	0.16	0.16	0.08	0.08	0.01	1.63	0.01	0.04	0.01
353226	plag	2008	11209	2652	140000	10311	79147	73.14	12.76	163.77	7123.96	0.05	9.88	15.60	2.27	579.56	0.16	0.28		0.44	0.42	24.67	0.48	0.86	0.12	0.48	0.06	0.15	0.04	0.02		0.04	0.00	0.69	0.01	0.00	0.01
353226	plag	2008	55292	2834	130000	8136	42991	190.54	16.38	130.45	6040.96	0.13	12.11	14.68	0.18	1112.52	0.23	0.90	0.04	0.73	0.05	141.55	0.41	0.79	0.10	0.41	0.04	0.10	0.01	0.04	0.04	0.05	0.00	0.95	0.01	0.02	0.01
353226	plag	2008	8621	283	130000	337	92409	38.10	0.35	50.68	3121.04	3.19	4.47	19.11		723.21	0.10		0.02	0.36		16.42	0.71	1.21	0.11	0.35	0.06	0.22		0.03	0.03	0.02	0.00	1.02		0.00	0.00
353226	plag	2008	7329	412	130000	266	94034	90.79	1.45	31.31	4157.95	0.44	2.13	15.00	0.00	672.23	0.18	0.15		0.09		14.39	0.52	0.96	0.11	0.40	0.02	0.15		0.03	0.02			0.34	0.00	0.01	0.00
353226	plag	2008	60030	3252	130000	19316	38883	149.20	27.39	219.07	5535.51	0.05	7.42	15.81	1.31	1015.07	0.98	4.96	0.00	0.78	0.12	336.12	0.26	0.60	0.10	0.54	0.13	0.12	0.21	0.10	0.15	0.21	0.04	1.57		0.03	0.00
353226	plag	2008	7016	351	140000	215	99206	75.32	0.83	30.81	4143.75	0.20	1.65	14.87	0.20	675.66	0.09	0.00	0.00	0.22	0.03	15.65	0.53	1.01	0.13	0.45	0.10	0.16		0.04		0.01	0.01	0.28			0.00
354019	plag	2008	47046	45	140000	2219	58605	32.25		26.83	1088.85		3.01	22.69		1569.15	0.06					105.07	6.12	6.77	0.52	1.28	0.07	0.49						6.67			
354019	plag	2008	41877	42	140000	1781	62518	37.75		30.83	1058.20		3.11	23.46		1516.44	0.08			0.55		92.26	5.51	6.44	0.44	1.23	0.06	0.48						6.26			
354019	plag	2008	44370	140	140000	2654	61684	36.32		31.64	1233.00		3.03	23.93		1520.35	0.10					103.13	5.61	6.69	0.45	1.36	0.11	0.48						6.23			
354019	plag	2008	48228	45	140000	2385	58082	33.66		26.36	1179.35		3.15	24.37		1549.80	0.04			0.63		117.35	6.78	7.50	0.51	1.29	0.11	0.51	0.12			0.06		6.23			
354019	plag	2008	44666	43	140000	1909	59427	35.52		28.25	1179.72		3.08	22.52		1350.36	0.03			0.78		96.83	5.18	5.88	0.43	1.30	0.11	0.50						5.49			
354019	plag	2008	101902	570	140000	8104	3198	12.42	12.69	19.65	780.79			13.83		668.60	0.27				0.37	38.35	0.15	0.35	0.04	0.08	0.15			0.07	0.05			1.85			
354019	plag	2008	64742	3378	140000	29889	2583	23.78	62.50	19.72	2612.26		3.35	21.53		467.67	0.34			2.93	0.23	56.42	0.15	0.42	0.03	0.10		0.03				0.05		1.97		0.02	0.03
354019	plag	2008	50039	58	140000	2636	56999	36.08		42.43	1317.12		5.32	22.46		1577.75	0.08	0.23		0.82		121.47	5.30	6.05	0.41	1.01	0.09	0.52						6.98		0.03	0.02
354019	plag	2008	51501	335	140000	4651	54002	36.50	0.64	26.45	1475.81		3.40	23.30		1484.25	0.05	0.18				122.59	5.26	6.49	0.42	1.16	0.10	0.47						6.73		0.03	0.02
354019	plag	2008	37501	42	140000	1479	67661	36.36		36.57	1076.19		2.39	21.74		1514.71	0.09	0.19		0.52		85.47	4.20	4.68	0.39	1.06		0.45			0.04			5.49		0.03	0.02
354510	plag	2008	37704	76	165000	963	90791	51.79		64.28	1993.27		4.95	27.33		1347.42	0.12					87.73	3.74	4.80	0.38	1.21		0.45						4.50			
354510	plag	2008	24130	1484	165000	3227	96750	16.36	6.43	133.11	1961.63	4.31	18.47	28.23		759.29	0.04		0.64	0.92	1.17	178.82	0.55	0.77	0.06	0.25		0.08						4.31			
354510	plag	2008	36608	336	165000	3064	104433	21.88	1.79	114.45	1264.70	4.94	5.31	28.71		1149.32	0.10					80.54	2.07	2.75	0.22	0.72		0.28		0.07				3.56			
354510	plag	2008	24453	3569	165000	13119	83339	63.07	31.87	210.39	2863.16	4.99	16.06	30.10		618.50	1.23	0.55	0.21	2.81	1.05	167.96	0.62	1.09	0.15	0.56	0.15	0.20	0.22	0.16	0.11	0.09	0.02	3.44			
354510	plag	2008	38838	451	165000	4734	83243	29.02	1.88	68.18	2713.19	1086.61	8.40	28.64		1129.04	0.06					131.84	2.21	3.17	0.33	0.73	0.13	0.35						4.83	0.29		
354510	plag	2008	32528	1125	165000	4234	91336	22.42	5.96	255.08	2192.55	15.32	13.64	28.39		927.92	0.11					115.98	0.69	0.93	0.07	0.28		0.17						3.77	0.06		
354510	plag	2008	32002	129	165000	1413	89896	39.15	2.32	57.19	1314.02	1.09	7.23	23.60		1226.02	0.14	0.07		0.80		71.06	2.46	3.35	0.27	0.82		0.49						5.26	0.05		
354510	plag	2008	34798	715	165000	10441	85930	12.65	5.97	159.95	998.17	4.38	18.85	28.57		806.08	0.19		2.03		0.50	215.34	0.92	1.36	0.13	0.29	0.10	0.17						5.11	0.03		
354510	plag	2008	30821	1790	165000	13754	114294	25.13	39.58	390.90	1695.29	2.69	9.34	29.70		709.30	3.22	0.07				337.79	1.11	2.18	0.23	1.36	0.23	0.15	0.44	0.42	0.39	0.35	0.06	2.50		0.15	
354510	plag	2008	33982	862	165000	7548	79801	22.92	11.04	54.97	1174.42	8.13	5.64	28.74		934.07	0.16	1.36		2.09	0.65	160.34	0.70	1.09	0.10	0.30		0.14						4.29	0.30	0.08	
354510	plag	2008	47218	1721	165000	17267	55398	591.64	20.30	107.57	3231.90		15.16	28.65		950.22	1.45	86.50		25.87	4.24	539.66	6.23	8.89	0.71	1.66	0.32	0.75		0.23	0.20	0.54	0.10	8.98		2.63	0.47
354510	plag	2008	30240	2844	165000	13949	80769	667.15	41.66	192.68	3878.80	1.67	12.18	28.81	1.72	890.91	1.19	11.75		0.58	0.47	195.24	1.44	2.03	0.16	0.51		0.22		0.18	0.15	0.27	0.04	3.46		0.50	0.14
354510	plag	2008	45465	264	165000	6489	75202	65.20	2.57	63.56	1164.75	1.59	6.31	27.74		1001.54	0.47	18.60			1.00	168.91	1.77	2.40	0.21	0.51	0.09	0.24			0.06	0.11	0.04	3.90		0.70	0.11
354510	plag	2008	27971	5615	165000	5417	132217	207.14	27.40	277.12	5909.29	4.06	18.93	28.53		1067.34	1.17	1.11	19.11	0.58	2.02	91.58	3.19	4.79	0.43	1.64	0.41	0.54	0.27	0.10		0.09		4.40		0.08	0.03
355195	plag	2008	87646	10647	140000	6963	6383	5.73	27.50	1021.43	11603.59		69.11	10.94	8.87	277.84	0.69	1.56	0.20	0.28	7.56	132.66	0.14	0.16	0.04				0.27	0.47		0.15	0.01	2.04		0.12	
355195	plag	2008	73175	977	140000	72750	4022	4.93	9.55	47.36	991.22	0.75	4.16	15.31	1.54	271.10	0.03	0.04	0.10	1.10	0.07	2009.50	0.02	0.05	0.02		0.04	0.02						3.22		0.00	
355195	plag	2008	7349	3636	140000	187461	15786	8089.51	106.95	583.21	13187.18	0.24	21.52	33.30	4.80	367.94	50.36	20.15	0.03	0.64	3.29	5484.67	42.16	96.90	12.07	53.10	11.43	4.10	11.81	9.27	5.11	5.03	0.80	14.00	0.09	0.42	0.42
355195	plag	2008	72218	38731	140000	26355	5586	38.59	111.07	1876.97	51161.67	0.05	234.32	19.24	1.81	306.29	5.54	47.57	0.07	1.11	0.87	641.64	0.78	2.21	0.28	1.81	0.50	0.14	0.43	0.72	0.67	1.16	0.18	1.68		1.87	0.39
355195	plag	2008	89695	3501	140000	8727	9773	14.05	15.30	241.95	3135.38	4.59	24.08	9.82	8.29	262.20	0.31	0.11		1.35	5.86	125.93	0.73	1.57	0.15	0.80					0.17		0.03	4.34	0.04	0.06	0.04
355195	plag	2008	70240	23155	140000	25961	5104	14.80	37.11	1887.09	21234.76	2.18	155.94	13.97	4.09	286.99	0.24	0.16			1.04	473.48	0.00						0.07	0.01	0.09	0.07	0.01	2.66		0.03	0.02
355195	plag	2008	82846	45852	140000	4935	4431	31.17	121.08	1612.07	47132.20	0.05	216.87	18.25	0.56	242.16	0.21	0.05	0.25	0.61	0.89	78.32	0.04	0.10	0.02	0.13	0.03	0.05	0.08	0.03				1.08		0.02	0.02
355195	plag	2008	26285	9739	140000	141094	2469	51.96	89.49	455.98	11673.01	0.45	55.39	22.73	0.31	254.85	0.13	0.13	0.03	1.67	1.48	3122.29	0.01	0.04	0.01	0.05		0.06	0.00		0.03		0.00	4.76	0.02	0.00	0.01
355195	plag	2008	103156	1794	140000	6992	7542	7.81	9.52	99.64	1930.64	0.30	9.77	7.47	0.10	438.45	0.02	0.05		0.41	0.10	108.44	0.02	0.00		0.00				0.02	0.01	0.00	0.01	1.56	0.01	0.01	0.01
355195	plag	2008	104940	960	140000	2915	5504	3.00	2.53	41.02	1045.04		6.95	8.29	1.33	320.57	0.06	0.06		0.20	0.09	26.54	0.05	0.12	0.00	0.25		0.00	0.03		0.03	0.06	0.01	1.11			0.00
BA08GS019	plag	2008	49695	51	145000	2963	60859	44.75		22.38	1390.62		3.90	24.08		1571.26						115.16	5.53	5.75	0.41	1.19		0.54						5.81			
BA08GS019	plag	2008	44046	45	145000	2540	65793	45.20		25.26	1478.14	1.19	4.40	23.57		1358.67	0.09					116.53	5.60	6.02	0.42	1.21	0.21	0.44						5.57			
BA08GS019	plag	2008	44526	50	145000	2784	63404	39.51		23.36	1496.82		4.40	21.82		1260.81	0.07					154.07	5.58	6.39	0.47	1.09	0.14	0.32						5.45			
BA08GS019	plag	2008	45106	38	145000	2818	64110	46.19		22.07	1291.30		2.87	22.44		1406.79						107.91	5.25	5.90	0.45	1.01	0.12	0.52						5.09			
BA08GS019	plag	2008	50455	37	145000	3246	59163	35.24		15.95	1361.80		2.34	23.45		1288.79	0.06					121.26	5.09	5.79	0.37	0.96		0.52						4.59			
BA08GS019	plag	2008	62125	35	145000	3737	49397	37.00		9.07	1538.48		1.94	22.05		1161.52						143.63	4.46	4.99	0.36	0.54		0.52						2.56			
BA08GS019	plag	2008	74712	43	145000	5276	37139	79.85		4.26	1881.48			27.38		910.32	0.06					199.14	2.92	3.37	0.29	0.77	0.12	0.61					0.02	1.75			
BA08GS019	plag	2008	66259	226	145000	12048	34017	64.23		35.11	1948.14	12.16		27.76		900.26	0.14		0.28			152.81	3.90	4.67	0.34	0.72		0.63						1.57			
BA08GS019	plag	2008	73104	23	145000	3420	38761	58.82	0.28	5.46	1792.50	19.48	1.66	30.53		693.62	0.08			0.68		152.61	4.11	4.63	0.35	1.02		0.90						1.73	0.06		
BA08GS019	plag	2008	69030	661	145000	66754	6302	185.83	20.33	45.33	1559.88	15.43		35.90		923.75	0.23	10.49				1743.00	1.34	1.83	0.11	0.33		0.53			0.14			2.25		0.11	0.06
BA08GS025	plag	2008	49832	72	150000	2657	63197	41.03		31.34	1601.41		4.37	26.71		1252.75	0.07					160.44	5.54	6.39	0.47	1.21		0.52						6.54			
BA08GS025	plag	2008	46951	57	150000	2362	67715	41.85		38.15	1654.27		3.39	24.04		1263.24	0.04					147.08	4.63	5.49	0.41	0.87		0.58						5.74			
BA08GS025	plag	2008	47274	73	150000	2374	66130	42.67		33.49	1610.46		4.42	25.79		1213.14	0.11					132.28	4.62	5.78	0.40	1.19	0.12	0.60						5.60			
BA08GS025	plag	2008	46057	132	150000	2401	67087	49.65		34.98	2099.98	1.73	8.19	25.90		1132.41	0.14					144.37	4.80	5.21	0.36	0.91		0.44	0.11					4.67			
BA08GS025	plag	2008	38868	94	150000	2138	73417	70.42		44.52	2314.09		4.96	25.73		1082.54	0.08					129.24	4.12	4.80	0.37	1.24		0.55	0.09					4.36			
BA08GS025	plag	2008	42455	88	150000	4416	69076	30.33	2.13	40.48	1490.60	1.47	6.86	22.09		1096.11	0.18		0.26			96.79	1.86	3.05	0.26	0.85	0.19	0.43	0.16					3.88			
BA08GS025	plag	2008	40131	62	150000	1804	68739	53.03		39.63	1619.15		4.27	22.85		1062.10	0.08	0.84				98.72	3.78	4.38	0.33	0.99		0.42	0.10					4.13		0.02	
BA08GS025	plag	2008	48177	333	150000	8386	60748	58.24	4.17	37.80	2413.13	1.47	9.89	26.14		1074.93	0.29	0.22		0.81		200.33	3.74	4.10	0.29	0.90		0.48		0.06				4.10		0.02	
BA08GS025	plag	2008	28898	83	150000	1218	80111	50.26		47.52	1740.08		3.59	20.34		1040.17	0.16					66.88	2.37	3.41	0.28	0.76		0.38						4.04		0.02	
BA08GS025	plag	2008	50766	772	150000	7977	55051	36.72	12.40	32.30	2051.90	12.55	11.12	24.51		931.83	0.20	0.14				120.74	3.60	4.33	0.31	0.86		0.48			0.04			4.61		0.02	0.02
BA08GS026	plag	2008	47453	41	144000	2179	63013	36.82		25.96	992.43		3.99	23.24		1502.29	0.06					97.23	5.02	5.61	0.40	0.86		0.54						8.96			
BA08GS026	plag	2008	49749	35	144000	2277	59695	34.33		21.70	959.05		2.73	23.13		1459.89						97.20	5.27	5.53	0.41	1.01	0.20	0.44						6.84			
BA08GS026	plag	2008	50215	43	144000	2269	59775	32.57		25.67	1081.82		6.03	22.76		1602.86	0.06					108.10	5.81	6.12	0.45	0.90		0.45						6.80			
BA08GS026	plag	2008	51493	38	144000	2430	57982	27.35		18.72	999.48		2.38	22.66		1507.56						91.43	4.51	5.13	0.37	0.93		0.39						6.66			
BA08GS026	plag	2008	45847	30	144000	1911	62916	37.42		22.97	932.07		2.63	22.19		1443.41	0.08					86.31	5.06	5.70	0.39	1.00		0.36						6.59			
BA08GS026	plag	2008	49979	38	144000	2433	60095	30.01		25.62	1121.23		3.17	23.77		1467.34						103.04	6.54	7.11	0.46	1.07	0.13	0.43						6.53			
BA08GS026	plag	2008	53144	39	144000	2767	56998	26.75		21.15	1167.34		2.57	22.19		1478.43	0.06					101.85	4.54	4.94	0.37	0.93	0.15	0.44						6.53			
BA08GS026	plag	2008	50388	263	144000	2460	58980	41.21	0.82	22.91	1210.72		10.04	23.30		1678.55		0.15				109.82	6.14	6.94	0.42	1.00		0.44						6.48			

Appendix 2.7 continued

Sample #	Mineral	Date Collected	Na	Mg	Al	K	Ca	Ti	V	Mn	Fe	Cu	Zn	Ga	As	Sr	Y	Zr	Mo	Sn	Sb	Ba	La	Ce	Pr	Nd	Sm	Eu	Gd	Dy	Er	Yb	Lu	Pb	Bi	Th	U
BA08GS026	plag	2008	51007	35	144000	2402	57615	26.80		32.68	949.31		1.78	22.84		1331.97						115.09	4.85	5.19	0.35	0.83		0.34						6.47			
BA08GS026	plag	2008	51256	31	144000	2399	59012	32.85		22.13	1201.09		3.28	23.00		1554.55						105.37	5.71	5.91	0.41	0.80	0.12	0.47						6.44			
BA08GS026	plag	2008	39745	33	144000	1543	69254	41.20		27.22	999.99		3.63	22.43		1523.78	0.08					88.04	5.31	6.43	0.48	0.89	0.12	0.45						6.44			
BA08GS026	plag	2008	45357	34	144000	1949	64715	33.47		26.67	1064.75		4.91	22.96		1466.81	0.05			0.50		91.95	5.31	6.18	0.45	1.18	0.17	0.42						6.03			
BA08GS026	plag	2008	47243	45	144000	2066	61441	37.43		23.50	1192.15		2.38	24.51		1604.87	0.07					98.57	6.74	7.16	0.47	1.03	0.13	0.52						5.87			
BA08GS026	plag	2008	48174	49	144000	2348	61676	31.67		21.96	1103.71		5.59	20.63		1400.01						98.40	4.57	5.07	0.30	0.78		0.36						5.86			
BA08GS026	plag	2008	47265	35	144000	2077	61639	28.66		22.99	1112.64		3.49	22.38		1460.17						92.37	4.88	5.80	0.41	1.11		0.43						5.75			
BA08GS026	plag	2008	38926	3734	144000	14824	66364	50.52	12.84	273.95	2996.70		32.61	30.32		813.26	0.22					775.17	0.08	0.06				0.12						5.01			
BA08GS026	plag	2008	34228	301	144000	34040	57675	5.99	0.45	35.86	619.13		7.07	31.88	2.21	1140.36					0.35	1373.50	0.11	0.15				0.17						4.80			
BA08GS026	plag	2008	34708	978	144000	16449	85035	32.03	0.77	473.53	1161.39		14.18	23.20		1087.00	0.17			0.65		462.59	2.76	3.41	0.29	0.72		0.32						4.67			
BA08GS026	plag	2008	37317	29	144000	1496	71414	16.65		31.43	735.31		6.11	22.77		1126.64						92.03	3.80	4.43	0.29	0.74		0.27						4.50			
BA08GS026	plag	2008	30434	262	144000	5829	74398	4.82	1.35	60.24	468.01		14.51	35.87		763.20						506.97	0.05					0.12						4.49			
BA08GS026	plag	2008	37452	39	144000	2014	71167	9.83		44.56	364.70		7.41	24.00		892.69						335.56	0.62	0.85	0.06	0.14		0.12						3.94			
BA08GS026	plag	2008	40267	211	144000	3385	71619	11.57	10.04	246.32	5822.21		11.22	31.37		909.34	0.24	0.14			0.89	600.46	1.28	1.69	0.12	0.43		0.16						6.56	0.06	0.14	0.10
BA08GS026	plag	2008	45712	681	144000	7440	63485	11.96	5.65	185.75	2186.49		20.12	27.41		806.47	0.10	0.19			0.49	623.97	0.74	0.92	0.06	0.22		0.14						4.90		0.03	0.05
BA08GS030	plag	2008	48145	45	150000	1206	64935	41.56		28.71	1282.89		3.61	23.32		1407.33	0.04					110.78	5.45	6.04	0.42	1.20	0.10	0.43						5.91			
BA08GS030	plag	2008	51527	42	150000	5805	62797	56.03		25.12	1429.59	2.97	3.69	27.88		1257.73	0.11					181.73	5.78	6.83	0.51	1.35	0.10	0.76						3.46			
BA08GS030	plag	2008	34803	78	150000	630	77769	96.26	0.33	38.17	2227.03	3.21	6.35	23.33		1377.82	0.34			0.48		77.96	3.27	4.36	0.40	1.33	0.14	0.47	0.09	0.06				3.04			
BA08GS030	plag	2008	38592	43	150000	1360	75305	59.30		43.26	1332.06		3.35	23.88		1391.40	0.25					97.69	5.28	6.62	0.52	1.47		0.46	0.08					5.33		0.03	
BA08GS033A	plag	2008	38948	72	150000	1688	74154	54.87		43.59	1867.03		4.58	25.96		1078.41	0.07			0.70		118.73	4.21	5.22	0.37	1.20	0.18	0.51						5.19			
BA08GS033A	plag	2008	45235	90	150000	2515	68423	42.67		35.98	1791.08		3.71	24.48		1219.60	0.10					119.82	4.54	5.37	0.36	1.03		0.51						5.06			
BA08GS033A	plag	2008	46008	73	150000	2453	66206	43.92	0.20	37.46	1861.94		4.43	21.96		1195.26	0.07					126.17	3.94	4.69	0.36	0.92	0.17	0.40						4.89			
BA08GS033A	plag	2008	46551	72	150000	2408	67135	52.06		35.72	1969.81		5.11	26.36		1109.20	0.07	0.07				137.83	4.17	4.44	0.40	0.89		0.46						4.76			
BA08GS033A	plag	2008	44831	62	150000	2422	68951	37.50		40.87	1886.90		4.38	24.96		1100.17	0.10					120.63	4.50	5.21	0.42	0.87	0.13	0.47	0.10					4.68			
BA08GS033A	plag	2008	44324	83	150000	2385	70134	62.51		39.19	2195.83		5.61	25.64		1135.29	0.09					134.70	4.09	4.66	0.32	0.91		0.51						4.53			
BA08GS033A	plag	2008	45654	139	150000	4539	62715	51.97	0.25	36.07	1822.41		5.10	23.79		1039.98	0.07			0.54		128.17	3.85	4.45	0.31	0.93		0.54						4.34			
BA08GS033A	plag	2008	56687	160	150000	7812	52227	77.21	0.31	30.42	1671.56		5.79	26.78		1041.22	0.06	0.10				182.71	4.05	4.67	0.34	0.93		0.41	0.09					3.75			
BA08GS033A	plag	2008	27502	2516	150000	15622	61502	45.49	6.01	56.67	3142.18	6.35	16.26	22.80		868.74	0.18	0.22				120.67	3.31	4.23	0.32	0.89		0.33						3.74			
BA08GS033A	plag	2008	67190	4715	150000	35836	32199	1073.87	40.12	93.05	5579.59	6.27	13.79	29.48		658.53	2.88	43.39	0.28	0.67		984.16	7.96	10.24	0.67	2.06	0.44	0.45	0.49	0.39	0.29	0.50	0.06	3.50	0.03	2.99	0.79
BA08GS033A	plag	2008	36064	91	150000	1619	78861	51.71	0.28	44.39	1680.62		4.35	23.34		1148.63	1.11	0.30		0.53		103.37	4.07	6.64	0.63	2.12	0.39	0.38	0.25	0.12	0.08	0.09		4.31		0.40	0.15
BA08GS033A	plag	2008	46009	103	150000	2824	67698	38.86		36.27	1580.48		4.38	24.35		1549.49	0.09	0.63				105.55	5.60	6.40	0.42	1.15		0.43		0.07				5.79		0.05	0.02
BA08GS033B	plag	2008	52986	67	150000	2421	61680	45.58		32.10	1529.56		4.33	24.58		1216.62	0.05					159.53	5.80	6.92	0.44	1.11		0.57	0.11					5.59			
BA08GS033B	plag	2008	42414	63	150000	11077	66617	54.30		36.72	1619.04		3.92	25.41		1249.51						263.98	4.18	4.94	0.31	1.00		0.51						5.36			
BA08GS033B	plag	2008	49917	103	147000	3553	63867	40.79		32.64	1789.47		4.65	25.25		1169.87						164.95	4.78	5.54	0.45	0.95		0.50						4.93			
BA08GS033B	plag	2008	45696	93	150000	2505	68955	58.04		36.31	2001.54		6.51	27.34		1189.10	0.12					148.25	5.07	5.66	0.39	0.95		0.52						4.45			
BA08GS033B	plag	2008	42594	62	150000	1833	68981	43.87		39.39	1738.85		4.49	23.04		1004.79	0.09					113.56	3.18	3.90	0.27	0.75		0.39						4.45			
BA08GS033B	plag	2008	49367	77	150000	2634	63061	38.63		30.60	1639.80		5.15	23.82		1116.78	0.05					126.53	4.27	4.67	0.33	0.70		0.52						4.20			
BA08GS033B	plag	2008	38783	680	150000	15864	52791	49.15	1.92	51.93	2043.55		8.52	26.30		854.00	0.15					133.63	3.03	3.60	0.25	0.58		0.32						3.72			
BA08GS033B	plag	2008	53327	1940	150000	89748	642717	28.69	8.17	1200.56	1895.46	1.39	6.24	36.47		1556.50	2.03	0.34				4700.01	50.23	58.95	4.44	12.47	0.90	2.28	0.78	0.35	0.14			3.20			
BA08GS033B	plag	2008	42071	84	147000	2450	68463	71.08	0.26	41.70	1758.87		4.90	22.90		936.90	0.17	1.64				134.33	4.04	4.81	0.36	0.96		0.41						4.62		0.10	0.05
BA08GS033B	plag	2008	33820	299	150000	2865	79319	62.15	0.60	47.95	1920.87		5.14	22.70		1073.02	0.55					96.96	4.25	6.07	0.54	2.12	0.32	0.49	0.18	0.15	0.06		0.02	3.73		0.08	0.03
BA08GS034	plag	2008	45705	44	150000	1337	67387	41.96		33.91	1234.72		3.05	23.11		1336.85						110.46	5.00	5.61	0.41	0.96		0.46	0.09	0.06				5.31			
BA08GS034	plag	2008	48153	1582	150000	4014	79669	43.94	3.64	407.55	3361.23		5.47	23.28		1310.53	3.18					128.51	6.13	7.51	0.73	2.47	0.52	0.76	0.65	0.39	0.21	0.14	0.03	5.40	0.04	0.03	
BA08GS034	plag	2008	47647	47	150000	2253	65921	31.72		32.93	1267.00	2.23	4.16	23.02		1309.25	0.08			0.66		112.26	4.76	5.41	0.36	1.14		0.41						5.93		0.02	
BA08GS036	plag	2008	46296	41	141000	2070	59581	32.73		23.95	1002.18		3.43	22.51		1400.61						98.42	5.07	5.33	0.34	0.92		0.48						6.47			
BA08GS036	plag	2008	45534	38	141000	1935	60753	37.21		24.43	1095.31		2.34	22.94		1489.91	0.07					103.46	6.50	7.13	0.50	1.10		0.47						6.28			
BA08GS036	plag	2008	46124	40	141000	2018	60216	38.71		22.61	1151.54		2.20	22.24		1430.12	0.04					92.15	5.36	5.67	0.38	0.88	0.13	0.40						6.23			
BA08GS036	plag	2008	43757	42	141000	1778	62119	26.49		25.43	1028.96		2.63	22.07		1323.11	0.04					78.67	5.20	6.24	0.43	1.04	0.08	0.41						6.03			
BA08GS036	plag	2008	45771	49	141000	2270	61129	27.65		27.78	1092.73		2.34	21.14		1417.70	0.08					96.43	4.79	5.72	0.40	1.02	0.12	0.43	0.11					5.88			
BA08GS036	plag	2008	40614	51	141000	1582	65738	47.37		26.39	1282.31		3.20	24.26		1581.80	0.08					94.82	5.42	6.19	0.40	1.17		0.38						5.80			
BA08GS036	plag	2008	48372	41	141000	2191	58222	34.51		21.09	1035.55		1.59	21.77		1424.99						99.79	5.90	6.25	0.42	1.05		0.42						5.77			
BA08GS036	plag	2008	37024	50	141000	1169	71558	27.73		34.58	1045.98		2.47	22.24		1177.26	0.08	0.09				78.80	3.83	4.64	0.31	0.93		0.27						4.76			
BA08GS037	plag	2008	49942	31	150000	2010	65203	35.03		36.23	1215.09		4.01	24.06		1319.76	0.05					118.35	4.94	5.38	0.40	0.88	0.16	0.40						5.87			
BA08GS037	plag	2008	47712	46	150000	2248	66779	69.42		27.57	1220.72		3.13	25.50		1578.82						126.20	4.82	5.22	0.34	0.95		0.40						5.74			
BA08GS037	plag	2008	47108	50	150000	2352	65214	39.33		31.89	1314.23		3.12	23.23		1372.18	0.07					112.05	5.25	5.67	0.39	1.11	0.11	0.43						5.69			
BA08GS037	plag	2008	47443	38	150000	1307	66929	32.16		28.06	1272.04		3.47	24.36		1264.68	0.04					114.09	5.04	5.73	0.36	1.04		0.52						5.49			
BA08GS037	plag	2008	44372	58	150000	1950	68546	40.36		41.70	1374.95		4.41	22.58		1300.16	0.08					105.55	4.85	5.58	0.36	1.02		0.43						5.14			
BA08GS037	plag	2008	48003	52	150000	1870	65507	48.08	0.18	32.54	1647.95	17.55	12.37	23.26		1313.52	0.16	0.45		0.49	0.39	114.94	4.40	5.08	0.32	0.96		0.41		0.06				6.08		0.04	0.02
BA08GS037	plag	2008	47370	145	150000	4838	65869	41.80		32.69	1397.99		4.23	22.69		1320.32	0.24					206.45	4.66	6.14	0.45	1.22	0.17	0.45	0.11	0.06			0.02	5.06		0.03	0.02
BA08GS038	plag	2008	46883	58	144000	2089	59805	31.76	0.29	30.65	1052.55	1.16	9.22	23.86		1452.36	0.04					84.01	4.91	5.71	0.38	0.84		0.34		0.00				7.21			
BA08GS038	plag	2008	50995	42	144000	2450	58009	35.18		20.86	1033.78		2.12	23.87		1586.20	0.05		0.08	0.27		103.93	5.61	6.20	0.43	1.11		0.45			0.01			7.02	0.01		
BA08GS038	plag	2008	36167	2295	144000	7784	69781	378.90	6.77	364.36	2864.30	2.14	46.00	19.48	0.71	984.54	1.32	11.14	1.25	0.27	0.19	79.72	2.51	4.73	0.44	1.55	0.26	0.28	0.16	0.19	0.10		0.03	3.27		0.59	0.24
BA08GS038	plag	2008	41378	367	144000	2968	67481	38.74	8.62	100.34	5000.93	18.66	23.29	24.54	2.26	1383.76	0.40	0.08			0.46	79.06	4.78	6.01	0.45	1.28	0.15	0.43		0.06	0.04	0.04		8.89		0.02	0.10
BA08GS038	plag	2008	44744	378	144000	2299	60602	233.75	2.09	41.35	1147.14	47.04	41.16	24.13		1409.01	0.59	0.65				84.93	4.62	5.14	0.39	1.04		0.41	0.11	0.11	0.05	0.07		6.68			0.07
BA08GS038	plag	2008	53402	260	144000	2718	54474	23.53	5.95	67.18	2479.65	22.81	64.78	20.79	0.94	1197.00	0.31	1.26			0.18	75.69	3.36	4.03	0.27	0.93		0.24	0.04		0.01			6.09	0.10	0.35	0.06
BA08GS038	plag	2008	49017	59	144000	2290	60685	36.82	0.15	38.00	930.27	0.64	7.57	21.19		1355.85	0.04		0.07			79.69	3.69	4.31	0.29	0.73		0.29	0.01					6.11		0.01	0.01
BA08GS038	plag	2008	47260	42	144000	2113	59541	28.47		24.71	1062.64		3.03	24.19		1348.28	0.04			0.27		87.18	4.92	5.49	0.34	1.02	0.06	0.37					0.00	6.04			0.00
BA08GS047	plag	2008	47479	896	150000	18994	52504	8.17	1.51	63.47	2436.83		9.12	18.15		895.02	0.05					116.48	0.09	0.15	0.02			0.09						3.15			
BA08GS047	plag	2008	6831	229	150000	203	105185	34.64	0.50	34.92	3637.86		2.05	17.80		850.28	0.06					13.41	0.75	1.28	0.11	0.44		0.19						0.54			
BA08GS047	plag	2008	6331	340	150000	3379	98409	37.52	0.50	35.23	4124.35		3.23	17.27		733.59	0.73					12.59	0.95	1.59	0.17	0.88	0.19	0.13	0.13	0.12				0.43			
BA08GS047	plag	2008	4816	275	150000	130	111927	33.16	0.61	29.27	3823.15		1.97	15.13		697.98						8.82	0.48	0.83	0.07	0.31		0.09						0.40			
BA08GS047	plag	2008	6118	282	150000	157	103638	45.59	0.95	33.31	4128.63		1.56	16.73		732.42	0.07	0.25		0.47		11.75	0.55	0.91	0.10	0.44		0.13						0.39			

Appendix 2.7 continued

Sample #	Mineral	Date Collected	Na	Mg	Al	K	Ca	Ti	V	Mn	Fe	Cu	Zn	Ga	As	Sr	Y	Zr	Mo	Sn	Sb	Ba	La	Ce	Pr	Nd	Sm	Eu	Gd	Dy	Er	Yb	Lu	Pb	Bi	Th	U
BA08GS047	plag	2008	58117	22619	150000	9550	68395	1173.41	326.91	600.23	65547.99	2.91	27.15	41.62		828.84	10.65	5.97		1.59		77.74	13.33	27.05	3.47	16.11	3.56	0.92	3.38	2.57	1.14	0.72	0.06	2.85		2.94	1.37
BA08GS047	plag	2008	13717	995	150000	28523	74401	34.86	3.00	64.81	4023.24	2.05	6.68	21.26		868.15	4.68	210.48				147.34	1.07	1.62	0.15	0.54	0.14	0.18		0.31	0.91	2.34	0.49	1.11		0.50	0.73
BA08GS052A	plag	2008	47425	982	140000	22444	47889	0.86	2.44	44.77	985.03		2.36	19.10		947.44	0.22	0.00				487.89	0.04	0.10	0.01	0.09		0.02				0.05	0.00				
BA08GS052A	plag	2008	35896	42	140000	1661	69741	34.21		49.41	1378.02		4.26	26.32		1201.10	0.18	0.02	0.06			78.87	4.67	6.13	0.47	1.39	0.07	0.51		0.03	0.05			5.66			
BA08GS052A	plag	2008	39849	49	140000	1585	64068	34.31		40.05	1504.25		4.86	24.39		1168.09	0.12	0.01		0.30		85.55	4.01	4.85	0.32	0.99	0.11	0.47	0.02		0.01			4.35			
BA08GS052A	plag	2008	47391	774	140000	12489	51865		0.26	89.58	1209.71		1.81	18.87		856.08	0.22	0.03				163.30	0.17	0.26	0.02	0.17		0.03			0.01			0.47			
BA08GS052A	plag	2008	39775	73	140000	1640	65396	89.53	0.48	44.18	1579.34	1.25	3.79	27.21		1332.27	0.18	0.35				87.10	3.84	4.97	0.37	1.06	0.07	0.57					0.01	4.87		0.05	
BA08GS052A	plag	2008	39491	475	140000	12900	79816		0.63	133.00	1733.74	1.68	4.35	21.56		782.15	0.54		0.07			135.00	0.33	0.49	0.07	0.22		0.05	0.08	0.08	0.03			1.20		0.00	
BA08GS052A	plag	2008	45339	110	140000	1122	59126	7.04	6.41	42.57	1494.97	1.12	3.69	18.63		649.23	1.79	0.18	0.00		0.15	126.68	3.43	5.92	0.80	2.62	0.49	0.17	0.60	0.29	0.11		0.01	1.55		0.46	0.22
BA08GS052A	plag	2008	43016	751	140000	34444	75105	109.67	8.50	160.53	5964.91	2.77	7.49	26.16	1.70	706.18	1.57	28.39	0.04		0.46	1045.29	2.56	3.05	0.25	0.81		0.33	0.15	0.13	0.14	0.20	0.05	1.82		0.45	0.17
BA08GS052A	plag	2008	37452	1644	140000	24743	65184	8.97	7.84	500.91	13740.53	2.08	6.18	24.40	0.56	764.17	0.84	0.11	0.11	0.18	0.17	157.41	0.87	1.58	0.16	0.62	0.10	0.17	0.14	0.10	0.04	0.07		4.05	0.04	0.01	0.04
BA08GS052A	plag	2008	35842	40	140000	1353	69632	38.89		49.12	1302.39		5.12	24.74		958.52	0.57			0.22	0.04	65.74	3.03	4.98	0.48	1.36	0.26	0.59	0.17	0.13	0.09			3.91		0.07	0.03
BA08GS052A	plag	2008	44549	58	140000	2070	60373	3.61	0.80	73.44	2495.32		0.65	22.69		620.56	0.41			0.22	0.15	60.49	0.63	1.20	0.13	0.43	0.07	0.05	0.11	0.12		0.02	0.01	1.56	0.04	0.05	0.03
BA08GS052A	plag	2008	43616	38	140000	1839	59596	21.57	0.25	34.66	1133.58		5.87	22.44		1266.32	0.16	0.02	0.09			100.88	4.99	6.14	0.47	1.13	0.00	0.40		0.03	0.00	0.00	0.00	5.64		0.02	0.02
BA08GS052A	plag	2008	35740	71	140000	1316	67954	50.72	0.26	41.60	1659.50		4.60	25.38		1109.45	0.11	0.10		0.30		77.26	3.88	4.95	0.41	0.88		0.43	0.05		0.01			4.25			0.00
BA08GS052A	plag	2008	37356	40	140000	1542	67871	29.65		41.98	1142.18		2.78	24.40		1202.01	0.11			0.25		81.02	4.25	5.65	0.42	1.31	0.11	0.47						5.77			0.00
BA08GS052A	plag	2008	45639	5	140000	760	60539	2.09		5.92	189.65			20.93		869.39		0.01				75.22					0.02	0.00						0.42	0.00	0.00	0.00
BA08GS052B	plag	2008	40933	49	145000	1537	66103	26.25		40.08	1306.54		4.95	24.25		1169.12	0.07		0.07			74.74	4.18	5.11	0.35	1.03	0.10	0.40		0.02			0.01	5.06			
BA08GS052B	plag	2008	42377	51	145000	1609	64456	26.88		37.83	1117.45		4.33	20.76		1159.23	0.06		0.00			86.30	3.50	4.83	0.38	1.07		0.40	0.02	0.03	0.04			4.88			
BA08GS052B	plag	2008	39204	60	145000	1434	67040	35.68		41.15	1534.43		5.61	25.57		1141.43	0.05		0.03	0.25		82.79	4.25	5.29	0.41	0.89	0.10	0.48				0.00	0.00	4.50			
BA08GS052B	plag	2008	29383	168	145000	793	78228	67.62	0.43	41.58	2742.71		5.64	22.95		1020.20	0.09	0.08	0.06	0.23		58.68	2.05	2.60	0.21	0.59	0.07	0.35		0.02		0.00		2.08			
BA08GS052B	plag	2008	109798	26	145000	1042	4828			3.66	60.50	1.01		12.48		390.49	0.01			0.32		28.42		0.02			0.00	0.02	0.00		0.00	0.01		0.13			
BA08GS052B	plag	2008	41881	41	145000	1543	65547	38.68		40.15	1225.63		4.27	24.39		1045.29	0.08					84.72	3.66	4.09	0.30	0.84		0.46		0.02				4.76	0.00		
BA08GS052B	plag	2008	45501	47	145000	1852	61388	26.49	0.13	35.93	1217.30		3.55	24.86		1170.46	0.04		0.02	0.21		97.20	5.54	6.56	0.46	1.32		0.49		0.02				5.63		0.00	
BA08GS052B	plag	2008	35541	50	145000	1243	71276	47.14		43.31	1304.00		3.76	22.47		1197.69	0.10		0.06	0.22		61.92	2.73	3.75	0.30	0.86	0.08	0.43	0.06					4.78		0.00	
BA08GS052B	plag	2008	65105	530	145000	11005	78255	2.62	0.36	239.38	1811.36	0.78	4.09	24.26		1386.60	0.18					126.21	0.05	0.12			0.03	0.06			0.01	0.01		1.96	0.00	0.00	
BA08GS052B	plag	2008	28690	1416	145000	26477	65926	164.20	2.81	100.06	3502.02		6.19	24.77	1.35	889.89	1.20	13.06	0.06	0.25	0.31	562.10	3.25	4.53	0.43	1.14	0.15	0.57	0.13	0.16	0.13	0.25	0.05	1.54	0.02	0.73	0.24
BA08GS052B	plag	2008	32239	261	145000	1576	76065	87.65	0.88	28.97	2584.13		6.72	21.20		1156.34	0.55	10.20		0.34		104.27	2.78	3.85	0.23	1.09		0.48		0.08	0.02		0.02	2.44		0.82	0.08
BA08GS052B	plag	2008	33508	193	145000	2072	72302	62.06	0.39	36.27	2292.90		6.56	23.79		1151.77	0.78	13.59	0.00			100.92	3.04	4.01	0.29	1.08	0.18	0.41		0.05	0.09	0.13	0.04	3.02	0.01	0.68	0.07
BA08GS052B	plag	2008	30999	781	145000	11213	67510	59.05	0.99	59.07	2633.76	0.81	5.30	25.67		1058.56	0.63	4.49		0.18	0.23	510.44	3.60	6.01	0.52	1.77	0.22	0.45	0.26	0.12	0.08		0.02	3.70		0.26	0.07
BA08GS052B	plag	2008	38849	97	145000	1983	68897	71.07	0.23	58.56	1747.60	0.89	4.55	25.40	0.48	1136.42	0.18	1.94				92.95	4.63	5.80	0.42	1.33	0.15	0.42		0.06		0.03		4.91		0.20	0.04
BA08GS052B	plag	2008	46226	997	145000	17645	52612	2.73	1.02	97.92	2280.06	0.75	5.02	17.95		768.87	0.34	0.35		0.23		133.76	0.27	0.52	0.06	0.24		0.04	0.03	0.03	0.04	0.01		1.14	0.02	0.02	0.02
BA08GS052B	plag	2008	32406	142	145000	3115	73543	47.68	0.65	42.57	1362.17	1.09	4.17	24.13		1209.86	0.12	0.31	0.02			95.72	3.37	4.51	0.34	1.06	0.10	0.39	0.08	0.04	0.01	0.01		4.97		0.04	0.01
BA08GS054	plag	2008	46078	46	145000	2097	62411	35.60	0.10	36.04	1198.05		3.81	25.28		1363.05	0.04					95.75	5.30	5.93	0.48	1.27		0.42			0.02			6.57			
BA08GS054	plag	2008	46478	43	145000	1977	61294	20.92		34.12	1088.94		4.31	24.39		1240.02	0.06	0.04				91.91	4.64	5.86	0.42	1.12		0.48						6.17			
BA08GS054	plag	2008	42245	47	145000	1561	66593	28.17		63.78	1211.19		6.19	23.56		1228.75	0.07			0.22		80.66	4.27	5.39	0.36	0.95		0.47						6.15			
BA08GS054	plag	2008	44809	52	145000	2067	63831	34.71	0.12	38.12	1394.03		4.63	23.38		1186.35	0.07			0.26	0.07	94.50	2.98	3.80	0.27	0.75		0.43	0.03		0.00			4.40			
BA08GS054	plag	2008	43928	164	145000	18769	53054	32.51	0.35	32.27	1012.10	0.32	3.43	23.02	1.00	1255.10	0.07	0.05	0.04			643.17	1.47	2.26	0.21	0.46		0.30			0.03		0.01	3.29			
BA08GS054	plag	2008	32501	78	145000	2381	74124	47.69		45.82	1922.48		5.55	24.32		1076.96	0.10					72.51	2.61	3.39	0.24	0.77	0.10	0.33	0.04	0.03		0.02		3.10			
BA08GS054	plag	2008	33880	47	145000	1148	73764	63.70		46.50	1202.31		3.58	21.64	0.52	1360.24	0.07	0.01				55.30	2.65	3.37	0.29	0.82	0.11	0.34	0.04		0.00	0.00		5.60	0.01		
BA08GS054	plag	2008	44217	48	145000	1837	64991	34.02		36.41	1200.67		3.84	25.10		1320.53	0.07				0.06	91.22	4.23	5.22	0.38	1.04	0.06	0.52					0.00	5.67	0.00		
BA08GS054	plag	2008	34304	709	145000	13051	61097	29.45	1.86	69.85	2131.42	0.62	4.23	24.01		1081.57	0.12	0.18	0.02	0.28		202.77	3.43	4.37	0.38	0.93		0.38	0.06		0.04			3.93		0.02	
BA08GS054	plag	2008	44358	183	145000	14632	56788	36.18	0.49	39.90	1439.37		4.12	23.80		1361.82	0.06				0.20	260.00	4.16	5.54	0.36	1.08	0.10	0.41	0.07	0.01			0.00	4.50		0.01	
BA08GS054	plag	2008	42797	731	145000	23028	47614	29.77	0.33	51.94	2396.57	3.51	5.86	30.88		1094.36	0.09	0.11		0.22		1254.24	3.52	4.33	0.35	1.04		0.49		0.02				4.36		0.01	
BA08GS054	plag	2008	36697	56	145000	1296	71451	51.77		43.73	1818.37		5.24	25.52		1148.35	0.08		0.03			76.90	3.34	4.22	0.33	0.85	0.08	0.45	0.06		0.01			3.89		0.00	
BA08GS054	plag	2008	73704	651	145000	3537	42626	2742.54	34.94	116.43	18801.11	1.67	8.81	29.24		837.86	10.87	172.57			0.95	451.30	27.04	40.87	3.33	9.95	1.63	0.79	1.55	1.71	1.12	1.36	0.26	15.46		12.18	4.02
BA08GS054	plag	2008	65354	12687	145000	4625	64712	2160.36	401.62	249.73	170633.76	8.33	21.64	27.36	7.50	785.13	21.69	308.50	0.09		1.08	302.47	14.33	35.25	4.86	24.29	3.99	1.03	3.91	3.03	2.30	3.81	0.77	3.73		10.34	1.71
BA08GS054	plag	2008	64384	128	145000	5849	43041	430.37	0.36	18.36	1774.03		5.26	25.15		848.91	3.63	116.82		0.49	0.35	333.81	7.35	9.12	0.81	2.66	0.35	0.47	0.27	0.43	0.55	1.13	0.17	5.14		5.61	1.02
BA08GS054	plag	2008	66805	342	145000	2934	51753	181.61	1.16	37.04	2233.05		5.92	27.54		856.68	5.82	28.71		0.43		265.16	11.39	18.73	2.11	8.56	1.45	0.75	2.05	1.18	1.03	0.75	0.08	4.58		1.48	0.34
BA08GS054	plag	2008	49247	168	145000	4699	98458	177.02	9.99	390.43	21309.20		3.22	32.79	2.90	732.30	3.21	1.85			0.43	60.50	5.47	9.95	1.09	4.20	0.64	0.28	0.83	0.47	0.28	0.34	0.03	4.45	0.03	0.73	0.27
BA08GS054	plag	2008	27161	801	145000	33016	56863	69.05	7.43	89.31	4292.54	0.70	6.31	23.69	0.89	895.91	1.28	4.18		0.20	0.21	615.95	3.16	4.79	0.45	1.49	0.23	0.34	0.17	0.25	0.08	0.13	0.03	1.82	0.03	1.90	0.12
BA08GS054	plag	2008	43927	61	145000	1702	67629	31.69	2.51	59.50	2785.63		4.38	25.25		1230.51	0.21		0.09			92.03	5.01	5.97	0.48	1.31		0.48	0.15	0.05		0.02		5.24			0.05
BA08GS054	plag	2008	51043	1869	145000	15371	41615	7.62	4.03	21.06	1966.35	0.69	3.43	17.90		761.05	0.08	0.14	0.13			80.94	0.19	0.44	0.06	0.22								0.38		0.03	0.02
BA08GS054	plag	2008	38348	778	145000	26418	51154	62.44	0.30	65.90	2025.22	0.94	6.15	26.25	1.14	1384.92	0.42				0.19	912.42	4.44	6.87	0.59	2.01	0.24	0.36	0.11	0.08				3.27		0.03	0.01
BA08GS054	plag	2008	41901	49	145000	1524	67719	34.73		39.72	1265.71		4.63	24.29		1349.11	0.08		0.02			101.00	3.68	4.65	0.38	0.93		0.51					0.00	6.07	0.00		0.01
BA08GS054	plag	2008	42200	421	145000	21918	44689	31.20	1.07	64.54	2141.62	0.51	5.70	24.10	0.66	1064.02	0.08	0.64				469.40	2.49	2.97	0.23	0.70		0.26			0.00			2.92		0.03	0.01
BA08GS054	plag	2008	45798	38	145000	1683	62489	22.95		37.43	1061.61		2.65	23.97		1252.07	0.06		0.02			90.12	4.93	6.00	0.40	1.02	0.13	0.43						6.01			0.00
BA08GS056	plag	2008	18032	5638	150000	48675	41154	217.97	18.05	194.31	9490.69	11.52	12.46	20.29	0.83	432.72	0.10	0.10			0.27	208.07	0.20	0.44		0.21		0.09						1.18			
BA08GS056	plag	2008	26593	2141	150000	18824	76062	28.99	8.57	98.13	4214.64	4.87	8.88	16.65		550.38	0.05					43.19	0.13	0.16	0.04	0.16		0.04						1.12			
BA08GS056	plag	2008	24978	3326	140000	10964	76880	113.12	73.36	334.68	41262.28	1.36	9.58	45.96	2.70	703.98	4.24	0.89			0.71	58.26	5.14	11.05	1.30	5.93	1.11	0.44	1.32	1.01	0.36	0.36	0.05	3.91	0.06	0.11	0.23

Appendix 2.8 – Individual laser ablation-inductively coupled plasma mass spectrometry spot analyses of hornblend (LA-ICPMS) generated for this thesis. All values reported in ppm; blank values indicate below detection limit concentrations.

Sample #	Mineral	Year	Na	Mg	Al	K	Ca	Ti	V	Mn	Fe	Cu	Zn	Ga	As	Sr	Y	Zr	Mo	Sn	Sb	Ba	La	Ce	Pr	Nd	Sm	Eu	Gd	Dy	Er	Yb	Lu	Pb	Bi	Th	U
353226	hbl	2008	19101	102369	77102	8899	88000	14675	652	558	100418	6.53	38.32	17.47		287.34	18.29	20.20		0.97		75.33	0.99	3.34	0.96	5.36	1.60	0.91	4.25	4.38	2.58	1.64	0.25				
353226	hbl	2008	19273	106959	77384	8691	88000	14382	714	760	99967	1.46	33.47	15.99		286.36	15.55	17.00		0.97		73.89	0.84	5.29	0.96	7.03	3.44	1.12	4.09	3.32	1.31	1.45	0.23	0.28			
353226	hbl	2008	16857	99199	73100	6766	83000	13929	576	990	93869	2.61	47.31	14.96		281.36	18.12	22.99		1.54		75.67	1.57	6.88	1.43	8.79	3.04	1.11	3.78	4.05	2.02	1.57	0.20	0.31	0.02	0.04	
353226	hbl	2008	16659	102528	74889	6977	88000	13751	655	732	94049	2.25	35.58	13.85		282.38	15.98	18.33		1.38		67.82	0.98	4.32	0.97	6.32	2.39	0.97	3.61	3.40	1.67	1.33	0.19	0.36		0.02	
353226	hbl	2008	17348	101394	69998	5921	83000	14428	616	1084	97595	3.96	53.85	14.43		249.75	19.85	21.38		1.56		56.45	1.29	5.77	1.25	8.10	3.32	1.07	4.00	4.29	2.25	1.79	0.25	0.40		0.02	
353226	hbl	2008	17269	102908	72500	6462	83000	13378	623	889	92589	3.06	42.60	14.11		262.81	16.71	19.94		1.26		61.20	1.35	5.43	1.11	7.48	2.75	0.94	3.40	3.42	1.82	1.48	0.21	0.43		0.02	
353226	hbl	2008	16910	112674	75366	8559	88000	12744	653	540	80052	1.83	27.62	12.78		250.48	10.97	12.68		1.27		64.23	0.74	3.21	0.65	4.52	1.78	0.67	2.49	2.53	1.25	0.67	0.10	0.24		0.02	
353226	hbl	2008	18253	110038	76123	6577	88000	14544	668	957	95556	3.71	44.84	15.33		283.72	20.29	24.46		1.56		63.66	1.41	6.02	1.26	8.47	3.16	1.15	4.33	4.47	2.24	1.92	0.27	0.42		0.02	
353226	hbl	2008	16889	103731	73271	6513	83000	12633	620	753	89468	2.89	38.42	13.73		262.05	14.94	16.72		1.29	0.19	57.41	1.03	4.20	0.89	6.22	2.30	0.84	3.01	3.10	1.52	1.19	0.15	0.33		0.02	
353226	hbl	2008	15288	107771	70206	9967	83000	11833	632	433	70251	2.31	21.79	11.30		234.79	9.30	11.27		1.13		81.39	0.95	3.88	0.78	5.39	1.89	0.72	2.31	2.21	0.92	0.71	0.09	0.18		0.02	
353226	hbl	2008	16699	100562	71771	6980	83000	14418	648	875	92754	3.40	42.27	14.05		279.43	17.97	24.29		1.20		80.69	1.76	7.03	1.46	9.02	3.40	1.17	3.84	3.86	1.90	1.59	0.20	0.35		0.02	
353226	hbl	2008	15399	107833	70369	9256	83000	11316	623	486	73598	2.39	23.99	11.46		244.48	10.60	12.68		1.07	0.21	72.87	1.14	4.51	0.97	6.19	2.20	0.71	2.58	2.50	1.13	0.96	0.12	0.30		0.01	
353226	hbl	2008	17474	109498	75605	7434	88000	14810	682	721	87510	3.57	34.49	14.58		264.03	16.80	15.90		1.27		68.10	0.88	3.89	0.98	6.60	2.61	1.02	3.87	3.94	1.99	1.42	0.16	0.34		0.01	
353226	hbl	2008	17522	113355	76786	7737	88000	13009	652	642	86858	2.16	32.52	12.79		250.80	12.55	14.24		1.45		59.52	0.84	3.54	0.79	5.20	2.13	0.75	2.79	2.91	1.32	1.12	0.15	0.28		0.01	
353226	hbl	2008	18573	108888	78311	9354	88000	13849	750	753	101324	5.33	39.37	16.44		311.17	14.19	15.81		0.63		84.22	0.85	4.47	0.70	6.64	2.55	0.79	2.71	3.13	1.06	1.18	0.14	0.34		0.06	0.02
353226	hbl	2008	17550	106712	77062	8369	88000	15181	713	940	92414	6.26	45.82	15.47		344.90	20.11	24.38		1.57		100.03	2.10	8.65	1.74	11.13	3.89	1.22	4.24	4.51	2.02	1.82	0.26	0.42		0.03	0.01
353226	hbl	2008	18914	108410	72744	6537	88000	16029	660	1397	104558	3.28	65.81	16.47		262.55	30.32	32.78		1.86		68.02	2.41	10.16	2.12	13.83	4.90	1.73	5.95	6.59	3.51	2.71	0.39	0.50		0.03	0.01
353226	hbl	2008	16387	97732	73461	6659	83000	12863	631	766	92808	4.58	38.25	13.69		261.85	15.76	16.99		1.26		62.11	1.05	4.34	0.91	6.72	2.78	0.89	3.25	3.62	1.82	1.52	0.19	3.42		0.01	0.01
354019	hbl	2008	25	90274	62034	94	74000	25171	423	3295	106302	19.59	425.16	24.42	2.73	61.82	103.21	82.20	0.50	7.15	0.27	6.17	5.57	30.77	8.44	56.84	20.12	4.89	20.65	21.88	10.72	9.33	1.12	4.53	0.03	0.24	0.69
354019	hbl	2008	11622	168510	113682	5205	74000	9268	740	4410	233522	44.49	541.42	50.63	1.83	90.45	49.21	39.26		2.86	0.95	62.27	9.40	35.73	5.98	32.02	7.72	2.59	8.79	9.32	5.85	5.41	0.77	7.83	0.04	0.17	0.08
354019	hbl	2008	10263	159382	97512	4119	74000	9438	827	4042	225531	2.99	536.68	47.46	2.13	82.64	45.66	38.38		3.86	0.79	54.48	12.97	44.89	7.36	37.77	8.72	2.34	8.72	8.79	5.02	4.93	0.78	15.09	0.03	0.44	0.06
354019	hbl	2008	11751	96130	61697	7396	74000	9729	489	2073	99556	5.42	139.78	18.26		109.43	22.74	30.82		2.26	0.20	70.44	5.53	17.59	2.75	13.55	3.95	1.26	4.54	4.63	2.39	2.22	0.39	4.55	0.03	0.17	0.06
354019	hbl	2008	11981	86084	58810	4799	74000	7717	419	2945	130215	1.73	195.35	26.27		69.35	46.71	39.83		2.80	0.11	35.93	10.19	41.53	7.12	36.81	9.55	2.47	9.04	9.03	5.11	5.57	0.75	1.24	0.02	0.16	0.06
354019	hbl	2008	11942	89986	57737	4857	74000	7751	433	2952	126498	0.97	197.61	25.86		66.35	52.41	36.62		2.72		35.36	12.00	49.43	8.77	44.26	11.56	2.81	10.60	10.35	5.99	5.65	0.80	0.86	0.03	0.13	0.05
354019	hbl	2008	12327	87357	65088	5674	74000	9049	444	2880	134165	38.27	222.28	27.08		89.62	48.29	45.48		3.55		47.26	9.80	40.03	6.98	37.56	9.90	2.77	9.51	9.16	5.31	5.43	0.71	1.07	0.02	0.11	0.05
354019	hbl	2008	11457	84730	56718	5356	74000	7405	436	2998	122099		206.44	25.52		59.67	52.11	33.11		2.90		31.27	11.40	47.28	8.30	41.73	10.98	2.86	10.38	10.17	5.69	5.61	0.74	0.84	0.02	0.11	0.04
354019	hbl	2008	11588	99360	59175	8407	74000	11486	460	2215	106663	0.94	152.89	19.58		134.89	25.55	45.72	0.13	2.41		78.97	5.39	19.69	3.34	18.39	5.18	1.53	5.74	5.35	2.72	2.33	0.34	0.99	0.03	0.11	0.04
354019	hbl	2008	8044	100307	68264	4176	74000	6337	498	3115	146530	29.41	297.13	31.56	1.00	72.30	40.88	33.67		2.93	0.62	40.97	9.61	36.55	6.40	31.99	8.22	2.27	8.25	7.69	4.52	4.18	0.62	14.83	0.01	0.12	0.04
354019	hbl	2008	11538	89948	59200	4962	74000	8674	489	2956	131025	21.09	213.90	25.17		72.85	44.98	42.38		2.37		42.28	10.10	38.91	6.42	33.26	8.20	2.31	8.53	8.86	5.13	5.04	0.75	4.04	0.02	0.10	0.04
354019	hbl	2008	12146	99153	65548	5514	74000	7838	481	2999	125788	34.60	211.96	24.72		55.95	45.66	26.14		2.64	0.41	23.84	9.35	36.88	6.38	32.18	7.93	2.12	8.20	7.96	4.42	4.06	0.60	37.23		0.10	0.04
354019	hbl	2008	11891	93456	66843	5729	74000	10144	532	3101	144950	145.49	244.00	30.11		114.99	38.17	48.48		2.68	0.30	50.60	7.71	29.98	5.11	25.49	6.26	2.04	7.06	7.04	4.13	3.84	0.57	2.08	0.03	0.09	0.03
354019	hbl	2008	12000	86949	57138	4959	74000	9202	436	2653	116710	0.60	180.62	21.33		82.88	36.26	42.28		2.40		36.61	7.98	30.51	5.02	25.02	6.16	1.72	6.74	6.70	3.74	3.60	0.55	0.87		0.09	0.03
354019	hbl	2008	10613	73090	54961	5116	74000	7316	420	2665	114553		176.80	23.64		78.00	43.35	31.70		2.78		33.83	7.61	31.81	5.57	29.36	7.80	2.21	8.64	8.52	4.78	4.68	0.66	0.98		0.09	0.03
354019	hbl	2008	2844	36811	23716	1279	74000	2279	168	2433	50932	40.86	115.45	11.49		62.72	40.61	10.54		1.08		9.90	12.68	42.43	6.96	35.08	8.61	2.09	8.30	7.47	4.22	4.23	0.65	4.10		0.08	0.03
354019	hbl	2008	11064	87404	60022	5378	74000	6862	455	2750	127980	7.62	213.31	28.17		42.62	44.42	26.39		3.01		25.53	5.60	23.74	4.36	23.35	6.89	1.99	7.50	8.42	4.58	4.28	0.63	2.42		0.08	0.02
354019	hbl	2008	12163	87348	59633	5616	74000	7710	427	2836	120066	0.69	197.15	25.36		64.35	47.10	32.85		2.98		31.60	9.55	38.99	6.83	34.90	8.82	2.31	8.84	8.65	4.83	4.78	0.67	0.76	0.03	0.12	0.02
354019	hbl	2008	11490	92801	57118	4263	74000	6627	449	2867	116698	26.54	193.19	22.98		48.44	32.47	24.02		2.81	0.81	15.84	6.89	28.30	4.96	24.68	5.90	1.77	6.09	5.65	3.25	3.21	0.44	0.79	0.02	0.08	0.02
354019	hbl	2008	15322	111151	59714	7238	74000	13840	480	1055	84429	35.87	65.17	13.55	0.80	291.34	23.32	60.03		2.14	0.51	40.66	2.57	10.09	2.08	12.14	4.08	1.36	5.16	4.73	2.51	2.04	0.26	19.09		0.03	0.01
354019	hbl	2008	290	115297	77424	162	74000	1425	398	4945	143395	5.90	591.46	38.47		76.12	15.02	5.65		0.50	0.12	7.55	4.59	15.10	2.37	11.75	2.74	0.74	2.90	2.41	1.64	1.67	0.31	3.66		0.03	0.01
BA08GS026	hbl	2008	12366	86037	63422	5655	79000	8869	492	2701	130524		185.03	25.37		76.86	35.99	37.63		2.26		35.32	10.10	35.99	5.71	27.50	7.10	2.02	6.84	6.86	3.74	3.94	0.50	1.09	0.02	0.18	0.07
BA08GS026	hbl	2008	11154	93294	53757	4117	79000	7284	456	2670	122852		187.27	24.21		56.18	39.39	34.53		2.61		22.10	12.56	49.53	8.18	39.72	9.33	2.51	8.71	7.43	4.01	3.53	0.55	0.82		0.15	0.04
BA08GS026	hbl	2008	6934	75198	37108	3525	79000	4550	408	2957	98899		160.79	17.24	0.99	54.27	26.31	23.31		1.56	0.24	17.70	6.50	25.24	4.25	21.00	5.09	1.48	4.84	4.87	2.64	2.62	0.36	0.85	0.02	0.09	0.04
BA08GS026	hbl	2008	10906	89442	57373	4557	79000	7350	517	3126	128385	0.85	226.88	26.12		64.09	38.02	32.52		2.03		26.16	8.71	34.44	5.74	29.05	7.04	2.03	7.32	7.47	4.09	3.89	0.59	1.20	0.02	0.14	0.03
BA08GS026	hbl	2008	11039	92433	53729	4673	79000	7277	465	2619	123502		181.72	23.77		46.38	47.86	25.77		2.83		19.43	11.45	45.13	7.72	39.45	9.95	2.54	10.30	9.18	4.67	4.38	0.62	0.83		0.12	0.03
BA08GS026	hbl	2008	11454	91447	55471	4475	79000	7141	465	2659	125506		190.83	25.77		49.94	35.77	26.42		2.46		19.19	10.57	42.47	7.23	35.09	8.44	2.27	7.93	6.74	3.81	3.62	0.49	0.70	0.03	0.13	0.03
BA08GS026	hbl	2008	6276	80444	36852	3129	79000	4770	354	4349	88331		200.23	17.19		59.19	27.67	20.68		1.82	0.12	18.14	6.84	25.73	4.24	21.23	5.23	1.40	5.38	5.15	2.91	2.75	0.47	2.10		0.14	0.03
BA08GS026	hbl	2008	11283	94808	56536	5313	79000	7507	486	2826	133713		191.34	24.17		46.23	43.55	24.30		2.64		21.51	10.08	41.13	6.66	33.91	8.73	2.27	8.73	8.44	4.45	4.12	0.59	0.76	0.03	0.12	0.02
BA08GS030	hbl	2008	9046	91122	61155	6000	80000	9446	492	3363	140962	57.82	207.45	25.30		73.80	56.20	46.45		2.54		48.37	10.91	42.01	7.29	37.48	10.41	2.72	10.21	10.77	6.21	5.90	0.86	0.99	0.02	0.15	0.29
BA08GS030	hbl	2008	9436	98574	64243	5825	82000	10254	484	2780	123881		177.85	21.93		85.97	39.34	65.82		2.15		42.78	9.21	34.16	5.81	29.52	8.01	2.31	7.98	7.75	4.58	4.28	0.58	0.83	0.04	0.21	0.07
BA08GS030	hbl	2008	4275	109034	33512	4404	82000	6980	393	4065	119875	1.05	171.72	18.32		16.85	95.06	28.43		4.34		12.65	22.89	81.19	12.84	61.76	16.59	2.55	17.12	18.60	9.79	9.57	1.34	0.49	0.02	0.18	0.05
BA08GS030	hbl	2008	9241	101471	59172	5152	82000	8083	480	2844	126941	10.18	188.01	24.58		64.66	48.90	34.80	0.16	2.68		29.94	11.69	44.72	7.61	38.37	10.23	2.59	9.77	9.76	5.08	5.09	0.74	0.78	0.02	0.19	0.05
BA08GS030	hbl	2008	6475	93095	48177	4260	82000	9403	511	3285	124243	0.86	212.46	26.28		49.81	46.53	32.54		3.64	0.14	33.64	8.03	31.62	5.52	27.86	8.25	2.20	8.98	9.23	5.01	4.73	0.74	0.61		0.13	0.04
BA08GS030	hbl	2008	8987	91470	60082	6068	80000	8613	476	3690	142324	2.87	195.93	26.15		57.27	57.36	40.31		2.80		41.64	11.17	42.85	7.20	38.31	9.45	2.61	10.15	10.44	6.18	6.01	0.90	0.88	0.03	0.14	0.04
BA08GS030	hbl	2008	9580	100081	58421	4902	82000	8169	488	2873	129727		193.11	24.11		61.29	40.84	32.96		2.22		26.98	10.95	41.74	6.98	33.45	8.62	2.31	8.12	7.85	4.38	4.40	0.63	0.76	0.02	0.16	0.03
BA08GS030	hbl	2008	3628	105166	29833	3260	82000	4261	399	4055	111940	7.72	188.44	14.03		9.68	54.48	11.20		3.70		12.78	8.77	25.96	4.12	22.69	6.78	1.36	8.85	10.00	5.76	5.38	0.83	0.56	0.01	0.07	0.02
BA08GS033A	hbl	2008	11123	93466	52638	5503	80000	10935	444	3246	127799		187.24	19.60		68.76	59.13	53.84	0.18	2.29		57.70	9.78	36.92	6.19	33.85	9.03	2.40	9.69	10.73	6.57	6.68	1.00	1.37	0.02	0.11	0.09
BA08GS033A	hbl	2008	11253	93828	51359	4498	80000	8756	416	3396	127463	4.76	202.41	21.40		61.44	53.67	46.53		2.20		40.84	8.21	31.23	5.69	30.13	9.01	2.22	9.64	10.42	5.63	6.00	0.83	1.01	0.02	0.09	0.07
BA08GS033A	hbl	2008	11578	94576	52741	5438	80000	12784	402	3638	126850		197.55	20.27		100.08	51.55	65.78		2.59		65.28	8.34	31.76	5.65	29.00	8.30	2.17	8.34	9.70	5.37	5.53	0.75	1.09	0.02	0.12	0.06
BA08GS033A	hbl	2008	10972	95676	50321	5325	80000	9569	429	3374	128372		200.09	20.37		65.37	54.27	46.79		2.46		51.31	10.41	38.42	6.50	33.48	9.83	2.49	9.20	10.38	5.72	5.76	0.85	0.76	0.02	0.20	0.05
BA08GS033A	hbl	2008	10743	106436	47721	4072	80000	8397	357	4335	124839		222.31	20.07		46.01	74.20	42.34		2.82		32.77	10.97	44.38	8.02	43.15	12.27	2.80	12.82	14.10	8.05	8.11	1.22	0.68	0.01	0.13	0.04
BA08GS033A	hbl	2008	11341	101778	50544	4392	80000	8597	408	3532	127185	0.54	195.44	21.09		56.72	55.69	49.70		2.34	0.15	34.92	9.55	39.17	6.77	34.97	9.91	2.53	10.17	10.14	6.00	6.28	0.87	0.81	0.02	0.13	0.03
BA08GS033A	hbl	2008	10384	101910	46908	4056	80000	6610	352	4216	130521		227.30	21.70		31.97	75.36	29.40		3.36		21.39	11.87	49.35	9.15	48.26	13.72	3.06	13.92	14.85	8.23	7.68	1.13	0.67	0.01	0.11	0.03
BA08GS033A	hbl	2008	9355	107343	43157	3614	80000	6599	314	4280	122925	1.27	220.70	19.51		31.32	82.03	29.90		3.38		22.85	13.12	53.59	9.57	49.49	14.03	3.08	14.89	15.86	8.67	8.29	1.12	0.66	0.01	0.10	0.03
BA08GS033A	hbl	2008	8467	108864	49004	3511	80000	6973	453	3427	127006	9.50	250.04	21.00		52.62	48.81	35.39		1.89		24.69	8.40	31.23	5.44	29.47	7.88	1.95	8.88	8.93	5.19	4.48	0.70	1.46	0.01	0.07	0.02
BA08GS033B	hbl	2008	15028	98151	71626	4304	81000	10336	519	1042	94989		62.68	13.43		202.88	15.90	13.27		0.90		45.38	0.62	2.99	0.72	5.27	2.09	0.86	3.06	3.23	1.76	1.35	0.19	0.45		0.02	
BA08GS033B	hbl	2008	9860	96238	47388	3767	81000	7972	367	3678	124138		208.89	19.91		56.63	56.77	392.14	0.14	1.92		33.29	13.73	46.21	7.44	37.39	9.90	2.43	10.11	9.97	6.02	6.55	0.96	0.61	0.02	0.42	0.33
BA08GS033B	hbl	2008	11505	101256	47949	4944	80000	8362	340	3818	113861	93.40	196.92	19.02		62.13	56.46	39.90		2.07		65.75	11.72	42.02	6.83	35.48	9.70	2.35	9.42	9.79	5.72	5.79	0.83	1.42	0.07	0.46	0.17
BA08GS033B	hbl	2008	11918	94758	55789	5520	80000	8204	451	3352	126466	7.31	206.19	22.57		53.63	58.40	32.90		2.26	0.32	38.79	10.04	41.20	7.10	36.01	10.17	2.59	10.18	10.46	6.06	5.86	0.89	1.51	0.02	0.13	0.05
BA08GS033B	hbl	2008	10435	106692	46171	4220	81000	8751	305	4000	125532		230.15	18.88		55.81	58.85	47.11	0.19	2.14		38.83	10.10	39.67	6.51	34.36	9.59	2.61	10.39	10.53	6.11	6.28	0.85	0.66		0.11	0.04
BA08GS033B	hbl	2008	13399	86503	67798	4860	81000	9989	472	2750	122346		168.38	19.44		172.71	24.30	23.94		1.36		50.25	3.17	12.43	2.24	11.88	3.92	1.23	4.31	4.50	2.49	2.65	0.33	0.76		0.07	0.04
BA08GS033B	hbl	2008	11173	96335	49720	5254	81000	13601	434	3701	125841	0.67	198.47	19.40		96.20	44.19	64.26		1.94		67.60	9.39	34.78	5.78	29.04	7.98	2.25	7.90	7.78	4.69	4.65	0.67	0.82		0.14	0.03
BA08GS033B	hbl	2008	8917	106757	44759	2952	81000	6062	334	4224	120696	0.48	238.34	18.61		36.87	59.96	26.24		2.15		19.25	9.67	41.11	7.11	37.51	10.24	2.63	10.15	11.11	6.24	6.20	0.97	0.54	0.01	0.09	0.03

Sample #	Mineral	Year	Na	Mg	Al	K	Ca	Ti	V	Mn	Fe	Cu	Zn	Ga	As	Sr	Y	Zr	Mo	Sn	Sb	Ba	La	Ce	Pr	Nd	Sm	Eu	Gd	Dy	Er	Yb	Lu	Pb	Bi	Th	U
BA08GS033B	hbl	2008	10519	101638	48264	3816	81000	7565	367	4134	128235		225.88	20.57		41.46	61.47	33.57		2.50		26.26	10.14	40.59	7.33	37.40	10.15	2.45	10.52	10.41	6.18	6.47	0.99	0.59		0.09	0.03
BA08GS033B	hbl	2008	11432	87951	53940	6131	81000	11717	509	2988	130342	0.92	191.63	21.20		101.50	35.75	59.19		1.94		65.62	8.59	31.00	4.96	25.34	6.93	2.09	6.86	6.88	4.12	3.63	0.60	0.99	0.03	0.10	0.03
BA08GS033B	hbl	2008	10165	107312	49084	4165	81000	9399	413	3593	131008	26.91	282.20	22.27	1.06	57.97	60.81	45.81		2.69		37.51	10.88	42.23	7.24	36.76	10.14	2.57	10.53	11.39	6.12	6.05	0.87	36.11	0.28	0.10	0.03
BA08GS033B	hbl	2008	14341	90579	71966	4539	81000	10382	516	1181	98565		73.70	14.08		207.45	14.44	12.15		0.90		44.05	0.60	2.69	0.60	4.52	1.95	0.78	2.57	2.77	1.60	1.43	0.17	0.54		0.03	0.02
BA08GS033B	hbl	2008	10808	98986	49799	5512	81000	9828	410	3768	129951		216.92	20.94		51.27	58.51	41.65		2.24		50.80	9.58	36.36	6.23	32.79	8.92	2.28	9.74	10.28	6.08	6.20	0.92	0.75	0.02	0.12	0.02
BA08GS033B	hbl	2008	10772	101241	48985	3780	81000	7977	374	4154	126876		220.12	21.30		45.62	61.31	36.36		2.19		26.73	9.26	38.38	6.87	35.73	9.76	2.69	10.97	10.85	6.33	6.37	1.00	0.59		0.10	0.01
BA08GS035	hbl	2008	14505	109370	70436	7431	87000	8761	536	1586	94776	4.90	106.63	11.50		177.33	10.15	5.86		0.88		43.57	0.51	2.17	0.41	3.41	1.34	0.54	1.92	2.00	1.22	1.07	0.11	0.75			
BA08GS035	hbl	2008	16226	99657	77692	5487	86000	11404	630	1229	110009	4.33	99.37	14.84		233.46	16.10	14.02		1.44		46.06	0.65	2.84	0.72	4.72	2.03	0.76	2.69	3.32	1.57	1.45	0.18	0.45			
BA08GS035	hbl	2008	16607	108773	80228	7484	86000	11209	612	1130	101203	3.91	115.40	14.10		205.67	12.55	7.78		0.91	0.22	50.58	0.46	2.09	0.47	3.83	1.63	0.62	2.34	2.88	1.47	1.16	0.14	0.40			
BA08GS035	hbl	2008	16953	101538	78345	6284	86000	11435	536	864	98641	2.53	44.98	13.34		237.01	16.20	10.32		1.40		44.75	0.50	2.51	0.61	4.61	2.08	0.79	3.04	3.65	1.84	1.45	0.17	0.37			
BA08GS035	hbl	2008	11432	103637	56363	5800	87000	6861	455	2487	93521	0.53	92.04	8.90		137.60	7.74	5.37		0.39	0.14	35.17	0.36	1.88	0.41	2.28	0.86	0.49	1.64	1.72	0.97	0.83	0.13	0.37			
BA08GS035	hbl	2008	16502	102760	82448	7726	86000	10434	510	910	100893	1.56	50.56	13.40		215.45	13.28	8.19		1.03		48.08	0.47	2.27	0.48	3.52	1.63	0.80	2.38	2.69	1.63	1.17	0.15	0.36			
BA08GS035	hbl	2008	16456	101822	75991	7653	86000	9837	539	900	100444	1.09	46.74	13.08		193.11	11.18	7.08		0.59		42.88	0.36	2.05	0.47	3.10	1.62	0.60	1.82	2.32	1.35	1.06	0.11	0.31			
BA08GS035	hbl	2008	17011	106797	75880	7864	86000	9846	509	836	99915	0.48	44.64	13.05		192.19	9.37	5.11		0.63		46.29	0.34	1.58	0.41	2.96	1.49	0.53	1.97	2.21	1.04	0.77	0.12	0.28			
BA08GS035	hbl	2008	17805	112888	76985	7343	87000	9026	500	852	94393	2.51	43.51	13.22		186.28	12.60	8.42		0.89		37.95	0.42	2.27	0.55	4.23	1.82	0.62	2.26	2.73	1.39	1.23	0.16	0.22			
BA08GS035	hbl	2008	2187	104688	16004	961	87000	1081	283	8318	117612	6.91	289.48	5.60	1.47	20.01	2.91	2.64			0.61	4.25	0.05	0.28	0.05	0.45	0.19	0.08	0.30	0.30	0.45	0.77	0.16	0.54	0.02		
BA08GS035	hbl	2008	14514	107816	77472	6545	87000	9252	584	2497	117020	17.31	224.47	16.77		196.97	12.46	8.92		1.07		45.32	0.54	2.36	0.52	3.71	1.62	0.62	2.50	2.73	1.45	1.10	0.18	0.49		0.02	
BA08GS035	hbl	2008	14702	95444	78128	5809	86000	10256	557	2014	114442	3.62	175.20	15.55		228.85	15.73	10.81		0.97		48.16	0.51	2.52	0.54	4.44	2.02	0.83	2.78	3.20	1.83	1.47	0.22	1.42		0.02	
BA08GS035	hbl	2008	16385	97472	80707	6978	86000	10717	531	993	103763		52.03	13.77		228.59	14.35	9.58		1.03		48.63	0.55	2.58	0.60	4.06	1.82	0.70	2.59	2.81	1.49	1.25	0.17	0.34		0.02	
BA08GS035	hbl	2008	16471	105194	77571	7432	86000	10448	558	911	100154	2.77	56.49	13.54		207.48	11.76	7.00		1.09		45.20	0.45	2.17	0.51	3.35	1.56	0.63	2.07	2.42	1.26	0.98	0.12	0.32		0.02	
BA08GS035	hbl	2008	17232	107617	78108	8546	87000	10220	577	760	96999	2.44	40.10	12.67		203.51	11.68	6.99		0.95		46.95	0.49	2.40	0.53	3.31	1.49	0.62	2.02	2.67	1.27	1.00	0.14	0.24		0.01	
BA08GS035	hbl	2008	16112	96389	80660	7015	86000	10624	499	948	100660	1.03	48.14	13.34		233.67	13.89	7.82		0.91		48.37	0.42	2.06	0.49	3.31	1.83	0.72	2.51	2.96	1.50	1.23	0.16	0.34	0.02	0.01	
BA08GS035	hbl	2008	16245	92727	81527	6377	86000	10893	519	1139	107935	2.01	58.69	14.59		237.37	16.10	10.41		0.99		46.97	0.51	2.63	0.58	4.75	2.14	0.78	2.83	3.20	1.78	1.49	0.21	0.36		0.01	
BA08GS035	hbl	2008	16651	102346	78497	7378	86000	10047	584	857	98164	2.21	45.36	13.19		211.72	12.75	8.67		0.70		46.92	0.52	2.53	0.58	4.04	1.89	0.67	2.29	2.67	1.41	1.05	0.15	0.30		0.01	
BA08GS035	hbl	2008	16549	100444	79967	6747	87000	10586	557	1030	103236	2.78	53.16	14.22		232.13	14.18	9.34		1.16		45.49	0.52	2.40	0.55	4.17	1.72	0.71	2.71	3.07	1.56	1.25	0.16	0.32		0.01	
BA08GS035	hbl	2008	16611	99264	79426	6734	87000	10437	545	957	101218	1.80	51.97	13.86		229.12	13.87	8.95		1.06		44.58	0.51	2.44	0.53	4.31	1.77	0.79	2.65	2.94	1.65	1.32	0.17	0.41		0.01	
BA08GS035	hbl	2008	15165	93575	79507	5156	86000	11056	563	1838	119996	4.96	114.68	18.21		234.25	22.73	14.40		1.37		44.67	1.79	6.04	1.18	7.16	2.98	1.02	3.89	4.41	2.50	2.09	0.29	0.95	0.04	0.17	0.08
BA08GS035	hbl	2008	17031	97855	82959	6743	87000	11294	547	976	103674		48.74	14.85		261.44	16.00	11.16		1.13		54.54	0.61	2.84	0.68	4.88	2.00	0.80	2.92	3.71	1.79	1.47	0.20	0.44			0.02
BA08GS035	hbl	2008	16159	105683	74272	7835	86000	9554	540	728	93306	4.69	46.26	12.32		188.74	9.82	6.25		0.93		45.00	0.51	2.04	0.42	3.32	1.61	0.54	1.96	2.23	1.03	0.80	0.12	0.20			0.01
BA08GS035	hbl	2008	17275	111060	75729	8872	87000	9647	653	893	95599	1.17	40.44	12.44		187.43	10.27	8.19		0.86		46.71	0.62	2.35	0.54	3.53	1.60	0.60	1.88	2.17	1.20	0.90	0.12	0.26		0.02	0.01
BA08GS038	hbl	2008	24	495	54047	133	77500	4565	336	769	51425		6.62	38.34	5.65	621.49	5.57	0.76	0.01	0.63	2.53	3.13	9.11	11.32	1.14	4.16	0.76	3.17	0.75	0.70	0.41	0.38	0.05	13.79	0.12	0.05	1.42
BA08GS038	hbl	2008	9	268	54378	62	77500	6540	396	677	50067	0.58	3.92	41.20	5.22	556.86	5.62	0.63		0.81	2.41	1.92	7.52	8.18	0.79	3.23	0.57	5.33	0.57	0.49	0.33	0.35	0.06	15.12	0.08		1.39
BA08GS038	hbl	2008	10200	127049	71148	4325	77500	7997	538	3443	139009	22.29	635.08	29.96	1.04	57.40	29.76	33.57		2.12	0.29	25.35	8.68	30.86	4.99	24.97	5.68	1.74	5.74	5.63	3.07	3.18	0.48	1.58	0.14	0.15	0.11
BA08GS038	hbl	2008	10405	89169	53810	4409	77500	7142	482	2786	123352	1.31	210.17	23.23		58.52	38.57	34.52	0.07	1.93	0.06	26.00	11.67	41.21	6.67	30.74	7.80	2.02	6.87	7.01	4.04	4.31	0.78	0.95	0.02	0.24	0.07
BA08GS038	hbl	2008	10821	91065	53093	4307	77500	7822	417	3071	120676	0.99	203.12	24.28	0.49	65.24	44.34	41.84		2.35		26.70	11.59	44.33	7.43	38.30	10.09	2.55	9.69	8.66	4.90	4.56	0.67	1.37	0.04	0.16	0.05
BA08GS038	hbl	2008	9314	131874	72564	3955	77500	6504	498	4031	146826	5.12	469.96	31.98	0.66	57.60	31.63	37.35	0.15	2.24	0.13	25.27	9.65	37.62	6.41	32.55	7.75	2.03	7.29	6.10	3.13	2.77	0.42	0.96		0.20	0.03
BA08GS038	hbl	2008	6064	94293	44864	2535	77500	3686	384	3670	107723	2.32	326.52	20.12	0.70	40.92	24.70	16.96	0.18	1.34	0.13	12.42	5.19	19.49	3.39	17.08	4.52	1.12	4.69	4.52	2.39	2.30	0.36	0.76		0.07	0.02
BA08GS047	hbl	2008	16802	104078	75976	6471	86500	10730	568	997	101480		52.62	15.23		259.93	18.25	20.86		1.50		50.77	1.12	4.74	1.01	6.36	2.46	0.92	3.40	3.89	2.14	1.52	0.21	0.37			
BA08GS047	hbl	2008	17787	105136	76328	6548	86500	10429	586	1027	105029		57.99	15.79		249.26	16.78	23.24		1.17		45.90	1.27	5.25	1.06	6.99	2.39	0.89	3.26	3.41	1.83	1.47	0.20	0.47		0.02	
BA08GS047	hbl	2008	13113	95426	71505	7225	86500	12058	592	2037	125748		121.83	19.82		232.17	24.57	44.69		1.43		57.41	3.09	11.99	2.33	13.45	3.77	1.42	4.97	4.99	2.73	2.58	0.37	0.79	0.02	0.04	0.02
BA08GS047	hbl	2008	13927	101725	73483	7158	86500	10703	574	1517	108792		79.88	16.85		253.56	20.48	29.62		1.17		57.30	2.05	8.48	1.66	10.27	3.51	1.13	3.67	4.21	2.11	1.85	0.27	0.92		0.04	0.02
BA08GS047	hbl	2008	14846	103597	73051	6037	86500	9744	540	1338	104673		69.62	15.23		235.71	18.63	25.04		1.00		43.44	1.31	5.64	1.27	7.62	2.63	1.02	3.41	3.60	2.11	1.72	0.24	0.85	0.02	0.02	0.01
BA08GS047	hbl	2008	15017	99399	74119	6562	86500	11082	589	1468	116719	1.06	91.80	17.42		248.75	19.19	25.58		1.31		50.65	1.41	5.63	1.20	7.53	2.82	0.94	3.53	3.84	1.99	1.87	0.24	1.27	0.03	0.03	0.01
BA08GS047	hbl	2008	16687	104722	75233	6385	86500	9962	561	1291	107249		82.00	15.13		252.50	17.37	21.11		1.12		50.02	1.21	4.93	1.06	6.63	2.33	0.93	3.26	3.40	1.97	1.65	0.21	2.03		0.04	0.01
BA08GS047	hbl	2008	15977	104535	75969	5885	86500	10684	555	1210	104507	5.07	70.10	14.76		208.93	17.95	17.04		1.16		35.57	0.98	3.77	0.81	5.34	1.78	0.79	2.89	3.45	2.13	1.59	0.21	0.47		0.01	0.01
BA08GS047	hbl	2008	16458	106504	73846	6394	86500	9712	555	961	97751		49.10	15.19		241.23	16.08	20.59		1.25		45.38	1.16	4.69	1.04	6.07	2.41	0.83	2.93	3.39	1.73	1.50	0.20	0.44		0.02	0.01
BA08GS056	hbl	2008	16217	103530	82389	5224	87000	9348	572	889	99040	1.12	48.63	14.77		253.87	13.62	10.77		1.05		45.29	0.49	2.18	0.54	3.53	1.70	0.60	2.40	2.75	1.50	1.43	0.19	0.51			
BA08GS056	hbl	2008	16123	109936	81993	5572	87000	9300	632	1128	98493	4.65	60.17	16.56		213.45	15.26	12.41		1.21		42.94	0.62	2.81	0.66	4.46	1.98	0.71	2.97	3.28	1.66	1.42	0.19	0.48			
BA08GS056	hbl	2008	16659	102456	82363	5823	87000	9738	635	1045	101944	0.94	60.70	16.27		220.67	15.31	11.18		1.00		44.27	0.51	2.57	0.62	4.43	1.93	0.74	2.65	3.10	1.70	1.49	0.20	0.46			
BA08GS056	hbl	2008	17500	119052	74739	6031	87000	9472	609	642	75956	0.89	30.77	11.83		199.37	11.21	8.78		0.76		39.37	0.41	1.70	0.39	2.74	1.36	0.55	1.87	2.15	1.14	1.07	0.13	0.37			
BA08GS056	hbl	2008	18110	120622	77207	6970	87000	8629	652	662	78036	1.34	34.99	11.90		175.52	11.55	6.24		0.68		36.47	0.31	1.46	0.36	2.85	1.41	0.53	1.99	2.53	1.33	1.04	0.15	0.27			
BA08GS056	hbl	2008	18022	121489	77057	7115	87000	8832	611	671	73640	2.76	33.85	12.25		185.75	11.86	7.34		0.65		45.37	0.43	1.81	0.45	2.85	1.54	0.65	2.15	2.36	1.19	1.11	0.12	0.26			
BA08GS056	hbl	2008	18265	124869	76169	7347	87000	8694	643	599	70607	0.68	29.58	11.57		174.66	10.72	6.38		0.81		36.19	0.36	1.71	0.38	2.70	1.33	0.53	1.97	2.25	1.27	0.85	0.13	0.25			
BA08GS056	hbl	2008	15701	106567	73339	4741	87000	12115	558	1383	96620	1.22	69.61	16.21	1.21	233.62	35.93	27.10		1.52		53.73	2.73	10.88	2.19	14.53	5.29	1.73	6.63	7.25	4.15	3.50	0.52	0.54		0.12	
BA08GS056	hbl	2008	15535	120866	69888	6371	87000	7816	666	1017	77807	0.75	47.92	10.87		152.90	9.86	5.96		0.82		32.76	0.30	1.38	0.31	2.26	1.17	0.49	1.75	1.94	1.03	0.90	0.14	0.37		0.03	
BA08GS056	hbl	2008	16352	95754	78739	5062	87000	10414	636	1315	114799	1.97	84.32	17.27		217.84	17.47	13.64		1.34		40.81	0.51	3.10	0.69	5.13	2.40	0.84	2.86	3.46	2.01	1.73	0.24	0.54		0.03	
BA08GS056	hbl	2008	17041	120518	74925	5463	87000	8456	550	750	80798	2.10	35.60	12.86		201.14	11.61	9.00		0.91		35.02	0.44	1.89	0.50	3.09	1.22	0.57	2.13	2.38	1.36	1.00	0.14	0.41		0.02	
BA08GS056	hbl	2008	16842	117268	75907	5029	87000	8506	541	853	87932		40.51	13.72		215.36	12.96	10.32		0.90		37.15	0.44	2.05	0.54	3.65	1.64	0.61	2.27	2.48	1.48	1.18	0.15	0.42	0.03	0.02	
BA08GS056	hbl	2008	17432	112694	77410	6172	87000	9723	591	808	90220	1.30	41.78	13.44		219.00	12.57	9.64		0.90		42.79	0.44	2.12	0.51	3.35	1.75	0.63	2.34	2.80	1.49	1.30	0.15	0.39		0.02	
BA08GS057	hbl	2008	6517	70624	36771	2412	86000	4432	454	1670	54210	0.33	39.53	10.97		120.30	18.50	5.47		8.04		13.62	0.42	1.76	0.42	3.34	1.71	0.86	2.85	3.34	2.01	1.64	0.24	1.53			
BA08GS057	hbl	2008	11284	80738	60028	3638	86000	6406	426	974	70693	0.92	42.48	11.42		194.82	9.72	7.95		0.59		32.82	0.48	1.96	0.41	2.96	1.08	0.48	1.75	1.90	1.11	1.01	0.13	0.70			
BA08GS057	hbl	2008	15196	162740	99434	4419	86000	9426	759	1599	131637	2.60	135.75	26.49		198.67	13.59	12.51	0.15	1.01		35.99	0.53	2.43	0.56	3.70	1.88	0.55	2.25	2.73	1.61	1.32	0.16	0.58			
BA08GS057	hbl	2008	16105	87884	83866	5167	86000	12156	556	1561	122107	1.40	95.72	17.81		268.11	21.35	12.60		1.21		42.85	0.69	3.39	0.87	6.18	2.79	1.09	3.70	4.14	2.34	1.92	0.29	0.47			
BA08GS057	hbl	2008	17888	121014	76082	7115	86000	8341	654	613	73196	0.36	28.60	11.28		165.50	10.92	5.82		0.71		36.54	0.26	1.46	0.38	2.74	1.40	0.53	1.84	2.40	1.07	1.10	0.14	0.30			
BA08GS057	hbl	2008	17465	118389	74584	5943	86000	9094	598	640	75934	0.76	32.33	12.47		197.25	11.72	8.12		0.79		38.53	0.41	1.78	0.41	2.93	1.27	0.54	2.10	2.42	1.30	0.96	0.13	0.29			
BA08GS057	hbl	2008	17645	118623	79007	7364	86000	8821	667	684	83411	0.88	36.58	12.93		183.69	11.20	6.54		0.82		36.86	0.42	1.94	0.45	3.21	1.49	0.59	2.07	2.36	1.28	0.97	0.14	0.29			
BA08GS057	hbl	2008	17048	115618	77472	8460	86000	9678	698	577	78809	0.54	27.73	11.80		180.61	9.35	5.89		0.91		41.26	0.36	1.66	0.35	2.62	0.98	0.46	1.54	1.89	0.96	0.74	0.10	0.18			
BA08GS057	hbl	2008	15152	108621	75723	4242	86000	9996	542	1211	98590	0.44	58.87	15.31		234.55	20.87	20.15		1.44		39.82	0.96	4.54	0.99	6.73	2.75	0.97	3.90	4.21	2.30	2.09	0.30	0.71	0.05	0.03	